PUBLICATION

20

DHL-publication 161

DISCHARGE MEASUREMENT STRUCTURES

INTERNATIONAL INSTITUTE FOR LAND RECLAMATION AND IMPROVEMENT/ILRI
DELFT HYDRAULICS LABORATORY
UNIVERSITY OF AGRICULTURE, DEPARTMENT OF HYDRAULICS AND IRRIGATION

DISCHARGE MEASUREMENT STRUCTURES

DISCHARGE MEASUREMENT STRUCTURES

Working Group on Small Hydraulic Structures

Editor: M. G. BOS

INTERNATIONAL INSTITUTE FOR LAND RECLAMATION AND IMPROVEMENT/ILRI
P.O. BOX 45, 6700 AA WAGENINGEN (THE NETHERLANDS) 1978

Represented in the Working Group on Small Hydraulic Structures are the following institutions:

INTERNATIONAL INSTITUTE FOR LAND RECLAMATION AND IMPROVEMENT / ILRI, WAGENINGEN

DELFT HYDRAULICS LABORATORY, DELFT

UNIVERSITY OF AGRICULTURE, DEPARTMENTS OF HYDRAULICS AND IRRIGATION, WAGENINGEN

The first edition of this book appeared as
Publication No. 20 ILRI, Wageningen
Publication No. 161, Delft Hydraulics Laboratory, Delft
Report No. 4, Laboratory of Hydraulics and Catchment Hydrology, Wageningen

First edition 1976
Second edition 1978

Printed in The Netherlands

Preface to the first edition

The Working Group on Small Hydraulic Structures was formed in September 1971 and charged with the tasks of surveying current literature on small structures in open channels and of conducting additional research as considered necessary. The members of the Working Group are all engaged in irrigation engineering, hydrology, or hydraulics, and are employed by the Delft Hydraulics Laboratory (DHL), the University of Agriculture (LH) at Wageningen, or the International Institute for Land Reclamation and Improvement (ILRI) at Wageningen.

The names of those participating in the Group are:

Ing. W.Boiten (DHL)
Ir. M.G.Bos (ILRI)
Prof.Ir. D.A.Kraijenhoff van de Leur (LH)
Ir. H.Oostinga (DHL) during 1975
Ir. R.H.Pitlo (LH)
Ir. A.H.de Vries (DHL)
Ir. J.Wijdieks (DHL)

The Group lost one of its initiators and most expert members in the person of Professor Ir. J.Nugteren (LH), who died on April 20, 1974.

The manuscripts for this publication were written by various group members. Ing. W.Boiten prepared the Sections 4.3, 4.4, and 7.4; Ir. R.H.Pitlo prepared Section 7.5; Ir. A.H.de Vries prepared the Sections 7.2, 7.3, 9.2, and 9.7, and the Appendices II and III. The remaining manuscripts were written by Ir. M.G.Bos. All sections were critically reviewed by all working group members, after which Ir. M.G.Bos prepared the manuscripts for publication.

Special thanks are due to Ir. E.Stamhuis and Ir. T.Meijer for their critical review of Chapter 3, to Dr P.T.Stol for his constructive comments on Appendix II and to Dr M.J.Hall of the Imperial College of Science and Technology, London, for proof-reading the entire manuscript.

This book presents instructions, standards, and procedures for the selection, design, and use of structures, which measure or regulate the flow rate in open channels. It is intended to serve as a guide to good practice for engineers concerned with the design and operation of such structures. It is hoped that the book will serve this purpose in three ways: (i) by giving the hydraulic theory related to discharge measurement structures; (ii) by indicating the major demands made upon the structures; and (iii) by providing specialized and technical knowledge on the more common types of structures now being used throughout the world.

The text is addressed to the designer and operator of the structure and gives the hydraulic dimensions of the structure. Construction methods are only given if they influence the hydraulic performance of the structure. Otherwise, no methods of construction nor specifications of materials are given since they vary greatly from country to country and their selection will be influenced by such factors as the availability of materials, the quality of workmanship, and by the number of structures that need to be built.

The efficient management of water supplies, particularly in the arid regions of the world, is becoming more and more important as the demand for water grows even greater with the world's increasing population and as new sources of water become harder to find. Water resources are one of our most vital commodities and they must be conserved by reducing the amounts of water lost through inefficient management. An essential part of water conservation is the accurate measurement and regulation of discharges.

We hope that this book will find its way, not only to irrigation engineers and hydrologists, but also to all others who are actively engaged in the management of water resources. Any comments which may lead to improved future editions of this book will be welcomed.

Wageningen, October 1975

M.G.Bos
editor

Preface to the second edition

The second edition of this book is essentially similar to the first edition in 1976, which met with such success that all copies have been sold.

The only new material in the second edition is found in Chapter 7, Sections 1 and 5.

Further all known errors have been corrected, a number of graphs have been redrawn and, where possible, changes in the lay-out have been made to improve the readability.

Remarks and criticism received from users and reviewers of the first edition have been very helpful in the revision of this book.

Wageningen, July 1978

M.G.Bos,
Editor

List of principal symbols

A	cross-sectional area	L^2
a	height of rectangular weir section (Sutro)	L
a	acceleration	LT^{-2}
B	channel surface width	L
b	breadth at bottom of control section	L
b_e	effective breadth of weir crest ($b + K_b$)	L
C_d	discharge coefficient	dimensionless
C_v	approach velocity coefficient	dimensionless
C_e	effective discharge coefficient (C_dC_v)	dimensionless
c	subscript for critical flow condition	dimensionless
D	diameter of float	L
D_p	diameter of pipe	L
D_n	thickness of n^{th} layer	L
D	drop number	dimensionless
d	diameter of circular weir	L
E	energy	ML^2T^{-2}
E	complete elliptical integral of the first kind	dimensionless
e	exponential number, 2.71828	dimensionless
F	force	MLT^{-2}
F	coefficient correction factor	dimensionless
Fr	Froude number, $Q(B/gA^3)^{\frac{1}{2}}$	dimensionless
f	friction coefficient in the Darcy-Weissbach equation	dimensionless
f	drowned flow reduction factor	dimensionless
G	weight	M
G	relative slope factor	dimensionless
g	gravitational acceleration	LT^{-2}
H	total energy head over crest	L
H_o	specific energy	L
H_1	total upstream energy head over crest	L
H_2	total downstream energy head over crest	L
h_1	upstream head above crest	L
h_2	tailwater head over crest	L
h_e	effective upstream head over crest ($h_1 + K_h$)	L
Δh	head loss over structure ($h_1 - h_2$)	L

K	weir constant	dimensionless
K	head loss coefficient	dimensionless
K	complete elliptical integral of the second kind	dimensionless
K_b & K_h	empirical quantities to correct for surface tension and viscosity	L
k	filling ratio circular weir $(h/d)^{0.5}$	dimensionless
k	acceleration due to mass forces	LT^{-2}
L	flowwise length of crest	L
L	length of channel reach	L
l	length of pipe	L
m	mass	M
m	cot θ	dimensionless
m	coordinate direction (binormal)	dimensionless
n	coordinate direction (principal normal)	dimensionless
n	number of data	dimensionless
P	wetted perimeter of flow cross-section	dimensionless
P	pressure intensity	$ML^{-1}T^{-2}$
p	height of crest above approach channel bed	L
p_2	height of crest above tailwater channel bed	L
Q	discharge rate	L^3T^{-1}
Q_r	discharge rate through rectangular section	L^3T^{-1}
Q_c	discharge rate through curved section	L^3T^{-1}
Q_{air}	volumetric air discharge rate	L^3T^{-1}
q	discharge per unit width	L^2T^{-1}
R	hydraulic radius (A/P)	L
R_b	radius of embankment	L
r	radius of circular weir	L
r	radius of curved streamline	L
r	radius of float-wheel	L
r	radius of round-nose weir crest	L
S	length of side weir	L
S_H	submergence ratio (H_2/H_1)	dimensionless
S_h	submergence ratio (h_2/h_1)	dimensionless
S_m	modular limit	dimensionless
s	coordinate direction (velocity direction)	dimensionless
T_f	resisting torque due to friction	ML^2T^{-2}

TW	tailwater level	L
t	time	T
u	power of head or of differential head	dimensionless
V	volume of fluid	L^3
v	fluid velocity	LT^{-1}
$\bar{v}$	average fluid velocity (Q/A)	LT^{-1}
W	friction force	MLT^{-2}
w	acceleration due to friction	LT^{-2}
w	underflow gate opening	L
X	relative error	dimensionless
X	horizontal distance	L
x	breadth of weir throat at height y above crest	L
x	factor due to boundary roughness	dimensionless
x	cartesian coordinate direction	dimensionless
Y	vertical distance	L
y	vertical depth of flow	L
y	coordinate direction	dimensionless
z	coordinate direction	dimensionless
Δz	drop height	L
α	velocity distribution coefficient	dimensionless
α	angle of circular section	degrees
α	diversion angle	degrees
β	half angle of circular section ($\frac{1}{2}\alpha$)	degrees
γ	Q_{max}/Q_{min}	dimensionless
δ	error	dimensionless
δ	contraction coefficient	dimensionless
Δ	small increment of	dimensionless
Δ	$(\rho_s - \rho)/\rho$: relative density	dimensionless
θ	weir notch angle	degrees
π	circular circumference-diameter ratio; 3.1416	dimensionless
ρ	mass density of water	ML^{-3}
ρ_{air}	mass density of air	ML^{-3}
ρ_s	mass density of bed material	ML^{-3}
ω	circular section factor	dimensionless
ξ	friction loss coefficient	dimensionless
τ	standard deviation	dimensionless
$\hat{\tau}$	estimate of standard deviation	dimensionless
τ'	relative standard deviation	dimensionless

Contents

APPENDIX III

SIDE WEIRS AND OBLIQUE WEIRS 419

APPENDIX IV

SUITABLE STILLING BASINS 431

APPENDIX V

TABLES 451

1 Basic principles of fluid flow as applied to measuring structures

1.1 General

The purpose of this chapter is to explain the fundamental principles involved in evaluating the flow pattern in weirs, flumes, orifices and other measuring structures, since it is the flow pattern that determines the head-discharge relationship in such structures.

Since the variation of density is negligible in the context of these studies, we shall regard the mass density (ρ) of water as a constant. Nor shall we consider any flow except time invariant or steady flow, so that a streamline indicates the path followed by a fluid particle.

The co-ordinate system, used to describe the flow phenomena at a point P of a streamline in space, has the three directions as illustrated in Figure 1.1.

Before defining the co-ordinate system, we must first explain some mathematical concepts. A tangent to a curve is a straight line that intersects the curve at two points which are infinitely close to each other. An osculating plane intersects the curve at three points which are infinitely close to each other. In other words, the curvature at a point P exists in the local osculating plane only. Hence the tangent is a line in the osculating plane. The normal plane to a curve at P is defined as the plane perpendicular to the tangent of the curve at P. All lines through P in this normal plane are called normals, the normal in the osculating plane being called the principal normal, and the one perpendicular to the osculating plane being called the bi-normal.

The three co-ordinate directions are defined as follows:

s-direction: The direction of the velocity vector at point P. By definition, this vector coincides with the tangent to the streamline at P ($v_s = v$).

n-direction: The normal direction towards the centre of curvature of the streamline at P. By definition, both the s- and n-direction are situated in the osculating plane.

m-direction: The direction perpendicular to the osculating plane at P as indicated in Figure 1.1.

It should be noted that, in accordance with the definition of the osculating plane, the acceleration of flow in the m-direction equals zero ($a_m = 0$).

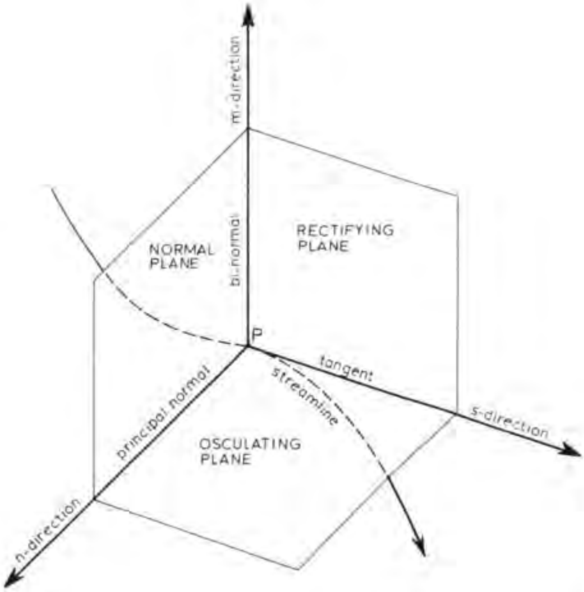

Fig.1.1.
The co-ordinate system.

Metric units (SI) will be used throughout this book, although sometimes for practical purposes, the equivalent Imperial units will be used in addition.

1.2 Continuity

An elementary flow passage bounded by streamlines is known as a stream tube. Since there is, per definition, no flow across these boundaries and since water is assumed here to be incompressible, fluid must enter one cross-section of the tube at the same volume per unit time as it leaves the other.

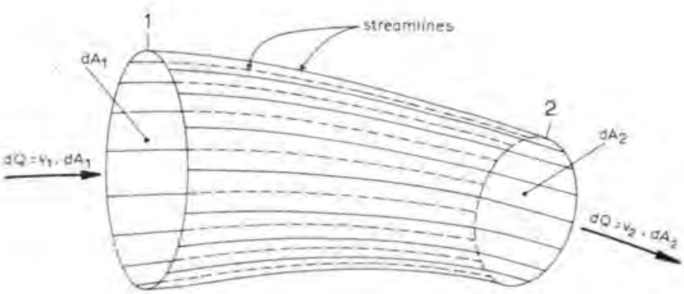

Fig.1.2.
The stream tube.

From the assumption of steady flow, it follows that the shape and position of the stream tube do not change with time. Thus the rate at which water is flowing across a section equals the product of the velocity component perpendicular to the section and the area of this section. If the subscripts 1 and 2 are applied to the two ends of the elementary stream tube, we can write:

$$\text{Discharge} = dQ = v_1 dA_1 = v_2 dA_2 \tag{1-1}$$

This continuity equation is valid for incompressible fluid flow through any stream tube. If Equation 1-1 is applied to a stream tube with finite cross-sectional area, as in an open channel with steady flow (the channel bottom, side slopes, and water surface being the boundaries of the stream tube), the continuity equation reads:

$$Q = \int^A v dA = \bar{v}A = \text{constant}$$

or

$$\bar{v}_1 A_1 = \bar{v}_2 A_2 \tag{1-2}$$

where $\bar{v}$ is the average velocity component perpendicular to the cross-section of the open channel.

1.3 Equation of motion in the s-direction

Since we do not regard heat and sound as being types of energy which influence the liquid flow in open channels, an elementary fluid particle has the following three interchangeable types of energy per unit of volume:

$\frac{1}{2}\rho v^2$ = kinetic energy per unit of volume
ρgz = potential energy per unit of volume
P = pressure energy per unit of volume.

Consider a fluid particle moving in a time interval Δt from Point 1 to Point 2 along a streamline, there being no loss of energy due to friction or increased turbulence. (See Fig.1.3.) Since, on the other hand, there is no gain of energy either, we can write:

$$(\tfrac{1}{2}\rho v^2 + \rho gz + P)_1 = (\tfrac{1}{2}\rho v^2 + \rho gz + P)_2 = \text{constant} \tag{1-3}$$

This equation is valid for points along a streamline only if the energy losses are negligible and the mass density (ρ) is a constant. According to Equation 1-3:

$$\tfrac{1}{2}\rho v^2 + \rho g z + P = \text{constant} \tag{1-4}$$

or

$$v^2/2g + P/\rho g + z = H = \text{constant} \tag{1-5}$$

where, as shown in Figure 1.3,

$v^2/2g$	= the velocity head
$P/\rho g$	= the pressure head
z	= the elevation head
$P/\rho g + z$	= the piezometric head
H	= the total energy head.

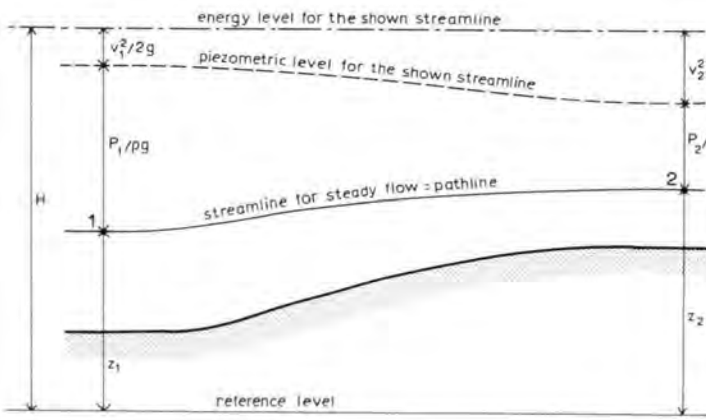

Fig.1.3.The energy of a fluid particle.

The last three heads all refer to the same reference level. The reader should note that each individual streamline may have its own energy head. Equations 1-3,1-4, and 1-5 are alternative forms of the well-known Bernoulli equation, of which a detailed derivation is presented in Appendix I.

1.4 Piezometric gradient in the n-direction

On a particle (ds, dn, dm) following a curved streamline, a force F is acting towards the centre of curvature in order to accelerate the particle in a sense perpendicular to its direction of motion. Since in Section 1.1 the direction of motion and the direction towards the centre of curvature have been defined as the s- and n-direction respectively, we consider here the movement of a particle along an elementary section of a streamline in the osculating plane.

By Newton's second law of motion

$$F = ma \tag{1-6}$$

the centripetal acceleration (a) in consequence of the passage along a circle with a radius (r) with a velocity (v), according to mechanics, equals:

$$a = \frac{v^2}{r} \tag{1-7}$$

Since the mass (m) of the particle equals ρ(ds dn dm), the force (F) can be expressed as

$$F = \rho \text{ ds dn dm } \frac{v^2}{r} \tag{1-8}$$

This force (F) is due to fluid pressure and gravitation acting on the fluid particle. It can be proved (see Appendix I) that the negative energy gradient in the n-direction equals the centripetal force per unit of mass (equals centripetal acceleration). In other words:

$$-\frac{d}{dn}\left(\frac{P}{\rho} + gz\right) = \frac{v^2}{r} \tag{1-9}$$

or

$$d\left(\frac{P}{\rho g} + z\right) = -\frac{1}{g}\frac{v^2}{r}\,dn \tag{1-10}$$

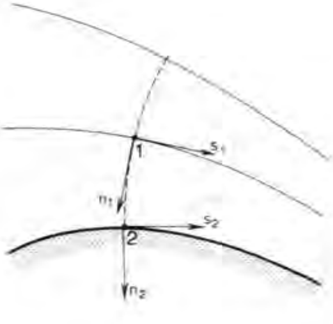

Fig.1.4. Key to symbols.

After integration of this equation from Point 1 to Point 2 in the n-direction we obtain the following equation for the fall of piezometric head in the n-direction (see Fig.1.4)

$$\left[\frac{P}{\rho g} + z\right]_1 - \left[\frac{P}{\rho g} + z\right]_2 = \frac{1}{g} \int_1^2 \frac{v^2}{r} \, dn \qquad (1\text{-}11)$$

In this equation

$\left[\frac{P}{\rho g} + z\right]_1$ = the piezometric head at Point 1

$\left[\frac{P}{\rho g} + z\right]_2$ = the piezometric head at Point 2

$\int_1^2 \frac{v^2}{gr} \, dn$ = the difference between the piezometric heads at Points 1 and 2 due to the curvature of the streamlines

From this equation it appears that, if the streamlines are straight ($r = \infty$), the integral has zero value, and thus the piezometric head at Point 1 equals that at Point 2, so that

$$\left[\frac{P}{\rho g} + z\right]_1 = \left[\frac{P}{\rho g} + z\right]_2 = \text{constant} \qquad (1\text{-}12)$$

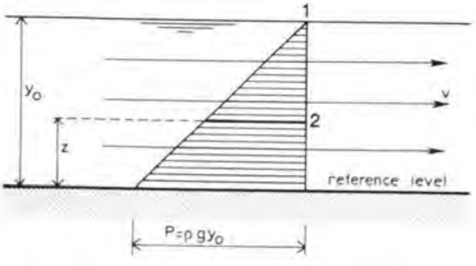

Fig.1.5.
Hydrostatic pressure distribution.

At the water surface in an open channel, $P_1 = 0$; hence

$$\frac{P_2}{\rho g} = y_o - z$$

or

$$P_2 = \rho g(y_o - z) \tag{1-13}$$

Thus, if $r = \infty$ there is what is known as a hydrostatic pressure distribution. If the streamlines are curved, however, and there is a significant flow velocity, the integral may reach a considerable value.

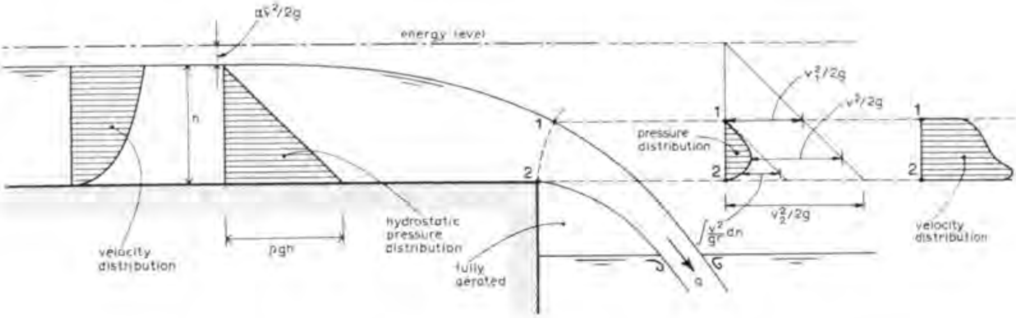

Fig.1.6.Pressure and velocity distribution at a free overfall.

At a free overfall with a fully aerated air pocket underneath the nappe, there is atmospheric pressure at both Points 1 and 2, while a certain distance upstream there is a hydrostatic pressure distribution. The deviation from the hydrostatic pressure distribution at the end of the weir is mainly caused by the value of the integral (see Fig.1.6). A decrease of piezometric head,which is due to the centripetal acceleration, necessarily induces a corresponding increase of velocity head:

$$\frac{v_2^2}{2g} - \frac{v_1^2}{2g} = \int_1^2 \frac{v^2}{gr} \, dn \tag{1-14}$$

To illustrate the effect of streamline curvature on the velocity distribution in the n-direction, Figure 1.6 shows the velocity distribution over a cross section where a hydrostatic pressure distribution prevails and the velocity distribution at the free overfall.

1.5 Hydrostatic pressure distribution in the m-direction

As mentioned in Section 1.1, in the direction perpendicular to the osculating plane, not only $v_m = 0$, but also

$$a_m = \frac{dv_m}{dt} = 0$$

Consequently, there is no net force acting in the m-direction, and therefore the pressure distribution is hydrostatic.

Consequently, in the m-direction

$$P + \rho g z = \text{constant} \tag{1-15}$$

or

$$\frac{P}{\rho g} + z = \text{constant} \tag{1-16}$$

1.6 The total energy head of an open channel cross-section

According to Equation 1-4, the total energy per unit of volume of a fluid particle can be expressed as the sum of the three types of energy:

$$\tfrac{1}{2}\,\rho v^2 + \rho g z + P \tag{1-17}$$

We now want to apply this expression to the total energy which passes through the entire cross-section of a channel. We therefore need to express the total kinetic energy of the discharge in terms of the average flow velocity of the cross-section.

In this context, the reader should note that this average flow velocity is not a directly measurable quantity but a derived one, defined by

$$\bar{v} = \frac{Q}{A} \tag{1-18}$$

Due to the presence of a free water surface and the friction along the solid channel boundary, the velocities in the channel are not uniformly distributed over the channel cross-section (Fig.1.7).

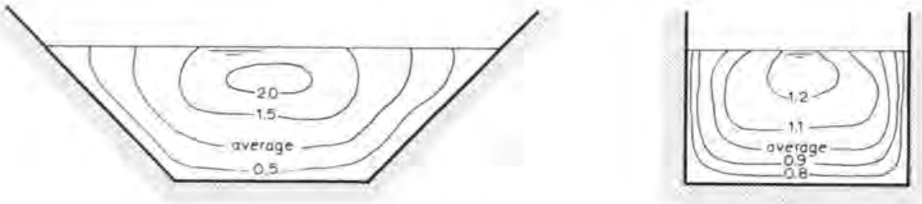

Fig.1.7. Examples of velocity profiles in a channel section.

Owing to this non-uniform velocity distribution, the true average kinetic energy per unit of volume across the section, $(\frac{1}{2}\rho v^2)_{average}$, will not necessarily be equal to $\frac{1}{2}\rho\bar{v}^2$.

In other words:

$$(\tfrac{1}{2}\rho v^2)_{average} = \alpha\,\tfrac{1}{2}\rho\bar{v}^2 \qquad (1\text{-}19)$$

The velocity distribution coefficient (α) always exceeds unity. It equals unity when the flow is uniform across the entire cross-section and becomes greater, the further flow departs from uniform.

For straight open channels with steady turbulent flow, α-values range between 1.03 and 1.10. In many cases the velocity head makes up only a minor part of the total energy head and $\alpha = 1$ can then be used for practical purposes. Thus, the average kinetic energy per unit of volume of water passing a cross-section equals:

$$\alpha\,\tfrac{1}{2}\rho\bar{v}^2$$

The variation of the remaining two terms over the cross-section is characterized by Equations 1-9 and 1-15. If we consider an open channel section with steady flow, where the streamlines are straight and parallel, there is no centripetal acceleration and, therefore, both in the n- and m-direction, the sum of the potential and pressure energy at any point is constant. In other words:

$$\rho gz + P = \text{constant} \qquad (1\text{-}20)$$

for all points in the cross-section. Since at the water surface $P = 0$, the piezometric level of the cross-section coincides with the local water surface. For the considered cross-section the expression for the average energy per unit of volume passing through the cross-section reads:

$$E = \alpha \tfrac{1}{2} \rho\bar{v}^2 + P + \rho g z \qquad (1\text{-}21)$$

or if expressed in terms of head

$$\alpha \frac{\bar{v}^2}{2g} + \frac{P}{\rho g} + z = H \qquad (1\text{-}22)$$

where H is the total energy head of a cross-sectional area of flow. We have now reached the stage that we are able to express this total energy head in the elevation of the water surface ($P/\rho g + z$) plus the velocity head $\alpha\bar{v}^2/2g$.

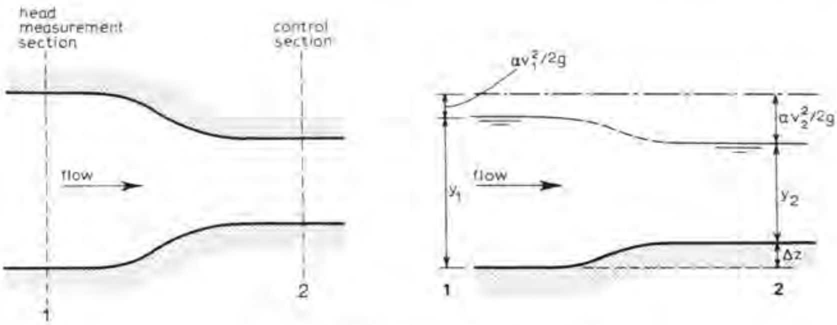

Fig.1.8. The channel transition.

In the following sections it will be assumed that over a short reach of accelerated flow, bounded by channel cross-sections perpendicular to straight and parallel streamlines, the loss of energy head is negligible with regard to the interchangeable types of energy (Fig.1.8). Hence:

$$\alpha \frac{\bar{v}_1^2}{2g} + \left[\frac{P}{\rho g} + z\right]_1 = H = \alpha \frac{\bar{v}_2^2}{2g} + \left[\frac{P}{\rho g} + z\right]_2 \qquad (1\text{-}23)$$

Thus, if we may assume the energy head (H) in both cross-sections to be the same, we have an expression that enables us to compare the interchange of velocity head and piezometric head in a short zone of acceleration.

1.7 Recapitulation

For a short zone of acceleration bounded by cross-sections perpendicular to straight and parallel streamlines, the following two equations are valid:

Continuity equation (1-2)

$$Q = \bar{v}_1 A_1 = \bar{v}_2 A_2$$

Bernoulli's equation (1-23)

$$H = \alpha \frac{\bar{v}_1^2}{2g} + \left[\frac{P}{\rho g} + z\right]_1 = \alpha \frac{\bar{v}_2^2}{2g} + \left[\frac{P}{\rho g} + z\right]_2$$

In both cross-sections the piezometric level coincides with the water surface and the latter determines the area A of the cross-section. We may therefore conclude that if the shapes of the two cross-sections are known, the two unknowns $\bar{v}_1$ and $\bar{v}_2$ can be determined from the two corresponding water levels by means of the above equations.

It is evident, however, that collecting and handling two sets of data per measuring structure is an expensive and time-consuming enterprise which should be avoided if possible. It will be shown that under critical flow conditions one water level only is sufficient to determine the discharge. In order to explain this critical condition, the concept of specific energy will first be defined.

1.8 Specific energy

The concept of specific energy was first introduced by Bakhmeteff in 1912, and is defined as the average energy per unit weight of water at a channel section as expressed with respect to the channel bottom. Since the piezometric level coincides with the water surface, the piezometric head with respect to the channel bottom is:

$$\frac{P}{\rho g} + z = y, \text{ the water depth} \qquad (1\text{-}24)$$

so that the specific energy head can be expressed as:

$$H_o = y + \alpha\bar{v}^2/2g \qquad (1\text{-}25)$$

We find that the specific energy at a channel section equals the sum of the water depth (y) and the velocity head, provided of course that the streamlines are straight and parallel. Since v = Q/A, Equation 1-25 may be written:

$$H_o = y + \alpha \frac{Q^2}{2gA^2} \tag{1-26}$$

where A, the cross-sectional area of flow, can also be expressed as a function of the water depth, y.

From this equation it can be seen that for a given channel section and a constant discharge (Q), the specific energy in an open channel section is a function of the water depth only. Plotting this water depth (y) against the specific energy (H_o) gives a specific energy curve as shown in Figure 1.9.

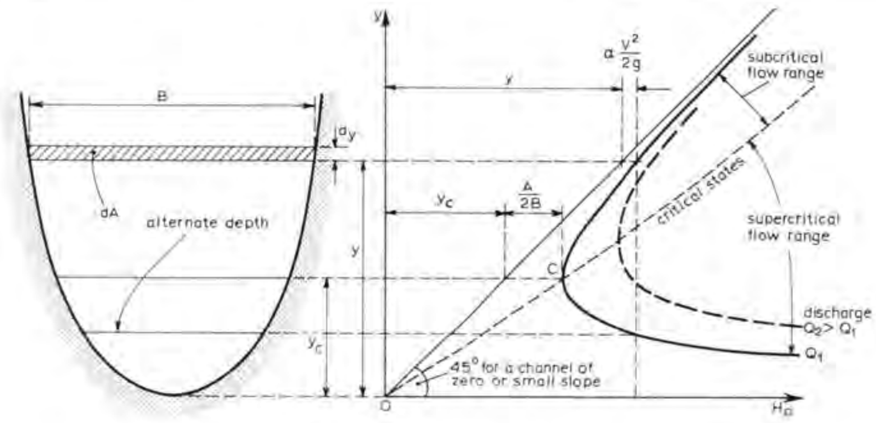

Fig.1.9. The specific energy curve.

The curve shows that, for a given discharge and specific energy, there are two "alternate depths" of flow. At Point C the specific energy is a minimum for a given discharge and the two alternate depths coincide. This depth of flow is known as "critical depth" (y_c).

When the depth of flow is greater than the critical depth, the flow is called subcritical; if it is less than the critical depth, the flow is called supercritical. Conversely we may say that the curve illustrates how a given discharge can occur at two possible flow regimes; slow and deep on the upper limb, fast and shallow on the lower limb, the limbs being separated by the critical flow condition (Point C).

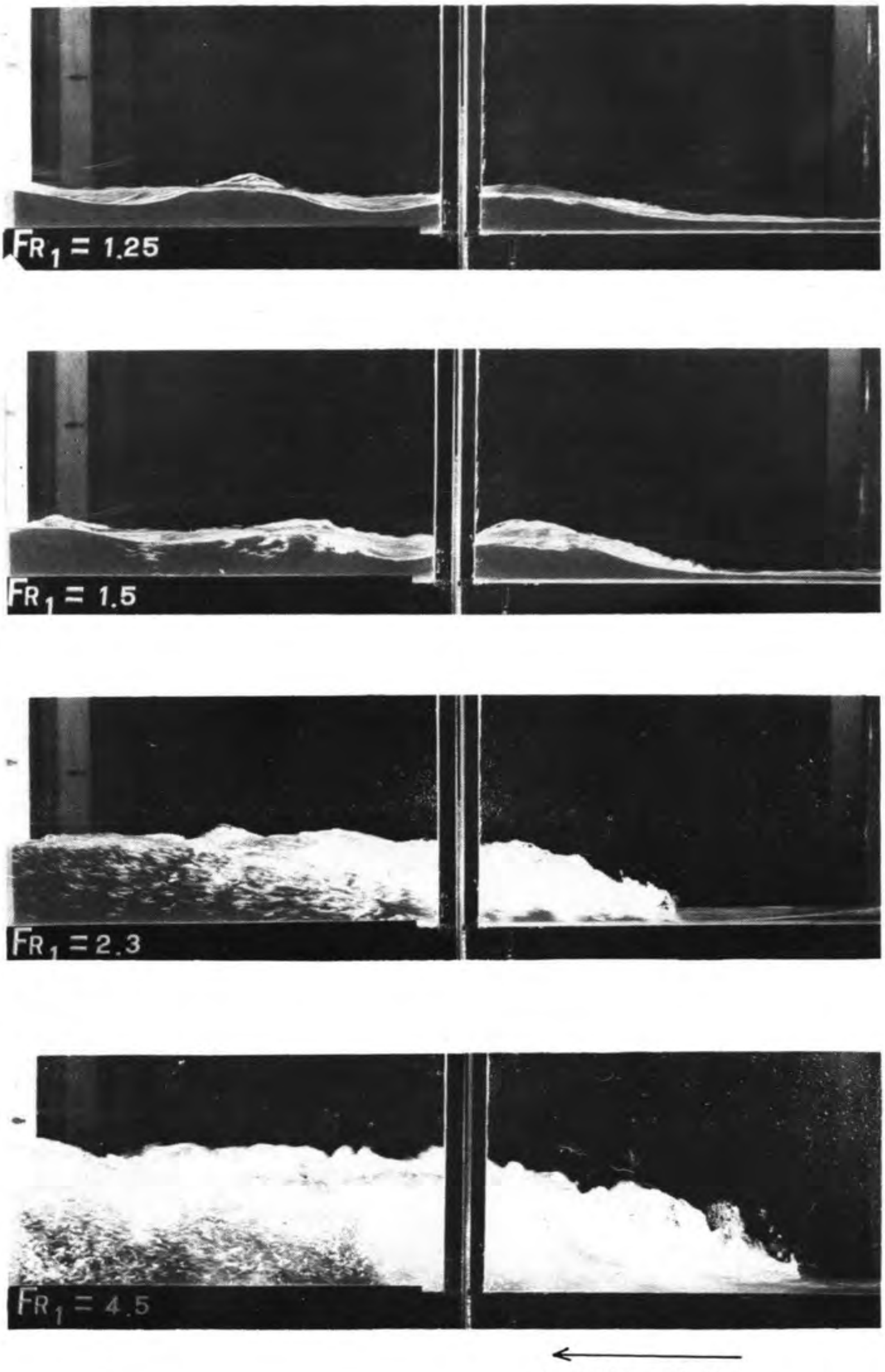

Photo 1: Hydraulic jumps.

When there is a rapid change in depth of flow from a high to a low stage, a steep depression will occur in the water surface; this is called a "hydraulic drop". On the other hand, when there is a rapid change from a low to a high stage, the water surface will rise abruptly; this phenomenon is called a "hydraulic jump" or "standing wave". The standing wave shows itself by its turbulence (white water), whereas the hydraulic drop is less apparent. However, if in a standing wave the change in depth is small, the water surface will not rise abruptly but will pass from a low to a high level through a series of undulations (undular jump), and detection becomes more difficult. The normal procedure to ascertain whether critical flow occurs in a channel contraction - there being subcritical flow upstream and downstream of the contraction - is to look for a hydraulic jump immediately downstream of the contraction.

From Figure 1.9 it is possible to see that if the state of flow is critical, i.e. if the specific energy is a minimum for a given discharge, there is one value for the depth of flow only. The relationship between this minimum specific energy and the critical depth is found by differentiating Equation 1-26 to y, while Q remains constant.

$$\frac{dH_o}{dy} = 1 - \alpha \frac{Q^2}{gA^3} \frac{dA}{dy} = 1 - \alpha \frac{\bar{v}^2}{gA} \frac{dA}{dy} \qquad (1-27)$$

Since dA = B dy, this equation becomes:

$$\frac{dH_o}{dy} = 1 - \alpha \frac{\bar{v}^2 B}{g\ A} \qquad (1-28)$$

If the specific energy is a minimum $dH_o/dy = 0$, we may write:

$$\alpha \frac{\bar{v}_c^2}{2g} = \frac{A_c}{2B_c} \qquad (1-29)$$

Equation 1-29 is valid only for steady flow with parallel streamlines in a channel of small slope. If the velocity distribution coefficient, α, is assumed to be unity, the criterion for critical flow becomes:

$$\bar{v}_c^2/2g = \tfrac{1}{2} A_c/B_c \quad \text{or} \quad \bar{v} = \bar{v}_c = (g\ A_c/B_c)^{0.50} \qquad (1-30)$$

Provided that the tailwater level of the measuring structure is low enough to enable the depth of flow at the channel contraction to reach critical depth, Equations 1-2, 1-23, and 1-30 allow the development of a discharge equation for each measuring device, in which the upstream total energy head (H_1) is the only independent variable.

Equation 1-30 states that at critical flow the average flow velocity

$$\bar{v}_c = (g\ A_c/B_c)^{0.50}$$

It can be proved that this flow velocity equals the velocity with which the smallest disturbance moves in an open channel, as measured relative to the flow. Because of this feature, a disturbance or change in a downstream level cannot influence an upstream water level if critical flow occurs in between the two cross-sections considered. The "control section" of a measuring structure is located where critical flow occurs and subcritical, tranquil, or streaming flow passes into supercritical, rapid, or shooting flow.
Thus, if critical flow occurs at the control section of a measuring structure, the upstream water level is independent of the tailwater level; the flow over the structure is then called "modular".

1.9 The broad-crested weir

A broad-crested weir is an overflow structure with a horizontal crest above which the deviation from a hydrostatic pressure distribution because of centripetal acceleration may be neglected. In other words, the streamlines are practically straight and parallel.To obtain this situation the length of the weir crest in the direction of flow (L) should be related to the total energy head over the weir crest as $0.08 \leqslant H_1/L \leqslant 0.50$. $H_1/L \geqslant 0.08$ because otherwise the energy losses above the weir crest cannot be neglected, and undulations may occur on the crest; $H_1/L \leqslant 0.50$, so that only slight curvature of streamlines occurs above the crest and a hydrostatic pressure distribution may be assumed.

If the measuring structure is so designed that there are no significant energy losses in the zone of acceleration upstream of the control section, according to Bernoulli's equation (1-23):

$$H_1 = h_1 + \alpha\ \bar{v}_1^2/2g = H = y + \alpha\ \bar{v}^2/2g$$

or:

$$\bar{v} = \{2g(H_1 - y)\}^{0.50}\alpha^{-0.50} \tag{1-31}$$

where H_1 equals the total upstream energy head over the weir crest as shown in Figure 1.10.

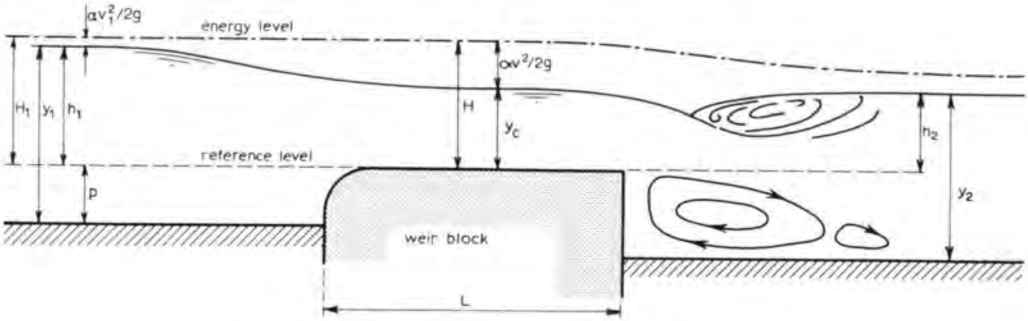

Fig.1.10.Flow pattern over a broad crested weir.

Substituting $Q = \bar{v}A$ and putting $\alpha = 1.0$ gives

$$Q = A\ \{2g(H_1 - y)\}^{0.50} \tag{1-32}$$

Provided that critical flow occurs at the control section ($y = y_c$), a head-discharge equation for various throat geometries can now be derived from

$$Q = A_c\ \{2g(H_1 - y_c)\}^{0.50} \tag{1-33}$$

1.9.1 Broad-crested weir with rectangular control section

For a rectangular control section in which the flow is critical, we may write $A_c = by_c$ and $A_c/B_c = y_c$ so that Equation 1-30 may be written as $\bar{v}^2/2g = \frac{1}{2}\ y_c$. Hence:

$$y_c = \frac{2}{3}\ H = \frac{2}{3}\ H_1 \tag{1-34}$$

Substitution of this relation and $A_c = b\ y_c$ into Equation 1-33 gives, after simplification:

$$Q = \frac{2}{3}\ (\tfrac{2}{3}g)^{0.50}\ b\ H_1^{\ 1.50} \tag{1-35}$$

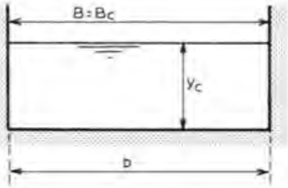

Fig.1.11. Dimensions of a rectangular control section.

This formula is based on idealized assumptions such as: absence of centripetal forces in the upstream and downstream cross-sections bounding the considered zone of acceleration, absence of viscous effects and increased turbulence, and finally a uniform velocity distribution so that also the velocity distribution coefficient can be omitted. In reality these effects do occur and they must therefore be accounted for by the introduction of a discharge coefficient C_d. The C_d-value depends on the shape and type of the measuring structure.

$$Q = C_d \frac{2}{3} (\frac{2}{3} g)^{0.50} b H_1^{1.50} \tag{1-36}$$

Naturally in a field installation it is not possible to measure the energy head H_1 directly and it is therefore common practice to relate the discharge to the upstream water level over the crest in the following way:

$$Q = C_d C_v \frac{2}{3} (\frac{2}{3} g)^{0.50} b h_1^{1.50} \tag{1-37}$$

where C_v is a correction coefficient for neglecting the velocity head in the approach channel, $\alpha_1 v_1^2/2g$.

Photo 2. Flow over a round-nose broad-crested weir with rectangular control section.

Generally, the approach velocity coefficient

$$C_v = \left[\frac{H_1}{h_1}\right]^u \tag{1-38}$$

where u equals the power of h_1 in the head-discharge equation, being u = 1.50 for a rectangular control section.

Thus C_v is greater than unity and is related to the shape of the approach channel section and to the power of h_1 in the head-discharge equation.

Values of C_v as a function of the area ratio $C_d A^*/A_1$ are shown in Figure 1.12 for various control sections, where A^* equals the imaginary wetted area at the control section if we assume that the water depth $y = h_1$; A_1 equals the wetted area at the head measurement station and C_d is the discharge coefficient. In Chapters IV to IX, the C_d-value is usually given as some function of H_1. Since it is common practice to measure h_1 instead of H_1, a positive correction equal to $v_1^2/2g$ should be made on h_1 to find the true C_d-value whenever the change in C_d as a function of H_1 is significant.

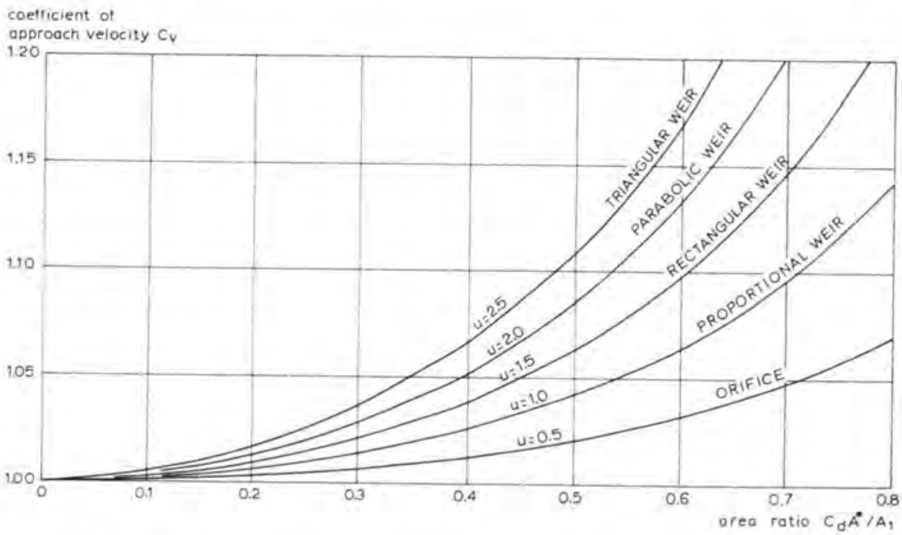

A^* = wetted area at control section if waterdepth equals $y = h_1$
A_1 = wetted area at head measurement station

Fig.1.12. Approach velocity coefficient for various control sections.

In the literature, Equation 1-37 is sometimes written as

$$Q = C''_d\ C_v\ b\ h_1^{1.50} \tag{1-39}$$

It should be noted that in this equation the coefficient C''_d has the dimension $\left[L^{\frac{1}{2}}\ T^{-1}\right]$. To avoid mistakes and to facilitate easy comparison of discharge coefficients in both the metric and the Imperial systems, the use of Equation 1-37 is recommended.

1.9.2 Broad-crested weir with parabolic control section

For a parabolic control section, having a focal distance equal to f, (see Fig. 1.13) with $A_c = \frac{2}{3} B_c y_c$ and $B_c = 2\sqrt{2fy_c}$, we may write Equation 1-30 as:

$$\bar{v}_c^2/2g = A_c/2B_c = \frac{1}{3}\ y_c \tag{1-40}$$

Hence

$$y_c = \frac{3}{4}\ H = \frac{3}{4}\ H_1 \tag{1-41}$$

Substituting those relations into Equation 1-33 gives:

$$Q = \sqrt{\frac{3}{4}\ fg}\ H_1^{2.0} \tag{1-42}$$

As explained in Section 1.9.1, correction coefficients have to be introduced to obtain a practical head-discharge equation. Thus

$$Q = C_d\ C_v \sqrt{\frac{3}{4}\ fg}\ h_1^{2.0} \tag{1-43}$$

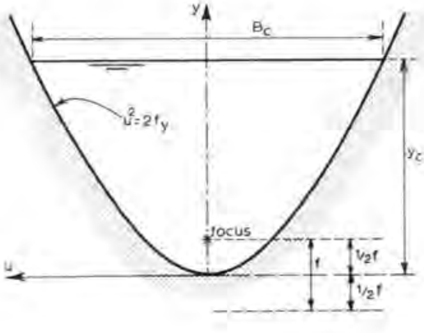

Fig. 1.13.
Dimensions of a parabolic control section.

1.9.3 Broad-crested weir with triangular control section

For a triangular control section with $A_c = y_c^2 \tan\frac{\theta}{2}$ and $B_c = 2y_c \tan\frac{\theta}{2}$ (see Fig.1.14), we may write Equation 1-30 as:

$$\bar{v}_c^2/2g = \tfrac{1}{4}\, y_c \qquad (1\text{-}44)$$

Hence,

$$y_c = \frac{4}{5}\, H = \frac{4}{5}\, H_1 \qquad (1\text{-}45)$$

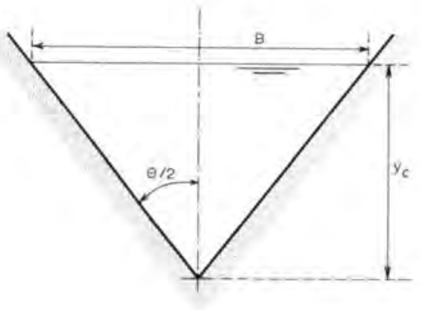

Fig.1.14.
Dimensions of a triangular control section.

Substituting those relations and $A_c = y_c^2 \tan\frac{\theta}{2}$ into Equation 1-33 gives:

$$Q = \frac{16}{25}\left[\frac{2}{5}\, g\right]^{0.50} \tan\frac{\theta}{2}\, H_1^{2.50} \qquad (1\text{-}46)$$

For similar reasons as explained in Section 1.9.1, a C_d- and C_v-coefficient have to be introduced to obtain a practical head-discharge equation. Thus

$$Q = C_d\, C_v\, \frac{16}{25}\left[\frac{2}{5}\, g\right]^{0.50} \tan\frac{\theta}{2}\;\, h_1^{2.50} \qquad (1\text{-}47)$$

1.9.4 Broad-crested weir with truncated triangular control section

For weirs with a truncated triangular control section, two head-discharge equations have to be used: one for the conditions where flow is confined within the triangular section, and the other, at higher stages, where the presence of the vertical side walls has to be taken into account. The first equation is analogous to Equation 1-47, being,

$$Q = C_d\, C_v\, \frac{16}{25}\left[\frac{2}{5}\, g\right]^{0.50} \tan\frac{\theta}{2}\, h_1^{2.50} \tag{1-48}$$

which is valid if $H_1 \leqslant 1.25\ H_b$.

The second equation will be derived below.

For a truncated triangular control section,

$$A_c = H_b^2 \tan\frac{\theta}{2} + B(y_c - H_b) = By_c - \frac{1}{2} BH_b$$

According to Equation 1-30 we may write (see Fig.1.15)

$$\bar{v}_c^2/2g = A_c/2B_c = \frac{1}{2}\, y_c - \frac{1}{4}\, H_b \tag{1-49}$$

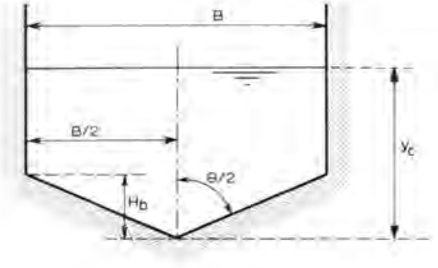

Fig.1.15. Dimension of a truncated triangular control section.

Hence

$$y_c = \frac{2}{3}\, H_1 + \frac{1}{6}\, H_b \tag{1-50}$$

Substituting those relations and $A_c = \frac{2}{3}\, BH_1 - \frac{1}{3}\, BH_b$ into Equation 1-33 gives

$$Q = B\, \frac{2}{3}\left[\frac{2}{3}\, g\right]^{0.50} (H_1 - \tfrac{1}{2}\, H_b)^{1.50} \tag{1-51}$$

For similar reasons as explained in Section 1.9.1, discharge and approach velocity coefficients have to be introduced to obtain a practical head-discharge equation. Thus

$$Q = C_d\, C_v\, B\, \frac{2}{3}\left[\frac{2}{3}\, g\right]^{0.50} (h_1 - \tfrac{1}{2}\, H_b)^{1.50} \tag{1-52}$$

which is valid provided $H_1 \geqslant 1.25\ H_b$.

Photo 3. Flow over a broad-crested weir with triangular control section.

1.9.5 Broad-crested weir with trapezoïdal control section

For weirs with a trapezoïdal control section with $A_c = by_c + my_c^2$ and $B_c = b + 2\ my_c$, we may write Equation 1-30 as (Fig.1.16):

$$v_c^2/2g = A_c/2B_c = \frac{by_c + my_c^2}{2b + 4\ my_c} \tag{1-53}$$

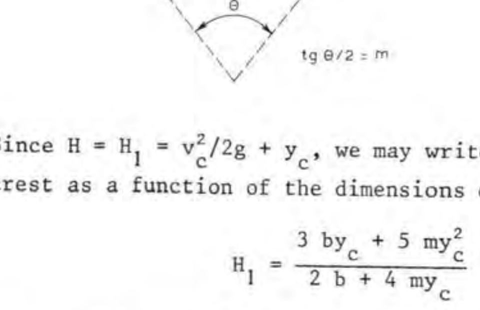

Fig.1.16. Dimensions of a trapezoïdal control section.

Since $H = H_1 = v_c^2/2g + y_c$, we may write the total energy head over the weir crest as a function of the dimensions of the control section as

$$H_1 = \frac{3\ by_c + 5\ my_c^2}{2\ b + 4\ my_c} \tag{1-54}$$

From this equation it appears that the critical depth in a trapezoïdal control section is a function of the total energy head H_1, of the bottom width b and of the side slope ratio m of the control section.

TABLE 1.1. VALUES OF THE RATIO y_c/H_1 AS A FUNCTION OF m AND H_1/b FOR TRAPEZOIDAL CONTROL SECTIONS

	Side slopes of channel ratio of horizontal to vertical (m:1)									
H_1/b	Vertical	1/4:1	1/2:1	3/4:1	1:1	1½:1	2:1	2½:1	3:1	4:1
.00		.667	.667	.667	.667	.667	.667	.667	.667	.667
.01	.667	.667	.667	.668	.668	.669	.670	.670	.671	.672
.02	.667	.667	.668	.669	.670	.671	.672	.674	.675	.678
.03	.667	.668	.669	.670	.671	.673	.675	.677	.679	.683
.04	.667	.668	.670	.671	.672	.675	.677	.680	.683	.687
.05	.667	.668	.670	.672	.674	.677	.680	.683	.686	.692
.06	.667	.669	.671	.673	.675	.679	.683	.686	.690	.696
.07	.667	.669	.672	.674	.676	.681	.685	.689	.693	.699
.08	.667	.670	.672	.675	.678	.683	.687	.692	.696	.703
.09	.667	.670	.673	.676	.679	.684	.690	.695	.698	.706
.10	.667	.670	.674	.677	.680	.686	.692	.697	.701	.709
.12	.667	.671	.675	.679	.684	.690	.696	.701	.706	.715
.14	.667	.672	.676	.681	.686	.693	.699	.705	.711	.720
.16	.667	.672	.678	.683	.687	.696	.703	.709	.715	.725
.18	.667	.673	.679	.684	.690	.698	.706	.713	.719	.729
.20	.667	.674	.680	.686	.692	.701	.709	.717	.723	.733
.22	.667	.674	.681	.688	.694	.704	.712	.720	.726	.736
.24	.667	.675	.683	.689	.696	.706	.715	.723	.729	.739
.26	.667	.676	.684	.691	.698	.709	.718	.725	.732	.742
.28	.667	.676	.685	.693	.699	.711	.720	.728	.734	.744
.30	.667	.677	.686	.694	.701	.713	.723	.730	.737	.747
.32	.667	.678	.687	.696	.703	.715	.725	.733	.739	.749
.34	.667	.678	.689	.697	.705	.717	.727	.735	.741	.751
.36	.667	.679	.690	.699	.706	.719	.729	.737	.743	.752
.38	.667	.680	.691	.700	.708	.721	.731	.738	.745	.754
.40	.667	.680	.692	.701	.709	.723	.733	.740	.747	.756
.42	.667	.681	.693	.703	.711	.725	.734	.742	.748	.757
.44	.667	.681	.694	.704	.712	.727	.736	.744	.750	.759
.46	.667	.682	.695	.705	.714	.728	.737	.745	.751	.760
.48	.667	.683	.696	.706	.715	.729	.739	.747	.752	.761
.5	.667	.683	.697	.708	.717	.730	.740	.748	.754	.762
.6	.667	.686	.701	.713	.723	.737	.747	.754	.759	.767
.7	.667	.688	.706	.718	.728	.742	.752	.758	.764	.771
.8	.667	.692	.709	.723	.732	.746	.756	.762	.767	.774
.9	.667	.694	.713	.727	.737	.750	.759	.766	.770	.776
1.0	.667	.697	.717	.730	.740	.754	.762	.768	.773	.778
1.2	.667	.701	.723	.737	.747	.759	.767	.772	.776	.782
1.4	.667	.706	.729	.742	.752	.764	.771	.776	.779	.784
1.6	.667	.709	.733	.747	.756	.767	.774	.778	.781	.786
1.8	.667	.713	.737	.750	.759	.770	.776	.781	.783	.787
2	.667	.717	.740	.754	.762	.773	.778	.782	.785	.788
3	.667	.730	.753	.766	.773	.781	.785	.787	.790	.792
4	.667	.740	.762	.773	.778	.785	.788	.790	.792	.794
5	.667	.748	.768	.777	.782	.788	.791	.792	.794	.795
10	.667	.768	.782	.788	.791	.794	.795	.796	.797	.798
∞		.800	.800	.800	.800	.800	.800	.800	.800	.800

It also shows that, if both b and m are known, the ratio y_c/H_1 is a function of H_1. Values of y_c/H_1 as a function of m and the ratio H_1/b are shown in Table 1.1.

Substitution of $A_c = by_c + my_c^2$ into Equation 1-33 and introduction of a discharge coefficient gives as a head-discharge equation

$$Q = C_d \{by_c + my_c^2\} \{2g(H_1 - y_c)\}^{0.50} \qquad (1\text{-}55)$$

Since for each combination of b, m, and H_1/b, the ratio y_c/H_1 is given in Table 1.1, the discharge Q can be computed because the discharge coefficient has a predictable value. In this way a Q-H_1 curve can be obtained. If the approach velocity head $v_1^2/2g$ is negligible, this curve may be used to measure the discharge. If the approach velocity has a significant value, $v_1^2/2g$ should be estimated and $h_1 = H_1 - v_1^2/2g$ may be obtained in one or two steps.

In the literature the trapezoïdal control section is sometimes described as the sum of a rectangular and a triangular control section. Hence, along similar lines as will be shown in Section 1.13 for sharp-crested weirs, a head-discharge equation is obtained by superposing the head-discharge equations valid for a rectangular and a triangular control section. For broad-crested weirs, however, this procedure results in a strongly variable C_d-value, since for a given H_1 the critical depth in the two superposed equations equals $\frac{2}{3} H_1$ for a rectangular and $\frac{4}{5} H_1$ for a triangular control section. This difference of simultaneous y_c-values is one of the reasons why superposition of various head-discharge equations is not allowed. A second reason is the significant difference in mean flow velocities through the rectangular and triangular portions of the control section.

1.9.6 Broad-crested weir with circular control section

For a broad-crested weir with a circular control section we may write (see Fig.1.17)

$$A_c = \frac{1}{8} d^2(\alpha - \sin \alpha)$$

$$B_c = d \sin \tfrac{1}{2} \alpha \qquad \text{and}$$

$$y_c = \frac{d}{2} (1 - \cos \tfrac{1}{2} \alpha) = d \sin^2 \tfrac{1}{4} \alpha$$

Substitution of values for A_c and B_c into Equation 1-30 gives

$$v_c^2/2g = A_c/2B_c = \frac{d}{16}\left[\frac{\alpha - \sin\alpha}{\sin\frac{1}{2}\alpha}\right] \tag{1-56}$$

and because $H = H_1 = y_c + v_c^2/2g$ we may write the total energy head over the weir crest as

$$H_1/d = y_c/d + v_c^2/2gd = \sin^2\tfrac{1}{4}\alpha + \frac{\alpha - \sin\alpha}{16\sin\frac{1}{2}\alpha} \tag{1-57}$$

For each value of $y_c/d = \sin^2\frac{1}{4}\alpha$ a matching value of the ratios A_c/d^2 and H_1/d can now be computed.

These values, and the additional values on the dimensionless ratios $v_c^2/2gd$ and y_c/H_1 are presented in Table 1.2.

For a circular control section we may use the general head-discharge relation given earlier (Eq.1-33)

$$Q = C_d\, A_c\{2g(H_1 - y_c)\}^{0.50} \tag{1-58}$$

where the discharge coefficient C_d has been introduced for similar reasons to those explained in Section 1.9.1. The latter equation may also be written in terms of dimensionless ratios as

$$Q = C_d\,\frac{A_c}{d^2}\,d^{2.50}\sqrt{2g\left[\frac{H_1}{d} - \frac{y_c}{d}\right]} \tag{1-59}$$

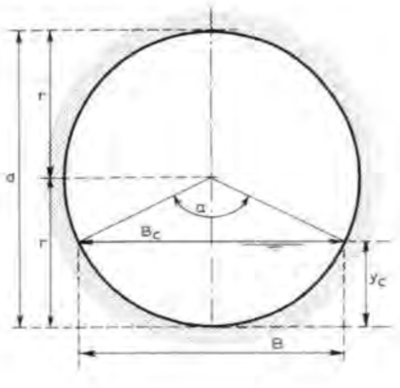

Fig.1.17.
Dimensions of a circular control section.

TABLE 1.2: RATIOS FOR DETERMINING THE DISCHARGE Q OF A BROAD-CRESTED WEIR AND LONG-THROATED FLUME WITH CIRCULAR CONTROL SECTION

y_c/d	$\frac{v_c^2/2g}{d}$	H_1/d	A_c/d^2	y_c/H_1	y_c/d	$\frac{v_c^2/2g}{d}$	H_1/d	A_c/d^2	y_c/H_1	y_c/d	$\frac{v_c^2/2g}{d}$	H_1/d	A_c/d^2	y_c/H_1
0.01	0.0033	0.0133	0.0013	0.752	0.36	0.1326	0.4926	0.2546	0.731	0.71	0.3286	1.0386	0.5964	0.684
.02	.0067	.0267	.0037	.749	.37	.1368	.5068	.2642	.730	.72	.3371	1.0571	.6054	.681
.03	.0101	.0401	.0069	.749	.38	.1411	.5211	.2739	.729	.73	.3459	1.0759	.6143	.679
.04	.0134	.0534	.0105	.749	.39	.1454	.5354	.2836	.728	.74	.3552	1.0952	.6231	.676
.05	.0168	.0668	.0147	.748	.40	.1497	.5497	.2934	.728	.75	.3648	1.1148	.6319	.673
.06	.0203	.0803	.0192	.748	.41	.1541	.5641	.3032	.727	.76	.3749	1.1349	.6405	.670
.07	.0237	.0937	.0242	.747	.42	.1586	.5786	.3130	.726	.77	.3855	1.1555	.6489	.666
.08	.0271	.1071	.0294	.747	.43	.1631	.5931	.3229	.725	.78	.3967	1.1767	.6573	.663
.09	.0306	.1206	.0350	.746	.44	.1676	.6076	.3328	.724	.79	.4085	1.1985	.6655	.659
.10	.0341	.1341	.0409	.746	.45	.1723	.6223	.3428	.723	.80	.4210	1.2210	.6735	.655
.11	.0376	.1476	.0470	.745	.46	.1769	.6369	.3527	.722	.81	.4343	1.2443	.6815	.651
.12	.0411	.1611	.0534	.745	.47	.1817	.6517	.3627	.721	.82	.4485	1.2685	.6893	.646
.13	.0446	.1746	.0600	.745	.48	.1865	.6665	.3727	.720	.83	.4638	1.2938	.6969	.641
.14	.0482	.1882	.0688	.744	.49	.1914	.6814	.3827	.719	.84	.4803	1.3203	.7043	.636
.15	.0517	.2017	.0739	.744	.50	.1964	.6964	.3927	.718	.85	.4982	1.3482	.7115	.630
.16	.0553	.2153	.0811	.743	.51	.2014	.7114	.4027	.717	.86	.5177	1.3777	.7186	.624
.17	.0589	.2289	.0885	.743	.52	.2065	.7265	.4127	.716	.87	.5392	1.4092	.7254	.617
.18	.0626	.2426	.0961	.742	.53	.2117	.7417	.4227	.715	.88	.5632	1.4432	.7320	.610
.19	.0662	.2562	.1039	.742	.54	.2170	.7570	.4327	.713	.89	.5900	1.4800	.7384	.601
.20	.0699	.2699	.1118	.741	.55	.2224	.7724	.4426	.712	.90	.6204	1.5204	.7445	.592
.21	.0736	.2836	.1199	.740	.56	.2279	.7879	.4526	.711	.91	.6555	1.5655	.7504	.581
.22	.0773	.2973	.1281	.740	.57	.2335	.8035	.4625	.709	.92	.6966	1.6166	.7560	.569
.23	.0811	.3111	.1365	.739	.58	.2393	.8193	.4724	.708	.93	.7459	1.6759	.7612	.555
.24	.0848	.3248	.1449	.739	.59	.2451	.8351	.4822	.707	.94	.8065	1.7465	.7662	.538
.25	.0887	.3387	.1535	.738	.60	.2511	.8511	.4920	.705	.95	.8841	1.8341	.7707	.518
.26	.0925	.3525	.1623	.738	.61	.2572	.8672	.5018	.703	.96	.9885	1.9485	.7749	.493
.27	.0963	.3663	.1711	.737	.62	.2635	.8835	.5115	.702	.97	1.1410	2.1110	.7785	.460
.28	.1002	.3802	.1800	.736	.63	.2699	.8999	.5212	.700	.98	1.3958	2.3758	.7817	.412
.29	.1042	.3942	.1890	.736	.64	.2765	.9165	.5308	.698	.99	1.9700	2.9600	.7841	.334
.30	.1081	.4081	.1982	.735	.65	.2833	.9333	.5404	.696	1.00	–	–	.7854	–
.31	.1121	.4221	.2074	.734	.66	.2902	.9502	.5499	.695					
.32	.1161	.4361	.2167	.734	.67	.2974	.9674	.5594	.693					
.33	.1202	.4502	.2260	.733	.68	.3048	.9848	.5687	.691					
.34	.1243	.4643	.2355	.732	.69	.3125	1.0025	.5780	.688					
.35	.1284	.4784	.2450	.732	.70	.3204	1.0204	.5872	.686					

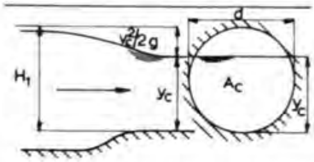

Provided that the diameter of the control section is known and H_1 is measured ($H_1 \approx h_1$ if the approach velocity is low), values for the ratios A_c/d^2 and y_c/d can be read from Table 1.2. Substitution of this information and a common C_d-value gives a value for Q, so that Equation 1-59 may be used as a general head-discharge equation for broad-crested weirs with circular control section.

If the approach velocity head $v_1^2/2g$ cannot be neglected, v_1 should be estimated and $h_1 = H_1 - v_1^2/2g$ calculated in one or two steps.

1.10 Short-crested weir

The basic difference between a broad-crested weir and a short-crested weir is that nowhere above the short crest can the curvature of the streamlines be neglected; there is thus no hydrostatic pressure distribution. The two-dimensional flow pattern over a short-crested weir can be described by the equations of motion in the s- and n-directions whereby the problem of determining the local values of v and r is introduced. This problem, like those involved in three-dimensional flow, is not tractable by existing theory and thus recourse must be made to hydraulic model tests.

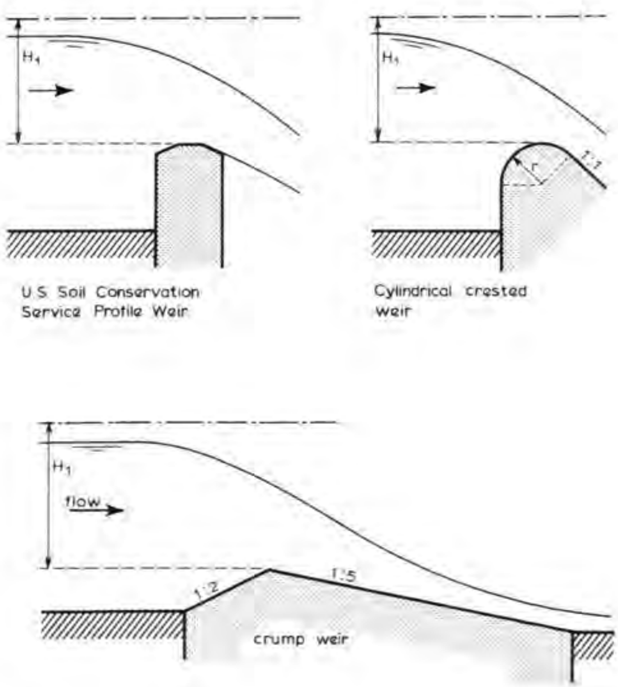

Fig.1.18. Various types of short-crested weirs.

Thus experimental data are made to fit a head-discharge equation which is structurally similar to that of a broad-crested weir but in which the discharge coefficient expresses the influence of streamline curvature in addition to those factors explained in Section 1.9.1.

In fact, the same measuring structure can act as a broad-crested weir for low heads ($H_1/L < 0.50$), while with an increase of head ($H_1/L > 0.50$) the influence of the streamline curvature becomes significant, and the structure acts as a short-crested weir. For practical purposes, a short-crested weir with rectangular control section has a head-discharge equation similar to Equation 1-37, i.e.

$$Q = C_d\, C_v\, \frac{2}{3} \left[\frac{2}{3}\, g\right]^{0.50} b h_1^{1.50} \qquad (1\text{-}60)$$

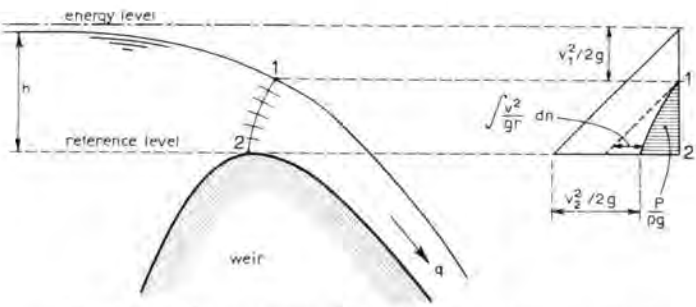

Fig.1.19. Velocity and pressure distribution above a short-crested weir.

The head-discharge equations of short-crested weirs with non-rectangular throats are structurally similar to those presented in Section 1.9.An exception to this rule is provided by those short-crested weirs which have basic characteristics in common with sharp-crested weirs. As an example we mention the WES-spillway which is shaped according to the lower nappe surface of an aerated sharp-crested weir and the triangular profile weir whose control section is situated above a separation bubble downstream of a sharp weir crest.

Owing to the pressure and velocity distributions above the weir crest,as indicated in Figure 1.19, the discharge coefficient (C_d) of a short-crested weir is higher than that of a broad-crested weir. The rate of departure from the hydrostatic pressure distribution is defined by the local centripetal acceleration v^2/r (see Eq. 1-10).

$$\frac{d}{dn}\left[\frac{p}{\rho g} + z\right] = -\frac{v^2}{gr} \qquad (1\text{-}61)$$

Depending on the degree of curvature in the overflowing nappe, an underpressure may develop near the weir crest, while under certain circumstances even vapour pressure can be reached (see also Appendix 1). If the overfalling nappe is not in contact with the body of the weir, the air pocket beneath the nappe should be aerated to avoid an underpressure, which increases the streamline curvature at the control section. For more details on this aeration demand the reader is referred to Section 1.14.

1.11 Critical depth flumes

A free flowing critical depth or standing wave flume is essentially a streamlined constriction built in an open channel where a sufficient fall is available so that critical flow occurs in the throat of the flume. The channel constriction may be formed by side contractions only, by a bottom contraction or hump only, or by both side and bottom contractions.

The hydraulic behaviour of a flume is essentially the same as that of a broad-crested weir. Consequently, stage-discharge equations for critical depth flumes are derived in exactly the same way as was illustrated in Section 1.9.

In this context it is noted that the stage-discharge relationships of several critical depth flumes have the following empirical shape:

$$Q = C'h^u \tag{1-62}$$

where C' is a coefficient depending on the breadth (b) of the throat, on the velocity head $v^2/2g$ at the head measurement station, and on those factors which influence the discharge coefficient; h is not the water level but the piezometric level over the flume crest at a specified point in the converging approach channel, and u is a factor usually varying between 1.5 and 2.5 depending on the geometry of the control section.

Examples of critical depth flumes that have such a head-discharge relationship are the Parshall flume, Cut-throat flume, and H-flume.

Empirical stage-discharge equations of this type (Eq.1-62) have always been derived for one particular structure, and are valid for that structure only. If such a structure is installed in the field, care should be taken to copy the dimensions of the tested original as accurately as possible.

Photo 4. If H_1/L < apr. 0.08, undulations may occur in the flume throat.

1.12 Orifices

The flow of water through an orifice is illustrated in Figure 1.20. Water approaches the orifice with a relatively low velocity, passes through a zone of accelerated flow, and issues from the orifice as a contracted jet. If the orifice discharges free into the air, there is modular flow and the orifice is said to have free discharge; if the orifice discharges under water it is known as a submerged orifice. If the orifice is not too close to the bottom, sides, or water surface of the approach channel, the water particles approach the orifice along uniformly converging streamlines from all directions. Since these particles cannot abruptly change their direction of flow upon leaving the orifice, they cause the jet to contract. The section where contraction of the jet is maximal is known as the vena contracta. The vena contracta of a circular orifice is about half the diameter of the orifice itself.

If we assume that the free discharging orifice shown in Figure 1.20 discharges under the average head H_1 (if $H_1 >> w$) and that the pressure in the jet is atmospheric, we may apply Bernoulli's theorem

$$H_1 = (h + v^2/2g)_1 = v^2/2g \qquad (1\text{-}63)$$

Hence

$$v = \sqrt{2gH_1} \tag{1-64}$$

This relationship between v and $\sqrt{H_1}$ was first established experimentally in 1643 by E.Torricelli.

If we introduce a C_v-value to correct for the velocity head and a C_d-value to correct for the assumptions made above, we may write:

$$v = C_d\ C_v\ \sqrt{2gh_1} \tag{1-65}$$

According to Equation 1-2, the discharge through the orifice equals the product of the velocity and the area at the vena contracta. This area is less than the orifice area, the ratio between the two being called the contraction coefficient, δ.

Therefore

$$Q = C_d\ C_v\ \delta\ \ A\sqrt{2gh_1} \tag{1-66}$$

The product of C_d, C_v and δ is called the effective discharge coefficient C_e. Equation 1-66 may therefore be written as

$$Q = C_e\ A\sqrt{2gh_1} \tag{1-67}$$

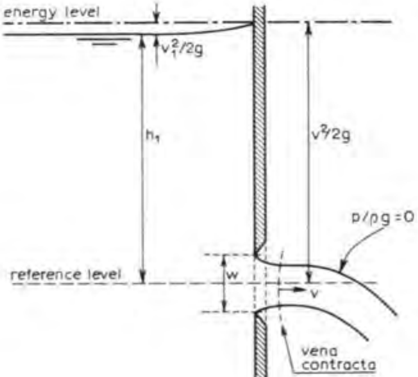

Fig.1.20. The free discharging jet.

Proximity of a bounding surface of the approach channel on one side of the orifice prevents the free approach of water and the contraction is partially suppressed on that side. If the orifice edge is flush with the sides or bottom of the approach channel, the contraction along this edge is fully suppressed. The contraction coefficient, however, does not vary greatly with the length of orifice perimeter that has suppressed contraction. If there is suppression of contraction on one or more edges of the orifice and full contraction on at least one remaining edge, more water will approach the orifice with a flow parallel to the face of the orifice plate on the remaining edge(s) and cause an increased contraction, which will compensate for the effect of partially or fully suppressed contraction.

Of significant influence on the contraction, however, is the roughness of the face of the orifice plate. If, for example, lack of maintenance has caused algae to grow on the orifice plate, the velocity parallel to the face will decrease, causing a decreased contraction and an increased contraction coefficient. Thus, unlike broad-crested weirs, an increase of boundary roughness of the structure will cause the discharge to increase if the head h_1 remains constant. This is also true for sharp-crested weirs.

Equation 1-67 is valid provided that the discharge occurs under the average head. For low heads, however, there is a significant difference between the flow velocity at the bottom and top of the orifice. If we take, for example, a rectangular orifice with a breadth b and a height w as shown in Figure 1.21 we may say that the theoretical discharge through an elementary strip of area bdz, discharging under a head $(h_b - z)$ equals

$$dQ = C_e\ b\ \sqrt{2g(h_b - z)}\ dz \qquad (1\text{-}68)$$

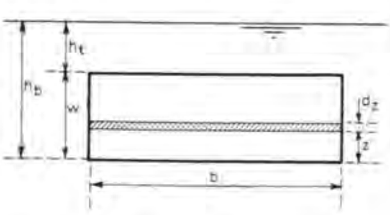

Fig.1.21. Rectangular orifice.

The total discharge through the orifice is obtained by integration between the limits o and $h_b - h_t$.

$$Q = C_e b \int_{o}^{h_b - h_t} \sqrt{2g(h_b - z)}\, dz \qquad (1\text{-}69)$$

or

$$Q = C_e\, b\, \frac{2}{3} \sqrt{2g}\, (h_b^{1.50} - h_t^{1.50}) \qquad (1\text{-}70)$$

If $h_t = 0$, the latter equation expresses the discharge across a rectangular sharp-crested weir (see also Section 1.13). In practice Equation 1-67 is used for all orifices, including those discharging under low heads, all deviations from the theoretical equation being corrected for in the effective discharge coefficient.

If the orifice discharges under water, it is known as a submerged orifice. Flow of water through a submerged orifice is illustrated in Figure 1.22.

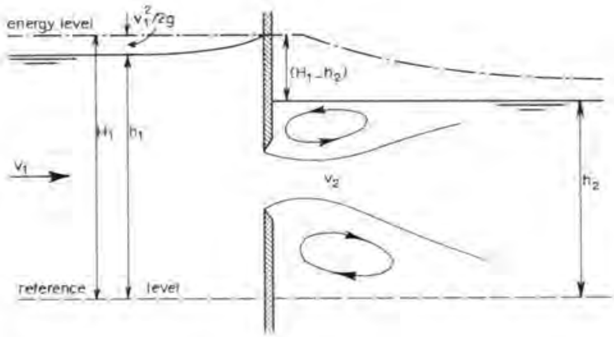

Fig.1.22. Flow pattern through a submerged orifice.

If we assume that there is no energy loss over the reach of accelerated flow, that the streamlines at the vena contracta are straight, and that the flow velocities in the eddy above the jet are relatively low, we may apply Bernoulli's theorem

$$H_1 = (p/\rho g + z)_1 + v_1^2/2g = (p/\rho g + z)_2 + v_2^2/2g \qquad (1\text{-}71)$$

and since $(p/\rho g + z)_2 = h_2$ we may write Equation 1-71 as

$$v = \{2g(H_1 - h_2)\}^{0.50} \qquad (1\text{-}72)$$

Using a similar argument to that applied in deriving Equation 1-64 we may obtain a formula that gives the total discharge through a submerged orifice as:

$$Q = C_e \, A\{2g(h_1 - h_2)\}^{0.50} \qquad (1\text{-}73)$$

1.13 Sharp-crested weirs

If the crest length in the direction of flow of a weir is short enough not to influence the head-discharge relationship of this weir (H_1/L greater than about 15) the weir is called sharp-crested. In practice, the crest in the direction of flow is generally equal to or less than 0.002 m so that even at a minimum head of 0.03 m the nappe is completely free from the weir body after passing the weir and no adhered nappe can occur. If the flow springs clear from the downstream face of the weir, an air pocket forms beneath the nappe from which a quantity of air is removed continuously by the overfalling jet. Precautions are therefore required to ensure that the pressure in the air pocket is not reduced, otherwise the performance of the weir will be subject to the following undesirable effects:

a) Owing to the increase of underpressure, the curvature of the overfalling jet will increase, causing an increase of the discharge coefficient (C_d).

b) An irregular supply of air to the air pocket will cause vibration of the jet resulting in an unsteady flow.

If the frequency of the overfalling jet, air pocket, and weir approximate each other there will be resonance, which may be disastrous for the structure as a whole.
To prevent these undesirable effects, a sufficient supply of air should be maintained to the air pocket beneath the nappe. This supply of air is especially important for sharp-crested weirs, since this type is used frequently for discharge measurements where a high degree of accuracy is required (laboratory, pilot scheme, etc.).

Figure 1.23 shows the profile of a fully aerated nappe over a rectangular sharp-crested weir without side contractions as measured by Bazin and Scimeni. This figure shows that for a sharp-crested weir the concept of critical flow is not applicable. For the derivation of the head-discharge equations it is assumed that sharp-crested weirs behave like orifices with a free water surface, and the following assumptions are made:

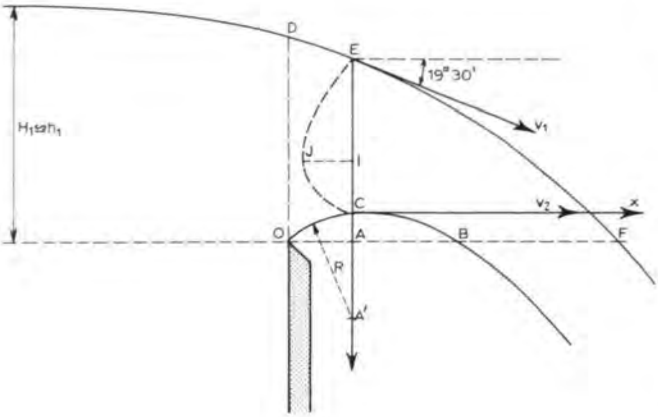

$$
\begin{aligned}
OA &= 0.25\ H_1\\
OD &= 0.85\ H_1\\
OB &= 0.67\ H_1\\
OF &= 1.38\ H_1\\
AC &= 0.112\ H_1\\
CE &= 0.65\ H_1\\
CI &= \frac{CE}{3} = 0.22\ H_1\\
IJ &= 0.18\ H_1\\
v_1 &= 0.475\ \sqrt{2gH_1}\\
v_2 &= 0.946\ \sqrt{2gH_1}
\end{aligned}
$$

Fig.1.23. Profile of nappe of a fully aerated two-dimensional weir (after BAZIN and SCIMENI).

(i) the height of the water level above the weir crest is $h = h_1$ and there is no contraction;

(ii) velocities over the weir crest are almost horizontal; and

(iii) the approach velocity head $v_1^2/2g$ is neglected.

The velocity at an arbitrary point of the control section is calculated with the equation of Torricelli, which was derived in Section 1.12 (Fig.1.24).

$$v = \{2g(h_1 + v_1^2/2g - z)\}^{0.50} \tag{1-74}$$

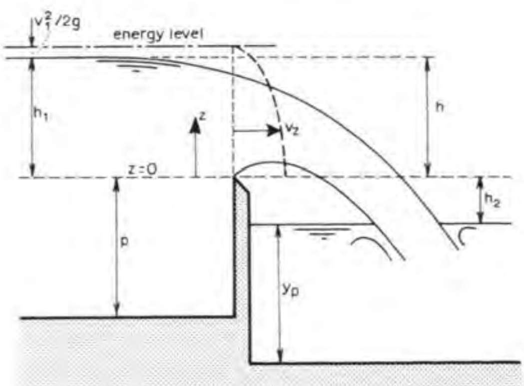

Fig.1.24. Parameters of a sharp-crested weir.

The total flow over the weir may be obtained by integration between the limits $z=0$ and $z=h_1$:

$$Q = (2g)^{0.50} \int_{o}^{h_1} x(h_1 - z)^{0.50}\, dz \qquad (1\text{-}75)$$

where x denotes the local width of the weir throat as a function of z. After the introduction of an effective discharge coefficient, C_e, to correct for the assumptions made, the general head-discharge equation of a sharp-crested weir reads (see also Section 1.12):

$$Q = C_e(2g)^{0.50} \int_{o}^{h_1} x(h_1 - z)^{0.50}\, dz \qquad (1\text{-}76)$$

The reader should note that the assumptions made above deviate somewhat from reality as shown in Figure 1.23 and are even partly in contradiction with the velocity distribution as calculated by Equation 1-74. In practice, however, Equation 1-76 has proved to be satisfactory and is widely used throughout the world. Since, also, the effective discharge coefficient is almost constant, a different set of head-discharge equations will be derived below for various kinds of sharp-crested weirs.

1.13.1 Sharp-crested weir with rectangular control section

For a rectangular control section, x = b = constant and Equation 1-76 may be written as

$$Q = C_e\ (2g)^{0.50} \int_{0}^{h_1} b(h_1 - z)^{0.50}\, dz \qquad (1\text{-}77)$$

or

$$Q = C_e\ \frac{2}{3}\ (2g)^{0.50}\ bh_1^{1.50} \qquad (1\text{-}78)$$

So, apart from a constant factor, Equation 1-78 has the same structure as the head-discharge relation for a broad-crested weir with rectangular control section (Equation 1-37).

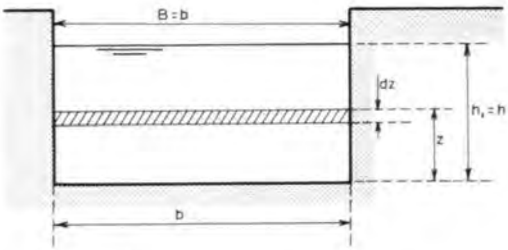

Fig.1.25. Dimensions of a rectangular control section.

1.13.2 Sharp-crested weir with a parabolic control section

For a parabolic control section $x = 2\sqrt{2fz}$, and Equation 1-76 may be written as

$$Q = C_e(2g)^{0.50} \int_0^{h_1} 2\{2fz(h_1 - z)\}^{0.50} \qquad (1\text{-}79)$$

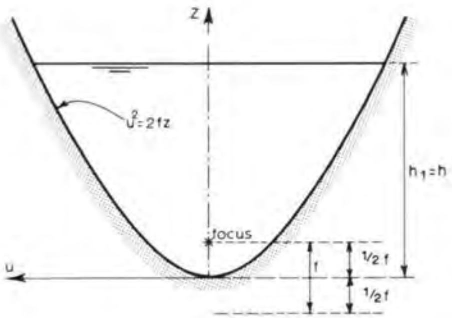

Fig.1.26. Dimensions of a parabolic control section.

After substituting $z = h(1 - \cos\alpha)/2$, Equation 1-79 is transformed into

$$Q = C_e(2g)^{0.50}\ 2(2f)^{0.50}\left[\frac{h_1}{2}\right]^2 \int_0^{\pi} (1 - \cos^2\alpha)^{0.50} \sin\alpha d\alpha$$

or

$$Q = C_e \frac{\pi}{2} \sqrt{fg}\ h_1^2 \qquad (1\text{-}80)$$

In the above α was introduced for mathematical purposes only.

1.13.3 Sharp-crested weir with triangular control section

For a triangular control section, $x = 2z \tan \theta/2$, and Equation 1-76 may be written as

$$Q = C_e (2g)^{0.50} \int_0^{h_1} \left[2 \tan\frac{\theta}{2}\right] z \; (h_1 - z)^{0.50} \, dz \qquad (1\text{-}81)$$

or

$$Q = C_e \frac{8}{15} (2g)^{0.50} \tan\frac{\theta}{2} \, h_1^{2.50} \qquad (1\text{-}82)$$

So, apart from a constant factor, Equation 1-82 has the same structure as the head-discharge relation for a broad-crested weir with triangular control section (Eq. 1-47).

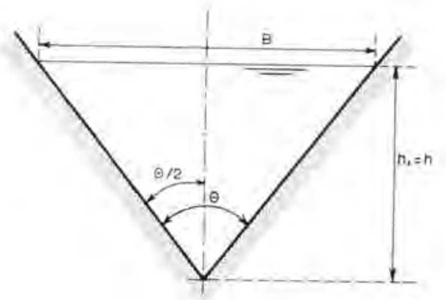

Fig.1.27. Dimensions of a triangular control section.

1.13.4 Sharp-crested weir with truncated triangular control section

The head-discharge relation for a truncated triangular control section as shown in Figure 1.28 is obtained by subtracting the head-discharge equation for a triangular control section with a head $(h_1 - H_b)$ from the head-discharge equation for a triangular control section with a head h_1. In general for sharp-crested weirs, superposing or subtracting head-discharge equations for parts of the control section is allowed, provided that each of the parts concerned contains a free water level.

The head-discharge equation $(h_1 > H_b)$ reads

$$Q = C_e \frac{8}{15} (2g)^{0.50} \tan\frac{\theta}{2} \left[h_1^{2.50} - (h_1 - H_b)^{2.50}\right] \qquad (1\text{-}83)$$

or

$$Q = C_e \frac{4}{15} (2g)^{0.50} \frac{B}{H_b} \left[h_1^{2.50} - (h_1 - H_b)^{2.50}\right] \quad (1\text{-}84)$$

If the head over the weir crest is less than H_b, Equation 1-82 should be used to calculate the discharge.

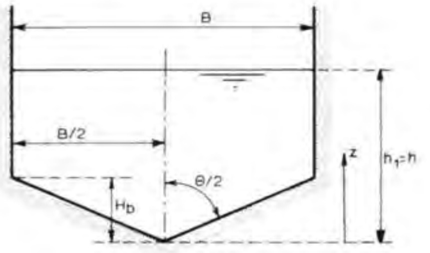

Fig.1.28. Dimensions of a truncated triangular control section.

1.13.5 Sharp-crested weir with trapezoidal control section

The head-discharge relation for a trapezoidal control section as shown in Figure 1.29 is obtained by superimposing the head-discharge equations for a rectangular and triangular control section respectively, resulting in

$$Q = C_e \frac{2}{3} (2g)^{0.50} \left[b + \frac{4}{5} h_1 \tan\frac{\theta}{2}\right] h_1^{1.50} \quad (1\text{-}85)$$

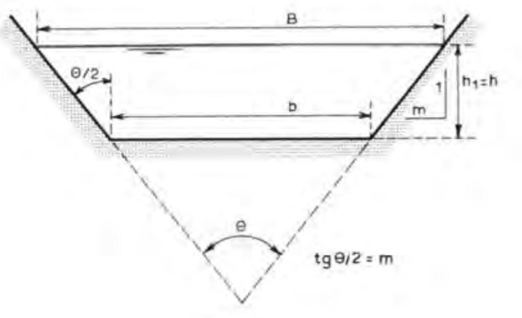

Fig.1.29. Dimensions of a trapezoidal control section.

1.13.6 Sharp-crested weir with circular control section

For a circular control section as shown in Figure 1.30, the values for x, z, and dz can be written as

$$x = 2\,r \sin\alpha = d \sin 2\beta = 2\,d \sin\beta \cos\beta$$

$$z = r(1 - \cos\alpha) = d \sin^2\beta$$

$$dz = 2\,d \sin\beta \cos\beta \, d\beta$$

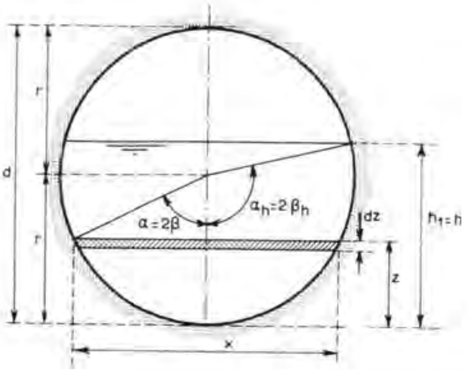

Fig.1.30.
Dimensions of a circular control section.

Substitution of this information into Equation 1-76 gives

$$Q = C_e (2g)^{0.5} \int_0^{\beta_h} (2d \sin\beta \cos\beta)^2 (h_1 - d \sin^2\beta)^{0.5} \, d\beta \qquad (1\text{-}86)$$

After introduction of $k^2 = \frac{h_1}{d}$ (being < 1) and some further modifications, Equation 1-86 reads

$$Q = C_e 4(2g)^{0.5} d^{2.5} \left[\int_0^{\beta_h} \sin^2\beta \, (k^2 - \sin^2\beta)^{0.5} \, d\beta - \right.$$

$$\left. - \int_0^{\beta_h} \sin^4\beta \, (k^2 - \sin^2\beta)^{0.5} \, d\beta \right] \qquad (1\text{-}87)$$

Substitution of $\sin\beta = k \sin\psi$ and introduction of $\Delta\psi = (1 - k^2 \sin^2\psi)^{0.5}$ leads to

$$Q = C_e 4(2g)^{0.5} d^{2.5} \left[\int_0^{\pi/2} \frac{\sin^2\psi}{\Delta\psi} \, d\psi - (1 + k^2) \int_0^{\pi/2} \frac{\sin^4\psi}{\Delta\psi} \, d\psi + \right.$$

$$\left. + k^2 \int_0^{\pi/2} \frac{\sin^6\psi}{\Delta\psi} \, d\psi \right] \qquad (1\text{-}88)$$

Now the complete elliptical integrals K and E of the first and second kind respectively, are introduced. K and E are functions of k only and are available in tables.

TABLE 1.3: VALUES OF ω and ϕ AS A FUNCTION OF THE FILLING RATIO $h_1/d = k^2$ OF A CIRCULAR SHARP-CRESTED WEIR

h_1/d	ω dimension-less	ϕ_i $m^{1/2}/s$	h_1/d	ω dimension-less	ϕ_i $m^{1/2}/s$	h_1/d	ω dimension-less	ϕ_i $m^{1/2}/s$
0.01	0.0004	0.00047	0.36	.3451	.4076	0.71	1.1804	1.3943
.02	.0013	.00154	.37	.3633	.4291	.72	1.2085	1.4275
.03	.0027	.00319	.38	.3819	.4511	.73	1.2368	1.4609
.04	.0046	.00543	.39	.4009	.4735	.74	1.2653	1.4946
.05	.0071	.00839	.40	.4203	.4965	.75	1.2939	1.5284
.06	.0102	.0120	.41	.4401	.5199	.76	1.3226	1.5623
.07	.0139	.0164	.42	.4603	.5437	.77	1.3514	1.5963
.08	.0182	.0215	.43	.4809	.5681	.78	1.3802	1.6303
.09	.0231	.0273	.44	.5019	.5929	.79	1.4091	1.6644
.10	.0286	.0338	.45	.5233	.6182	.80	1.4380	1.6986
.11	.0346	.0409	.46	.5451	.6439	.81	1.4670	1.7328
.12	.0412	.0487	.47	.5672	.6700	.82	1.4960	1.7671
.13	.0483	.0571	.48	.5896	.6965	.83	1.5250	1.8013
.14	.0560	.0661	.49	.6123	.7233	.84	1.5540	1.8356
.15	.0642	.0758	.50	.6354	.7506	.85	1.5830	1.8699
.16	.0728	.0860	.51	.6588	.7782	.86	1.6120	1.9041
.17	.0819	.0967	.52	.6825	.8062	.87	1.6410	1.9384
.18	.0914	.1080	.53	.7064	.8344	.88	1.6699	1.9725
.19	.1014	.1198	.54	.7306	.8630	.89	1.6988	2.0066
.20	.1119	.1322	.55	.7551	.8920	.90	1.7276	2.0407
.21	.1229	.1452	.56	.7799	.9212	.91	1.7561	2.0743
.22	.1344	.1588	.57	.8050	.9509	.92	1.7844	2.1077
.23	.1464	.1729	.58	.8304	.9809	.93	1.8125	2.1409
.24	.1589	.1877	.59	.8560	1.0111	.94	1.8403	2.1738
.25	.1719	.2030	.60	.8818	1.0416	.95	1.8678	2.2063
.26	.1854	.2190	.61	.9079	1.0724	.96	1.8950	2.2384
.27	.1994	.2355	.62	.9342	1.1035	.97	1.9219	2.2702
.28	.2139	.2527	.63	.9608	1.1349	.98	1.9484	2.3015
.29	.2289	.2704	.64	.9876	1.1666	.99	1.9744	2.3322
.30	.2443	.2886	.65	1.0147	1.1986	1.00	2.000	-
.31	.2601	.3072	.66	1.0420	1.2308			
.32	.2763	.3264	.67	1.0694	1.2632			
.33	.2929	.3460	.68	1.0969	1.2957			
.34	.3099	.3660	.69	1.1246	1.3284			
.35	.3273	.3866	.70	1.1524	1.3612			

$$Q = C_e \frac{4}{15}\sqrt{2g}\,\omega d^{2.5} \quad \text{or}$$

$$Q = C_e\,\phi_i\,d^{2.5}$$

Values of ω from J.C.STEVENS, 1957

$$E = \int_0^{\pi/2} \frac{d\psi}{\Delta\psi} \qquad (1\text{-}89)$$

$$K = \int_0^{\pi/2} \Delta\psi \; d\psi \qquad (1\text{-}90)$$

For the separate integrals of Equation 1-88 the following general reduction formula can be derived (n being an arbitrary even number):

$$\int_0^{\pi/2} \frac{\sin^n\psi}{\Delta\psi} = \frac{n-2}{n-1}\,\frac{1+k^2}{k^2} \int_0^{\pi/2} \frac{\sin^{n-2}\psi}{\Delta\psi}\,d\psi - \frac{n-3}{n-1}\,\frac{1}{k^2} \int_0^{\pi/2} \frac{\sin^{n-4}\psi}{\Delta\psi}\,d\psi \qquad (1\text{-}91)$$

Combinations of Equations 1-88, 1-89, 1-90, and 1-91 gives

$$Q = C_e \frac{4}{15}\,(2g)^{0.5}\,d^{2.5}\,\{2(1 - k^2 + k^4)\,E - (2 - 3k^2 + k^4)\,K\} \qquad (1\text{-}92)$$

or

$$Q = C_e \frac{4}{15}(2g)^{0.5}\,d^{2.5}\,\omega = C_e\,\phi_i\,d^{2.5} \qquad (1\text{-}93)$$

Equation 1-93 was first obtained by A.Staus and K.von Sanden in 1926.

Values of $\omega = \{2(1 - k^2 + k^4)\,E - (2 - 3k^2 + k^4)\,K\}$ and of $\phi_i = \frac{4}{15}(2g)^{0.5}\,\omega$ are presented in Table 1.3.

1.13.7 Sharp-crested proportional weir

A proportional weir is defined as a weir in which the discharge is linearly proportional to the head over the weir crest. In other words, the control section over a proportional weir is shaped in such a way that the sensitivity of the weir

$$\frac{dQ}{dh_1}\,\frac{h_1}{Q} = 1.0 \qquad (1\text{-}94)$$

In order to satisfy this identity the curved portion of the weir profile must satisfy the relation $x = cz^{-0.5}$ (c is a constant), so that the theoretical head-discharge equation, according to Equation 1-76, reads

$$Q = C_e(2g)^{0.5}\ c \int_0^h \left[\frac{h_1}{z} - 1\right]^{0.5} dz \qquad (1\text{-}95)$$

Substitution of a new dummy variable β into $\tan\beta = \left[\frac{h_1}{z} - 1\right]^{0.5}$ leads, after some modification, to

$$Q = C_e(2g)^{0.5}\ c\ \frac{\pi}{2}\ h_1 \qquad (1\text{-}96)$$

This mathematical solution, however, is physically unrealizable because of the infinite wings of the weir throat at $z = 0$. To overcome this practical limitation, H.H.SUTRO (1908) proposed that the weir profile should consist of a rectangular portion at the base of the throat and a curved portion above it, which must have a different profile law to maintain proportionality.

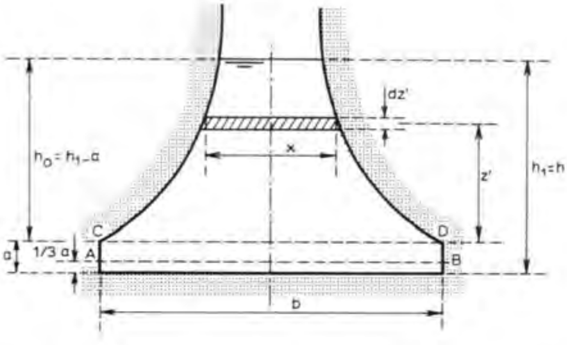

Fig.1.31. Dimensions of a proportional SUTRO weir notch.

The discharge through the rectangular section under a head h_1 above the weir crest equals, according to Equation 1-78

$$Q_r = C_e\ \frac{2}{3}\ (2g)^{0.5}\ b\left[h_1^{1.5} - h_o^{1.5}\right] \qquad (1\text{-}97)$$

where b equals the width of the rectangular portion, $h_o = (h_1 - a)$ equals the head over the boundary line CD, and "a" equals the height of the rectangular portion of the control section as shown in Figure 1.31.

The discharge through the curved portion of the weir equals, according to Equation 1-76

$$Q_c = C_e(2g)^{0.5} \int_0^{h_o} (h_o - z')^{0.5}\ x dz' \qquad (1\text{-}98)$$

Thus the total discharge through the weir equals

$$Q = Q_r + Q_c = C_e (2g)^{0.5} \left[\frac{2}{3} b \left(h_1^{1.5} - h_o^{1.5} \right) + \right.$$

$$\left. + \int_0^{h_o} (h_o - z')^{0.5} \, x dz' \right] \qquad (1\text{-}99)$$

The discharge through the weir must be proportional to the head above an arbitrarily chosen reference level situated in the rectangular portion of the weir. The reference level AB is selected at a distance of one-third of the rectangular portion above the weir crest to facilitate further calculations. So the total discharge through the weir also reads

$$Q = K(h_1 - a/3) \qquad (1\text{-}100)$$

where K is a weir constant.

Since proportionality is valid for heads equal to or above the boundary line CD, it must hold also if $h_o = 0$. Substitution of $h_o = 0$ and $h_1 = a$ into Equations 1-99 and 1-100 gives

$$Q = C_e \frac{2}{3} (2g)^{0.5} \, ba^{1.5} \quad \text{and}$$

$$Q = \frac{2}{3} Ka$$

Consequently the weir constant equals

$$K = C_e b \, (2ga)^{0.5} \qquad (1\text{-}101)$$

Substitution of the latter equation into Equation 1-100 gives

$$Q = C_e \, (2ga)^{0.5} \, b(h_1 - a/3) \qquad (1\text{-}102)$$

as a head-discharge equation.

The relationship between x and z' for the curved position of the weir can be obtained from the condition that Equations 1-99 and 1-102 should be equal to each other, thus

$$\frac{2}{3}\, b \left[h_1^{1.5} - h_o^{1.5} \right] + \int_0^{h_o} (h_o - z')^{0.5}\, x dz' = ba^{0.5}\, (h_1 - a/3)$$

From this equation h_1 and h_o can be eliminated and the following relationship between x and z can be obtained:

$$x/b = 1 - \frac{2}{\pi} \tan^{-1} \sqrt{(z'/a)} \qquad (1\text{-}103)$$

The derivation of this equation was presented by E.A.Pratt (1914).

1.14 The aeration demand of weirs

Under those circumstances where the overfalling jet is not in contact with the body of the weir, an air pocket exists under the nappe from which a quantity of air is removed continuously by the overfalling jet. If the air pocket is insufficiently aerated, an underpressure is created. This underpressure increases the curvature of the nappe. One of the results of this feature is an increase of the discharge coefficient (C_d). For a given head (h_1) the discharge is increased, and if the discharge is fixed, the measured head over the weir is reduced. Obviously, this phenomenon is not a desirable one as far as discharge measuring weirs are concerned.

Based on data provided by HOWE (1955) the writers have been able to find a relationship that gives the maximum demand of air (q_{air}) required for full aeration in m^3/sec per metre breadth of weir crest as

$$q_{air} = 0.1 \frac{q_w}{(y_p/h_1)^{1.5}} \qquad (1\text{-}104)$$

where q_w equals the unit discharge over the weir, h_1 is the head over the weir, and y_p equals the water depth in the pool beneath the nappe as shown in Figure 1.32.

The poolwater depth y_p is either a function of the tailwater level or of the unit discharge q and the drop height Δz.

If a free hydraulic jump is formed downstream of the weir, y_p may be calculated with Equation 1-105, which reads

$$y_p = \Delta z \left[\frac{q^2}{g\Delta z^3} \right]^{0.22} \tag{1-105}$$

The dimensionless ratio $q^2/g\Delta z^3$ is generally known as the drop number. If the jump downstream of the weir is submerged, the poolwater-depth may be expected to be about equal to the tailwater depth; $y_p \approx y_2$.

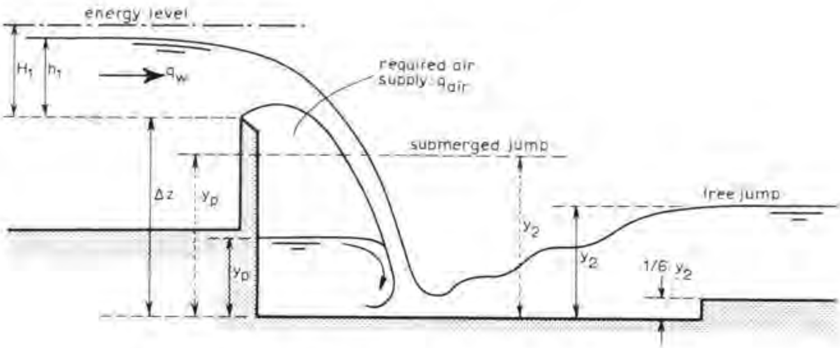

Fig.1.32. Definition sketch aeration demand.

As an example we consider a fully suppressed weir with a breadth b = 6.50 m and water discharging over it under a head h_1 = 0.60 m, giving a unit discharge of 0.86 m^3/sec per metre, while the pool depth y_p = 0.90 m. Equation 1-104 gives the maximum air demand for full aeration under these conditions as

$$q_{air} = 0.1 \frac{0.86}{(0.90/0.60)^{1.5}} = 0.047 \text{ m}^3\text{/sec per metre}$$

or 6.5 × 0.047 = 0.305 m^3/sec for the full breadth of the weir. The diameter of the air vent(s) to carry this air flow can be determined by use of the ordinary hydrodynamical equations, provided the underpressure beneath the nappe is low so that the mass density of air (ρ_{air}) can be considered a constant. In calculating the air discharge, however, the effective head over the vent must be stated in metres air-column rather than in metres water-column. For air at 20 °C, the ratio ρ_{air}/ρ_{water} equals approximately 1/830.

To facilitate the flow of air through the vent(s) a differential pressure is required over the vent, resulting in an underpressure beneath the nappe. In this example we suppose that the maximum permissible under-pressure equals 0.04 m water column.

Photo 5.
Non-aerated air pocket.

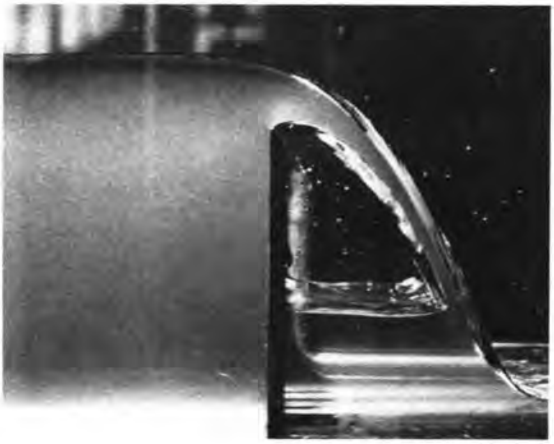

Photo 6.
Fully aerated air pocket.

Suppose that the most convenient way of aeration is by means of one steel pipe 2.50 m long with one-right angle elbow and a sharp cornered entrance; the head-loss over the vent due to the maximum air discharge then equals

$$(p/\rho g)_2 = \frac{\rho_{air}}{\rho_w}\left[K_e + \frac{fL}{D_p} + K_b + K_{ex}\right]\frac{v^2_{air}}{2g} \qquad (1\text{-}106)$$

where

$(p/\rho g)_2$ = permissible underpressure beneath the nappe in metres water-column

K_e = entrance loss coefficient (use $K_e = 0.5$)

f = friction coefficient in the Darcy-Weisbach equation, being:

$h_f = f\,\frac{L}{D}\,v^2/2g$ (use $f = 0.02$)

L	=	length of vent pipe
D_p	=	diameter of vent pipe
K_b	=	bend loss coefficient (use $K_b = 1.1$)
K_{ex}	=	exit loss coefficient (use $K_{ex} = 1.0$)
v_{air}	=	average flow velocity of the air through the vent pipe.

According to continuity, the total flow of air through the vents equal

$$Q_{air} = bq_{air} = \frac{1}{4} \pi D_p^2 \, v_{air} \tag{1-107}$$

Substitution of the data of the example and the latter equation into Equation 1-106 gives

$$0.04 = \frac{1}{830} \left[2.6 + \frac{0.02 \times 2.50}{D_p}\right] \frac{0.305^2}{12.14 \, D_p^4}$$

so that the internal diameter of the vent pipe should be about 0.16 m.

An underpressure beneath the nappe will deflect the nappe downwards and thus give a smaller radius to the streamlines, which results in a higher discharge coefficient. Consequently, for a measured head over the weir crest h_1, the discharge will be greater than the one calculated by the head-discharge equation (see Appendix I).

Based on experimental data provided by JOHNSON (1935), HICKOX (1942) and our own data a curve has been produced on double log paper (see Fig.1.33),resulting in the following empirical formula for the positive percentage error in the discharge:

$$X_Q = 20(p_2/\rho g h_1)^{0.92} \tag{1-108}$$

In our example, where $p_2/\rho g = 0.04$, and $h_1 = 0.60$ m; the ratio $p_2/\rho g h_1 = 0.067$, resulting in a positive error of 1.7% in the discharge.

Figure 1.33 shows that if the underpressure beneath the nappe increases, due to underdimensioning of the air-vent(s), the percentage error in the discharge increases rapidly, and the weir becomes of little use as a discharge measuring device.

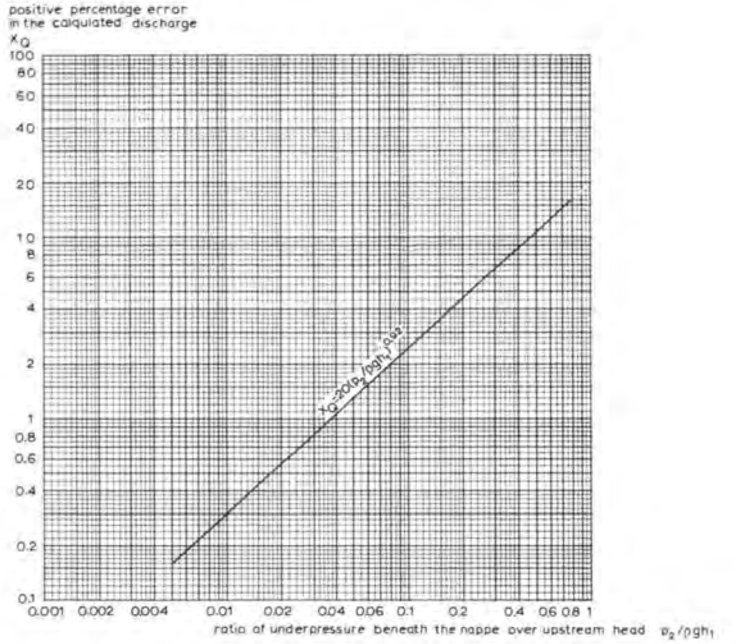

Fig.1.33. Increment of the discharge over a rectangular weir with no side contractions (after data from JOHNSON, HICKOX and present writers).

1.15 Channel expansions

1.15.1 General

As specified in Section 1.8 all discharge measuring structures which have a head-discharge relationship independent of the tailwater level (h_2) require a transition of subcritical to supercritical flow at their control section. The reversion to subcritical flow, however, entails a certain loss of energy. This loss of energy is a minimum if the submergence ratio H_2/H_1 is so great that the discharge is just not influenced significantly by the tailwater level. The minimum loss of head required for modular flow consists of the friction loss and the conversion losses. Of these, for well-designed streamlined structures, the friction loss can be calculated per section by means of an accepted formula for uniform flow such as that of Chézy or Manning. Because of the relatively short channel reach involved, the total loss of energy due to friction is usually small compared with the conversion losses.

With a proper hydraulic design of the measuring structure, the energy losses upstream of the control section in the zone of acceleration are negligible (see Section 1.6). On the other hand, however, the loss of energy due to the conversion of kinetic into potential energy downstream of the control section has to be reconciled with the afflux at the measuring site. Consequently, the downstream expansions of measurement structures have either discontinuous boundaries and sharp breaks in wall alignment, with extensive separation zones and local eddying whenever economy of construction is more important than the loss of energy head, or are carefully streamlined with very gradual expansions when the modular limit of the structure has to be increased because of the limited available head.

Photo 7. If no kinetic energy needs to be recovered a sudden downstream expansion is adequate.

1.15.2 Influence of tapering the side walls

If the discharge measuring structure operates at its modular limit, i.e. if the submergence ratio H_2/H_1 is such that the theoretical discharge is just on the verge of being reduced because of the tailwater level, flow in the entire downstream expansion is sub-critical. It is common practice to express the loss of energy head over such a channel expansion in terms of the average flow velocities upstream and downstream of the expansion as follows:

$$\Delta H = \xi \frac{(v - v_2)^2}{2g} \tag{1-109}$$

This equation is based on the derivation of the energy loss in a sudden expansion in a closed conduit. Because of its simplicity, however, it is generally applied to open channel expansions as well.

If we now consider two alternative channel expansions as shown in Figure 1.34 and apply Equation 1-109, we see that the energy head loss for Expansion A equals

$$\Delta H_A = \xi \frac{(v - v_2)^2}{2g} \tag{1-110}$$

and for two sufficiently spaced expansions (B)

$$\Delta H_B = \xi \frac{(v - v_o)^2}{2g} + \xi \frac{(v_o - v_2)^2}{2g} \tag{1-111}$$

If we substitute, for example, $v = 2v_o = 4v_2$ into both equations we find

$$\Delta H_A = \xi \frac{9}{16} \frac{v^2}{2g} \quad \text{and} \quad \Delta H_B = \xi \frac{5}{16} \frac{v^2}{2g}$$

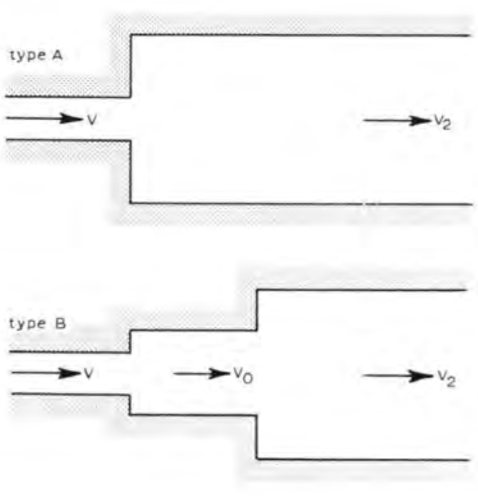

Fig.1.34. Comparison of channel expansions.

Thus the loss of energy for Expansion B is about 44% lower. A gradual expansion may be considered an extreme case of many successive sudden expansions and, consequently, a discharge measuring structure with a gradual expansion (Type B) will have a higher modular limit than a measuring structure with a sudden expansion (Type A).

For subcritical flow passing through channel expansions, experiments with various designs were made by G.FORMICA (1955). These are shown in Figure 1.35. Formica's experiments clearly illustrate how the energy loss in a sudden expansion can be reduced by gradually enlarging the transition reach and how this reduction may be partly nullified by such modifications as those shown in Designs 6 to 8.

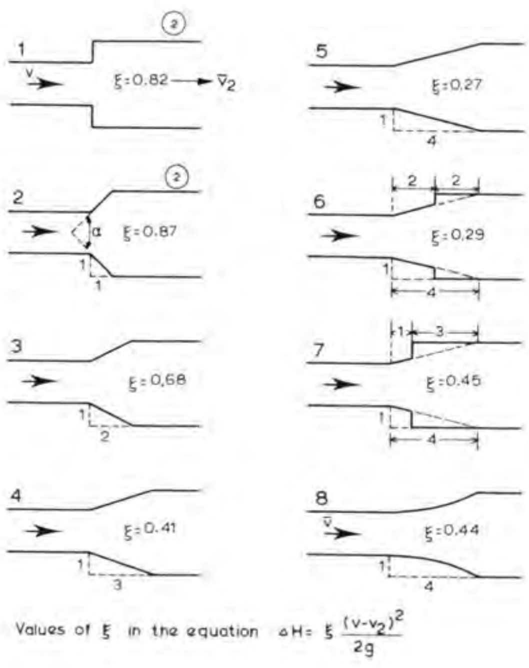

Fig.1.35. Energy loss in channel expansions (after G.FORMICA, 1955). (Channel width 355 mm for wider sections and 205 mm for narrower sections.)

No data are known giving ξ-values for open channel transitions where flow changes from critical to sub-critical. IDELCIK, 1969, however, gives data on expansions in closed conduits with a rectangular cross section. Curves, showing ξ-values as a function of the angle of divergence, α, for two- and three-dimensional transitions are shown in Figure 1.36. Comparison of FORMICA's and IDELCIK's data shows that the latter gives more unfavourable ξ-values.

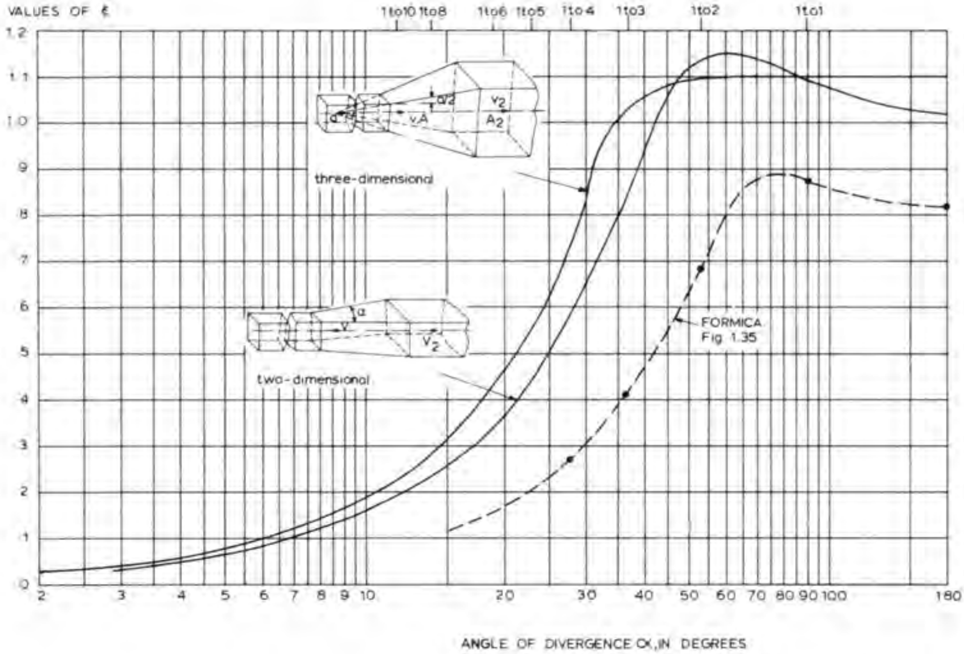

Fig. 1.36. Values of ξ as a function of α.

If IDELCIK's data are used to calculate the modular limit of broad-crested weirs and long-throated flumes by the equations derived in Section 1.15.3, a fair estimate can be made of the true modular limit (see also Section 7.1.3).

A more gradual taper than 1-to-8 does not usually result in savings in energy head commensurate with the extra expense, so that this angle of divergence is recommended as an economical minimum for expansions downstream of measuring devices.

1.15.3 Calculation of modular limit for downstream transitions

Long throated flumes are usually equipped with gradual expansions downstream of their control section to obtain a gradual conversion of kinetic into potential energy and thus to obtain a favourable modular limit.

As shown in Section 1.9 the head discharge relationship of a long-throated flume can be written as

$$Q = \text{constant } C_d \; bH_1^u \tag{1-112}$$

In this equation C_d is a coefficient which corrects for deviations from the assumptions that the upstream energy head H_1 would be equal to the energy head, H, at the control section and that the streamlines at the control are straight and parallel. For heads which are low with respect to the throat length ($0.10 \leqslant H_1/L \leqslant 0.33$) we may safely assume, however, that the C_d-value is mainly influenced by the first assumption so that replacement of H_1 by H in Equation 1-112 results in

$$Q = \text{constant } \; bH^u \tag{1-113}$$

Combination of the Equations 1-112 and 1-113 gives

$$H_1 C_d^{1/u} = H \qquad \text{or,} \tag{1-114}$$

$$H_1 - H = H_1(1 - C_d^{1/u}) \tag{1-115}$$

being an approximate expression for the loss of energy head between the head measurement station and the control section.

Downstream of the control section the loss of energy head may be expressed by

$$H - H_2 = \xi \frac{(v - v_2)^2}{2g} + \Delta H_f \tag{1-116}$$

where ΔH_f denotes the loss of energy head over the downstream transition due to friction.

Substitution of Equation 1-114 into Equation 1-116 gives after some transformation

$$\frac{H_2}{H_1} = C_d^{1/u} - \xi \frac{(v - v_2)^2}{2gH_1} - \frac{\Delta H_f}{H_1} \tag{1-117}$$

Equation 1-117 is an expression for the modular limit of a long-throated flume or broad-crested weir ($C_d < 1$). To obtain modular flow obviously

$$\frac{H_2}{H_1} \leqslant C_d^{1/u} - \xi \frac{(v - v_2)^2}{2gH_1} - \frac{\Delta H_f}{H_1} \qquad (1\text{-}118)$$

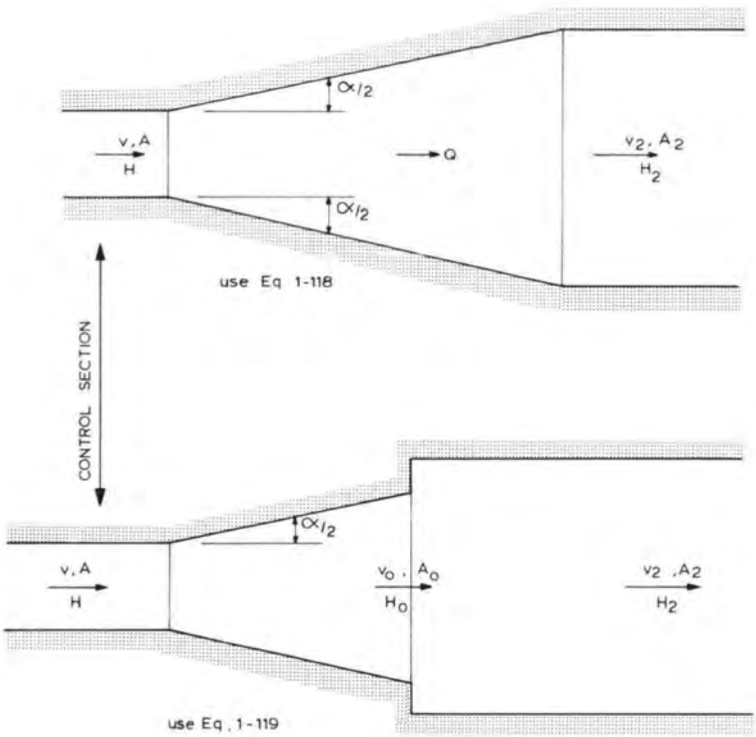

Fig.1.37. Downstream transitions.

If the transition is truncated, the above equation must be rewritten by use of Equation 1-111 to read

$$\frac{H_2}{H_1} \leqslant C_d^{1/u} - \xi \frac{(v - v_o)^2}{2gH_1} - \xi_{180} \frac{(v_o - v_2)^2}{2gH_1} - \frac{\Delta H_f}{H_1} \qquad (1\text{-}119)$$

1.16 Selected list of literature

1. BASIN, H.E.: Expériments nouvelles sur l'écoulement en déversoir. Annales des Ponts et Chaussées. Vol.7, 1896, pp.249-357.

2. CARLIER, M.: Hydraulique générale et appliquée. Collection du Centre de recherches et d'essais de Chatou. Eyrolles, Paris, 1972.

3. FORMICA, G.: Esperienze preliminari sulle perdite di carico nei canali, dovute a cambiamenti di sezione.
L'Energia elettrica. Milano, Vol.32, No.7. pp.554-568. July 1955.

4. HENDERSON, F.M.: Open channel flow. The Macmillan Company, New York,1966.

5. HICKOX, G.H.: Aeration of spillways. Transactions of the American Society of Civil Engineers. Vol.109, pp.537-556. 1944.

6. HOWE, J.W., SHIEH, G.C. and OBADIA, A.O.: Aeration demand of a weir calculated. Civil Engineering Vol.25, No.5, p.289. 1955. Easton, Pa. & Personal Communication, 1972 (HOWE).

7. IDELČIK, I.E.: Memento des pertes de charge. Coll.du Centre de recherche et d'essais de Chatou. Eyrolles, Paris, 1969. (Transl.from Russian.)

8. KING, H.W. and BRATER, E.F.: Handbook of hydraulics. 5° Edition. McGraw-Hill Book Comp.

9. KNAPP, F.H.: Ausfluss, Überfall und Durchfluss im Wasserbau. Verl.G.Braun, Karlsruhe, 1960.

10. PRATT, E.A.: Another proportional-flow weir; Sutro weir. Engineering News, Vol.72, No.9, p.462. August 1914.

11. ROUSE, H.: Fluid Mechanics for hydraulic engineers. Dover Publications, Inc. New York, 1938. Reprint 1961.

12. ROUSE, H.: Engineering Hydraulics. John Wiley & Sons, Inc., New York, 1950, Fourth printing 1964.

13. SCIMENI, E.: Sulla forme delle vene tracimani. L'Energia elettrica, Milano, Vol.7, No.4, pp.293-305. April 1930.

14. STEVENS, J.C.: Flow through circular weirs. J.of the Hydraulics Division of the American Society of Civil Engineers, Vol.83,No.HY 6, Dec.1957, Paper 1455.

15. VEN TE CHOW:Open-channel hydraulics.McGraw-Hill Book Comp.New York,1959.

2 Auxiliary equipment for measuring structures

2.1 Introduction

Most structures built for the purpose of measuring or regulating discharges consist of a converging section with accelerating subcritical flow, a control section with a transition to supercritical flow, and a downstream transition where the flow velocity is reduced to an acceptable value.

Upstream of the structure is an approach channel, which influences the velocity distribution of the approaching flow. Downstream of the structure is a tailwater channel, which is of fundamental importance in the design of the structure because of the range of tailwater levels that will result from varying discharges.

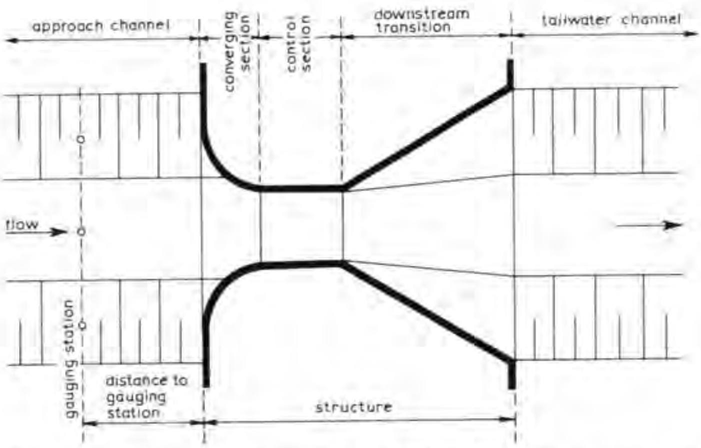

Fig.2.1. General lay-out of a discharge measurement structure.

The difference in elevation between the crest of the control section and the piezometric head in the approach channel is known as the upstream head over the crest of the structure and is denoted by h_1. If the structure is located in a channel where the discharge is determined upstream, h_1 corresponds with the discharge and the structure serves as a measuring device only. If the structure is located at a canal bifurcation, h_1 can be altered so that the structure can be used both as a measuring and as a regulating device. The upstream head over the crest can be determined by reading the water surface elevation in the approach channel on a staff gauge whose gauge datum elevation coincides with the crest of the structure. Determining the gauge datum elevation is generally known as zero-setting and this should be repeated at regular intervals to avoid serious errors in the measurement of h_1. That part of the approach channel where the water surface elevation is measured is known as the head measurement or gauging station.

2.2 Head measurement station

The head measurement station should be located sufficiently far upstream of the structure to avoid the area of surface draw-down, yet it should be close enough for the energy loss between the head measurement station and the structure to be negligible. This means that it will be located at a distance equal to between two and four times h_1max from the structure. For several standard measuring flumes, this general rule has been disregarded and the piezometric head is measured at a well-prescribed point in the converging section where there is a significant acceleration of flow. Thus the measured piezometric head is lower than the real upstream head over the crest, which hampers the comparison of stage-discharge equations and the minimum required loss of head (modular limit, see also Section 1.8). The stage-discharge relationship of such flumes can only be obtained by calibration (tables and/or formulae). The only advantage of this procedure is that an approach velocity coefficient is not needed.

The water level upstream of the structure may be measured by a vertical or an inclined gauge. A hook, point, or staff gauge can be used where incidental measurements are required, or a float-operated recording gauge where a continuous record is needed. Regardless of the type of gauge used, it should be located to one side of the approach channel so that it will not interfere with the flow pattern over the structure.

Photo 1. The elevation of a movable weir can be read from a fixed gauge.

Photo 2. Sharp-nosed intermediate piers tend to trap floating trash.

2.3 The approach channel

All structures for measuring and regulating discharges require an approach channel with a flow free from disturbance and with a regular velocity distribution. This can be obtained by having a straight section free of projections at the sides and on the bottom. The channel should have reasonably uniform cross-sections and be straight for a length equal to approximately 10 times its average width, provided that the breadth of the control section is equal to or greater than half the width of the approach channel. If the breadth of the control section is less than this, the length of the approach channel should be at least 20 times the breadth of the control section. In canals that carry no debris, the desired flow conditions can be provided by suitably placed baffles formed by vertical vanes or laths. These baffles should not be located nearer to the head measurement station than 10 times h_1.

If super-critical flow occurs upstream of the structure, a hydraulic jump should be introduced to ensure a regular velocity distribution at the head measurement station. This jump should be located at a distance of not less than 30 times h_1 from the structure.

In cases where the entry to the converging section is through a bend, where the approach channel is too short, or where a hydraulic jump occurs within the distance mentioned above, either the approach channel must be modified or the structure must be calibrated in situ, for example by use of the velocity-area method or salt dilution method.

2.4 Tailwater level

The difference between the water level immediately below the downstream transition (tailwater level) and the elevation of the crest of the structure is known as the downstream head over the crest and is denoted by h_2. Tailwater level, and thus the submergence ratio h_2/h_1, is affected by the hydraulic properties of the tailwater channel and by the occurrence of transitions in that channel.

The measuring structure should be so designed that modular flow is maintained under all operating conditions. If there is only a limited head loss available, both the elevation of the crest in relation to the downstream energy level and the length and shape of the downstream transition should be selected in such a way that modular flow is ensured (see also Section 1.15).

If the tailwater channel is relatively wide or if the tailwater level is affected by a downstream structure, it may occur that the measuring structure is modular at its maximum design capacity, but non-modular with lesser discharges. Under such circumstances a decrease in the upstream head means an increase in the submergence ratio h_2/h_1. The crest of the control section should then be raised so that h_2, and thus the ratio h_2/h_1, decreases to below the modular limit.

If the measuring structure is modular over its entire operating range, it is not necessary to make tailwater measurements (see Section 1.8). If the flow conditions are non-modular, however, both h_1 and h_2 must be recorded to allow the discharge to be calculated. The tailwater level should be measured immediately downstream of the deceleration transition where normal channel velocities occur. The equipment to be used for this purpose may be the same as that used for measuring the upstream water level or it may be of a lower accuracy, and thus more simple, depending on the frequency with which submerged flow occurs (see also Section 2.12).

It is evident that collecting and handling two sets of data per measuring structure is an expensive and time-consuming enterprise, which should be avoided as much as possible. Other even more important reasons for applying a modular structure are that in an irrigation canal system a water user with his own canal inlet cannot increase the discharge by lowering the tailwater level while, on the other hand, all persons concerned have a simple way of checking whether they receive their proper share of the available water.

2.5 Staff gauge

Where no detailed information on the discharge is needed or in stream channels where the flow fluctuation is gradual, periodic readings on a calibrated staff gauge may provide adequate data. A staff gauge should also be provided if the head is registered by a float-operated recorder as it will enable comparison of the outside water level with the head in the float well.

Supports for the staff gauge should not interfere with the flow pattern in the structure, and should be independent of the stilling well. Most permanent gauges are plates of enamelled steel, cast aluminium, or polyester, bolted or screwed in sections to a timber or steel pole. A typical gauge is shown in Figure 2.2. The gauge should be placed in such a manner that the water level can be read from the canal bank. Care should be taken that the staff gauge is firmly secured.The following type of support has proved satisfactory for permanent installations: a section of 180 mm channel iron is embedded about 0.50 m in a concrete block and extended above the block to the maximum height required. The concrete block should extend well below the maximum expected frost penetration and at least 0.60 m below the minimum bed level of a natural stream. The top of the block should be 0.10 m below the lowest head to be measured. A staff of durable hardwood, 0.05 × 0.15 m, is bolted to the channel iron above the concrete block, and the enamelled gauge section is fastened to this staff with brass screws. Staff gauges may be fastened to any other supporting structure, provided that its elevation is constant.

Fig. 2.2 Typical staff gauge.

2.6 Stilling well

The primary purpose of a stilling well is to facilitate the accurate registration of a piezometric or water level in open channels where the water surface is disturbed by surges or wave action.

The stilling well should be vertical and of sufficient height and depth to cover the entire range of expected water levels. In natural streams it should have a minimum margin of 0.60 m above the estimated maximum level to be recorded. In canals the minimum margin should be equal to the canal freeboard. Whenever the stilling well is used in combination with a float-operated recorder, it is common practice to extend the well to about 1.00 m above ground/platform level, so that the recorder can be placed at a suitable working height.

Care should be taken to ensure that if the float is rising its counterweight does not land on top of the float, but keeps well above it or passes the float.If a high degree of accuracy is required, the counterweight should not be permitted to become submerged over part of the operating range since this will change the submergence rate of the float and thus affect the recorded water level. This systematic error may be prevented

(i) by locating the counterweight inside a separate water-tight and water-free pipe

Photo 3. A stilling well made of steel pipes.

(ii) by mounting two different-sized wheels on the axle of the recorder, the large-diameter wheel serving to coil up the float wire and the small-diameter wheel coiling up the counterweight wire

(iii) by extending the stilling well pipe to such a height that the counterweight neither touches the float wheel at low stage nor the water surface at maximum expected stage.

The cross-sectional dimensions of the well depend on a number of factors:

(i) whether a dip-stick, staff gauge, or a float-operated recorder is used

(ii) type of construction material

(iii) height of the well

(iv) possible protection against freezing

(v) required stability

(vi) the necessity to have access to the inside.

If the well is used in combination with a dip-stick, a minimum diameter of 0.10 m to 0.15 m is advised to give access to a hand. A reference point, on which the stick will rest and whose elevation coincides with the exact crest elevation, is provided inside the well. A dip-stick can supply very accurate information on head.

If the well is used in combination with a staff gauge, the length of the well, as measured from the face of the gauge, should not be less than twice the depth to minimum water level in the well. The well width should not be less than 0.20 m to allow sufficient room for the gauge to be fixed by screws to the side of the well.

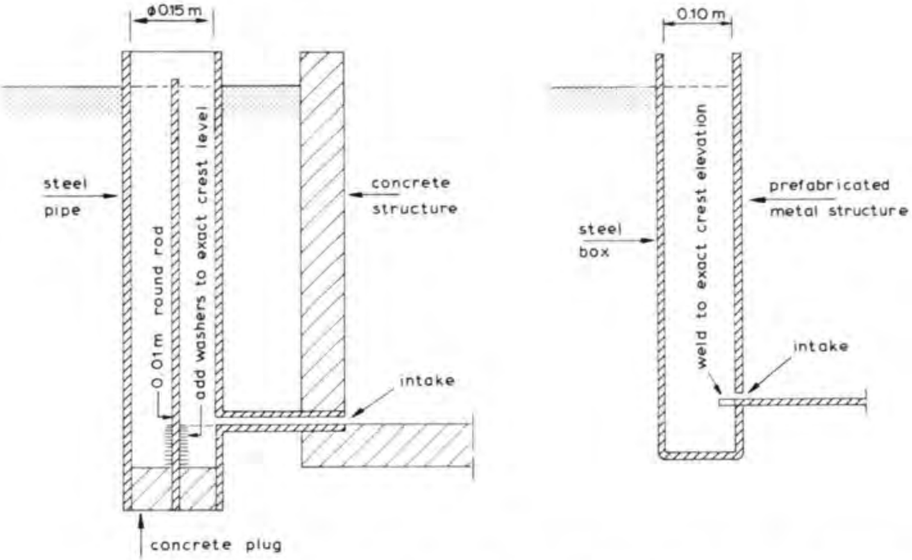

Fig.2.3. Examples of a stilling well used in combination with a dip-stick.

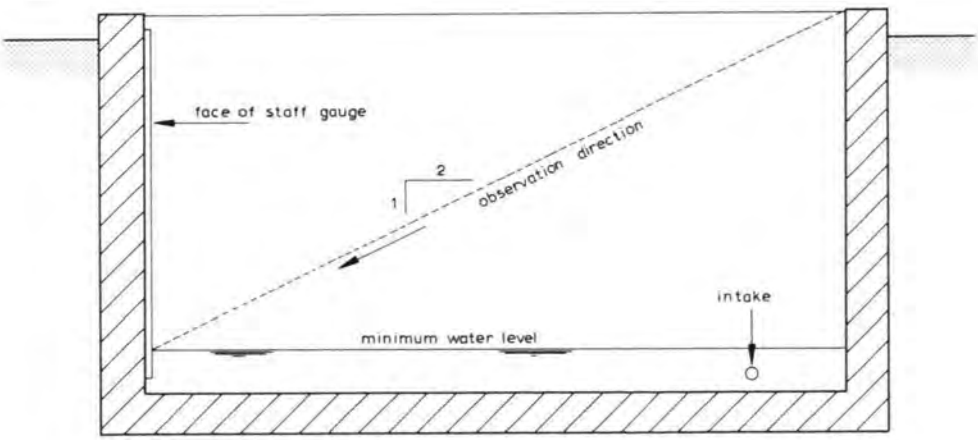

Fig.2.4. Stilling well used in combination with a staff gauge.

If the well is to accommodate the float of an automatic water level recorder, it should be of adequate size and depth to give clearance around the float at all stages. If the well is a metal, PVC, or concrete pipe, its diameter should be 0.06 m larger than the diameter of the float to avoid capillary effect; if the well is rectangular and constructed of brickwork, concrete, wood, or similar materials, the float should not be nearer than 0.08 m to the wall of the well. The bottom of the well should be some distance, say 0.15 m, below the lowest intake, to avoid the danger of the float touching the bottom or any silt that might have accumulated. This silt should be removed at regular intervals. In general, an access door should be provided to allow the recorder setting to be checked and to permit the removal of silt without the well having to be entered. If the well is set back into the channel embankment, the access door should be placed just above the embankment; if the well is installed in the channel, the door should be placed just slightly above low water. A second access door will allow the float tape length to be adjusted and gears to be changed without the recorder having to be removed. To avoid corrosion problems, it is recommended that the hinges of these access doors be of a rust-resistant metal such as stainless steel, brass, or bronze. A more simple solution is to support the door by wing nuts on short bolts welded to the well.

The foundation level of both the structure and the stilling well should be well below the maximum expected frost penetration and sufficiently below minimum bed level of canal or stream to provide stability and eliminate undercutting. To prevent the stilling well plus intake from functioning as a short-cut for groundwater flow and to facilitate zero-setting of a recorder, the well should be watertight. The inner base of a steel well should be sealed with bitumen where it meets the concrete foundation.

Since the primary purpose of the stilling well is to eliminate or reduce the effects of surging water and wave action in the open channel, the cross-sectional area of the intake should be small. On the other hand, the loss of head in the intake during the estimated maximum rate of change in stage should be limited to say 0.005 m. This head loss causes a systematic error; a rising water level is always recorded too low and a falling water level too high (see also Section 2.9). As a general guide to the size and number of intakes, their total cross-sectional area should be approximately 1 per cent of the inside horizontal cross-sectional area of the well.

The intake pipe or slot should have its opening at least 0.05 m below the lowest level to be gauged, and it should terminate flush with and perpendicular to the boundary of the approach channel. The area surrounding the intake pipe or slot should be carefully finished with concrete or equivalent material over a distance of 10 times the diameter of the pipe or width of the slot. Although the minimum requirement is one slot or pipe, on field installations it is advisable to install at least two at different levels to avoid the loss of valuable data if one intake should become clogged.

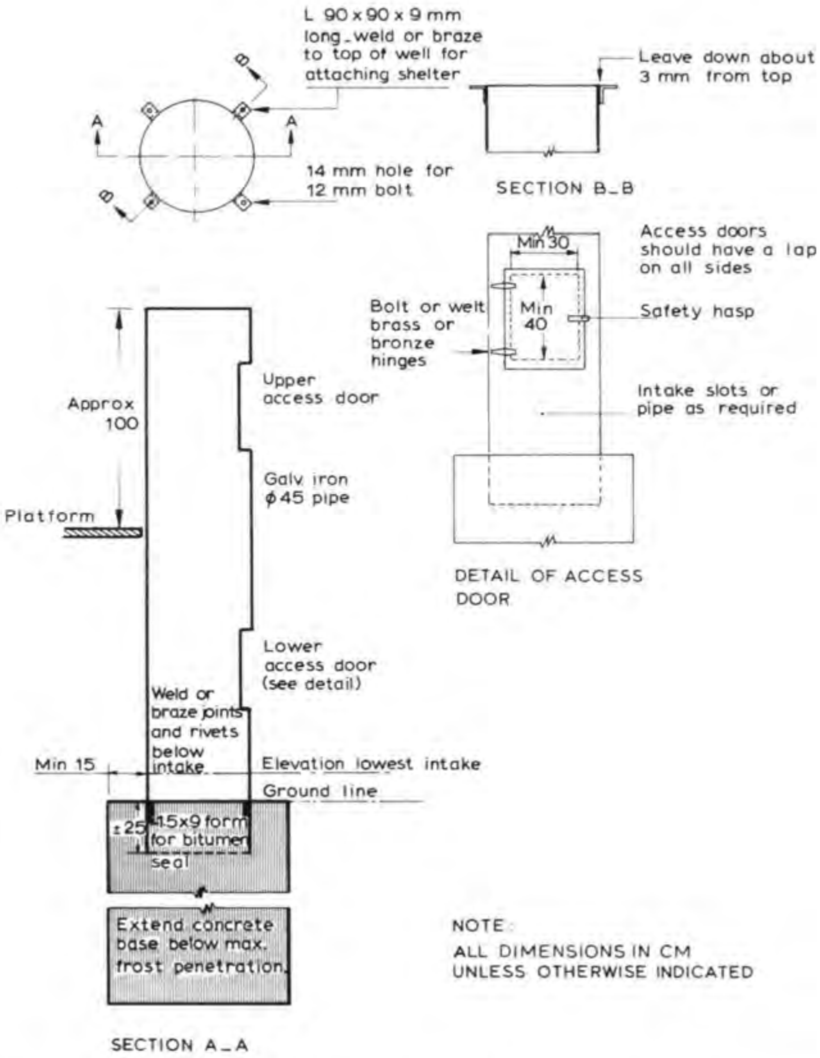

Fig.2.5. Example of a steel stilling well for low head installations (after U.S.Dept.of Agriculture).

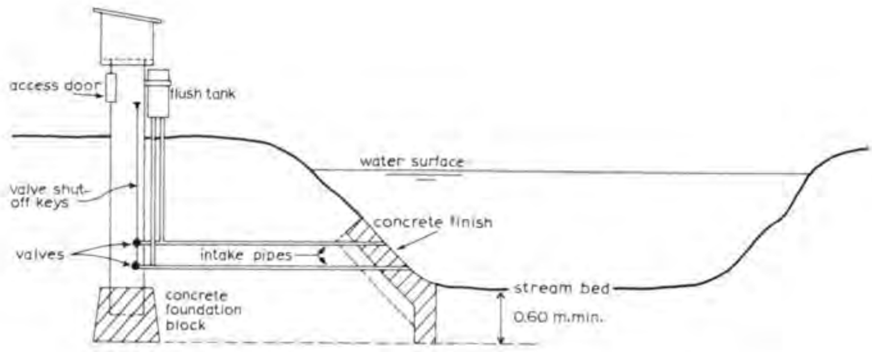

Fig.2.6. Example of an intake pipe system with flush tank.

In most stilling wells, the intake pipes will require periodical cleaning, especially those in rivers carrying sediments. Permanent installations can be equipped with a flushing tank as shown in Figure 2.6. The tank is filled either by hand pump or with a bucket, and a sudden release valve will flush water through the intake pipe, thereby removing the sediment. For tightly clogged pipes and on temporary or semi-permanent structures, a sewer rod or "snake" will usually provide a satisfactory way of cleaning.

A method that delays plugging involves the construction of a large cavity in the floor of the approach channel at the head measurement station. Its size may be of the order of 0.1 m^3. The stilling well pipe then enters this cavity and is fitted with a pipe elbow which is turned down so that sediment cannot fall directly into the pipe. The cavity must fill with sediment before the stilling well pipe can be clogged. The cavity must be covered with a steel plate coincident with the bottom of the approach channel. Taking into consideration the probable increased bedload trapping of transverse slots in this plate and the low quality pressure detection likely with parallel slots, REPLOGLE and FRAZIER (1973) advised the use of a battery of ∅ 4 mm holes drilled into the 8 mm grating plate. They reported that laboratory use showed no pressure detection anomalies and that field use showed no sedimentation plugging problems, although periodic grating and cavity cleaning is required.

2.7 Maximum stage gauge

If records are kept to gain information on maximum flow and no continuously operating recorder is installed, a flood gauge may be used to protect and retain a high-water mark for subsequent observations. The types recommended by the U.S.Department of Agriculture all use powdered cork to mark the maximum water level. As an example, Figure 2.7 shows a gauge that consists of a pipe containing a removable calibrated stick, 2.5 cm square, from which the cork is wiped off after each observation. A small metal or plastic cap, 4.0 cm in diameter and 1.5 cm deep, is attached to the bottom end of the stick to hold a supply of powdered cork.

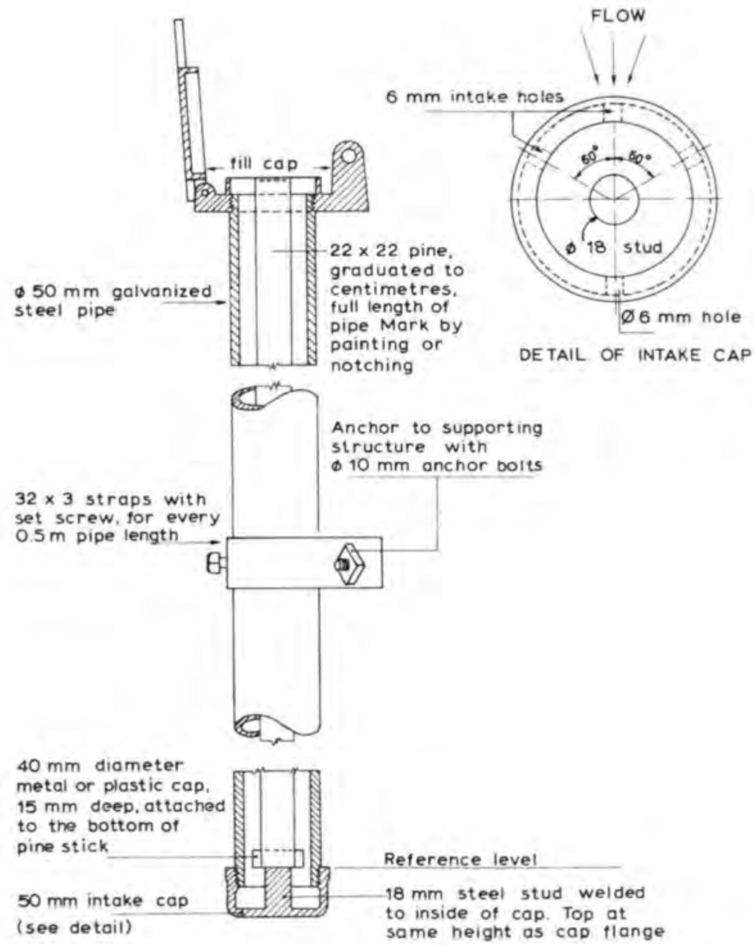

Fig.2.7. Details of a maximum stage gauge (after U.S.Department of Agriculture).

The 50 mm galvanized pipe is equipped with a perforated cap (4 perforations of ϕ 6 mm) at the bottom and another cap at the top. The top cap should be easily removable to allow observations but should have provisions for a padlock to prevent vandalism. The pipe should be securely anchored in an upright position as described in Section 2.5 for a staff gauge. The top of the pipe should be accessible, also at flood stages, to facilitate observations. Since the flood gauge is intended to register high water marks, the pipe should be long enough to extend from the moderate high water mark, which is expected on an average of say twice per year, to a point above the maximum stage expected.

2.8 Recording gauge

Automatic water stage recorders are instruments that produce graphical or punched paper tape records of water surface elevation in relation to time. The usual accessories to a recorder and its clock are a float, a counterweight, a calibrated float tape, two tape clamps with rings, a box of charts or paper tapes, and the manufacturer's instructions.

The use of such a recorder, in combination with a float well, has the following advantages over an ordinary attendant-read staff gauge:

(i) In rivers with daily fluctuations, continuous records provide the most accurate means of determining the daily average

(ii) The entire hydrograph is recorded with the maximum and minimum stages as a function of time

(iii) Observations can be made at remote places where observers are not available or in locations that are not accessible under all weather conditions.

Various meteorological instrument manufacturers produce a variety of commercially available recorders. Most recorders operate on the principle of a reducing mechanism that permits the accurate registration of a wide range in stage on a scale which can be read easily.

Most recorders have several time- and stage-scale ratios available, and may run as long as 60 days before the clock has to be rewound or the chart or tape replaced.

Some recorders are driven by clocks operated either by spring or weight; the digital recorder is an electrically operated device. No further details of recorders are given here, since the manufacturer's description and instructions are both detailed and complete, while technical progress soon makes any description obsolete.

Regardless of the type of water level recorder selected, it should be equipped with a calibrated float tape that passes over the float wheel. The float and counterweight should be attached to the ends of the tape by ring connectors. If the recorder is not equipped with a tape index pointer, one should be attached either to the shelterhouse floor or to the instrument case. The purpose of the calibrated tape and the index pointer is to enable the observer to check the registered water level against the actual water level in the float well and that shown on the independently placed staff gauge. As such,they provide an immediate check on whether recorder, float, and inlet pipe or slots are functioning properly.

2.9 Diameter of float

All water level recorders operate only if a certain initial resistance is overcome. This resistance, which is due to friction in the recorder and on the axle, can be expressed as a resisting torque, T_f, on the shaft of the float wheel.

If the counterweight exerts a tensile force, F, on the float-tape, this force must increase or decrease by ΔF before the recorder will operate so that:

$$\Delta F \; r > T_f \tag{2-1}$$

where

ΔF = change in tensile force on float-tape between float and float wheel
r = radius of the float wheel
T_f = resisting torque due to friction on the float wheel axle.

When we have, for example, a continuously rising water level in the well, a decrease in the tensile force, ΔF, is required, which is possible only if the upward force acting on the submerged part of the float increases. Consequently, the float has to lag behind the rising water table by a distance Δh, so that the volume of the submerged float section will increase by

$$\Delta V = \frac{\pi}{4} D^2 \Delta h \qquad (2\text{-}2)$$

where D equals the diameter of the float. According to Archimedes' law, the upward force will increase linearly with the weight of the displaced volume of water, hence

$$\Delta F = \frac{\pi}{4} D^2 \Delta h \rho g \qquad (2\text{-}3)$$

Substitution of Equation 2-3 into Equation 2-1 shows that the friction in the recorder and on the axle causes a registration error of the water level

$$\Delta h > \frac{4T_f}{\rho g \pi D^2 r} \qquad (2\text{-}4)$$

This lagging behind of the float causes a systematic error; a rising water level is always registered too low and a falling water level too high.

Accepting the recorder's internal friction moment, T_f, as a basic datum, this systematic error can only be reduced by enlarging either the float diameter, D, or the radius of the float-wheel, r.

Submergence of the counterweight and an increase of weight of the float tape or cable on one side of the float wheel (and consequently a decreasing weight on the other side) cause a known change in tape force at the float. This change in force, ΔF, results in a systematic registration error, Δh, which can be calculated by Equation 2-3. These systematic errors can also be reduced by enlarging the float diameter.

The reader should note that the phenomena just described produce a systematic error that adds to the one mentioned in Section 2.6, i.e. that due to the head loss in the intakes.

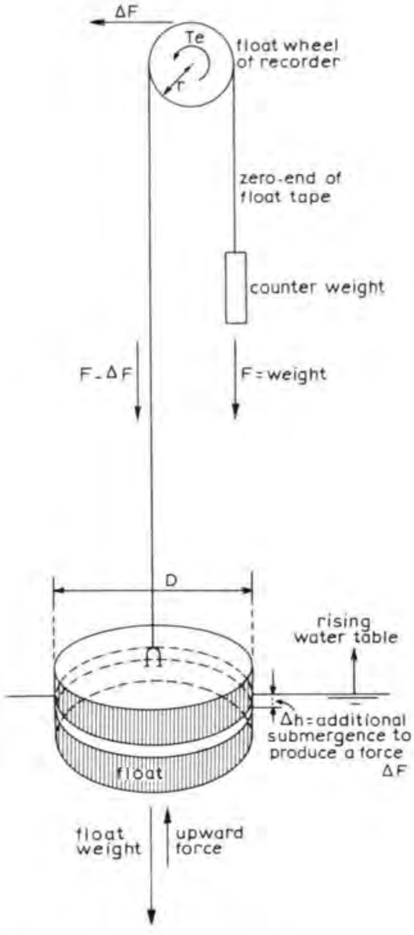

Fig.2.8. Forces acting on a float tape.

2.10 Instrument shelter

The housing of the recorder can vary from those used for permanent stations on large streams, which allow the observer to enter, to very simple ones, just large enough to cover the recorder and hinged to lift in the same direction as the instrument cover. A major disadvantage of the latter type is that it is impossible to service the recorder during bad weather, and further that the shelter provides no room for the storage of charts and other supplies. For our purposes, the instrument shelter should meet the following criteria:
The shelter should be ventilated to prevent excessive humidity from distorting the chart paper. All ventilation openings should be covered with a fly screen.

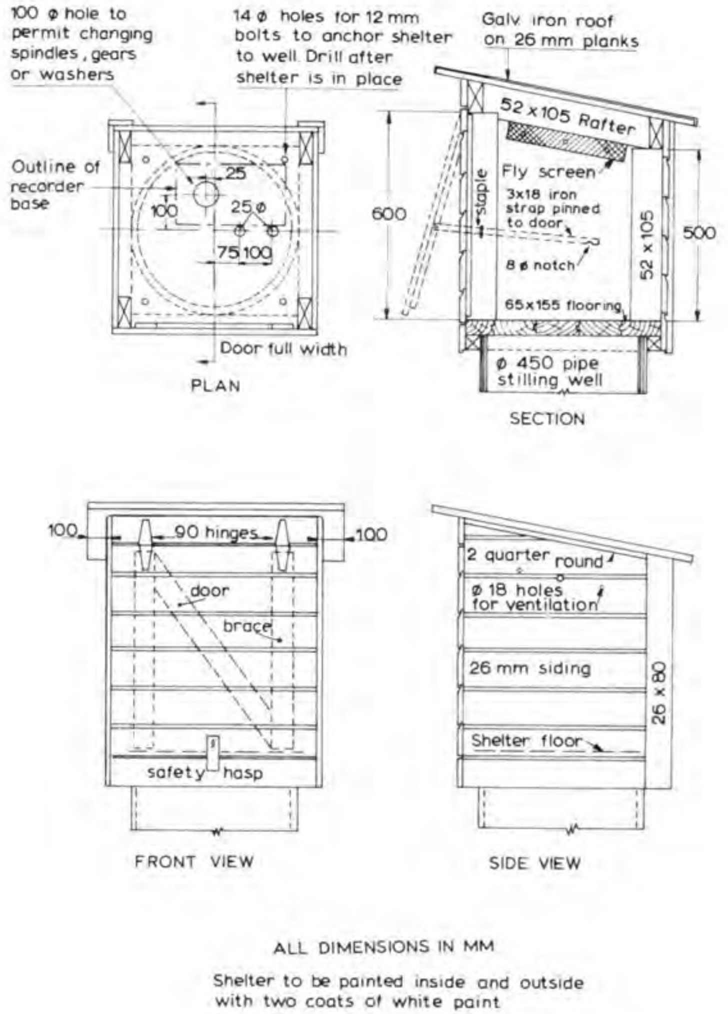

Fig.2.9. Example of an instrument shelter (after U.S.Dept.of Agriculture).

The shelter door should be hinged at the top so that when it is opened it will provide cover for the observer. An iron strip with a small notch near one end should be attached to either side of the door and should run through a staple on each side of the door opening, thus holding the opened door in position. To prevent vandalism, all hinges and safety hasps should be placed so that they cannot be removed while the door is locked. The flooring should be solid and of a suitable hardwood which will not warp. The shelter floor should be anchored to the well, for instance by bolting it at the four corners to small angle irons welded to the top of the float well. Condensation can be reduced by gluing or spraying a 3 mm layer of cork to the inside of both the metal shelter and the recorder cover. Silica gel can be utilized as a desiccant, but the moisture should be removed from the gel at regular intervals by heating it in an oven to about 150 °C (300 °F).

2.11 Protection against freezing

During winter it may be necessary to protect the stagnant water in the float well against freezing. This can be done by employing one or more of the following methods, depending on location and climate. If the well is set into the bank, an isolating subfloor can be placed inside the well just below ground level. Care should be taken, however, that both the float and counterweight can still move freely over the range of water levels expected during winter. If the well is heated with an electric heater or cluster of lights, or when a lantern or oil heater is suspended just above the water level, the subfloor will reduce the loss of heat. A reflector to concentrate the light or heat energy on the water surface will increase the heating efficiency.

A layer of low-freezing-point oil, such as fuel oil, around the float can be used as protection. The thickness of the oil layer required equals the greatest thickness of ice expected, plus some allowance for water-stage fluctuations. To prevent leakage of oil and erroneous records, a watertight float well will be necessary. Since the mass density of oil is less than that of water, the oil will stand higher in the float well than the water surface in the open channel. Consequently, the recorder must be adjusted to give the true water stage. If the stilling well is large compared with the float, it is advisable to accommodate the float in an inner pipe and to place the oil in this pipe to avoid the danger of oil being spilled into the open channel. The inner pipe should be open at the bottom so that water may pass freely in and out of it.

2.12 Differential head meters

The differential head meter is an important device in structures where the difference between two piezometric heads or water levels has to be known. Examples of such structures are the constant head orifice and other submerged orifices.

The importance of the differential head meter is such that the success or failure of the measuring and/or regulating structure often depends entirely upon the efficiency of the particular meter used. Four types, all employing two adjacent stilling wells, will be described here.

U-hook type

This most simple and sturdy of differential head meters has no moving parts and consists merely of two scales fixed to one short beam.

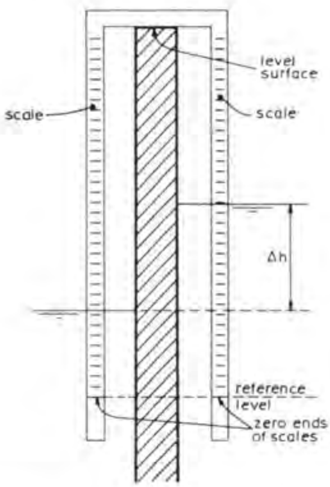

Fig.2.10. U-hook type differential head meter.

When the u-hook is placed over the divide wall between the two stilling wells, both scales are hanging in the water. The differential head is obtained by reading both scales independently and calculating the difference in immersion.

Hanging scale type

A differential head meter of the hanging scale type is a rather simple and inexpensive device from which the full differential head can be read from a free hanging scale. The meter consists of a float and an index which are hung over two disc wheels and a second float plus scale which hang over a third disc wheel. The three disc wheels are mounted on the same beam. Bicycle axles could be used for this purpose (see Fig.2.11).

The length of the scale should be about 0.10 m more than the maximum expected head differential.The height of the beam above ground level should be such that

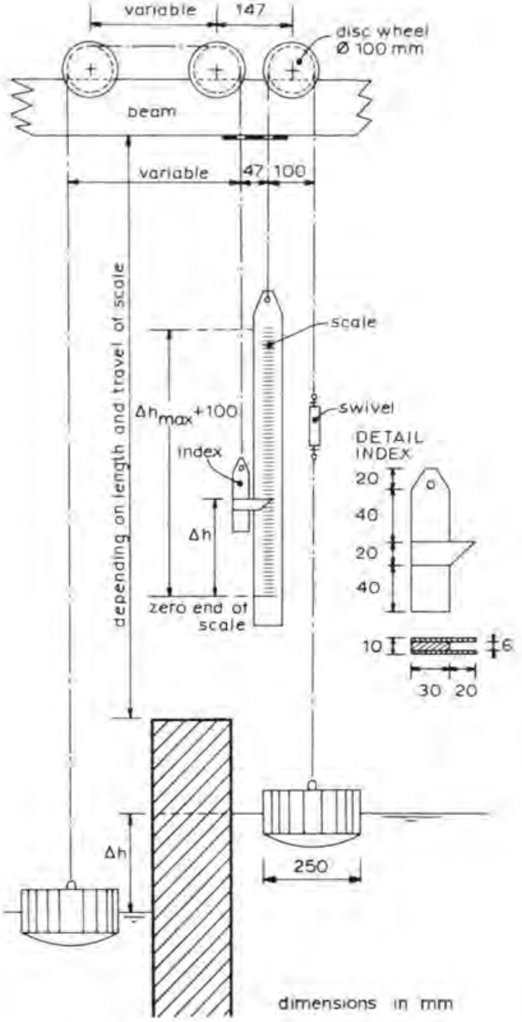

Fig.2.11. Differential head meter with hanging scale.

the scale stays clear of the steel stop-plate at low stage while the scale should remain hanging free at high stages. Zero-setting of the index should preferably be done by turning a swivel in the cable between the upstream float and scale. The device cannot be coupled to an automatic recorder.

Tube-float type

This robust differential head meter, which works without interruption under field conditions, can be constructed by using two tube-floats. These floats can be made from a section of ϕ 150 mm galvanized pipe, welded closed at the bottom and equipped with a screw cap plus hook at the top. Ballast is placed inside the watertight tube-floats so that they are heavier than the water they replace. Two of these floats, hanging over a bicycle wheel equipped with a zinc "tyre", form a balance which, after immersion of the floats, adjusts itself in such a way that the pipes have either the same draught or a constant difference in draught, the latter occurring if the weights of the two tube-floats are not exactly the same.

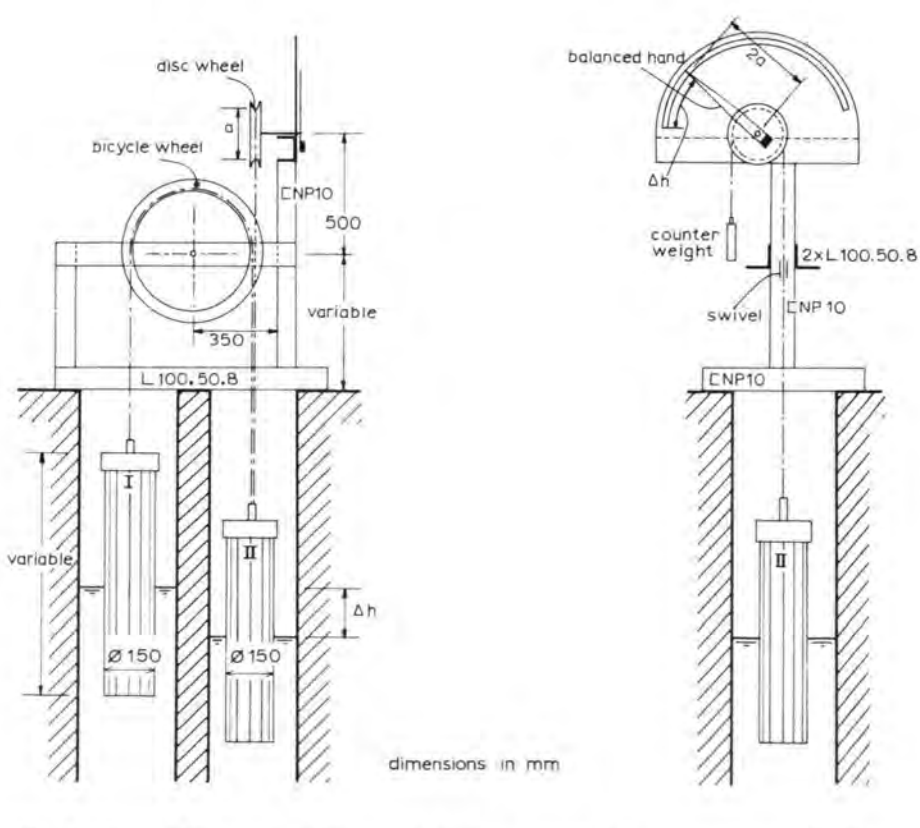

Fig.2.12. Tube-float differential head meter (after D.G.ROMIJN 1938).

When the head between the two stilling wells is changing, each of the floats will move over half the change in head. By transmitting the movement of the floats, as illustrated in Figure 2.12, a differential head meter is obtained, which shows the difference in head on a real or enlarged scale depending on the diameter of the disc-wheel and the length of the balanced hand. The diameter of the disc-wheel should be such that half its circumference is equal to or slightly larger than half the maximum difference in head to be measured. In this case the scale only fills half a circle, which facilitates observations.

A change of head will cause a point on the circumference of the disc-wheel to move over half that dimension. Provided the hand is twice as long as the radius of the wheel, its point moves over a distance twice as far as the movement of one float. Hence, it shows the real change in head. The length of the tube-floats should be such that, at both maximum and minimum stages, the floats are neither submerged nor hanging free above the water surface.

Index-setting of the hand should preferably be done by turning a swivel in the cable between the downstream float (II) and the disc-wheel. If required, the differential head can be recorded by an automatic recorder.

Suction lift type

A portable differential head meter which facilitates accurate observation is the suction lift type. This instrument consists of two glass tubes which are joined at the top by a tee that is connected to a transparent conduit in which a partial vacuum can be created by means of a simple hand-operated pump.

The lower ends of the glass tubes are connected with the stilling wells for the upstream and downstream heads. The meter is operated as follows. The stopcock valve is opened and a partial vacuum is created by means of the hand pump so that water flows into the container and all air is removed from the conduits. Then the stopcock valve is closed. Subsequently, by operating the valve, some air is admitted so that the two liquid levels become visible in the glass tubes. The difference in head can now be obtained by reading the elevation of each liquid level independently on a scale placed behind the tubes.

A device developed by the Iowa Institute simplifies this process by the use of a continuous tape over pulleys mounted at the top and bottom of the gauge. The zero end of the tape is set at one liquid level and a sliding indicator moved to the other level. Subsequently, the difference in head is given as a direct reading on the tape.

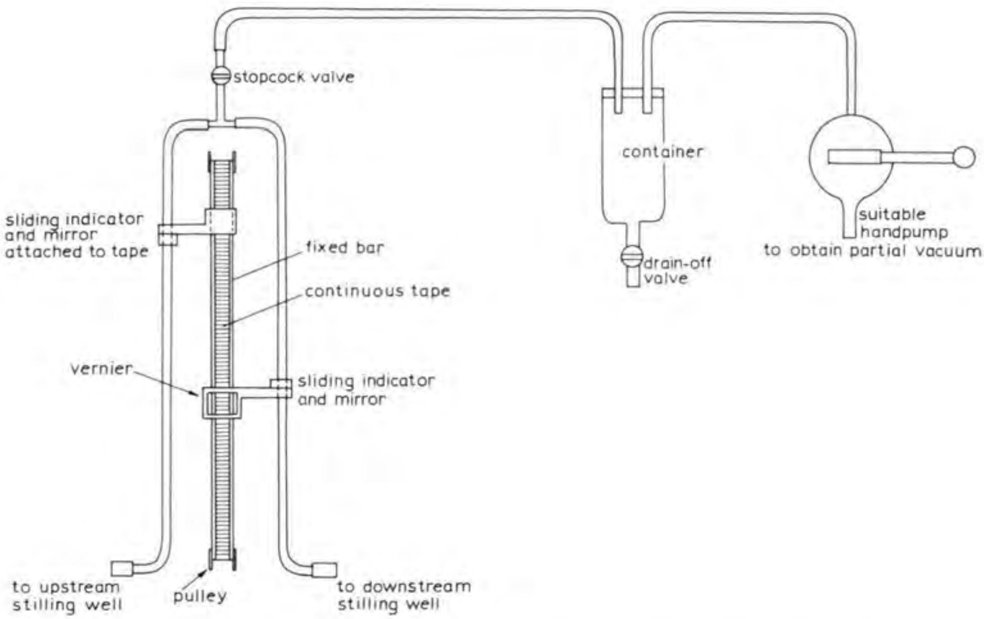

Fig.2.13. Differential head meter of the suction lift type with direct reading scale.

To prevent the small diameter conduits from becoming clogged, they should be used in combination with stilling wells and the conduit openings should be carefully screened. A conduit diameter of 0.5 to 1.0 cm will usually be adequate.

2.13 Selected list of references

1. BRITISH STANDARDS INSTITUTION: Methods of Measurement of Liquid Flow in Open Channels. B.S.3680: Part 4A: Thin plate weirs and venturi flumes. Part 4B: Long base weirs. British Standards House, London W.1. 1965, 1969.

2. REPLOGLE, J.A. and G.FRAZIER: Depth detection in critical depth flumes. Annual Report 1973. U.S.Water Conservation Laboratory, USDA, Phoenix, AZ.

3. ROMIJN, D.G.: Meetsluizen ten behoeve van Irrigatiewerken. Vereniging van Waterstaats Ingenieurs in Nederlandsch-Indië. Bandung 1938.

4. ROUSE, H.: Engineering Hydraulics. John Wiley & Sons, Inc., New York, London. 4th printing 1964.

5. TROSKOLANSKI, A.T.: Hydrometry. Theory and practice of hydraulic measurements. Pergamon Press, Oxford, London, New York, Paris. 1960.

6. U.S.DEPARTMENT OF AGRICULTURE: Field manual for research in Agricultural Hydrology. Agriculture Handbook No.224. Washington, D.C. 1962.

7. U.S.DEPARTMENT OF THE INTERIOR. Water Measurement Manual. U.S.Bureau of Reclamation. 2nd Ed. Denver, Colorado. 1967. Repr.1971.

3 The selection of structures

3.1 Introduction

In selecting a suitable structure to measure or regulate the flow rate in open channels, all demands that will be made upon the structure should be listed. For discharge measuring and regulating structures, hydraulic performance is fundamental to the selection, although other criteria such as construction cost and standardization of structures may tip the balance in favour of another device.

The hydraulic dimensions of the discharge measuring or regulating structures described in the following chapters are standardized. The material from which the device is constructed, however, can vary from wood to brick-work, concrete, polyester, metal, or any other suitable material. The selection of the material depends on such criteria as the availability and cost of local material and labour, the life-time of the structure, pre-fabrication etc. Constructional details are not given in this book except for those steel parts whose construction can influence the hydraulic performance of the structure.

Although the cost of construction and maintenance is an important criterion in the selection of structures, the ease with which a discharge can be measured or regulated is frequently more important since this will reduce the cost of operation. This factor can be of particular significance in irrigation schemes, where one ditchrider or gatesman has to control and adjust 10 to 20 or more structures daily. Here, ease of operation is labour saving and ensures a more efficient distribution of water over the irrigated area.

Although other criteria will come into play in the final selection of a discharge measuring or regulating structure, the remarks in this chapter will be limited to a selection based solely on hydraulic criteria.

3.2 Demands made upon a structure

3.2.1 Function of the structure

Broadly speaking, there are four different types of structures, each with its own particular function:

- discharge measuring structure
- discharge regulating structure
- flow divider
- flow totalizer

Discharge measuring structure

The function of such a structure is to enable the flow rate through the channel in which it is placed to be determined. If the structure is not required to fulfil any other function, such as water-level control, it will have no movable parts. Discharge measurement structures can be found in natural streams and drainage canals, and also in hydraulic laboratories or in industries where flow rates need to be measured. All flumes and fixed weirs are typical examples of discharge measurement structures.

Discharge regulating structure

These structures are frequently found in irrigation canals where, as well as having a discharge measuring function, they also serve to regulate the flow and so distribute the water over the irrigated area. Discharge regulating structures can be used when water is drawn from a reservoir or when a canal is to be split up into two or more branches. A discharge regulating structure is equipped with movable parts. If the structure is a weir, its crest will be movable in a vertical direction; if an orifice (gate) is utilized, the area of the opening will be variable. Almost all weirs and orifices can be used as discharge regulating structures. In this context it is curious to note that in many irrigation canal systems, the discharge is regulated and measured by two structures placed in line in the same canal. The first structure is usually a discharge regulating gate and, the second downstream of the first, is a discharge measuring flume. It would seem to be a waste of money to build two such structures, when one would suffice. Moreover, the use of two structures requires a larger loss of head to operate within the modular flow range than if only one is used. Another even more serious disadvantage is that setting the required discharge with two structures is a more time consuming and complicated procedure than if a single regulating structure is used. Obviously, such procedures do not contribute to the efficient management of the available water.

Flow divider

It may happen that in an irrigated area we are only interested in the percentage distribution of the incoming flow into two or more branch canals. This percentage distribution can be achieved by constructing a group of weirs all having the same crest level but with different control widths. If the percentage distribution has to vary with the flow rate in the undivided canal, the crest level of the weirs may differ or the control sections may have different shapes. Sometimes the required percentage distribution of flow over two canals has to vary while the incoming flow remains constant. This problem can be solved by using a movable partition (or divisor) board which is adjusted and locked in place above a fixed weir crest (see Section 9.1).

Although a flow divider needs no head measurement device to fulfil its function, a staff gauge placed in the undivided canal can give additional information on the flow rate, if this is required by the project management.

Flow totalizer

If we want to know the volume of water passing a particular section in a given period, we can find this by using a flow totalizer. Such information will be required, for instance, if a farmer is charged for the volume of water he diverts from the irrigation canal system, or if an industry is charged for the volume of effluent it discharges into a stream. The two flow totalizers treated in this book both have a rotating part and a revolution counter which can be fitted with an additional counter or hand to indicate the instantaneous flow rate.

3.2.2 Required fall of energy head to obtain modular flow

Flumes and weirs

The available head and the required head at the discharge measuring site influence both the type and the shape of the structure that will be selected. For weirs and flumes, the minimum required head ΔH to operate in the modular flow range can be expressed as a fraction of the upstream energy head H_1 or as $(H_1 - H_2)/H_1$. This ratio can also be written as $1 - H_2/H_1$, the last term of which describes the limit of the modular flow range, i.e., the modular limit (see also Section 1.15).

The modular limit is defined as the value of submergence ratio H_2/H_1 at which the real discharge deviates by 1% from the discharge calculated by the head-discharge equation. We can compare the required fall over weirs of equal width by considering their respective modular limits. The modular limit of weirs and flumes depends basically on the degree of streamline curvature at the control section and on the reduction of losses of kinetic energy if any, in the downstream expansion. Broad-crested weirs and long-throated flumes, which have straight and parallel streamlines at their control section and where part of the kinetic energy is recovered, can obtain a modular limit as high as $H_2/H_1 = 0.95$. As mentioned in Chapter I, the discharge coefficient of a weir increases if the streamline curvature at the control section increases. At the same time, however, a rising tailwater level tends to reduce the degree of streamline curvature, and thus reduces the discharge. Consequently we can state that the modular limit of a weir or flume will be lower as the streamlines are more strongly curved under normal operation. The extreme examples are the rectangular sharp-crested weir and the Cipoletti weir, where the tailwater level must remain at least 0.05 m below crest level, so that streamline curvature at the control section will not be affected. Modular limits are given for each structure and are summarized in Section 3.3.

The available head and the required head over a structure are determining factors for the crest elevation, width and shape of the control section, and for the shape of the downstream expansion of a discharge measurement structure. This can be shown by the following example.
Suppose a 0.457 m (1.5 ft) wide Parshall flume is to be placed in a trapezoidal concrete-lined farm ditch with 1-to-1.5 side slopes, a bottom width of 0.50 m, and its crest at ditch bottom level. In the ditch the depth-discharge relationship is controlled by its roughness, geometry, and slope.

If we use the Manning equation, $v = \frac{1}{n} R^{2/3} s^{\frac{1}{2}}$, with a value of $n = 0.014$ and $s = 0.002$, we obtain a satisfactory idea of the tailwater depth in the ditch. Tailwater depth data are shown in Figure 3.1, together with the head-discharge curve of the Parshall flume and its 70% submergence line (modular limit).

An examination of the 70% submergence curve and the stage-discharge curve shows that submerged flow will occur at all discharges below 0.325 m^3/s, when the flume crest coincides with the ditch bottom. Figure 3.1 clearly shows that if a design engineer only checks the modularity of a device at maximum stage, he may unknowingly introduce submerged flow conditions at lower stages.

The reason for this phenomenon is to be found in the depth-discharge relationships of ditch and of control section. In the given example,a measuring structure with a rectangular control section and a discharge proportional to about the 1.5 power of

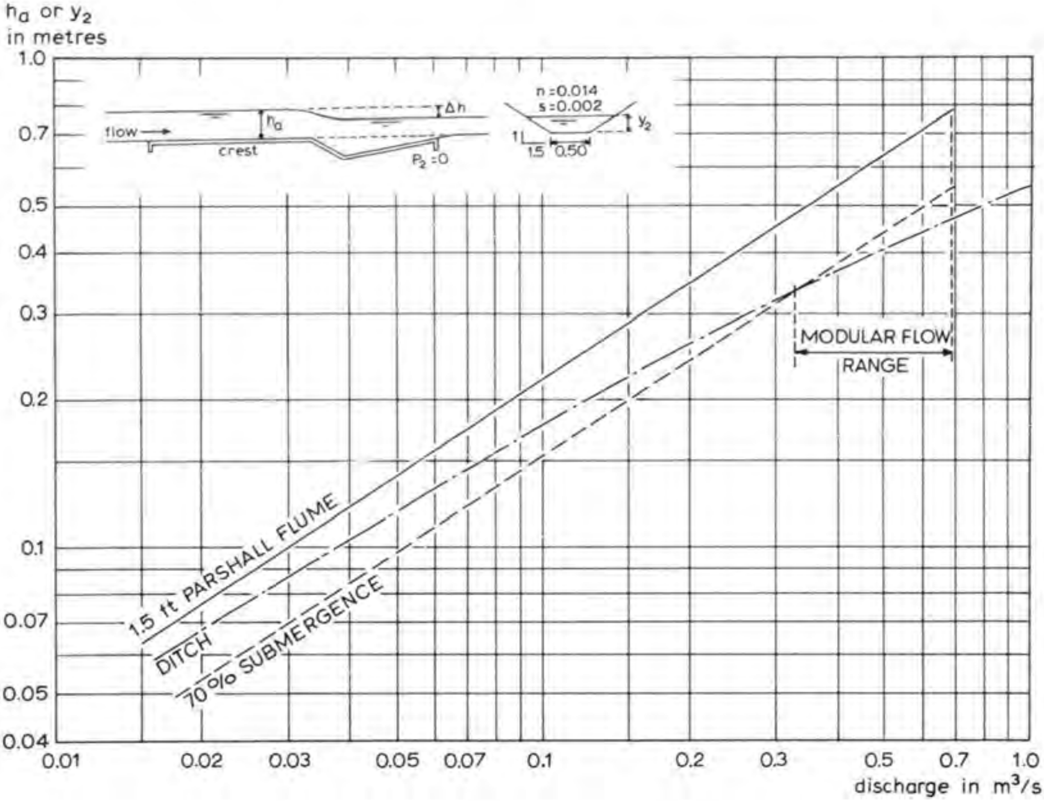

Fig.3.1. Stage-discharge curves for 1.5 ft Parshall flume and for a concrete-lined ditch. Flume crest coincides with ditch bottom.

upstream head is used in a trapezoidal channel which has a flow rate proportional to a greater power of water depth than 1.5. The average ditch discharge is proportional to $y_2^{1.8}$. On log-log paper the depth-discharge curve (ditch) has a flatter slope than the head-discharge curve of the flume (see Fig.3.1).

To avoid submerged flow conditions, the percentage submergence line of the measuring device in this log-log presentation must be to the left of the channel discharge curve throughout the anticipated range of discharges. The coefficient of roughness, n, will depend on the nature of the surface of the downstream channel. For conservative design the roughness coefficient should be maximized when evaluating tailwater depths.

Various steps can be taken to avoid submergence of a discharge measuring device. These are:

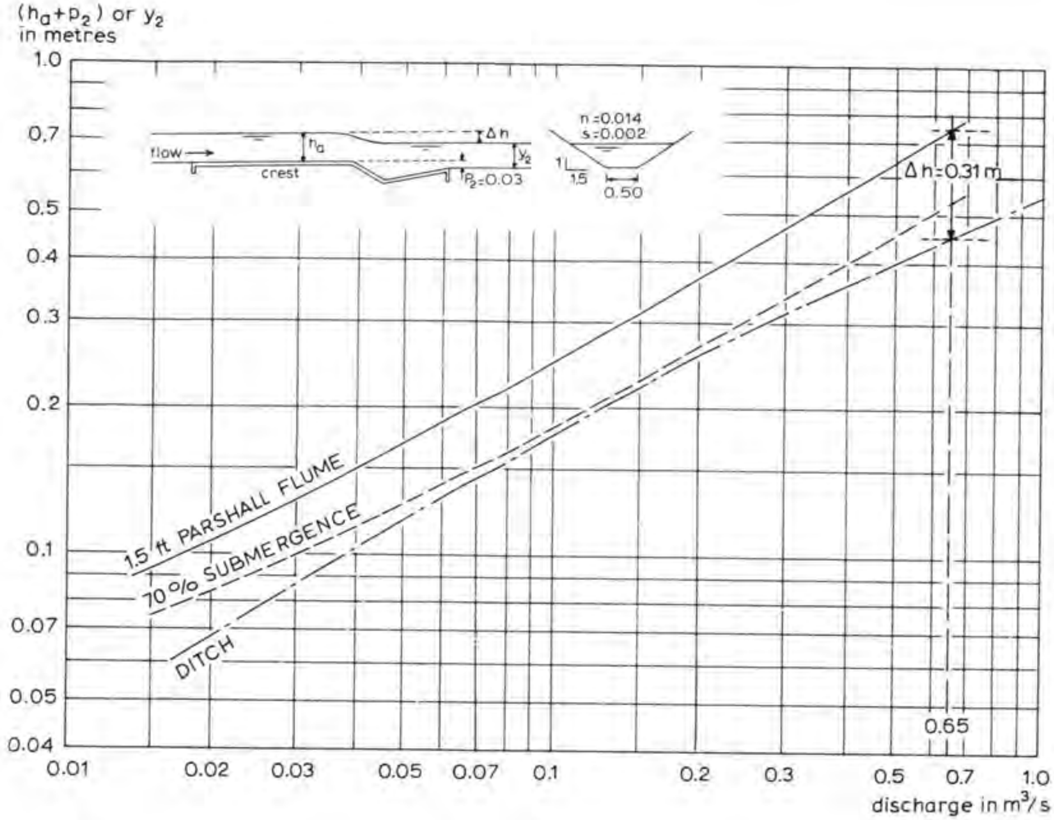

Fig.3.2. Stage-discharge curves for flume and ditch of Figure 3.1, but flume crest 0.03 m above ditch bottom.

The 1.5 ft Parshall flume of Figure 3.1 can be raised 0.03 m above ditch bottom. The stage-discharge curve of the flume in terms of h_a + 0.03 m plots as a curve shown in Figure 3.2. The corresponding 70% submergence curve plots to the left of the stage- discharge curve of the ditch.

The 1.5 ft Parshall flume of Figure 3.1 can be replaced either by a flume which requires more head for the same discharge, thus with a rating curve that plots more to the left on log-log paper, or by a flume which has a higher modular limit than 70%. A flat-bottom long-throated flume with 0.45 m wide control and 1 to 6 downstream expansion will be suitable.

It must be recognized that the two previous solutions require a loss of head of at least 0.31 m at the maximum discharge capacity of the flume, being $Q = 0.65$ m^3/s (see Figure 3.2). If this head loss exceeds the available head, the design engineer must select a structure with a discharge proportional to an equal or greater power of head than the power of the depth y_2 of the ditch. For example, he may select a flat-bottom, long-throated flume with a trapezoidal control section and a gradual downstream expansion. Such a flume can be designed in such a way that at $Q = 0.65\ m^3/s$ an upstream head $h_1 = 0.53$ m and a modular limit of about 0.85 occur resulting in a required head loss of only 0.08 m. He could also use a flume with a (truncated) triangular, parabolic, or semi-circular control section.

Orifices

At the upstream side of free flowing orifices or undershot gates, the upper edge of the opening must be submerged to a depth which is at least equal to the height of the opening. At the downstream side the water level should be sufficiently low so as not to submerge the jet (see Chapter 8). For this reason free flowing orifices, especially at low flows, require high head losses and are less commonly used than submerged orifices. The accuracy of a discharge measurement obtained with a submerged orifice depends on the accuracy with which the differential head over the orifice can be measured. Depending on the method by which this is done and the required accuracy of the discharge measurement, a minimum fall can be calculated with the aid of Appendix II. In general, we do not recommend the use of differential heads of less than 0.10 m.

3.2.3 Range of discharges to be measured

The flow rate in an open channel tends to vary with time. The range between Q_{min} and Q_{max} through which the flow should be measured strongly depends on the nature of the channel in which the structure is placed. Irrigation canals, for example, have a considerably narrower range of discharges than do natural streams. The anticipated range of discharges to be measured may be classified by the ratio

$$\gamma = Q_{max}/Q_{min} \tag{3-1}$$

From the limits of application of several weirs, a maximum attainable γ-value can be calculated. Taking the example of the round-nosed horizontal broad-crested weir (Section 4.1), the limits of application indicate that H_1/L can range between 0.05 and 0.50 m. As a result we obtain a maximum value of γ which is

$$\gamma = \frac{Q_{max}}{Q_{min}} = \frac{C_d max}{C_d min} \frac{(0.50)^{1.5}}{(0.05)^{1.5}} \simeq 35 \tag{3-2}$$

This illustrates that whenever the ratio $\gamma = Q_{max}/Q_{min}$ exceeds about 35 the round-nosed horizontal broad-crested weir described in Section 4.1 cannot be used. Weirs or flumes that utilize a larger range of head, or which have a head-discharge relationship proportional to a power of head greater than 1.5, or both, can be used in channels where $\gamma = Q_{max}/Q_{min}$ exceeds 35. The following example shows how the γ-value, in combination with the available upstream channel water depth y_1, influences the choice of a control section. The process of selection is as follows:

Find a suitable flume and weir for

$$Q_{min} = 0.015\ m^3/s$$

$$Q_{max} = 3.00\ m^3/s \rightarrow \gamma = 200$$

$$y_1 = h_1 + p \leqslant 0.80\ m$$

The flume is to be placed in an existing trapezoidal channel with a 4-m wide bottom and 1-to-2 side slopes. At maximum water depth $y_1 = 0.80$ m, the Froude number in the approach channel is $Fr = v_1/(gA_1/B_1)^{\frac{1}{2}} = 0.27$. For $Fr < 0.50$ the water surface will be sufficiently stable.

From the relatively high γ-value of 200 we can conclude that the control section of the structure should be narrower at minimum stage than at maximum stage. Meeting the requirements of this example are control sections with a narrow bottomed trapezium, or a triangular or truncated triangular shape. Because of the limited available width we select a truncated triangular control section of which two solutions are illustrated below.

Triangular profile flat-V weir (Fig.3.3)

According to Section 6.4.2 the basic head-discharge equation of this weir reads

$$Q = C_d C_v \frac{4}{15} (2g)^{0.5} \frac{B}{H_b} \left[h_e^{2.5} - (h_e - H_b)^{2.5} \right] \qquad (3\text{-}3)$$

in which the term $(h_e - H_b)^{2.5}$ should be deleted if h_e is less than H_b. If we use the 1-to-2/1-to-5 weir profile and a 1-to-10 cross slope, the minimum channel discharge can be measured at the minimum required head, since Q at 0.06 m head is

$$Q_{0.06} = 0.66 \times 1 \times \frac{4}{15} (2g)^{0.5} \times \frac{10}{2} (0.06 - 0.0008)^{2.5}$$

$$Q_{0.06} = 0.0133 \text{ m}^3/\text{s}$$

Another restriction for the application of this type is the ratio h_1/p, which should not exceed 3.0. The required width of the weir can be found by trial and error:

Since $y_1 = h_1 + p \leqslant 0.80$ m, the maximum head over the weir crest $h_1 max = 0.60$ m when $p = 0.20$ m. Using a width B of 4 m, we find for the discharge capacity at $h_1 = 0.60$ m (for C_v see Fig.6.10):

$$Q_{0.60} = 0.66 \times 1.155 \times \frac{4}{15} (2g)^{\frac{1}{2}} \times \frac{4.00}{0.20} \times$$

$$\times \left[(0.60 - 0.0008)^{5/2} - (0.60 - 0.0008 - 0.20)^{5/2}\right]$$

$$Q_{0.60} = 3.205 \text{ m}^3/\text{s}$$

This shows that the full discharge range can be measured with the selected weir.

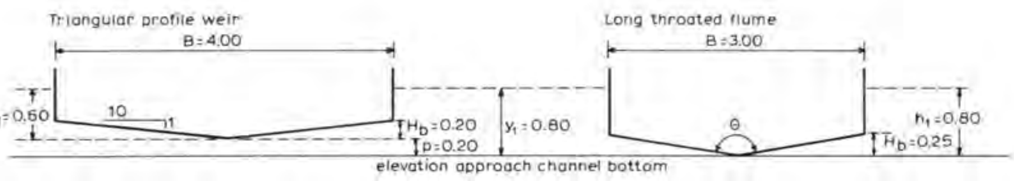

Fig.3.3. Two examples of suitable control sections.

Long-throated flume with truncated triangular control (see Fig.3.3)

According to Section 7.1.2, the head-discharge relationships for this flume read

$$Q = C_d C_v \frac{16}{25}\left[\frac{2}{5} g\right]^{\frac{1}{2}} \tan\theta/2 \; h_1^{5/2} \qquad (3\text{-}4)$$

for $H_1 \leqslant 1.25 H_b$, and

$$Q = C_d C_v \frac{2}{3}\left[\frac{2}{3} g\right]^{\frac{1}{2}} B(h_1 - \tfrac{1}{2} H_b)^{3/2} \qquad (3\text{-}5)$$

if $H_1 \geqslant 1.25 H_b$.

Using a flat-bottomed flume with a throat length of L = 0.80 m ($H_1/L \leqslant 1$), we can select a suitable control section. After some experience has been acquired two trials will usually be sufficient to find a control section which will pass the maximum discharge. For the section shown in Figure 3.3 the C_d- and C_v-values can be found as follows:

For $h_1 = 0.80$ m, $H_1/L \approx 1$, Figure 7.3 shows that $C_d = 1.0$

The area ratio

$$C_d \frac{A^*}{A_1} = \frac{0.25 \times 1.5 + 0.55 \times 3.0}{0.80 \times 5.60} = 0.45$$

and we find in Figure 1.12 that the related C_v-value is about 1.06 ($1.5 < u < 2.0$). Substitution of these values into Equation 3-5 yields a discharge capacity at $h_1 = 0.80$ m equal to

$$Q_{0.80} = 1.0 \times 1.06 \times \frac{2}{3} (\frac{2}{3}\, 9.81)^{\frac{1}{2}} \times 3(0.80 - 0.125)^{3/2}$$

$$Q_{0.80} = 3.01 \text{ m}^3/\text{s}$$

At minimum applicable head of $h_1 = 0.1\ L = 0.08$ m (see Section 7.1.4) $C_d = 0.88$ and $C_v \approx 1.0$.

Using Equation 3-4 we find that at $h_1 = 0.08$ m the discharge capacity is

$$Q_{0.08} = 0.88 \times 1.0 \times \frac{16}{25} (\frac{2}{5}\, 9.81)^{\frac{1}{2}} \frac{1.50}{0.25} \times 0.08^{\ 5/2}$$

$$Q_{0.08} = 0.0121 \text{ m}^3/\text{s}$$

This shows that both minimum and maximum discharges can be measured with the selected structure. These structures are only two of the many which meet the demands set on the discharge range and upstream water depth.

3.2.4 Sensitivity

The accuracy to which a discharge can be measured will depend not only on the errors in the C_d- and C_v-values but also on the variation of the discharge because of a unit change of upstream head. Hence, on the power u of h_1 in the head-discharge equation.

In various countries, the accuracy of discharge measuring structure is expressed in the sensitivity, S, of the structure. This is defined as the fractional change of discharge of the structure that is caused by the unit rise, usually $\Delta h_1 = 0.01$ m, of the upstream water level. For modular flow

$$S = \frac{\Delta Q}{Q} = \frac{(dQ/dh_1)\Delta h_1}{Q} \qquad (3\text{-}6)$$

Using the relationship

$$Q = \text{Constant} \times h_1^u \tag{3-7}$$

we can also write Equation 3-6 as

$$S = \frac{\text{Const} \times u h_1^{u-1}\ \Delta h_1}{\text{Const} \times h_1^u} \tag{3-8}$$

$$S = \frac{u}{h_1}\ \Delta h_1 \tag{3-9}$$

The value of Δh_1 can refer to a change in waterlevel, head reading error, mis-location of gauging station, etc.
In Figure 3.4 values of $S \times 100$ in per cent are shown as a function of $\Delta h_1/h_1$ and the u-value, the latter being indicative of the shape of the control section.

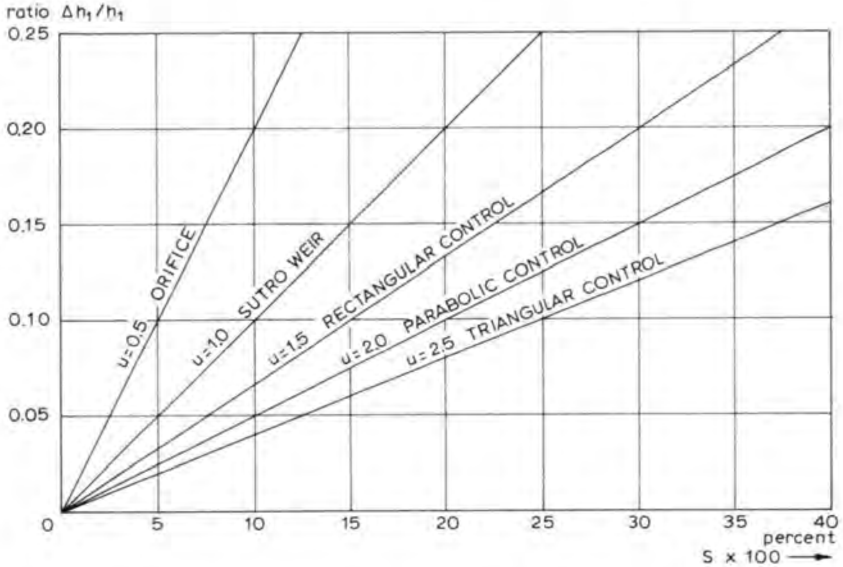

Fig.3.4. Sensitivity as a function of relative change in head and shape of control section (modular flow).

Presented as an example is a 90-degree V-notch sharp-crested weir which discharges at $h_1 = 0.05$ m. If the change in head (error) $\Delta h_1 = 0.005$ m, we find

$$S \times 100 = 100\ \frac{2.5}{0.05}\ 0.005 = 25\%$$

This shows that especially at high u-values and low heads the utmost care must be taken to obtain accurate h_1 values if an accurate discharge measurement is required.

In irrigated areas, where fluctuations of the head in the conveyance canals or errors in head reading are common and the discharge through a turn-out structure has to be near constant, a structure having a low sensitivity should be selected.

3.2.5 Flexibility

Because of a changing flow rate, the head upstream of an (irrigation) canal bifurcation usually changes. Depending on the characteristics of the structures in the supply canal and that in the off-take canal, the relative distribution of water may change because of the changing head. To describe this relative change of distribution the term flexibility is used, which has been defined as the ratio of the rate of change of discharge of the off-take or outlet Q_o to the rate of change of discharge of the continuing supply canal Q_s or:

$$F = \frac{dQ_o/Q_o}{dQ_s/Q_s} \tag{3-10}$$

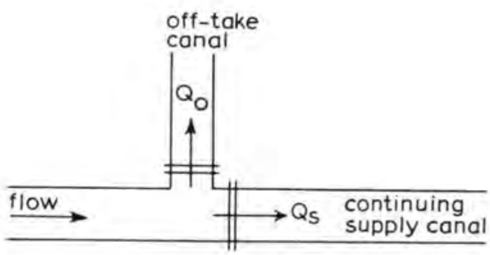

Fig. 3.5. Definition sketch.

In general the discharge of a structure or channel can be expressed by the Equation

$$Q = \text{Const } h_1^u \tag{3-11}$$

Hence we can write

$$dQ/dh_1 = \text{Const } uh_1^{u-1} \tag{3-12}$$

Division by Q and by Const h_1^u gives

$$dQ/Q = u\ dh_1/h_1 \tag{3-13}$$

Substitution of Equation 3-13 into Equation 3-10 for both Q_s and Q_o results in

$$F = \frac{u_o}{u_s}\frac{dh_{1,o}}{dh_{1,s}}\frac{h_{1,s}}{h_{1,o}} \tag{3-14}$$

Since a change in water level in the upstream reach of the supply canal causes an exactly equal change in $h_{1,o}$ and $h_{1,s}$, the quotient $dh_{1,o}/dh_{1,s} = 1$, and thus

$$F = \frac{u_o h_{1,s}}{u_s h_{1,o}} \tag{3-15}$$

The proportional distribution of water over two or more canals may be classified according to the flexibility as follows:

a) $F = 1$

For $F = 1$ we may write

$$\frac{u_o}{u_s} = \frac{h_{1,o}}{h_{1,s}} \tag{3-16}$$

To meet this requirement for various heads, the structures on the off-take and supply canal must be of the same type and their crest or sills must be at the same level.

b) $F < 1$

If less variation is allowed in the off-take discharge than in the supply canal discharge, the flexibility of the bifurcation has to be less than unity and is said to be sub-proportional.

The easiest way to obtain $F < 1$ is to select two different types of structures, for example:

an orifice as off-take; $u = 0.5$

a weir with rectangular (or other) control in the supply canal: $u = 1.5$ (or more).

We now find that

$$F = \frac{0.5}{1.5} \frac{h_{1,s}}{h_{1,o}}$$

Usually $h_{1,s}$ is less than 3 $h_{1,o}$, and then the flexibility of the bifurcation will be less than unity.
$F < 1$ can be an advantage in irrigation projects where, during the growing season, canal water level rises due to silting and weed growth. A low flexibility here helps to avoid a water shortage at the downstream end of the supply canal.

c) $F > 1$

If more variation is allowed in the off-take discharge than in the supply canal discharge, the flexibility of the bifurcation has to be greater than unity and is said to be hyper-proportional. Here again, the easiest way this can be obtained is by using two different types of structures. Now, however, the structure with low u-value (orifice) is placed in the supply canal while the off-take has a weir with a u-value of 1.5 or more. Thus

$$F = \frac{1.5}{0.5} \frac{h_{1,s}}{h_{1,o}}$$

Since in this case $h_{1,s}$ is always greater than $h_{1,o}$, the flexibility of the bifurcation will be much more than unity. This is especially useful, for example, if the off-take canal leads to a surface drain which can be used to evacuate excess water from the supply canal system.

3.2.6 Sediment discharge capability

Besides transporting water, almost all open channels will transport sediments. The transport of sediments is often classified according to the transport mechanism or to the origin of the sediments, as follows

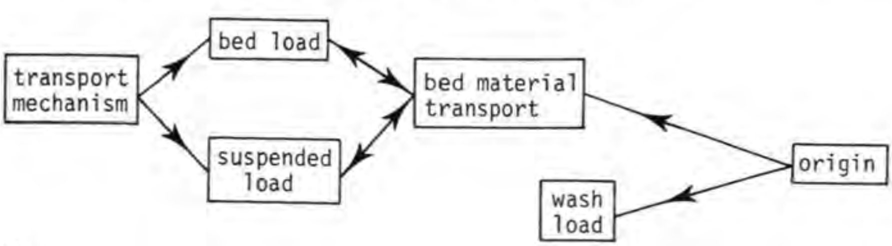

The expressions used in this diagram are defined as follows:

Bed-load

Bed-load is the transport of sediment particles sliding, rolling, or jumping over and near the channel-bed, generally in the form of moving bed forms such as dunes and ripples. Many formulae have been developed to describe the mechanism of the bed-load, some being completely based upon experiment, while others are founded upon a model of the transport mechanism. Most of these equations, however, have in common that they contain a number of "constants" which have to be modified according to the field data collected for a certain river. In fact, all the deviations in bed-load from the theoretical results are counteracted by selecting the right "constants".

Most of the available bed-load functions can be written as a relation between the transport parameter

$$X = T/\sqrt{\Delta g D^3}$$

and the flow parameter

$$Y = \mu y s/\Delta D$$

where

- T = transport in solid volume per unit width (sometimes expressed in terms of the transport including voids, S, according to $T = S(1 - \varepsilon)$, where ε is the porosity
- y = depth of flow (often y is replaced by the hydraulic radius R)
- D = grain diameter
- Δ = relative density = $(\rho_s - \rho)/\rho$
- s = hydraulic gradient
- μ = so-called ripple factor, in reality a factor of ignorance, used to obtain agreement between measured and computed values of T.

As an example of such an X versus Y relation the well known MEYER-PETER/MÜLLER bed-load function may be given;

$$X = A(Y - 0.047)^{3/2} \qquad (3\text{-}17)$$

with $A = 8$.

Typical bed-load equations like the Meyer-Peter/Müller equation do not include suspended-load. Equation (3-17) differs from the total-load equation given below, although the construction of both equations will appear to be similar.

Suspended-load

Suspended-load is the transport of bed particles when the gravity force is counterbalanced by upward forces due to the turbulence of the flowing water. This means that the particles make larger or smaller jumps, but return eventually to the river-bed. By that time, however, other particles from the bed will be in suspension and, consequently, the concentration of particles transported as suspended-load does not change rapidly in the various layers.

A strict division between bed-load and suspended-load is not possible; in fact, the mechanisms are related. It is therefore not surprising that the so-called total-load (bed-load and suspended-load together) equations have a similar construction to that of the bed-load equations.

An example of a total-load equation is the equation of ENGELUND and HANSEN (1967), which reads

$$X = 0.05\ Y^{5/2} \tag{3-18}$$

in the flow parameter Y;

$$\mu = \left[\frac{C^2}{g}\right]^{2/5}$$

C = roughness coefficient of Chézy

$D = D_{50}$

Wash-load

Wash-load is the transport of small particles finer (generally < 50 μm) than the bulk of the bed material and rarely found in the bed. Transport quantities found from bed-load, suspended-load, and total-load formulae do not include wash-load quantities.

Whereas for a certain cross-section quantities of suspended-load and bed-load can be calculated with the use of the locally valid hydraulic conditions, this is not the case for wash-load. The rate of wash-load is mainly determined by climatological characteristics and the erosion features of the whole catchment area.

Since there is normally no interchange with bed particles, wash-load is not important for local scour or silting. Owing to the very low fall velocity of the wash-load particles, wash-load only contributes to sedimentation in areas with low current velocities (reservoirs, dead river branches, on the fields). Owing to the small fall velocity, in turbulent water the concentration of the particles over a vertical (generally expressed in parts per million, p.p.m.) is rather uniform, so that even with one water sample a fairly good impression can be obtained. However, the wash-load concentration over the width of a channel may vary considerably.

The most appropriate method of avoiding sediment deposition in the channel reach upstream from a structure is to avoid a change of the flow parameter $Y = \mu Rs/\Delta D$. This can be done, for example, by avoiding a backwater effect in the channel. To do so, a structure should be selected whose head-discharge curve coincides with the stage-discharge curve of the upstream channel at uniform flow.

Since the u-value of most (trapezoidal) channels varies between $u \simeq 2.2$ for narrow bottomed channels and $u \simeq 1.7$ for wide channels, the most appropriate structures are those with a trapezoidal, parabolic, semicircular, or (truncated) triangular control section.
To avoid the accumulation of sediments between the head measurement station and the control section, a structure that has either a flat bottom or a low bottom hump with sloping upstream apron is recommended. Flat bottomed long-throated flumes, which can be tailored to fit the channel stage-discharge curve, are very suitable.
Many well-designed irrigation canal systems are equipped with a sand trap situated immediately downstream of the head works or diversion dam. The diversion dam will usually be dimensioned in such a way that a minimal volume of sediments is diverted from the river. Other systems draw their water from reservoirs or wells. As a result most irrigation canals do not have bed-load transport but will have a certain amount of suspended-load and wash-load. Because of the flow regulating function of the structure, the deposition of silt immediately upstream of it can-

Photo 1. Most weirs can be fitted with a movable gate.

not always be avoided even if uniform flow is maintained upstream of the head measurement station.

If an adjustable orifice is used as a discharge regulating structure, it is recommended that a bottom sill be avoided. If a movable weir is used, it should be fitted with a movable bottom gate that can be lifted to wash out sediments. This gate arrangement is described in Section 4.2. Its use is not restricted solely to the Romijn weir; it can be used in combination with all weirs described in Chapters 4, 5, and 6.

3.2.7 Passing of floating and suspended debris

All open channels, and especially those which pass through forested or populated areas, transport all kinds of floating and suspended debris. If this debris is trapped by the discharge measuring structure, the approach channel and control section become clogged and the structure ceases to act as a discharge measuring device.

In irrigation canals it may be practical to install a trash rack at strategic points to alleviate the problem of frequently clogged structures. This applies especially if narrow openings, V-notches, or orifices are used. In drainage channels, however, because of their larger dimensions, the installation of trash-racks would not be practical. For drainage canals therefore one should select structures that are not vulnerable to clogging. All sharp-crested weirs and orifices are easily clogged and are thus not recommended if floating debris has to be passed. Weirs with a sloping upstream face or weirs with a rounded nose or crest and all flumes will pass debris relatively easily. Piers which have no rounded nose or are less than 0.30 m wide, which thus includes sharp-edged movable partition boards, tend to trap the bulkier debris.

3.2.8 Undesirable change in discharge

Structures may be damaged through vandalism or by persons who stand to benefit from a faulty or non-operating structure. To prevent such damage, the design engineer should keep structures as simple as possible and any movable parts should be as sturdy as is economically justified. It may also happen that attempts will be made to alter the discharge of a structure by changing the hydraulic conditions under which the structure should operate.

Particularly vulnerable to damage are the sharp-crested weir and sharp-edged orifices. It is possible to increase the discharge of these structures by rounding (i.e.damaging) the sharp edge, roughening the upstream face, or by blocking the aeration vent to the air pocket beneath a fully contracted nappe. Because of this and also because of their vulnerability to clogging, sharp-crested weirs and sharp-edged orifices are only recommended for use in laboratories or in pilot schemes or at other places where frequent inspection of the structures is common.

It is obvious that the discharge of structures which operate under submerged flow can easily be influenced by altering the water level in the tailwater channel. It is therefore recommended that modular structures be used wherever off-takes, outlets, or turn-outs are required.

Lack of maintenance will usually cause algal growth to occur on a structure. On a sharp-crested weir, algal growth will lead to a roughening of the upstream weir face and a rounding of the sharp edge. Both phenomena cause the contraction to decrease and thus lead to an increase in the weir discharge at constant head.

On a broad-crested weir algal growth causes a roughening of the weir crest and a rise in its height. This phenomenon, however, causes the weir discharge to decrease at constant head.

The least influenced by algal growth is the short-crested weir. Its discharge will scarcely be affected because of the strong influence of streamline curvature on the discharge coefficient relative to the influence of a change of roughness of the weir crest. In selecting a discharge measuring or regulating structure and organizing its maintenance, this phenomena should be taken into account.

3.2.9 Minimum water level in upstream channel

Several discharge measurement structures have as a second function,which is to retain water in the upstream channel reach, especially at low flows. In flat areas in moderate climates, structures in drainage channels can be used to maintain a minimum water level in the channels during the dry season, thus controlling the groundwater level in the area. To perform this function, the weir crest elevation must be above the upstream channel bottom. If the variation between required minimum and required maximum water levels in the channel is small and the discharge varies considerably, a movable weir may be the only possible solution.

On the other hand, in hot climates it may be desirable to design discharge measurement structures so that the channels in which they are placed will go dry if no flow occurs. This may be a necessary precaution to prevent the spread of serious diseases like malaria and bilharzia. It may also be convenient to have irrigation canals go dry by gravity flow so that maintenance work can be performed. This will require that all structures in supply canals and drainage channels have zero crest elevation. If a raised weir crest is needed during other periods, a movable weir will provide the answer.

3.2.10 Required accuracy of measurement

In the head-discharge equation of each structure there is a discharge coefficient and an approach velocity coefficient, or a combination of these coefficients. The accuracy with which a discharge can be measured with a particular structure depends to a great extent on the variation of these coefficients determined under similar hydraulic conditions.

For all of the structures described, an expected error in the product C_dC_v or in the combined coefficient is given in the relevant section on the evaluation of discharge. These errors are also listed in Section 3.3. Often, the error in C_dC_v is not constant but decreases if the C_d-value increases, which usually occurs if the head over a crest increases.

Besides the error in the coefficients, the most important error in a discharge measurement is the error inherent to the determination of a head or head differential.

The error in head mainly depends on the method and accuracy of zero setting and the method used to measure the head. It can be expressed in a unit of length independently of the value of head to be measured. As a result enormous errors often occur in a discharge measurement if the structure operates under minimal applicable head or head differential (see also Sensitivity, Section 3.2.5).

3.2.11 Standardization of structures in an area

It may happen that in a certain area, several structures will be considered suitable for use, each being able to meet all the demands made of discharge measuring or regulating structures. It may also happen that one of these suitable structures is already in common use in the area. If so, we would recommend the continued use of the familiar device, especially if one person or one organization is charged with the operation and maintenance of the structures. Standardization of structures is a great advantage, particularly for the many small structures in an irrigation canal system.

3.3 Properties and limits of application of structures

3.3.1 General

In Section 3.2 the most common demands made of discharge measuring or regulating structures are described. In Chapters 4 to 9, the properties and limits of application of each separate structure are given in the sections entitled Description and Limits of application. To aid the design engineer in selecting a suitable structure, we have tabulated the most relevant data.

3.3.2 Tabulation of data

Table 3.1 consists of 18 columns giving data on the following subjects:

Column 1: Name of the standard discharge measuring or regulating device. In brackets is the section number in which the device is discussed. Each section generally consists of sub-sections entitled: Description, Evaluation of discharge, Modular limit, Limits of application.

Column 2: A three-dimensional sketch of the structure.

Column 3: Shape of the control section perpendicular to the direction of flow and the related power u to which the head or differential head appears in the head-discharge equation.

Column 4: Possible function of the structure. If the area of the control section cannot be changed, the structure can only be used to measure discharges; this is indicated by the letter M in the column. If the weir crest can be made movable by use of a gate arrangement as shown in Section 4.2, or if the area of an orifice is variable, the structure can be used to measure and regulate discharges and has the letters MR in the column. The Dethridge and propeller meters can measure a flow rate in m^3/s and totalize the volume in m^3. The discharge can be regulated by a separate gate, which is, however, incorporated in the standard design. These two devices have the letters MRV in the column.

TABLE 3.1. DATA ON VARIOUS STRUCTURES

1	2	3	4	5	6	7	8	9
Name of structure and section number in which structure is described	Sketch of structure	Shape of control section perpendicular to flow and u-value	M = measuring MR = measuring & regulating	H_1 min or Δh min	H_1 max or Δh max	minimum crest height above approach channel bottom p	minimum size of control b or B, w and D_p	range of notch angle θ degrees
Round-nose horizontal broad-crested weir (4.1)	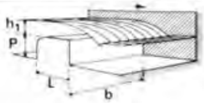	rectangular u = 1.5	MR	0.06 m 0.05 L	0.5 L	0.15 m 0.33 H_1	0.30 m H_1 max 0.2 L	–
Romijn movable measuring/ regulating weir (4.2)		rectangular u = 1.5	MR	0.05 m 0.12 L	0.78 L	0.15 m 0.33 H_1	0.30 m H_1 max	–
Triangular broad-crested weir (4.3)		(truncated) triangular u=1.7 to 2.5	MR	0.06 m 0.05 L	0.5 L to 0.7 L	0.15 m 0.33 H_1	0.30 m H_1 max 0.2 L	30 to 180
Broad-crested rectangular profile weir (4.4)		rectangular u = 1.5	MR	0.06 m 0.08 L	0.85 L* → 1.50 L →	0.15 m if 0.4 h_1 if 0.65 h_1	0.30 m h_1 max 0.2 L	–
Faiyum weir (4.5)		rectangular u = 1.6	M	0.06 m 0.08 L	1.6 L	0.15 m	0.05 m $3h_1/A_1$	–
Rectangular sharp-crested weirs (5.1)		rectangular u = 1.5	M → or MR →	0.07 m 0.03 m	0.60 m 0.5 b 2.4 p	0.30 m 2 h_1 0.10 m 0.5 h_1	0.30 m B-b>4 h_1 0.15 m	–
V-notch sharp-crested weirs (5.2)		triangular u = 2.5	M M	0.05 m 0.05 m	0.60 m 1.2 p 0.38 m 0.4 p	0.10 m 0.45 m	$B_1 \geq 2.5\ h_1$ $B_1 \geq 5.0\ h_1$	90 25 to 100
Cipoletti weir (5.3)		trapezoidal u = 1.5	MR	0.06 m	0.60 m	0.30 m 2 h_1	b≥0.30 m 0.5 h_1	–
Circular weir (5.4)		circular u is variable but ≤ 2.0	M	0.03 m 0.1 d	0.9 d	0.10 m 0.5 d	d≥0.20 m	–
Proportional weir (5.5)		proportional u = 1.0	M	0.03 m 2 a	such that x≤0.005 m	p = 0 or p≥0.15 m	0.15 m	–
Weir sill with rectangular control section (6.1)		rectangular u = 1.5	M	0.09 m 0.75 L	0.90 m 0.5 b	0	0.30 m b≥1.25 b_1	–
V-notch weir sill (6.2)		triangular u = 2.5	M	h_1=0.03m	h_1=1.83 m	0.15 m	–	126°52'* 143°08' 157°22'
Triangular profile two-dimensional weir (6.3)		rectangular u = 1.5	M	0.03 m* steel 0.06 m concrete	3.00 m 3.0 p	0.06 m 0.33 H_1	0.30 m 2 H_1	–

10 Q_{min} m^3/s	11 Q_{max} in m^3/s or q max in m^2/s	12 $\gamma = \frac{Q_{max}}{Q_{min}}$	13 modular limit H_2/H_1 or head loss	14 error in C_dC_v or C_e (%)	15 sensitiveness at minimum head % per 0.01 m	16 debris passing capacity	17 sediment passing capacity	18 Remarks
						+ + very good; + good; □ fair; - poor; - - very poor		
0.0066 b = 0.30 m	q = 4.7 H_1=2.0 m	35	0.70 to* 0.95	2(21-20 C_d)	25	+	□	* value depends on slope backface and on ratio p_2/H_2
0.0057* b=0.30 m	Q=0.860* b=1.50 m	30	0.30	3	30	+	+	* values refer to standard weir with L = 0.60 m
0.0026 at θ=30°	variable	830*	0.80 to 0.95	2(21-20 C_d)	42	+ to □ depending on θ	□	* triangular control 0.05 L≤H_1≤0.7 L
0.0064	q=5.07 H_1=2.0 m	35* 81	0.66 to 0.38	10F-8 1≤F≤1.24	25	□	□	* depending on weir height p
0.0011	q=5.1 H_1=2.0 m	90	0.66*	5	25	□	-	*usually lower
0.00997	q=0.813	24.5 if b≥1.2 m	head loss= H_1 +0.05 m	1	25	- -	- -	Fully contracted weir
0.00137	variable	about 30	head loss= H_1 +0.05 m	1	25	–	- -	Full width & partially contracted weirs
0.0008 about	Q=0.390 about	about 500	head loss ≥ H_1	2	50	- -	- -	partially contracted
0.0002 if θ=28°4'	Q=0.145 if θ=100°	about 150	head loss ≥ H_1	1	50	- -	- -	fully contracted
Q=0.0082 b=0.30 m	q=0.864	36.4	head loss H_1+0.05 m	5	25	- -	- -	
0.00091 d=0.20 m	variable	55.9 if d≥0.30 m	head loss H_1+0.05 m	2	67	- -	- -	
0.0058 a=0.006 m b=0.15 m	variable	small, but depends on a-value	head loss H_1+0.05 m	2	33	- -	- - good if p = 0	a ≥ 0.005 m
0.013 b=0.30 m	q=1.366	32	0.20	5	17	+	+	
0.0005 0.0007 0.0010	Q=25.4** Q=30.6 Q=49.4	50000* 43000 49000	0.30	3	83	□	-	*three notch angles only **depending on A_1-values
0.0031 h_1=0.03m 0.0088 b=0.30 m h_1=0.06m	q=10,18	1000* or 350	0.75	10 C_v-9	50 or 25	+ +	+	* depends on crest material. Applies to 1-to-5 back face

TABLE 3.1. DATA ON VARIOUS STRUCTURES (cont.)

1	2	3	4	5	6	7	8	9
Name of structure and section number in which structure is described	Sketch of structure	Shape of control section perpendicular to flow and u-value	M = measuring MR = measuring & regulating	H_1 min or Δh min	H_1 max or Δh max	minimum crest height above approach channel bottom p	minimum size of control b or B, w and D_p	range of notch angle θ degrees
Triangular profile flat-vee weir (6.4)		(truncated) triangular u = 1.7 to 2.5	M	0.03 m steel 0.06 m concrete	3.00 m 3.0 p	0.06 m 0.33 H_1	0.30 m 2 H_1	168°34' 174°16'
Butcher's movable standing wave weir (6.5)		rectangular u = 1.6	MR	0.05 m	1.00 m	1.4 $h_1$max	0.30 m 2 h_1	–
WES-Standard spillway (6.6)		rectangular u = 1.5	M	0.06 m	depends* on h_d 5.0 p	0.15 m 0.2 h_1	0.30 m 2 H_1	–
Cylindrical crested weir (6.7)	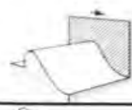	rectangular u = 1.5	MR	0.06 m 0.1 r	depends* on r 3.0 p	0.15 m 0.33 h_1	0.30 m 2 H_1	–
Long-throated flumes (5 basic shapes) (7.1)	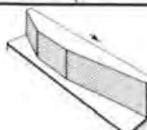	rectangular u = 1.5	M	0.06 m 0.1 L for all flumes	1.0 L 1.0 B for all flumes *Note: in general $H_1 \leq 3.0$ m*	0 but Fr≤0.5 for all flumes	0.30 m*	–
		(truncated) triangular u=1.7 to 2.5	M				B≥0.10 m*	30 to 180
		trapezoidal u=1.6 to 2.4	M				B≥0.30 m*	side slope variable**
		parabolic u = 2.0	M				f ≥0.10 m*	–
		(semi)-circular u is variable but ≤ 2.0	M				d ≥ 0.20 m*	–
Throatless flumes with rounded transition (7.2)		rectangular u = 1.5	M	0.06 m	2.00 m 1.5 R	0	0.20 m H_1 max	–
Throatless flumes with broken plane transition (7.3)		rectangular u = 1.5	M	0.06 m	1.80 m	0	0.305 m only	–
Parshall flumes (22 types) (7.4)		rectangular u = 1.55	M	0.015 m and 0.03 m	0.21 m to 0.33 m	0 level floor	0.0254 m to 0.0762 m	–
		u = 1.522 to u = 1.607	M	0.03 m, 0.045 m, and 0.076 m	0.45 m to 0.76 m		0.1524 m to 2.438 m	–
		u = 1.60	M	0.09 m	1.07 m to 1.83 m		3.048 m to 15.24 m	–
H-flumes (3 types) (7.5)		sloping trapezium u = 2.0 to 2.4	M	0.01 m to 0.04 m	0.11 m to 0.30 m	0	see Figure 7.21	–
				0.01 m to 0.03 m	0.14 m to 1.36 m			
				0.03 m	1.06 m and 1.21 m			
Circular sharp-edged orifice (8.1)		circular u = 0.5	M	Δh≥0.03 m h_1 ≥ d	–	0.5 d	A ≤ 10 A_1 d ≥ 0.02 m	–
Rectangular sharp-edged orifice (8.2)	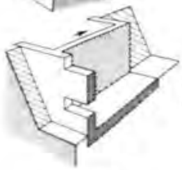	rectangular u = 0.5	M but MR if suppressed	Δh≥0.03 m y_1≥0.15 m	–	0	b≥0.30 m w≥0.02 m	–
Constant head orifice (8.3)		rectangular u = 0.5	MR	Δh≡0.06 m y_1 ≥ 2.5 w	Δh=0.06 m	0	usually* b=0.60 m and b=0.75 m	–

10	11	12	13	14	15	16	17	18
Q_{min} m^3/s	Q_{max} in m^3/s or q max in m^2/s	$\gamma = \frac{Q_{max}}{Q_{min}}$	modular limit H_2/H_1 or head loss	error in C_dC_v or C_e (%)	sensitiveness at minimum head % per 0.01 m	debris passing capacity + + very good; + good; □ fair; - poor; - - very poor	sediment passing capacity	Remarks
0.0137 h=0.03 m	depends on degree of truncation	100,000* $h_1 \geq 0.03$ m	0.67	10 C_v-8	83 if h_1=0.03 m	+ +	+	Applies to 1-to-5 back face only.
0.0275 h_1=0.06 m b=0.30 m		17,500 $h_1 \geq 0.06$ m			42 if h_1=0.06 m			*γ-values decrease if control is more truncated
0.0077 b=0.30 m	q=2.30	120	0.70	3	32	+	-*	* good if gate arrangement as in Section 4.2
0.025 b=1.0 m	variable*	about 1000 but depends on h_d-value	0.30	5	25	+ +	+	* minimum pressure on crest limited to -4.0 m water column (see Fig.6.17)
0.0064 b=0.30 m	variable*	about 750, but depends on ratio H_1/r	0.33	5	25	+ +	+	* minimum pressure on crest limited to -4.0 m water column (see Fig.6.23)
0.0066 b=0.30 m	variable with throat length	35	0.70 to 0.95 depending on downstream transition	2(21-20C_d) for all flumes	25	+ +	+	* for all flumes; at maximum stage: B > 0.30 m B > H_1max B > L/5
0.00098 θ=90°		≤315			28 to 42	+ +	+ +	
0.0036 b=0.08 m slope 1:2		≤250			27 to 40	+ +	+ +	**side slope ratio horz : vert. varies between ½:1 to 4:1
0.0027 f=0.10 m		100			33	+ +	+ +	
0.0026 d=0.20 m		100 if d≥0.60 m			≤ 33	+ +	+ +	
0.0050 b=0.20 m	q=4.82 H_1=2.00 m	190	about* 0.50	8	25	+ +	+	* if radii of rounding and if downstream transition comply with Section 7.2.2
-	-	-	-	-	25	+ +	+	not recommended to be constructed due to lack of data
0.00009 to 0.00077	0.0054 to 0.0321	about 55	0.50	3	103 to 52	+ +	+	very small flumes; 1,2, and 3 inch wide
0.0015 to 0.0972	0.111 to 3,949	about 75	0.60 and 0.70	3	53 to 21	+ +	+	small flumes; 0.5,0.75, 1.0, 1.5, 2,3 to 8 feet wide
0.16 to 0.75 m^3/s	8.28 to 93.04 m^3/s	about 105	0.80	3	18	+ +	+	large flumes; 10 to 50 feet wide
0.000012 to 0.00034	0.0003 to 0.0223	about 100	0.25	3	≤240	-	□	HS-flumes, D=0.4, 0.6, 0.8 and 1.0 ft
0.000031 to 0.0014	0.009 to 2.336	about 750	0.25	3	≤240	□	□	H-flumes,D=0.5, 0.75, 1.0, 1.5, 2.0, 2.5, 3.0, and 4.5 ft
0.0018 and 0.0020	2.370 and 3.298	about 1500	0.30	3	≤ 80	+	□	HL-flumes, D=3.5 and 4.0 ft
0.00014 d=0.02 m	variable	5.8*	submerged	1	17	- -	- -	*0.03 m ≤ Δh ≤ 1.0 m
0.0028	variable	5.8*	submerged	2 to 3	17	- -	□ if p=0	*0.03 m ≤Δ h ≤ 1.0 m and A = constant
0.0086* 0.0107	Q=0.140* Q=0.280	16** 26	submerged, but usually $\Delta H_t \geq 0.30$ m	≥ 7	8	- -	-	* Two sizes of orifice gates,0.60×0.45 m & 0.75 ×0.60 m are com.used ** If A varies

1	2	3	4	5	6	7	8	9
Name of structure and section number in which structure is described	Sketch of structure	Shape of control section perpendicular to flow and u-value	M = measuring MR = measuring & regulating	H_1 min or Δh min	H_1 max or Δh max	minimum crest height above approach channel bottom p	minimum size of control b or B, w and D_p	range of notch angle θ degrees
Radial or Tainter gate (8.4)	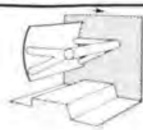	rectangular $u = 0.5$	MR	$y_1 \geq 0.15$ m $y_1 \geq 1.25$ w $y_1 \geq 0.1$ r	$y_1 < 1.2$ r	0	$b \geq 0.30$ m $w \geq 0.02$ m	-
Crump-de Gruyter adjustable orifice (8.5)		rectangular $u = 0.5$	MR	0.03 m 1.58 w	0.60 m	0.20 m p = b	$b \geq 0.20$ m 0.02 m $< w$ ≤ 0.38 m $w \leq 0.63\ h_1$	-
Meter gate (8.6)		Section of circle $u=0.5$	MR	$h_1 \geq 1.0\ D_p$ $\Delta h \geq 0.05$ m	$\Delta h \leq 0.45$ m	0.17 D_p	$D_p \geq 0.30$ m $w \leq 0.75\ D_p$ $w \geq 0.02$ m	-
Neyrpic modules (8.7)	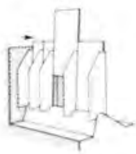	rectangular $u = 0.5$	MR	$h_d = 0.17$m $h_d = 0.28$m	$h_d \leq p$ and $h_d \leq 0.35\ p_2$	0.16 m 0.26 m	0.05 m 0.05 m	- -
Danaidean tub (8.8)		circular or rectangular $u = 0.5$	M	approx. 0.10 m	approx. 5.0 m	-	$d \geq 0.02$ m $b \geq 0.02$ m	$0^o \leq \theta \leq 180^o$
Divisors (9.1)	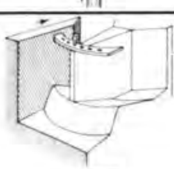	rectangular $u = 1.5$	MR	0.06 m 0.50 r	1.0 p 0.35 p_2 4.0 r	0.15 m 0.33 H_1	0.30 m 2.0 H_1	-
Pipes and small siphons (9.2)		circular $u = 0.5$	M	0.03 m	1.20 m	1.0 D_p	$D_p \geq 0.015$ m $D_p \geq 0.03$ m	-
Fountain flow from vertical pipe (9.3)		circular $u = 1.35$ or $u = 0.53$	M	0.03 m	4.00 m	-	$0.025 \leq D_p$ $D_p \leq 0.609$	-
Flow from horizontal pipes (9.4)	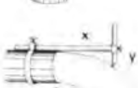	circular $1.5 < u \leq 2$ $u = 1.5$ (versus Y)	M M	$y_e = 0.02$m 0.1 D_p $y_e \geq D_p$ $Y \geq 0.025$	$y_e \leq$ 0.56 D_p $Y \leq 0.15$ m*	- -	$D_p \geq 0.05$ m $0.05 \leq D_p$ ≤ 0.15 m	- -
Brink depth method for rectangular canals (9.5)		rectangular $u = 1.5$	M	$y_e \geq 0.03$m	-*	p = 0	0.30 m 3 y_c	-
Dethridge meters (9.6)	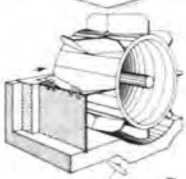	rectangular no u-value	MRV	$y_1 = 0.30$m $y_1 = 0.38$m	$y_1 = 0.90$m $y_1 = 0.90$m	- -	0.52 m 0.78 m	- -
Propeller meters (9.7)		usually circular no u-value	MRV	$v > 0.45$ m/s	$v < 5.0$ m/s	-	0.05 m $\leq D_p \leq 1.82$ m	-

10	11	12	13	14	15	16	17	18
Q_{min} m^3/s	Q_{max} in m^3/s or q max in m^2/s	$\gamma = \frac{Q_{max}}{Q_{min}}$	modular limit H_2/H_1 or head loss	error in C_dC_v or C_e (%)	sensitiveness at minimum head % per 0.01 m	debris passing capacity + + very good; + good; ☐ fair; - poor; - - very poor	sediment passing capacity	Remarks
0.005 y_1=0.15 m	variable	about* 35	variable	5	8	-	+ +	* If A varies γ is greater if gate is lifted entirely
0.0088	q=0.742	10	up to* 0.25	[illegible]	8	-	-	* If w/h_1 is small
0.0076 D_p=0.30 m	Q=2.10 D_p=1.22 m	7 to 45	$h_2 \geqslant 0.15$ m $\Delta H_c \geqslant 0.30$ m	3 to 6	8	-	-	Usually 0.20 m ≤ D_p ≤ 1.22 m
0.0005 0.0010	q=0.100 q=0.200	1* 1	0.60 0.60	5 5	3 1.8	- - - -	☐ ☐	Type X 1 Type XX 2 * Discharge is regulated by opening/closing gates
0.00027 d=0.02 m h_1=0.10 m	variable	7	$h_1+\delta d$*	2	5	- -	☐	* δ = contraction coefficient
0.0075 b=0.30 m	q=5.69 H_1=2.00 m	30*	0.60	[illegible]	25	- -	+	* Other weir profiles are possible
0.00006 0.00037	variable	6 6	usually submerged	10 10	17 17	- - - -	- - - -	L > 20 D_p 6 D_p ≤ L ≤ 20 D_p
0.00048 D_p=0.025 m	Q=2.45 D_p=0.609 m	237	pipe must discharge free into the air	15 to 20	50	- -	- -	
0.00062 D_p=0.05 m	variable	42	pipe must discharge free into the air	3	100	- -	- -	Brink depth method
0.0020 D_p=0.05 m	Q=0.100 D_p=0.15 m	2.5		15	20	- -	- -	Trajectory method; X=0.152, 0.305 and 0.457 m
0.0081 b=0.30 m	q=4.82 H_1=2.0 m	about 175	head loss 2.1 H_1	3	25	+	+	y_e/y_c=0.715 * Approach canal length ≥ 12 y_c
0.015	Q=0.070	4.6	head loss ≥ 0.08 m	5	-	+	+	Small meter
0.040	Q=0.140	3.5	≥ 0.09 m at y_1 min.	5	-	+	+	Large meter
0.00088 D_p=0.05 m	Q=13.0 D_p=1.82 m	10	usually Δh ≥ 0.50 m	5*	-	☐	+	* If propeller is maintained frequently

Column 5: Minimum value of H_1 or Δh in metres or in terms of structural dimensions.

Column 6: As Column 5, but giving maximum values.

Column 7: Minimum height of weir crest or invert of orifice above approach channel bottom; in metres or in terms of structural dimensions.

Column 8: Minimum dimensions of control section; b, B, w, and D_p.

Column 9: Range of notch angle θ for triangular control sections.

Column 10: Minimum discharge (Q_{min}) in $m^3/s \times 10^{-3}$ or l/s of the smallest possible structure of the relevant type, being determined by the minima given in Columns 5, 8, and 9.

Column 11: Maximum discharge: q in m^2/s, being the discharge per metre crest width if this width is not limited to a maximum value, or Q in m^3/s if both the head (differential) and control section dimensions are limited to a maximum. No maximum discharge value is shown if neither the head (differential) nor the control dimensions are limited by a theoretical maximum. Obviously, in such cases, the discharge is limited because of various practical and constructional reasons.

Column 12: Value of $\gamma = Q_{max}/Q_{min}$ of the structure. If Q_{max} cannot be calculated directly, the γ-value can usually be determined by substituting the limitations on head (differential) in the head-discharge equation, as shown in Section 3.2.3.

Column 13: Modular limit H_2/H_1 or required total head loss over the structure. The modular limit is defined as that submergence ratio H_2/H_1 whereby the modular discharge is reduced by 1% due to an increasing tailwater level.

Column 14: Error in the product C_dC_v or in the coefficient C_e.

Column 15: Maximum value of the sensitivity of the structure times 100, being

$$100\ S = \frac{u}{h_1} \Delta h_1\ 100$$

where the minimum absolute value of h_1 is used with the assumption Δh_1=0.01 m. The figures shown give a percentage error in the minimum discharge if an error in the determination of h_1 equal to 0.01 m is made. The actual error Δh_1 obviously depends on the method by which the head is determined.

Column 16: Classifies the structures as to the ease with which they pass floating and suspended debris.

Column 17: Classifies the structures as to the ease with which they pass bed-load and suspended load.

Column 18: Remarks.

3.4 Selecting the structure

Although it is possible to select a suitable structure by using Table 3.1, an engineer may need some assistance in selecting the most appropriate one. To help him in this task, we will try to illustrate the process of selection. To indicate the different stages in this process we shall use differently shaped blocks, with connecting lines between them. A set of blocks convenient for this purpose is defined in Figure 3.6.

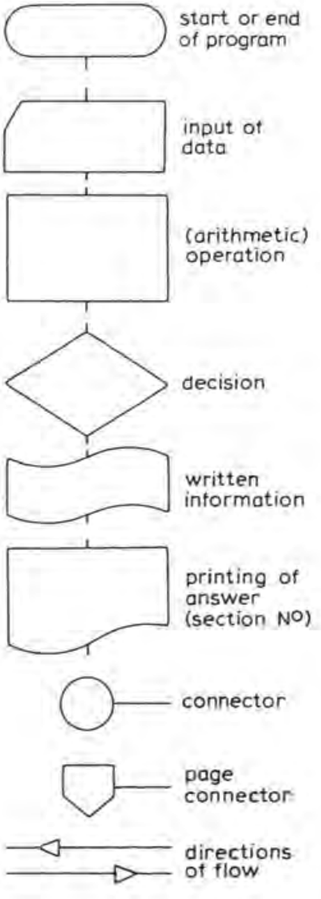

Fig.3.6. Legend of blocks diagram.

All blocks except the terminal block, which has no exit, and logical decision blocks, which have two or more exits, may have any number of entry paths but only one exit path. A test for a logical decision is usually framed as a question to which the answer is "Yes" or "No", each exit from the Lozenge block being marked by the appropriate answer.
A block diagram showing the selection process is shown in Figure 3.7.

The most important parts of this process are:

The weighing of the hydraulic properties of the structure against the actual situation or environment in which the structure should function (boundary conditions);

The period of reflection, being the period during which the engineer tests the type of structure and decides whether it is acceptable.

Both parts of the selection process should preferably be passed through several times to obtain a better understanding of the problem.

To assist the engineer to find the most appropriate type of structure, and thus the relevant section number in the next chapters of this book, we have included Figure 3.8, which treats approximately that part of the selection process enclosed by the dotted line in Figure 3.7. In constructing the diagram of Figure 3.8 we have only used the most important criteria. The use of more criteria would make the diagram longer and more complex.

After one or more suitable structures (sections) are found we recommend that Table 3.1 be consulted for a first comparative study, after which the appropriate section should be studied. During the latter study one takes the secondary boundary conditions into account and continues through the "reflection branch" of Figure 3.7 until the proper structure has been selected.

It is stressed again that in this chapter the selection of structures is based purely upon the best hydraulic performance. In reality it is not always desirable to alter the existing situation so that all limits of application of a standard structure are fulfilled. If, however, a structure is to be used to measure discharges and its head-discharge relationship is not known accurately, the structure must either be calibrated in a hydraulic laboratory or calibrated in situ. Calibration in situ can be performed by using the area-velocity method or the salt dilution method.

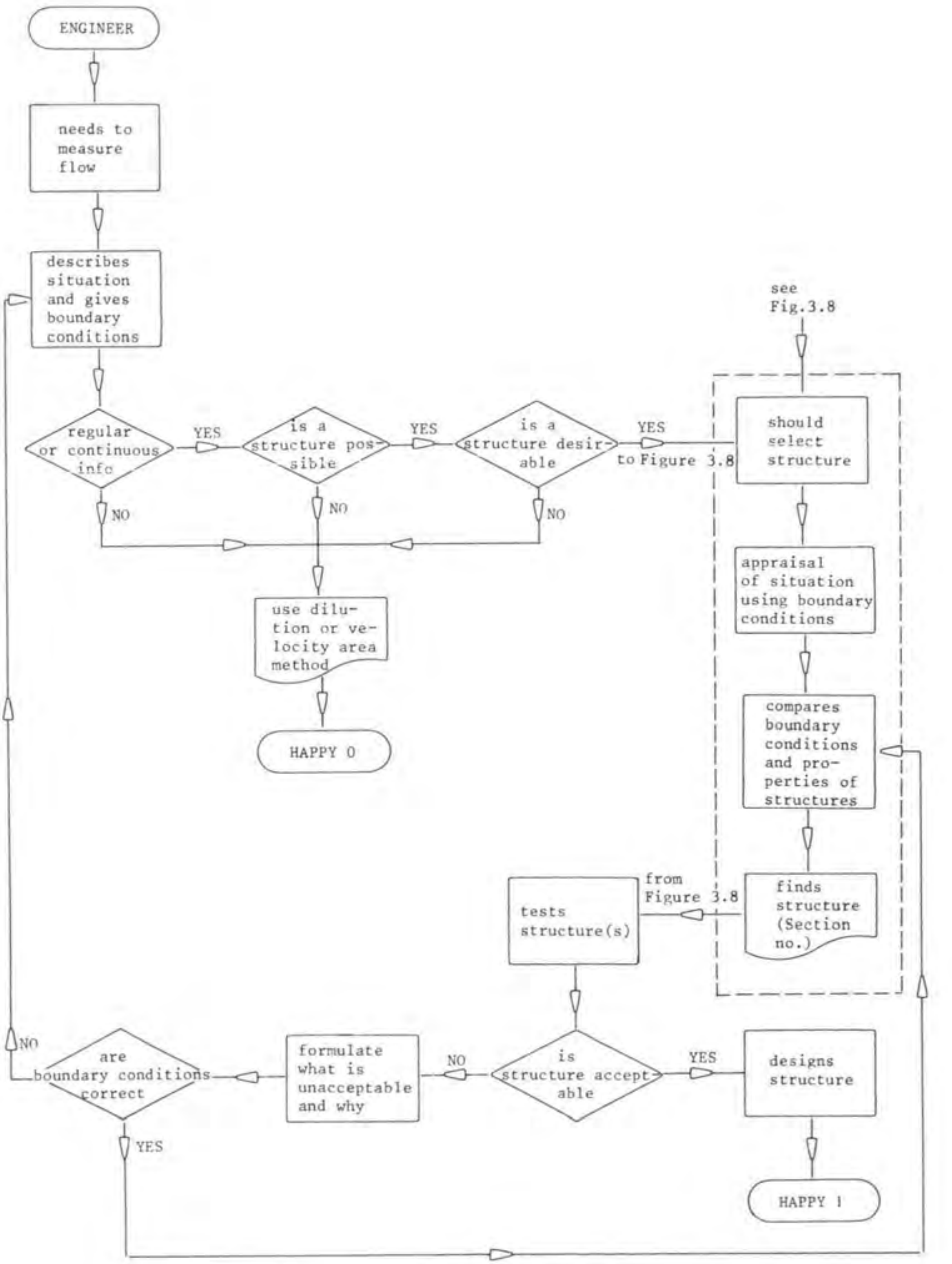

Fig. 3.7. Selecting process of a discharge measuring or regulating structure.

Photo 2. The side walls of the channel in which the weir is placed are not parallel.

Photo 3. If the limits of application of a measuring structure cannot be fulfilled, laboratory tests can provide a head-discharge curve.

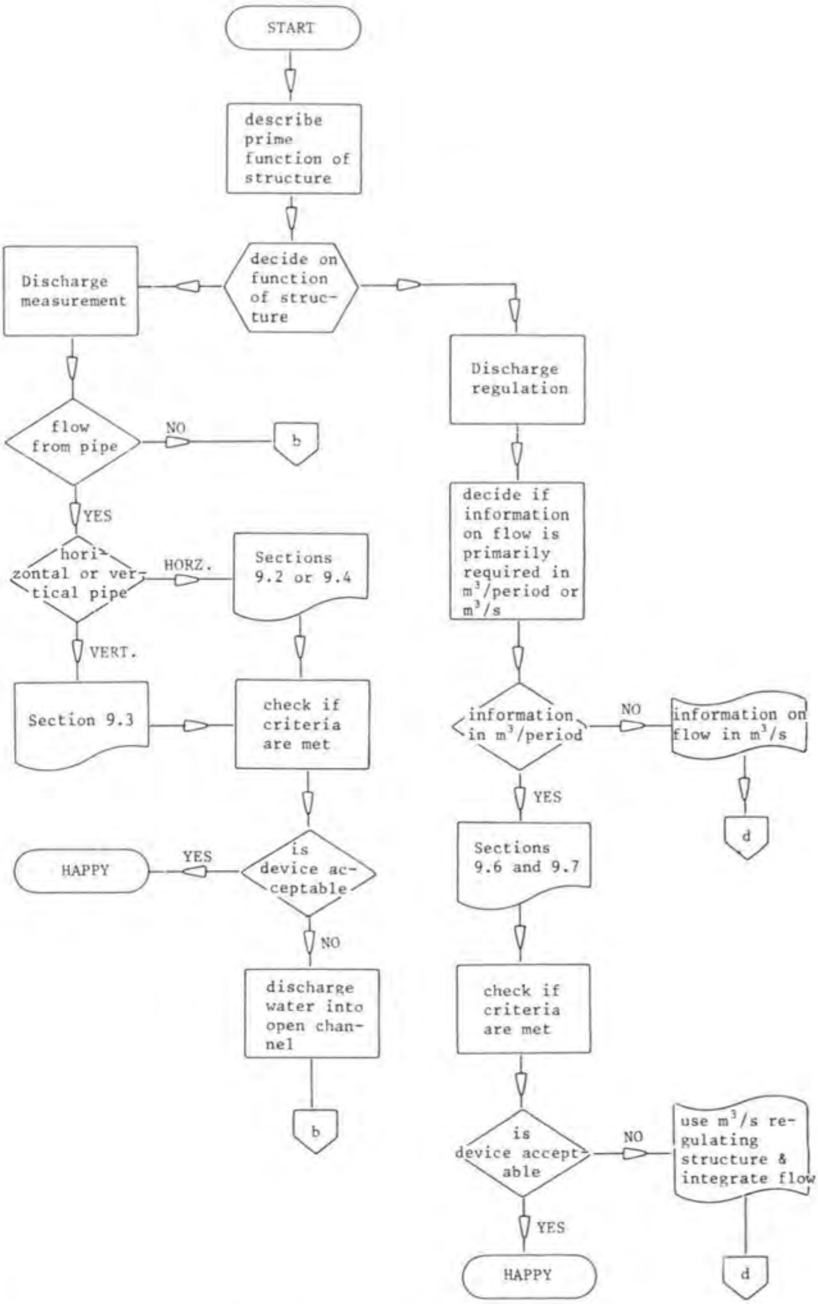

Fig.3.8 a. Finding the relevant structure (or section).

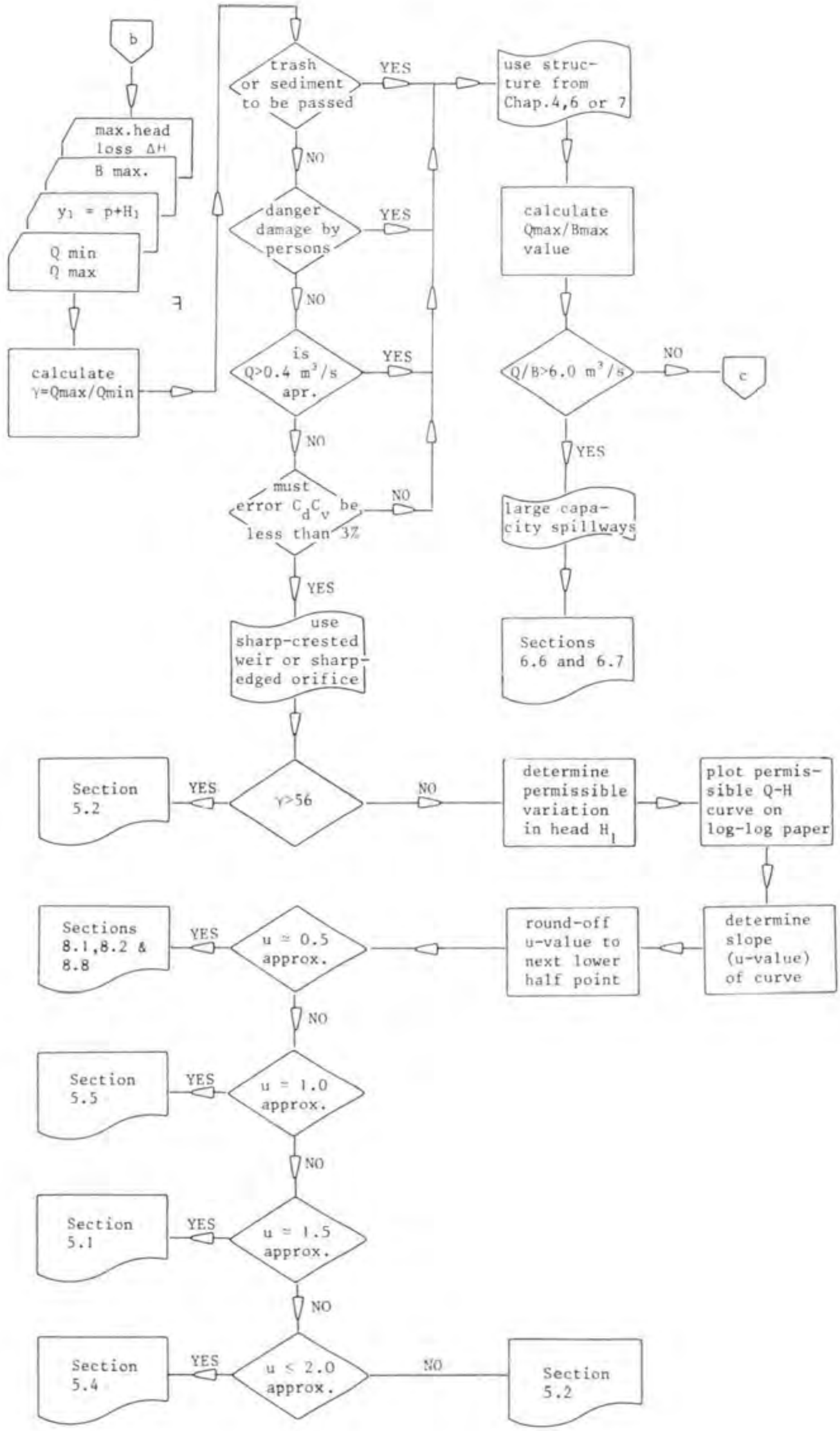

b
max.head loss ΔH
B max.
y₁ = p+H₁
Q min
Q max
calculate γ=Qmax/Qmin
trash or sediment to be passed
YES
NO
danger damage by persons
YES
NO
is Q>0.4 m³/s apr.
YES
NO
must error CdCv be less than 3%
NO
YES
use sharp-crested weir or sharp-edged orifice
use structure from Chap.4,6 or 7
calculate Qmax/Bmax value
Q/B>6.0 m³/s
NO
c
YES
large capacity spillways
Sections 6.6 and 6.7
Section 5.2
YES
γ>56
NO
determine permissible variation in head H₁
plot permissible Q-H curve on log-log paper
determine slope (u-value) of curve
round-off u-value to next lower half point
Sections 8.1,8.2 & 8.8
YES
u ≃ 0.5 approx.
NO
Section 5.5
YES
u ≃ 1.0 approx.
NO
Section 5.1
YES
u ≃ 1.5 approx.
NO
Section 5.4
YES
u ≤ 2.0 approx.
NO
Section 5.2

Fig.3.8 b.

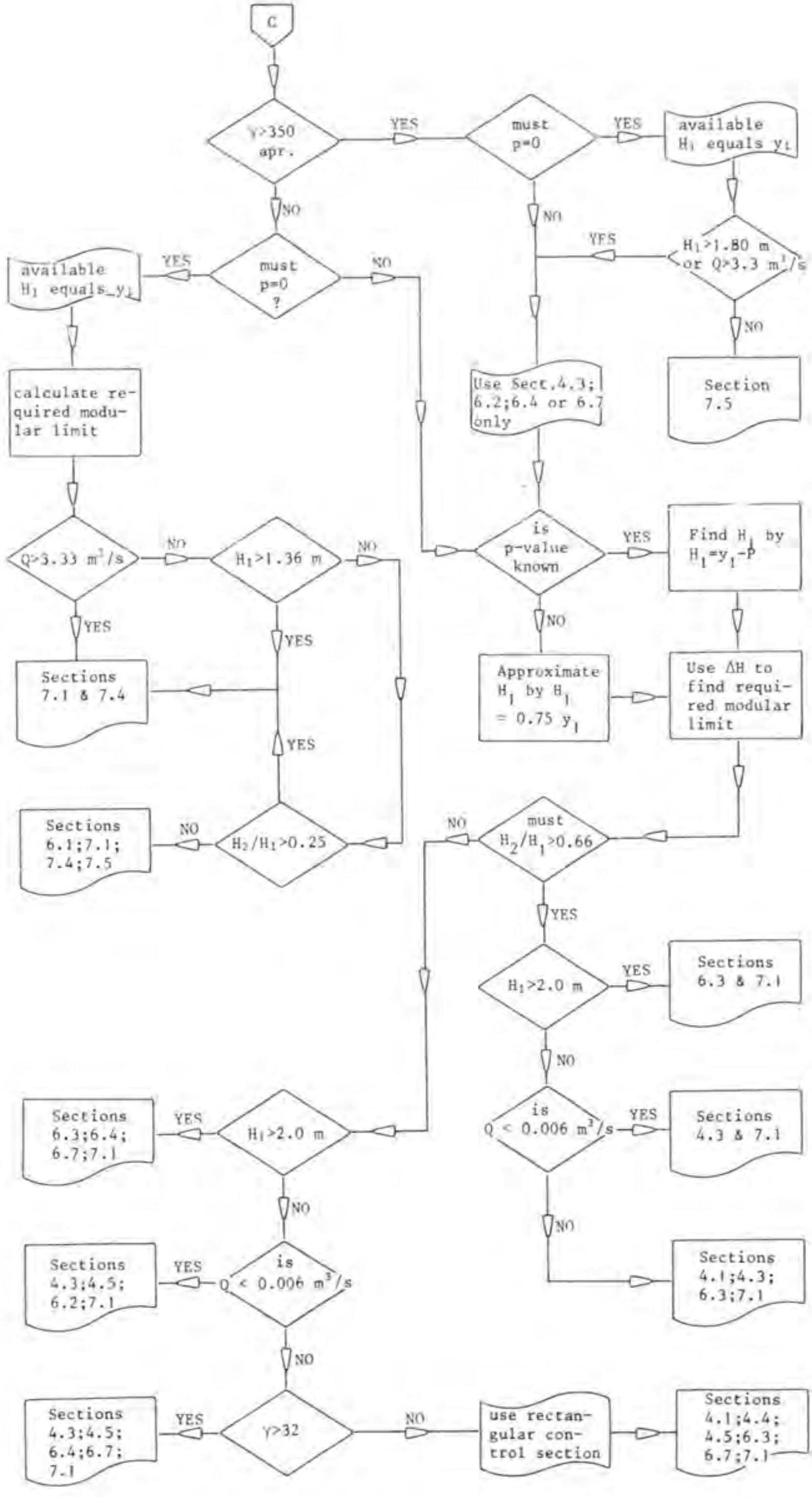
C
y>350 apr.
YES
NO
must p=0
available H1 equals y1
H1>1.80 m or Q>3.3 m3/s
must p=0 ?
calculate required modular limit
Use Sect.4.3; 6.2;6.4 or 6.7 only
Section 7.5
Q>3.33 m3/s
H1>1.36 m
is p-value known
Find H1 by H1=y1-P
Sections 7.1 & 7.4
Approximate H1 by H1 = 0.75 y1
Use ΔH to find required modular limit
Sections 6.1;7.1; 7.4;7.5
H2/H1>0.25
must H2/H1>0.66
H1>2.0 m
Sections 6.3 & 7.1
is Q < 0.006 m3/s
Sections 4.3 & 7.1
Sections 6.3;6.4; 6.7;7.1
Sections 4.1;4.3; 6.3;7.1
Sections 4.3;4.5; 6.2;7.1
Sections 4.3;4.5; 6.4;6.7; 7.1
y>32
use rectangular control section
Sections 4.1;4.4; 4.5;6.3; 6.7;7.1

Fig.3.8 c.

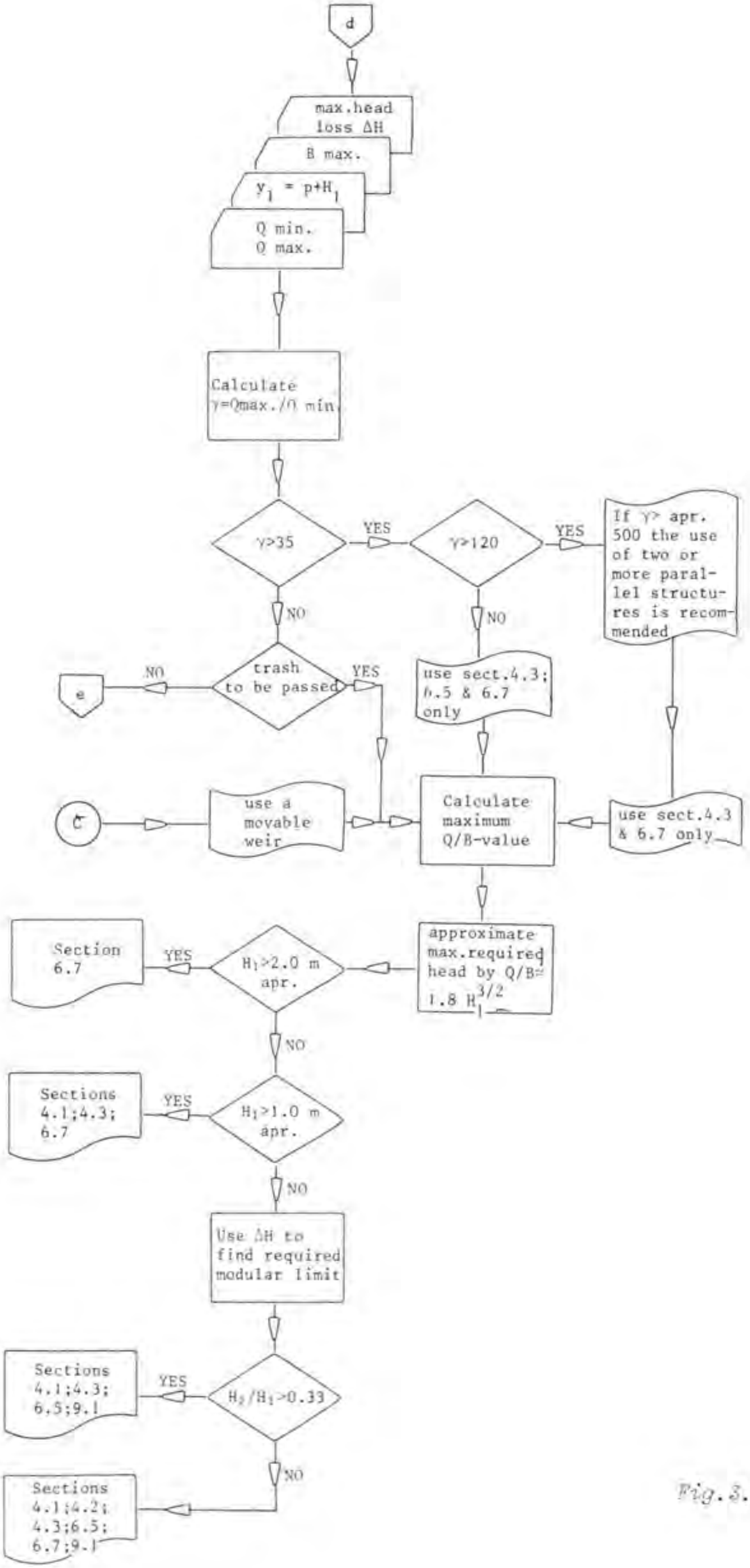
d
max.head loss ΔH
B max.
y1 = p+H1
Q min. Q max.
Calculate γ=Qmax./Q min.
γ>35
YES
γ>120
YES
If γ> apr. 500 the use of two or more parallel structures is recommended
NO
NO
trash to be passed
NO
e
YES
use sect.4.3; 6.5 & 6.7 only
C
use a movable weir
Calculate maximum Q/B-value
use sect.4.3 & 6.7 only
approximate max.required head by Q/B≈ 1.8 H1^3/2
H1>2.0 m apr.
YES
Section 6.7
NO
H1>1.0 m apr.
YES
Sections 4.1;4.3; 6.7
NO
Use ΔH to find required modular limit
H2/H1>0.33
YES
Sections 4.1;4.3; 6.5;9.1
NO
Sections 4.1;4.2; 4.3;6.5; 6.7;9.1

Fig. 3.8 d.

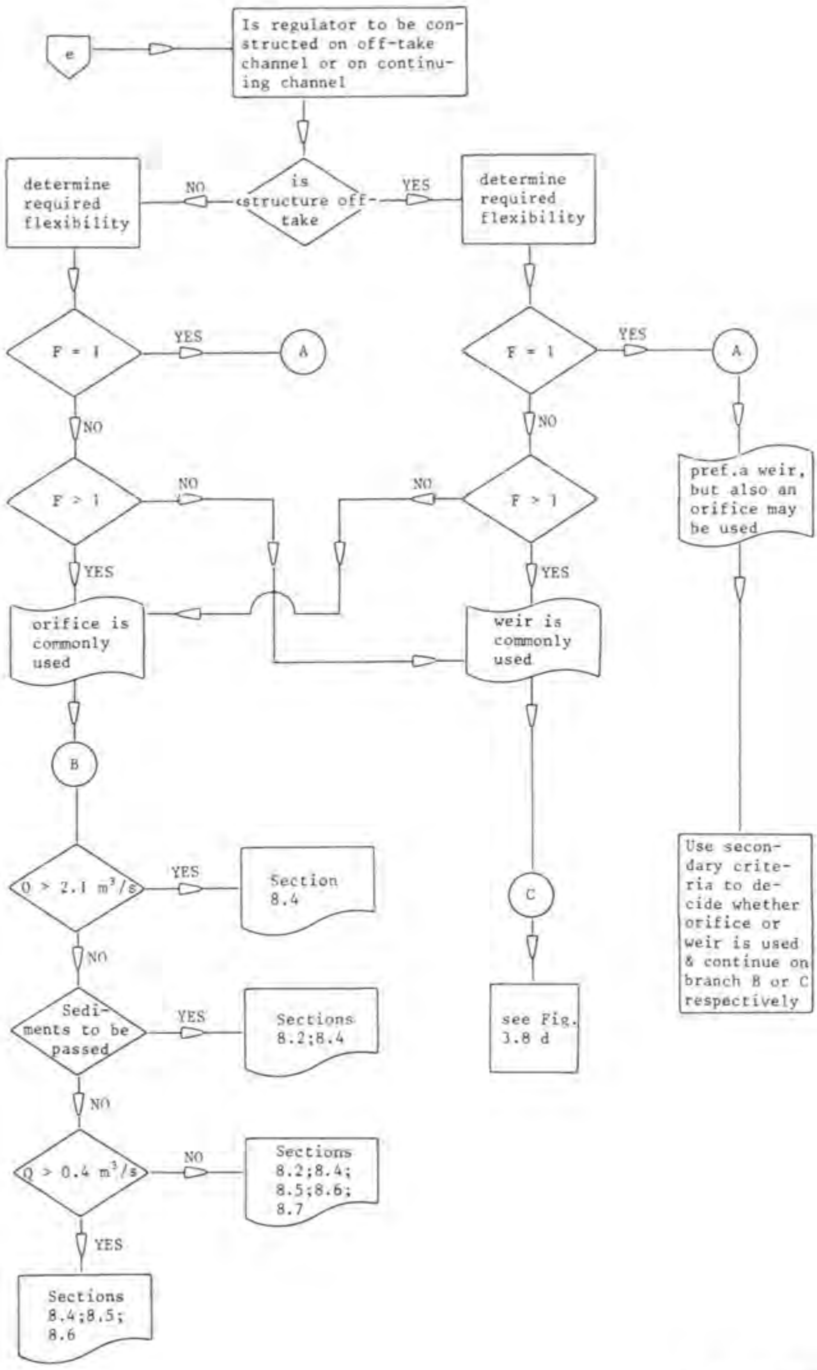
e
Is regulator to be constructed on off-take channel or on continuing channel
is structure off-take
NO
YES
determine required flexibility
determine required flexibility
F = 1
YES
A
F = 1
YES
A
NO
NO
F > 1
NO
NO
F > 1
pref.a weir, but also an orifice may be used
YES
YES
orifice is commonly used
weir is commonly used
B
Q > 2.1 m³/s
YES
Section 8.4
C
NO
Sediments to be passed
YES
Sections 8.2;8.4
see Fig. 3.8 d
Use secondary criteria to decide whether orifice or weir is used & continue on branch B or C respectively
NO
Q > 0.4 m³/s
NO
Sections 8.2;8.4; 8.5;8.6; 8.7
YES
Sections 8.4;8.5; 8.6

Fig.3.8 e.

3.5 Selected list of references

1. BERKHOUT, F.M.C.: Lecture notes on irrigation engineering. F 18. University of Technology, Delft. 1965.

2. ENGELUND, F. and HANSEN, E.: A monograph on sediment transport in alluvial streams. Teknisk Forlag, Copenhagen. 1967.

3. MAHBUB, S.I., and GULHATI, N.D.: Irrigation outlets. Atma Ram & Sons, India, 1951. 184 pp.

4. MEIJER-PETER, E. and MÜLLER, R.: Formulas for bed-load transport. Proc.Second meeting of the International Association for Hydraulic Structures Res., Stockholm 1948. Vol.2, Paper 2.

5. NETHERLANDS ENGINEERING CONSULTANTS (NEDECO): Río Magdalena and Canal del dique survey project. The Hague 1973.

6. REPLOGLE, J.A.: Discussion of Rectangular cutthroat flow measuring flumes (Proc.Paper 5628). J.of the Irrigation and Drainage Division of the ASCE. Vol.94. No.IR3. Sept. 1968, pp.359-362.

4 Broad-crested weirs

Classified under the term "broad-crested weirs" are those structures over which the streamlines run parallel to each other at least for a short distance, so that a hydrostatic pressure distribution may be assumed at the control section. To obtain this condition, the length in the direction of flow of the weir crest (L) is restricted to the total upstream energy head over the crest (H_1). In the following sections the limitation on the ratio H_1/L will be specified for the following types of broad-crested weirs:
4.1 Round-nose horizontal broad-crested weir; 4.2 The Romijn movable measuring/regulating weir; 4.3 Triangular broad-crested weir; 4.4 Broad-crested rectangular profile weir; 4.5 Faiyum weir.

4.1 Round-nosed horizontal broad-crested weir

4.1.1 Description

This weir is in use as a standard discharge measuring device and, as such, is described in the British Standard 3680, 1969, which is partly quoted below. The weir comprises a truly level and horizontal crest between vertical abutments. The upstream corner is rounded in such a manner that flow separation does not occur. Downstream of the horizontal crest there may be

(i) a vertical face

(ii) a downward slope or

(iii) a rounded corner, depending on the submergence ratio under which the weir should operate at modular flow.

The weir structure should be rigid and watertight and be at right angles to the direction of flow.

The dimensions of the weir and its abutments should comply with the requirements indicated in Figure 4.1. The minimum radius of the upstream rounded nose (r) is 0.11 H_1 max, although for the economic design of field structures a value r = 0.2 H_1max is recommended. The length of the horizontal portion of the weir crest should not be less than 1.75 H_1max. To obtain a favourable (high) discharge coefficient (C_d) the crest length (L) should be close to the permissible minimum. In accordance with Section 2.2 the head measurement section should be located a distance of between two and three times H_1max upstream of the weir block.

Photo 1. Downstream view of a broad-crested weir.

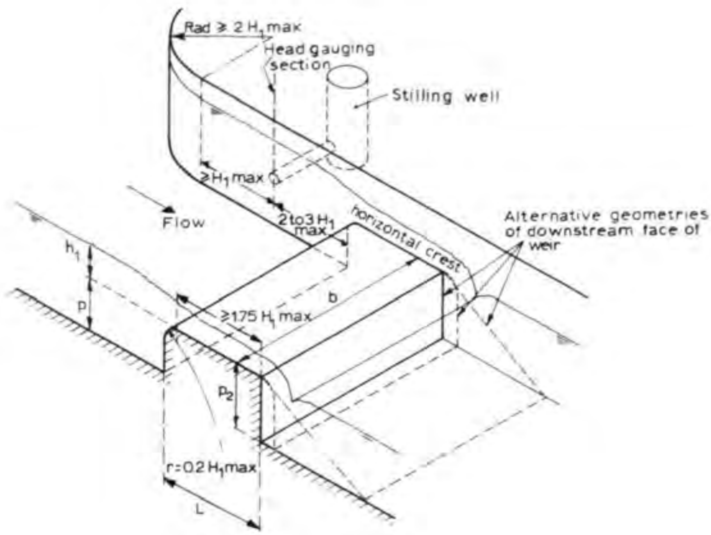

Fig.4.1. Dimensions of round-nose broad-crested weir and its abutments (adapted from British Standards Institution, 1969).

4.1.2 Evaluation of discharge

According to Equation 1-37 Section 1.9.1,the basic stage-discharge equation for a broad-crested weir with a rectangular throat reads

$$Q = C_d \ C_v \ \frac{2}{3}\left[\frac{2}{3}\ g\right]^{0.50} bh_1^{1.50} \tag{4-1}$$

For water of ordinary temperatures, the discharge coefficient (C_d) is a function of the upstream head over the crest (h_1), the length of the weir crest in the direction of flow (L),the roughness of the crest, and the breadth (b) of the crest. It can be expressed by the equation

$$C_d = \left[1 - 2x(L - r)/b\right] \left[1 - x(L - r)/h_1\right]^{1.50} \tag{4-2}$$

where x is a factor which allows for the influence of the boundary layer on the crest and abutments.For field installations of well-finished concrete or similar construction, x≃0.005.For well-finished structures such as those that might be used in laboratories for gauging clean water, $x = 0.003$.

The appropriate value of the approach velocity coefficient (C_v) can be read from Figure 1.12 (Chapt.1).

The error in the product C_dC_v of a well maintained round-nose broad-crested weir, which has been constructed with reasonable care and skill, can be deduced from the equation

$$X_c = \pm 2(21 - 20\ C_d) \text{ per cent} \qquad (4\text{-}3)$$

The method by which this error is to be combined with other sources of error is shown in Appendix II.

4.1.3 Modular limit

The flow over a weir is modular when it is independent of variations in tail-water level. For this to occur, assuming subcritical conditions in the tail-water channel, the tailwater level (h_2) must not rise beyond a certain percentage of the upstream head over the weir crest (H_1). Hence, the height of the weir above the bottom of the tailwater channel (p_2) should be such that the weir operates at modular flow at all discharges. The modular limit can be read from Figure 4.2 as a function of H_1/p_2 and the slope of the back face of the weir. The design value of p_2 should be established by a trial and error method.

4.1.4 Limits of application

a) The practical lower limit of h_1 is related to the magnitude of the influence of fluid properties, to the boundary roughness, and to the accuracy with which h_1 can be determined. The recommended lower limit is 0.06 m or 0.05 times L, whichever is greater.

b) The limitations on H_1/p arise from difficulties experienced when the Froude number $Fr = v_1/(gA_1/B)^{0.5}$ in the approach channel exceeds 0.5, coupled with inadequate experimental confirmation at high values of H_1/p. The recommended upper limit is $H_1/p = 3.0$, while p should be greater than or equal to 0.15 m.

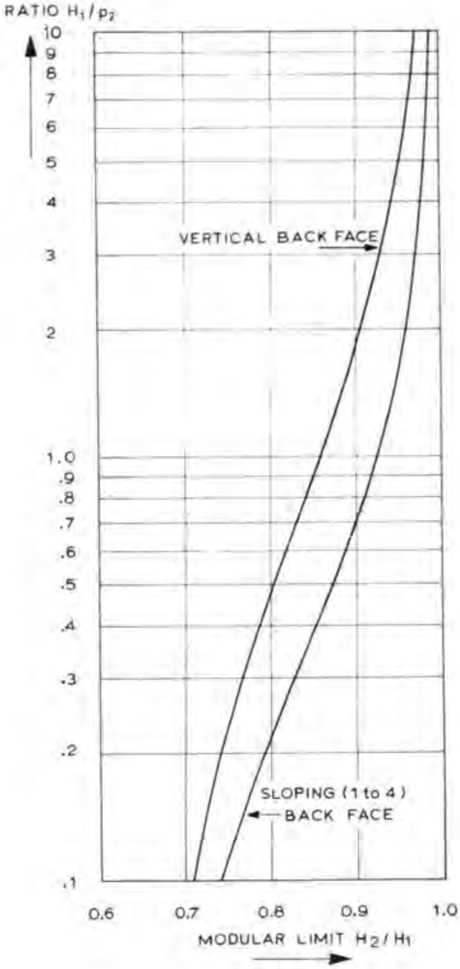

Fig.4.2. The modular limit as a function of H_1/p_2 (after Harrison, 1967).

c) The limitations on H_1/L arise from the necessity of ensuring a sensible hydrostatic pressure distribution at the critical section of the crest and of preventing the formation of undulations above the weir crest. Values of the ratio H_1/L should therefore range between 0.05 and 0.50.

d) The breadth (b) of the weir crest should not be less than 0.30 m, nor less than H_1max, nor less than L/5.

4.2 The Romijn movable measuring/regulating weir

4.2.1 Description

The Romijn weir was developed by the Department of Irrigation in Indonesia as a regulating and measuring device for use in relatively flat irrigated regions where the water demand is variable because of different requirements during the growing season and because of crop rotation. A description of the weir was published in 1932 by D.G.ROMIJN, after whom the structure is named.

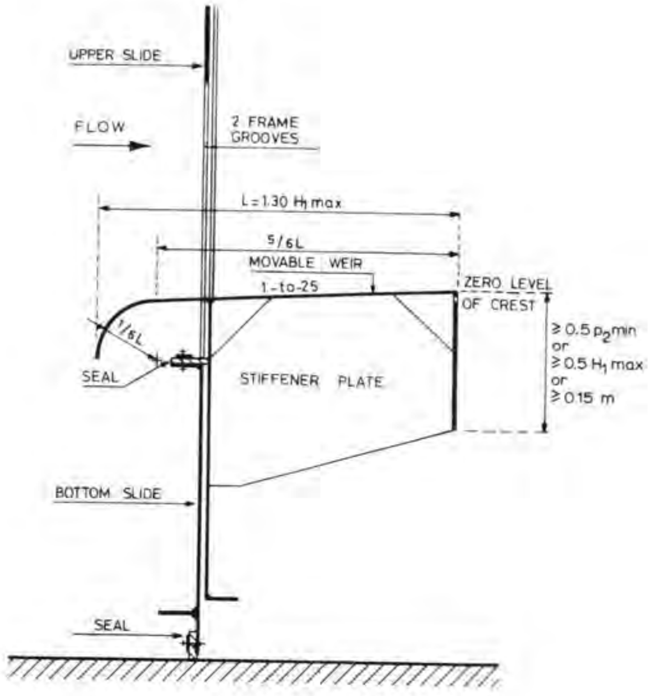

Fig.4.3. The Romijn movable weir.

The telescoping Romijn weir consists of two sliding blades and a movable weir which are mounted on a steel guide frame:

a) the bottom slide is blocked in place under operational conditions and acts as a bottom terminal for the movable weir

b) the upper slide is connected to the bottom slide by means of two steel strips placed in the frame grooves and acts as a top terminal for the movable weir

c) the movable weir is connected by two steel strips to a horizontal lifting beam. The weir crest is horizontal perpendicular to the flow and slopes 1-to-25 upward in the direction of flow. Its upstream nose is rounded off in such a way that flow separation does not occur. The operating range of the weir equals the maximum upstream head (h_1) which has been selected for the dimensioning of the regulating structure (see Fig.4.3).

Although the Romijn weir has been included in this chapter on broad-crested weirs, from a purely hydraulic point of view this is not quite correct. Above the 1-to-25 sloping weir crest the streamlines are straight but converging so that the equipotential lines are curved. At the same time, the control section is situated more towards the end of the crest than if the crest were truly horizontal. Therefore, the degree of downward curvature of the overflowing nappe has a significant influence on the C_d-value. To prevent the formation of a relatively strong eddy beneath the weir crest and the overflowing nappe, the weir should have a vertical downstream face. The reason for this is that especially under submerged flow conditions the nappe will deflect upwards due to the horizontal thrust of the eddy, resulting in up to 7% lower weir flows. The downstream weir face, which breaks the force of the eddy should have a minimum height of 0.5 p_2 min or 0.5 H_1 max or 0.15 m, whichever is greater.

As mentioned, the bottom slide, and thus the upper slide, is blocked in place during normal flow conditions. However, to flush sediments that have collected upstream of the weir, both slides can be unlocked and raised by moving the weir crest upward. After flushing operations the slides are pushed in place again by lowering the weir crest.

The weir abutments are vertical and are rounded in such a way that flow separation does not occur. A rectangular approach channel is formed to assure an even flow distribution. The upstream head over the weir, h_1, is measured in this approach channel at a distance of between two and three times H_1 max upstream of the weir face.The dimensions of the abutment should comply with the requirements indicated in Figure 4.4.The radius of the upstream rounding-off of the abutments may be reduced to $r \geq H_1$ max if the centre line of the weir structure is parallel to or coincides with the centre line of the undivided supply canal (in-line structure) or if the water is drawn direct from a (storage) basin.

If several movable weirs are combined in a single structure, intermediate piers should be provided so that two-dimensional flow is preserved over each weir unit, allowing the upstream head over the weir to be measured independently per unit.

The parallel section of the pier should therefore commence at a point located at a distance of H_1max upstream of the head measurement station and extend to the downstream edge of the weir-crest. Piers should have streamlined noses, i.e. of semi-circular or tapered semi-elliptical profile (1-to-3 axis). To avoid extreme velocity differences over short distances, the thickness of the intermediate piers should be equal to or more than 0.65 H_1max, with a minimum of 0.30 m.

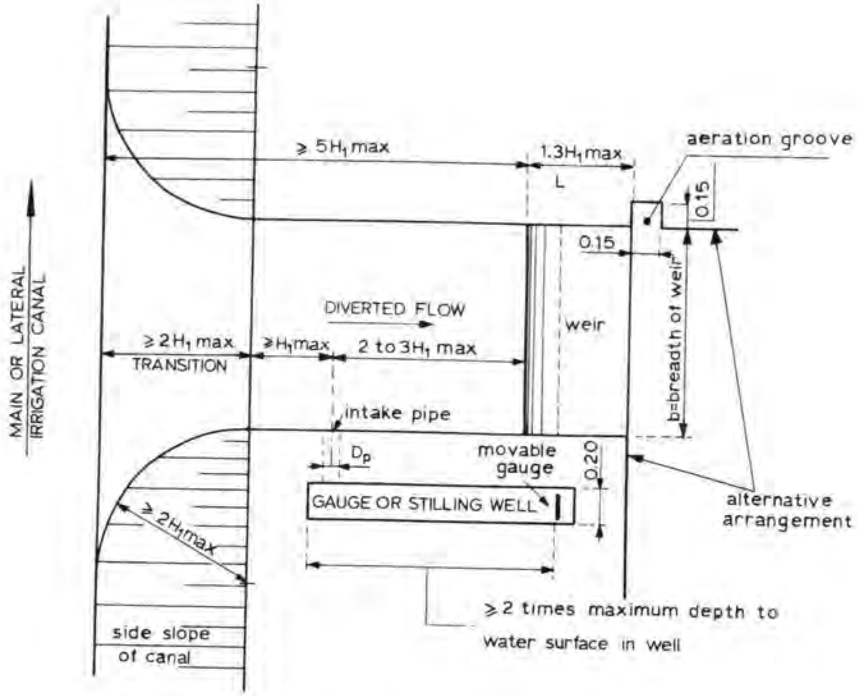

Fig.4.4. Hydraulic dimensions of weir abutments.

Since the weir crest moves up and down, a fixed staff gauge at the head measurement station does not provide a value for the upstream head over the crest unless the weir crest elevation is registered separately in terms of gauged head. To avoid this procedure, the weir is equipped with a gauge that moves up and down with the weir crest (see Fig.4.4). Zero level of this gauge coincides with the downstream edge of the weir crest, so that the upstream head over the crest equals the immersed depth of the gauge and can be read without time lag. The movable gauge is attached to the extended lifting beam as shown in Figure 4.7.

4.2.2 Evaluation of discharge

According to Equation 1-37, Section 1.9.1, the basic head discharge equation for a broad-crested weir with a rectangular control section reads

$$Q = C_d C_v \frac{2}{3} \left[\frac{2}{3} g\right]^{0.50} b h_1^{1.50} \qquad (4\text{-}4)$$

Values of the discharge coefficient C_d may be read from Figure 4.5 as a function of the ratio H_1/L.

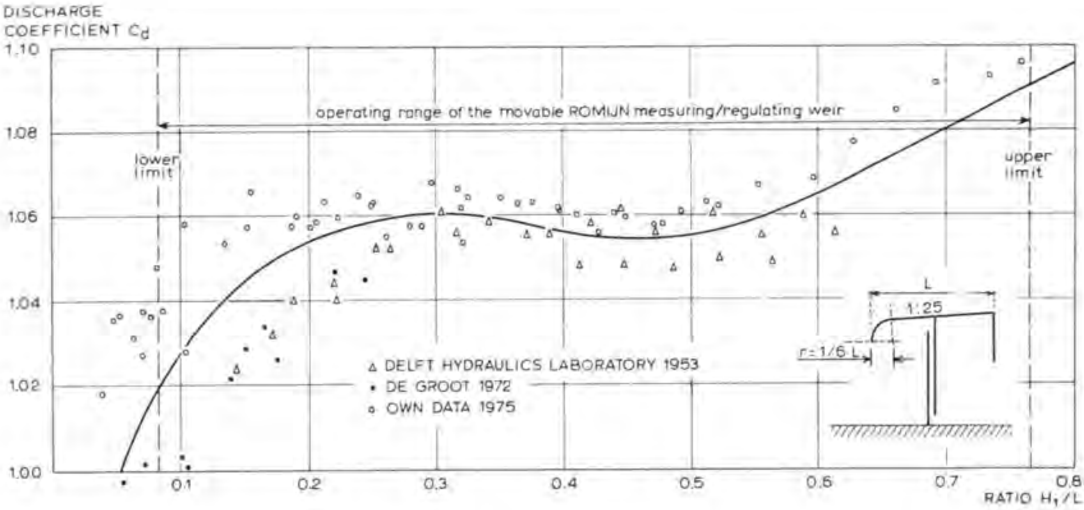

Fig.4.5. Values of C_d as a function of H_1/L for the Romijn weir.

Since the weir crest height above the approach channel bed (p) is variable and to a certain extent independent of the head over the weir crest h_1, the approach velocity cannot be predicted unless p is known. Engineers therefore tend to use either a constant C_d-value of 1.055 for all values of h_1/L or to use Figure 4.5 to determine C_d by assuming that $h_1 \simeq H_1$.

Values for the approach velocity coefficient C_v may be read from Figure 1.12 as a function of the dimensionless ratio $C_d h_1/(h_1 + p)$, where p is the variable height of the movable weir crest above the bottom of the rectangular approach channel. Over the range of p-values, an average C_v-value may be used in Equation 4-4 (see also Fig.4.8).

If the reader compares the C_d-value of the round-nose broad-crested weir as described in Section 4.1.2 and the C_d-value presented in Figure 4.5, he will note that a weir with 1-to-25 upward sloping weir crest as introduced by VLUGTER (1940), has the advantage that C_d varies less as a function of H_1/L and that C_d has a value about 7% higher.

As a result, the length of the Romijn weir in the direction of flow can be rather short, which makes the movable structure cheaper yet more sturdy while at the same time the weir discharge is increased.

If a movable Romijn weir has been constructed and installed with reasonable care and skill, its discharge coefficient C_d may be expected to have an error of less than 3%. If an average value of $C_d = 1.055$ is used for all ratios of H_1/L, this C_d-values may be expected to have an error of less than 4%. To obtain these accuracies the weir should be properly maintained. The error in the C_v-coefficient depends on the minimum value of p and the operating range of the movable weir. For the two most common weir types the error in C_v may be obtained from Section 4.2.4 and Figure 4.8. The method by which the coefficient errors have to be combined with other sources of error is shown in Appendix II.

4.2.3 Modular limit

In order to obtain modular flow, the modular limit, i.e. the submergence ratio H_2/H_1 for which the modular discharge is reduced by 1% owing to the increasing tailwater level, should not exceed 0.3.
Results of laboratory tests have shown that the drowned flow reduction factor, and thus the modular limit, depends on a number of factors, such as the value of the ratio H_1/L and the crest height above the tailwater channel bottom p_2. Since most energy loss occurs in the bottom eddy immediately downstream of the weir crest, little or no influence on the modular limit was observed if the side walls of the weir either terminated abruptly or flared under 1-to-6. Values of the average drowned flow reduction factor, f, (i.e.the factor whereby the equivalent modular discharge is decreased due to submergence) varies with H_2/H_1, as shown in Figure 4.6.

To prevent underpressure beneath the nappe influencing the discharge, the air pocket beneath the nappe should be fully aerated, for example by means of the two aeration grooves as shown in Figure 4.4.

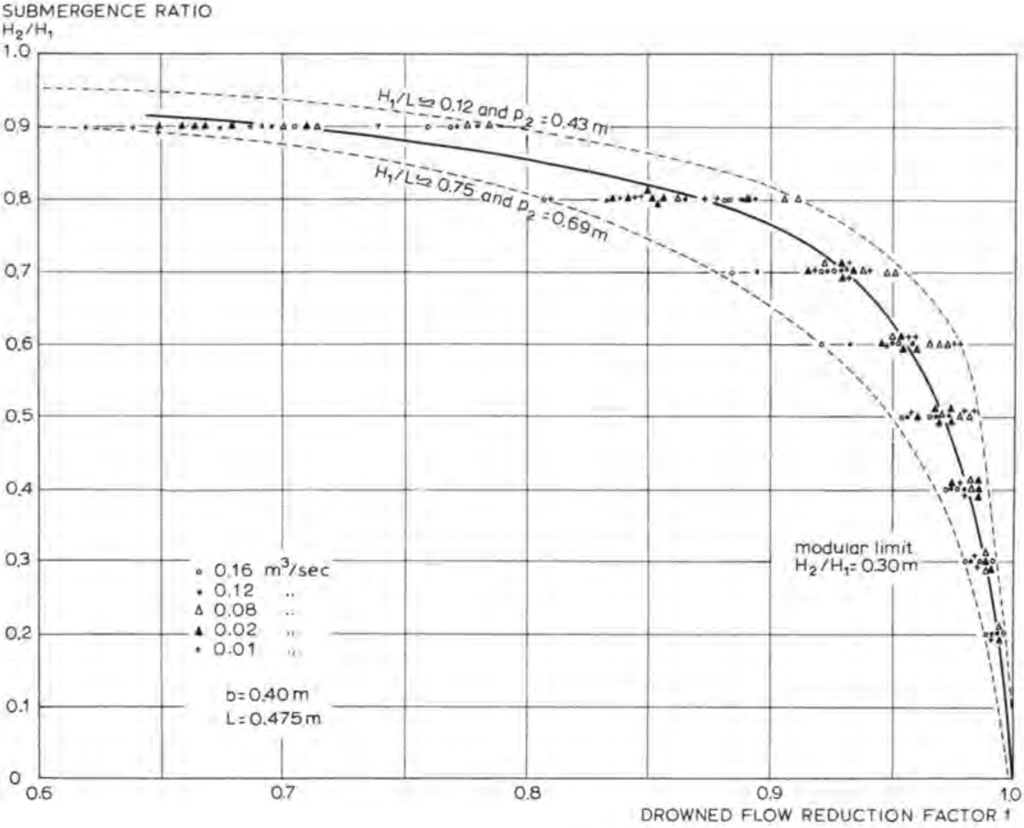

Fig.4.6. Drowned flow reduction factor for Romijn weir.

4.2.4 Commonly used weir dimensions

The reader will have noted that all dimensions of both the weir and its abutments are related to the maximum value selected for the total energy head over the weir crest (H_1max). The loss of head required for modular flow is also related to the total energy head as $\Delta h = h_1 - h_2 \geqslant 0.70\ H_1max$.

Since the limiting factor in most relatively flat irrigated areas is the available head for open canal and weir flow, the maximum value of h_1 is limited to a certain practical value which approximates 0.45 m. The length of the weir crest in the direction of flow consequently equals L=0.60 m, of which 0.50 m is straight and sloping 1:25 upward in the direction of flow and the remaining 0.10 m forms the rounded nose, its radius also being 0.10 m.

Theoretically any weir breadth greater or equal to 0.30 m may be used, but to obtain a degree of standardization in the structures of an irrigation project a limited number of breadths should be employed. It is often practicable to use a breadth not greater than b = 1.50 m, since a central handwheel can then be used to move the weir while the groove arrangement can be a relatively simple one consisting of steel blades sliding in narrow (0.01 m) grooves. If the breadth b exceeds 1.50 m, a groove arrangement as shown in Section 6.5.1 may be used. Examples of constructional drawings are shown in Figure 4.7.

If the Romijn weir is installed in accordance with Figure 4.6, which is the normal method of installation, the values for h_1 and p vary in such a way that

$$0.05 \text{ m} \leqslant h_1 \leqslant 0.45 \text{ m}$$
$$0.55 \text{ m} \leqslant p \leqslant 0.95 \text{ m}$$
$$0.60 \text{ m} \leqslant h_1 + p \leqslant 1.00 \text{ m}$$

Due to the variation of both h_1 and p, the approach velocity coefficient is not a function of h_1 alone, but ranges between the broken lines shown in Figure 4.8.

In irrigation practice it is confusing to work with several C_v-values for the same upstream head. Therefore the use of an average C_v-value, as a function of the upstream head h_1 only, is advised. It follows from Figure 4.8 that this average C_v-value may be expected to have an error of less than 1%. The discharge in m^3/s per metre width of weir crest can be calculated from Equation 4-4 and Figures 4.5 and 4.8. Values of q for each 0.01 m of head are presented in Table 4.1, Column 2.

An alternative method of installing the weir is to use no bottom slide. The movable weir is then lowered behind a drop in the channel bottom, this drop acting as a bottom terminal. With this method, the height of the weir crest above the bottom of approach channel is less than with the normal method of installation. Consequently, the approach velocity and thus the C_v-value is significantly higher.For a standard weir with a length of the weir crest in the direction of flow L = 0.60 m, values of p and h_1 range in such a way that:

$$0.05 \text{ m} \leqslant h_1 \leqslant 0.45 \text{ m}$$
$$0.15 \text{ m} \leqslant p \leqslant 0.55 \text{ m}$$
$$0.20 \text{ m} \leqslant h_1 + p \leqslant 0.60 \text{ m}$$

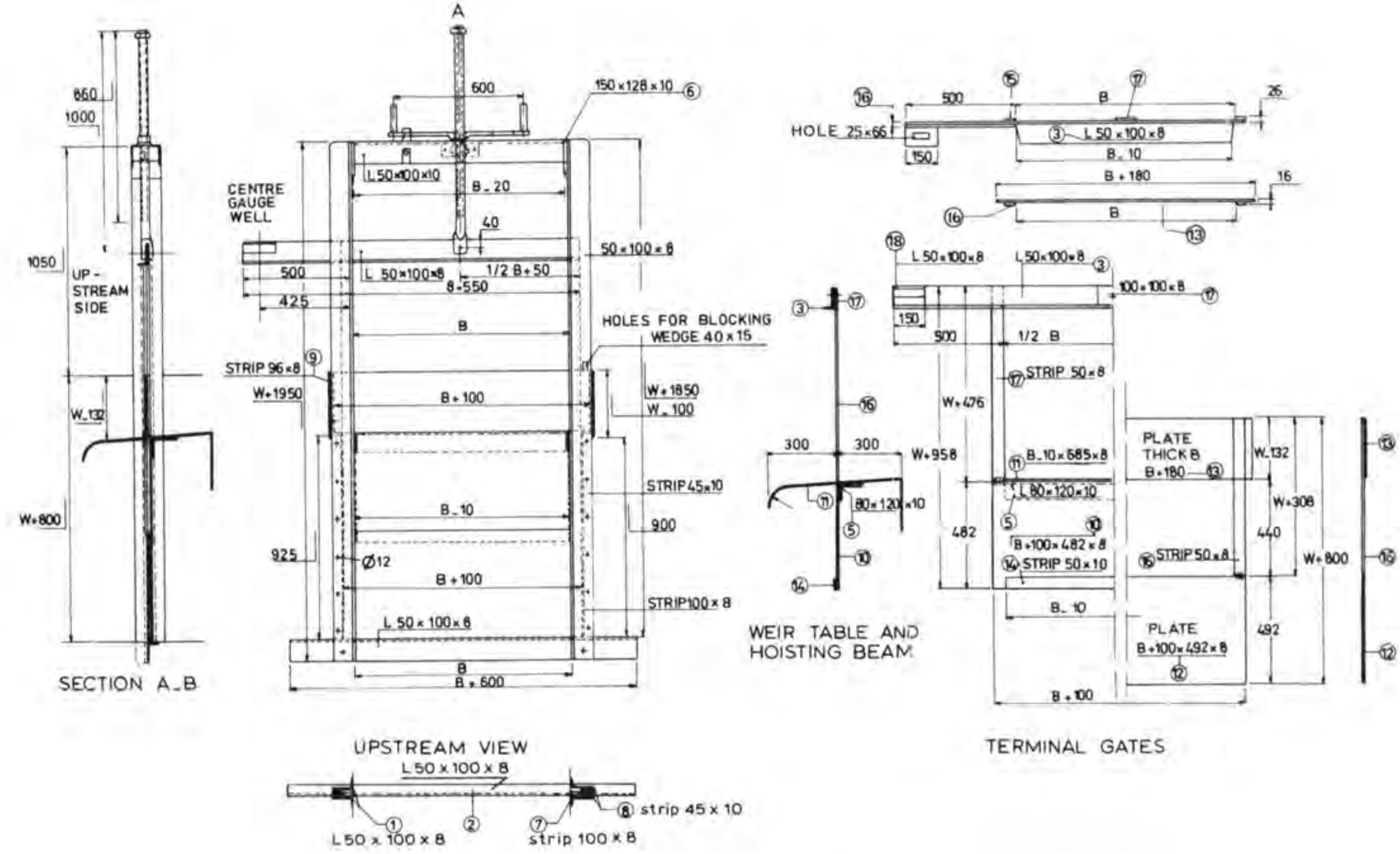

Fig.4.7. The Romijn movable measuring/regulating weir (dimensions in mm).

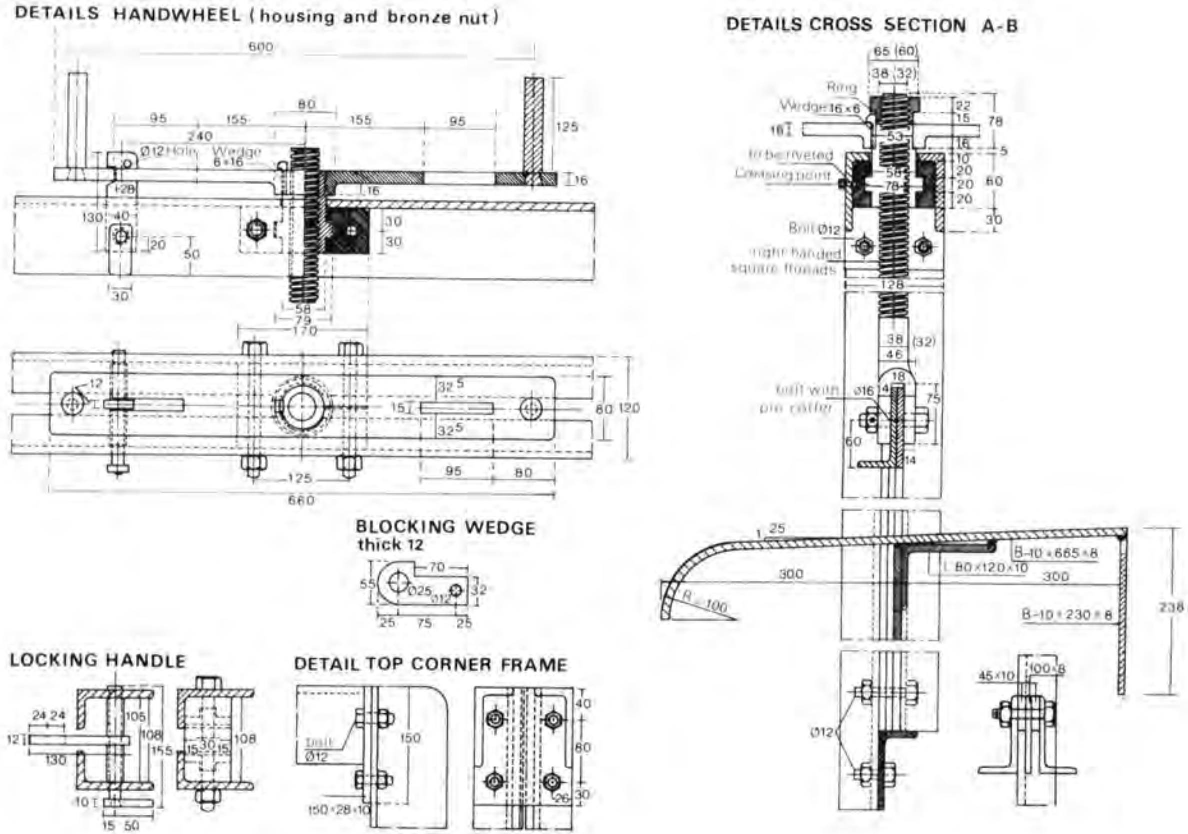

Fig.4.7 (cont.). The Romijn movable measuring/regulating weir (dimensions in mm).

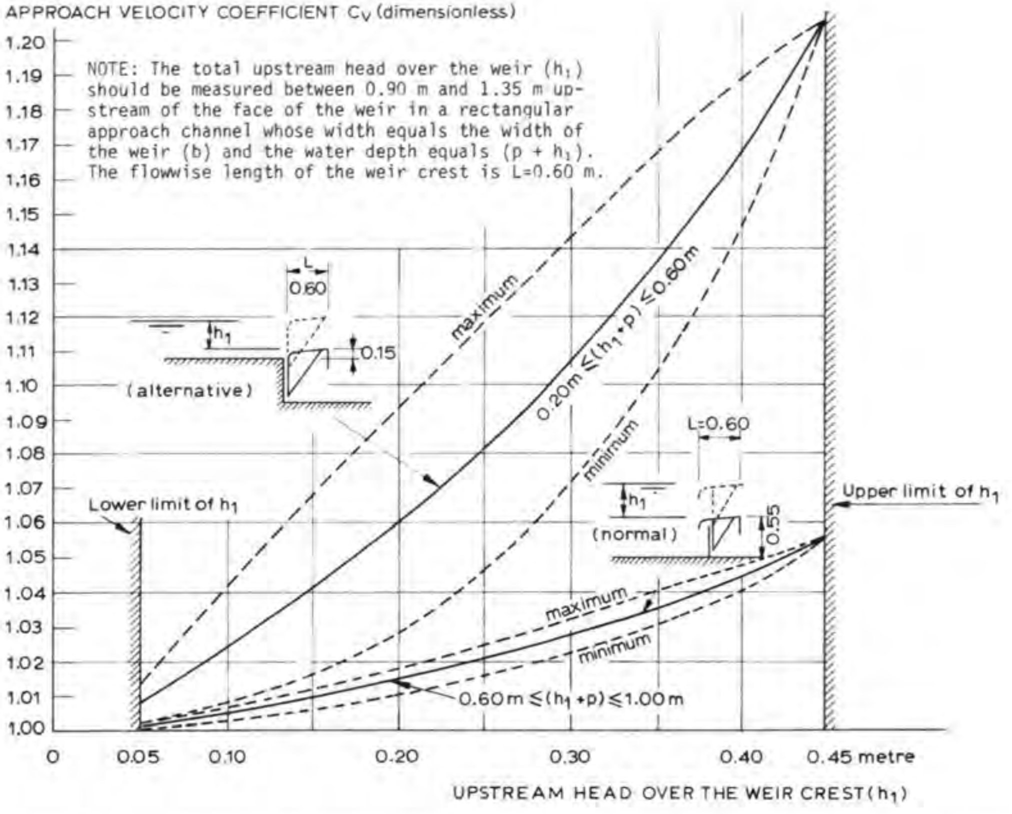

Fig.4.8. Approach velocity coefficient (C_v) as a function of the head over the movable weir crest (h_1).

Values of the ratio $C_d h_1/(h_1+p)$ thus range more widely than before, as do C_v values as a function of h_1. Minimum and maximum possible C_v-values are shown in Figure 4.8. Here, the average C_v-value to be used may be expected to have an error of less than 4%. Values of q for each 0.01 m of head may be calculated from Equation 4-4 and from Figures 4.5 and 4.8, and are presented in Table 4.1, Column 3.

4.2.5 Limits of application

The limits of application of a movable Romijn weir for reasonable accuracy are

a) The practical lower limit of h_1 is related to fluid properties and to the accuracy with which gauge readings can be made. The recommended lower limit of h_1 is 0.05 m or 0.08 L, whichever is greater.

TABLE 4.1: DISCHARGE PER METRE WIDTH OF WEIR CREST FOR THE MOVABLE ROMIJN MEASURING/REGULATING WEIR

Head h_1 metre	Method of installation: normal $0.55\ m < p < 0.95\ m$	Method of installation: alternative $0.15\ m < p < 0.55\ m$
	discharge q in m^3/s per metre width	
0.05	0.0195	0.0196
0.06	.0258	.0260
0.07	.0327	.0332
0.08	.0402	.0408
0.09	.0483	.0491
0.10	.0568	.0579
0.11	.0658	.0672
0.12	.0752	.0770
0.13	.0850	.0873
0.14	.0952	.0980
0.15	.106	.109
0.16	.117	.121
0.17	.128	.133
0.18	.140	.145
0.19	.152	.158
0.20	.164	.171
0.21	.176	.185
0.22	.189	.199
0.23	.202	.213
0.24	.216	.228
0.25	.230	.243
0.26	.244	.259
0.27	.258	.275
0.28	.273	.292
0.29	.288	.310
0.30	.304	.327
0.31	.319	.345
0.32	.336	.365
0.33	.353	.384
0.34	.370	.404
0.35	.388	.426
0.36	.407	.448
0.37	.425	.470
0.38	.444	.493
0.39	.464	.517
0.40	.484	.541
0.41	.504	.566
0.42	.525	.592
0.43	.547	.619
0.44	.569	.646
0.45	.591	.675

NOTE: The number of corresponding figures given in the columns for discharge should not be taken to imply a corresponding accuracy of the values given, but only to assist in the interpolation and rounding off for various values of head

b) To reduce the influence of boundary layer effects at the sides of the weir, the weir breadth b should not be less than 0.30m nor less than the maximum value of H_1.

c) The height of the weir crest above the bottom of the approach channel should not be less than 0.15 m nor less than 0.33 H_1max.

d) To obtain a sensibly constant discharge coefficient, the ratio H_1/L should not exceed 0.75.

e) The submergence ratio H_2/H_1 should not exceed 0.30 to obtain modular flow.

4.3 Triangular broad-crested weir

4.3.1 Description

On natural streams and irrigation canals where it is necessary to measure a wide range of discharges, a triangular control has several advantages. Firstly it provides a large breadth at high flows so that the backwater effect is not excessive. Secondly, at low flows the breadth is reduced so that the sensitivity of the weir remains acceptable. These advantages, combined with the fact that a triangular control section has a critical depth equal to 0.8 H_1 so that the weir can take a high submergence before its capacity is affected, makes this weir type an interesting flow measuring device. A description of the weir, although slightly different in shape, was published in 1963 by R.J.BOS[1].

The weir profile in the direction of flow shows an upstream rounded nose with a minimum radius r equal to 0.11 H_1max to prevent flow separation.For the economic design of field structures, however, a value r=0.20 H_1max is recommended. To obtain

[1] *Bos tested a weir type with 1-to-25 sloping crest similar to that of the Romijn weir. Since sufficient data are not available, however, no further details on this weir type will be given.*

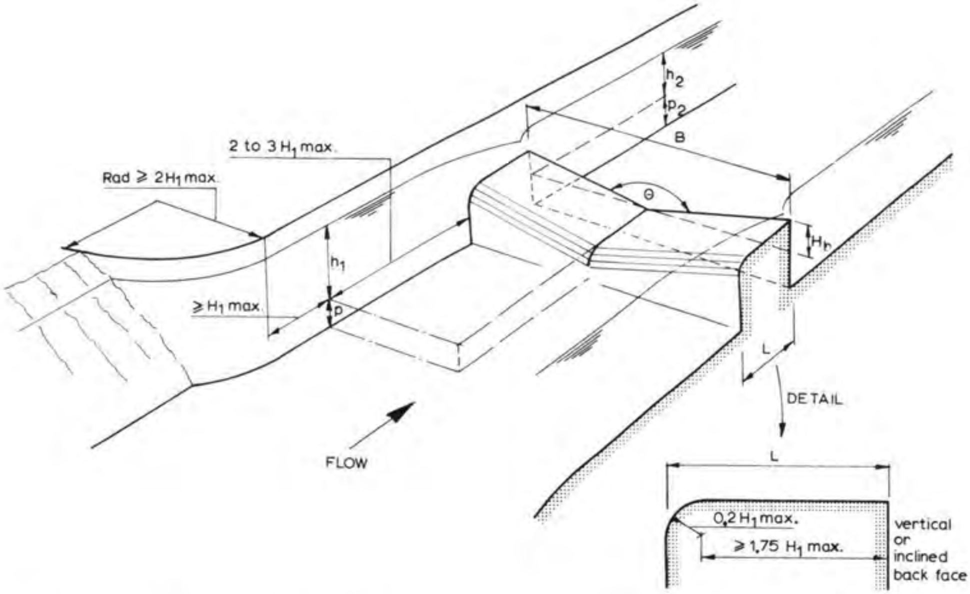

Fig.4.9. Definition sketch for triangular broad-crested weir.

Photo 2. Triangular broad-crested weir.

a sensibly hydrostatic pressure distribution above the weir crest, the length of the horizontal portion of the crest should not be less than 1.75 H_1max. To obtain a favourable (high) discharge coefficient the crest length L should be close to the permissible minimum. The weir should be placed between vertical abutments and be at right angles to the direction of flow. The upstream head over the weir crest should be measured in the rectangular approach channel at a distance of between two and three times H_1max upstream from the weir face (see also Chapter 2).

Essentially, there are two types of triangular broad-crested weirs:

(i) If the maximum weir width is unrestricted (i.e. if the available weir width is such that in combination with a selected weir notch angle θ, the water level in the control section does not reach the intersection of side slopes and vertical abutments), the weir type is referred to as "less-than-full". For this type of weir, one head-discharge equation applies for the entire operating range from H_1min to H_1max.

(ii) If the weir is installed in a channel with restricted width, the water level at the control section may sometimes rise above the top of the side slopes. This weir type is referred to as "over-full", and somewhere in between H_1min and H_1max we have to change over from the head-discharge equation for a triangular control section to that of a truncated triangular control section. As shown in Sections 1.9.3 and 1.9.4, critical depth in a triangular control section equals $y_c = 0.80\ H_1$, so that the weir is just full if $H_b = 0.80\ H_1$ or $H_1 = 1.25\ H_b$, where H_b denotes the difference in elevation between the top of the side slopes and the vertex of the weir notch (see Fig.4.9) and equals $H_b = \frac{1}{2}\ B \cot \theta/2$.

4.3.2 Evaluation of discharge

As discussed already in Section 4.3.1 we can distinguish between two different cases of head-discharge relationships, as follows

"Less-Than-Full" ($H_1 \leqslant 1.25\ H_b$)

In this case the basic-head-discharge equation for a triangular control section is applicable, which, according to Section 1.9.3, reads

$$Q = C_d C_v \frac{16}{25} \left[\frac{2}{5}\, g\right]^{0.50} \tan\frac{\theta}{2}\, h_1^{2.50} \tag{4-5}$$

where the discharge coefficient may be read as a function of the ratio H_1/L from Figure 4.10. The approach velocity coefficient may be read from Figure 1.12 as a function of the dimensionless ratio

$$C_d A^* / A_1 = (C_d h_1^2 \tan\frac{\theta}{2})/B(h_1 + p)$$

"Over-Full" ($H_1 \geqslant 1.25\ H_b$)

In this case the basic head-discharge equation for a truncated triangular control section applies (see Section 1.9.4)

$$Q = C_d C_v \frac{2}{3} \left[\frac{2}{3}\, g\right]^{0.50} B(h_1 - \tfrac{1}{2}H_b)^{1.50} \tag{4-6}$$

where values of C_d again may be read from Figure 4.10 as a function of the ratio H_1/L. It should be noted that if H_1/L exceeds 0.50 the weir cannot be termed broad-crested. If ratios $H_1/L \geqslant 0.50$ are used, the overfalling nappe should be fully aerated, and it should be noted that the modular limits given in Section 4.3.2 will decrease significantly with increasing H_1/L-values. C_v-values may be obtained from Figure 1.12 as a function of the dimensionless ratio $C_d A^* / A_1 = C_d(h_1 - \tfrac{1}{2}H_b)/(h_1 + p)$.

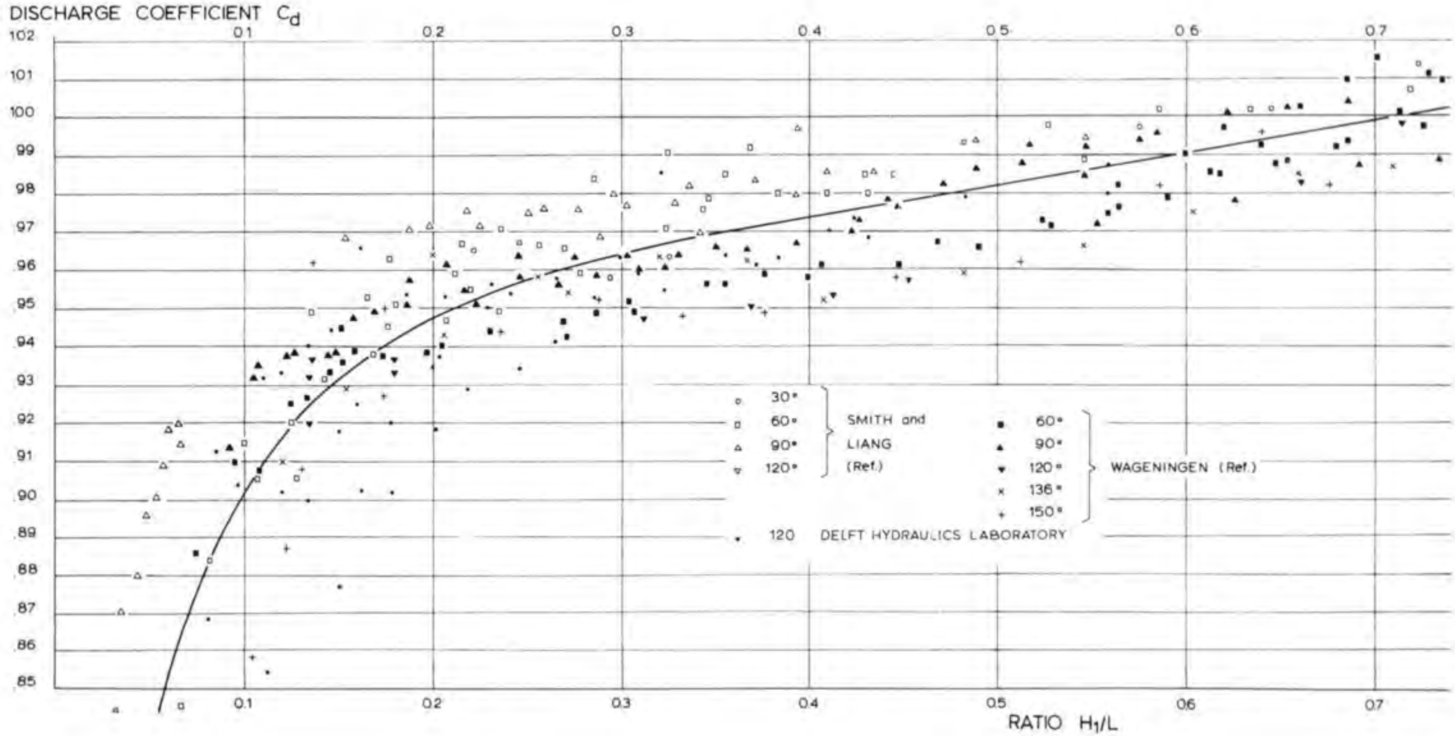

Fig.4.10. Discharge coefficient as a function of H_1/L.

The error in the discharge coefficient (including C_v) of a round-nose triangular broad-crested (truncated) weir, which has been constructed with reasonable care and skill, may be deduced form the equation

$$X_c = \pm 2(21 - 20\ C_d) \text{ per cent} \tag{4-7}$$

The method by which this error has to be combined with other sources of error is shown in Appendix II.

4.3.3 Modular limit

a) "Less-than-full" case

The modular limit,or that submergence ratio H_2/H_1 which produces a 1% reduction in the equivalent modular discharge, depends on a number of factors, such as the value of the ratio H_1/H_b and the slope of the downstream weir face. Results of various tests by the Hydraulic Laboratory, Agricultural University, Wageningen, 1964-1971, and by C.D.Smith and W.S.Liang (1969), showed that for the less-than-full type weir ($H_1/H_b \leqslant 1.25$) the drowned flow reduction factor (f) (i.e. the factor whereby the equivalent modular discharge is decreased due to submergence), varies with H_2/H_1, as shown in Figure 4.11. The modular limit for weirs with a vertical back-face equals $H_2/H_1 = 0.80$. This modular limit may be improved by constructing the downstream weir face under a slope of 1-to-4 (see also Fig.4.2) or by decreasing p_2.

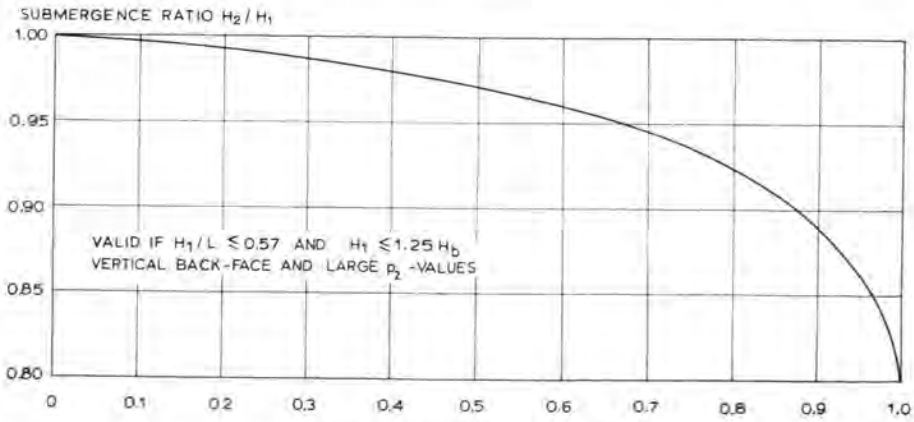

Fig.4.11. Drowned flow reduction factor as a function of H_2/H_1.

b) "Over-full-case"

No systematic research has been done on the evaluation of the modular limit of "over-full" type weirs. It may be expected, however, that the modular limit will change gradually to that of a broad-crested weir as described in Section 4.1.1 if the ratio H_1/H_b increases significantly above 1.25.

4.3.4 Limits of application

The limits of application of the triangular broad-crested weir and truncated weir for reasonable accuracy are:

a) The practical lower limit of h_1 is related to the magnitude of the influence of fluid properties, boundary roughness, and the accuracy with which h_1 can be determined. The recommended lower limit is 0.06 m or 0.05 times L, whichever is greater.

b) The weir notch angle θ should not be less than 30°.

c) The recommended upper limit of the ratio $H_1/p = 3.0$, while p should not be less than 0.15 m.

d) The limitation on H_1/L arises from the necessity of ensuring a sensible hydrostatic pressure distribution at the control section. Values of the ratio H_1/L should therefore not exceed 0.50 (0.70 if sufficient head is available).

e) The breadth B of a truncated triangular broad-crested weir should not be less than 0.30 m, nor less than H_1max, nor less than L/5.

4.4 Broad-crested rectangular profile weir

4.4.1 Description

From a constructional point of view the broad-crested rectangular profile weir is a rather simple measuring device. The weir block shown in Figure 4.12 has a truly flat and horizontal crest. Both the upstream and downstream weir faces should be smooth vertical planes. The weir block should be placed in a rectangular approach channel perpendicular to the direction of flow. Special care should be taken that the crest surface makes a straight and sharp 90-degree intersection with the upstream weir face.

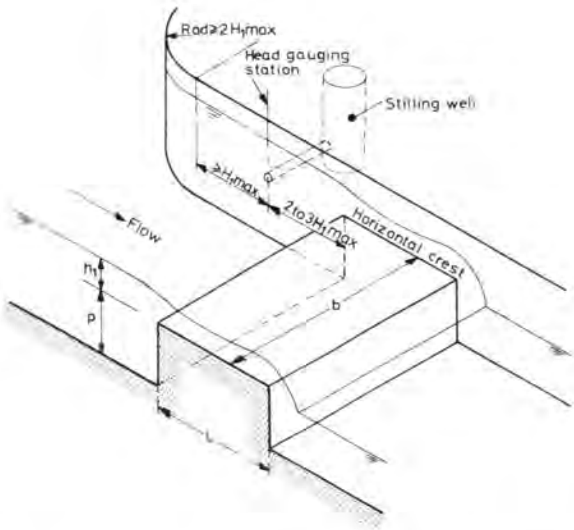

Fig.4.12. Broad-crested rectangular profile weir (after BSI, 1969).

The upstream head over the weir crest should be measured in a rectangular approach channel as shown in Figure 4.12. The head measurement station should be located at a distance of between two and three times H_1max upstream from the weir face.

Depending on the value of the ratio H_1/L, four different flow regimes over the weir may be distinguished:

a) $H_1/L < 0.08$

The depth of flow over the weir crest is such that sub-critical flow occurs above the crest. The control section is situated near the downstream edge of the weir crest and the discharge coefficient is determined by the resistance characteristics of the crest surface. Over this range the weir cannot be used as a measuring device.

b) $0.08 \leq H_1/L \leq 0.33$

At these values of H_1/L a region of parallel flow will occur somewhere midway above the crest. The water surface slopes downward at the beginning of the crest and again near the end of the crest. From a hydraulic point of view the weir may be described as broad-crested over this range of H_1/L only. The control section is located at the end of the section where parallel flow occurs. Provided that the approach velocity has no significant influence on the shape of the separation bubble (see Fig.4.13) the discharge coefficient has a constant value over this H_1/L-range.

c) $0.33 < H_1/L <$ about 1.5 to 1.8

In this range of H_1/L values the two downward slopes of the water surface will merge and parallel flow will not occur above the crest. Streamline curvature at the control has a significant positive effect on the discharge, resulting in higher C_d-values. In fact the weir cannot be termed broad-crested over this range but should be classified as short-crested. The control section lies at station A above the separation bubble shown in Figure 4.13.

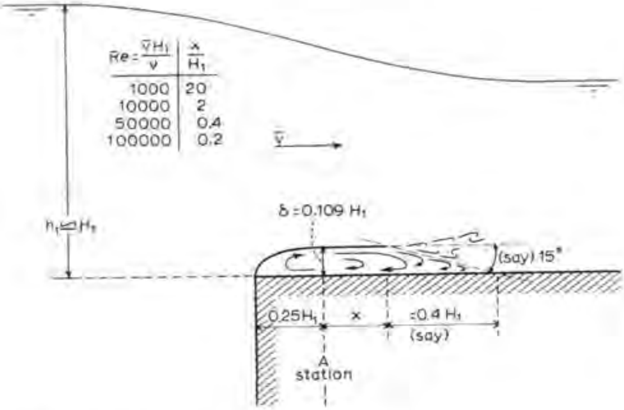

Fig.4.13. Assumed structure of entry-edge separation bubble as a function of H_1 and the Reynolds number (after G.W.Hall, 1962).

d) $H_1/L >$ about 1.5

Here the ratio H_1/L has such a high value that the nappe may separate completely from the crest and the weir in fact acts as a sharp-crested weir. If H_1/L becomes larger than about 1.5 the flow pattern becomes unstable and is very sensitive to the "sharpness" of the upstream weir edge. For H_1/L values greater than 3.0 the flow pattern becomes stable again and similar to that over a sharp-crested measuring weir (see Chapter 5).

To prevent underpressures beneath the overflowing nappe from influencing the head-discharge relationship, the air pocket beneath the nappe should be fully aerated whenever H_1/L exceeds 0.33. Dimensions of the aeration duct should be determined as shown in Section 1.14.

The modular limit, or that submergence ratio H_2/H_1 which produces a 1% reduction from the equivalent modular discharge, depends on the ratio H_1/L. If $0.08 \leq H_1/L \leq 0.33$, the modular limit may be expected to be 0.66. If $H_1/L = 1.5$, however, the modular limit is about 0.38 and over the range $0.33 < H_1/L < 1.5$ the modular limit may be obtained by linear interpolation between the given values. Provided that the ratio $h_1/(h_1 + p) \leq 0.35$, Figure 4.18, too, can be used to obtain information on the reduction of modular flow due to submergence.

4.4.2 Evaluation of discharge

The basic head-discharge equation derived in Section 1.9.1 can be used to evaluate the flow over the weir. This equation reads

$$Q = C_d C_v \frac{2}{3}\left[\frac{2}{3} g\right]^{0.50} b h_1^{1.50} \qquad (4\text{-}8)$$

where the approach velocity coefficient C_v may be read from Figure 1.12 as a function of the dimensionless ratio $C_d A^*/A_1 = C_d h_1/(h_1 + p)$. Experimental results have shown that under normal field conditions the discharge coefficient is a function of the two ratios h_1/L and $h_1/(h_1 + p)$. As mentioned in the previous section, the discharge coefficient remains constant if there is parallel flow at the control section and if the approach velocity does not influence the shape of the separation pocket. Hence C_d remains fairly constant if both

$$0.08 < h_1/L \leq 0.33 \quad \text{and}$$

$$h_1/(h_1 + p) \leq 0.35$$

The average value of C_d within these limits is 0.848 and is referred to as the basic discharge coefficient. If one of the limits is not fulfilled the basic coefficient should be multiplied by a coefficient correction factor F which is always greater than unity since both streamline curvature at the control section and a depression of the separation bubble have a positive influence on weir flow. Values of F as a function of h_1/L and $h_1/(h_1 + p)$ can be read from Figure 4.14.

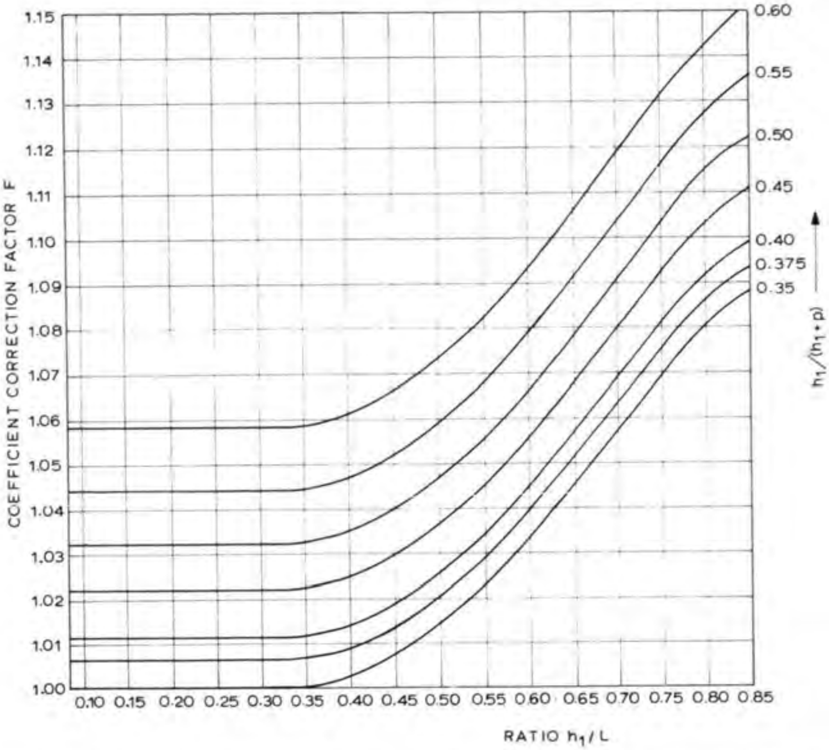

Fig.4.14. Coefficient correction factor F as a function of h_1/L and $h_1/(h_1+p)$ (adapted from J.SINGER, 1964).

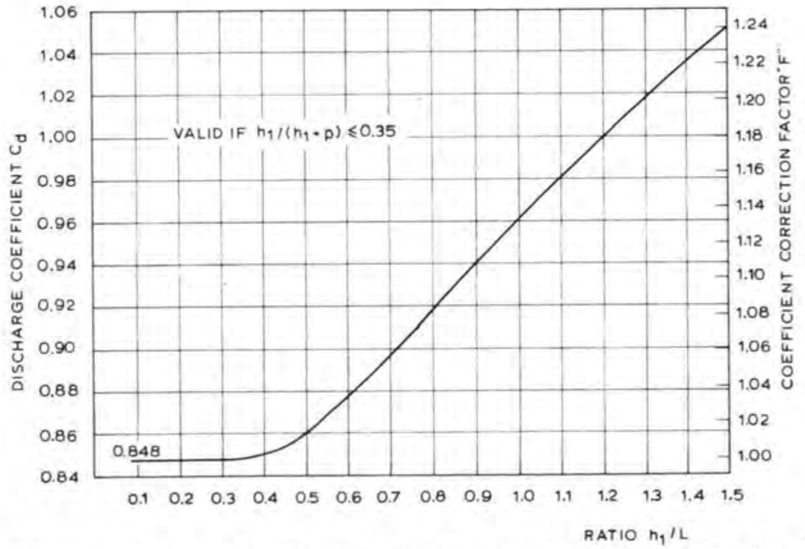

Fig.4.15. C_d-values and F-values as a function of h_1/L, provided that $h_1/(h_1 + p) \leq 0.35$.

There are not enough experimental data available to give the relation between C_d and the ratios h_1/L and $h_1/(h_1 + p)$ with satisfactory accuracy over the entire range. If, however, the influence of the approach velocity on C_d is negligible, (i.e. if $h_1/(h_1 + p) \leq 0.35$), C_d-values can be read as a function of h_1/L from Figure 4.15.

The error in the discharge coefficient (including C_v) of a rectangular profile weir, constructed with reasonable care and skill, may be obtained from the equation

$$X_c = \pm (10F - 8) \text{ per cent} \tag{4-9}$$

To obtain this accuracy the structure should be properly maintained. The method by which this error should be combined with other sources of error is shown in Appendix II.

4.4.3 Limits of application

The limits of application of the rectangular profile weir essential for reasonable accuracy are:

a) The practical lower limit of h_1 is related to the magnitude of the influence of fluid properties, to boundary roughness, and to the accuracy with which h_1 can be determined. The recommended lower limit of h_1 is 0.06 m or 0.08 times L, whichever is greater.

b) The recommended upper limit of the ratio $h_1/(h_1 + p) = 0.60$, while p should not be less than 0.15 m.

c) The ratio h_1/L should not be less than 0.08 and should not exceed 1.50. If, however, the influence of the approach velocity on C_d is significant (i.e. if $h_1/(h_1 + p) > 0.35$), C_d-values are only available provided that the ratio $h_1/L \leq 0.85$.

d) The breadth b of the weir should not be less than 0.30 m nor less than $h_1$max, nor less than L/5.

e) The air pocket beneath the nappe should be fully aerated whenever the ratio h_1/L exceeds 0.33.

4.5 Faiyum weir

4.5.1 Description

The Faiyum weir is essentially a rectangular profile weir with a crest shape identical to that described in Section 4.4. The only significant difference is that with the latter weir two-dimensional weir flow was assured by placing the weir block in a rectangular approach channel. In contrast, the Faiyum weir consists of a rectangular control section placed in a "wall" across an open channel of arbitrary cross-section. The weir originates from the Faiyum Province in Egypt and a detailed description of it was given in 1923 by A.D.Butcher.

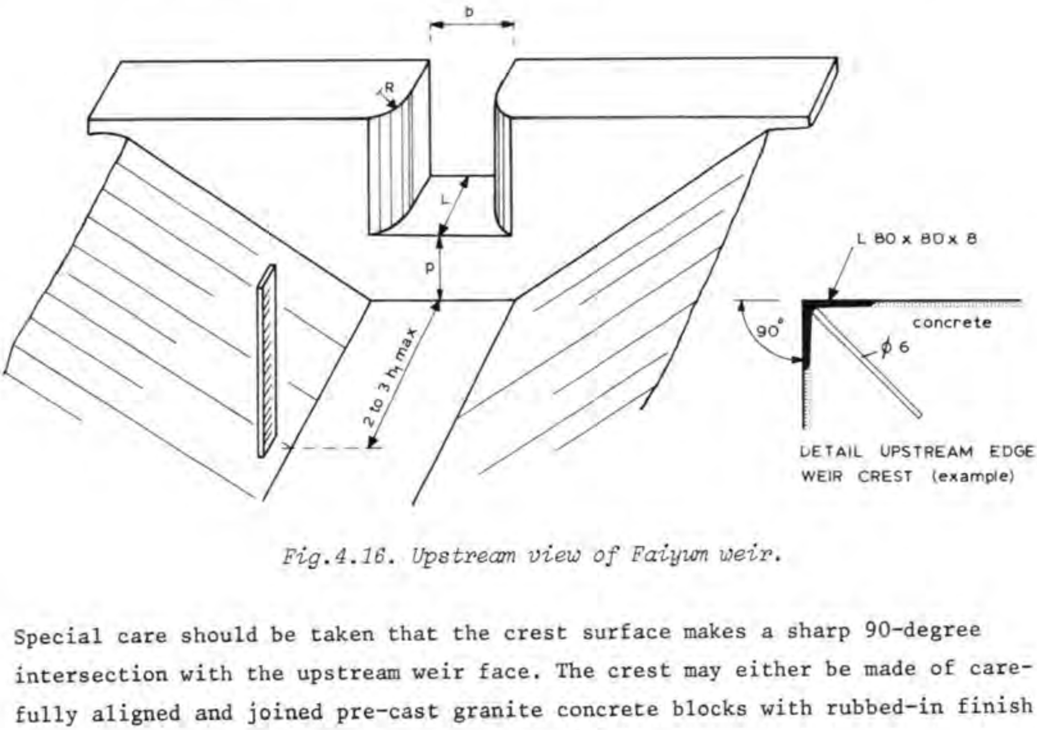

Fig.4.16. Upstream view of Faiyum weir.

Special care should be taken that the crest surface makes a sharp 90-degree intersection with the upstream weir face. The crest may either be made of carefully aligned and joined pre-cast granite concrete blocks with rubbed-in finish or it may have a metal profile as upstream edge.

Although one is free to instal the Faiyum weir across an approach channel of arbitrary cross-section, care should be taken that the approach velocity is sufficiently low so that it does not influence the contraction at the upstream edge of the weir crest. For this to occur, the area ratio bh_1/A_1 should not exceed 0.35 for all values of h_1. A_1 denotes the cross-sectional area of the approach channel at the head measurement station. This head measurement station should be located a distance of between two and three times $h_1$max upstream from the weir face.

The upstream corners of the vertical and parallel side walls are known to have a significant influence on both contraction of the weir flow and the boundary layer displacement thickness of the side walls.

Both effects make it impossible to apply the basic two-dimensional head-discharge equation to the full width of the control section unless the upstream corners of the side walls are dimensioned in such a way that the combined effects of lateral contraction and side-wall boundary layers are counterbalanced.

One way of ensuring that the weir discharge is proportional to the breadth b of the control section is to make the radius R of the upstream corners dependent on the weir breadth b and the crest length L. As a result of his experimental research work on the Faiyum weir, Butcher produced a diagram giving the radius R as a function of the weir breadth b for the most common crest length (L = 0.50 m) of the weir. Figure 4.17 shows a dimensionless rendering of Butcher's diagram. The two dotted curves in the figure show the eventual limits of variation of the radius R, corresponding to a maximum difference of ± 1% in the two-dimensional weir discharge.

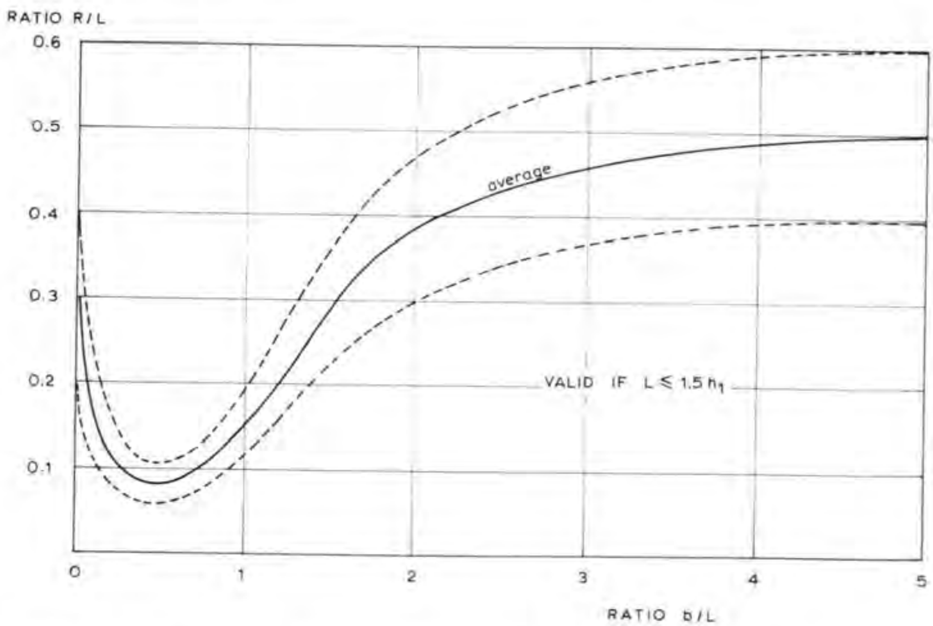

Fig.4.17. Radius of upstream corner of side wall as a function of b and L (adapted from A.D.BUTCHER, 1923).

To prevent underpressure beneath the overflowing nappe influencing the head-discharge relationship, the air pocket beneath the nappe should be fully aerated.

4.5.2 Modular limit

The modular limit, or the submergence ratio H_2/H_1 that produces a 1% reduction in the equivalent modular discharge of the Faiyum weir, is a function of the ratio H_1/L. If $0.08 \leqslant H_1/L \leqslant 0.33$ the weir acts as a broad-crested weir and the modular limit may be expected to be 0.66. If streamline curvature occurs at the control section, however, the weir becomes more sensitive to submergence and consequently has a lower modular limit, which may be obtained from Figure 4.18.

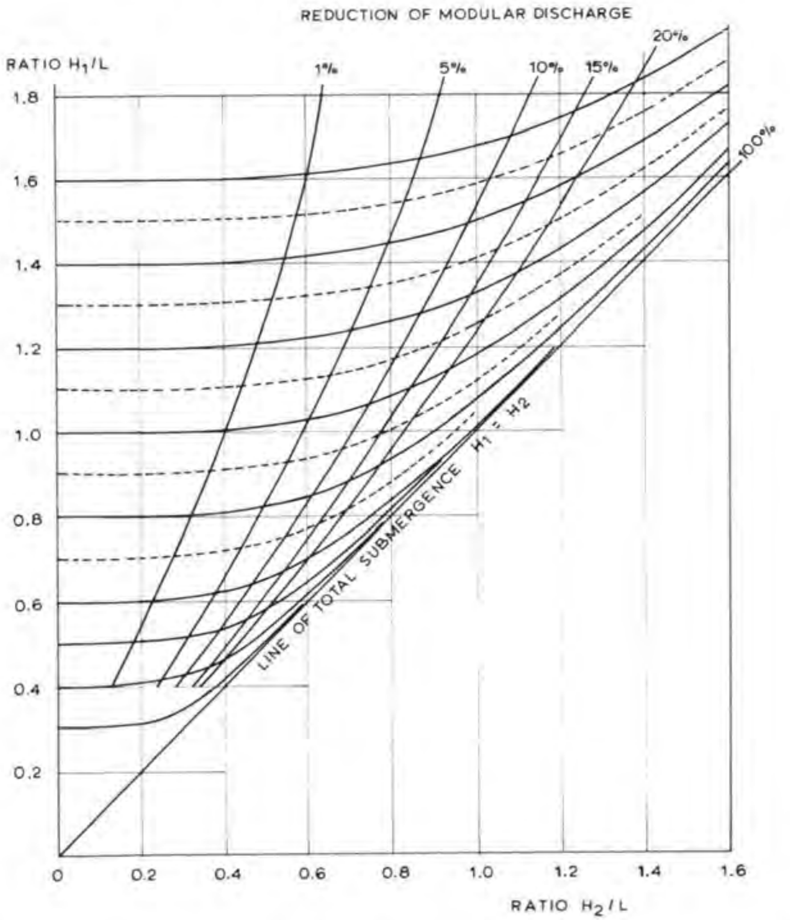

Fig.4.18. Diagram showing both reduction of modular discharge and variation of H_1/L due to submergence (adapted from A.D.Butcher, 1923).

We can read from Figure 4.18 that if, for example, $H_1/L = 1.0$ the modular limit equals 0.40 and that if, for this H_1/L value, the submergence ratio increases to $H_2/H_1 = 0.71$, the modular discharge is reduced by 10%. Figure 4.18 can also be used for the rectangular profile weirs described in Section 4.4, provided that the area ratio bh_1/A_1 does not exceed 0.35.

4.5.3 Evaluation of discharge

The basic head-discharge equation derived in Section 1.9.1 for modular flow through a rectangular control section can be used to evaluate the weir flow. This equation reads

$$Q = C_d C_v \frac{2}{3} \left[\frac{2}{3} g\right]^{0.50} bh_1^{1.50} \qquad (4\text{-}10)$$

where values of C_d are similar to those shown in Figure 4.15 and where the approach velocity coefficient C_v can be obtained from Figure 1.12 as a function of the ratio $C_d A^* / A_1 = C_d bh_1/A_1$. The reader will note that due to the restriction on the area ratio bh_1/A_1, C_v has a maximum value of 1.035.

The accuracy of the discharge coefficient of the Faiyum weir is unknown. A well maintained structure, however, constructed with reasonable care and accuracy has an acceptable accuracy for field conditions. The percentage error in the product $C_d C_v$ is expected to be less than 5% over the entire range of h_1/L. The method by which this percentage error should be combined with other sources of error is shown in Appendix II.

4.5.4 Limits of application

The limits of application of the Faiyum weir for reasonable accuracy are:

a) The upstream corners of the parallel and vertical side walls should be selected in accordance with Figure 4.17.

b) The practical lower limit of h_1 is related to the magnitude of the influence of fluid properties, to boundary roughness, and to the accuracy with which h_1 can be determined. The recommended lower limit is 0.06 m.

c) The area ratio bh_1/A_1 should not exceed 0.35.

d) The breadth of the control section should not be less than 0.05 m.

e) The ratio h_1/L should not be less than 0.08 and should not exceed 1.6.

f) The airpocket beneath the nappe should be fully aerated whenever h_1/L exceeds 0.33.

4.6 Selected list of references

1. AGRICULTURAL UNIVERSITY WAGENINGEN: Various laboratory reports on the V-notch broad-crested weir. Hydraulic Laboratory Agric.Univ.,Wageningen.

2. BOS, M.G.: The Romijn movable measuring/regulating weir. Publ.in joint FAO-ICID publication on small hydraulic structures in irrigation distribution systems. Irrigation and Drainage Paper, No.26.

3. BOS, R.J.: De lange meetoverlaat met V-vormige kruin. Polytechnisch Tijdschrift No.7B, 1964 pp.254-259; No.8B, pp.301-310.

4. BRITISH STANDARDS INSTITUTION: Methods of measurement of liquid flow in open channels. British Standard 3680, Part 4B, Long base weirs. London 1969.

5. BUTCHER, A.D.: Submerged weirs and standing wave weirs. Government Press, Cairo, 1923. 17 pp.

6. DELFT HYDRAULICS LABORATORY: Invloed van stromingsvorm van een Romijn meetoverlaat op de afvoer-coefficient. Report Hydraulics Laboratory, Delft, 1953.

7. HALL, G.W.: Analytic determination of the discharge characteristics of broad-crested weirs using boundary layer theory. Proceedings of the Inst.of Civil Engineers, 1967. Vol.22, June, Paper 6607. pp.177-190.

8. HARRISON, A.J.M.: The streamlined broad-crested weir. Proceedings of the Inst.of Civil Engineers, 1967. Dec. Vol.38, pp.657-678.

9. HORTON, R.E.: Weir experiments, Coefficients and Formulas. Water Supply Paper 200, Geological Survey, U.S.Department of the Interior, Washington D.C. 1907.

10. ISO, TC 113-WG 2, THE NETHERLANDS: A reference document on the round-nose broad-crested weir. Wageningen, Agric.Univ.Hydraul.Laboratory, May 1967, unpubl.

11. KEUTNER, C.: Strömungsvorgänge an breitkronigen Wehrkörpern Einlaufbauwerken. Der Bauingenieur, Vol.15, 1934, p.366.

12. LELIAVSKY, S.: Irrigation Engineering: Siphons, Weirs and Locks. Design textbook in Civil Engineering, Vol.II, Chapman and Hall Ltd., London 1965.

13. PITLO, R.H., and SMIT, M.: Discussion to reference 17. Proc.of the Am. Soc.of Civil Engineers, Irrigation and Drainage Division,R3, Sept.1970, pp. 364-369.

14. ROMIJN, D.G.· Een regelbare meetoverlaat als tertiaire aftapsluis. De Waterstaatsingenieur, Bandung, 1932, Nr.9.

15. ROMIJN, D.G.: Meetsluizen ten behoeve van irrigatiewerken. Handleiding door "De Vereniging van Waterstaats Ingenieurs in Nederlandsch Indië, 1938, pp.58.

16. SINGER, J.: Square-edged broad-crested weir as a flow measuring device. Water and Water Engineering, June 1964, Vol.68, Nr.820, pp.229-235.

17. SMITH, C.D., and LIANG, W.S.: Triangular broad-crested weir. Proc.of the Am.Soc.of Civil Engineers, Irrigation and Drainage Division, IR 4, Dec. 1969, Paper 6954. pp.493-502 and closure in IR 4, Dec.1971, pp.637-640.

18. VLUGTER, H.: De regelbare meetoverlaat. De Waterstaatsingenieur, Bandung, 1940, Nr.10.

19. WOODBURN, J.G.: Tests of broad-crested weirs. Proc.of the Am.Soc.of Civil Engineers, Vol.56, 1930, Sept.,No.7,pp.1583-1612.Also:Trans.ASCE,Vol.96,1932, Paper 1797, pp.387-408.

5 Sharp-crested weirs

Classified unter the term "sharp-crested" or "thin-plate" weirs are those overflow structures whose length of crest in direction of flow is equal to or less than two millimetres.The weir plate should be smooth and plane,especially on the upstream face, while the crest surface and the sides of the notch should have plane surfaces which make sharp 90-degree intersections with the upstream weir face. The downstream edge of the notch should be bevelled if the weir plate is thicker than two millimetres. The bevelled surfaces should make an angle of not less than 45-degrees with the surface of a rectangular notch and an angle of not less than 60 degrees if the throat section is non-rectangular (see Fig.5.1).

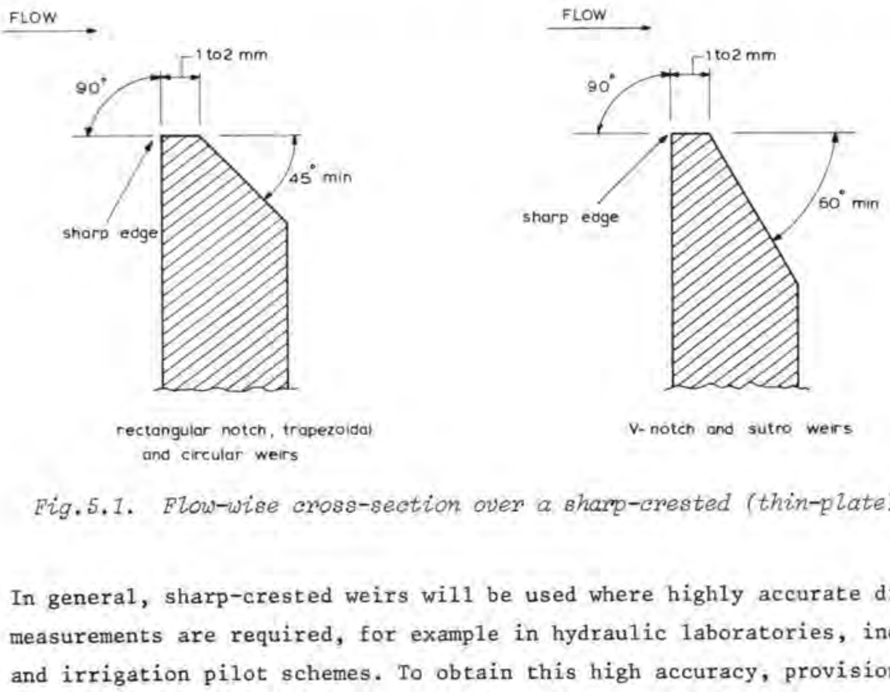

Fig.5.1. Flow-wise cross-section over a sharp-crested (thin-plate) weir.

In general, sharp-crested weirs will be used where highly accurate discharge measurements are required, for example in hydraulic laboratories, industry, and irrigation pilot schemes. To obtain this high accuracy, provision should be made for ventilating the nappe to ensure that the pressure on the sides and surfaces of the nappe is atmospheric (see Section 1.14). The downstream water level should be low enough to ensure that it does not interfere with the ventilation of the air pocket beneath the nappe. Consequently, the required loss of head for modular flow will always exceed the upstream head over the weir crest (h_1) by about 0.05 m, which is one of the major disadvantages of a sharp-crested weir.

5.1 Rectangular sharp-crested weirs

5.1.1 Description

A rectangular notch, symmetrically located in a vertical thin (metal) plate which is placed perpendicular to the sides and bottom of a straight channel, is defined as a rectangular sharp-crested weir. Rectangular sharp-crested weirs comprise the following three types:

a) "Fully contracted weirs", i.e. a weir which has an approach channel whose bed and walls are sufficiently remote from the weir crest and sides for the channel boundaries to have no significant influence on the contraction of the nappe.

b) "Full width weirs", i.e. a weir which extends across the full width of the rectangular approach channel ($B/b = 1.0$). In literature this weir is frequently referred to as a rectangular suppressed weir or Rehbock weir.

c) "Partially contracted weir", i.e. a weir the contractions of which are not fully developed due to the proximity of the walls and/or the bottom of the approach channel.

In general, all three types of rectangular weirs should be located in a rectangular approach channel. If, however, the approach channel is sufficiently large $\{B(h_1 + p) \geqslant 10bh_1\}$ to render the velocity of approach negligible, and the weir is fully contracted, the shape of the approach channel is unimportant. Consequently, the fully contracted weir may be used with non-rectangular approach channels. The sides of the rectangular channel above the level of the crest of a full-width weir should extend at least $0.3\ h_1max$ downstream of the weir crest.

The fully contracted weir may be described by the limitations on $B-b$, b/B, h_1/p, h_1/b, h_1, b, and p as shown in Table 5.1.

TABLE 5.1. LIMITATIONS OF A RECTANGULAR SHARP-CRESTED FULLY CONTRACTED WEIR

$B - b$	$\geqslant 4\ h_1$
h_1/p	$\leqslant 0.5$
h_1/b	$\leqslant 0.5$
$0.07\ m \leqslant h_1 < 0.60\ m$	
b	$\geqslant 0.30\ m$
p	$\geqslant 0.30\ m$

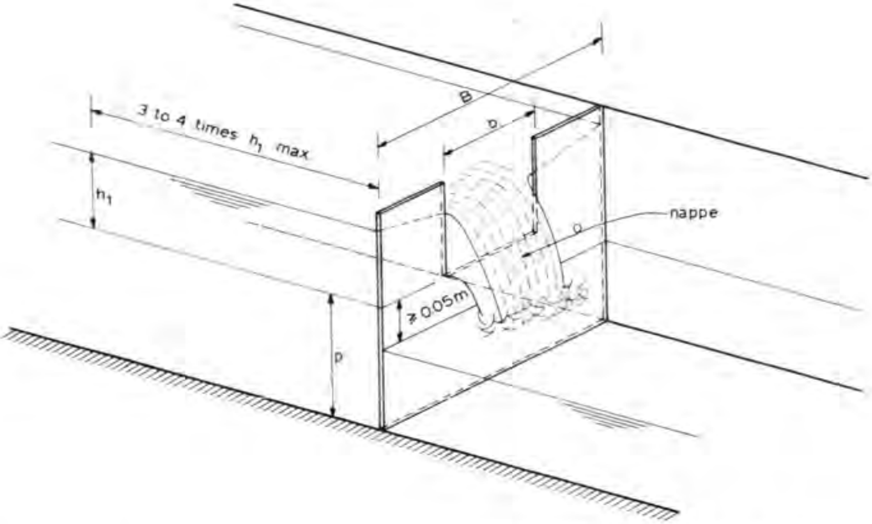

Fig.5.2. The rectangular sharp-crested weir (thin-plate weir).

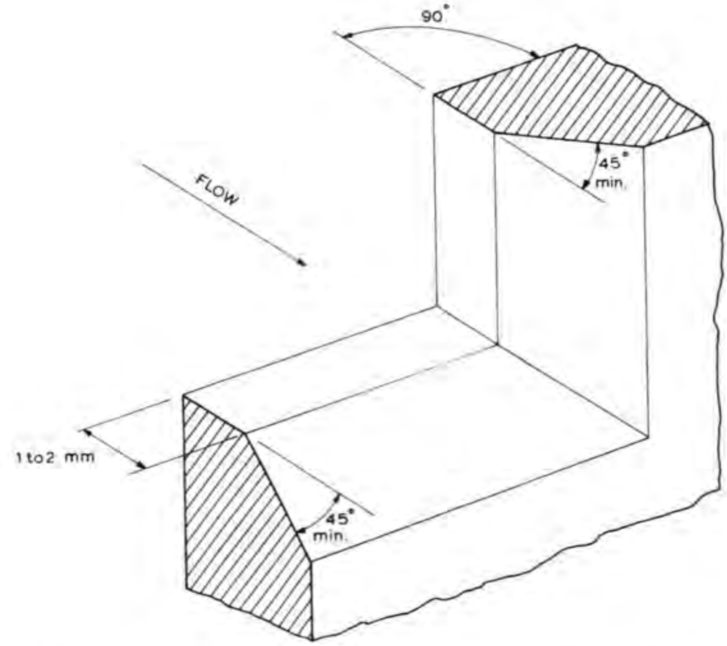

Fig.5.3. Enlarged view of crest and side of rectangular sharp-crested weir.

A comparison of these limitations with those given in Section 5.1.3 shows that the fully contracted weir has limitations that are both more numerous and more stringent than the partially contracted weir and full width weir.

Photo 1. Rectangular sharp-crested weir.

5.1.2 Evaluation of discharge

As mentioned in Section 1.13.1, the basic head-discharge equation for a rectangular sharp-crested weir is

$$Q = C_e \frac{2}{3}\sqrt{2g}\, b h_1^{1.5} \qquad (5\text{-}1)$$

To apply this equation to fully contracted, full-width, and partially contracted thin-plate weirs, it is modified as proposed by KINDSVATER and CARTER (1957),

$$Q = C_e \frac{2}{3}\sqrt{2g}\, b_e h_e^{1.5} \qquad (5\text{-}2)$$

where the effective breadth (b_e) equals $b + K_b$ and the effective head (h_e) equals $h_1 + K_h$. The quantities K_b and K_h represent the combined effects of the several phenomena attributed to viscosity and surface tension. Empirically defined values for K_b as a function of the ratio b/B are given in Figure 5.4 and a constant positive value for K_h = 0.001 m is recommended for all values of the ratios b/B and h_1/p.

C_e is an effective discharge coefficient which is a function of the ratios b/B and h_1/p and can be determined from Figure 5.5 or from Table 5.2.

TABLE 5.2. VALUES FOR C_e AS A FUNCTION OF THE RATIOS b/B AND h_1/p (FROM GEORGIA INSTITUTE OF TECHNOLOGY)

b/B	C_e
1.0	0.602 + 0.075 h_1/p
0.9	0.599 + 0.064 h_1/p
0.8	0.597 + 0.045 h_1/p
0.7	0.595 + 0.030 h_1/p
0.6	0.593 + 0.018 h_1/p
0.5	0.592 + 0.011 h_1/p
0.4	0.591 + 0.0058 h_1/p
0.3	0.590 + 0.0020 h_1/p
0.2	0.589 - 0.0018 h_1/p
0.1	0.588 - 0.0021 h_1/p
0	0.587 - 0.0023 h_1/p

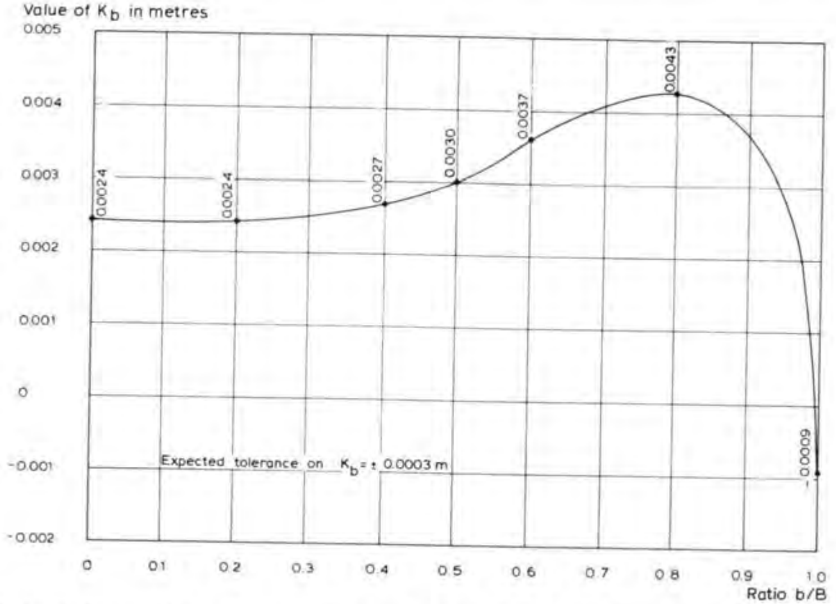

Fig.5.4. Values of K_b as a function of b/B (derived from tests at the Georgia Institute of Technology by Kindsvater and Carter, 1957).

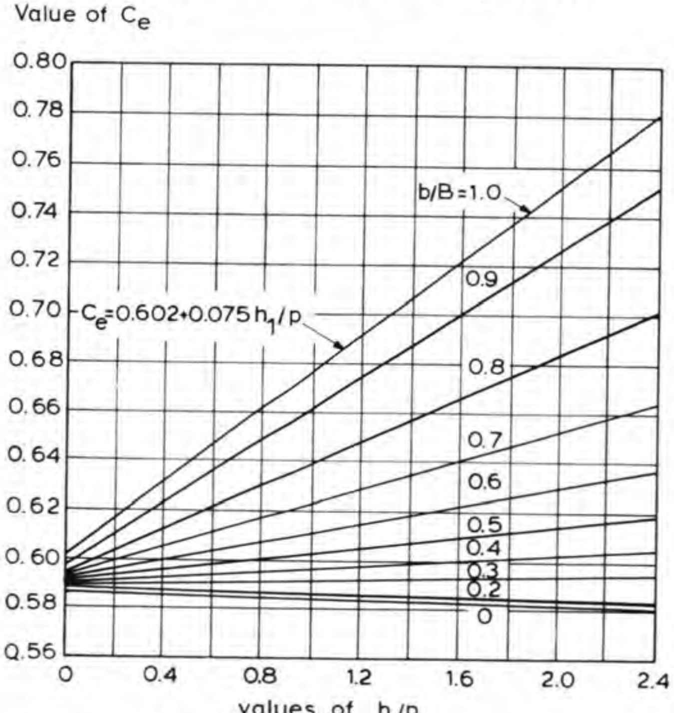

Fig.5.5. C_e as a function of the ratios b/B and h_1/p (after Georgia Institute of Technology).

For a rectangular sharp-crested weir which has been constructed with reasonable care and skill, the error in the effective discharge coefficient (C_e) in the modified Kindsvater and Carter equation is expected to be less than 1%. The tolerance on both K_b and K_h is expected to be of the order of $\pm$ 0.0003 m. The method by which these errors are to be combined with other sources of error is shown in Appendix II.

5.1.3 Limits of application

a) The practical lower limit of h_1 is related to the magnitude of the influence of fluid properties and the accuracy with which h_1 can be determined. The recommended lower limit is 0.03 m.

b) Böss (1929) has shown that critical depth will occur in the approach channel upstream from a weir if the ratio h_1/p exceeds about 5. Thus, for values of h_1/p greater than 5 the weir is not a control section as specified in Section 1.13. Further limitations on h_1/p arise from observational difficulties and measurement errors. For precise discharge measurements the recommended upper limit for h_1/p equals 2.0, while p should be at least 0.10 m.

c) The breadth (b) of the weir crest should not be less than 0.15 m.

d) To facilitate aeration of the nappe the tailwater level should remain at least 0.05 m below crest level.

5.2 V-notch sharp-crested weirs

5.2.1 Description

A V-shaped notch in a vertical thin plate which is placed perpendicular to the sides and bottom of a straight channel is defined as a V-notch sharp-crested weir.
The line which bisects the angle of the notch should be vertical and at the same distance from both sides of the channel (see Section 5). The V-notch sharp-crested weir is one of the most precise discharge measuring devices suitable for a wide range of flow. In international literature, the V-notch sharp-crested-weir is frequently referred to as the "Thomson weir". The weir is shown diagrammatically in Figures 5.6 and 5.7.

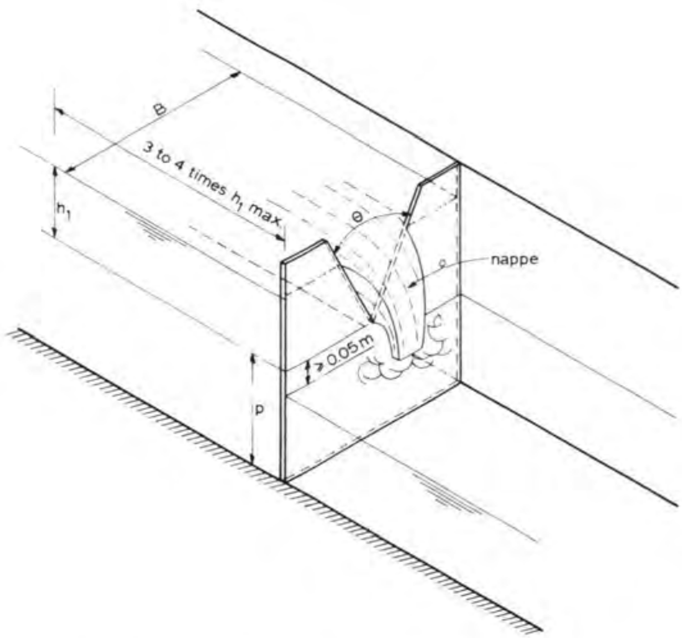

Fig.5.6. V-notch sharp-crested weir.

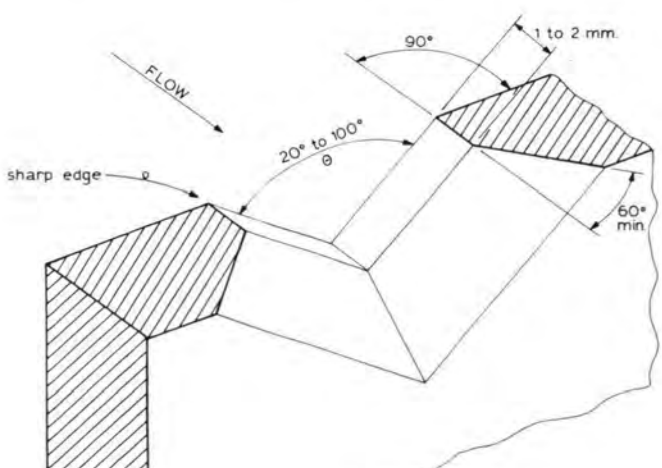

Fig.5.7. Enlarged view of V-notch.

The following flow regimes are encountered with V-notch sharp-crested or thin-plate weirs:

a) "Partially contracted weir", i.e. a weir the contractions of which along the sides of the V-notch are not fully developed due to the proximity of the walls and/or bed of the approach channel.

b) "Fully contracted weir", i.e. a weir which has an approach channel whose bed and sides are sufficiently remote from the edges of the V-notch to allow for a sufficiently great approach velocity component parallel to the weir face so that the contraction is fully developed.

These two types of V-notch sharp-crested weirs may be classified by the following limitations on h_1/p, h_1/B, h_1, p and B. It should be noted that in this classification fully contracted flow is a subdivision of partially contracted flow.

TABLE 5.3. CLASSIFICATION AND LIMITS OF APPLICATION OF V-NOTCH SHARP-CRESTED (THIN-PLATE) WEIRS (AFTER ISO, 1971, FRANCE)

Partially contracted weir	Fully contracted weir
$h_1/p \leqslant 1.2$	$h_1/p \leqslant 0.4$
$h_1/B \leqslant 0.4$	$h_1/B \leqslant 0.2$
$0.05\ m < h_1 \leqslant 0.6\ m$	$0.05\ m < h_1 \leqslant 0.38\ m$
$p \geqslant 0.1\ m$	$p \geqslant 0.45\ m$
$B_1 \geqslant 0.6\ m$	$B_1 \geqslant 0.90\ m$

From this table it appears that from a hydraulical point of view a weir may be fully contracted at low heads while at increasing h_1 it becomes partially contracted.

The partially contracted weir should be located in a rectangular approach canal. Owing to a lack of experimental data relating to the discharge coefficient over a sufficiently wide range of the ratios h_1/p and p/B, only the 90-degree V-notch should be used as a partially contracted V-notch weir. The fully contracted weir may be placed in a non-rectangular approach channel provided that the cross-sectional area of the selected approach channel is not less than that of the rectangular channel as prescribed in Table 5.3.

5.2.2 Evaluation of discharge

As shown in Section 1.13.3, the basic head-discharge equation for a V-notch sharp-crested weir is

$$Q = C_e \frac{8}{15} (2g)^{0.5} \tan\frac{\theta}{2} h_1^{2.5} \tag{5-3}$$

To apply this equation to both fully and partially contracted sharp-crested weirs, it is modified to a form proposed by Kindsvater and Carter

$$Q = C_e \frac{8}{15} (2g)^{0.5} \tan\frac{\theta}{2} h_e^{2.5} \tag{5-4}$$

where θ equals the angle induced between the sides of the notch and h_e is the effective head which equals $h_1 + K_h$. The quantity K_h represents the combined effects of fluid properties. Empirically defined values for K_h as a function of the notch angle (θ) are shown in Figure 5.8.

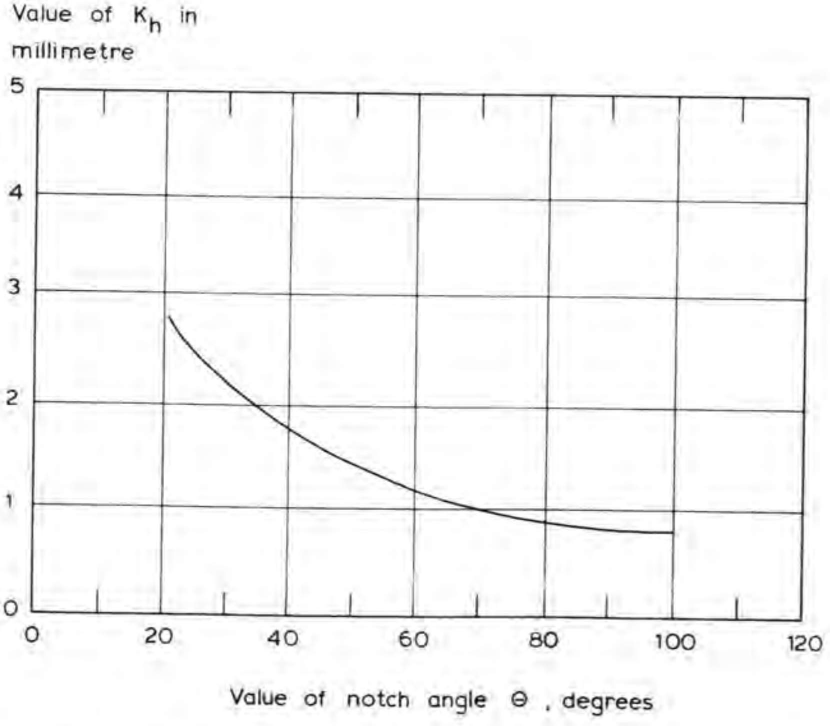

Fig.5.8. Value of K_h as a function of the notch angle.

For water at ordinary temperature, i.e. 5 °C to 30 °C or 40 °F to 85 °F, the effective coefficient of discharge (C_e) for a V-notch sharp-crested weir is a function of three variables:

$$C_e = f\left[\frac{h_1}{p}, \quad \frac{p}{B_1}, \quad \theta\right] \tag{5-5}$$

If the ratios $h_1/p \leq 0.4$ and $p/B_1 \leq 0.2$, the V-notch weir is fully contracted and C_e becomes a function of only the notch angle θ, as illustrated in Fig.5.9.

If on the other hand the contraction of the nappe is not fully developed, the effective discharge coefficient (C_e) can be read from Figure 5.10 for a 90-degree V-notch only.
Insufficient experimental data are available to produce C_e-values for non-90-degree partially contracted V-notch weirs.

The coefficients given in Figures 5.9 and 5.10 for a V-notch sharp-crested weir can be expected to have an accuracy of the order of 1.0% and of 1.0% to 2.0% respectively, provided that the notch is constructed and installed with reasonable care and skill in accordance with the requirements of Sections 5 and 5.2.1. The tolerance on K_h is expected to be of the order of 0.0003 m. The method by which these errors are to be combined with other sources of error is shown in Appendix II.

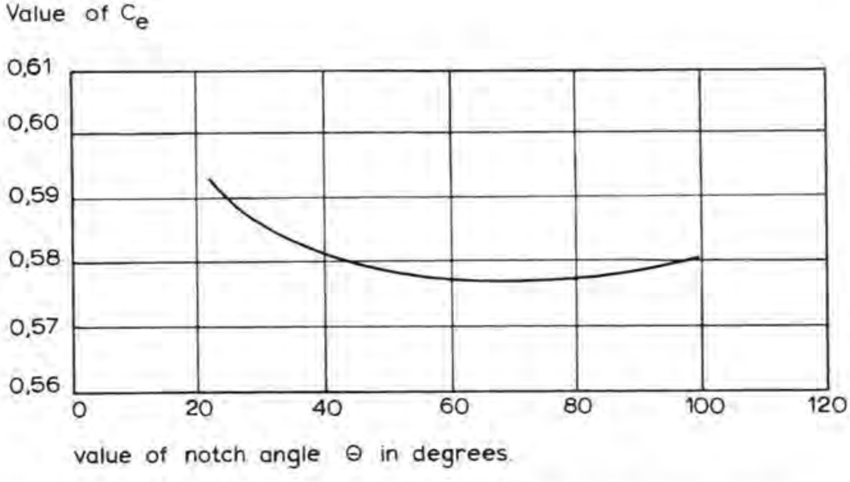

Fig.5.9. Coefficient of discharge C_e as a function of notch angle for fully contracted V-notch weirs.

TABLE 5.4: DISCHARGES FOR V-NOTCH SHARP-CRESTED WEIRS FOR HEADS IN METRES. (ADAPTED FROM ISO/TC 113/GT 2 (FRANCE-10) 152).

HEAD	DISCHARGE l/sec			HEAD	DISCHARGE l/sec			HEAD	DISCHARGE l/sec			HEAD	DISCHARGE l/sec		
metre	90°	½ 90°	¼ 90°	metre	90°	½ 90°	¼ 90°	metre	90°	½ 90°	¼ 90°	metre	90°	½ 90°	¼ 90°
0.050	0.803	0.406	0.215	0.100	4.420	2.249	1.161	0.150	12.066	6.130	3.140	0.200	24.719	12.506	6.379
0.051	0.843	0.427	0.225	0.101	4.530	2.305	1.190	0.151	12.267	6.231	3.192	0.201	25.028	12.662	6.458
0.052	0.884	0.448	0.236	0.102	4.641	2.362	1.219	0.152	12.471	6.334	3.245	0.202	25.339	12.819	6.537
0.053	0.926	0.469	0.247	0.103	4.754	2.420	1.249	0.153	12.676	6.437	3.297	0.203	25.652	12.977	6.617
0.054	0.970	0.491	0.259	0.104	4.869	2.478	1.278	0.154	12.883	6.542	3.350	0.204	25.969	13.136	6.698
0.055	1.015	0.514	0.271	0.105	4.985	2.537	1.309	0.155	13.093	6.648	3.404	0.205	26.288	13.296	6.780
0.056	1.061	0.537	0.283	0.106	5.103	2.598	1.339	0.156	13.304	6.755	3.458	0.206	26.610	13.457	6.862
0.057	1.108	0.561	0.295	0.107	5.222	2.659	1.371	0.157	13.517	6.863	3.513	0.207	26.934	13.620	6.944
0.058	1.156	0.586	0.308	0.108	5.344	2.720	1.402	0.158	13.732	6.971	3.568	0.208	27.261	13.784	7.028
0.059	1.206	0.611	0.321	0.109	5.467	2.783	1.434	0.159	13.950	7.081	3.624	0.209	27.590	13.949	7.111
0.060	1.257	0.637	0.334	0.110	5.592	2.847	1.466	0.160	14.169	7.192	3.680	0.210	27.921	14.115	7.196
0.061	1.309	0.663	0.348	0.111	5.719	2.911	1.499	0.161	14.391	7.304	3.737	0.211	28.254	14.282	7.281
0.062	1.362	0.691	0.362	0.112	5.847	2.976	1.533	0.162	14.614	7.417	3.794	0.212	28.588	14.450	7.366
0.063	1.417	0.718	0.376	0.113	5.977	3.042	1.566	0.163	14.840	7.531	3.852	0.213	28.924	14.620	7.453
0.064	1.473	0.747	0.391	0.114	6.108	3.109	1.601	0.164	15.067	7.646	3.911	0.214	29.264	14.264	7.539
0.065	1.530	0.776	0.406	0.115	6.242	3.177	1.635	0.165	15.297	7.762	3.969	0.215	29.607	14.964	7.627
0.066	1.588	0.806	0.421	0.116	6.377	3.246	1.670	0.166	15.529	7.879	4.029	0.216	29.953	15.138	7.715
0.067	1.648	0.836	0.437	0.117	6.514	3.315	1.706	0.167	15.763	7.998	4.089	0.217	30.301	15.313	7.803
0.068	1.710	0.867	0.453	0.118	6.653	3.386	1.742	0.168	15.999	8.117	4.149	0.218	30.651	15.489	7.893
0.069	1.772	0.899	0.470	0.119	6.793	3.457	1.778	0.169	16.237	8.237	4.210	0.219	31.004	15.666	7.982
0.070	1.836	0.932	0.486	0.120	6.935	3.529	1.815	0.170	16.477	8.358	4.272	0.220	31.359	15.844	8.073
0.071	1.901	0.965	0.503	0.121	7.079	3.602	1.853	0.171	16.719	8.481	4.334	0.221	31.717	16.024	8.164
0.072	1.967	0.999	0.521	0.122	7.224	3.677	1.891	0.172	16.964	8.604	4.397	0.222	32.077	16.204	8.255
0.073	2.035	1.033	0.539	0.123	7.372	3.751	1.929	0.173	17.210	8.728	4.460	0.223	32.439	16.386	8.347
0.074	2.105	1.069	0.557	0.124	7.522	3.827	1.968	0.174	17.459	8.854	4.524	0.224	32.803	16.570	8.441
0.075	2.176	1.105	0.575	0.125	7.673	3.904	2.007	0.175	17.709	8.980	4.588	0.225	33.168	16.754	8.535
0.076	2.248	1.141	0.594	0.126	7.827	3.982	2.046	0.176	17.963	9.108	4.653	0.226	33.535	16.940	8.629
0.077	2.322	1.179	0.613	0.127	7.982	4.060	2.086	0.177	18.219	9.237	4.718	0.227	33.907	17.127	8.724
0.078	2.397	1.217	0.633	0.128	8.139	4.140	2.127	0.178	18.478	9.367	4.784	0.228	34.282	17.315	8.819
0.079	2.473	1.256	0.653	0.129	8.298	4.220	2.168	0.179	18.738	9.497	4.851	0.229	34.659	17.504	8.915
0.080	2.551	1.296	0.673	0.130	8.458	4.302	2.209	0.180	19.001	9.629	4.918	0.230	35.039	17.695	9.011
0.081	2.630	1.336	0.694	0.131	8.621	4.384	2.251	0.181	19.265	9.762	4.986	0.231	35.421	17.886	9.108
0.082	2.710	1.377	0.715	0.132	8.785	4.467	2.294	0.182	19.531	9.896	5.054	0.232	35.806	18.079	9.207
0.083	2.792	1.419	0.737	0.133	8.951	4.551	2.337	0.183	19.800	10.032	5.122	0.233	36.139	18.274	9.306
0.084	2.876	1.462	0.759	0.134	9.119	4.636	2.380	0.184	20.071	10.168	5.192	0.234	36.582	18.469	9.405
0.085	2.961	1.505	0.781	0.135	9.289	4.722	2.424	0.185	20.345	10.305	5.261	0.235	36.974	18.666	9.504
0.086	3.048	1.549	0.803	0.136	9.461	4.809	2.468	0.186	20.621	10.444	5.332	0.236	37.369	18.864	9.605
0.087	3.136	1.594	0.826	0.137	9.634	4.897	2.513	0.187	20.899	10.584	5.403	0.237	37.766	19.063	9.706
0.088	3.225	1.640	0.850	0.138	9.810	4.986	2.559	0.188	21.180	10.726	5.475	0.238	38.166	19.263	9.808
0.089	3.316	1.686	0.874	0.139	9.987	5.075	2.604	0.189	21.463	10.867	5.547	0.239	38.568	19.465	9.910
0.090	3.409	1.734	0.898	0.140	10.167	5.166	2.651	0.190	21.748	11.010	5.620	0.240	38.973	19.668	10.013
0.091	3.503	1.782	0.922	0.141	10.348	5.258	2.697	0.191	22.034	11.155	5.693	0.241	39.380	19.872	10.116
0.092	3.598	1.830	0.947	0.142	10.532	5.351	2.744	0.192	22.322	11.300	5.766	0.242	39.790	20.079	10.220
0.093	3.696	1.880	0.973	0.143	10.717	5.444	2.792	0.193	22.612	11.447	5.841	0.243	40.202	20.287	10.325
0.094	3.795	1.930	0.998	0.144	10.904	5.539	2.840	0.194	22.906	11.595	5.916	0.244	40.617	20.496	10.430
0.095	3.895	1.981	1.025	0.145	11.093	5.635	2.889	0.195	23.203	11.743	5.992	0.245	41.034	20.705	10.536
0.096	3.997	2.033	1.051	0.146	11.284	5.732	2.938	0.196	23.501	11.893	6.068	0.246	41.454	20.916	10.642
0.097	4.101	2.086	1.078	0.147	11.476	5.830	2.988	0.197	23.802	12.044	6.145	0.247	41.877	21.127	10.750
0.098	4.206	2.139	1.106	0.148	11.671	5.929	3.038	0.198	24.106	12.197	6.222	0.248	42.302	21.340	10.858
0.099	4.312	2.194	1.133	0.149	11.867	6.029	3.089	0.199	24.411	12.351	6.300	0.249	42.730	21.555	10.967

HEAD	DISCHARGE l/sec			HEAD	DISCHARGE l/sec			HEAD	DISCHARGE l/sec		
metre	90°	½ 90°	¼ 90°	metre	90°	½ 90°	¼ 90°	metre	90°	½ 90°	¼ 90°
0.250	43.160	21.772	11.077	0.300	68.106	34.268	17.410	0.350	100.19	50.313	25.512
0.251	43.593	21.990	11.187	0.301	68.675	34.552	17.555	0.351	100.91	50.672	25.693
0.252	44.028	22.209	11.299	0.302	69.246	34.837	17.700	0.352	101.63	51.033	25.875
0.253	44.466	22.429	11.410	0.303	69.821	35.124	17.845	0.353	102.36	51.397	26.057
0.254	44.907	22.649	11.523	0.304	70.398	35.412	17.992	0.354	103.08	51.758	26.240
0.255	45.350	22.873	11.635	0.305	70.980	35.702	18.139	0.355	103.81	52.121	26.424
0.256	45.796	23.098	11.749	0.306	71.568	35.995	18.287	0.356	104.54	52.487	26.609
0.257	46.245	23.323	11.863	0.307	72.159	36.290	18.435	0.357	105.28	52.856	26.794
0.258	46.696	23.549	11.978	0.308	72.750	36.585	18.585	0.358	106.02	53.227	26.981
0.259	47.150	23.777	12.094	0.309	73.341	36.880	18.735	0.359	106.77	53.596	27.168
0.260	47.606	24.005	12.210	0.310	73.936	37.177	18.885	0.360	107.52	53.967	27.355
0.261	48.065	24.235	12.326	0.311	74.534	37.477	19.037	0.361	108.27	54.340	27.544
0.262	48.527	24.466	12.443	0.312	75.135	37.779	19.189	0.362	109.02	54.717	27.733
0.263	48.991	24.699	12.561	0.313	75.738	38.081	19.342	0.363	109.78	55.096	27.923
0.264	49.458	24.933	12.680	0.314	76.344	38.384	19.495	0.364	110.54	55.473	28.114
0.265	49.928	25.168	12.799	0.315	76.954	38.687	19.650	0.365	111.30	55.852	28.306
0.266	50.400	25.404	12.920	0.316	77.566	38.995	19.805	0.366	112.06	56.231	28.498
0.267	50.876	25.642	13.041	0.317	78.181	39.304	19.960	0.367	112.84	56.616	28.691
0.268	51.353	25.881	13.162	0.318	78.802	39.615	20.117	0.368	113.62	57.003	28.885
0.269	51.834	26.121	13.284	0.319	79.428	39.927	20.274	0.369	114.39	57.391	29.080
0.270	52.317	26.363	13.407	0.320	80.057	40.241	20.432	0.370	115.17	57.780	29.275
0.271	52.802	26.606	13.529	0.321	80.685	40.553	20.590	0.371	115.95	58.171	29.472
0.272	53.291	26.851	13.653	0.322	81.314	40.867	20.750	0.372	116.73	58.560	29.669
0.273	53.782	27.098	13.778	0.323	81.947	41.184	20.910	0.373	117.52	58.950	29.867
0.274	54.276	27.347	13.903	0.324	82.583	41.503	21.071	0.374	118.31	59.345	30.065
0.275	54.772	27.596	14.030	0.325	83.222	41.824	21.232	0.375	119.11	59.742	30.264
0.276	55.272	27.845	14.157	0.326	83.863	42.147	21.395	0.376	119.91	60.141	30.465
0.277	55.774	28.097	14.284	0.327	84.508	42.471	21.558	0.377	120.71	60.542	30.666
0.278	56.282	28.351	14.413	0.328	85.155	42.796	21.721	0.378	121.52	60.944	30.867
0.279	56.794	28.607	14.542	0.329	85.806	43.123	21.886	0.379	122.32	61.346	31.070
0.280	57.306	28.863	14.671	0.330	86.459	43.451	22.051	0.380	123.13	61.747	31.273
0.281	57.819	29.119	14.802	0.331	87.116	43.779	22.217	0.381	123.94	62.150	31.477
0.282	58.335	29.377	14.933	0.332	87.775	44.107	22.384				
0.283	58.853	29.638	15.065	0.333	88.438	44.438	22.551				
0.284	59.375	29.901	15.197	0.334	89.103	44.773	22.719				
0.285	59.899	30.163	15.330	0.335	89.772	45.108	22.888				
0.286	60.425	30.427	15.464	0.336	90.448	45.446	23.058				
0.287	60.955	30.691	15.598	0.337	91.128	45.785	23.228				
0.288	61.487	30.959	15.734	0.338	91.811	46.125	23.400				
0.289	62.023	31.229	15.870	0.339	92.491	46.467	23.572				
0.290	62.560	31.499	16.006	0.340	93.175	46.810	23.744				
0.291	63.101	31.769	16.143	0.341	93.862	47.153	23.910				
0.292	63.645	32.040	16.281	0.342	94.551	47.497	24.092				
0.293	64.195	32.315	16.420	0.343	95.244	47.842	24.267				
0.294	64.748	32.591	16.559	0.344	95.940	48.191	24.442				
0.295	65.303	32.869	16.699	0.345	96.638	48.542	24.619				
0.296	65.858	33.146	16.840	0.346	97.340	48.895	24.796				
0.297	66.416	33.424	16.982	0.347	98.045	49.249	24.974				
0.298	66.976	33.704	17.124	0.348	98.753	49.604	25.152				
0.299	67.539	33.985	17.267	0.349	99.471	49.958	25.332				

90° – V – $\theta = 90^\circ$

½ 90° – V – $\theta = 53^\circ 8'$

¼ 90° – V – $\theta = 28^\circ 4'$

See Fig.6.11.

NOTE: The number of significant figures given for the discharge does not imply a corresponding accuracy in the knowledge of the values given.

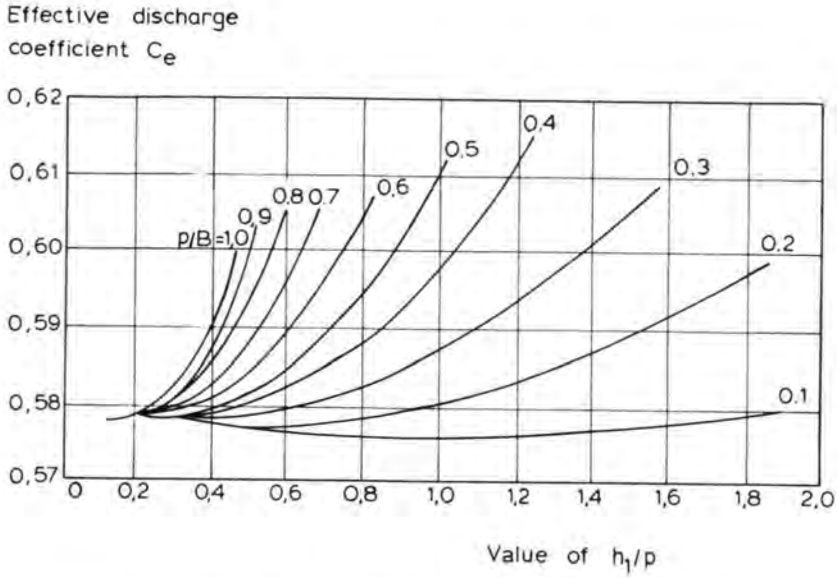

Fig.5.10. C_e as a function of h_1/p and p/B for 90-degree V-notch sharp-crested weir. (From British Standard 3680:Part 4A and ISO/TC 113/GT 2 (France-10) 152).

5.2.3 Limits of application

The limits of application of the Kindsvater and Carter equation for V-notch sharp-crested weirs are:

a) The ratio h_1/p should be equal to or less than 1.2
b) The ratio h_1/B should be equal to or less than 0.4
c) The head over the vertex of the notch h_1 should not be less than 0.05 m nor more than 0.60 m
d) The height of the vertex of the notch above the bed of the approach channel (p) should not be less than 0.10 m
e) The width of the rectangular approach channel shall exceed 0.60 m
f) The notch angle of a fully contracted weir may range between 25 and 100 degrees. Partially contracted weirs have a 90-degree notch only.
g) Tailwater level should remain below the vertex of the notch.

5.2.4 Rating tables

Commonly used sizes of V-notches for fully contracted thin-plate weirs are the 90-degree, ½ 90-degree and ¼ 90-degree notches in which the dimensions across the top are twice, equal to and half the vertical depth respectively, as shown in Figure 5.11.

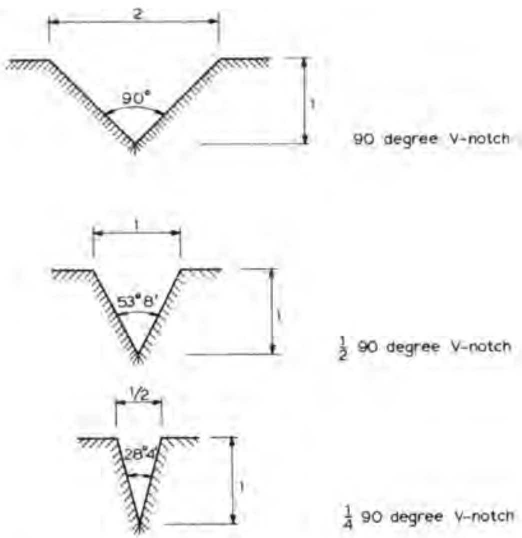

Fig.5.11. Commonly used V-notch control sections.

5.3 Cipoletti weir

5.3.1 Description

A Cipoletti weir is a modification of a fully contracted rectangular sharp-crested weir and has a trapezoidal control section, the crest being horizontal and the sides sloping outward with an inclination of 1 horizontal to 4 vertical.

Cipoletti (1886) assumed that, due to the increase of side-contraction with an increasing head, the decrease of discharge over a fully contracted rectangular sharp-crested weir with breadth b would be compensated by the increase of discharge due to the inclination of the sides of the control-section. This compensation thus allows the head-discharge equation of a full width rectangular weir to be used.

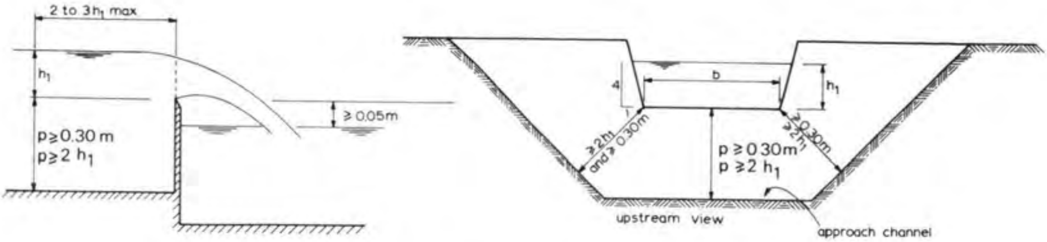

Fig.5.12. Definition sketch of a Cipoletti weir.

It should be noted, however, that experiments differ as to the degree to which this compensation occurs. Inherently, the accuracy of measurements obtained with a Cipoletti weir is not as great as that obtainable with the rectangular or V-notch sharp-crested weirs described in Section 5.1 and 5.2 respectively.

Photo 2. Cipoletti weir.

5.3.2 Evaluation of discharge

The basic-head-discharge equation for the Cipoletti weir is the same as that of a rectangular fully contracted weir. Hence

$$Q = C_d C_v \frac{2}{3} (2g)^{0.5} bh_1^{1.5} \qquad (5\text{-}6)$$

where, within certain limits of application, the discharge coefficient C_d equals 0.63. The approach velocity coefficient C_v may be obtained from Figure 1.12. A rating table for the discharge q in m^3/sec/m with negligible approach velocity is presented in Table 5.5.

The accuracy of the discharge coefficient for a well maintained Cipoletti weir is reasonable for field conditions. The error in the product $C_d C_v$ is expected to be less than 5%. The method by which this coefficient error is to be combined with other sources of error is shown in Appendix II.

5.3.3 Limits of application

The limits of application of the Cipoletti (fully contracted) weir are:

a) The height of the weir crest above the bottom of the approach channel should be at least twice the head over the crest with a minimum of 0.30 m.

b) The distance from the sides of the trapezoidal control section to the sides of the approach channel should be at least twice the head over the crest with a minimum of 0.30 m.

c) The upstream head over the weir crest h_1 should not be less than 0.06 m not more than 0.60 m.

d) The ratio h_1/b should be equal to or less than 0.50.

e) To enable aeration of the nappe, the tailwater level should be at least 0.05 m below crest level.

Provided the Cipoletti weir conforms to the above limits of application, it may be placed in a non-rectangular approach channel.

TABLE 5.5. DISCHARGE OF THE STANDARD CIPOLETTI WEIR IN $m^3/sec/m$

Head metre	Discharge $m^3/sec/m^1$	Head metre	Discharge $m^3/sec/m^1$
0.06	0.0273	0.36	0.402
0.07	0.0344	0.37	0.418
0.08	0.0421	0.38	0.435
0.09	0.0502	0.39	0.453
0.10	0.0588	0.40	0.470
0.11	0.0678	0.41	0.488
0.12	0.0773	0.42	0.506
0.13	0.0871	0.43	0.524
0.14	0.0974	0.44	0.543
0.15	0.108	0.45	0.561
0.16	0.119	0.46	0.580
0.17	0.130	0.47	0.599
0.18	0.142	0.48	0.618
0.19	0.154	0.49	0.638
0.20	0.166	0.50	0.657
0.21	0.179	0.51	0.677
0.22	0.192	0.52	0.697
0.23	0.205	0.53	0.717
0.24	0.219	0.54	0.738
0.25	0.232	0.55	0.758
0.26	0.247	0.56	0.779
0.27	0.261	0.57	0.800
0.28	0.275	0.58	0.821
0.29	0.290	0.59	0.843
0.30	0.306	0.60	0.864
0.31	0.321		
0.32	0.337		
0.33	0.352		
0.34	0.369		
0.35	0.385		

NOTE: The approach velocity has been neglected (C_v = 1.00)

5.4 Circular weir

5.4.1 Description

A circular control section located in a vertical thin (metal) plate, which is placed perpendicular to the sides and bottom of a straight approach channel, is defined as a circular thin plate weir. These weirs have the advantage that the crest can be turned and bevelled with precision in a lathe, and more particularly that they do not have to be levelled.

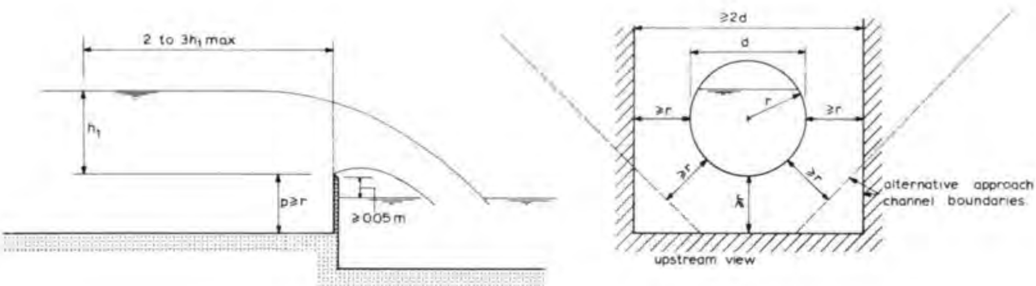

Fig.5.13. Circular weir dimensions

Circular sharp-crested weirs, in practice, are fully contracted so that the bed and sides of the approach channel should be sufficiently remote from the control section to have no influence on the development of the nappe.

The fully contracted weir may be placed in a non-rectangular approach channel provided that the general installation conditions comply with those laid down in Section 5.4.3.

TABLE 5.6. VALUES OF ω AND ϕ AS A FUNCTION OF THE FILLING RATIO $h_1/d = k^2$ OF A CIRCULAR SHARP-CRESTED WEIR

h_1/d	ω dimension-less	ϕ_i $m^{\frac{1}{2}}/s$	h_1/d	ω dimension-less	ϕ_i $m^{\frac{1}{2}}/s$	h_1/d	ω dimension-less	ϕ_i $m^{\frac{1}{2}}/s$
0.01	0.0004	0.00047	0.36	.3451	.4076	0.71	1.1804	1.3943
.02	.0013	.00154	.37	.3633	.4291	.72	1.2085	1.4275
.03	.0027	.00319	.38	.3819	.4511	.73	1.2368	1.4609
.04	.0046	.00543	.39	.4009	.4735	.74	1.2653	1.4946
.05	.0071	.00839	.40	.4203	.4965	.75	1.2939	1.5284
.06	.0102	.0120	.41	.4401	.5199	.76	1.3226	1.5623
.07	.0139	.0164	.42	.4603	.5437	.77	1.3514	1.5963
.08	.0182	.0215	.43	.4809	.5681	.78	1.3802	1.6303
.09	.0231	.0273	.44	.5019	.5929	.79	1.4091	1.6644
.10	.0286	.0338	.45	.5233	.6182	.80	1.4380	1.6986
.11	.0346	.0409	.46	.5451	.6439	.81	1.4670	1.7328
.12	.0412	.0487	.47	.5672	.6700	.82	1.4960	1.7671
.13	.0483	.0571	.48	.5896	.6965	.83	1.5250	1.8013
.14	.0560	.0661	.49	.6123	.7233	.84	1.5540	1.8356
.15	.0642	.0758	.50	.6354	.7506	.85	1.5830	1.8699
.16	.0728	.0860	.51	.6588	.7782	.86	1.6120	1.9041
.17	.0819	.0967	.52	.6825	.8062	.87	1.6410	1.9384
.18	.0914	.1080	.53	.7064	.8344	.88	1.6699	1.9725
.19	.1014	.1198	.54	.7306	.8630	.89	1.6988	2.0066
.20	.1119	.1322	.55	.7551	.8920	.90	1.7276	2.0407
.21	.1229	.1452	.56	.7799	.9212	.91	1.7561	2.0743
.22	.1344	.1588	.57	.8050	.9509	.92	1.7844	2.1077
.23	.1464	.1729	.58	.8304	.9809	.93	1.8125	2.1409
.24	.1589	.1877	.59	.8560	1.0111	.94	1.8403	2.1738
.25	.1719	.2030	.60	.8818	1.0416	.95	1.8678	2.2063
.26	.1854	.2190	.61	.9079	1.0724	.96	1.8950	2.2384
.27	.1994	.2355	.62	.9342	1.1035	.97	1.9219	2.2702
.28	.2139	.2527	.63	.9608	1.1349	.98	1.9484	2.3015
.29	.2289	.2704	.64	.9876	1.1666	.99	1.9744	2.3322
.30	.2443	.2886	.65	1.0147	1.1986	1.00	2.000	-
.31	.2601	.3072	.66	1.0420	1.2308			
.32	.2763	.3264	.67	1.0694	1.2632			
.33	.2929	.3460	.68	1.0969	1.2957			
.34	.3099	.3660	.69	1.1246	1.3284			
.35	.3273	.3866	.70	1.1524	1.3612			

$$Q = C_e \frac{4}{15} \sqrt{2g}\, \omega\, d^{2.5}$$

or

$$Q = C_e\, \phi_i\, d^{2.5}$$

Values of ω from J.C.STEVENS, 1957

5.4.2 Determination of discharge

According to Equation 1-93, the basic head-discharge equation for a circular sharp-crested weir reads

$$Q = C_e \, \omega \, \frac{4}{15} \sqrt{2g} \, d^{2.5} = C_e \, \phi_i \, d^{2.5} \qquad (5\text{-}7)$$

where ω is a function of the filling ratio $h_1/d = k^2$. Values of ω and $\phi_i = \frac{4}{15} \sqrt{2g}. \omega$ are shown in Table 5.6.

For water at ordinary temperatures, the discharge coefficient is a function of the filling ratio h_1/d. A.STAUS (1931) determined experimental values of C_e for various weir diameters. Average values of C_e as a function of h_1/d are shown in Table 5.7.

TABLE 5.7. AVERAGE DISCHARGE COEFFICIENT FOR CIRCULAR SHARP-CRESTED WEIRS

h_1/d	C_e	h_1/d	C_e	h_1/d	C_e
1.00	0.606	0.65	0.595	0.30	0.600
0.95	0.604	0.60	0.594	0.25	0.604
0.90	0.602	0.55	0.593	0.20	0.610
0.85	0.600	0.50	0.593	0.15	0.623
0.80	0.599	0.45	0.594	0.10	0.650
0.75	0.597	0.40	0.595	0.05	0.75
0.70	0.596	0.35	0.597	0	-

So far as is practicable, circular weirs should be installed and maintained so as to make the approach velocity negligible ($H_1 \simeq h_1$).

The error in the effective discharge coefficients for a well maintained circular sharp-crested weir, as presented in Table 5.7, may be expected to be less than 2%. The method by which this error is to be combined with other sources of error is shown in Appendix II.

The lower quarter of a circular weir is sometimes described as a parabola of which the focal distance equals the radius of the circle. According to Equation 1-80, the head-discharge relationship then reads

$$Q = C_e \frac{\pi}{2} \sqrt{\tfrac{1}{2}\, gd}\; h_1^{2.0} \tag{5-8}$$

where the effective discharge coefficient differs less than 5% from those presented in Table 5.7, provided that $h_1/d \leqslant$ about 0.25.

5.4.3 Limits of application

The limits of application of the circular sharp-crested weir are:

a) The height of the crest above the bed of the approach channel should not be less than the radius of the control section with a minimum of 0.10 m.

b) The sides (boundary of the rectangular, trapezoïdal, or circular approach channel) should not be nearer than r to the weir notch.

c) The ratio H_1/d should be equal to or more than 0.10.

d) The practical lower limit of H_1 is 0.03 m.

e) To enable aeration of the nappe the tailwater level should be at least 0.05 m below crest level.

If only the lower half of the circular control section is used, the same limits of application should be observed.

5.5 Proportional weir

5.5.1 Description

The proportional or Sutro weir is defined as a weir in which the discharge is linearly proportional to the head over an arbitrary reference level which, for the Sutro weir,has been selected at a distance of one-third of the height (a) of the rectangular section above the weir crest.

The Sutro weir consists of a rectangular portion joined to a curved portion which, according to Equation 1-103, has as a profile law (see Section 1.13.7)

$$x/b = (1 - \frac{2}{\pi}\tan^{-1} \sqrt{z'/a}) \qquad (5\text{-}9)$$

to provide proportionality for all heads above the boundary line CD (Fig.5.14).

Photo 3. Portable Sutro weir equipped with recorder.

This somewhat complex equation of the curved profile may give the impression that the weir is difficult to construct.In practice, however, it is quite easy to make from sheet metal and, by using modern taped profile cutting machines, very fine tolerances can be obtained. Table 5.8 gives values for z'/a and x/b from which the coordinates of the curved portion can be computed when the two controlling dimensions, a and b, are known. The values of z'/a and x/b are related by the Equation 5-9.

TABLE 5.8. VALUES OF z'/a AND x/b RELATED BY EQUATION 5-9

z'/a	x/b	z'/a	x/b	z'/a	x/b
0.1	0.805	1.0	0.500	10	0.195
0.2	0.732	2.0	0.392	12	0.179
0.3	0.681	3.0	0.333	14	0.166
0.4	0.641	4.0	0.295	16	0.156
0.5	0.608	5.0	0.268	18	0.147
0.6	0.580	6.0	0.247	20	0.140
0.7	0.556	7.0	0.230	25	0.126
0.8	0.536	8.0	0.216	30	0.115
0.9	0.517	9.0	0.205		
1.0	0.500	10.0	0.195		

Several types of the Sutro proportional weirs have been tested, both symmetrical and unsymmetrical forms being shown in Figure 5.14.

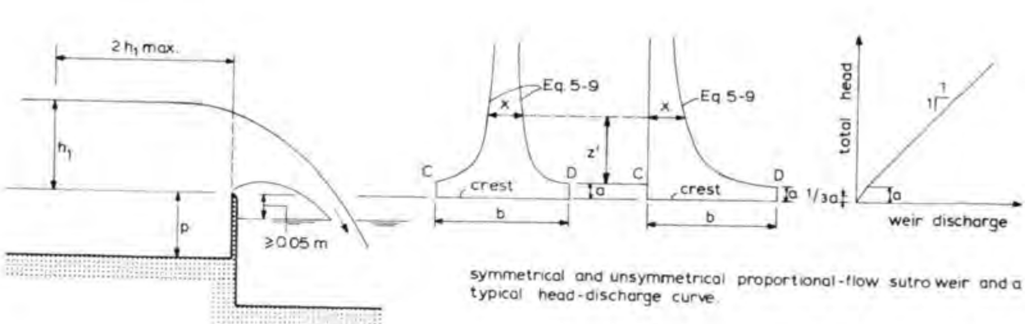

Fig.5.14. Sutro weir dimensions.

Both types are fully contracted along the sides and along the crest. Ventilation of the nappe is essential for accurate measurements so that the tailwater level should be at least 0.05 m below crest level. Of special interest are the so-called crestless weirs in which the symmetrical weir profile has been superimposed directly on the bottom of the approach channel to prevent the accumulation of sediments upstream of the weir plate. With all three types, the weir crest should be truly horizontal and perpendicular to the flow. Weirs with a linear head-discharge relationship are particularly suitable for use as downstream control on rectangular canals with constant flow velocity, as controls for float regulated chemical dosing or sampling devices, or as a flow meter whereby the average discharge over any period is a direct function of the average recorded head.

5.5.2 Evaluation of discharge

As shown in Section 1.13.7, the basic head-discharge equation for a linearly proportional weir is

$$Q = C_d\, b(2ga)^{\frac{1}{2}}\, (h_1 - a/3) \tag{5-10}$$

where the discharge coefficient C_d is mainly determined by the geometrical portions of the control section, which, according to Equation 5-9, is governed by the values of a and b. The values of C_d for symmetrical and unsymmetrical weirs are presented in Tables 5.9 and 5.10 respectively.

TABLE 5.9. DISCHARGE COEFFICIENTS OF SYMMETRICAL SUTRO WEIRS AS A FUNCTION OF a AND b (AFTER SOUCEK, HOWE AND MAVIS)

a	b (metres)				
(metres)	0.15	0.23	0.30	0.38	0.46
0.006	0.608	0.613	0.617	0.6185	0.619
0.015	0.606	0.611	0.615	0.617	0.6175
0.030	0.603	0.608	0.612	0.6135	0.614
0.046	0.601	0.6055	0.610	0.6115	0.612
0.061	0.599	0.604	0.608	0.6095	0.610
0.076	0.598	0.6025	0.6065	0.608	0.6085
0.091	0.597	0.602	0.606	0.6075	0.608

TABLE 5.10. DISCHARGE COEFFICIENTS OF UNSYMMETRICAL SUTRO WEIRS AS A FUNCTION OF a AND b (AFTER SOUCEK, HOWE AND MAVIS)

a (metres)	b (metres) 0.15	0.23	0.30	0.38	0.46
0.006	0.614	0.619	0.623	0.6245	0.625
0.015	0.612	0.617	0.621	0.623	0.6235
0.030	0.609	0.614	0.618	0.6195	0.620
0.046	0.607	0.6115	0.616	0.6175	0.618
0.061	0.605	0.610	0.614	0.6155	0.616
0.076	0.604	0.6085	0.6125	0.614	0.6145
0.091	0.603	0.608	0.612	0.6135	0.614

The coefficients given in Tables 5.9 and 5.10 can be expected to have an accuracy of the order of 2%, provided the control is constructed and installed with reasonable care and skill. To maintain this coefficient accuracy, the weir should be cleaned frequently. The method by which this error is to be combined with other sources of error is shown in Appendix II.

If contraction is fully suppressed along the weir crest, contraction along the curved edges of the weir will increase to such an extent that the wetted area of the jet at the "vena contracta" remains about constant (see orifices Section 1.12).Experimental results obtained by J.SINGER and D.C.G.LEWIS (1966) showed that the coefficient values in Tables 5.9 and 5.10 may be used for crestless weirs provided that the weir breadth b is not less than 0.15 m.

5.5.3 Limits of application

The weir discharge is linearly proportional to the head provided that the head is greater than about 1.2 a. However, to obtain a sensibly constant discharge coefficient, it is advised to use $h_1 = 2a$ as a lower limit. In addition, h_1 has a practical lower limit which is related to the magnitude of the influence of fluid properties and the accuracy with which h_1 can be determined. The recommended lower limit is 0.03 m.

The maximum value of h_1 is related to the magnitude of the influence of fluid properties. Further, $h_1 - a = z'$ is restricted to a value whereby the value of x, as computed by Equation 5-9, is not less than 0.005 m. For similar reasons, the height of the rectangular portion (a) should not be less than 0.005 m.

The breadth (b) of the weir crest should not be less than 0.15 m to allow the use of the standard discharge coefficient.

To achieve a fully contracted weir, the ratio b/p should be equal to or greater than 1.0 and the ratio B/b not less than 3.0.

Linearly proportional weirs that do not comply with the limits on the breadth of the crest can be employed satisfactorily provided that such weirs are first calibrated to obtain the proper coefficient value. Due to lack of experimental data, no standard C_d-values are yet available if $b < 0.15$ m.

To allow sufficient aeration of the nappe, tailwater-level should be at least 0.05 m below crest level.

5.6 Selected list of references

1. BANKS, W.H.H., BURCH, C.R. and SHAW, T.L.: The design of proportional and logarithmic thin-plate weirs. J.of Hydraulic Research, Vol.6, 1968, No.2, pp.75-106, Delft.

2. BÖSS, P.: Berechnung der Abflussmengen und der Wasserspiegellage bei Abstürzen und Schwellen unter besonderer Berücksichtigung der dabei auftretenden Zusatzspannungen. Wasserkraft u.Wasserwirtschaft, Vol.22,1929, pp.13-33.

3. BRITISH STANDARDS INSTITUTION. Methods of measurement of liquid flow in open channels. BS 3680, Part 4A: Thin-plate weirs and venturi flumes.1965.London.

4. CIPOLETTI, C.: Modulo per la dispensa delle acque atramazzo libero di forma trapezia e coefficiente di contrazione constante. Esperimenti e formole per grandi stramazzi a soglia inclinata e orizontale. Milano, Hocpli, 1886,88 p.

5. FRANKE, P.G.: Messüberfälle. Das Gas- und Wasserfläche, 103 Jahrg., 1962, Nr.40, pp.1072-1075. Nr.42, pp.1137-1140 and Nr.44, pp.1178-1181.

6. KINDSVATER, C.E. and R.W.C.CARTER: Discharge characteristics of rectangular thin-plate weirs. Journal of the Hydraulics Division of the ASCE, Vol.83, No.HY 6, Dec.1957, Paper 1453.

7. L'ASSOCIATION FRANÇAISE DE NORMALISATION: Mesure de débit de l'eau dans les chenaux au moyen de déversoire en mince paroi. X 10-311, Dec.1971, ISO/TC 113/GT 2 (France-10), 152.

8. PRATT, E.A.: Another proportional-flow weir. Sutro weir. Engineering News, Vol.72, No.9, p.462, Aug.27, 1914.

9. REHBOCK, Th.: Die Ausbildung der Überfälle beim Abfluss von Wasser über Wehre nebst Beschreibung der Anlage zur Beobachtung von Überfällen im Flusslaboratorium zu Karlsruhe, Karlsruhe 1909. Festschrift der Grossherzoglichen Technischen Hochschule Fridericiana.

10. REHBOCK, Th.: Wassermessung mit scharfkantigen Überfallwehren. Z.des Vereines deutscher Ingenieure. 73 (1929), No.24, pp.817-823, Berlin.

11. SINGER, J. and LEWIS, D.C.G.: Proportional-flow weirs for automatic sampling or dosing. Water & Water Engineering,March 1966,V.70, No.841,pp.105-111.

12. SOUCEK, J., HOWE, H.E., and MAVIS, F.T.: Sutro weir investigations furnish discharge coefficients. Engineering New-Record, November 12, 1936.

13. STAUS, A.: Der Beiwert kreisrunder Überfälle. Wasserkraft u.Wasserwirtschaft, 1931, p.42, No.4.

14. STEVENS, J.C.: Flow through circular weirs. J.of the Hydraulics Div. of the ASCE, Vol.83, No.HY 6, Dec.1957, Paper 1455.

15. THIJSSE, J.Th.: Discharge meters. Waterloopkundig Laboratorium, Delft.

16. THOMSON, J.: On experiments on the measurement of water by triangular notches in weir-boards. Report of the 28th meeting British Ass.for Advancement of Science, held at Leeds, Sept.1858, pp.181-185, London 1859.

17. UNITED STATES BUREAU OF RECLAMATION: Water measurement manual. Second edition, Denver, Col., 1971.

18. WELLS, J.R.: Discharge characteristics of rectangular notch weirs in rectangular channels. MSc.Thesis presented to the Georgia Institute of Technol., Atlanta, Ga., 1954.

6 Short-crested weirs

In general, short-crested weirs are those overflow structures, in which the streamline curvature above the weir crest has a significant influence on the head-discharge relationship of the structure.

6.1 Weir sill with rectangular control section

6.1.1 Description

A common and simple structure used in open waterways as either a drop or a check structure is the concrete rectangular control shown in Figure 6.1.

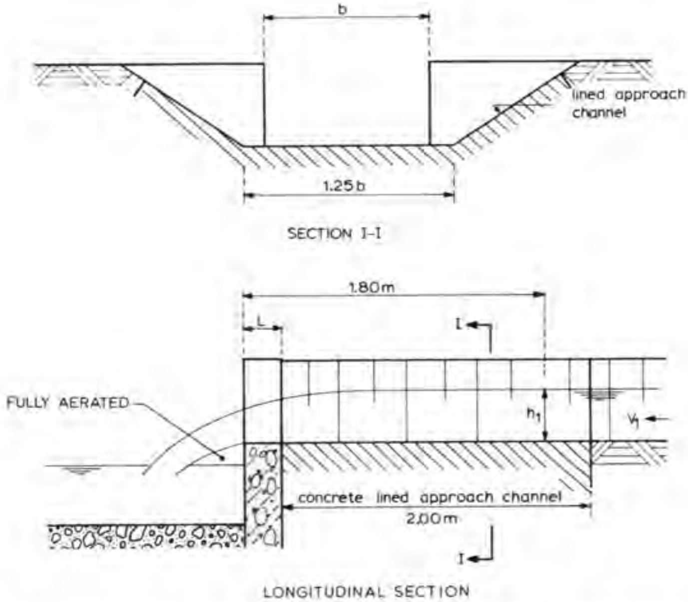

Fig.6.1. Weir sill with rectangular control section (after W.O.Ree, 1938).

The control is placed in a trapezoidal approach channel, the bottom of which has the same elevation as the weir crest (p = 0). The upstream head over the weir crest h_1 is measured a distance of 1.80 m from the downstream weir face in the trapezoidal approach channel. To prevent a significant change in the roughness or configuration in the approach channel boundary from influencing the weir discharge, the approach channel should be lined with concrete or equivalent material over the 2 metres immediately upstream of the weir. The crest surface and sides of the notch should have plane surfaces which make sharp 90-degree intersections with the upstream weir face. These sharp edges may be reinforced by a non-corrodible angle iron. If a movable gate is required on the (check) structure, the grooves should be located at the downstream side of the weir and should not interfere with the flow pattern through the control section.

No specific data are available on the rate of change of the weir discharge if the tailwater level rises above the weir crest. It may be expected, however, that no significant change in the $Q - h_1$ relationship will occur provided that the submergence ratio h_2/h_1 does not exceed 0.20.

6.1.2 Evaluation of discharge

As stated in Section 1.10, the basic head-discharge equation for a short-crested weir with rectangular control section is

$$Q = C_d\ C_v\ \frac{2}{3}\left[\frac{2}{3}\ g\right]^{0.50}\ bh_1^{1.5} \qquad (6\text{-}1)$$

where values of the discharge coefficient C_d may be obtained from Figure 6.2 as a function of the dimensionless ratios b/h_1 and L/h_1.

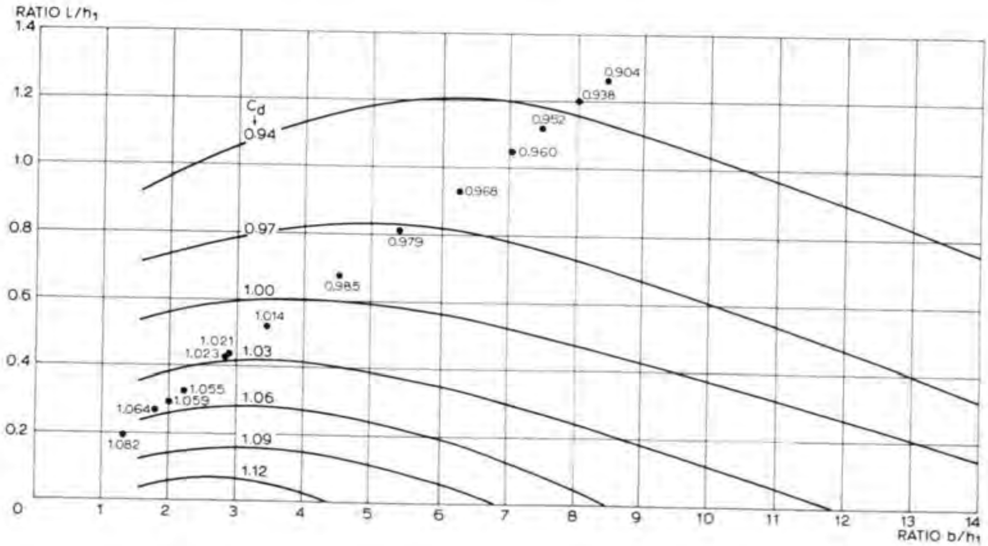

Fig.6.2. Values of C_d as a function of b/h_1 and L/h_1 (adapted from W.O.REE, 1938, Spartanborg Outdoor Hydr.Lab. and after own data points).

Values of the approach velocity coefficient C_v can be read as a function of $C_d A^*/A_1$ in Chapter I, Figure 1.12, where $A^* = bh_1$.

For a weir which has been constructed and maintained with reasonable care and skill the error in the product C_dC_v in Equation 6-1, may be expected to be less than 5%. The method by which the coefficient error is to be combined with other sources of error is shown in Appendix II.

6.1.3 Limits of application

For reasonable accuracy, the limits of application of a weir sill with rectangular control section are:

a) The practical lower limit of h_1 is related to the magnitude of the influence of fluid properties, to the boundary roughness in the approach section, and to the accuracy with which h_1 can be determined. The recommended lower limit is 0.09 m.

b) The crest surface and sides of the control section should have plane surfaces which make sharp 90-degree intersections with the upstream weir face.

c) The bottom width of the trapezoidal approach channel should be 1.25 b.

d) The upstream head h_1 should be measured 1.80 m above the downstream weir face. Consequently, h_1 should not exceed half of this distance, i.e. 0.90 m.

e) To obtain modular flow the submergence ratio h_2/h_1 should not exceed 0.20.

6.2 V-notch weir sill

6.2.1 Description

In natural streams, where it is necessary to measure a wide range of discharge, a triangular control section has the advantage of providing a wide opening at high flows so that it causes no excessive backwater effects, whereas at low flows its opening is reduced so that the sensitivity of the structure remains acceptable.

The U.S. Soil Conservation Service developed a V-notch weir sill with 2-to-1, 3-to-1, and 5-to-1 crest slopes to measure flows up to a maximum of 50 m^3/s in small streams, Dimensions of this standard structure are shown in Figure 6.3.

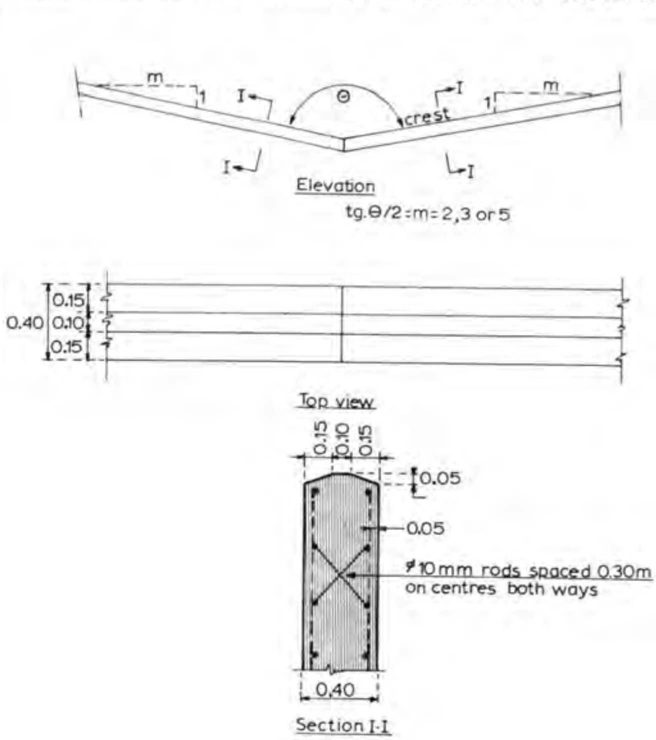

Fig.6.3. Dimension sketch of a V-notch weir sill (after U.S.Soil Cons.Serv.)

The upstream head over the weir crest h_1 should be measured a distance of 3.00 m upstream from the weir, which equals about 1.65 times the maximum value of h_1 of 1.83 m (6 ft). A reasonably straight and level approach channel of arbitrary shape should be provided over a distance of 15 m upstream of the weir. The weir notch should be at least 0.15 m from the bottom or the sides of the approach channel. To prevent the structure from being undermined, a reinforced concrete apron is required. This should extend for about 3.50 m downstream from the weir, 0.60 m below the vertex of the notch, 6.0 m across the channel, and it should have a 1.0 m end cutoff wall. The middle 3.0 m section of this apron should be level and the two 1.50 m sides should slope slightly more than the weir crest.

No specific data are available on the rate of change of the weir discharge if the tailwater level rises above the weir crest. It may be expected, however, that there will be no significant change in the Q-h_1 relationship provided that the submergence ratio h_2/h_1 does not exceed 0.30.

6.2.2 Evaluation of discharge

The basic head-discharge equation for a short-crested weir with a triangular control section is as shown in Section 1.9.3:

$$Q = C_d C_v \frac{16}{25} \left[\frac{2}{5} g\right]^{0.5} \tan \theta/2 \; h_1^{2.5} \qquad (6\text{-}2)$$

where $\tan \theta/2$ equals m.

Based on hydraulic laboratory tests conducted by the U.S.Soil Conservation Service at Cornell University, Ithaca, N.Y., rating tables have been developed giving the discharge in m^3/s at each 0.3048 m (1 foot) of head for a number of wetted areas, A_1, at the head measurement station. These are presented in Table 6.1.

From this table, it is possible to read, for example, that the discharge over a 5-to-1 V-notch weir under a head $h_1 = 0.915$ m and a wetted area of the approach channel of $A_1 = 6.50\ m^2$ equals $7.70\ m^3/s$. For a wetted area of $A_1 = 15.0\ m^2$, and therefore with a lower approach velocity, the weir discharge equals $6.56\ m^3/s$ under the same head. The head-discharge relationship for these weirs can be obtained by plotting the discharge for each 0.3048 m (1 foot) of head and the corresponding wetted area of the approach channel.

Discharges for heads up to 0.20 m can be obtained from Table 6.2. A smooth line is drawn through the plotted points and a rating table for each 0.01 m of head is produced from this curve.It should be understood that any significant change in the approach cross-section, due either to cutting or filling, requires a revision of the $Q - h_1$ curve.

It can be expected that for a well-maintained V-notch weir which has been constructed with reasonable care and skill the error in the discharges shown in Tables 6.1 and 6.2 will be less than 3%. The method by which this error is to be combined with other sources of error is shown in Appendix II.

6.2.3 Limits of application

For reasonable accuracy, the limits of application of the V-notch weir sill are:

a) The head over the weir crest should be at least 0.03 m and should be measured a distance of 3.00 m upstream from the weir.

TABLE 6.1. RATING TABLE FOR V-NOTCH WEIR SILL

(ADAPTED FROM DATA OF U.S.SOIL CONSERVATION SERVICE AT CORNELL UNIVERSITY, ITHACA)

h_1=0.305 m (1 ft)		h_1=0.610 m (2 ft)		h_1=0.915 m (3 ft)		h_1=1.219 m (4 ft)		h_1=1.524 m (5 ft)		h_1=1.829 m (6 ft)	
A_1 in m^2	Q in m^3/s	A_1 in m^2	Q in m^3/s	A_1 in m^2	Q in m^3/s	A_1 in m^2	Q in m^3/s	A_1 in m^2	Q in m^3/s	A_1 in m^2	Q in m^3/s
2-to-1 V-NOTCH WEIR											
0.55	0.159	1.20	1.17	2.40	3.74	4.30	7.56	6.75	13.7	9.50	25.4
0.60	0.157	1.25	1.13	2.45	3.60	4.50	7.00	7.00	12.5	9.75	21.3
0.65	0.156	1.30	1.09	2.50	3.48	4.75	6.64	7.25	11.8	10.00	19.6
0.70	0.156	1.35	1.06	2.65	3.23	5.00	6.38	7.50	11.4	10.25	19.0
0.75	0.155	1.40	1.03	3.00	2.93	5.50	6.06	7.75	11.2	10.50	18.5
0.80	0.154	1.45	1.02	3.50	2.78	6.00	5.84	8.00	10.9	11.0	17.6
0.90	0.154	1.50	1.00	4.00	2.70	6.50	5.69	8.50	10.6	12.0	16.8
1.00	0.153	1.60	0.980	4.50	2.64	7.00	5.61	9.00	10.4	13.0	16.2
1.50	0.153	1.75	0.962	5.00	2.61	7.50	5.54	9.75	10.2	14.0	15.8
2.00	0.152	2.00	0.942	6.00	2.57	8.00	5.46	10.50	9.96	17.0	15.1
3.00	0.152	2.50	0.927	7.50	2.55	10.0	5.30	12.00	9.74	20.0	14.8
4.00	0.152	5.00	0.898	10.00	2.52	13.0	5.24	15.00	9.35	25.0	14.6
5.00	0.151	7.50	0.895	15.00	2.50	16.0	5.21	20.0	9.16	30.0	14.4
6.00	0.151	10.0	0.895	20.00	2.49	23.0	5.18	30.0	9.01	40.0	14.3
7.00	0.151	14.0	0.895	25.00	2.49	32.0	5.18	40.0	9.00	60.0	14.2

h_1=0.305 m (1 ft)		h_1=0.610 m (2 ft)		h_1=0.915 m (3 ft)		h_1=1.219 m (4 ft)		h_1=1.524 m (5 ft)		h_1=1.829 m (6 ft)	
A_1 in m^2	Q in m^3/s	A_1 in m^2	Q in m^3/s	A_1 in m^2	Q in m^3/s	A_1 in m^2	Q in m^3/s	A_1 in m^2	Q in m^3/s	A_1 in m^2	Q in m^3/s
3-to-1 V-NOTCH WEIR											
0.75	0.237	1.85	1.62	3.75	5.24	6.50	12.0	10.5	19.2	15.0	30.6
0.80	0.234	2.00	1.56	4.00	4.83	6.75	10.8	11.0	18.0	15.5	28.8
0.90	0.232	2.50	1.44	4.50	4.43	7.00	10.3	12.0	16.8	16.0	27.6
1.00	0.230	2.75	1.42	5.00	4.25	7.50	9.69	13.0	16.0	16.5	27.0
1.20	0.228	3.00	1.40	5.50	4.14	8.00	9.31	14.0	15.5	17.0	26.5
1.50	0.226	3.50	1.38	6.00	4.06	8.50	9.02	15.0	15.1	18.0	25.9
2.00	0.225	4.00	1.37	6.50	4.02	9.00	8.81	16.0	14.9	19.0	24.9
3.00	0.224	4.50	1.36	7.00	3.98	9.50	8.67	17.0	14.7	20.0	24.4
5.00	0.224	5.00	1.35	8.00	3.91	10.0	8.55	18.0	14.5	22.5	23.6
7.50	0.224	5.50	1.35	9.00	3.88	11.0	8.37	20.0	14.4	25.0	23.1
		6.00	1.34	10.0	3.85	12.0	8.25	22.5	14.2	27.5	22.8
		7.00	1.34	12.5	3.79	15.0	8.03	25.0	14.0	30.0	22.5
		8.00	1.33	15.0	3.77	20.0	7.90	30.0	13.9	40.0	22.0
		10.00	1.33	20.0	3.75	30.0	7.80	40.0	13.8	50.0	21.8
		14.00	1.33	25.0	3.74	45.0	7.79	55.0	13.7	60.0	21.7
5-to-1 V-NOTCH WEIR											
1.50	0.386	2.80	2.77	5.60	8.76	11.0	16.4	16.0	30.0	22.0	49.4
2.00	0.382	3.00	2.67	5.75	8.49	11.25	16.1	17.0	27.8	23.0	46.3
3.00	0.378	3.25	2.58	6.00	8.17	11.5	15.8	18.5	26.9	25.0	43.4
6.00	0.376	3.50	2.52	6.25	7.87	12.0	15.5	20.0	26.0	27.5	41.1
10.00	0.376	3.75	2.49	6.50	7.70	12.5	15.2	22.5	25.0	30.0	39.8
		4.00	2.45	7.00	7.42	13.0	15.0	25.0	24.5	32.5	39.1
		4.50	2.42	7.50	7.26	14.0	14.6	27.5	24.1	35.0	38.5
		5.00	2.39	8.00	7.10	15.0	14.4	30.0	23.8	37.5	38.0
		6.00	2.35	9.00	6.99	16.0	14.2	32.5	23.7	40.0	37.6
		7.00	2.33	10.0	6.84	17.5	14.0	35.0	23.6	45.0	37.1
		8.50	2.32	12.0	6.67	20.0	13.8	40.0	23.4	50.0	36.6
		10.00	2.30	15.0	6.56	25.0	13.5	50.0	23.3	55.0	36.4
		15.00	2.23	20.0	6.48	30.0	13.4	60.0	23.2	60.0	36.2
		20.00	2.28	30.0	6.42	40.0	13.3	75.0	23.0	75.0	36.0
		25.00	2.28	45.0	6.40	65.0	13.2	90.0	22.8	90.0	36.0

TABLE 6.2. DISCHARGE VALUES FOR HEADS UP TO 0.20 m OF V-NOTCH WEIRS $m^3/s \times 10^{-3}$

Head (metres)	Discharge in litres per second for V-notch weirs 2-to-1 (a)	3-to-1 (b)	5-to-1 (c)
0.03	0.5	0.7	1.0
0.04	0.9	1.3	2.0
0.05	1.7	2.3	3.7
0.06	2.6	3.7	6.0
0.07	3.7	5.3	8.6
0.08	5.2	7.3	12.1
0.09	6.9	9.9	16.1
0.10	8.9	12.9	21.1
0.11	11.2	16.4	26.8
0.12	13.9	20.5	33
0.13	17.0	25.3	41
0.14	21.8	31	52
0.15	24.5	37	59
0.16	28.3	43	68
0.17	34	51	80
0.18	39	59	93
0.19	45	67	107
0.20	51	77	123

NOTE:

Applicable to stations with cross-sectional areas through intake equal to or greater than

(a) 0.55 m^2 for 0.30 m head

(b) 0.75 m^2 for 0.30 m head

(c) 1.40 m^2 for 0.30 m head

b) The notch should be at least 0.15 m from the bottom or the sides of the approach channel.

c) The approach channel should be reasonably straight and level for 15.0 m upstream from the weir.

d) To obtain modular flow the submergence ratio h_2/h_1 should not exceed 0.30.

6.3 Triangular profile two-dimensional weir

6.3.1 Description

The triangular profile two-dimensional weir is sometimes referred to in the literature as the Crump weir, a name credited to E.S.CRUMP, who described the device for the first time in a paper in 1952. The profile of the weir in the direction of flow shows an upstream slope of 1 (vertical) to 2 (horizontal) and a downstream slope of either 1 to 5 or 1 to 2. The intersection of the two sloping surfaces forms a straight horizontal crest at right angles to the flow direction in the approach channel. Care should be taken that the crest has a well-defined corner of durable construction. The crest may either be made of carefully aligned and joined precast concrete sections or have a cast-in non-corrodible metal profile.

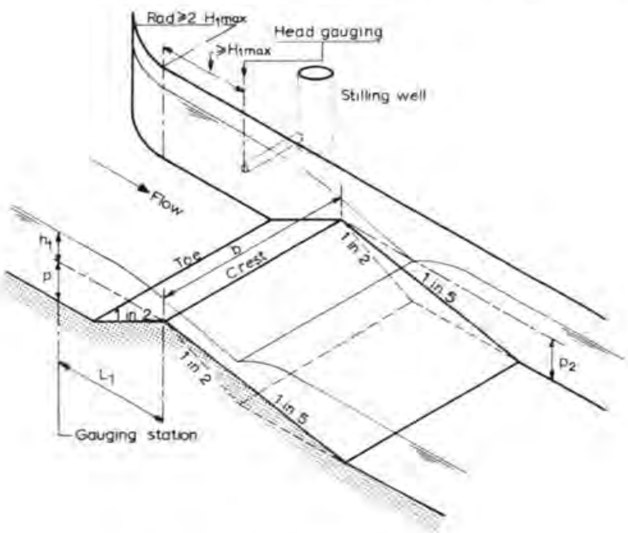

Fig.6.4. Triangular profile two-dimensional weir.

Tests were carried out at the Hydraulics Research Station at Wallingford (U.K.) to determine the maximum permissible truncation of the weir block in the direction of flow whereby the discharge coefficient was to be within 0.5% of its constant value. It was found that for a 1-to-2 / 1-to-5 weir the minimum horizontal distance from the weir crest to point of truncation of the weir block equals 1.0 H_1max for the 1-to-2 slope and 2.0 H_1 max for the 1-to-5 slope. For a 1-to-2 / 1-to-2 weir, these minimum distances equal 0.8 H_1 max for the upstream slope and 1.2 H_1 max for the downstream slope.

The upstream head over the weir crest h_1 should be measured in a rectangular approach channel at a sufficient distance upstream from the crest to avoid the area of surface draw-down,but close enough to the crest for the energy loss between the head measurement station and the control section to be negligible. For this to occur, the head measurement station should be at a distance $L_1 = 6$ p upstream from the weir crest for a 1-to-2 / 1-to-5 weir and at $L_1 = 4$ p for a 1-to-2 / 1-to-2 weir. If no particularly high degree of accuracy is required in the maximum discharges to be measured, savings can be made in the construction cost of the structure by reducing the distance from the crest to head measurement station to 2p + 0.5 H_1 max. The additional error introduced will be of the order of 0.25% at an H_1/p value of 1, of 0.5% at an H_1/p value of 2, and of 1% at an H_1/p value of 3.

If the weir is to be used for discharge measuring beyond the modular range, crest tappings should be provided to measure the piezometric level in the separation pocket formed immediately downstream of the crest. The crest tapping should consist of a sufficient number (usually 4 to 12) of ø 0.01 m holes drilled in the weir crest block on 0.10 m centres 0.019 m downstream from the weir crest as shown in Figure 6.5. The edges of the holes should not be rounded or burred.

Preferably, the crest tapping should be located at the centre of the weir, but may be off-centre provided that the side walls do not interfere with the pressure distribution in the separation pocket. A distance of about 1.20 m from the side walls should be sufficient. Weirs with a breadth b of less than 2.5 m should have the crest tapping in the centre.

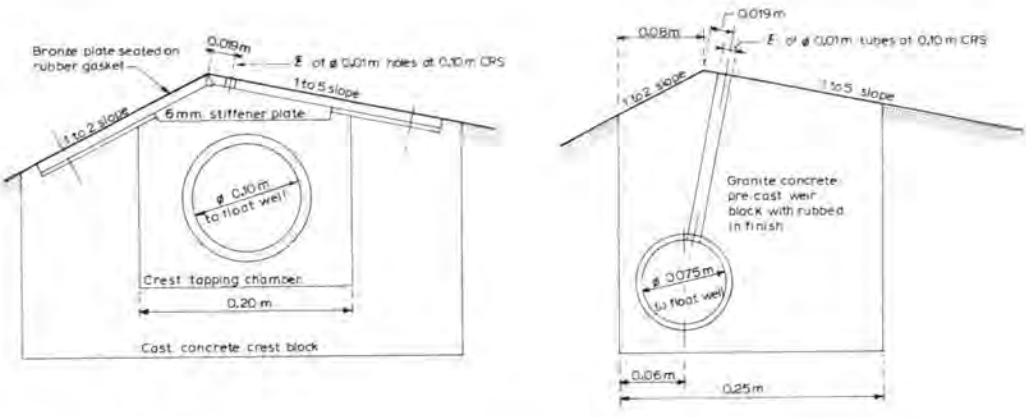

Fig.6.5. Alternative solutions for crest tappings.

6.3.2 Evaluation of discharge

According to Sections 1.10 and 1.13.1, the basic head-discharge equation for a short-crested weir with rectangular control section reads

$$Q = C_d C_v \frac{2}{3} \left[2g\right]^{0.5} b h_e^{1.5} \qquad (6\text{-}3)$$

where the effective head over the weir crest $h_e = h_1 - K_h$, K_h being an empirical quantity representing the combined effects of several phenomena attributed to viscosity and surface tension. A constant value of $K_h = 0.0003$ m for 1-to-2 / 1-to-5 weirs, and of $K_h = 0.00025$ for 1-to-2 / 1-to-2 weirs is recommended.

For field installations where it is not practicable to determine h_1-values accurate to the nearest 0.001 m the use of K_h is inappropriate. Consequently values of $h_e \simeq h_1$ may be used on these installations.

Over the selected range of ratio h_1/p, being $h_1/p < 3$, the discharge coefficient is a function of the dimensionless ratio H_1/p_2 as illustrated in Figure 6.6.

The curve for the 1-to-2/1-to-2 weir shows that the discharge coefficient for low values of p_2 begins to fall at a value $H_1/p_2 = 1.0$ and is 0.5% below the average deep downstream value at $H_1/p_2 = 1.25$. The curve for the 1-to-2/1-to-5 weir shows corresponding values of $H_1/p_2=2.0$ and $H_1/p_2=3.0$,thereby indicating that the discharge coefficient for a 1-to-5 downstream slope is considerably more constant in terms of the proximity of the downstream bed.For high p_2 values, the discharge coefficient of the 1-to-2/1-to-2 weir has a higher value (C_d = 0.723) than the 1-to-2/1-to-5 weir (C_d = 0.674) since the streamlines above the crest of the latter have a larger radius of curvature (see also Section 1.10).

The approach velocity coefficient $C_v = (H_1/h_1)^{3/2}$ is related to the ratio $\{C_d\ h_1/(h_1 + p)\}\ b/B$ and can be read from Figure 1.12.

The error in the product C_dC_v of a well-maintained triangular profile weir with modular flow, constructed and installed with reasonable care, may be deduced from the equation

$$X_c = \pm\ (10\ C_v - 9)\ \text{percent} \tag{6-4}$$

The method by which this error is to be combined with other sources of error is shown in Appendix II.

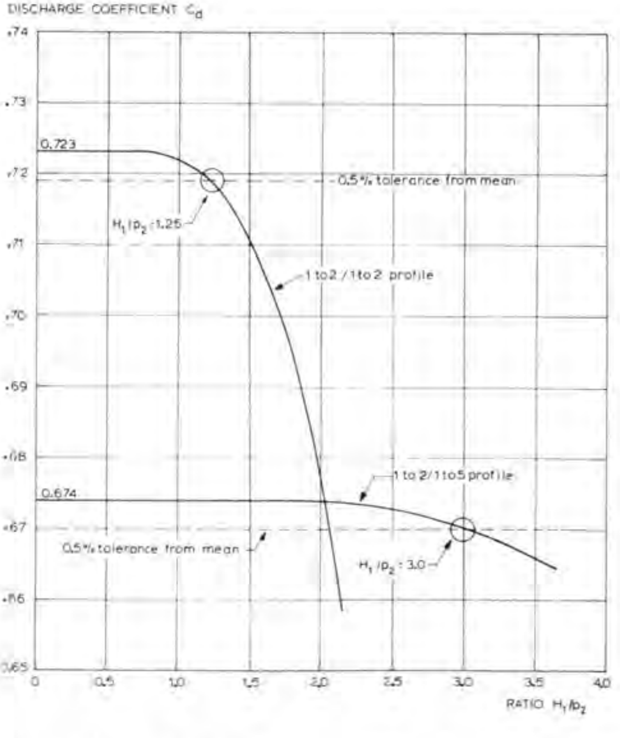

Fig.6.6. Two-dimensional triangular profile weirs, effect of downstream bed level on modular C_d-value.
(After W.R.White, 1971.)

6.3.3 Modular limit

The modular limit, or that submergence ratio H_2/H_1 which produces a 1% reduction from the equivalent modular discharge, depends on the height of the crest above the average downstream bed level. The results of various tests are shown in Figure 6.7, where the modular limit H_2/H_1 is given as a function of the dimensionless ratio H_1/p_2.

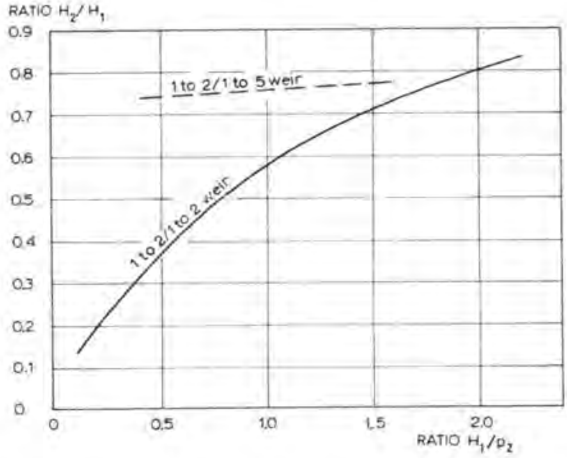

Fig.6.7. Modular limit as a function of H_1/p_2 (after E.S.Crump, 1952, and H.R.S.Wallingford, 1966 and 1971).

For non-modular flow conditions, the discharge as calculated by Equation 6-3, i.e. the discharge that would occur with low tailwater levels, has to be reduced by a factor which is a function of the downstream head over the weir crest. For non-modular flow, the discharge thus equals

$$Q = C_d C_v \ f \ \frac{2}{3} \ (2 \ g)^{0.5} \ bh_e^{1.5} \qquad (6\text{-}5)$$

The drowned flow reduction factor f is easier to define and evaluate for weirs which have a constant discharge coefficient. Figure 6.7 shows that the 1-to-2/1-to-5 weir has a more favourable modular limit, while Figure 6.6 shows that the C_d-coefficient is constant over a wider range of H_1/p_2. The Hydraulics Res. Station, Wallingford therefore concentrated its study on the drowned flow performance of the 1-to-2/1-to-5 weir. A graph has been produced giving values of the product $C_v f$ as a function of the two-dimensionless ratios $\{C_d h_e/(h_e+p)\}b/B$

and h_p/h_e, where h_p equals the piezometric pressure within the separation pocket.

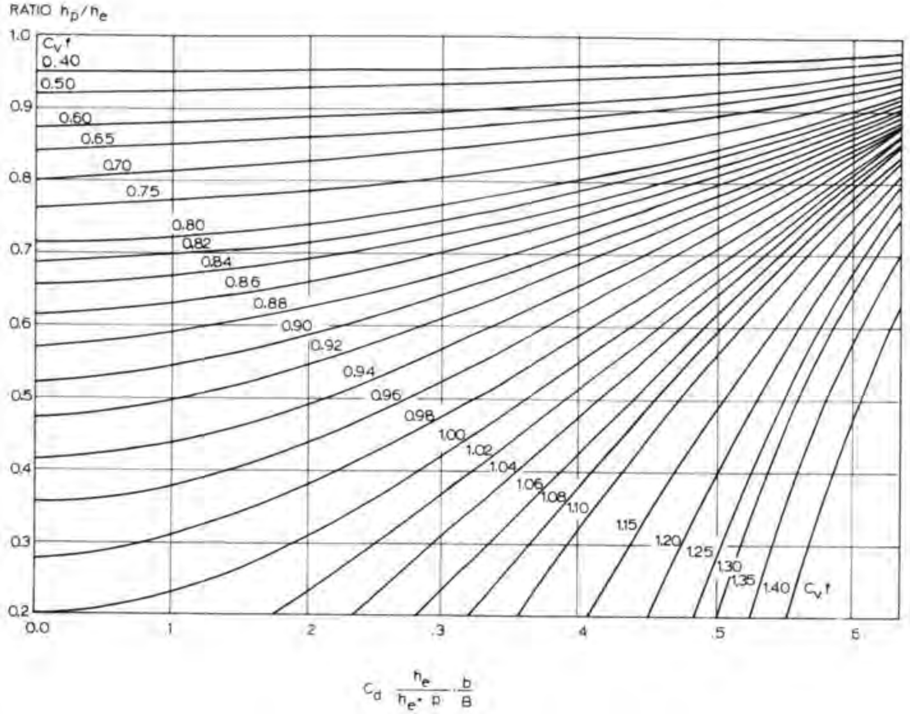

Fig.6.8. Two-dimensional 1-to-2/1-to-5 weir, submerged flow product $C_v f$ (after W.R.WHITE, 1971).

The product $C_v f$ can be extracted from Figure 6.8 for values of the two ratios. Substitution of $C_v f$ into Equation 6-5 then gives the weir discharge for its non-modular range.

6.3.4 Limits of application

For reasonable accuracy, the limits of application of the triangular profile weir are:

a) For a well-maintained weir with a non-corrodible metal insert at its crest, the recommended lower limit of h_1 = 0.03 m. For a weir with a crest made of precast concrete sections or similar materials, h_1 should not be less than 0.06 m.

b) The weir, in common with other weirs and flumes, becomes inaccurate when the Froude number, $Fr = V/(gA_1/B_1)^{\frac{1}{2}}$, in the approach channel exceeds 0.5, due to the effects of surface instability in the form of stationary waves. The limitation $Fr \leqslant 0.5$ may be stated in terms of h_1 and p. The recommended upper limit of h_1/p is 3.0.

c) The height of the weir crest should not be less than 0.06 m above the approach channel bottom ($p \geqslant 0.06$ m).

d) To reduce the influence of boundary layer effects at the sides of the weir, the breadth of the weir b should not be less than 0.30 m and the ratio b/H_1 should not be less than 2.0.

e) To obtain a sensibly constant discharge coefficient for 1-to-2/1-to-2 profile weirs, the ratio H_1/p_2 should not exceed 1.25. For 1-to-2/1-to-5 profile weirs, this ratio should be less than 3.0.

6.4 Triangular profile flat-V weir

6.4.1 Description

In natural streams where it is necessary to measure a wide range of discharges, a triangular control has the advantage of providing a wide opening at high flows so that it causes no excessive backwater effects, whereas at low flows its opening is reduced so that the sensitivity of the structure remains acceptable. The Hydraulics Research Station, Wallingford investigated the characteristics of a triangular profile flat-V weir with cross-slopes of 1-to-10 and 1-to-20. (For the two-dimensional triangular profile weir, see Section 6.3.) The profile in the direction of flow shows an upstream slope of 1-to-2 and a downstream slope of either 1-to-5 or 1-to-2. The intersections of the upstream and downstream surfaces form a crest at right angles to the flow direction in the approach channel. Care should be taken that the crest has a well-defined corner made either of carefully aligned and joined precast concrete sections or of a cast-in non-corrodible metal profile.

The permissible truncation of the weir block is believed to be the same as that of the two-dimensional weir (see Section 6.3.1). Therefore the minimum horizontal distance from the weir crest to point of truncation whereby the C_d-value is within 0.5% of its constant value, equals 1.0 H_1 max for the upstream and 2.0 H_1 max for the downstream slope of a 1-to-2/1-to-5 weir. For a 1-to-2/1-to-2 weir these minimum distances equal 0.8 H_1max for the upstream slope and 1.2 H_1max for the downstream slope.

The upstream head over the weir crest h_1 should be measured in a rectangular approach channel at a distance of ten times the V-height upstream of the crest, i.e. $L_1 = 10\ H_b$. At this station, differential drawdown across the width of the approach channel is negligible and a true upstream head can be measured accurately.

If a 1-to-2/1-to-5 weir is to be used for discharge measuring beyond its modular range, three crest tappings should be provided to measure the piezometric level in the separation pocket, h_p, immediately downstream (0.019 m) of the crest (see also Figure 6.5).

One crest tapping should be at the centre line, the other two at a distance of 0.1 B offset from the centre line.

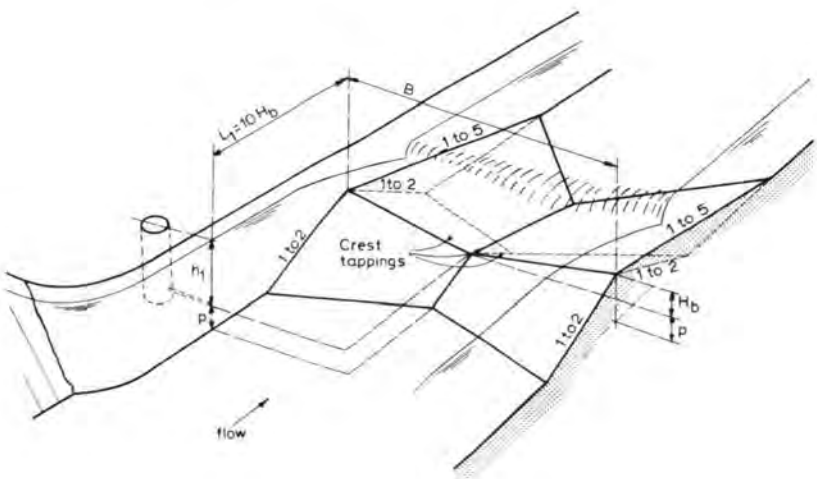

Fig.6.9. Triangular profile flat-V weir.

6.4.2 Evaluation of discharge

According to Section 1.10, the basic head-discharge equation for a short-crested flat-V weir with vertical side walls reads

$$Q = C_d C_v \frac{4}{15} (2g)^{0.5} \frac{B}{H_b} \left[h_e^{2.5} - (h_e - H_b)^{2.5} \right] \qquad (6\text{-}6)$$

in which the term $(h_e - H_b)^{2.5}$ should be deleted if h_e is less than H_b. The effective head over the weir crest $h_e = h_1 - K_h$, K_h being an empirical quantity representing the combined effects of several phenomena attributed to viscosity and surface tension. Values for K_h are presented in Table 6.3.

TABLE 6.3. K_h-VALUES FOR TRIANGULAR PROFILE FLAT-V WEIRS (AFTER W.R.WHITE, 1971)

weir profile	1-to-20 cross slope	1-to-10 cross slope
1-to-2/1-to-2	0.0004 m	0.0006 m
1-to-2/1-to-5	0.0005 m	0.0008 m

For the 1-to-2/1-to-5 weir, an average C_d-value of 0.66 may be used for both cross slopes provided that the ratio $h_e/p_2 < 3.0$. The C_d-value of a 1-to-2/1-to-2 weir is more sensitive to the bottom level of the tailwater channel with regard to crest level. An average value of $C_d = 0.71$ may be used provided that h_e/p_2 does not exceed 1.25.

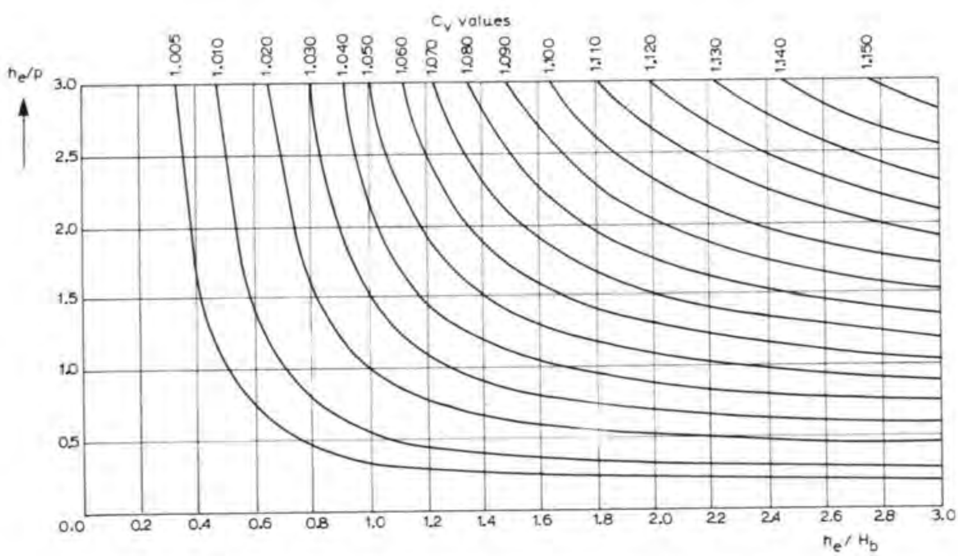

Fig.6.10. C_v-values as a function of h_e/p and h_e/H_b (after W.R.White, 1971).

The approach velocity coefficient C_v can be read as a function of the ratios h_e/p and h_e/H_b in Figure 6.10.

The error in the product C_dC_v of a well-maintained triangular profile weir with modular flow, constructed with reasonable care and skill, may be expected to be

$$X_c = \pm (10\ C_v - 8) \text{ percent} \qquad (6\text{-}7)$$

The method by which this error is to be combined with other sources of error is shown in Appendix II.

6.4.3 Modular limit and non-modular discharge

The modular limit again is defined as that submergence ratio H_2/H_1 which produces a 1% reduction from the equivalent modular discharge as calculated by Equation 6-6.

Results of various tests have shown that for a 1-to-2/1-to-2 weir the drowned flow reduction factor, f, and thus the modular limit, are functions of the dimensionless ratios H_2/H_1, H_1/H_b, H_1/p, H_1/p_2, and the cross slope of the weir crest.

Because of these variables, the modular limit characteristics of a 1-to-2/1-to-2 weir are rather complex and sufficient data are not available to predict the influence of the variables. A limited series of tests in which only discharge, cross-slope, and downstream bed level (p_2) were varied was undertaken at Wallingford. The results of these tests, which are shown in Figure 6.11, are presented mainly to illustrate the difficulties.

For a 1-to-2/1-to-5 profile weir, the drowned flow reduction factor is a less complex phenomenon, and it appears that the f-value is a function of the ratios H_2/H_1 and H_1/H_b only (Fig.6.12). Tests showed that there is no significant difference between the modular flow characteristics of the weirs with either 1-to-10 or 1-to-20 cross slopes. As illustrated in Figure 6.12, the drowned flow reduction factor f equals 0.99 for modular limit values between 0.67 and 0.78, depending on the modular value of H_1/H_b.

For non-modular flow conditions, the discharge over the weir is reduced because of high tailwater levels, and the weir discharge can be calculated from Equation 6-8, which reads

$$Q = C_dC_v\ f\ \frac{4}{15}\ (2g)^{0.5}\ \frac{B}{H_b}\left[h_e^{2.5} - (h_e - H_b)^{2.5}\right] \qquad (6\text{-}8)$$

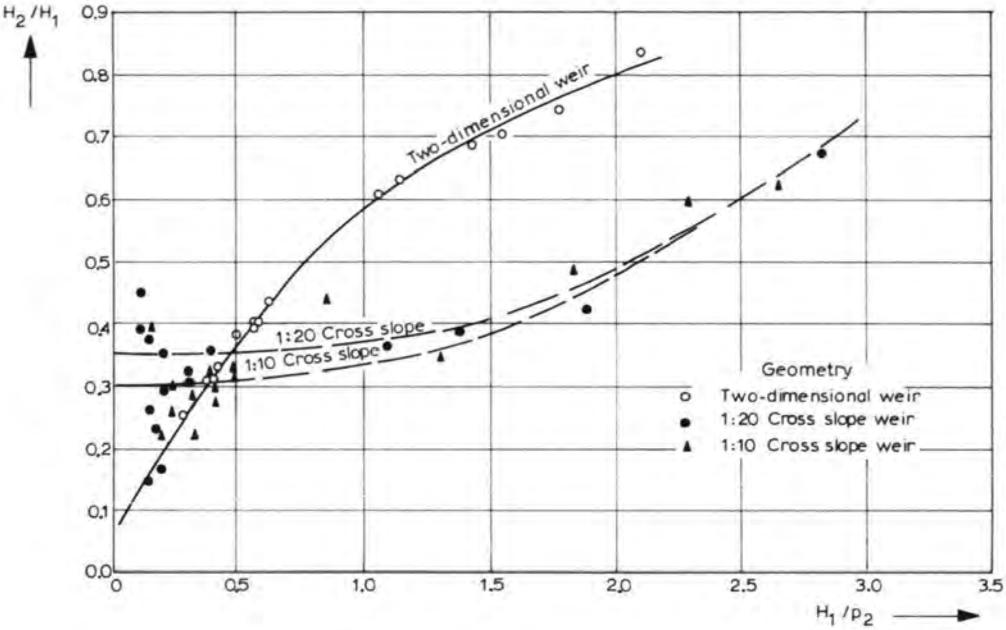

Fig.6.11. Modular limit conditions, triangular profile 1-to-2/1-to-2 flat-V (after W.R.WHITE, 1971).

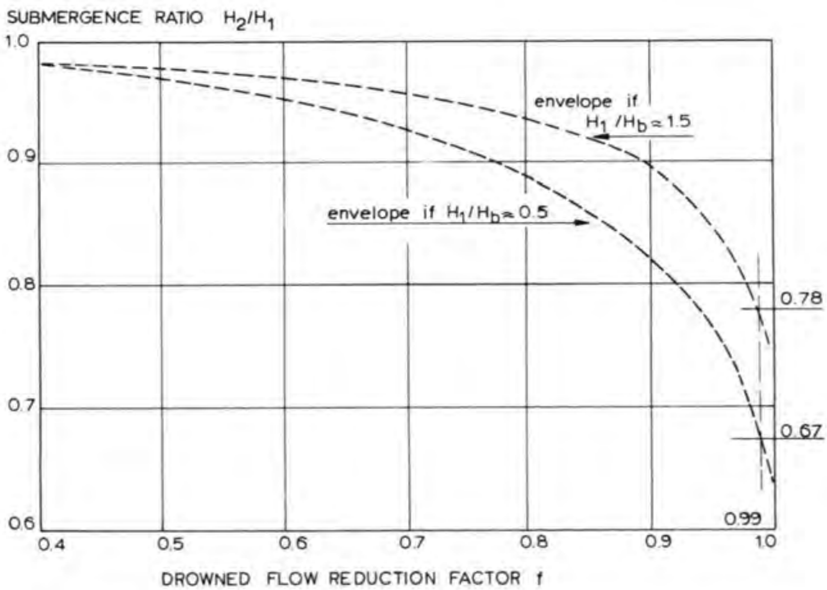

Fig.6.12. Modular limit conditions, 1-to-2/1-to-5 flat-V weir (adapted from W.R.WHITE, 1971).

This equation is similar to Equation 6-6 except that a drowned flow reduction factor f has been introduced.For 1-to-2/1-to-5 profile weirs, f-values have been determined and,in order to eliminate an intermediate step in the computation of discharge,they have also been combined with the approach velocity coefficient as a product $C_v f$. This product is a function of h_e/H_b, h_p/h_e, and H_b/p and as such is presented in Figure 6.13. To find the proper $C_v f$-value, one enters the figure by values of h_e/H_b and h_p/h_e and by use of interpolation in terms of H_b/p a value of the product $C_v f$ is obtained. Substitution of all values into Equation 6-8 gives the non-modular discharge.

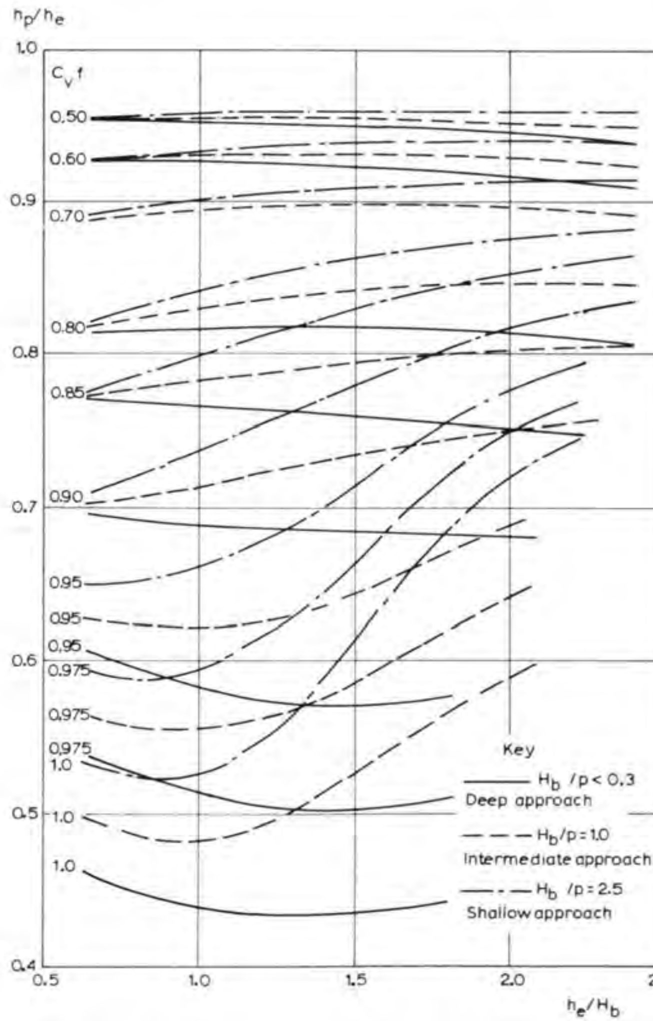

Fig.6.13. Values of $C_v f$ for a 1-to-2/1-to-5 flat-V weir as a function of h_e/H_b, h_p/h_e and H_b/p (after W.R.WHITE, 1971).

6.4.4 Limits of application

For reasonable accuracy, the limits of application of a triangular profile flat-V weir are:

a) For a well-maintained weir with a non-corrodible metal insert at its crest, the recommended lower limit of $h_1 = 0.03$ m. For a crest made of pre-cast concrete sections or similar materials, h_1 should not be less than 0.06 m.

b) To prevent water surface instability in the approach channel in the form of stationary waves, the ratio h_1/p should not exceed 3.0.

c) The height of the vertex of the weir crest should not be less than 0.06 m above the approach channel bottom.

d) To reduce the influence of boundary layer effects at the sides of the weir, the width of the weir B should not be less than 0.30 m and the ratio B/H_1 should not be less than 2.0.

e) To obtain a sensibly constant discharge coefficient for 1-to-2/1-to-2 profile weirs, the ratio H_1/p_2 should not exceed 1.25. For 1-to-2/1-to-5 profile weirs, this ratio should be less than 3.0.

f) The upstream head over the weir crest should be measured a distance of 10 H_b upstream from the weir crest in a rectangular approach channel.

g) To obtain modular weir flow, the submergence ratio H_2/H_1 should not exceed 0.30 for 1-to-2/1-to-2 profile weirs and should be less than 0.67 for 1-to-2/1-to-5 profile weirs. For the latter weir profile, however, non-modular flows may be calculated by using Equation 6-8 and Figure 6.13.

6.5 Butcher's movable standing wave weir

6.5.1 Description

Butcher's weir was developed to meet the particular irrigation requirements in the Sudan, where the water supplied to the fields varies because of different requirements during the growing season and because of crop rotation. A description of the weir was published for the first time in 1922 by A.D.BUTCHER, after whom the structure has been named.[1]

[1] *Nowadays the structure is manufactured commercially by Newton Chambers Engineering Ltd., Thorncliff, Sheffield, England.*

The weir consists of a round-crested movable gate with guiding grooves and a self-sustaining hand gear for raising and lowering it. The cylindrical crest is horizontal perpendicular to the flow direction. The profile in the direction of flow shows a vertical upstream face connected to a 1-to-5 downward sloping face by a 0.25 $h_1$max radius circle, where $h_1$max is the upper limit of the range of heads to be expected at the gauge located at a distance 0.75 $h_1$max upstream from the weir face.

The side walls are vertical and are rounded at the upstream end in such a way that flow separation does not occur. Thus a rectangular approach channel is formed to assure two-dimensional weir flow. The upstream water depth over the weir crest h_1 is measured in this approach channel by a movable gauge mounted on two supports. The lower support is connected to the movable gate and the upper support is bolted to the hoisting beam. The gauge must be adjusted so that its zero corresponds exactly with the weir crest. Because of their liability to damage the supports have been kept rather short; a disadvantage of this shortness is that the water surface elevation is measured in the area of surface drawdown so that the hydraulic dimensions of both the approach channel and weir cannot be altered without introducing an unknown change in the product of C_dC_v. The centre line of the gauge should be 0.75 $h_1$max upstream from the weir face.

The weir can be raised high enough to cut off the flow at full supply level in the feeder canal and, when raised, leakage is negligible. In practice it has been found advantageous to replace the lower fixed weir, behind which the weir moves, with a concrete or masonry sill whose top width is about 0.10 m and whose upstream face is not flatter than 2-to-1.

The maximum water depth over the weir crest, and thus the maximum permissible discharge per metre weir crest, influences the weir dimensions. Used in the Sudan are two standard types with maximum values of h_1 = 0.50 m and h_1 = 0.80 m respectively. It is recommended that 1.00 m be the upper limit for h_1. The breadth of the weir varies from 0.30 m to as much as 4.00 m, the larger breadths used in conjunction with high $h_1$max-values. As shown in Figure 6.14, p = 1.4 $h_1$max, which results in low approach velocities.

The modular limit is defined as the submergence ratio h_2/h_1 which produces a 1% reduction from the equivalent modular discharge. Results of various tests showed that the modular limit is h_2/h_1 = 0.70. The average rate of reduction from the equivalent modular discharge is shown in percentages in Figure 6.15.

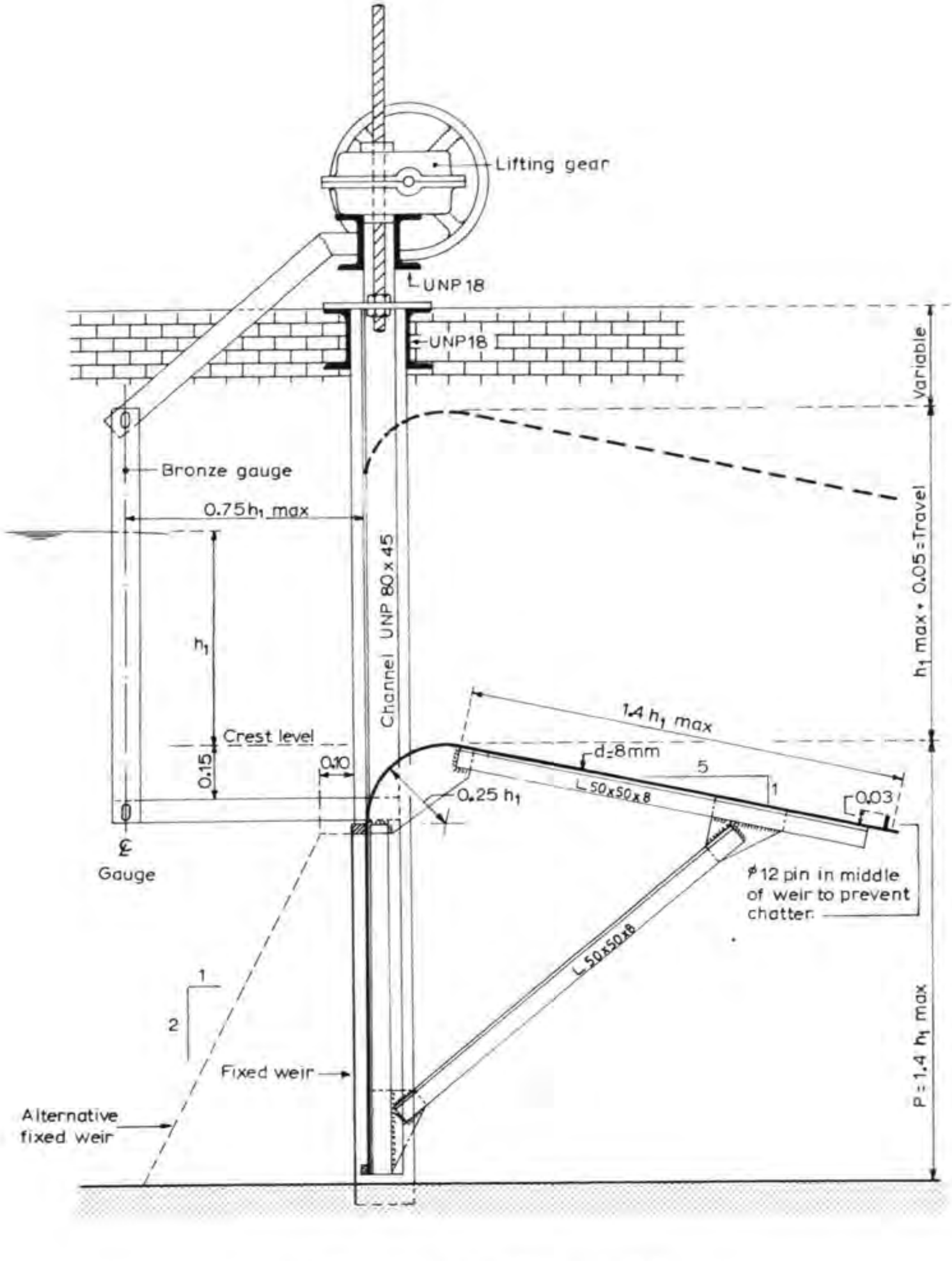

Fig.6.14. Butcher's movable gate.

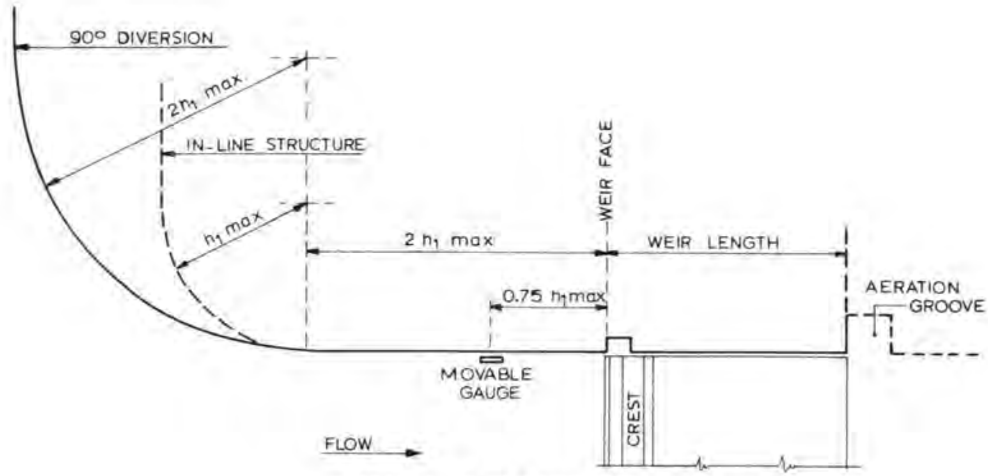

DETAILS OF WEIR ABUTMENT

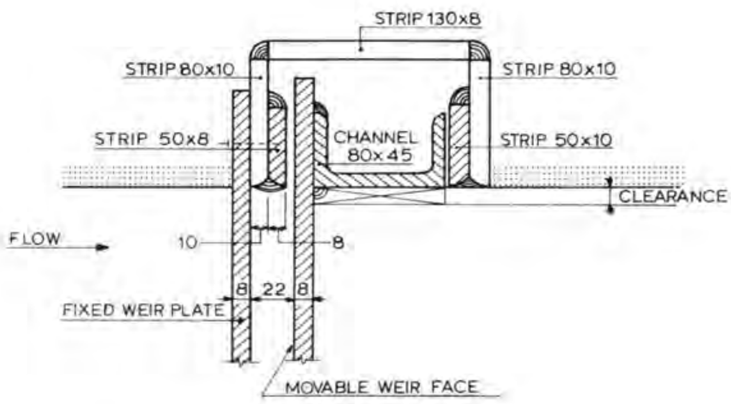

DETAILS GROOVE ARRANGEMENT

Fig.6.14. (cont.)

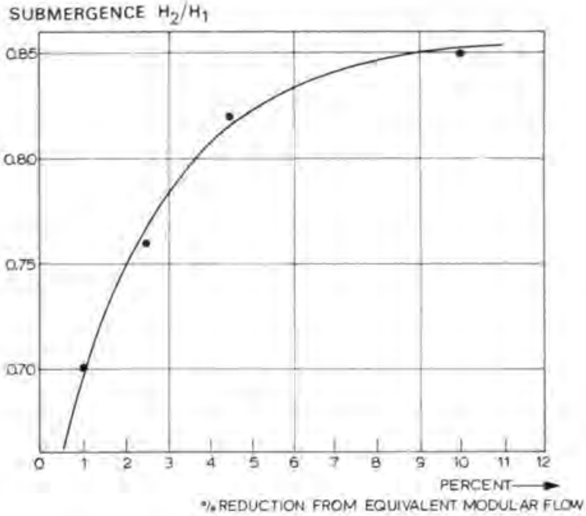

Fig.6.15. Modular flow conditions.

6.5.2 Evaluation of discharge

Since the water depth over the weir crest is measured in the area of water surface drawdown at a distance of 0.75 $h_1$max upstream from the weir face, i.e. $h_1$max upstream from the weir crest, the stage-discharge relationship of the weir has the following empirical shape:

$$Q = cbh_1^{1.6} \tag{6-9}$$

where h_1 equals the water depth at a well-prescribed distance, L_1 = 0.75 $h_1$max, upstream from the weir face. It should be noted that this water depth is somewhat lower than the real head over the weir crest. For weirs that are constructed in accordance with the dimensions shown in Figure 6.14, the effective discharge coefficient equals c = 2.30 $m^{0.4}$ sec^{-1}. The influence of the approach velocity on the weir flow is included in this coefficient value and in the exponent value 1.6.

To facilitate calculations of discharge, Table 6.4 gives values of $h_1^{1.6}$ for each 0.01 m of water depth.

The error in the discharge coefficient c of a well-maintained Butcher movable weir which has been constructed with reasonable care and skill may be expected to be less than 3%. The method by which this error is to be combined with other sources of error is shown in Appendix II.

TABLE 6.4. 1.6 POWERS OF NUMBERS FOR USE IN EQUATION 6-9

h_1	0	1	2	3	4	5	6	7	8	9
0.01	.00063	.00074	.00085	.00096	.00109	.00121	.00134	.00148	.00163	.00177
0.02	.00191	.00207	.00223	.00239	.00256	.00274	.00291	.00310	.00329	.00347
0.03	.00366	.00386	.00406	.00427	.00448	.00468	.00490	.00513	.00535	.00558
0.04	.00580	.00601	.00628	.00652	.00676	.00700	.00726	.00752	.00780	.00805
0.05	.00829	.00856	.00883	.00911	.00938	.00965	.00994	.01023	.01052	.01081
0.06	.01109	.01140	.01170	.01200	.01230	.01261	.01292	.01324	.01356	.01388
0.07	.01420	.01453	.01486	.01519	.01552	.01586	.01620	.01665	.01689	.01724
0.08	.01758	.01793	.01829	.01864	.01900	.01936	.01973	.02010	.02047	.02084
0.09	.02121	.02160	.02198	.02237	.02275	.02314	.02354	.02393	.02433	.02472
0.1	.02512	.02925	.03362	.03826	.04303	.04806	.05327	.05869	.06434	.07017
0.2	.07610	.08231	.08867	.09521	.10200	.1087	.1159	.1231	.1305	.1380
0.3	.1456	.1536	.1615	.1696	.1780	.1865	.1950	.2037	.2127	.2217
0.4	.2309	.2402	.2496	.2592	.2689	.2787	.2887	.2988	.3089	.3194
0.5	.3299	.3406	.3513	.3621	.3731	.3842	.3955	.4068	.4182	.4299
0.6	.4417	.4534	.4654	.4774	.4897	.5019	.5142	.5270	.5395	.5522
0.7	.5652	.5782	.5912	.6043	.6176	.6313	.6446	.6583	.6780	.6857
0.8	.6998	.7139	.7280	.7423	.7567	.7709	.7856	.8002	.8151	.8299
0.9	.8447	.8598	.8752	.8904	.9057	.9210	.9369	.9526	.9681	.9840
1.0	1.000	1.016	1.032	1.048	1.065	1.081	1.097	1.114	1.131	1.148

6.5.3 Limits of application

For reasonable accuracy, the limits of application of Equation 6-9 for Butcher's movable weir are:

a) All dimensions of both the weir and the approach channel should be strictly in accordance with the dimensions shown in Figure 6.14.

b) The width of the weir b should not be less than 0.30 m and the ratio b/h_1 should not be less than 2.0.

c) The upstream water depth should be measured with a movable gauge at a distance of 0.75 $h_1$max upstream from the weir face.

d) To obtain modular flow, the submergence ratio h_2/h_1 should not exceed 0.70.

e) The recommended lower limit of h_1 = 0.05 m, while h_1 should preferably not exceed 1.00 m.

6.6 WES-Standard spillway

6.6.1 Description

From an economic point of view, spillways must safely discharge a peak flow under the smallest possible head, while on the other hand the negative pressures on the crest must be limited to avoid the danger of cavitation. Engineers therefore usually select a spillway crest shape that approximates the lower nappe surface of an aerated sharp crested weir as shown in Figure 6.16.

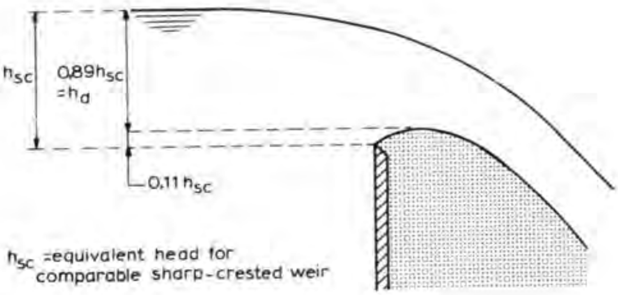

Fig.6.16. Spillway crest and equivalent sharp-crested weir.

Theoretically, there should be atmospheric pressure on the crest. In practice, however, friction between the surface of the spillway and the nappe will introduce some negative pressures. If the spillway is operating under a head lower than its design head, the nappe will normally have a lower trajectory so that positive pressures occur throughout the crest region and the discharge coefficient is reduced. A greater head will cause negative pressures at all points of the crest profile and will increase the discharge coefficient.

The magnitude of the local minimum pressure at the crest $(P/\rho g)_{min}$ has been measured by various investigators. Figure 6.17 shows this minimum pressure as a function of the ratio of actual head over design head as given by H.ROUSE and L.REID (1935) and O.DILLMAN (1933).

The avoidance of severe negative pressures on the crest, which may cause cavitation on the crest or vibration of the structure, should be considered an important design criterion on high-head spillways. In this context it is recommended that the minimum pressure on the weir crest be -4 m water column. This recommendation, used in combination with Figure 6.17, gives an upper limit for the actual head over the crest of a spillway.

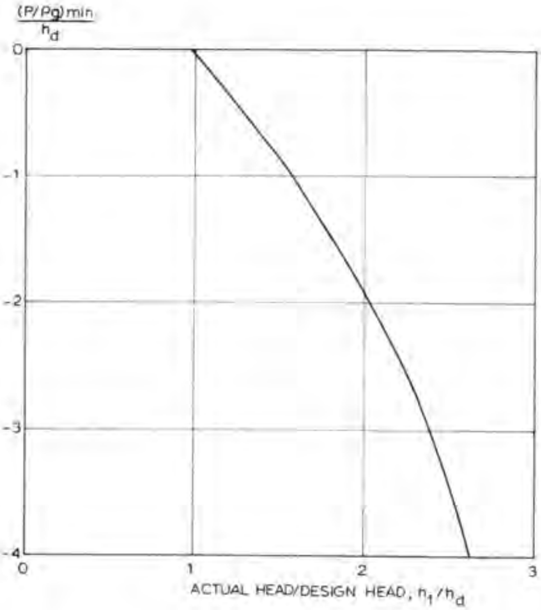

Fig.6.17. Negative pressure on spillway crest (after H.Rouse and L.Reid, 1935, and O.Dillman, 1933).

On the basis of experiments by the U.S.Bureau of Reclamation the U.S.Army Corps of Engineers conducted additional tests at their Waterways Experimental Station and produced curves which can be described by the following equation:

$$X^n = K\, h_d^{n-1}\, Y \tag{6-10}$$

which equation may also be written as

$$\frac{Y}{h_d} = \frac{1}{K}\left[\frac{X}{h_d}\right]^n \tag{6-11}$$

where X and Y are coordinates of the downstream crest slope as indicated in Figure 6.18 and h_d is the design head over the spillway crest. K and n are parameters, the values of which depend on the approach velocity and the inclination of the upstream spillway face. For low approach velocities, K and n-values for various upstream slopes are as follows:

slope of upstream face	K	n
vertical	2,000	1,850
3 to 1	1,936	1,836
3 to 2	1,939	1,810
1 to 1	1,873	1,776

Because the derived equations involve powers for which tables are not commonly available, Table 6.5 has been compiled.

TABLE 6.5. POWERS OF NUMBERS

a	$a^{1.850}$	$a^{1.836}$	$a^{1.810}$	$a^{1.776}$
0.10	.0141	.0146	.0155	.0167
0.15	.0299	.0307	.0323	.0344
0.20	.0509	.0521	.0543	.0574
0.25	.0769	.0785	.0813	.0853
0.30	.1078	.1097	.1131	.1179
0.35	.1434	.1455	.1495	.1550
0.40	.1836	.1859	.1904	.1965
0.45	.2283	.2308	.2357	.2422
0.50	.2774	.2801	.2852	.2920
0.60	.3887	.3915	.3967	.4036
0.70	.5169	.5195	.5244	.5308
0.80	.6618	.6639	.6677	.6728
0.90	.8229	.8241	.8264	.8293
1.00	1.000	1.000	1.000	1.000
1.20	1.401	1.398	1.391	1.382
1.40	1.864	1.855	1.839	1.818
1.60	2.386	2.370	2.341	2.304
1.80	2.967	2.942	2.898	2.840
2.00	3.605	3.570	3.506	3.425
2.50	5.447	5.378	5.251	5.090
3.00	7.633	7.517	7.304	7.037
3.50	10.151	9.975	9.655	9.253
4.00	12.996	12.746	12.295	11.729
4.50	16.160	15.823	15.217	14.458
5.00	19.638	19.200	18.413	17.433
6.00	27.516	26.834	25.613	24.099
7.00	36.596	35.612	33.855	31.688
8.00	46.851	45.507	43.111	40.169
9.00	58.257	56.492	53.355	49.515
10.00	70.795	68.549	64.565	59.704

The upstream surface of the crest profile varies with the slope of the upstream spillway face as shown in Figure 6.18.

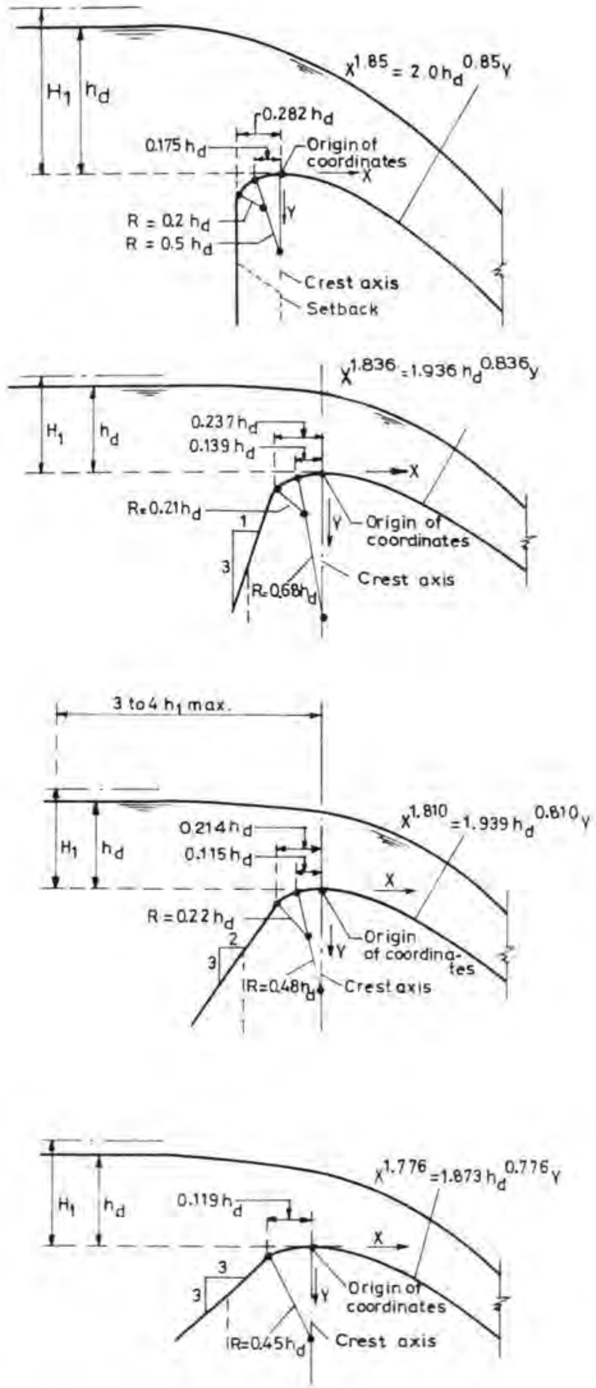

Fig.8.18. WES-standard spillway shapes (U.S.Army Corps of Engineers, Waterways Exp.Sta.)

6.6.2 Evaluation of discharge

The basic head discharge equation for a short-crested weir with a rectangular control section reads

$$Q = C_e \frac{2}{3} \left[\frac{2}{3} g\right]^{0.5} bH_1^{1.5} \tag{6-12}$$

Since the WES-standard spillway evolved from the sharp-crested weir, we might also use an equation similar to that derived in Section 1.13.1, being

$$Q = C_e^* \frac{2}{3}\left[2g\right]^{0.5} bH_1^{1.5} \tag{6-13}$$

A comparison of the two equations shows that $C_e^* = C_e/\sqrt{3}$, so that it is possible to use whichever equation suits one's purpose best.

In these two equations the effective discharge coefficient C_e (or C_e^*) equals the product of C_o (or C_o^*), C_1 and C_2 $(C_e = C_oC_1C_2)$.

C_o (or C_o^*) is a constant, C_1 is a function of p/h_d and H_1/h_d, and C_2 is a function of p/h_1 and the slope of the upstream weir face.

As illustrated in Figure 6.16 the high point of the nappe, being the spillway crest, is 0.11 h_{sc} above the crest of the alternative sharp-crested weir (see also Fig.1.23). As a result, the spillway discharge coefficient at design head, h_d, is about 1.2 times that of a sharp-crested weir discharging under the same head, provided that the approach channel is sufficiently deep so as not to influence the nappe profile. Model tests of spillways have shown that the effect of the approach velocity on C_e is negligible when the height, p, of the weir is equal to or greater than 1.33 h_d, where h_d is the design head excluding the approach velocity head. Under this condition and with an actual head, H_1, over the spillway crest equal to design head h_d, the basic discharge coefficient equals $C_o = 1.30$ in Equation 6-12 and $C_o^* = 0.75$ in Equation 6-13.

C_1 can be determined from a dimensionless plot by VEN TE CHOW (1959), which is based on data of the U.S.Bureau of Reclamation and of the Waterways Experimental Station (1952), and is shown in Figure 6.19.

The values of C_1 in Figure 6.19 are valid for WES-spillways with a vertical upstream face. If the upstream weir face is sloping, a second dimensionless correction coefficient C_2 on the basic coefficient should be introduced; this is a function of both the weir face slope and the ratio p/H_1. Values of C_2 can be obtained from Figure 6.20.

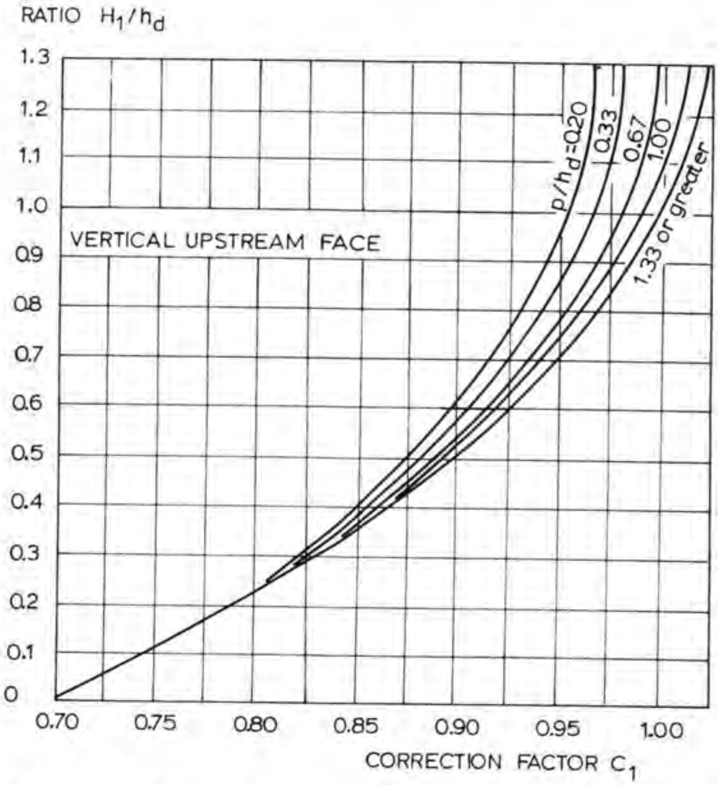

Fig.6.19. Correction factor for other than design head on WES-spillway (after VEN TE CHOW, 1959, based on data of USBR and WES).

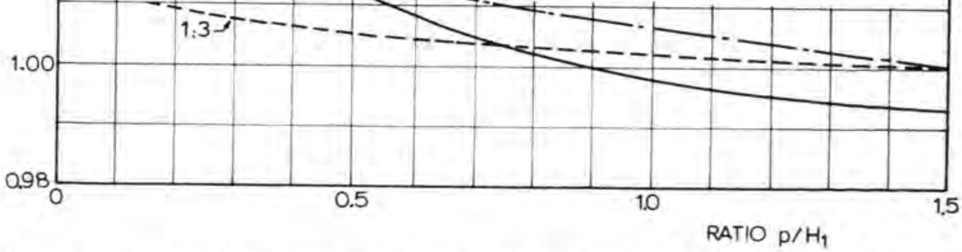

Fig.6.20. Correction factor for WES-spillway with sloping upstream face (after U.S.Bureau of Reclamation, 1960).

By use of the product $C_e = C_0C_1C_2$ an energy head-discharge relationship can now be determined provided that the weir flow is modular. After calculation of the approximate approach velocity, v_1, this Q-H_1 relationship can be transformed to a Q-h_1 curve.

To allow the WES-spillway to function as a high capacity overflow weir, the height p_2 of the weir crest above the downstream channel bed should be such that this channel bed does not interfere with the formation of the overflowing jet. It is evident that when p_2 approaches zero the weir will act as a broad-crested weir, which results in a reduction of the effective discharge coefficient by about 23 percent. This feature is clearly shown in Figure 6.21. This figure also shows that in order to obtain a high C_e-value, the ratio p_2/H_1 should exceed 0.75.

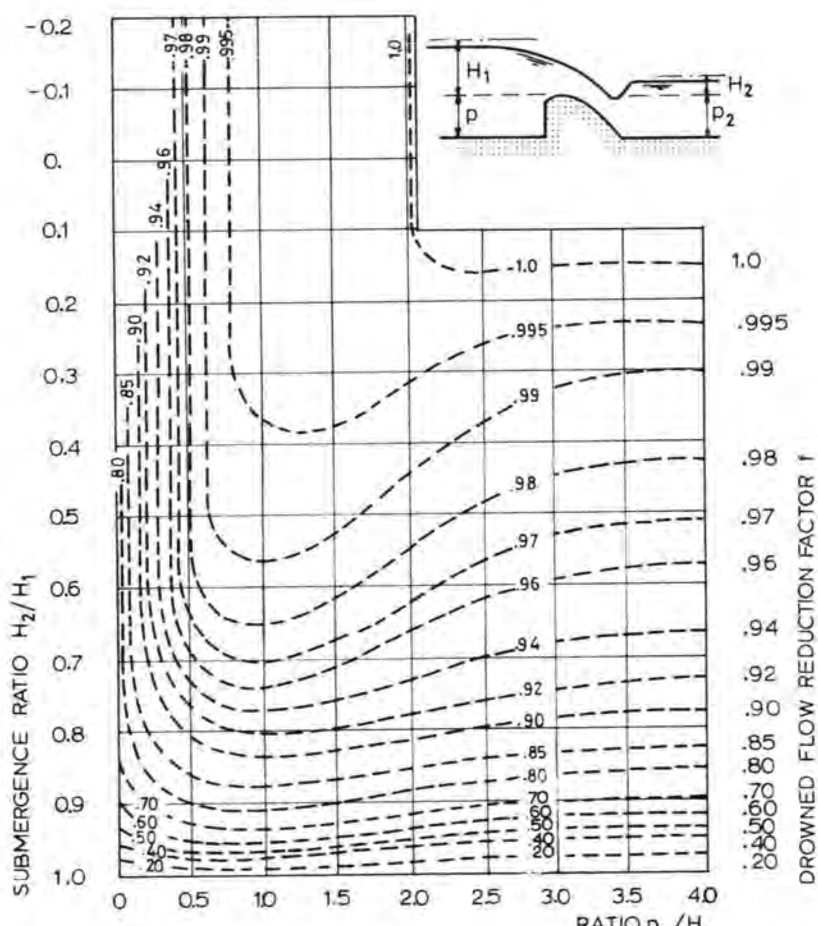

Fig.6.21. Drowned flow reduction factor as a function of p_2/H_1 and H_2/H_1. (Adapted from U.S.Army Corps of Engineers, Waterways Experimental Station.)

Figure 6.21 also shows that, provided $p_2/H_1 \geqslant 0.75$, the modular discharge as calculated by Equation 6-12 is decreased to about 99% of its theoretical value if the submergence ratio H_2/H_1 equals 0.3. Values of the drowned flow reduction factor f, by which the theoretical discharge is reduced under the influence of both p_2/H_1 and H_2/H_1, can be read from Figure 6.21.

The accuracy of the discharge coefficient $C_e = C_0C_1C_2$ of a WES-spillway which has been constructed with care and skill and is regularly maintained will be sufficient for field conditions. The error of C_e may be expected to be less than 5%. The method by which this error is to be combined with other sources of error is shown in Appendix II.

6.6.3 Limits of application

For reasonable accuracy, the limits of application of a weir with a WES-spillway crest are:

a) The upstream head over the weir crest h_1 should be measured a distance of 2 to 3 times $h_1$max upstream from the weir face. The recommended lower limit of h_1 is 0.06 m.

b) To prevent water surface instability in the approach channel, the ratio p/h_1 should not be less than 0.20.

c) To reduce the influence of boundary layer effects at the side walls of the weir, the ratio b/H_1 should not be less than 2.0.

d) To obtain a high C_e-value, the ratio p_2/H_1 should not be less than about 0.75.

e) The modular limit $H_2/H_1 = 0.3$, provided that the tailwater channel bottom does not interfere with the flow pattern over the weir ($p_2/H_1 \geqslant 0.75$).

f) The minimum allowable pressure at the weir crest equals - 4.00 m water column ($P/\rho g \geqslant -4.0$ m).

6.7 Cylindrical crested weir

6.7.1 Description

A cylindrical crested weir is an overflow structure with a rather high discharge coefficient and is, as such, very useful as a spillway. The weir consists of a vertical upstream face, a cylindrical crest which is horizontal perpendicular to the direction of flow, and a downstream face under a slope 1-to-1 ($\alpha = 45^{o}$) as shown in Figure 6.22. The abutments are vertical and should be rounded in such a manner that flow separation does not occur.

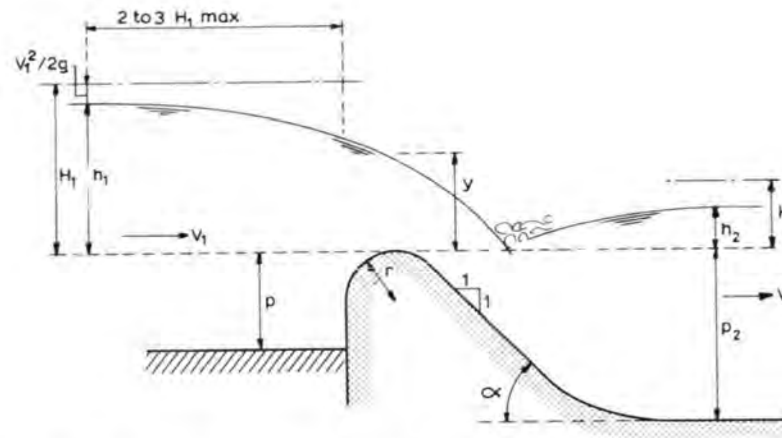

Fig.6.22. The cylindrical crested weir.

If the energy head over the weir crest as a function of the radius of the crest is small (H_1/r is small), the pressure on the weir crest is positive; if,however, the ratio H_1/r becomes large, the position of the overfalling nappe is depressed below that of a free falling nappe and the pressure of the crest becomes negative (sub-atmospheric) and at the same time causes an increase of the discharge coefficient. The magnitude of the local minimum pressure at the crest $(P/\rho g)$ min was measured by L.ESCANDE and F.SANANES (1959), who established the following equation from which $P/\rho g$ minimum can be calculated:

$$P/\rho g = H_1 - (H_1 - y) \{(r + ny)/r\}^{2/n} \qquad (6\text{-}14)$$

where $n = 1.6 + 0.35 \cot \alpha$ and y equals the water depth above the weir crest, which approximates 0.7 H_1 provided that the approach velocity is negligible.
For a weir with a 1-to-1 sloping downstream face ($\cot \alpha = 1$) the minimum pressure at the weir crest in metres water column $(P/\rho g)$min with regard to the energy head H_1 is given as a function of the ratio h_1/r in Figure 6.23.
To avoid the danger of local cavitation, the minimum pressure at the weir crest should be limited to -4 m water column. This limitation, together with the

maximum energy head over the weir crest, will give a limitation on the ratio H_1/r which can be obtained from Figure 6.23.

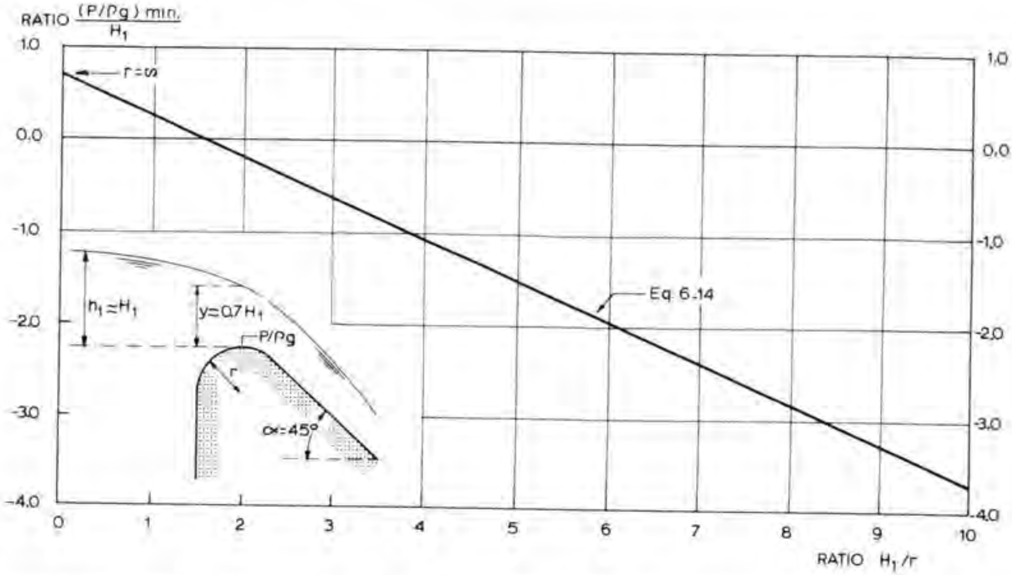

Fig.6.23. Minimum pressure at cylindrical weir crest as a function of the ratio H_1/r.

To allow the cylindrical-crested weir to function as a high capacity overflow weir, the crest height above the downstream channel bed should be such that this channel bed does not interfere with the formation of the overflowing nappe. Therefore the ratio p_2/H_1 should not be less than unity.

6.7.2 Evaluation of discharge

The basic head-discharge equation for a short-crested weir with a rectangular control section reads, according to Section 1.10

$$Q = C_e \frac{2}{3}\sqrt{\frac{2}{3} g} \; bH_1^{1.5} \tag{6-15}$$

where the effective discharge coefficient C_e equals the product of C_0 (which is a function of H_1/r), of C_1 (which is a function of p/H_1), and of C_2 (which is a function of p/H_1 and the slope of the upstream weir face) ($C_e = C_0C_1C_2$). The basic discharge coefficient is a function of the ratio H_1/r and has a maximum value of $C_0 = 1.49$ if H_1/r exceeds 5.0 as shown in Figure 6.24.

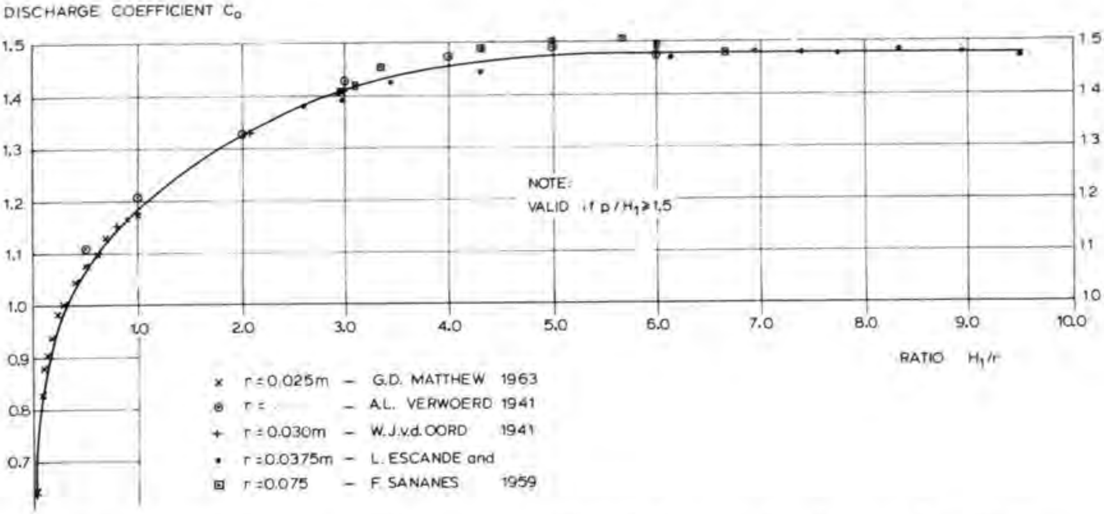

Fig.6.24. Discharge coefficient for cylindrical crested weir as a function of the ratio H_1/r.

The C_o-values in Figure 6.24 are valid if the weir crest is sufficiently high above the average bed of the approach channel ($p/H_1 \geq$ about 1.5). If, on the other hand, p approaches zero, the weir will perform as a broad-crested weir and have a C_e-value of about 0.98, which corresponds with a discharge coefficient reduction factor, C_1, of $0.98/1.49 \approx 0.66$. Values of the reduction factor as a function of the ratio p/H_1 can be read from Figure 6.25.

No results of laboratory tests on the influence of an upstream sloping weir face are available. It may be expected, however, that the correction factor on the basic discharge coefficient, C_2, will be about equal to those given in Figure 6.20 for WES-spillway shapes.

For each energy head over the weir crest, a matching discharge can be calculated with the available data, resulting in a Q-H_1 curve. With the aid of Figure 6.26, this Q-H_1 relationship can be changed rather simply into a Q-h_1 relationship. For each value of the ratio $(H_1 + p)/y_c$ a corresponding value of $(v_1^2/2g)/y_c$ can be obtained, where y_c is the critical depth in the approach channel, so that $h_1 = H_1 - v_1^2/2g$ can be calculated.

If we define the modular limit as that submergence ratio H_2/H_1 which produces a 1% reduction from the equivalent discharge ($f = 0.99$), we see in Figure 6.27 that the modular limit equals about 0.33. Values of the drowned flow reduction factor as a function of the submergence ratio can be obtained from Figure 6.27.

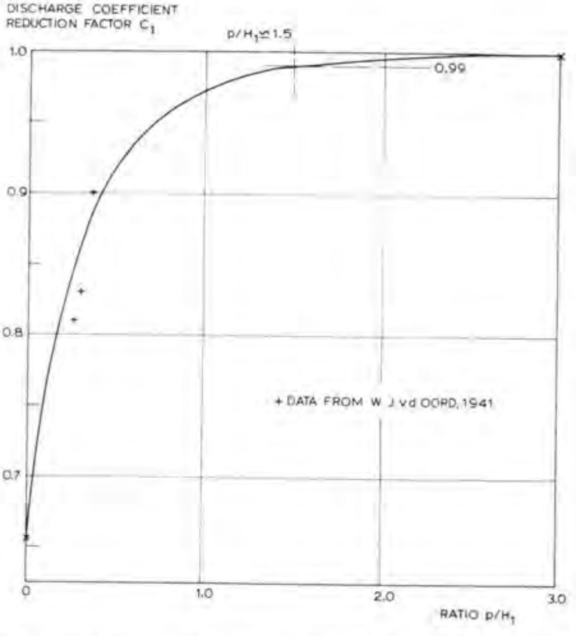

Fig.6.25. Reduction factor C_1 as a function of the ratio p/H_1.

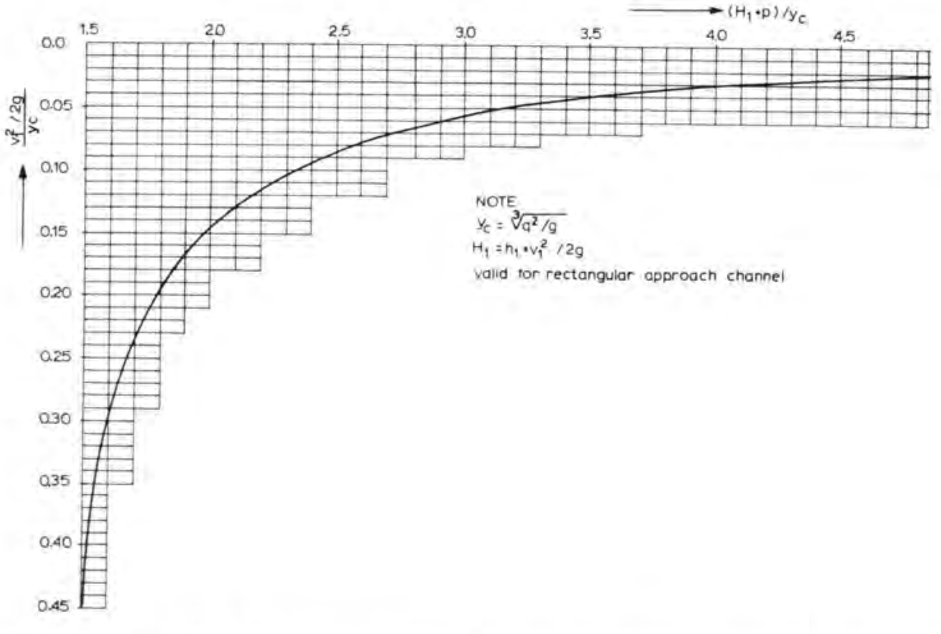

Fig.6.26. Graph for the conversion of H_1 into h_1 (after Technical University, Delft).

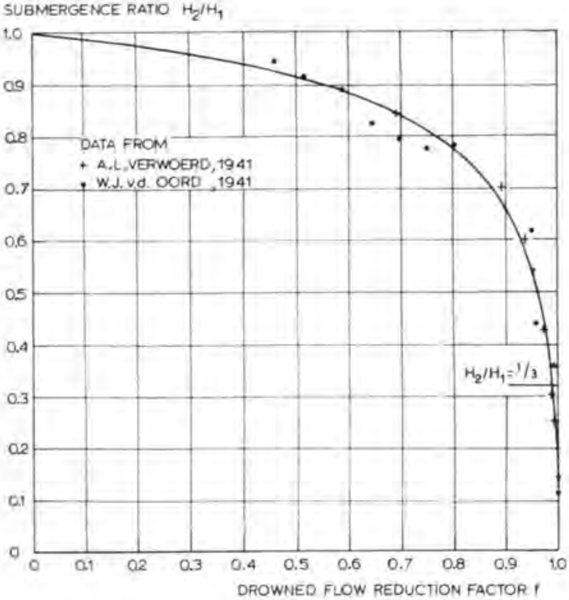

Fig.6.27. Drowned flow reduction factor as a function of H_2/H_1.

The accuracy of the effective discharge coefficient of a well-maintained cylindrical-crested weir which has been constructed with reasonable care and skill will be sufficient for field conditions. It can be expected that the error of $C_e = C_0C_1C_2$ will be less than 5%. The method by which this error is to be combined with other sources of error is shown in Appendix II.

6.7.3 Limits of application

For reasonable accuracy, the limits of application of a cylindrical crested weir are:

a) The upstream head over the weir crest h_1 should be measured a distance of 2 to 3 times $h_1$max upstream from the weir face. The recommended lower limit of $h_1 = 0.06$ m.

b) To prevent water surface instability in the approach channel, the ratio p/h_1 should not be less than 0.33.

c) To reduce the boundary layer effects of the vertical side walls, the ratio b/H_1 should not be less than 2.0.

d) On high head installations, the ratio h_1/r should be such that the local pressure at the crest is not less than −4 m water column.

e) To prevent the tailwater channel bottom from influencing the flow pattern over the weir, the ratio p_2/H_1 should not be less than unity.

f) The modular limit $H_2/H_1 = 0.33$.

6.8 Selected list of references

1. BAZIN, H.E.: Expériences nouvelles sur l'écoulement en déversoir. Annales des Ponts et Chaussées. Vol.7, 1896, pp.249-357.

2. BRITISH STANDARDS INSTITUTION: Methods of measurement of Liquid flow in open channels. British Standard 3680, Part 4B, Long base weirs. 1969. 39 pp.

3. BUTCHER, A.D.: Submerged weirs and standing wave weirs. Min.of Public Works, Cairo 1923. 17 pp.

4. BUTCHER, A.D.: Clear overfall weirs. Res.Work Delta Barrage. Min.of Public Works, Cairo 1921/22.

5. CHOW, VEN TE: Open-Channel Hydraulics. McGraw-Hill Book Company Inc., New York, 1959. 680 pp.

6. CRUMP, E.S.: A new method of gauging stream flow with little afflux by means of a submerged weir of triangular profile. Proc.Inst.Civil Engrs., Part 1, Vol.1 (March), 1952. pp.223-242.

7. DILLMAN, O.: Untersuchungen an Überfällen. Mitt.des Hydr.Inst.der Tech.Hochschule München. 1933. No.7. pp.26-52.

8. ESCANDE, L. and SANANES, F.: Etude des seuils déversants à fente aspiratrice. La Houklle Blanche, 14 (1959), No.B, Dec. Grenoble. pp.892-902.

9. LELIAVSKY, S.: Irrigation Engineering: Syphons, Weirs and Locks. Vol.II. Chapman & Hall Ltd., London 1965. 296 pp.

10. MATTHEW, G.D.: On the influence of curvature, surface tension and viscosity on flow over round-crested weirs. Proc.Inst.Civil Engrs., Vol.25 (Aug.), 1962. pp.511-524.

11. OORD, W.J., van der: Stuw met cirkelvormige kruin. MSc Thesis. Techn. University Delft 1941.

12. ROUSE, H. and REID, L.: Model research on spillway crests. Civil Eng. Vol.5, 1935. January, p.10.

13. U.S.ARMY CORPS OF ENGINEERS: Corps of Engineers Hydraulic Design Criteria. Prepared for Office of the Chief of Engineers. Waterways Experimental Station Vicksburg, Miss. 1952. Revised in subsequent years.

14. U.S.BUREAU OF RECLAMATION: Design of small dams. USBR Denver 1960. 611 pp.

15. U.S.BUREAU OF RECLAMATION: Studies of crests for overfall dams. Boulder Canyon Project Final Reports. Part VI. USBR Denver, Hydraulic Investigations, Bull.3, 1948.

16. U.S.DEPARTMENT OF AGRICULTURE: Field manual for research in agricultural hydrology. Agric.Handbook No.224, Washington 1962. 215 pp.

17. VERWOERD, A.L.: Capaciteitsbepaling van volkomen en onvolkomen overlaten met afgeronde kruinen. Waterstaatsingenieur in Nederlandsch-Indië, 1941, Juli, No.7. pp.65-78 (II).

18. VLUGTER, H.: De volkomen overlaat. (Modular weirs.) De Waterstaats Ingenieur, No.4, Bandung 1932.

19. WALLINGFORD HYDRAULIC RESEARCH STATION: The triangular profile Crump weir. Effects of a bend in the approach channel. Report EX 518, 1970. W.HRS, England.

20. WATER RESOURCES BOARD: Crump Weir Design. Reading Bridge House, England, 1970 TN 8 (rev.), 92 pp.

21. WHITE, W.R. and BURGESS, J.S.: Triangular profile weir with 1:2 up-stream and downstream slopes. Hydr.Res.Sta.Wallingford, England, Oct. 1967. Rep.No.INT 64, pp.41-47.

22. WHITE, W.R.: The flat vee weir. Water & Water Eng., Jan. 1968, V 72 No.863, pp.13-19.

23. WHITE, W.R.: The performance of two-dimensional and flat-V triangular profile weirs. Proc.Inst.Civil Engrs. 1971. Suppl. (ii), Paper 7350 S. 48 pp.

7 Flumes

A critical depth-flume is essentially a geometrically specified constriction built in an open channel where sufficient fall is available for critical flow to occur in the throat of the flume. Flumes are "in-line" structures, i.e. their centre line coincides with the centre line of the undivided channel in which the flow is to be measured. The flume cannot be used in structures like turnouts, controls and other regulating devices.

In this chapter the following types of critical-depth flumes will be described: Long-throated flumes (7.1), Throatless flumes with rounded transition (7.2), Throatless flumes with broken plane transition (7.3), Parshall flumes (7.4), H-flumes (7.5). The name "Venturi flume" is not used in this chapter, since this term is reserved for flumes in which flow in the constriction is sub-critical. The discharge through such a constriction can be calculated by use of the equations presented in Section 1.7.

7.1 Long-throated flumes

7.1.1 Description

Classified under the term "long-throated flumes" are those structures which have a throat section in which the streamlines run parallel to each other at least over a short distance. Because of this, hydrostatic pressure distribution can be assumed at the control section. This assumption allowed the various head-discharge equations to be derived, but the reader should note that discharge coefficients are also presented for high H_1/L ratios when the streamlines at the control are curved.

The flume comprises a throat of which the bottom (invert) is truly horizontal in the direction of flow. The crest level of the throat should not be lower than the dead water level in the channel, i.e. the water level downstream at zero flow. The throat section is prismatic but the shape of the flume cross-section is rather arbitrary, provided that no horizontal planes, or planes that are nearly so, occur in the throat above crest (invert) level, since this will cause a discontinuity in the head-discharge relationship. Treated in this section will be the most common flumes, i.e. those with a rectangular, V-shaped, trapezoidal, truncated V, parabolic, or circular throat cross-section.

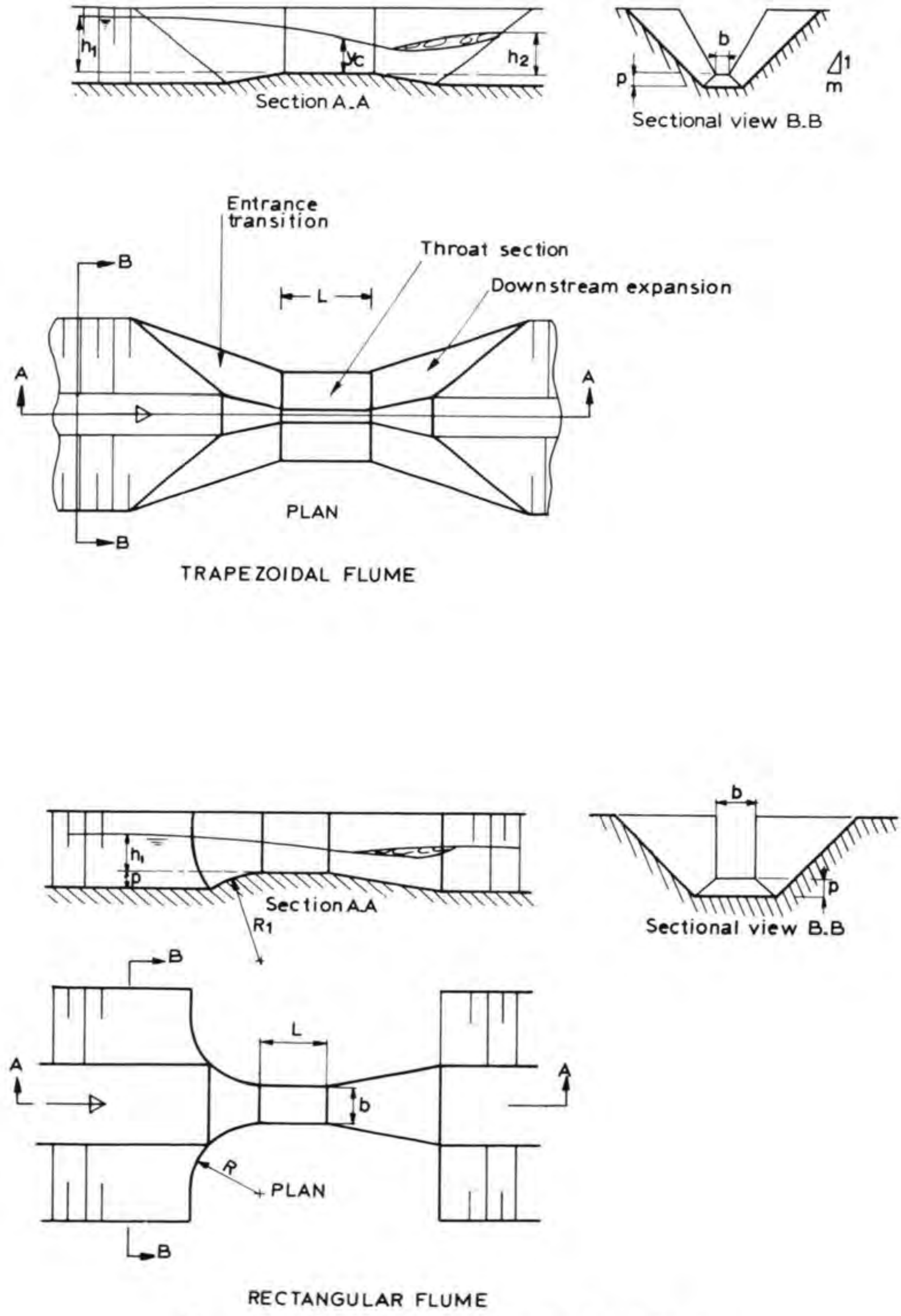

Fig.7.1. Alternative examples of flume lay-out.

The entrance transition should be of sufficient length, so that no flow separation can occur either at the bottom or at the sides of the transition. The transition can be formed of elliptical, cylindrical, or plane surfaces. For easy construction, a transition formed of either cylindrical or plane surfaces, or a combination of both, is recommended. If cylindrical surfaces are used, their axes should be parallel to the planes of the throat and should lie in the cross-section through the entrance of the throat. Their radii should preferably be about 2 H_1 max. With a plane surfaced transition, the convergence of side walls and bottom should be about 1:3. According to WELLS and GOTAAS (1956), minor changes in the slope of the entrance transition will have no effect upon the accuracy of the flume.

It is suggested that, where the flume has a bottom contraction or hump, the transitions for the crest and for the sides should be of equal lengths, i.e. the bottom and side contraction should begin at the same point at the approach channel bottom as shown in Figure 7.1.

With flat bottomed flumes, the floor of the entrance transition and of the approach channel should be flat and level and at no point higher than the invert of the throat, up to a distance 1.0 H_1 max upstream of the head measurement station. This head measurement station should be located upstream of the flume at a distance equal to between 2 and 3 times the maximum head to be measured.

Even if a flume is fitted with a curved entrance transition, it is recommended that the downstream expansion beyond the throat be constructed of plane surfaces. The degree of expansion influences the loss of energy head over the expansion and thus the modular limit of the flume.

7.1.2 Evaluation of discharge

The basic stage-discharge equations for long-throated flumes with various control sections have been derived in Section 1.9 and are shown in Fig.7.2. As indicated, the reader should use Table 7.1 to find y_c-values for a trapezoidal flume, and Table 7.2 to find the ratios A_c/d^2 and y_c/d as a function of H_1/d for circular flumes.

For all control sections shown, the discharge coefficient C_d is a function of the ratio H_1/L and is presented in Fig.7.3. The approach velocity coefficient C_v may be read from Fig.1.12 as a function of the dimensionless ratio $C_d\ A^*/A_1$.

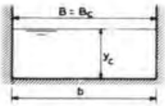

$$Q = C_d C_v \frac{2}{3} \left(\frac{2}{3} g\right)^{\frac{1}{2}} b h_1^{3/2}$$

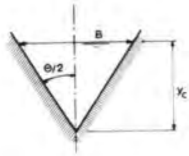

$$Q = C_d C_v \frac{16}{25} \left(\frac{2}{5} g\right)^{\frac{1}{2}} \tan\frac{\theta}{2}\, h_1^{5/2}$$

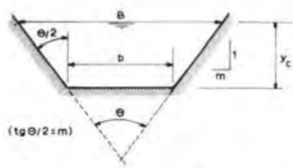

$$Q = C_d \left[b y_c + m y_c^2 \right] \left[2g(H_1 - y_c) \right]^{\frac{1}{2}}$$

use Table 7.1 to find y_c

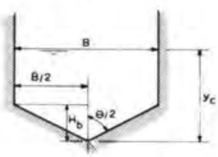

If $H_1 \leqslant 1.25\ H_b$

$$Q = C_d C_v \frac{16}{25} \left(\frac{2}{5} g\right)^{\frac{1}{2}} \tan\frac{\theta}{2}\, h_1^{5/2}$$

If $H_1 \geqslant 1.25\ H_b$

$$Q = C_d C_v \frac{2}{3} \left(\frac{2}{3} g\right)^{\frac{1}{2}} B\left(h_1 - \tfrac{1}{2} H_b\right)^{3/2}$$

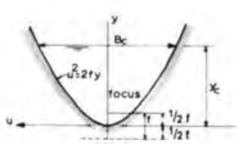

$$Q = C_d C_v \left(\frac{3}{4} f g\right)^{\frac{1}{2}} h_1^2$$

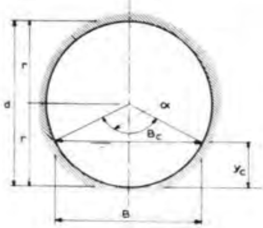

$$Q = C_d \frac{A_c}{d^2}\, d^{5/2} \left[2g \left(\frac{H_1}{d} - \frac{y_c}{d}\right) \right]^{\frac{1}{2}}$$

use Table 7.2 to find ratios

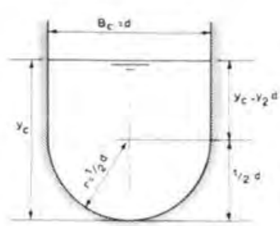

If $H_1 \leqslant 0.70\ d$

$$Q = C_d \frac{A_c}{d^2}\, d^{5/2} \left[2g \left(\frac{H_1}{d} - \frac{y_c}{d}\right) \right]^{\frac{1}{2}}$$

use Table 7.2 to find ratios

If $H_1 \geqslant 0.70\ d$

$$Q = C_d C_v\, 2d(2g)^{\frac{1}{2}} \left(\frac{1}{3} h_1 - 0.0358\ d\right)^{3/2}$$

Fig.7.2. Head-discharge relationship for long-throated flumes (from BOS, 1977).

TABLE 7.1. VALUES OF THE RATIO y_c/H_1 AS A FUNCTION OF m AND H_1/b FOR TRAPEZOIDAL CONTROL SECTIONS

		Side slopes of channel ratio of horizontal to vertical (m:1)								
H_1/b	Vertical	1/4:1	1/2:1	3/4:1	1:1	1½:1	2:1	2½:1	3:1	4:1
.00		.667	.667	.667	.667	.667	.667	.667	.667	.667
.01	.667	.667	.667	.668	.668	.669	.670	.670	.671	.672
.02	.667	.667	.668	.669	.670	.671	.672	.674	.675	.678
.03	.667	.668	.669	.670	.671	.673	.675	.677	.679	.683
.04	.667	.668	.670	.671	.672	.675	.677	.680	.683	.687
.05	.667	.668	.670	.672	.674	.677	.680	.683	.686	.692
.06	.667	.669	.671	.673	.675	.679	.683	.686	.690	.696
.07	.667	.669	.672	.674	.676	.681	.685	.689	.693	.699
.08	.667	.670	.672	.675	.678	.683	.687	.692	.696	.703
.09	.667	.670	.673	.676	.679	.684	.690	.695	.698	.706
.10	.667	.670	.674	.677	.680	.686	.692	.697	.701	.709
.12	.667	.671	.675	.679	.684	.690	.696	.701	.706	.715
.14	.667	.672	.676	.681	.686	.693	.699	.705	.711	.720
.16	.667	.672	.678	.683	.687	.696	.703	.709	.715	.725
.18	.667	.673	.679	.684	.690	.698	.706	.713	.719	.729
.20	.667	.674	.680	.686	.692	.701	.709	.717	.723	.733
.22	.667	.674	.681	.688	.694	.704	.712	.720	.726	.736
.24	.667	.675	.683	.689	.696	.706	.715	.723	.729	.739
.26	.667	.676	.684	.691	.698	.709	.718	.725	.732	.742
.28	.667	.676	.685	.693	.699	.711	.720	.728	.734	.744
.30	.667	.677	.686	.694	.701	.713	.723	.730	.737	.747
.32	.667	.678	.687	.696	.703	.715	.725	.733	.739	.749
.34	.667	.678	.689	.697	.705	.717	.727	.735	.741	.751
.36	.667	.679	.690	.699	.706	.719	.729	.737	.743	.752
.38	.667	.680	.691	.700	.708	.721	.731	.738	.745	.754
.40	.667	.680	.692	.701	.709	.723	.733	.740	.747	.756
.42	.667	.681	.693	.703	.711	.725	.734	.742	.748	.757
.44	.667	.681	.694	.704	.712	.727	.736	.744	.750	.759
.46	.667	.682	.695	.705	.714	.728	.737	.745	.751	.760
.48	.667	.683	.696	.706	.715	.729	.739	.747	.752	.761
.5	.667	.683	.697	.708	.717	.730	.740	.748	.754	.762
.6	.667	.686	.701	.713	.723	.737	.747	.754	.759	.767
.7	.667	.688	.706	.718	.728	.742	.752	.758	.764	.771
.8	.667	.692	.709	.723	.732	.746	.756	.762	.767	.774
.9	.667	.694	.713	.727	.737	.750	.759	.766	.770	.776
1.0	.667	.697	.717	.730	.740	.754	.762	.768	.773	.778
1.2	.667	.701	.723	.737	.747	.759	.767	.772	.776	.782
1.4	.667	.706	.729	.742	.752	.764	.771	.776	.779	.784
1.6	.667	.709	.733	.747	.756	.767	.774	.778	.781	.786
1.8	.667	.713	.737	.750	.759	.770	.776	.781	.783	.787
2	.667	.717	.740	.754	.762	.773	.778	.782	.785	.788
3	.667	.730	.753	.766	.773	.781	.785	.787	.790	.792
4	.667	.740	.762	.773	.778	.785	.788	.790	.792	.794
5	.667	.748	.768	.777	.782	.788	.791	.792	.794	.795
10	.667	.768	.782	.788	.791	.794	.795	.796	.797	.798
∞		.800	.800	.800	.800	.800	.800	.800	.800	.800

TABLE 7.2: RATIOS FOR DETERMINING THE DISCHARGE Q OF A BROAD-CRESTED WEIR AND LONG-THROATED FLUME WITH CIRCULAR CONTROL SECTION

y_c/d	$\frac{v_c^2/2g}{d}$	H_1/d	A_c/d^2	y_c/H_1	y_c/d	$\frac{v_c^2/2g}{d}$	H_1/d	A_c/d^2	y_c/H_1	y_c/d	$\frac{v_c^2/2g}{d}$	H_1/d	A_c/d^2	y_c/H_1
0.01	0.0033	0.0133	0.0013	0.752	0.36	0.1326	0.4926	0.2546	0.731	0.71	0.3286	1.0386	0.5964	0.684
.02	.0067	.0267	.0037	.749	.37	.1368	.5068	.2642	.730	.72	.3371	1.0571	.6054	.681
.03	.0101	.0401	.0069	.749	.38	.1411	.5211	.2739	.729	.73	.3459	1.0759	.6143	.679
.04	.0134	.0534	.0105	.749	.39	.1454	.5354	.2836	.728	.74	.3552	1.0952	.6231	.676
.05	.0168	.0668	.0147	.748	.40	.1497	.5497	.2934	.728	.75	.3648	1.1148	.6319	.673
.06	.0203	.0803	.0192	.748	.41	.1541	.5641	.3032	.727	.76	.3749	1.1349	.6405	.670
.07	.0237	.0937	.0242	.747	.42	.1586	.5786	.3130	.726	.77	.3855	1.1555	.6489	.666
.08	.0271	.1071	.0294	.747	.43	.1631	.5931	.3229	.725	.78	.3967	1.1767	.6573	.663
.09	.0306	.1206	.0350	.746	.44	.1676	.6076	.3328	.724	.79	.4085	1.1985	.6655	.659
.10	.0341	.1341	.0409	.746	.45	.1723	.6223	.3428	.723	.80	.4210	1.2210	.6735	.655
.11	.0376	.1476	.0470	.745	.46	.1769	.6369	.3527	.722	.81	.4343	1.2443	.6815	.651
.12	.0411	.1611	.0534	.745	.47	.1817	.6517	.3627	.721	.82	.4485	1.2685	.6893	.646
.13	.0446	.1746	.0600	.745	.48	.1865	.6665	.3727	.720	.83	.4638	1.2938	.6969	.641
.14	.0482	.1882	.0688	.744	.49	.1914	.6814	.3827	.719	.84	.4803	1.3203	.7043	.636
.15	.0517	.2017	.0739	.744	.50	.1964	.6964	.3927	.718	.85	.4982	1.3482	.7115	.630
.16	.0553	.2153	.0811	.743	.51	.2014	.7114	.4027	.717	.86	.5177	1.3777	.7186	.624
.17	.0589	.2289	.0885	.743	.52	.2065	.7265	.4127	.716	.87	.5392	1.4092	.7254	.617
.18	.0626	.2426	.0961	.742	.53	.2117	.7417	.4227	.715	.88	.5632	1.4432	.7320	.610
.19	.0662	.2562	.1039	.742	.54	.2170	.7570	.4327	.713	.89	.5900	1.4800	.7384	.601
.20	.0699	.2699	.1118	.741	.55	.2224	.7724	.4426	.712	.90	.6204	1.5204	.7445	.592
.21	.0736	.2836	.1199	.740	.56	.2279	.7879	.4526	.711	.91	.6555	1.5655	.7504	.581
.22	.0773	.2973	.1281	.740	.57	.2335	.8035	.4625	.709	.92	.6966	1.6166	.7560	.569
.23	.0811	.3111	.1365	.739	.58	.2393	.8193	.4724	.708	.93	.7459	1.6759	.7612	.555
.24	.0848	.3248	.1449	.739	.59	.2451	.8351	.4822	.707	.94	.8065	1.7465	.7662	.538
.25	.0887	.3387	.1535	.738	.60	.2511	.8511	.4920	.705	.95	.8841	1.8341	.7707	.518
.26	.0925	.3525	.1623	.738	.61	.2572	.8672	.5018	.703	.96	.9885	1.9485	.7749	.493
.27	.0963	.3663	.1711	.737	.62	.2635	.8835	.5115	.702	.97	1.1410	2.1110	.7785	.460
.28	.1002	.3802	.1800	.736	.63	.2699	.8999	.5212	.700	.98	1.3958	2.3758	.7817	.412
.29	.1042	.3942	.1890	.736	.64	.2765	.9165	.5308	.698	.99	1.9700	2.9600	.7841	.334
.30	.1081	.4081	.1982	.735	.65	.2833	.9333	.5404	.696	1.00	–	–	.7854	–
.31	.1121	.4221	.2074	.734	.66	.2902	.9502	.5499	.695					
.32	.1161	.4361	.2167	.734	.67	.2974	.9674	.5594	.693					
.33	.1202	.4502	.2260	.733	.68	.3048	.9848	.5687	.691					
.34	.1243	.4643	.2355	.732	.69	.3125	1.0025	.5780	.688					
.35	.1284	.4784	.2450	.732	.70	.3204	1.0204	.5872	.686					

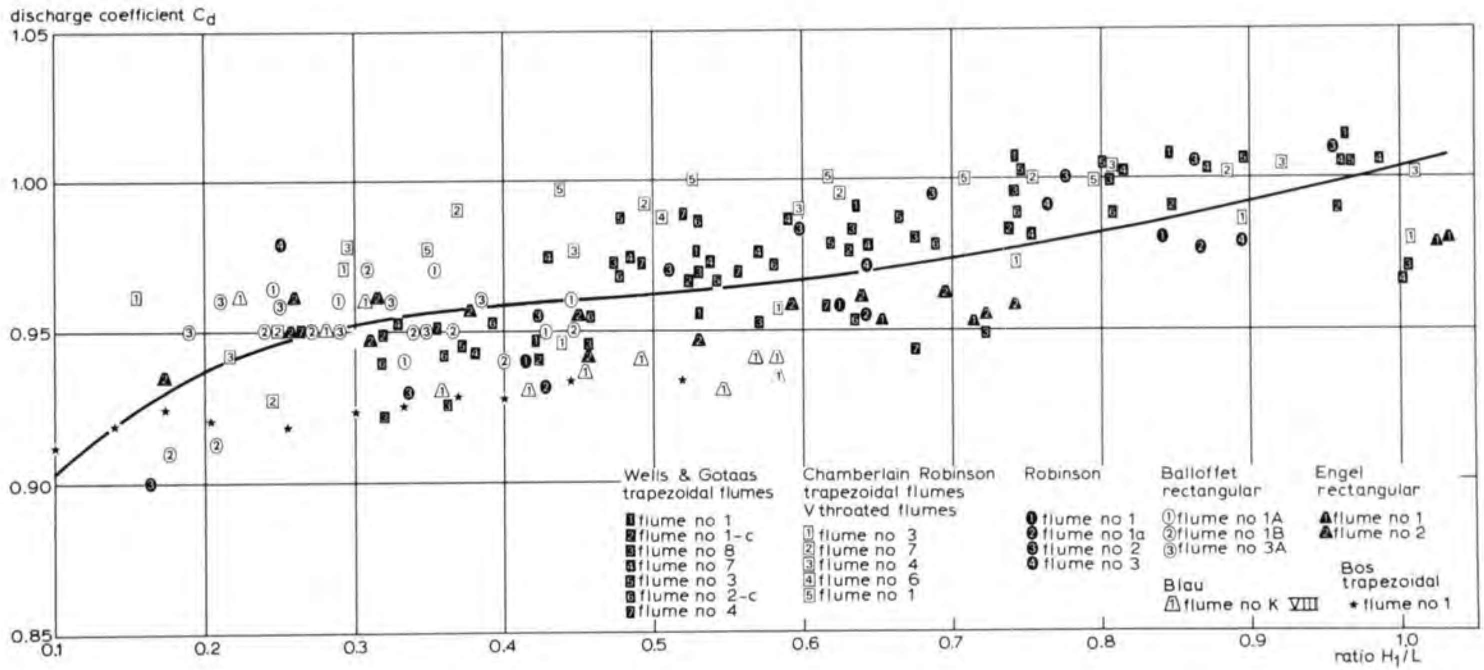

Fig.7.3. C_d-value as a function of H_1/L (from BOS, 1977).

The error in the product C_dC_v of a well maintained long-throated flume which has been constructed with reasonable care and skill may be deduced from the equation

$$X_c = \pm 2\ (21 - 20\ C_d) \text{ per cent} \qquad (7\text{-}1)$$

The method by which this coefficient error is to be combined with other sources of error is shown in Appendix II.

7.1.3 Modular limit

Although the available evidence is insufficient to define the relation between the modular limit and the angle of expansion, some information can be obtained from Section 1.15. Practice varies between very gentle and costly expansions of about 1-to-15, to ensure a high modular limit, and short expansions of 1-to-4. It is recommended that the divergences of each plane surface be not more abrupt than 1-to-4. If in some circumstances it is desirable to construct a short downstream expansion, it is better to truncate the transition rather than to enlarge the angle of divergence (see also Fig.1.35). At one extreme if no velocity head needs to be recovered, the downstream transition can be fully truncated. It will be clear from Section 1.15 that no expanding section will be needed if the tailwater level is always less than y_c above the invert of the flume throat.

At the other extreme, when almost all velocity head needs to be recovered, a transition with a very gradual expansion of sides and bed is required. The modular limit of long-throated flumes with various control cross sections and downstream expansions can be estimated with the aid of Section 1.15.3. As an illustration, we shall estimate the modular limit of the flume shown in Figure 7.4, flowing under an upstream energy head H_1 = 0.20 m. As can be read from Figure 7.3, the C_d-value for H_1/L = 0.33 equals 0.952. Hence for this flume

$$Q = 0.952\ \frac{2}{3}\ \sqrt{\frac{2}{3}\ 9.81}\quad 0.30\quad 0.20^{3/2} = 0.0436\ \text{m}^3/\text{s}$$

Since we know that the water depth at the control is $y_c = \frac{2}{3}\ H_1$ = 0.133 m, we can calculate v_c with the equation

$$v_c = \frac{Q}{y_c b} = 1.09\ \text{m/s}$$

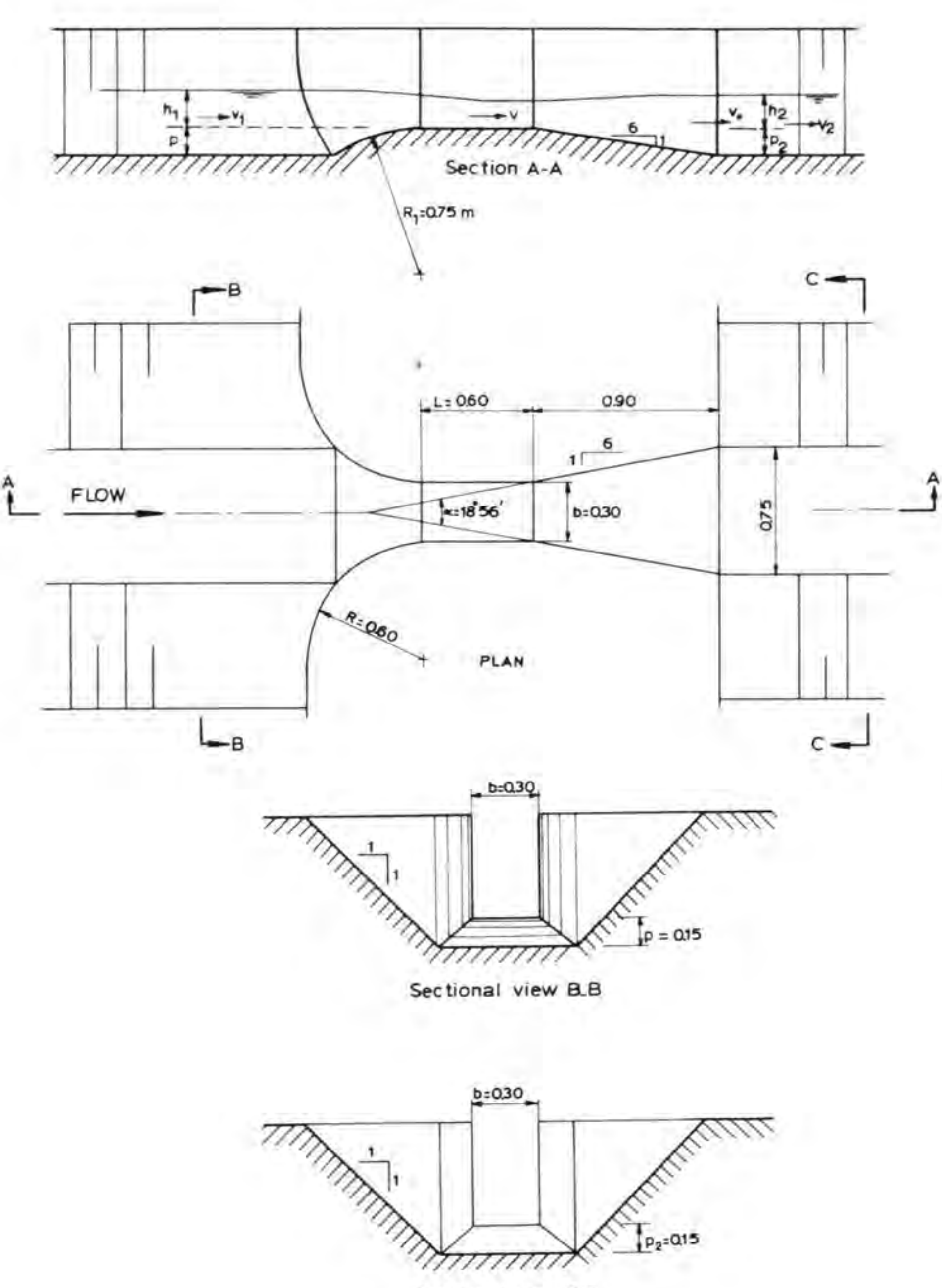

Fig.7.4. Long-throated flume dimensions (example).

To find the modular limit we now have to equalize by trial and error the Equation 1-119, which was presented in Section 1.15.3. This equation, which is valid for a truncated expansion reads

$$\frac{H_2}{H_1} \leqslant C_d^{1/u} - \xi_{19} \frac{(v_c - v_o)^2}{2gH_1} - \xi_{180} \frac{(v_o - v_2)^2}{2gH_1} - \frac{\Delta H_f}{H_1} \qquad (7\text{-}2)$$

In the above equation u = 1.5, the ξ-values can be taken from Figure 1.36, and ΔH_f may be estimated by using the Chézy or Manning equation. For a three-dimensional expansion $\xi_{19} = 0.42$ and $\xi_{180} = 1.10$. Energy losses over the downstream expansion are estimated to be $\Delta H_f = 0.005$ m, resulting in a $\Delta H_f/H_1$ value of 0.025. It should be noted that for low values of H_1 and relatively long expansions (small angles of divergence α), the ratio $\Delta H_f/H_1$ becomes significantly more important.

Substitution of the already known values into Equation 7-2 yields

$$\frac{H_2}{0.20} \leqslant 0.943 - 0.255 \left[0.42\ (1.09 - v_o)^2 + 1.10\ (v_o - v_2)^2 \right] \qquad (7\text{-}3)$$

This relationship must now be equalized by using different H_2 values.

Step 1

$H_2 = 0.16$ m and thus $v_o \simeq 0.19$ m/s, $v_2 \simeq 0.13$ m/s

and Equation 7-3 becomes

$0.80 \leqslant 0.943 - 0.255\ \{0.340 + 0.004\}$
$0.80 \leqslant 0.855$

Step 2

$H_2 = 0.17$ m and thus $v_o \simeq 0.18$ m/s, $v_2 \simeq 0.13$ m/s

and Equation 7-3 becomes

$0.85 \leqslant 0.943 - 0.255\ \{0.348 + 0.003\}$
$0.85 \leqslant 0.853$

which fits to the second decimal so that we may state that the modular limit of the shown flume at $H_1 = 0.20$ m is $H_2/H_1 \simeq 0.85$. Since in the example both velocities v_1 and v_2 are low (both values of $v^2/2g < 0.001$ m) we can state, that the minimum loss of head over the flume to obtain modular flow is $H_1 - H_2 = 0.03$ m.

The same procedure can be followed to predict the modular limit for other heads and other flumes. Modular limits as high as 0.96 can be achieved in gentle transitions.

Flumes whose throat is shorter than 2 H_1 do not have straight and parallel streamlines at the control section; streamlines become increasingly curved as H_1 increases. The available data are insufficient to define the relation of the modular limit and the degree of streamline curvature. It can be stated that, in general, the modular limit, however, decreases with an increasing value of H_1/L. As a conservative rule we may assume that if the ratio H_1/L increases from 0.5 to 1.0, the modular limit H_2/H_1 decreases linearly from the value calculated when using Section 1.15.3 to a value of about 0.5 y_c/H_1, where y_c is the critical depth at the control.

7.1.4 Limits of application

The limits of application of a long-throated flume for reasonably accurate flow measurements are:

a) The practical lower limit of h_1 is related to the magnitude of the influence of fluid properties, boundary roughness, and the accuracy with which h_1 can be determined. The recommended lower limit is 0.06 m or 0.1 L, whichever is greater.

b) To prevent water surface instability in the approach channel the Froude number $Fr = v_1/(gA_1/B_1)^{\frac{1}{2}}$ should not exceed 0.5.

c) The lower limitation on the ratio H_1/L arises from the necessity to prevent undulations in the flume throat. Values of the ratio H_1/L should range between 0.1 and 1.0.

d) The width B of the water surface in the throat at maximum stage should not be less than 0.30 m, nor less than H_1 max, nor less than L/5.

e) The width at the water surface in a triangular throat at minimum stage should not be less than 0.20 m.

7.2 Throatless flumes with rounded transition

7.2.1 Description

Throatless flumes may be regarded as shorter, and thus cheaper, variants of the long-throated flumes described in Section 7.1. Although their construction costs are lower, throatless flumes have a number of disadvantages, compared with long-throated flumes. These are:

- The discharge coefficient C_d is rather strongly influenced by H_1 and because of streamline curvature at the control section also by the shape of the downstream transition and H_2.
- The modular limit varies with H_1.
- In general, the C_d-value has a rather high error of about 8 percent.

Two basic types of throatless flumes exist, one having a rounded transition between the converging section and the downstream expansion, and the other an abrupt (broken plane) transition. The first type is described in this section, the second in Section 7.3.

Photo 1. Throatless flume with rounded transition.

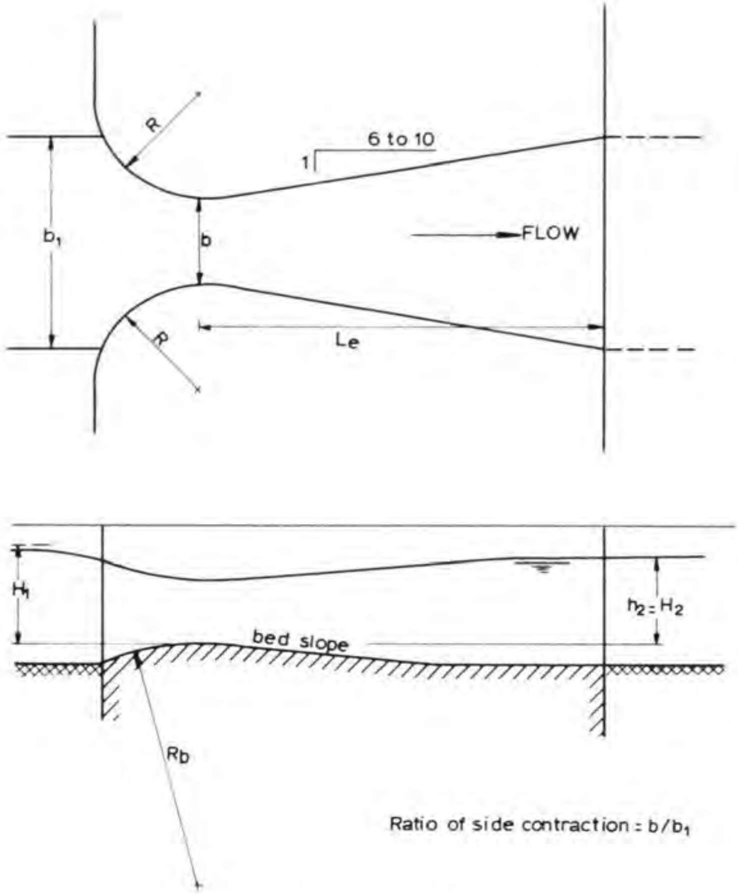

Fig.7.5. The throatless flume with rounded transition.

A throatless flume with rounded transition is shown in Figure 7.5. In contradiction to its shape, the flow pattern at the control section of such a flume is, rather complicated and cannot be handled by theory. Curvature of the streamlines is three-dimensional, and a function of such variables as the contraction ratio and curvature of the side walls, shape of any bottom hump if present, shape of the downstream expansion, and the energy heads on both ends of the flume. Laboratory data on throatless flumes are insufficient to determine the discharge coefficient as a function of any one of the above parameters.

The Figure 7.6 illustrates the variations in C_d. Laboratory data from various investigators are so divergent that the influence of parameters other than the ratio H_1/R is evident.

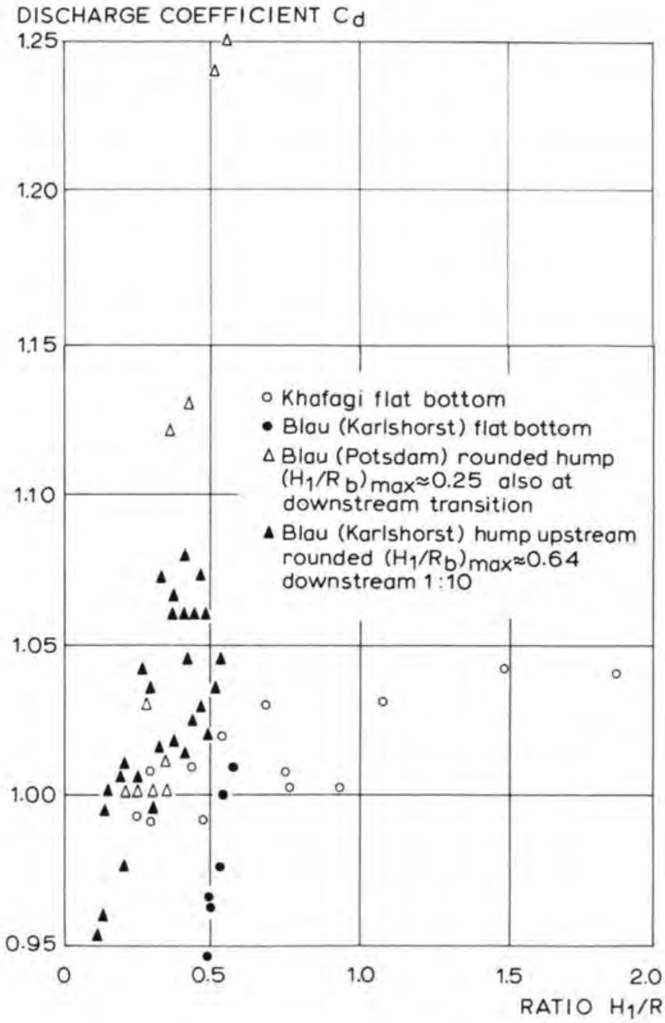

Fig.7.6. C_d-values for various throatless flumes.

7.2.2 Evaluation of discharge

The basic head-discharge equation for flumes with a rectangular control section equals

$$Q = C_d C_v \frac{2}{3} \left[\frac{2}{3} g\right]^{\frac{1}{2}} b h_1^{3/2} \qquad (7\text{-}4)$$

From the previous section it will be clear that a C_d-value can only be given if we introduce some standard flume design. We therefore propose the following:

- The radius of the upstream wing walls, R, and the radius, R_b, of the bottom hump, if any, ranges between 1.5 H_1 max and 2.0 H_1 max.

- The angle of divergence of the side walls and the bed slope should range between 1-to-6 and 1-to-10. Plane surface transitions only should be used.

- If the downstream expansion is to be truncated, its length should not be less than 1.5 (B_2-b), where B_2 is the average width of the tailwater channel.

If this standard design is used, the discharge coefficient C_d equals about unity. The appropriate value of the approach velocity coefficient, C_v, can be read from Figure 1.12 (Chapter 1).

Even for a well-maintained throatless flume which has been constructed with reasonable care and skill, the error in the above indicated product C_dC_v is rather high, and can be expected to be about 8 percent. The method by which this coefficient error is to be combined with other sources of error is shown in Appendix II.

7.2.3 Modular limit

Investigating the modular limit characteristics of throatless flumes is a complex problem and our present knowledge is extremely limited. Tests to date only scratch the surface of the problem, and are presented here mainly to illustrate the difficulties. Even if we take the simplest case of a flume with a flat bottom, the plot of H_2/H_1 versus H_1/b, presented in Figure 7.7 shows unpredictable variation of the modular limit for different angles of divergence and expansion ratios b/B_2.

It may be noted that KHAFAGI (1942) measured a decrease of modular limit with increasing expansion ratio b/B_2 for 1-to-8 and 1-to-20 flare angles. For long-throated flumes this tendency would be reversed and in fact Figure 7.7 shows this reversed trend for 1-to-6 flare angle. The modular limits shown in Figure 7.7 are not very favourable if we compare them with long-throated flumes having the same b/B_2 ratio and an abrupt ($\alpha = 180^\circ$) downstream expansion. The modular limit of the latter equals 0.70 if $b/B_2 = 0.4$ and 0.75 if $b/B_2 = 0.5$.

The variation in modular limit mentioned by KHAFAGI is also present in data reported by BLAU (1960). Blau reports the lowest modular limit for throatless flumes, which equals 0.5; for $H_1/b = 0.41$, $A/A_2 = 0.21$, $b/B_2 = 0.49$, wingwall divergence and bed slope both 1-to-10.

There seems little correlation between the available data, which would indicate that the throatless flume is not a suitable modular discharge measurement structure if the ratio H_2/H_1 exceeds about 0.5.

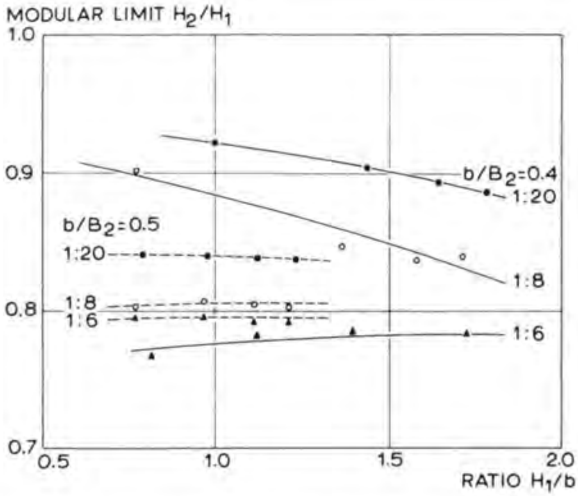

Fig.7.7. Modular limit conditions of flat bottomed throatless flumes (after Khafagi, 1942).

7.2.4 Limits of application

The limits of application of a throatless flume with rounded transition for reasonably accurate flow measurements are:

a) Flume design should be in accordance with the standards presented in Section 7.2.2.

b) The practical lower limit of h_1 depends on the influence of fluid properties, boundary roughness, and the accuracy with which h_1 can be determined. The recommended lower limit is 0.06 m.

c) To prevent water surface instability in the approach channel the Froude number $Fr = v_1/(gA_1/B_1)^{\frac{1}{2}}$ should not exceed 0.5.

d) The width b of the flume throat should not be less than 0.20 m nor less than H_1 max.

7.3 Throatless flumes with broken plane transition

7.3.1 Description

The geometry of the throatless flume with broken plane transition was first developed in irrigation practice in the Punjab and as such is described by HARVEY (1912). Later, BLAU (1960) reports on two geometries of this flume type. Both sources relate discharge and modular limit to heads upstream and downstream of the flume, h_1 and h_2 respectively. Available data are not sufficient to warrant inclusion in this manual.

Since 1967 SKOGERBOE et al. have published a number of papers on the same flume, referring to it as the "cutthroat flume". In the cutthroat flume, however, the flume discharge and modular limit are related to the piezometric heads at two points, in the converging section (h_a) and in the downstream expansion (h_b) as with the Parshall flume. Cutthroat flumes have been tested with a flat bottom only. A dimension sketch of this structure is shown in Figure 7.8.

Because of gaps in the research performed on cutthroat flumes, reliable head-discharge data are only available for one of the tested geometries (b = 0.305 m, overall length is 2.743 m). Because of the non-availability of discharge data as a function of h_1 and h_2 (or H_1 and H_2) the required loss of head over the flume to maintain modularity is difficult to determine.

In the original cutthroat flume design, various discharge capacities were obtained by simply changing the throat width b. Flumes with a throat width of 1, 2, 3, 4, 5, and 6 feet (1 ft = 0.3048 m) were tested for heads h_a ranging from 0.06 to 0.76 m. All flumes were placed in a rectangular channel 2.44 m wide. The upstream wingwall had an abrupt transition to this channel as shown in Figure 7.8.

Obviously, the flow pattern at the upstream piezometer tap is influenced by the ratio b/B_1. EGGLESTON (1967) reports on this influence for a 0.3048 m wide flume. A variation of discharge at constant h_a up to 2 percent was found. We expect, however, that this variation will increase with increasing width b and upstream head. Owing to the changing entrance conditions it even is possible that the piezometer tap for measuring h_a will be in a zone of flow separation. As already mentioned in Section 7.2.3, the ratios b/B_2 and b/L_2 are also expected to influence the head-discharge relationship.

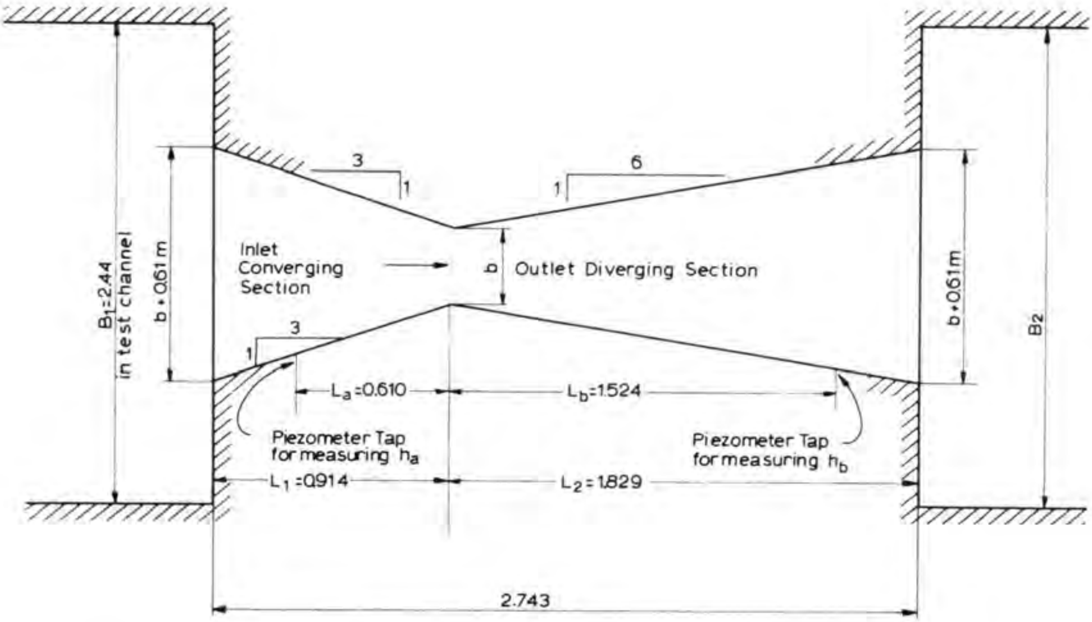

Fig.7.8. Cutthroat flume dimensions (after SKOGERBOE et al., 1967).

BENNETT (1972) calibrated a number of cutthroat flumes having other overall lengths than 2.743 m. He reported large-scale effects between geometrically identical cutthroat flumes, each of them having sufficiently large dimensions (b ranged from 0.05 to 0.305 m). Those scale effects were also mentioned by EGGLESTON (1967), SKOGERBOE and HYATT (1969), and SKOGERBOE, BENNETT, and WALKER (1972).

In all cases, however, the reported large-scale effects are attributed to the improper procedure of comparing measurements with extrapolated relations.

As a consequence of the foregoing, no head-discharge relations of cutthroat flumes are given here. Because of their complex hydraulic behaviour, the use of cutthroat flumes is not recommended by the present writers.

7.4 Parshall flumes

7.4.1 Description

Parshall flumes are calibrated devices for the measurement of water in open channels. They were developed by R.PARSHALL (1922) after whom the device was named.

The flume consists of a converging section with a level floor, a throat section with a downward sloping floor, and a diverging section with an upward sloping floor.

Because of this unconventional design, the control section of the flume is not situated in the throat but near the end of the level "crest" in the converging section. The modular limit of the Parshall flume is lower than that of the other long-throated flumes described in Section 7.1.

In deviation from the general rule for long-throated flumes where the upstream head must be measured in the approach channel, Parshall flumes are calibrated against a piezometric head, h_a, measured at a prescribed location in the converging section. The "downstream" piezometric head h_b is measured in the throat. This typical American practice is also used in the cutthroat and H flumes.

Parshall flumes were developed in various sizes, the dimensions of which are given in Table 7.3. Care must be taken to construct the flumes exactly in accordance with the structural dimensions given for each of the 22 flumes, because the flumes are not hydraulic scale models of each other. Since throat length and throat bottom slope remain constant for series of flumes while other dimensions are varied, each of the 22 flumes is an entirely different device. For example, it cannot be assumed that a dimension in the 12-ft flume will be three times the corresponding dimension in the 4-ft flume.

On the basis of throat width, Parshall flumes have been somewhat arbitrarily classified into three main groups for the convenience of discussing them, selecting sizes, and determining discharges.

These groups are "very small" for 1-, 2-, and 3-in flumes, "small" for 6-in through 8-ft flumes and "large" for 10-ft up to 50-ft flumes (USBR, 1971).

TABLE 7.3. PARSHALL FLUME DIMENSIONS (MILLIMETRES)

		Dimensions as shown in Fig.7.9																
b		A	a	B	C	D	E	L	G	H	K	M	N	P	R	X	Y	Z
1"	25.4	363	242	356	93	167	229	76	203	206	19	-	29	-	-	8	13	3
2"	50.8	414	276	406	135	214	254	114	254	257	22	-	43	-	-	16	25	6
3"	76.2	467	311	457	178	259	457	152	305	309	25	-	57	-	-	25	38	13
6"	152.4	621	414	610	394	397	610	305	610	-	76	305	114	902	406	51	76	-
9"	228.6	879	587	864	381	575	762	305	457	-	76	305	114	1080	406	51	76	-
1'	304.8	1372	914	1343	610	845	914	610	914	-	76	381	229	1492	508	51	76	-
1'6"	457.2	1448	965	1419	762	1026	914	610	914	-	76	381	229	1676	508	51	76	-
2'	609.6	1524	1016	1495	914	1206	914	610	914	-	76	381	229	1854	508	51	76	-
3'	914.4	1676	1118	1645	1219	1572	914	610	914	-	76	381	229	2222	508	51	76	-
4'	1219.2	1829	1219	1794	1524	1937	914	610	914	-	76	457	229	2711	610	51	76	-
5'	1524.0	1981	1321	1943	1829	2302	914	610	914	-	76	457	229	3080	610	51	76	-
6'	1828.8	2134	1422	2092	2134	2667	914	610	914	-	76	457	229	3442	610	51	76	-
7'	2133.6	2286	1524	2242	2438	3032	914	610	914	-	76	457	229	3810	610	51	76	-
8'	2438.4	2438	1626	2391	2743	3397	914	610	914	-	76	457	229	4172	610	51	76	-
10'	3048	-	1829	4267	3658	4756	1219	914	1829	-	152	-	343	-	-	305	229	-
12'	3658	-	2032	4877	4470	5607	1524	914	2438	-	152	-	343	-	-	305	229	-
15'	4572	-	2337	7620	5588	7620	1829	1219	3048	-	229	-	457	-	-	305	229	-
20'	6096	-	2845	7620	7315	9144	2134	1829	3658	-	305	-	686	-	-	305	229	-
25'	7620	-	3353	7620	8941	10668	2134	1829	3962	-	305	-	686	-	-	305	229	-
30'	9144	-	3861	7925	10566	12313	2134	1829	4267	-	305	-	686	-	-	305	229	-
40'	12192	-	4877	8230	13818	15481	2134	1829	4877	-	305	-	686	-	-	305	229	-
50'	15240	-	5893	8230	17272	18529	2134	1829	6096	-	305	-	686	-	-	305	229	-

Photo 2. Transparent model of a Parshall flume.

Very small flumes (1", 2", and 3")

The discharge capacity of the very small flumes ranges from 0.09 l/s to 32 l/s. The capacity of each flume overlaps that of the next size by about one-half the discharge range (see Table 7.4). The flumes must be carefully constructed. The exact dimensions of each flume are listed in Table 7.3. The maximum tolerance on the throat width b equals $\pm$ 0.0005 m.

The relatively deep and narrow throat section causes turbulence and makes the h_b gauge difficult to read in the very small flumes. Consequently, an h_c-gauge, located near the downstream end of the diverging section of the flume is added. Under submerged flow conditions, this gauge may be read instead of the h_b-gauge. The h_c readings are converted to h_b readings by using a graph, as will be explained in Section 7.4.3, and the converted h_b readings are then used to determine the discharge.

Small flumes (6", 9", 1', 1'6", 2' up to 8')

The discharge capacity of the small flumes ranges from 0.0015 m^3/s to 3.95 m^3/s. The capacity of each size of flume considerably overlaps that of the next size. The length of the side wall of the converging section, A, of the flumes with 1' up to 8' throat width is in metres:

$$A = \frac{b}{2} + 1.219 \tag{7-5}$$

where b is the throat width in metres. The piezometer tap for the upstream head, h_a, is located in one of the converging walls a distance of a = 2/3 A upstream from the end of the horizontal crest (see Fig.7.9). The location of the piezometer tap for the downstream head, h_b, is the same in all the "small" flumes, being 51 mm (X = 2 inch) upstream from the low point in the sloping throat floor and 76 mm (Y = 3 inch) above it. The exact dimensions of each size of flume are listed in Table 7.3.

Large flumes (10' up to 50')

The discharge capacity of the large flumes ranges from 0.16 m^3/s to 93.04 m^3/s. The capacity of each size of flume considerably overlaps that of the next size. The axial length of the converging section is considerably longer than it is in the small flumes to obtain an adequately smooth flow pattern in the upstream

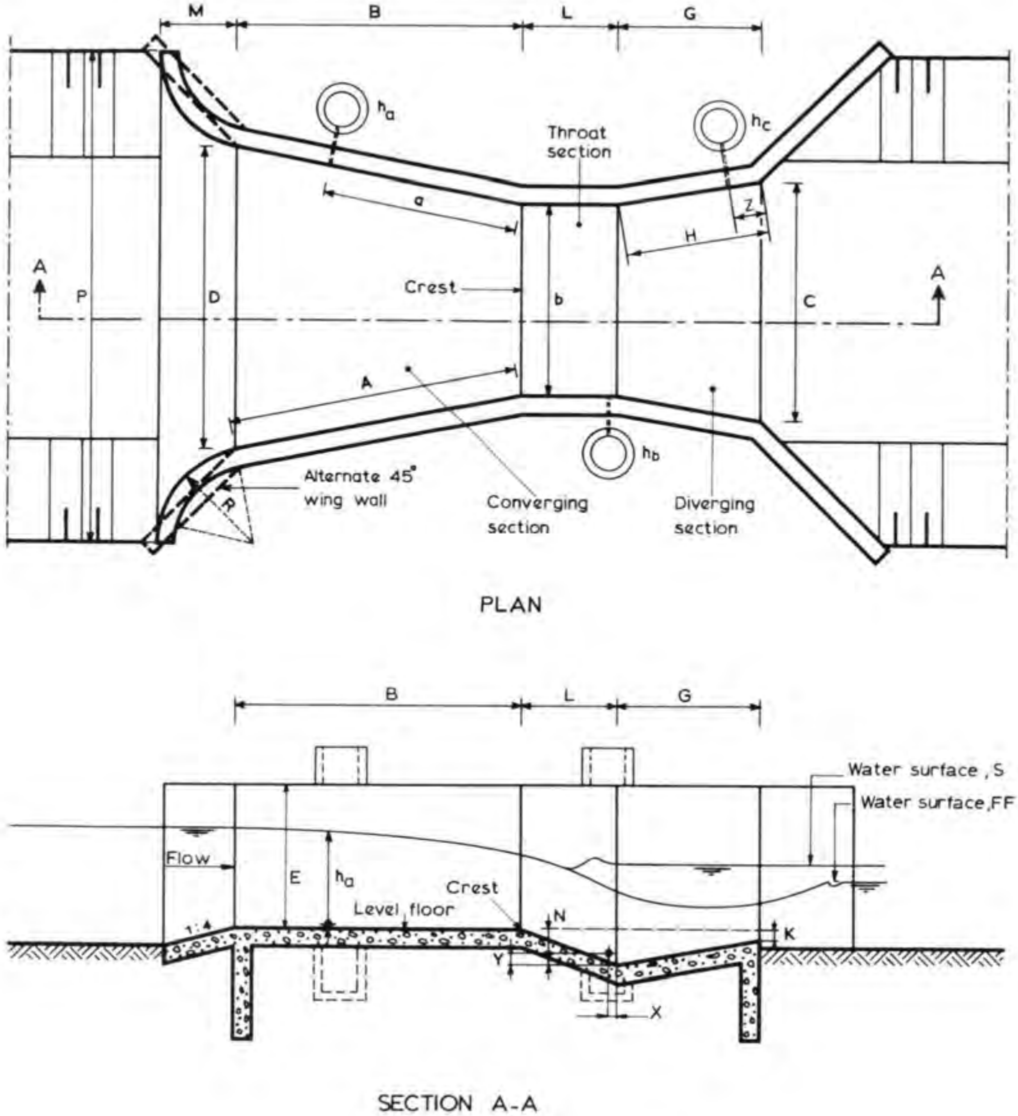

Fig.7.9. Parshall flume dimensions.

part of the structure. The measuring station for the upstream head, h_a, however, is maintained at $a = b/3 + 0.813$ m upstream from the end of the horizontal crest. The location of the piezometer tap for the downstream head, h_b, is the same in all the "large" flumes, being 305 mm (12 in) upstream from the floor at the downstream edge of the throat and 229 mm (9 in) above it. The exact dimensions of each size of flume are listed in Table 7.3.

All flumes must be carefully constructed to the dimensions listed, and careful levelling is necessary in both longitudinal and transverse directions if standard discharge table is to be used. When gauge zeros are established, they should be set so that the h_a-, h_b-, and h_c-gauges give the depth of water above the level crest - not the depths above pressure taps.

If the Parshall flume is never to be operated above the 0.60 submergence limit, there is no need to construct the portion downstream of the throat. The truncated Parshall flume (without diverging section) has the same modular flow characteristics as the standard flume. The truncated flume is sometimes referred to as the "Montana flume".

7.4.2 Evaluation of discharge

The upstream head-discharge (h_a-Q) relationship of Parshall flume of various sizes, as calibrated empirically, is represented by an equation, having the form:

$$Q = Kh_a^u \tag{7-6}$$

where K denotes a dimensional factor which is a function of the throat width. The power u varies between 1.522 and 1.60. Values of K and u for each size of flume are given in Table 7.4. In the listed equations Q is the modular discharge in m^3/s, and h_a is the upstream gauge reading in metres.

The flumes cover a range of discharges from 0.09 l/s to 93.04 m^3/s and have overlapping capacities to facilitate the selection of a suitable size. Each of the flumes listed in Table 7.4 is a standard device and has been calibrated for the range of discharges shown in the table. Detailed information on the modular discharge for each size of flume as a function of h_a are presented in the Tables 7.5 to 7.11.

TABLE 7.4. DISCHARGE CHARACTERISTICS OF PARSHALL FLUMES

Throat width b in feet or inches	Discharge range in $m^3/s \times 10^{-3}$ minimum	maximum	Equation $Q = K h_a^u$ (Q in m^3/s)	Head range in metres minimum	maximum	Modular limit h_b/h_a
1"	0.09	5.4	$0.0604\ h_a^{1.55}$	0.015	0.21	0.50
2"	0.18	13.2	$0.1207\ h_a^{1.55}$	0.015	0.24	0.50
3"	0.77	32.1	$0.1771\ h_a^{1.55}$	0.03	0.33	0.50
6"	1.50	111	$0.3812\ h_a^{1.58}$	0.03	0.45	0.60
9"	2.50	251	$0.5354\ h_a^{1.53}$	0.03	0.61	0.60
1'	3.32	457	$0.6909\ h_a^{1.522}$	0.03	0.76	0.70
1'6"	4.80	695	$1.056\ h_a^{1.538}$	0.03	0.76	0.70
2'	12.1	937	$1.428\ h_a^{1.550}$	0.046	0.76	0.70
3'	17.6	1427	$2.184\ h_a^{1.566}$	0.046	0.76	0.70
4'	35.8	1923	$2.953\ h_a^{1.578}$	0.06	0.76	0.70
5'	44.1	2424	$3.732\ h_a^{1.587}$	0.06	0.76	0.70
6'	74.1	2929	$4.519\ h_a^{1.595}$	0.076	0.76	0.70
7'	85.8	3438	$5.312\ h_a^{1.601}$	0.076	0.76	0.70
8'	97.2	3949	$6.112\ h_a^{1.607}$	0.076	0.76	0.70
	in m^3/s					
10'	0.16	8.28	$7.463\ h_a^{1.60}$	0.09	1.07	0.80
12'	0.19	14.68	$8.859\ h_a^{1.60}$	0.09	1.37	0.80
15'	0.23	25.04	$10.96\ h_a^{1.60}$	0.09	1.67	0.80
20'	0.31	37.97	$14.45\ h_a^{1.60}$	0.09	1.83	0.80
25'	0.38	47.14	$17.94\ h_a^{1.60}$	0.09	1.83	0.80
30'	0.46	56.33	$21.44\ h_a^{1.60}$	0.09	1.83	0.80
40'	0.60	74.70	$28.43\ h_a^{1.60}$	0.09	1.83	0.80
50'	0.75	93.04	$35.41\ h_a^{1.60}$	0.09	1.83	0.80

TABLE 7.5. FREE-FLOW DISCHARGE THROUGH 1" PARSHALL MEASURING FLUME IN l/sec COMPUTED FROM THE FORMULA $Q = 0.0604\ h_a^{1.55}$

Head h_a (m)	0	1	2	3	4	5	6	7	8	9
.01						0.09	0.10	0.11	0.12	0.13
.02	0.14	0.15	0.16	0.17	0.19	0.20	0.21	0.22	0.24	0.25
.03	0.26	0.28	0.29	0.31	0.32	0.33	0.35	0.36	0.38	0.40
.04	0.41	0.43	0.44	0.46	0.48	0.49	0.51	0.53	0.55	0.56
.05	0.58	0.60	0.62	0.64	0.66	0.67	0.69	0.71	0.73	0.75
.06	0.77	0.79	0.81	0.83	0.85	0.87	0.89	0.92	0.94	0.96
.07	0.98	1.00	1.02	1.05	1.07	1.09	1.11	1.14	1.16	1.18
.08	1.20	1.23	1.25	1.28	1.30	1.32	1.35	1.37	1.40	1.42
.09	1.45	1.47	1.50	1.52	1.55	1.57	1.60	1.62	1.65	1.68
.10	1.70	1.73	1.76	1.78	1.81	1.84	1.86	1.89	1.92	1.95
.11	1.97	2.00	2.03	2.06	2.09	2.11	2.14	2.17	2.20	2.23
.12	2.26	2.29	2.32	2.35	2.38	2.41	2.44	2.47	2.50	2.53
.13	2.56	2.59	2.62	2.65	2.68	2.71	2.74	2.77	2.80	2.84
.14	2.87	2.90	2.93	2.96	3.00	3.03	3.06	3.09	3.13	3.16
.15	3.19	3.22	3.26	3.29	3.32	3.36	3.39	3.43	3.46	3.49
.16	3.53	3.56	3.60	3.63	3.66	3.70	3.73	3.77	3.80	3.84
.17	3.87	3.91	3.95	3.98	4.02	4.05	4.09	4.12	4.16	4.20
.18	4.23	4.27	4.31	4.34	4.38	4.42	4.45	4.49	4.53	4.57
.19	4.60	4.64	4.68	4.72	4.75	4.79	4.83	4.87	4.91	4.95
.20	4.98	5.02	5.06	5.10	5.14	5.18	5.22	5.26	5.30	5.34
.21	5.38									

TABLE 7.6. FREE-FLOW DISCHARGE THROUGH 2" PARSHALL MEASURING FLUME IN l/sec COMPUTED FROM THE FORMULA $Q = 0.1207\ h_a^{1.55}$

Head h_a (m)	0	1	2	3	4	5	6	7	8	9
.01						0.18	0.20	0.22	0.24	0.26
.02	0.28	0.30	0.33	0.35	0.37	0.40	0.42	0.45	0.47	0.50
.03	0.53	0.55	0.58	0.61	0.64	0.67	0.70	0.73	0.76	0.79
.04	0.82	0.85	0.89	0.92	0.95	0.99	1.02	1.06	1.09	1.13
.05	1.16	1.20	1.23	1.27	1.31	1.35	1.38	1.42	1.46	1.50
.06	1.54	1.58	1.62	1.66	1.70	1.74	1.79	1.83	1.87	1.91
.07	1.96	2.00	2.04	2.09	2.13	2.18	2.22	2.27	2.31	2.36
.08	2.41	2.45	2.50	2.55	2.60	2.64	2.69	2.74	2.79	2.84
.09	2.89	2.94	2.99	3.04	3.09	3.14	3.19	3.24	3.30	3.35
.10	3.40	3.45	3.51	3.56	3.62	3.67	3.72	3.78	3.83	3.89
.11	3.94	4.00	4.06	4.11	4.17	4.22	4.28	4.34	4.40	4.45
.12	4.51	4.57	4.63	4.69	4.75	4.81	4.87	4.93	4.99	5.05
.13	5.11	5.17	5.23	5.29	5.35	5.42	5.48	5.54	5.60	5.67
.14	5.73	5.79	5.86	5.92	5.99	6.05	6.12	6.18	6.25	6.31
.15	6.38	6.44	6.51	6.58	6.64	6.71	6.78	6.84	6.91	6.98
.16	7.05	7.12	7.19	7.25	7.32	7.39	7.46	7.53	7.60	7.67
.17	7.74	7.81	7.88	7.96	8.03	8.10	8.17	8.24	8.31	8.39
.18	8.46	8.53	8.61	8.68	8.75	8.83	8.90	8.98	9.05	9.12
.19	9.20	9.27	9.35	9.43	9.50	9.58	9.65	9.73	9.81	9.88
.20	9.96	10.04	10.12	10.19	10.27	10.35	10.43	10.51	10.59	10.66
.21	10.74	10.82	10.90	10.98	11.06	11.14	11.22	11.30	11.38	11.47
.22	11.55	11.63	11.71	11.79	11.87	11.96	12.04	12.12	12.20	12.29
.23	12.37	12.45	12.54	12.62	12.71	12.79	12.87	12.96	13.04	13.13
.24	13.21									

TABLE 7.7. FREE-FLOW DISCHARGE THROUGH 3" PARSHALL MEASURING FLUME IN l/sec COMPUTED FROM THE FORMULA $Q = 0.1771\ h_a^{1.55}$

Upper-head h_a (m)	0	1	2	3	4	5	6	7	8	9
.03	0.77	0.81	0.85	0.90	0.94	0.98	1.02	1.07	1.11	1.16
.04	1.21	1.25	1.30	1.35	1.40	1.45	1.50	1.55	1.60	1.65
.05	1.70	1.76	1.81	1.87	1.92	1.98	2.03	2.09	2.15	2.20
.06	2.26	2.32	2.38	2.44	2.50	2.56	2.62	2.68	2.75	2.81
.07	2.87	2.94	3.00	3.06	3.13	3.20	3.26	3.33	3.40	3.46
.08	3.53	3.60	3.67	3.74	3.81	3.88	3.95	4.02	4.09	4.17
.09	4.24	4.31	4.39	4.46	4.53	4.61	4.69	4.76	4.84	4.91
.10	4.99	5.07	5.15	5.23	5.30	5.38	5.46	5.54	5.62	5.70
.11	5.79	5.87	5.95	6.03	6.12	6.20	6.28	6.37	6.45	6.54
.12	6.62	6.71	6.79	6.88	6.97	7.05	7.14	7.23	7.32	7.41
.13	7.50	7.59	7.68	7.77	7.80	7.95	8.04	8.13	8.22	8.32
.14	8.41	8.50	8.60	8.69	8.78	8.88	8.97	9.07	9.16	9.26
.15	9.36	9.45	9.55	9.65	9.75	9.85	9.94	10.04	10.14	10.24
.16	10.34	10.44	10.54	10.64	10.75	10.85	10.95	11.05	11.15	11.26
.17	11.36	11.46	11.57	11.67	11.78	11.88	11.99	12.09	12.20	12.31
.18	12.41	12.52	12.63	12.74	12.84	12.95	13.06	13.17	13.28	13.39
.19	13.50	13.61	13.72	13.83	13.94	14.05	14.16	14.28	14.39	14.50
.20	14.62	14.73	14.84	14.96	15.07	15.19	15.30	15.42	15.53	15.65
.21	15.76	15.88	16.00	16.11	16.23	16.35	16.47	16.59	16.70	16.82
.22	16.94	17.06	17.18	17.30	17.42	17.54	17.66	17.79	17.91	18.03
.23	18.15	18.27	18.40	18.52	18.64	18.77	18.89	19.01	19.14	19.26
.24	19.39	19.51	19.64	19.77	19.89	20.02	20.15	20.27	20.40	20.53
.25	20.66	20.78	20.91	21.04	21.17	21.30	21.43	21.56	21.69	21.82
.26	21.95	22.08	22.21	22.34	22.48	22.61	22.74	22.87	23.01	23.14
.27	23.27	23.41	23.54	23.67	23.81	23.94	24.08	24.21	24.35	24.49
.28	24.62	24.76	24.89	25.03	25.17	25.31	25.44	25.58	25.72	25.86
.29	26.00	26.14	26.28	26.42	26.56	26.70	26.84	26.98	27.12	27.26
.30	27.40	27.54	27.68	27.83	27.97	28.11	28.25	28.40	28.54	28.68
.31	28.83	28.97	29.12	29.26	29.41	29.55	29.70	29.84	29.99	30.14
.32	30.28	30.43	30.58	30.72	30.87	31.02	31.17	31.32	31.46	31.61
.33	31.76	31.91	32.06							

TABLE 7.8. FREE-FLOW DISCHARGE THROUGH 6" PARSHALL MEASURING FLUME IN 1/sec COMPUTED FROM THE FORMULA $Q = 0.3812\ h_a^{1.580}$

Upper-head h_a (m)	0	1	2	3	4	5	6	7	8	9
.03	1.5	1.6	1.7	1.7	1.8	1.9	2.0	2.1	2.2	2.3
.04	2.4	2.4	2.6	2.6	2.7	2.8	2.9	3.0	3.1	3.2
.05	3.4	3.5	3.6	3.7	3.8	3.9	4.0	4.1	4.2	4.4
.06	4.5	4.6	4.7	4.8	5.0	5.1	5.2	5.3	5.4	5.6
.07	5.7	5.8	6.0	6.1	6.2	6.4	6.5	6.6	6.8	6.9
.08	7.0	7.2	7.3	7.5	7.6	7.8	7.9	8.0	8.2	8.3
.09	8.5	8.6	8.8	8.9	9.1	9.2	9.4	9.6	9.7	9.9
.10	10.0	10.2	10.4	10.5	10.7	10.8	11.0	11.2	11.3	11.5
.11	11.7	11.8	12.0	12.2	12.3	12.5	12.7	12.8	13.0	13.2
.12	13.4	13.6	13.7	13.9	14.1	14.3	14.4	14.6	14.8	15.0
.13	15.2	15.4	15.6	15.7	15.9	16.1	16.3	16.5	16.7	16.9
.14	17.1	17.3	17.4	17.6	17.8	18.0	18.2	18.4	18.6	18.8
.15	19.0	19.2	19.4	19.6	19.8	20.0	20.2	20.4	20.7	20.9
.16	21.1	21.3	21.5	21.7	21.9	22.1	22.3	22.5	22.8	23.0
.17	23.2	23.4	23.6	23.8	24.1	24.3	24.5	24.7	24.9	25.2
.18	25.4	25.6	25.8	26.0	26.3	26.5	26.7	27.0	27.2	27.4
.19	27.6	27.9	28.1	28.3	28.6	28.8	29.0	29.3	29.5	29.7
.20	30.0	30.2	30.4	30.7	30.9	31.2	31.4	31.6	31.9	32.1
.21	32.4	32.6	32.9	33.1	33.4	33.6	33.8	34.1	34.4	34.6
.22	34.8	35.1	35.4	35.6	35.8	36.1	36.4	36.6	36.9	37.1
.23	37.4	37.6	37.9	38.2	38.4	38.7	38.9	39.2	39.5	39.7
.24	40.0	40.2	40.5	40.8	41.0	41.3	41.6	41.8	42.1	42.4
.25	42.6	42.9	43.2	43.5	43.7	44.0	44.3	44.6	44.8	45.1
.26	45.4	45.6	45.9	46.2	46.5	46.8	47.0	47.3	47.6	47.9
.27	48.2	48.4	48.7	49.0	49.3	49.6	49.9	50.2	50.4	50.7
.28	51.0	51.3	51.6	51.9	52.2	52.5	52.8	53.0	53.3	53.6
.29	53.9	54.2	54.5	54.8	55.1	55.4	55.7	56.0	56.3	56.6
.30	56.9	57.2	57.5	57.8	58.1	58.4	58.7	59.0	59.3	59.6
.31	59.9	60.2	60.5	60.8	61.1	61.4	61.8	62.1	62.4	62.7
.32	62.0	63.3	63.6	63.9	64.2	64.6	64.9	65.2	65.5	65.8
.33	66.1	66.4	66.8	67.1	67.4	67.7	68.0	68.4	68.7	69.0
.34	69.3	69.6	70.0	70.3	70.6	70.9	71.3	71.6	71.9	72.2
.35	72.6	72.9	73.2	73.6	73.9	74.2	74.6	74.9	75.2	75.5
.36	75.9	76.2	76.5	76.9	77.2	77.6	77.9	78.2	78.6	78.9
.37	79.2	79.6	79.9	80.2	80.6	80.9	81.3	81.6	82.0	82.3
.38	82.6	83.0	83.3	83.7	84.0	84.4	84.7	85.1	85.4	85.8
.39	86.1	86.5	86.8	87.2	87.5	87.9	88.2	88.6	88.9	89.3
.40	89.6	90.0	90.3	90.7	91.0	91.4	91.8	92.1	92.5	92.8
.41	93.2	93.6	93.9	94.3	94.6	95.0	95.4	95.7	96.1	96.4
.42	96.8	97.2	97.5	97.9	98.3	98.6	99.0	99.4	99.7	100.1
.43	100.5	100.8	101.2	101.6	102.0	102.3	102.7	103.1	103.4	103.8
.44	104.2	104.6	104.9	105.3	105.7	106.1	106.4	106.8	107.2	107.6
.45	108.0	108.3	108.7	109.1	109.5	109.8	110.2	110.6		

TABLE 7.9. FREE-FLOW DISCHARGE THROUGH 9" PARSHALL MEASURING FLUME IN l/sec COMPUTED FROM THE FORMULA $Q = 0.5354\ h_a^{1.53}$

Upper-head h_a (m)	0	1	2	3	4	5	6	7	8	9
.03	2.5	2.6	2.8	2.9	3.0	3.2	3.3	3.4	3.6	3.7
.04	3.9	4.0	4.2	4.3	4.5	4.7	4.8	5.0	5.1	5.3
.05	5.5	5.6	5.8	6.0	6.2	6.3	6.5	6.7	6.9	7.0
.06	7.2	7.4	7.6	7.8	8.0	8.2	8.4	8.6	8.8	9.0
.07	9.2	9.4	9.6	9.8	10.0	10.2	10.4	10.6	10.8	11.0
.08	11.2	11.4	11.7	11.9	12.1	12.3	12.5	12.8	13.0	13.2
.09	13.4	13.7	13.9	14.1	14.4	14.6	14.8	15.1	15.3	15.6
.10	15.8	16.0	16.3	16.5	16.8	17.0	17.3	17.5	17.8	18.0
.11	18.3	18.5	18.8	19.0	19.3	19.6	19.8	20.1	20.4	20.6
.12	20.9	21.2	21.4	21.7	22.0	22.2	22.5	22.8	23.0	23.3
.13	23.6	23.9	24.2	24.4	24.7	25.0	25.3	25.6	25.9	26.2
.14	26.4	26.7	27.0	27.3	27.6	27.9	28.2	28.5	28.8	29.1
.15	29.4	29.7	30.0	30.3	30.6	30.9	31.2	31.5	31.8	32.1
.16	32.4	32.7	33.0	33.4	33.7	34.0	34.3	34.6	35.0	35.3
.17	35.6	35.9	36.2	36.6	36.9	37.2	37.5	37.8	38.2	38.5
.18	38.8	39.2	39.5	39.8	40.2	40.5	40.8	41.2	41.5	41.8
.19	42.2	42.5	42.9	43.2	43.6	43.9	44.2	44.6	44.9	45.3
.20	45.6	46.0	46.3	46.7	47.0	47.4	47.7	48.1	48.4	48.8
.21	49.2	49.5	49.9	50.2	50.6	51.0	51.3	51.7	52.1	52.4
.22	52.8	53.2	53.5	53.9	54.3	54.6	55.0	55.4	55.8	56.1
.23	56.5	56.9	57.3	57.6	58.0	58.4	58.8	59.2	59.5	59.9
.24	60.3	60.7	61.1	61.5	61.9	62.2	62.6	63.0	63.4	63.8
.25	64.2	64.6	65.0	65.4	65.8	66.2	66.6	67.0	67.4	67.8
.26	68.2	68.6	69.0	69.4	69.8	70.2	70.6	71.0	71.4	71.8
.27	72.2	72.6	73.0	73.4	73.9	74.3	74.7	75.1	75.5	75.9
.28	76.4	76.8	77.2	77.6	78.0	78.4	78.9	79.3	79.7	80.1
.29	80.6	81.0	81.4	81.8	82.3	82.7	83.1	83.6	84.0	84.4
.30	84.8	85.3	85.7	86.2	86.6	87.0	87.5	87.9	88.3	88.8
.31	89.2	89.7	90.1	90.5	91.0	91.4	91.9	92.3	92.8	93.2
.32	93.7	94.1	94.6	95.0	95.5	95.9	96.4	96.8	97.3	97.7
.33	98.2	98.6	99.1	99.5	100.0	100.5	100.9	101.4	101.8	102.3
.34	102.8	103.2	103.7	104.2	104.6	105.1	105.6	106.0	106.5	107.0
.35	107.4	107.9	108.4	108.8	109.3	109.8	110.2	110.7	111.2	111.7
.36	112.2	112.6	113.1	113.6	114.1	114.6	115.0	115.5	116.0	116.5
.37	117.0	117.4	117.9	118.4	118.9	119.4	119.9	120.4	120.8	121.3
.38	121.8	122.3	122.8	123.3	123.8	124.3	124.8	125.3	125.8	126.3
.39	126.8	127.3	127.8	128.3	128.8	129.3	129.8	130.3	130.8	131.3
.40	131.8	132.3	132.8	133.3	133.8	134.3	134.8	135.3	135.8	136.3
.41	136.8	137.4	137.9	138.4	138.9	139.4	139.9	140.4	141.0	141.5
.42	142.0	142.5	143.0	143.5	144.1	144.6	145.1	145.6	146.2	146.7
.43	147.2	147.7	148.2	148.8	149.3	149.8	150.4	150.9	151.4	151.9
.44	152.5	153.0	153.5	154.1	154.6	155.1	155.6	156.2	156.7	157.3
.45	157.8	158.3	158.9	159.4	160.0	160.5	161.0	161.6	162.1	162.6
.46	163.2	163.7	164.3	164.8	165.4	165.9	166.5	167.0	167.6	168.1
.47	168.6	169.2	169.8	170.3	170.8	171.4	172.0	172.5	173.1	173.6
.48	174.2	174.7	175.3	175.8	176.4	177.0	177.5	178.1	178.6	179.2
.49	179.8	180.3	180.9	181.4	182.0	182.6	183.1	183.7	184.3	184.8
.50	185.4	186.0	186.5	187.1	187.7	188.2	188.8	189.4	190.0	190.5
.51	191.1	191.7	192.2	192.8	193.4	194.0	194.6	195.1	195.7	196.3
.52	196.9	197.4	198.0	198.6	199.2	199.8	200.4	200.9	201.5	202.1
.53	202.7	203.3	203.9	204.4	205.0	205.6	206.2	206.8	207.4	208.0
.54	208.6	209.2	209.8	210.3	210.9	211.5	212.1	212.7	213.3	213.0
.55	214.5	215.1	215.7	216.3	216.9	217.5	218.1	218.7	219.3	219.9
.56	220.5	221.1	221.7	222.3	222.9	223.5	224.1	224.7	225.3	225.9
.57	226.6	227.2	227.8	228.4	229.0	229.6	230.2	230.8	231.4	232.0
.58	232.7	233.3	233.9	234.5	235.1	235.7	236.4	237.0	237.6	238.2
.59	238.8	239.4	240.1	240.7	241.3	241.9	242.6	243.2	243.8	244.4
.60	245.0	245.7	246.3	246.0	247.6	248.2	248.8	249.4	250.1	250.7
.61	251.3									

TABLE 7.10. FREE-FLOW DISCHARGE THROUGH PARSHALL MEASURING FLUMES 1-TO-8 FOOT SIZE IN l/sec COMPUTED FROM THE FORMULA $Q = 4\ bh_a^{1.522}\ b^{0.026}$ (b = WIDTH IN FEET)

Upper-head h_a (mm)	Discharge per l/sec for flumes of various throat widths								
	1 feet	1.5 feet	2 feet	3 feet	4 feet	5 feet	6 feet	7 feet	8 feet
30	3.3	4.8							
32	3.7	5.3							
34	4.0	5.8							
36	4.4	6.4							
38	4.8	6.9							
40	5.2	7.5							
42	5.6	8.1							
44	6.0	8.7							
46	6.4	9.3	12.1	17.6					
48	6.8	9.9	12.9	18.8					
50	7.2	10.5	13.7	20.0					
52	7.7	11.2	14.6	21.3					
54	8.1	11.9	15.5	22.6					
56	8.6	12.5	16.4	23.9					
58	9.1	13.2	17.3	25.3					
60	9.5	14.0	18.2	26.7					
62	10.0	14.7	19.2	28.1	36.7	45.2			
64	10.5	15.4	20.2	29.5	38.6	47.6			
66	11.0	16.2	21.1	31.0	40.5	50.0			
68	11.6	16.9	22.1	32.4	42.5	52.4			
70	12.1	17.7	23.2	33.9	44.4	54.8			
72	12.6	18.5	24.2	35.5	46.5	57.4			
74	13.1	19.2	25.2	37.0	48.5	59.9			
76	13.7	20.1	26.3	38.6	50.6	62.5	74.1	85.8	97.2
78	14.2	20.9	27.4	40.2	52.7	65.1	77.3	89.4	101.3
80	14.8	21.7	28.5	41.8	54.9	67.8	80.4	93.1	105.6
82	15.4	22.0	29.6	43.5	57.0	70.5	83.7	96.9	109.8
84	15.9	23.4	30.7	45.2	59.3	73.2	87.0	100.7	114.2
86	16.5	24.3	31.9	46.8	61.5	76.0	90.3	104.6	118.6
88	17.1	25.1	33.0	48.6	63.8	78.9	93.6	108.5	123.0
90	17.7	26.0	34.2	50.3	66.1	81.7	97.1	112.5	127.5
92	18.3	26.9	35.4	52.1	68.4	84.6	100.5	116.5	132.1
94	18.9	27.8	36.6	53.8	70.8	87.6	104.0	120.6	136.8
96	19.5	28.7	37.8	55.6	73.2	90.5	107.6	124.7	141.5
98	20.1	29.7	39.0	57.5	75.6	93.5	111.2	128.9	146.2
100	20.8	30.6	40.2	59.3	78.0	96.6	114.8	133.1	151.1
102	21.4	31.5	41.5	61.2	80.5	99.7	118.5	137.4	156.0
104	22.0	32.5	42.8	63.1	83.0	102.8	122.2	141.8	160.9
106	22.7	33.5	44.0	65.0	85.6	106.0	126.0	146.1	165.9
108	23.4	34.4	45.4	66.9	88.1	109.1	129.8	150.6	171.0
110	24.0	35.4	46.6	68.9	90.7	112.4	133.7	155.1	176.1
112	24.7	36.4	48.0	70.8	93.3	115.6	137.6	159.6	181.2
114	25.4	37.4	49.3	72.8	96.0	118.9	141.5	164.2	186.5
116	26.0	38.4	50.7	74.8	98.6	122.2	145.5	168.8	191.8
118	26.7	39.5	52.0	76.9	101.3	125.6	149.5	173.5	197.1
120	27.4	40.5	53.4	78.9	104.0	129.0	153.6	178.2	202.5
122	28.1	41.5	54.8	81.0	106.8	132.4	157.7	183.0	208.0

(*Table 7.10. cont.*)

Upper-head h_a (mm)	Discharge per l/sec for flumes of various throat widths								
	1 feet	1.5 feet	2 feet	3 feet	4 feet	5 feet	6 feet	7 feet	8 feet
124	28.8	42.6	56.2	83.1	109.6	135.9	161.8	187.9	213.5
126	29.5	43.6	57.6	85.2	112.4	139.4	166.0	192.7	219.0
128	30.2	44.7	59.0	87.3	115.2	142.9	170.2	197.6	224.6
130	31.0	45.8	60.4	89.5	118.0	146.5	174.5	202.6	230.3
132	31.7	46.9	61.9	91.6	120.9	150.1	178.8	207.6	236.0
134	32.4	48.0	63.4	93.8	123.8	153.7	183.1	212.7	241.8
136	33.2	49.1	64.8	96.0	126.8	157.4	187.5	217.8	247.6
138	33.9	50.2	66.3	98.2	129.7	161.0	191.9	223.0	253.5
140	34.7	51.3	67.8	100.5	132.7	164.8	196.4	228.1	259.4
142	35.4	52.5	69.3	102.7	135.7	168.5	200.9	233.4	265.4
144	36.2	53.6	70.8	105.0	138.7	172.3	205.4	238.7	271.4
146	37.0	54.8	72.4	107.3	141.8	176.1	210.0	244.0	277.5
148	37.7	55.9	73.9	109.6	144.9	180.0	214.6	249.4	283.7
150	38.5	57.1	75.4	112.0	148.0	183.8	219.2	254.8	289.8
152	39.3	58.3	77.0	114.3	151.1	187.7	223.9	260.2	296.1
154	40.1	59.4	78.6	116.7	154.2	191.7	228.6	265.8	302.4
156	40.9	60.6	80.2	119.0	157.4	195.6	233.4	271.3	308.7
158	41.7	61.8	81.8	121.4	160.6	199.6	238.2	276.9	315.1
160	42.5	63.0	83.4	123.8	163.8	203.6	243.0	282.5	321.5
162	43.3	64.2	85.0	126.3	167.1	207.7	247.9	288.2	328.0
164	44.1	65.5	86.6	128.7	170.3	211.8	252.8	293.9	334.5
166	44.9	66.7	88.3	131.2	173.6	215.9	257.7	299.7	341.1
168	45.7	68.0	89.9	133.7	176.9	220.0	262.7	305.5	347.7
170	46.6	69.2	91.6	136.2	180.3	224.2	267.7	311.3	354.4
172	47.4	70.4	93.3	138.7	183.6	228.4	272.7	317.2	361.1
174	48.2	71.7	95.0	141.2	187.0	232.6	277.8	223.1	367.9
176	49.1	73.0	96.7	143.8	190.4	236.9	282.9	329.1	374.7
178	50.0	74.3	98.4	146.4	193.8	241.2	288.0	335.1	381.6
180	50.8	75.6	100.1	148.9	197.3	245.5	293.2	341.2	388.5
182	51.7	76.8	101.8	151.5	200.8	249.8	298.4	347.2	395.5
184	52.5	78.2	103.6	154.2	204.2	254.2	303.7	353.4	402.5
186	53.4	79.5	105.3	156.8	207.8	258.6	309.0	359.5	409.5
188	54.3	80.8	107.1	159.4	211.3	263.0	314.3	365.8	416.6
190	55.2	82.1	108.8	162.1	214.8	267.5	319.6	372.0	423.8
192	56.0	83.4	110.6	164.8	218.4	272.0	325.0	378.3	431.0
194	56.9	84.8	112.4	167.5	222.0	276.5	330.4	384.6	438.2
196	57.8	86.1	114.2	170.2	225.6	281.0	335.9	391.0	445.5
198	58.7	87.5	116.0	172.9	229.3	285.6	341.4	397.4	452.8
200	59.6	88.8	117.8	175.7	233.0	290.2	346.9	403.8	460.2
202	60.6	90.2	119.7	178.4	236.6	294.8	352.4	410.3	467.6
204	61.5	91.6	121.5	181.2	240.4	299.4	358.0	416.8	475.1
206	62.4	93.0	123.4	184.0	244.1	304.1	363.6	423.4	482.6
208	63.3	94.4	125.2	186.8	247.8	308.8	369.3	430.0	490.1
210	64.2	95.8	127.1	189.6	251.6	313.6	375.0	436.6	497.7
212	65.2	97.2	129.0	192.4	255.4	318.3	380.7	443.3	505.4
214	66.1	98.6	130.9	195.3	259.2	323.1	386.4	450.0	513.0
216	67.1	100.0	132.8	198.2	263.0	327.9	392.2	456.8	520.8
218	68.0	101.4	134.7	201.0	266.9	332.7	398.0	463.6	528.6
220	69.0	102.9	136.6	203.9	270.8	337.6	403.8	470.4	536.4
222	69.9	104.3	138.5	206.8	274.7	342.5	409.7	477.3	544.2
224	70.9	105.8	140.5	209.8	278.6	347.4	415.6	484.2	552.1
226	71.8	107.2	142.4	212.7	282.3	352.3	421.6	491.1	560.1

(*Table 7.10. cont.*)

Upper-head h_a (mm)	Discharge per l/sec for flumes of various throat widths								
	1 feet	1.5 feet	2 feet	3 feet	4 feet	5 feet	6 feet	7 feet	8 feet
228	72.8	108.7	144.4	215.7	286.5	357.3	427.5	498.1	568.0
230	73.8	110.2	146.4	218.6	290.4	362.2	433.5	505.1	576.1
232	74.8	111.6	148.3	221.6	294.4	367.3	439.5	512.2	584.2
234	75.8	113.1	150.3	224.6	298.5	372.3	445.6	519.2	592.3
236	76.7	114.6	152.3	227.6	302.5	377.4	451.7	526.4	600.4
238	77.7	116.1	154.3	230.7	306.6	382.4	447.8	533.5	608.6
240	78.7	117.6	156.3	233.7	310.6	387.6	464.0	540.7	616.8
245	81.2	121.4	161.4	241.4	320.9	400.4	479.5	558.9	637.6
250	83.8	125.2	166.6	249.1	331.3	413.5	495.2	577.2	658.7
255	86.3	129.1	171.7	257.0	341.8	426.7	511.1	595.8	680.0
260	88.9	133.0	177.0	264.9	352.4	440.0	527.1	614.6	701.5
265	91.5	137.0	182.3	272.9	363.2	453.6	543.4	633.7	723.3
270	94.2	141.0	187.6	281.0	374.1	467.2	559.8	652.9	745.4
275	96.8	145.0	193.1	289.2	385.1	481.1	576.5	672.4	767.7
280	99.5	149.1	198.5	297.5	396.2	495.0	593.3	692.1	790.2
285	102.3	153.2	204.0	305.9	407.4	509.1	610.3	712.0	813.0
290	105.0	157.3	209.6	314.3	418.7	523.3	627.4	732.1	836.1
295	107.8	161.5	215.2	322.8	430.2	537.7	644.8	752.4	859.4
300	110.6	165.8	220.9	331.4	441.7	552.2	662.3	772.9	882.9
305	113.4	170.0	226.7	340.2	453.4	566.9	680.0	793.6	906.7
310	116.2	174.3	232.4	348.9	465.2	581.7	697.8	814.6	930.7
315	119.1	178.7	238.3	357.8	477.1	596.7	715.9	835.7	954.9
320	122.0	183.1	244.2	366.7	489.1	611.8	734.1	857.0	979.4
325	124.9	187.5	250.1	375.7	501.2	627.0	752.5	878.6	1004
330	127.8	191.9	256.1	384.8	513.4	642.4	771.0	900.3	1029
335	130.8	196.4	262.2	394.0	525.8	657.9	789.8	922.3	1054
340	133.8	201.0	268.2	403.2	538.2	673.6	808.6	944.4	1080
345	136.8	205.5	274.4	412.6	550.7	689.4	827.7	966.7	1105
350	139.8	210.1	280.6	422.0	563.4	705.3	846.9	989.3	1131
355	142.8	214.7	286.8	431.3	576.1	721.4	866.3	1012	1157
360	145.9	219.4	293.1	441.0	589.0	737.6	885.8	1035	1183
365	149.0	224.1	299.4	450.6	602.0	753.9	905.5	1058	1210
370	152.1	228.8	305.8	460.3	615.0	770.3	925.4	1081	1237
375	155.3	233.6	312.2	470.1	628.2	786.9	945.4	1105	1264
380	158.4	238.4	318.7	480.0	641.4	803.6	965.6	1128	1291
385	161.6	243.3	325.2	489.9	654.8	820.5	985.9	1152	1318
390	164.8	248.2	331.8	499.9	668.3	837.4	1006	1176	1346
395	168.0	253.1	338.4	510.0	681.9	854.6	1027	1201	1374
400	171.3	258.0	345.1	520.1	695.5	871.8	1048	1225	1402
405	174.6	263.0	351.8	530.3	709.3	889.2	1069	1250	1430
410	177.9	268.0	358.5	540.6	723.2	906.6	1090	1274	1459
415	181.2	273.0	365.3	551.0	737.1	924.2	1111	1299	1487
420	184.5	278.1	372.2	561.4	751.2	942.0	1133	1325	1516
425	187.9	283.2	379.1	571.9	765.4	959.8	1154	1350	1545
430	191.2	288.4	386.0	582.5	779.6	977.8	1176	1375	1575
435	194.6	293.5	393.0	593.1	794.0	995.9	1198	1401	1604
440	198.0	298.7	400.0	603.8	808.4	1014	1220	1427	1634
445	201.5	304.0	407.1	614.6	823.0	1032	1242	1453	1664
450	204.9	309.2	414.2	625.4	837.6	1051	1264	1479	1694
455	208.4	314.6	421.4	636.4	852.3	1070	1287	1506	1724
460	211.9	319.9	428.6	647.3	867.2	1088	1310	1532	1755
465	215.4	325.2	435.8	658.4	882.1	1107	1332	1559	1786
470	219.0	330.6	443.1	669.5	897.1	1126	1355	1586	1817
475	222.5	336.1	450.4	680.7	912.2	1145	1378	1613	1848
480	226.1	341.5	457.8	692.0	927.4	1164	1402	1640	1879

(Table 7.10. cont.)

Upper-head h_a (mm)	Discharge per 1/sec for flumes of various throat widths 1 feet	1.5 feet	2 feet	3 feet	4 feet	5 feet	6 feet	7 feet	8 feet
485	229.7	347.0	465.2	703.3	942.7	1184	1425	1668	1911
490	233.3	352.5	472.6	714.7	958.1	1203	1448	1695	1942
495	236.9	358.1	480.1	726.1	973.5	1223	1472	1723	1974
500	240.6	363.6	487.7	737.6	989.1	1242	1496	1751	2006
505	244.2	369.2	495.3	749.2	1005	1262	1520	1779	2039
510	247.9	374.9	502.9	760.9	1020	1282	1544	1808	2071
515	251.6	380.6	510.5	772.6	1036	1302	1568	1836	2104
520	255.4	386.3	518.2	784.4	1052	1322	1592	1865	2137
525	259.1	392.0	526.0	796.2	1068	1342	1617	1893	2170
530	262.9	397.7	533.8	808.1	1084	1363	1642	1922	2203
535	266.7	403.5	541.6	820.1	1101	1383	1666	1951	2239
540	270.5	409.3	549.5	832.1	1117	1404	1691	1981	2271
545	274.3	415.2	557.4	844.2	1133	1424	1716	2010	2304
550	278.1	421.1	565.3	856.4	1150	1445	1741	2040	2339
555	282.0	427.0	573.3	868.6	1166	1466	1767	2070	2373
560	285.9	432.9	581.3	880.9	1183	1487	1792	2099	2407
565	289.8	438.8	589.4	893.2	1199	1508	1818	2130	2442
570	293.7	444.8	597.5	905.6	1216	1529	1844	2160	2477
575	297.6	450.8	605.6	918.1	1233	1551	1869	2190	2512
580	301.6	456.9	613.8	930.6	1250	1572	1895	2221	2547
585	305.5	463.0	622.0	943.2	1267	1594	1922	2252	2582
590	309.5	469.1	630.3	955.9	1284	1615	1948	2282	2618
595	313.5	475.2	638.6	968.6	1302	1637	1974	2313	2654
600	317.5	481.4	646.9	981.4	1319	1659	2001	2345	2690
605	321.6	487.5	655.3	994.2	1336	1681	2027	2376	2726
610	325.6	493.7	663.7	1007	1354	1703	2054	2408	2762
615	329.7	500.0	672.2	1020	1371	1725	2081	2439	2798
620	333.8	506.2	680.7	1033	1389	1748	2108	2471	2835
625	337.9	512.5	689.2	1046	1407	1770	2135	2503	2872
630	342.0	518.9	697.8	1059	1424	1793	2163	2535	2909
635	346.1	525.2	706.4	1072	1442	1815	2190	2567	2946
640	350.3	531.6	715.0	1086	1460	1838	2218	2600	2983
645	354.5	538.0	723.7	1099	1478	1861	2245	2632	3021
650	358.6	544.4	732.4	1112	1496	1884	2273	2665	3059
655	362.9	550.9	741.1	1126	1515	1907	2301	2698	3097
660	367.1	557.3	749.9	1139	1533	1930	2529	2731	3135
665	371.3	563.8	758.8	1153	1551	1953	2357	2764	3173
670	375.6	570.4	767.6	1166	1570	1977	2386	2798	3211
675	379.8	576.9	776.5	1180	1588	2000	2414	2831	3250
680	384.1	583.5	785.4	1194	1607	2024	2443	2865	3289
685	388.4	599.1	794.4	1208	1625	2047	2472	2899	3328
690	392.8	596.8	803.4	1221	1644	2071	2500	2933	3367
695	397.1	603.4	812.5	1235	1663	2095	2529	2967	3406
700	401.5	610.1	821.5	1249	1682	2119	2558	3001	3446
705	405.8	616.8	839.7	1263	1701	2143	2588	3035	3485
710	410.2	623.6	839.8	1277	1720	2167	2617	3070	3525
715	414.6	630.4	849.0	1292	1739	2191	2646	3105	3565
720	419.1	637.2	858.2	1306	1758	2216	2676	3139	3605
725	423.5	644.0	867.5	1320	1778	2240	2706	3174	3645
730	428.0	650.8	876.8	1334	1797	2265	2736	3210	3686
735	432.4	657.7	886.1	1349	1817	2289	2765	3245	3727
740	436.9	664.6	895.4	1363	1836	2314	2796	3280	3767
745	441.4	671.5	904.8	1377	1856	2339	2826	3316	3808
750	445.9	678.4	914.3	1392	1875	2364	2856	3351	3850
755	450.4	685.4	923.7	1406	1895	2389	2886	3387	3891
760	455.0	692.4	933.2	1421	1915	2414	2917	3423	3932

TABLE 7.11. FREE-FLOW DISCHARGE THROUGH PARSHALL MEASURING FLUMES IN m^3/s.
COMPUTED FROM THE FORMULA $Q = (3.6875\ b + 2.5)\ h_a^{1.6}$ (b = width in feet)

Upper-head h_a (mm)	Discharge per m^3/s for flumes of various throat widths							
	10 feet	12 feet	15 feet	20 feet	25 feet	30 feet	40 feet	50 feet
90	0.158	0.188	0.233	0.307	0.381	0.455	0.603	0.751
95	0.173	0.205	0.254	0.334	0.415	0.496	0.658	0.819
100	0.187	0.223	0.275	0.363	0.451	0.539	0.714	0.889
105	0.203	0.241	0.298	0.392	0.487	0.582	0.772	0.962
110	0.218	0.259	0.321	0.423	0.525	0.627	0.832	1.04
115	0.234	0.278	0.344	0.454	0.564	0.674	0.893	1.11
120	0.251	0.298	0.369	0.486	0.603	0.721	0.956	1.19
125	0.268	0.318	0.393	0.519	0.644	0.770	1.02	1.27
130	0.285	0.339	0.419	0.552	0.686	0.819	1.09	1.35
135	0.303	0.360	0.445	0.587	0.728	0.870	1.15	1.44
140	0.321	0.381	0.472	0.622	0.772	0.923	1.22	1.52
145	0.340	0.403	0.499	0.658	0.817	0.976	1.29	1.61
150	0.359	0.426	0.527	0.694	0.862	1.03	1.37	1.70
155	0.378	0.449	0.555	0.732	0.909	1.09	1.44	1.79
160	0.398	0.472	0.584	0.770	0.956	1.14	1.51	1.89
165	0.418	0.496	0.613	0.809	1.00	1.20	1.59	1.98
170	0.438	0.520	0.643	0.848	1.05	1.26	1.67	2.08
175	0.459	0.545	0.674	0.889	1.10	1.32	1.75	2.18
180	0.480	0.570	0.705	0.930	1.15	1.38	1.83	2.28
185	0.502	0.595	0.737	0.971	1.21	1.44	1.91	2.38
190	0.524	0.621	0.769	1.01	1.26	1.50	1.99	2.48
195	0.546	0.648	0.801	1.06	1.31	1.57	2.08	2.59
200	0.568	0.675	0.835	1.100	1.37	1.63	2.16	2.70
205	0.591	0.702	0.868	1.14	1.42	1.70	2.25	2.80
210	0.614	0.739	0.902	1.19	1.48	1.77	2.34	2.92
215	0.638	0.757	0.937	1.24	1.53	1.83	2.43	3.03
220	0.662	0.786	0.972	1.28	1.59	1.90	2.52	3.14
225	0.686	0.814	1.01	1.33	1.65	1.97	2.61	3.26
230	0.711	0.844	1.04	1.38	1.71	2.04	2.71	3.37
235	0.736	0.873	1.08	1.42	1.77	2.11	2.80	3.49
240	0.761	0.903	1.12	1.47	1.83	2.19	2.90	3.61
245	0.786	0.933	1.15	1.52	1.89	2.26	3.00	3.73
250	0.812	0.964	1.19	1.57	1.95	2.33	3.09	3.85
255	0.838	0.995	1.23	1.62	2.02	2.41	3.19	3.98
260	0.865	1.03	1.27	1.67	2.08	2.48	3.29	4.10
265	0.891	1.06	1.31	1.73	2.14	2.56	3.40	4.23
270	0.919	1.09	1.35	1.78	2.21	2.64	3.50	4.36
275	0.946	1.12	1.39	1.83	2.27	2.72	3.60	4.49
280	0.974	1.16	1.43	1.89	2.34	2.80	3.71	4.62
285	1.002	1.19	1.47	1.94	2.41	2.88	3.82	4.75
290	1.030	1.22	1.51	1.99	2.48	2.96	3.92	4.89
295	1.058	1.26	1.55	2.05	2.54	3.04	4.03	5.02
300	1.087	1.29	1.60	2.11	2.61	3.12	4.14	5.16
305	1.116	1.33	1.64	2.16	2.68	3.21	4.25	5.30
310	1.146	1.36	1.68	2.22	2.75	3.29	4.36	5.44
315	1.175	1.40	1.73	2.28	2.83	3.38	4.48	5.58
320	1.205	1.43	1.77	2.33	2.90	3.46	4.59	5.72
325	1.236	1.47	1.81	2.39	2.97	3.55	4.71	5.86
330	1.266	1.50	1.86	2.45	3.04	3.64	4.82	6.01
335	1.297	1.54	1.90	2.51	3.12	3.73	4.94	6.15

(Table 7.11. cont.)

Upper-head h_a (mm)	Discharge per m^3/s for flumes of various throat widths 10 feet	12 feet	15 feet	20 feet	25 feet	30 feet	40 feet	50 feet
340	1.328	1.58	1.95	2.57	3.19	3.82	5.06	6.30
345	1.360	1.61	2.00	2.63	3.27	3.91	5.18	6.45
350	1.391	1.65	2.04	2.69	3.34	4.00	5.30	6.60
355	1.423	1.69	2.09	2.76	3.42	4.09	5.42	6.75
360	1.455	1.73	2.14	2.82	3.50	4.18	5.54	6.91
365	1.488	1.77	2.19	2.88	3.58	4.27	5.67	7.06
370	1.521	1.81	2.23	2.94	3.66	4.37	5.79	7.22
375	1.554	1.84	2.28	3.01	3.73	4.46	5.92	7.37
380	1.587	1.88	2.33	3.07	3.81	4.56	6.05	7.53
385	1.621	1.92	3.38	3.14	3.90	4.66	6.17	7.69
390	1.65	1.96	2.43	3.20	3.98	4.75	6.30	7.85
395	1.69	2.00	2.48	3.27	4.06	4.85	6.43	8.01
400	1.72	2.04	2.53	3.34	4.14	4.95	6.56	8.17
405	1.76	2.09	2.58	3.40	4.22	5.05	6.69	8.34
410	1.79	2.13	2.63	3.47	4.31	5.15	6.83	8.50
415	1.83	2.17	2.68	3.54	4.39	5.25	6.96	8.67
420	1.86	2.21	2.74	3.61	4.48	5.35	7.10	8.84
425	1.90	2.25	2.79	3.68	4.56	5.45	7.23	9.01
430	1.93	2.30	2.84	3.74	4.65	5.56	7.37	9.18
435	1.97	2.34	2.89	3.81	4.74	5.66	7.51	9.35
440	2.01	2.38	2.95	3.89	4.82	5.76	7.64	9.52
445	2.04	2.43	3.00	3.96	4.91	5.87	7.78	9.69
450	2.08	2.47	3.05	4.03	5.00	5.98	7.92	9.87
455	2.12	2.51	3.11	4.10	5.09	6.08	8.06	10.0
460	2.15	2.56	3.16	4.17	5.18	6.19	8.21	10.2
465	2.19	2.60	3.22	4.24	5.27	6.30	8.35	10.4
470	2.23	2.65	3.27	4.32	5.36	6.41	8.49	10.6
475	2.27	2.69	3.33	4.39	5.45	6.52	8.64	10.8
480	2.31	2.74	3.39	4.47	5.54	6.63	8.79	10.9
485	2.34	2.78	3.44	4.54	5.64	6.74	8.93	11.1
490	2.38	2.83	3.50	4.62	5.73	6.85	9.08	11.3
495	2.42	2.88	3.56	4.69	5.82	6.96	9.23	11.5
500	2.46	2.92	3.62	4.77	5.92	7.07	9.38	11.7
505	2.50	2.97	3.67	4.84	6.01	7.19	9.53	11.9
510	2.54	3.02	3.73	4.92	6.11	7.30	9.68	12.1
515	2.58	3.06	3.79	5.00	6.20	7.42	9.83	12.2
520	2.62	3.11	3.85	5.08	6.30	7.53	9.99	12.4
525	2.66	3.16	3.91	5.15	6.40	7.65	10.1	12.6
530	2.70	3.21	3.97	5.23	6.50	7.76	10.3	12.8
535	2.74	3.26	4.03	5.31	6.59	7.88	10.5	13.6
540	2.78	3.31	4.09	5.39	6.69	8.00	10.6	13.0
550	2.87	3.40	4.21	5.55	6.89	8.24	10.9	13.6
560	2.95	3.50	4.33	5.71	7.09	8.48	11.2	14.0
570	3.04	3.60	4.46	5.88	7.30	8.72	11.6	14.4
580	3.12	3.71	4.58	6.04	7.50	8.97	11.9	14.8
590	3.21	3.81	4.71	6.21	7.71	9.22	12.2	15.2
600	3.30	3.91	4.84	6.38	7.92	9.47	12.6	15.6
610	3.38	4.02	4.97	6.55	8.13	9.72	12.9	16.1
620	3.47	4.12	5.10	6.73	8.35	9.98	13.2	16.5
630	3.56	4.23	5.23	6.90	8.57	10.2	13.6	16.9
640	3.65	4.34	5.37	7.08	8.78	10.5	13.9	17.3
650	3.75	4.45	5.50	7.25	9.00	10.8	14.3	17.8
660	3.84	4.56	5.64	7.43	9.23	11.0	14.6	18.2
670	3.93	4.67	5.77	7.61	9.45	11.3	15.0	18.7

(Table 7.11. cont.)

Upper-head h_a (mm)	Discharge per m^3/s for flumes of various throat widths 10 feet	12 feet	15 feet	20 feet	25 feet	30 feet	40 feet	50 feet
680	4.03	4.78	5.91	7.80	9.68	11.6	15.3	19.1
690	4.12	4.89	6.05	7.98	9.91	11.8	15.7	19.6
700	4.22	5.01	6.19	8.17	10.1	12.1	16.1	20.0
710	4.31	5.12	6.34	8.35	10.4	12.4	16.4	20.5
720	4.41	5.24	6.48	8.54	10.6	12.7	16.8	20.9
730	4.51	5.35	6.62	8.73	10.8	13.0	17.2	21.4
740	4.61	5.47	6.77	8.93	11.1	13.2	17.6	21.9
750	4.71	5.59	6.92	9.12	11.3	13.5	17.9	22.3
760	4.81	5.71	7.06	9.31	11.6	13.8	18.3	22.8
770	4.91	5.83	7.21	9.51	11.8	14.1	18.7	23.3
780	5.01	5.95	7.36	9.71	12.1	14.4	19.1	23.8
790	5.12	6.08	7.52	9.91	12.3	14.7	19.5	24.3
800	5.22	6.20	7.67	10.1	12.6	15.0	19.9	24.8
810	5.33	6.32	7.82	10.3	12.8	15.3	20.3	25.3
820	5.43	6.45	7.98	10.5	13.1	15.6	20.7	25.8
830	5.54	6.58	8.13	10.7	13.3	15.9	21.1	26.3
840	5.65	6.70	8.29	10.9	13.6	16.2	21.5	26.8
850	5.75	6.83	8.45	11.1	13.8	16.5	21.9	27.3
860	5.86	6.96	8.61	11.4	14.1	16.8	22.3	27.8
870	5.97	7.09	8.77	11.6	14.4	17.2	22.8	28.3
880	6.08	7.22	8.93	11.8	14.6	17.5	23.2	28.9
890	6.19	7.35	9.10	12.0	14.9	17.8	23.6	29.4
900	6.31	7.48	9.26	12.2	15.2	18.1	24.0	29.9
910	6.42	7.62	9.42	12.4	15.4	18.4	24.4	30.5
920	6.53	7.75	9.59	12.6	15.7	18.8	24.9	31.0
930	6.64	7.89	9.76	12.9	16.0	19.1	25.3	31.5
940	6.76	8.02	9.93	13.1	16.2	19.4	25.8	32.1
950	6.87	8.16	10.1	13.3	16.5	19.8	26.2	32.6
960	6.99	8.30	10.3	13.5	16.8	20.1	26.6	33.2
970	7.11	8.44	10.4	13.8	17.1	20.4	27.1	33.7
980	7.23	8.58	10.6	14.0	17.4	20.8	27.5	34.3
990	7.34	8.72	10.8	14.2	17.7	21.1	28.0	34.8
1000	7.46	8.86	11.0	14.4	17.9	21.4	28.4	35.4
1010	7.58	9.00	11.1	14.7	18.2	21.8	28.9	36.0
1020	7.70	9.14	11.3	14.9	18.5	22.1	29.3	36.5
1030	7.82	9.29	11.5	15.1	18.8	22.5	29.8	37.1
1040	7.95	9.43	11.7	15.4	19.1	22.8	30.3	37.7
1050	8.07	9.58	11.8	15.6	19.4	23.2	30.7	38.3
1060	8.19	9.72	12.0	15.9	19.7	23.5	31.2	38.9
1070		9.87	12.2	16.1	20.0	23.9	31.7	39.5
1080		10.0	12.4	16.3	20.3	24.2	32.2	40.1
1090		10.2	12.6	16.6	20.6	24.6	32.6	40.6
1100		10.3	12.8	16.8	20.9	25.0	33.1	41.2
1110		10.5	13.0	17.1	21.2	25.3	33.6	41.8
1120		10.6	13.1	17.3	21.5	25.7	34.1	42.4
1130		10.8	13.3	17.6	21.8	26.1	34.6	43.1
1140		10.9	13.5	17.8	22.1	26.4	35.1	43.7
1150		11.1	13.7	18.1	22.4	26.8	35.6	44.3
1160		11.2	13.9	18.3	22.7	27.2	36.1	44.9
1170		11.4	14.1	18.6	23.1	27.6	36.5	45.5
1180		11.5	14.3	18.8	23.4	27.9	37.0	46.1
1190		11.7	14.5	19.1	23.7	28.3	37.6	46.8
1200		11.9	14.7	19.3	24.0	28.7	38.1	47.4

(Table 7.11. cont.)

Upper-head h_a (mm)	Discharge per m^3/s for flumes of various throat widths 10 feet	12 feet	15 feet	20 feet	25 feet	30 feet	40 feet	50 feet
1210		12.0	14.9	19.6	24.3	29.1	38.6	48.0
1220		12.2	15.1	19.9	24.7	29.5	39.1	48.7
1230		12.3	15.3	20.1	25.0	29.9	39.6	49.3
1240		12.5	15.5	20.4	25.3	30.2	40.1	50.0
1250		12.7	15.7	20.7	25.6	30.6	40.6	50.6
1260		12.8	15.9	20.9	26.0	31.0	41.1	51.3
1270		13.0	16.1	21.2	26.3	31.4	41.7	51.9
1280		13.1	16.3	21.4	26.6	31.8	42.2	52.6
1290		13.3	16.5	21.7	27.0	32.2	42.7	53.2
1300		13.5	16.7	22.0	27.3	32.6	43.3	53.9
1310		13.6	16.9	22.3	27.6	33.0	43.8	54.5
1320		13.8	17.1	22.5	28.0	33.4	44.3	55.2
1330		14.0	17.3	22.8	28.3	33.8	44.9	55.9
1340		14.1	17.5	23.1	28.7	34.2	45.4	56.6
1350		14.3	17.9	23.4	29.0	34.7	46.0	57.2
1360		14.5	17.9	23.6	29.3	35.1	46.5	57.9
1370		14.7	18.1	23.9	29.7	35.5	47.0	58.6
1380			18.3	24.2	30.0	35.9	47.6	59.3
1390			18.6	24.5	30.4	36.3	48.2	60.0
1400			18.8	24.8	30.7	36.7	48.7	60.7
1410			19.0	25.0	31.1	37.2	49.3	61.4
1420			19.2	25.3	31.4	37.6	49.8	62.1
1430			19.4	25.6	31.8	38.0	50.4	62.8
1440			19.6	25.9	32.2	38.4	51.0	63.5
1450			19.9	26.2	32.5	38.9	51.5	64.2
1460			20.1	26.5	32.9	39.3	52.1	64.9
1470			20.3	26.8	33.2	39.7	52.7	65.7
1480			20.5	27.1	33.6	40.1	53.2	66.3
1490			20.7	27.4	34.0	40.6	53.8	67.0
1500			21.0	27.6	34.3	41.0	54.4	67.7
1510			21.2	27.9	34.7	41.5	55.0	68.5
1420			21.4	28.2	35.1	41.9	55.6	69.2
1530			21.6	28.5	35.4	42.3	56.1	69.9
1540			21.9	28.8	35.8	42.8	56.7	70.7
1550			22.1	29.1	36.2	43.2	57.3	71.4
1560			22.3	29.4	36.5	43.7	57.9	72.1
1570			22.6	29.7	36.9	44.1	58.5	72.9
1580			22.8	30.0	37.3	44.6	59.1	73.6
1590			23.0	30.3	37.7	45.0	59.7	74.4
1600			23.2	30.7	38.1	45.5	60.3	75.1
1610			23.5	31.0	38.4	45.9	60.9	75.9
1620			23.7	31.3	38.8	46.4	61.5	76.6
1630			24.0	31.6	39.2	46.9	62.1	77.4
1640			24.2	31.9	39.6	47.3	62.7	78.1
1650			24.4	32.2	40.0	47.8	63.4	78.9
1660			24.7	32.5	40.4	48.2	64.0	79.7
1670			24.9	32.8	40.8	48.7	64.6	80.4
1680				33.1	41.1	49.2	65.2	81.2
1690				33.5	41.5	49.6	65.8	82.0
1700				33.8	41.9	50.1	66.5	82.8
1710				34.1	42.3	50.6	67.1	83.5
1720				34.4	42.7	51.1	67.7	84.3
1730				34.7	43.1	51.5	68.3	85.1
1740				35.1	43.5	52.0	69.0	85.9
1750				35.4	43.9	52.5	69.6	86.7
1760				35.7	44.3	53.0	70.2	87.5
1770				36.0	44.7	53.5	70.9	88.3
1780				36.4	45.1	53.9	71.5	89.1
1790				36.7	45.5	54.4	72.2	89.9
1800				37.0	45.9	54.9	72.8	90.7
1810				37.3	46.4	55.4	73.5	91.5
1820				37.7	46.8	55.9	74.1	92.3

7.4.3 Submerged flow

When the ratio of gauge reading h_b to h_a exceeds the limits of 0.60 for 3-,6-,and 9-in flumes, 0.70 for 1- to 8-ft flumes and 0.80 for 10- to 50-ft flumes, the modular flume discharge is reduced due to submergence. The non-modular discharge of Parshall flumes equals

$$Q_s = Q - Q_E \tag{7-7}$$

where

Q = the modular discharge (Tables 7.5 to 7.11)

Q_E = the reduction on the modular discharge due to submergence

The diagrams in Figures 7.10 to 7.16 give the corrections, Q_E, for submergence for Parshall flumes of various sizes. The correction for the 1-ft flume is made applicable to the 1.5-ft up to 8-ft flumes by multiplying the correction Q_E for the 1-ft flume by the factor given below for the particular size of the flume in use.

size of flume		correction
b in ft	b in m	factor
1	0.3048	1.0
1.5	0.4572	1.4
2	0.6096	1.8
3	0.9144	2.4
4	1.2191	3.1
5	1.5240	3.7
6	1.8288	4.3
7	2.1336	4.9
8	3.4384	5.4

Similarly, the correction for the 10-ft flume is made applicable to the larger flumes by multiplying the correction for the 10-ft flume by the factor given below for the particular flume in use.

size of flume		correction
b in ft	b in m	factor
10	3.048	1.0
12	3.658	1.2
15	4.572	1.5
20	6.096	2.0
25	7.620	2.5
30	9.144	3.0
40	12.192	4.0
50	15.240	5.0

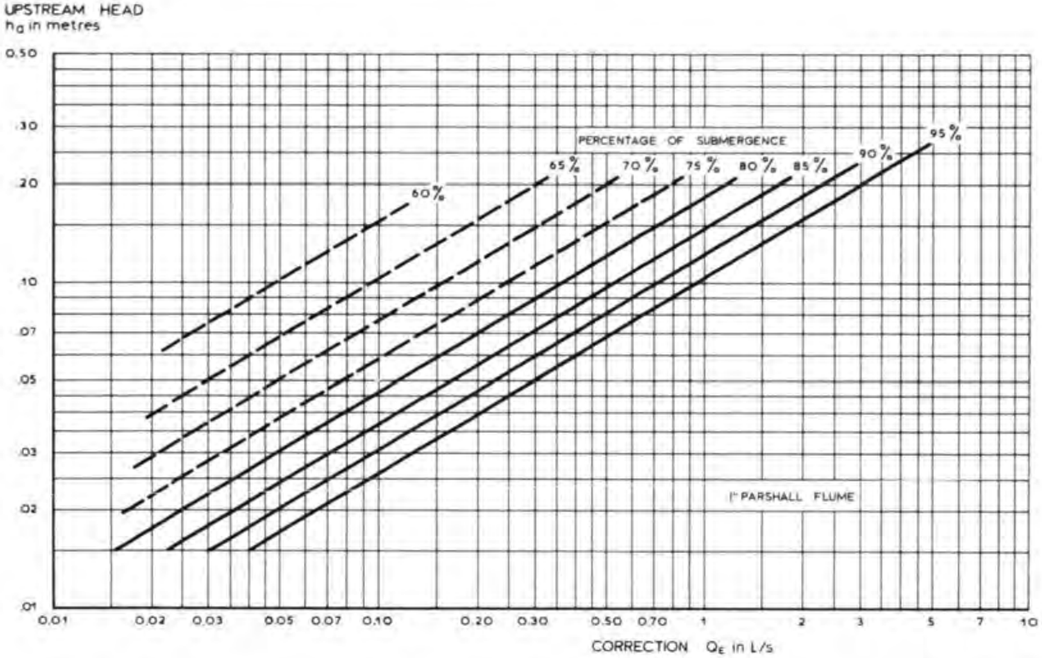

Fig.7.10. Discharge correction for submerged flow. 1" Parshall flume.

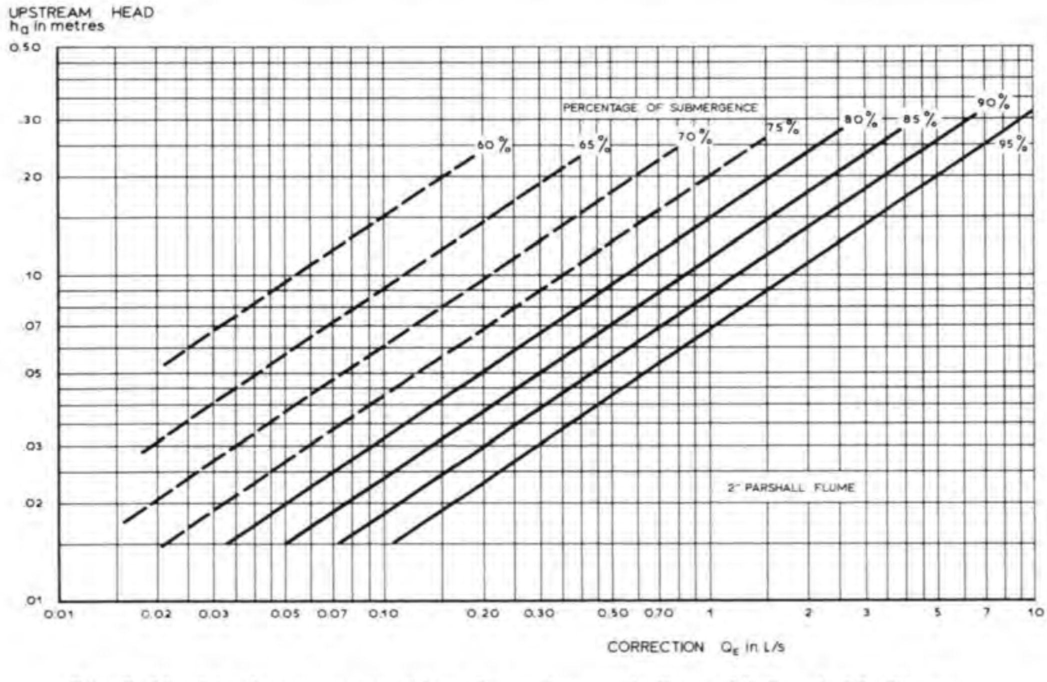

Fig.7.11. Discharge correction for submerged flow. 2" Parshall flume.

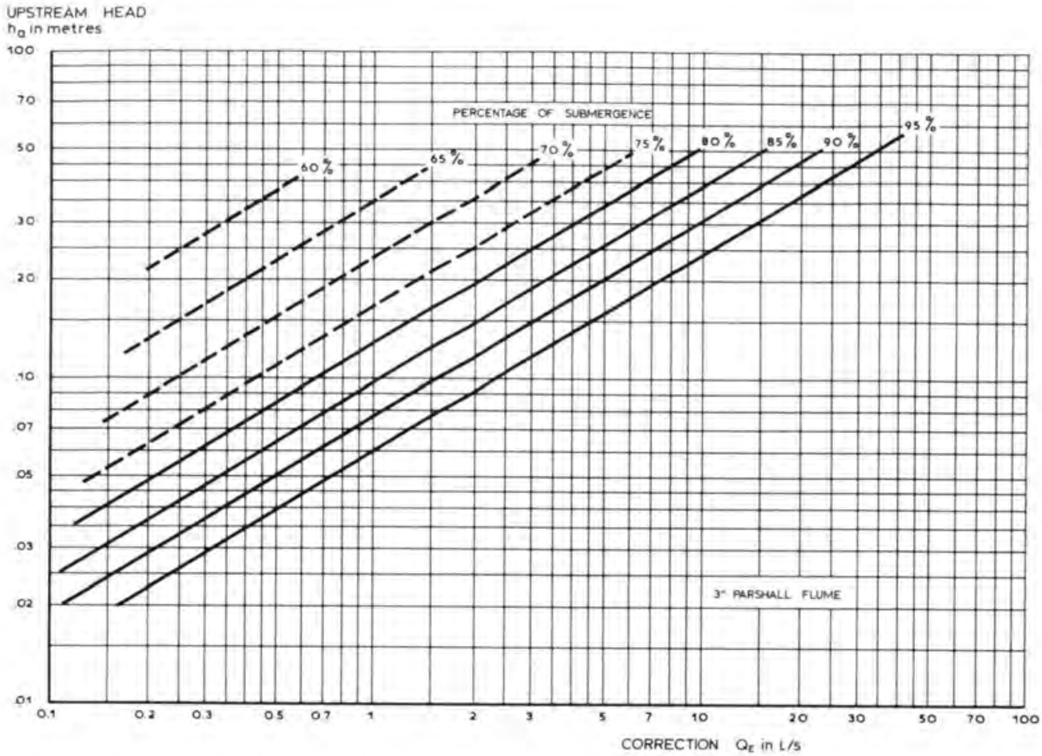

Fig. 7.12. Discharge correction for submerged flow. 3" Parshall flume.

If the size and elevation of the flume cannot be selected to permit modular-flow operation, the submergence ratio h_b/h_a should be kept below the practical limit of 0.95, since the flume ceases to be a measuring device if submergence exceeds this limit.

As mentioned, turbulence in the relatively deep and narrow throat of the "very small" flumes makes the h_b-gauge difficult to read. If an h_c-gauge is used under submerged flow conditions, the h_c-readings should be converted to h_b-readings with the aid of Figure 7.17, and the converted h_b-values are then used to determine the submerged discharge with the aid of Figures 7.10 to 7.14.

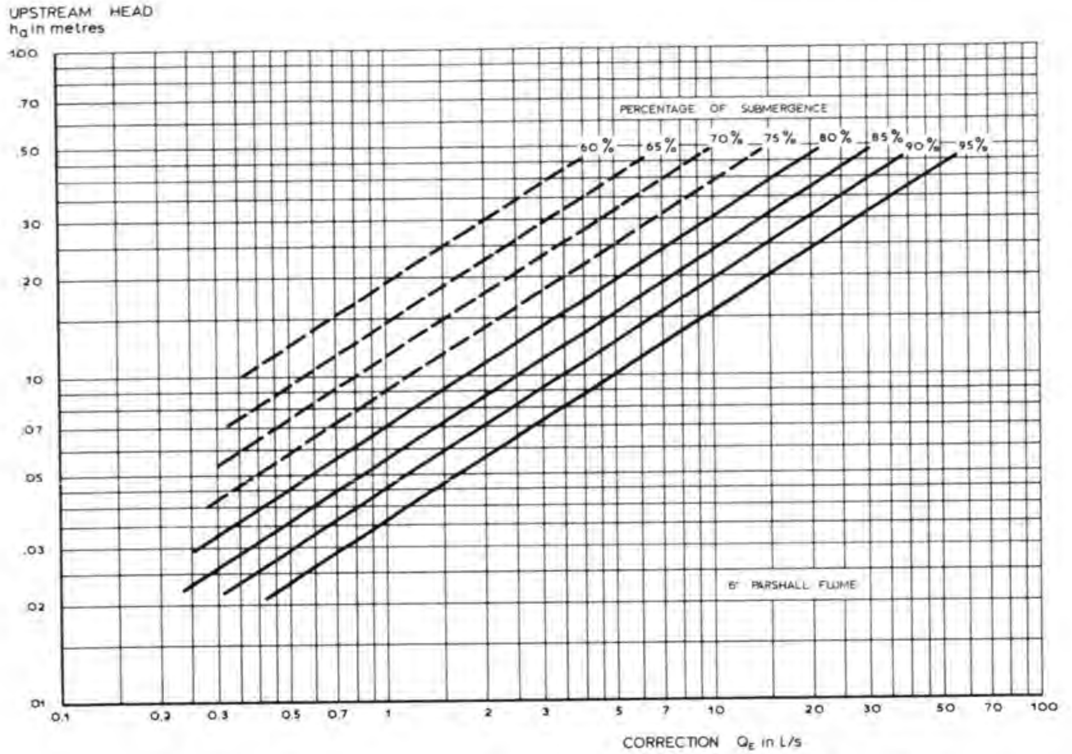

Fig.7.18. Discharge correction for submerged flow. 6" Parshall flume.

7.4.4 Accuracy of discharge measurement

The error in the modular discharge read from the Tables 7.5 to 7.11 is expected to be about 3%. Under submerged flow conditions the error in the discharge becomes greater, until at 95% submergence the flume ceases to be a measuring device. The method by which this discharge error is to be combined with errors in h_a, h_b, and the flume dimensions are shown in Appendix II.

7.4.5 Loss of head through the flume

The size and elevation of the crest of the flume depend on the available loss of head through the flume $\Delta h(\approx\Delta H)$. Since for the Parshall flume h_a and h_b are measured at rather arbitrary locations, the loss of head through the flume Δh is not equal to the difference between h_a and h_b but has a greater value. The head loss Δh can be determined from the diagrams in Figures 7.19 and 7.20 for small and large flumes. For very small flumes no data on Δh are available.

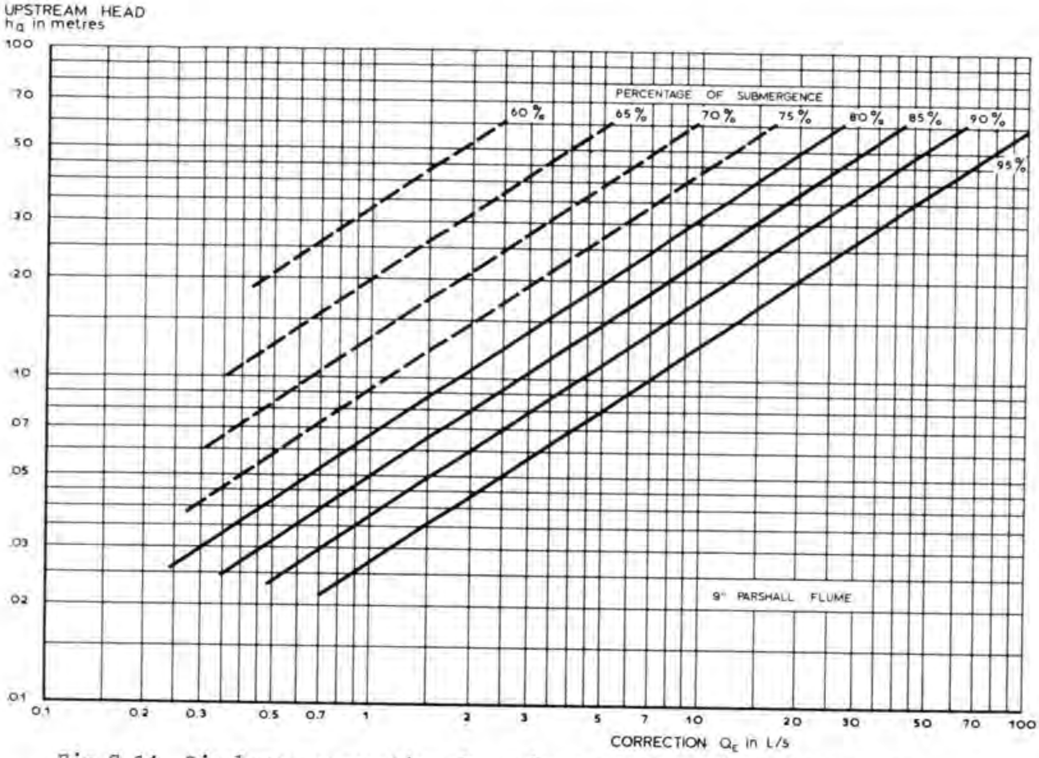

Fig.7.14. Discharge correction for submerged flow.9" Parshall flume.

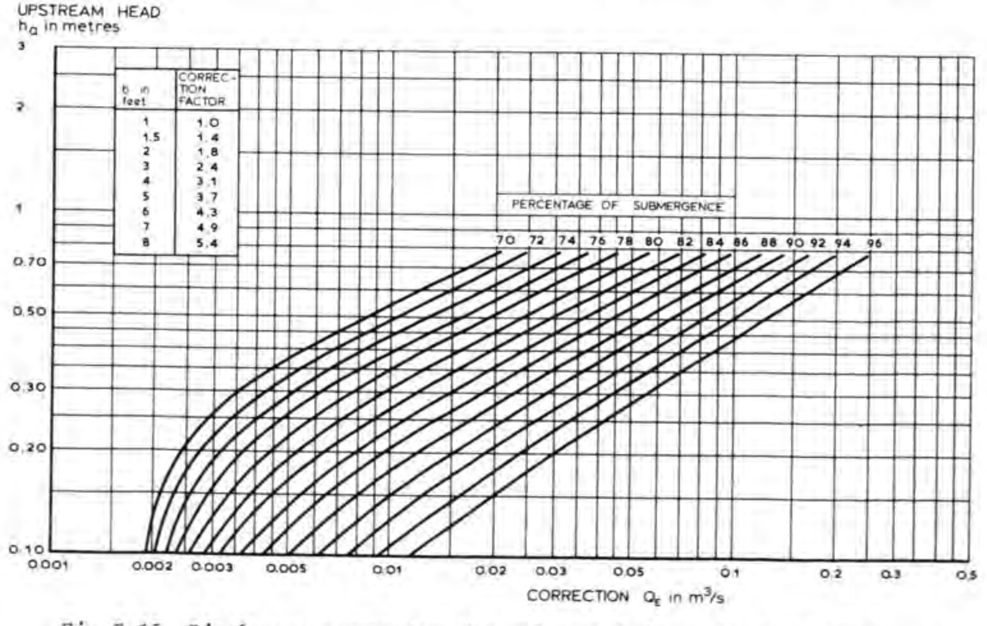

Fig.7.15. Discharge correction for submerged flow. 1' Parshall flume, correction Q_E (m^3/s).

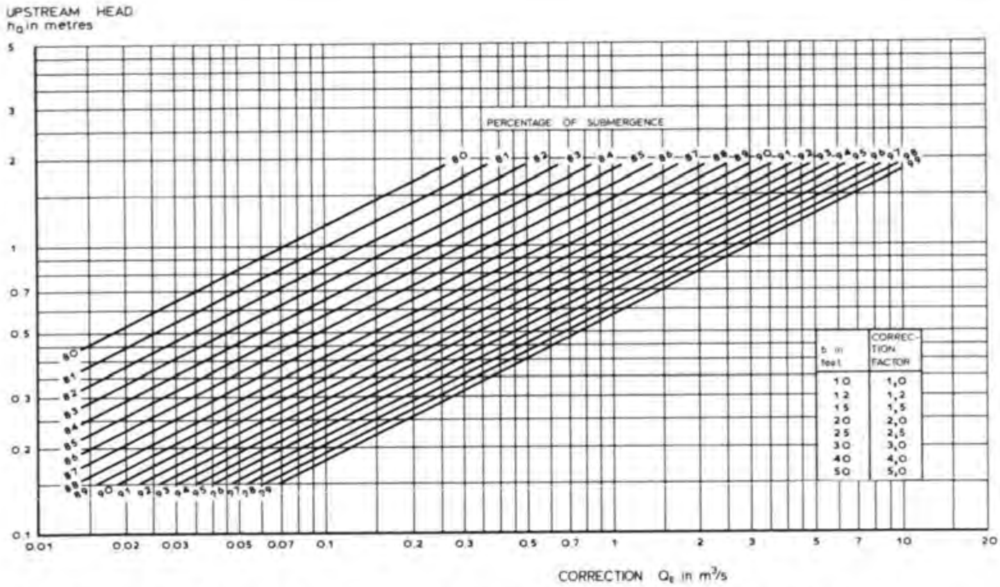

Fig.7.16. Diagram for determining correction to be subtracted from free-discharge flow to obtain submerged flow discharges through 10' Parshall flumes.

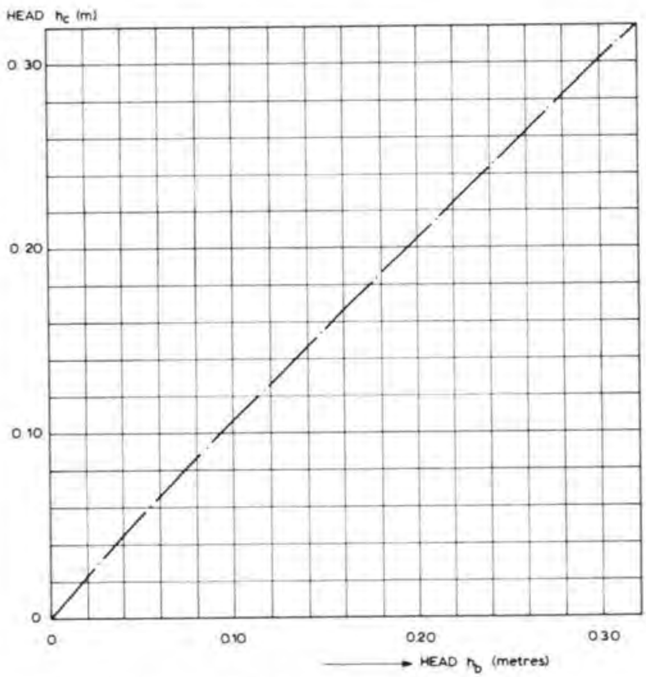

Fig.7.17. Relationship of h_c and h_b gauges for 1",2",and 3" Parshall flumes for submergences greater than 50 percent (after Colorado State Univ.)

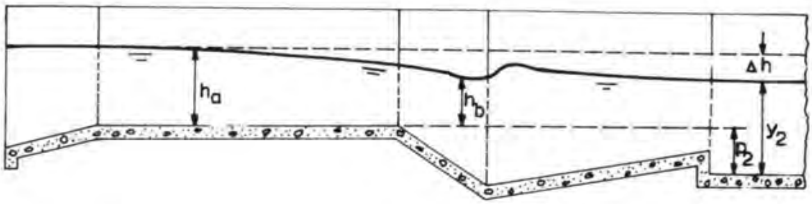

Fig.7.18. Section of Parshall flume.

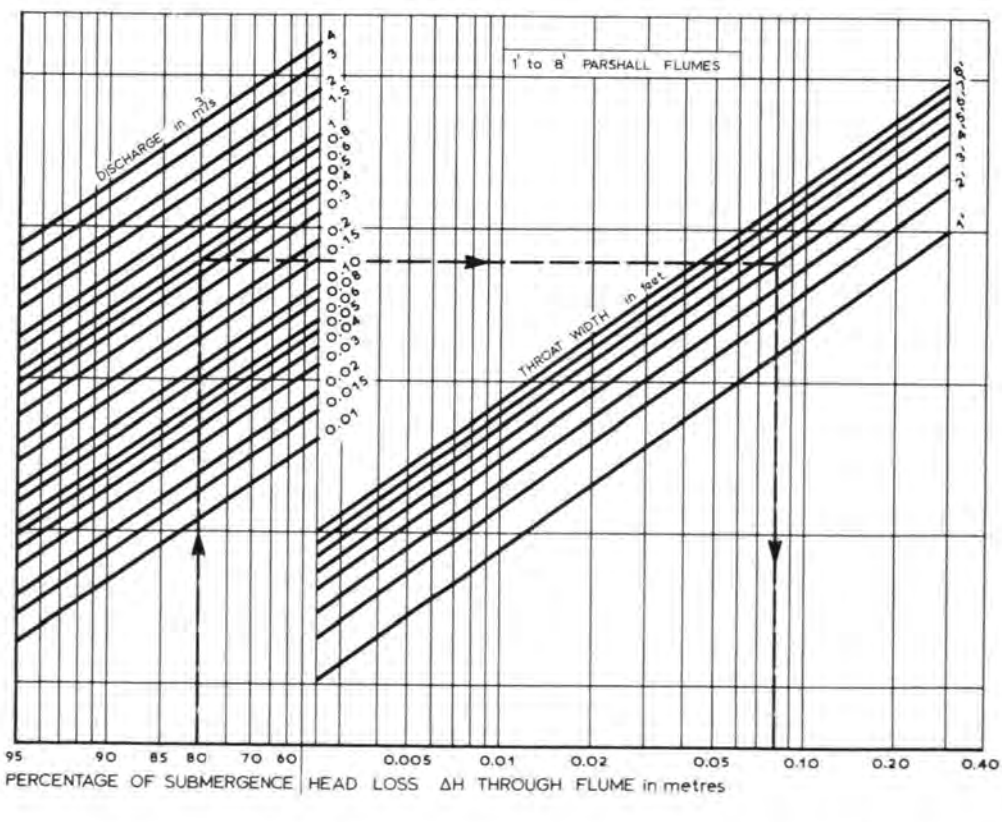

Fig.7.19. Head-loss through Parshall flumes. 1' up to 8' Parshall flumes.

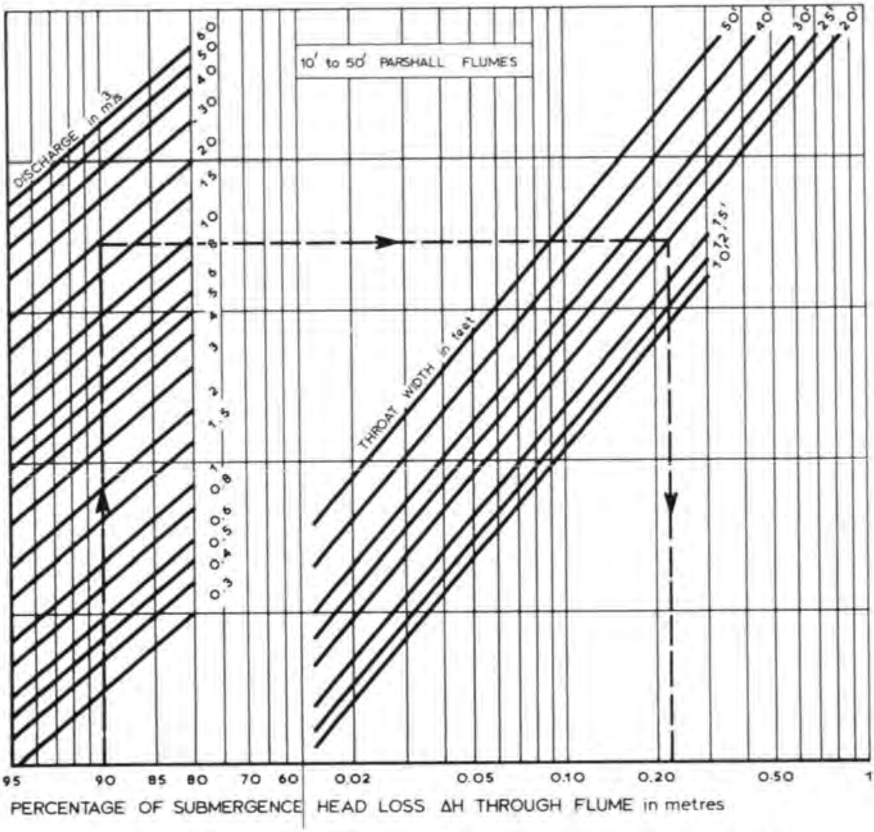

Fig.7.20. Head-loss through Parshall flumes (10-50 feet wide).

7.4.6 Limits of application

The limits of application of the Parshall measuring flumes essential for reasonable accuracy are:

a) Each type of flume should be constructed exactly to the dimensions listed in Table 7.3.

b) The flume should be carefully levelled in both longitudinal and transverse directions.

c) The practical range of heads h_a for each type of flume as listed in Table 7.4 is recommended as a limit on h_a.

d) The submergence ratio h_b/h_a should not exceed 0.95.

7.5 H-flumes

7.5.1 Description

On natural streams where it is necessary to measure a wide range of discharges, a structure with a V-type control has the advantage of providing a wide opening at high flows so that it causes no excessive backwater effects, whereas at low flows its opening is reduced so that the sensitivity of the structure remains acceptable. To serve this purpose the U.S.Soil Conservation Service developed the H-type flume, of which three geometrically different types are available. Their proportions are shown in Figure 7.21. They are:

HS-flumes

Of this "small" flume, the largest size has a depth D equal to 0.305 m (1 ft) and a maximum capacity of 0.022 m^3/s.

H-flumes

Of this "normal" flume, the largest size has a depth D equal to 1.37 m (4.5 ft) and a maximum capacity of 2.36 m^3/s.

Photo 1. H-flume.

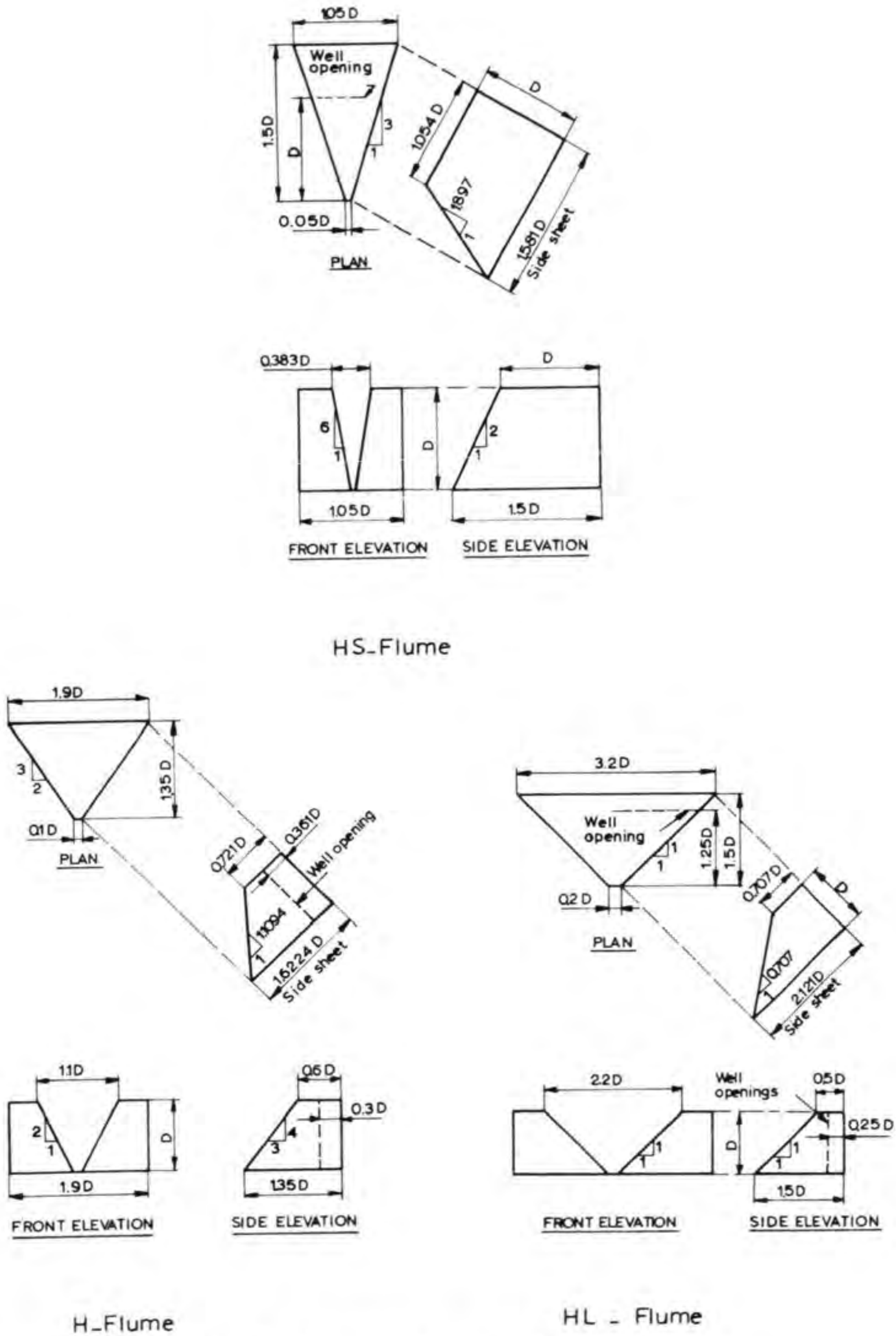

Fig.7.21. Dimensions of the types HS-, H- and HL-flume (after Holtan, Minshall & Harrold, 1961).

HL-flumes

The use of this "large" flume is only recommended if the anticipated discharge exceeds the capacity of the normal H-flume. The largest HL-flume has a depth D equal to 1.37 m (4.5 ft) and a maximum capacity of 3.32 m^3/s.

Since all three types are calibrated measuring devices, they should be constructed in strict accordance with the drawings in Figure 7.21. It is especially important that the slanting opening be bounded by straight sharp edges, that it has precisely the proportional dimensions shown, and that it lies in a plane with an inclination of the exact degree indicated in Figure 7.21. All cross sections of the flume should be symmetrical about the longitudinal axis. The flume floor should be truly level. All plates should be flat and should display no appreciable warp, dent, or other form of distortion.

All three types of flume should be located downstream of a rectangular approach channel which has the same bottom width as the entrance of the flume, i.e., 1.05D for the HS-flumes; 1.90D for the H-flumes; and 3.20D for the HL-flumes. The minimum length of this approach channel is 2D. In practice, the flume sections are frequently constructed from sheet steel or other suitable material, while the approach section is made of concrete, masonry, etc. The two parts should be given a watertight join with the use of bolts and a gasket. The bolts should be suitable for both fastening and levelling the flume. To prevent silting in the approach channel, its longitudinal slope may vary from flat to about 0.02.

The upstream head h_a is measured in the flume at a well defined location which is shown separately for each flume in Figure 7.21. The piezometric head should be measured in a separate well having a piezometer tap immediately above the flume bottom. Since the head is measured at a location of accelerating flow and where streamlines are curved it is essential that the piezometer tap be located in its precise position if accurate flow measurements are to be obtained.

To assure reliable head readings despite heavy sediment loads and the accompanying sediment deposition in the flume,an 1 to 8 sloping floor was provided for H-flumes. This false floor concentrates flows along the side wall having the stilling well intake. Low flows can scour the sediment from the little channel formed along this wall. The proportions of the sloping floor for the H-flume are given in Fig.7.22.

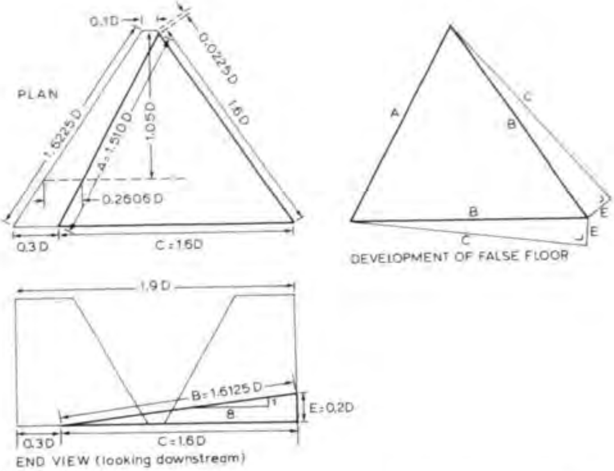

Fig.7.22. Sloping false floor for use in H-flumes (from GWINN & PARSON, 1976). Original drawing prepared by L.L.DeFabritis, 1938.

If the H-flume is equiped with a false floor, the true flow rate differs slightly from the figures given in Table 7.14. The percentage deviation in the free flow rate is shown in Fig.7.23.

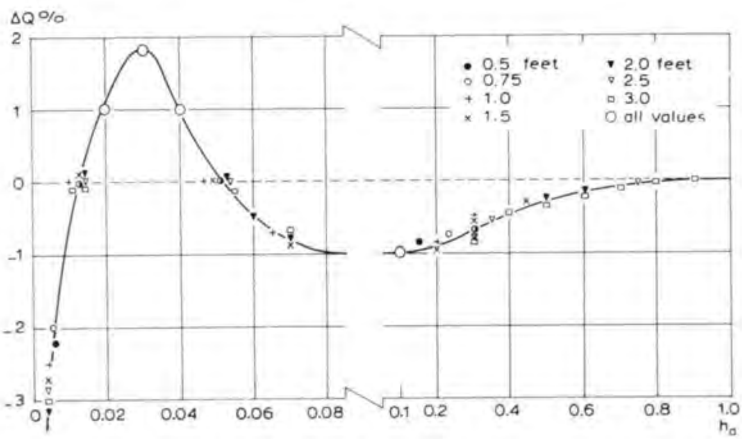

Fig.7.23. Deviation in free flow rate through H-flumes with a sloping floor from rating Tables 7.14 for H-flumes with a flat floor (after GWINN).

7.5.2 Evaluation of discharge

All three types of H-flumes have a rather arbitrary control while an upstream piezometric head h_a is measured at a station in the area of water surface drawdown. Under these circumstances, the only accurate method of finding a head-discharge relationship is by calibration in a hydraulic laboratory.

Based on this calibration, an empirical formula, expressing the discharge in m^3/s as a function of the head h_a in metres, could be established of the general form

$$\log Q = A + B \log h_a + C\left[\log h_a\right]^2 \tag{7-8}$$

Values of the numbers A, B, and C appear in Table 7.12 for each flume type. Based on Eq.7-8, calibration tables were prepared for each flume; see Tables 7.13 for the HS-flumes, Table 7.14 for the H-flumes and Table 7.15 for the HL-flumes.

TABLE 7.12. DATA ON THREE TYPE H-FLUMES

Flume type	Flume depth "D" ft	m	Maximum capacity $m^3/s \times 10^{-3}$	Number in Eq. 7-8 A	B	C	Calibration table
HS	0.4	.122	2.27	-0.4361	+2.5151	+0.1379	7.13.a
HS	0.6	.183	6.14	-0.4430	+2.4908	+0.1657	7.13.b
HS	0.8	.244	12.7	-0.4410	+2.4571	+0.1762	7.13.c
HS	1.0	.305	22.3	-0.4382	+2.4193	+0.1790	7.13.d
H	0.5	.152	9.17	+0.0372	+2.6629	+0.1954	7.14.a
H	0.75	.229	26.9	+0.0351	+2.6434	+0.2243	7.14.b
H	1.0	.305	53.5	+0.0206	+2.5902	+0.2281	7.14.c
H	1.5	.457	150	+0.0238	+2.5473	+0.2540	7.14.d
H	2.0	.610	309	+0.0237	+2.4918	+0.2605	7.14.e
H	2.5	.762	542	+0.0268	+2.4402	+0.2600	7.14.f
H	3.0	.914	857	+0.0329	+2.3977	+0.2588	7.14.g
H	4.5	1.37	2366	+0.0588	+2.3032	+0.2547	7.14.h
HL	3.5	1.07	2370	+0.3081	+2.3935	+0.2911	7.15.a
HL	4.0	1.22	3298	+0.3160	+2.3466	+0.2794	7.15.b

The error in the modular discharge given in Tables 7.13, 7.14 and 7.15 may be expected to be less than 3%. The method by which this error is to be combined with other sources of error is shown in Appendix II.

7.5.3 Modular limit

The modular limit is defined as the submergence ratio h_2/h_a which produces a 1% reduction from the equivalent modular discharge as calculated by Eq.7-8. Results of various tests showed that the modular limit for HS- and H-flumes is $h_2/h_a = 0.25$, for HL-flumes this limit is 0.30. Raising tailwater levels cause an increase of the equivalent upstream head h_a at modular flow as shown in Fig.7.24. Because of the complex method of calculating submerged flow, all HS- and H-flumes should be installed with a submergence ratio of less than 0.25 (for HL-flumes 0.30).

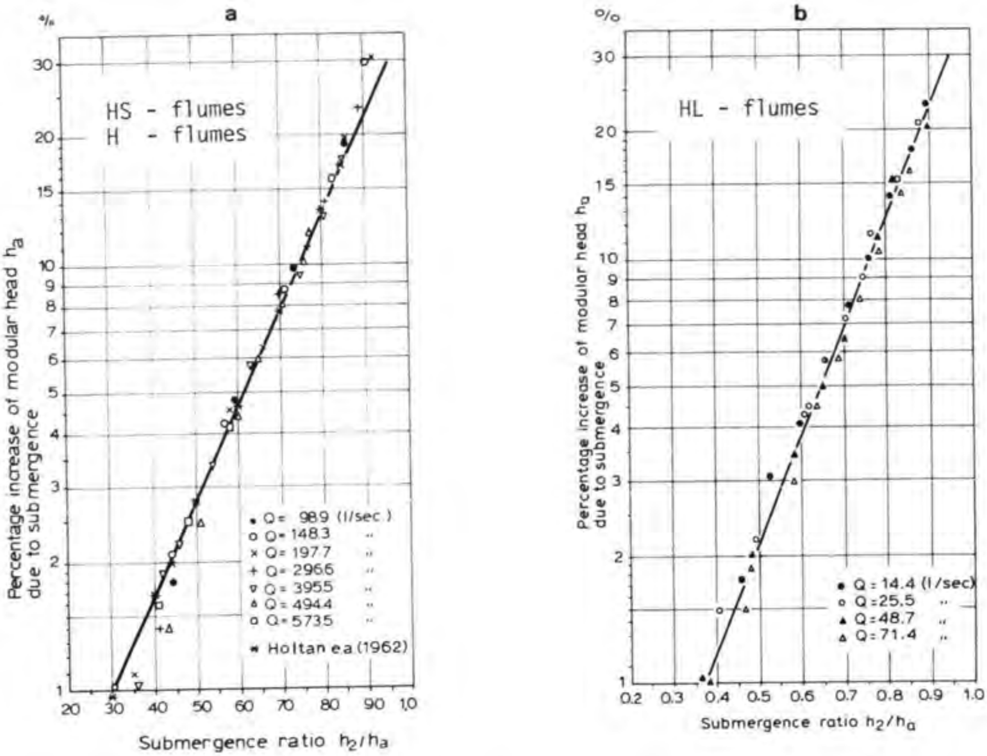

Fig.7.24a/b. Influence of submergence on the modular head of HS-, H-, and HL-flumes. (Data on HL-flumes based on personal communication, W.R.GWINN, 1977.)

7.5.4 Limits of application

The limits of application of all H-flumes are:

a) The inside surface of the flume should be plane and smooth while the flume dimensions should be in strict accordance with Figure 7.21.

b) The practical lower limit of h_a is mainly related to the accuracy with which h_a can be determined. For heads less than 0.06 m, point gauge readings are required to obtain a reasonably accurate measurement. The lower limit of h_a for each type of flume can be read from Tables 7.13 to 7.15.

c) To obtain modular flow the submergence ratio h_2/h_a should not exceed 0.25.

d) To prevent water surface instability in the approach channel, the Froude number $Fr = v_1/(gA_1/B)^{\frac{1}{2}}$ should not exceed 0.5.

TABLE 7.13. FREE-FLOW DISCHARGE THROUGH 0.4 ft HS-FLUME IN $m^3/s \times 10^{-3}$ (1/s)

h_a (m)	.000	.001	.002	.003	.004	.005	.006	.007	.008	.009
0.00										
0.01	0.012	0.015	0.017	0.020	0.024	0.027	0.031	0.035	0.039	0.044
0.02	0.049	0.054	0.059	0.065	0.071	0.077	0.084	0.091	0.098	0.105
0.03	0.113	0.121	0.130	0.138	0.147	0.156	0.166	0.176	0.186	0.197
0.04	0.208	0.219	0.230	0.242	0.255	0.267	0.280	0.293	0.307	0.321
0.05	0.335	0.350	0.365	0.380	0.396	0.412	0.428	0.445	0.462	0.480
0.06	0.497	0.516	0.534	0.553	0.573	0.592	0.612	0.633	0.654	0.675
0.07	0.697	0.719	0.741	0.764	0.787	0.811	0.835	0.860	0.884	0.910
0.08	0.935	0.961	0.988	1.01	1.04	1.07	1.10	1.13	1.16	1.19
0.09	1.21	1.25	1.28	1.31	1.34	1.37	1.40	1.44	1.47	1.50
0.10	1.54	1.57	1.61	1.64	1.68	1.71	1.75	1.79	1.83	1.87
0.11	1.90	1.94	1.98	2.02	2.06	2.10	2.15	2.19	2.23	2.27

FREE-FLOW DISCHARGE THROUGH 0.6 ft HS-FLUME IN 1/s

h_a (m)	.000	.001	.002	.003	.004	.005	.006	.007	.008	.009
0.00										
0.01										
0.02	0.064	0.070	0.076	0.083	0.091	0.098	0.106	0.114	0.123	0.131
0.03	0.141	0.150	0.160	0.170	0.181	0.191	0.202	0.214	0.226	0.238
0.04	0.251	0.263	0.277	0.290	0.304	0.318	0.333	0.348	0.363	0.379
0.05	0.395	0.412	0.429	0.446	0.463	0.481	0.500	0.518	0.537	0.557
0.06	0.577	0.597	0.618	0.639	0.660	0.682	0.704	0.727	0.750	0.773
0.07	0.797	0.821	0.846	0.871	0.896	0.922	0.948	0.975	1.00	1.03
0.08	1.06	1.09	1.11	1.14	1.17	1.20	1.23	1.26	1.30	1.33
0.09	1.36	1.39	1.43	1.46	1.49	1.53	1.56	1.60	1.63	1.67
0.10	1.71	1.74	1.78	1.82	1.86	1.90	1.93	1.97	2.01	2.06
0.11	2.10	2.14	2.18	2.22	2.27	2.31	2.35	2.40	2.44	2.49
0.12	2.53	2.58	2.63	2.68	2.72	2.77	2.82	2.87	2.92	2.97
0.13	3.02	3.07	3.12	3.18	3.23	3.28	3.34	3.39	3.45	3.50
0.14	3.56	3.61	3.67	3.73	3.78	3.84	3.90	3.96	4.02	4.08
0.15	4.14	4.20	4.27	4.33	4.39	4.46	4.52	4.58	4.65	4.72
0.16	4.78	4.85	4.92	4.98	5.05	5.12	5.19	5.26	5.33	5.40
0.17	5.47	5.55	5.62	5.69	5.77	5.84	5.92	5.99	6.07	6.14

TABLE 7.13. FREE-FLOW DISCHARGE THROUGH 0.8 ft HS-FLUME IN
(cont.) $m^3/s \times 10^{-3}$ (l/s)

h_a (m)	.000	.001	.002	.003	.004	.005	.006	.007	.008	.009
0.00										
0.01										
0.02										
0.03						0.227	0.239	0.252	0.266	0.280
0.04	0.294	0.308	0.324	0.339	0.355	0.371	0.388	0.404	0.422	0.440
0.05	0.458	0.476	0.495	0.514	0.534	0.554	0.574	0.595	0.617	0.638
0.06	0.660	0.683	0.706	0.729	0.753	0.777	0.802	0.827	0.852	0.878
0.07	0.904	0.931	0.958	0.986	1.01	1.04	1.07	1.10	1.13	1.16
0.08	1.19	1.22	1.25	1.29	1.32	1.35	1.38	1.42	1.45	1.49
0.09	1.52	1.56	1.59	1.63	1.67	1.70	1.74	1.78	1.82	1.86
0.10	1.90	1.94	1.98	2.02	2.06	2.10	2.15	2.19	2.23	2.28
0.11	2.32	2.37	2.41	2.46	2.50	2.55	2.60	2.65	2.69	2.74
0.12	2.79	2.84	2.89	2.94	2.99	3.05	3.10	3.15	3.20	3.26
0.13	3.31	3.37	3.42	3.48	3.54	3.59	3.65	3.71	3.77	3.83
0.14	3.89	3.95	4.01	4.07	4.13	4.19	4.25	4.32	4.38	4.45
0.15	4.51	4.58	4.64	4.71	4.77	4.84	4.91	4.98	5.05	5.12
0.16	5.19	5.26	5.33	5.40	5.48	5.55	5.62	5.70	5.77	5.85
0.17	5.92	6.00	6.08	6.15	6.23	6.31	6.39	6.47	6.55	6.63
0.18	6.71	6.79	6.88	6.96	7.04	7.13	7.21	7.30	7.39	7.47
0.19	7.56	7.65	7.74	7.82	7.91	8.00	8.10	8.19	8.28	8.37
0.20	8.47	8.56	8.65	8.75	8.84	8.94	9.04	9.14	9.23	9.33
0.21	9.43	9.53	9.63	9.73	9.83	9.94	10.0	10.1	10.2	10.4
0.22	10.5	10.6	10.7	10.8	10.9	11.0	11.1	11.2	11.3	11.4
0.23	11.5	11.7	11.8	11.9	12.0	12.1	12.2	12.3	12.5	12.6
0.24	12.7									

(Table 7.13 cont.)

FREE-FLOW DISCHARGE THROUGH 1.0 ft HS-FLUME IN l/s

h_a (m)	.000	.001	.002	.003	.004	.005	.006	.007	.008	.009
0.00										
0.01										
0.02										
0.03										
0.04	0.339	0.355	0.372	0.389	0.407	0.425	0.443	0.462	0.482	0.501
0.05	0.521	0.542	0.563	0.584	0.606	0.629	0.651	0.674	0.698	0.722
0.06	0.746	0.771	0.797	0.822	0.849	0.875	0.902	0.930	0.958	0.986
0.07	1.02	1.04	1.07	1.10	1.14	1.17	1.20	1.23	1.26	1.30
0.08	1.33	1.36	1.40	1.43	1.47	1.50	1.54	1.58	1.61	1.65
0.09	1.69	1.73	1.77	1.81	1.85	1.89	1.93	1.97	2.01	2.05
0.10	2.10	2.14	2.18	2.23	2.27	2.32	2.36	2.41	2.46	2.51
0.11	2.55	2.60	2.65	2.70	2.75	2.80	2.85	2.90	2.96	3.01
0.12	3.06	3.11	3.17	3.22	3.28	3.33	3.39	3.45	3.50	3.56
0.13	3.62	3.68	3.74	3.80	3.86	3.92	3.98	4.04	4.11	4.17
0.14	4.23	4.30	4.36	4.43	4.49	4.56	4.63	4.69	4.76	4.83
0.15	4.90	4.97	5.04	5.11	5.18	5.25	5.32	5.40	5.47	5.54
0.16	5.62	5.69	5.77	5.85	5.92	6.00	6.08	6.16	6.24	6.32
0.17	6.40	6.48	6.56	6.64	6.73	6.81	6.89	6.98	7.06	7.15
0.18	7.23	7.32	7.41	7.50	7.58	7.67	7.76	7.85	7.94	8.04
0.19	8.13	8.22	8.31	8.41	8.50	8.60	8.69	8.79	8.89	8.98
0.20	9.08	9.18	9.28	9.38	9.48	9.58	9.69	9.79	9.89	9.99
0.21	10.1	10.2	10.3	10.4	10.5	10.6	10.7	10.8	11.0	11.1
0.22	11.2	11.3	11.4	11.5	11.6	11.7	11.9	12.0	12.1	12.2
0.23	12.3	12.4	12.6	12.7	12.8	12.9	13.0	13.2	13.3	13.4
0.24	13.5	13.6	13.8	13.9	14.0	14.2	14.3	14.4	14.5	14.7
0.25	14.8	14.9	15.1	15.2	15.3	15.5	15.6	15.7	15.9	16.0
0.26	16.1	16.3	16.4	16.5	16.7	16.8	17.0	17.1	17.3	17.4
0.27	17.5	17.7	17.8	18.0	18.1	18.3	18.4	18.6	18.7	18.9
0.28	19.0	19.2	19.3	19.5	19.6	19.8	19.9	20.1	20.2	20.4
0.29	20.6	20.7	20.9	21.0	21.2	21.4	21.5	21.7	21.8	22.0
0.30	22.2	22.3								

TABLE 7.14. FREE-FLOW DISCHARGE THROUGH 0.5 ft H-FLUME IN $m^3/s \times 10^{-3}$ (l/s)

h_a (m)	0	2	4	6	8
0.00					
0.01	0.031	0.044	0.059	0.077	0.097
0.02	0.119	0.145	0.172	0.203	0.236
0.03	0.272	0.311	0.353	0.398	0.446
0.04	0.497	0.551	0.609	0.669	0.733
0.05	0.801	0.871	0.946	1.02	1.10
0.06	1.19	1.28	1.37	1.47	1.57
0.07	1.67	1.78	1.89	2.00	2.12
0.08	2.25	2.37	2.51	2.64	2.78
0.09	2.93	3.07	3.23	3.38	3.55
0.10	3.71	3.88	4.06	4.24	4.42
0.11	4.61	4.81	5.01	5.21	5.42
0.12	5.63	5.85	6.08	6.31	6.54
0.13	6.78	7.02	7.27	7.53	7.79
0.14	8.05	8.32	8.60	8.88	9.17

FREE-FLOW DISCHARGE THROUGH 0.75 ft H-FLUME in l/s

0.00					
0.01	0.044	0.061	0.080	0.103	0.128
0.02	0.155	0.186	0.220	0.256	0.296
0.03	0.339	0.384	0.433	0.486	0.541
0.04	0.600	0.662	0.728	0.797	0.869
0.05	0.945	1.03	1.11	1.20	1.29
0.06	1.38	1.48	1.58	1.69	1.80
0.07	1.91	2.03	2.15	2.28	2.41
0.08	2.54	2.68	2.83	2.97	3.13
0.09	3.28	3.44	3.61	3.78	3.95
0.10	4.13	4.31	4.50	4.70	4.89
0.11	5.10	5.30	5.52	5.73	5.96
0.12	6.18	6.42	6.65	6.90	7.14
0.13	7.40	7.65	7.92	8.19	8.46
0.14	8.74	9.03	9.32	9.61	9.91
0.15	10.2	10.5	10.9	11.2	11.5
0.16	11.8	12.2	12.5	12.9	13.2
0.17	13.6	14.0	14.4	14.7	15.1
0.18	15.5	15.9	16.3	16.7	17.2
0.19	17.6	18.0	18.5	18.9	19.4
0.20	19.8	20.3	20.8	21.2	21.7
0.21	22.2	22.7	23.2	23.7	24.2
0.22	24.8	25.3	25.8	26.4	26.9

TABLE 7.14. FREE-FLOW DISCHARGE THROUGH 1.0 ft H-FLUME IN
(cont.) $m^3/s \times 10^{-3}$ (l/s)

h_a (m)	0	2	4	6	8	h_a (m)	0	2	4	6	8
0.00						0.15	11.0	11.3	11.7	12.0	12.3
0.01				0.127	0.157	0.16	12.7	13.1	13.4	13.8	14.2
0.02	0.190	0.226	0.265	0.308	0.354	0.17	14.5	14.9	15.3	15.7	16.1
0.03	0.403	0.455	0.511	0.571	0.634	0.18	16.5	16.9	17.4	17.8	18.2
0.04	0.701	0.771	0.845	0.922	1.00	0.19	18.7	19.1	19.6	20.0	20.5
0.05	1.09	1.18	1.27	1.37	1.47	0.20	21.0	21.4	21.9	22.4	22.9
0.06	1.57	1.68	1.79	1.91	2.03	0.21	23.4	23.9	24.5	25.0	25.5
0.07	2.16	2.28	2.42	2.56	2.70	0.22	26.1	26.6	27.2	27.7	28.3
0.08	2.84	2.99	3.15	3.31	3.47	0.23	28.9	29.4	30.0	30.6	31.2
0.09	3.64	3.82	3.99	4.18	4.36	0.24	31.8	32.4	33.1	33.7	34.2
0.10	4.56	4.75	4.95	5.16	5.37	0.25	35.0	35.6	36.3	37.0	37.6
0.11	5.59	5.81	6.04	6.27	6.50	0.26	38.3	39.0	39.7	40.4	41.1
0.12	6.74	6.99	7.24	7.50	7.76	0.27	41.8	42.6	43.3	44.0	44.8
0.13	8.03	8.30	8.58	8.86	9.15	0.28	45.5	46.3	47.1	47.9	48.6
0.14	9.45	9.75	10.1	10.4	10.7	0.29	49.4	50.2	51.0	51.9	52.7
						0.30	53.5				

FREE-FLOW DISCHARGE THROUGH 1.5 ft H-FLUME in l/s

h_a (m)	0	2	4	6	8	h_a (m)	0	2	4	6	8
0.00						0.25	38.2	38.9	39.6	40.3	41.0
0.01						0.26	41.7	42.5	43.2	43.9	44.7
0.02	0.269	0.316	0.367	0.421	0.479	0.27	45.4	46.2	47.0	47.8	48.5
0.03	0.542	0.608	0.677	0.751	0.829	0.28	49.3	50.1	51.0	51.8	52.6
0.04	0.910	0.996	1.09	1.18	1.28	0.29	53.4	54.3	55.1	56.0	56.8
0.05	1.38	1.49	1.60	1.71	1.83	0.30	57.7	58.6	59.5	60.4	61.3
0.06	1.75	2.08	2.21	2.35	2.49	0.31	62.2	63.1	64.1	65.0	66.0
0.07	2.64	2.78	2.94	3.10	3.26	0.32	66.9	67.9	68.8	69.8	70.8
0.08	3.43	3.60	3.78	3.96	4.15	0.33	71.8	72.8	73.8	74.9	75.9
0.09	4.34	4.54	4.74	4.95	5.16	0.34	76.9	78.0	79.0	80.1	81.2
0.10	5.38	5.60	5.83	6.06	6.29	0.35	82.3	83.4	84.5	85.6	86.7
0.11	6.54	6.78	7.04	7.30	7.56	0.36	87.8	89.0	90.1	91.3	92.4
0.12	7.83	8.10	8.38	8.67	8.96	0.37	93.6	94.8	96.0	97.2	98.4
0.13	9.25	9.55	9.86	10.2	10.5	0.38	99.6	101	102	103	105
0.14	10.8	11.1	11.5	11.8	12.2	0.39	106	107	108	110	111
0.15	12.5	12.9	13.2	13.6	14.0	0.40	112	114	115	116	118
0.16	14.4	14.8	15.1	15.5	16.0	0.41	119	120	122	123	125
0.17	16.4	16.8	17.2	17.6	18.1	0.42	126	127	129	130	132
0.18	18.5	19.0	19.4	19.9	20.4	0.43	133	135	136	138	139
0.19	20.8	21.3	21.8	22.3	22.8	0.44	141	142	144	145	147
0.20	23.3	23.8	24.3	24.9	25.4	0.45	148	150			
0.21	25.9	26.5	27.0	27.6	28.2						
0.22	28.7	29.3	29.9	30.5	31.1						
0.23	31.7	32.3	33.0	33.6	34.2						
0.24	34.9	35.5	36.2	36.9	37.5						

TABLE 7.14. FREE-FLOW DISCHARGE THROUGH 2.0 ft H-FLUME IN
(cont.) $m^3/s \times 10^{-3}$ (l/s)

h_a (m)	0	2	4	6	8	h_a (m)	0	2	4	6	8
0.00						0.30	61.9	62.9	63.8	64.7	65.7
0.01						0.31	66.6	67.6	68.6	69.5	70.5
0.02			0.469	0.535	0.606	0.32	71.5	72.5	73.5	74.6	75.6
0.03	0.681	0.760	0.844	0.932	1.02	0.33	76.6	77.7	78.7	79.7	80.8
0.04	1.12	1.22	1.33	1.44	1.55	0.34	81.9	83.0	84.1	85.2	86.3
0.05	1.67	1.79	1.92	2.05	2.19	0.35	87.5	88.6	89.7	90.9	92.0
0.06	2.33	2.48	2.63	2.79	2.95	0.36	93.2	94.4	95.6	96.7	97.9
0.07	3.11	3.29	3.46	3.64	3.83	0.37	99.2	100	102	103	104
0.08	4.02	4.21	4.41	4.62	4.83	0.38	105	107	108	109	110
0.09	5.04	5.27	5.49	5.72	5.96	0.39	112	113	114	116	117
0.10	6.20	6.45	6.70	6.96	7.22	0.40	118	120	121	123	124
0.11	7.49	7.76	8.04	8.33	8.62	0.41	125	127	128	130	131
0.12	8.91	9.22	9.52	9.84	10.2	0.42	132	134	135	137	138
0.13	10.5	10.8	11.1	11.5	11.8	0.43	140	141	143	144	146
0.14	12.2	12.5	12.9	13.3	13.7	0.44	147	148	150	152	154
0.15	14.0	14.4	14.8	15.2	15.6	0.45	155	157	158	160	162
0.16	16.1	16.5	16.9	17.3	17.8	0.46	163	165	167	168	170
0.17	18.2	18.7	19.1	19.6	20.1	0.47	172	173	175	177	179
0.18	20.5	21.0	21.5	22.0	22.5	0.48	180	182	184	186	187
0.19	23.0	23.5	24.1	24.6	25.1	0.49	189	191	193	195	196
0.20	25.7	26.2	26.8	27.3	27.9	0.50	198	200	202	204	206
0.21	28.5	29.1	29.7	30.2	30.9	0.51	208	210	211	213	215
0.22	31.5	32.1	32.7	33.3	34.0	0.52	217	219	221	223	225
0.23	34.6	35.3	35.9	36.6	37.3	0.53	227	229	231	233	235
0.24	38.0	38.7	39.4	40.1	40.8	0.54	237	240	242	244	246
0.25	41.5	42.2	42.9	43.7	44.4	0.55	248	250	252	254	256
0.26	45.2	46.0	46.7	47.5	48.3	0.56	259	261	263	265	267
0.27	49.1	50.0	50.7	51.5	52.3	0.57	270	272	274	276	279
0.28	53.2	54.0	54.9	55.7	56.6	0.58	281	283	286	288	290
0.29	57.5	58.3	59.2	60.1	61.0	0.59	293	295	297	300	302
						0.60	305	307	309		

TABLE 7.14. FREE-FLOW DISCHARGE THROUGH 2.5 ft H-FLUME IN $m^3/s \times 10^{-3}$ (l/s)
(cont.)

h_a (m)	0	2	4	6	8
0.00					
0.01					
0.02				0.649	0.732
0.03	0.820	0.912	1.01	1.11	1.22
0.04	1.33	1.45	1.57	1.69	1.82
0.05	1.96	2.10	2.25	2.40	2.55
0.06	2.71	2.88	3.05	3.23	3.41
0.07	3.59	3.78	3.98	4.18	4.39
0.08	4.60	4.82	5.04	5.27	5.51
0.09	5.75	5.99	6.24	6.50	6.76
0.10	7.02	7.30	7.58	7.86	8.15
0.11	8.44	8.75	9.05	9.36	9.68
0.12	10.0	10.3	10.7	11.0	11.4
0.13	11.7	12.1	12.4	12.8	13.2
0.14	13.6	14.0	14.4	14.8	15.2
0.15	15.6	16.0	16.4	16.9	17.3
0.16	17.6	18.2	18.7	19.1	19.6
0.17	20.1	20.6	21.1	21.6	22.1
0.18	22.6	23.1	23.6	24.2	24.7
0.19	25.2	25.8	26.4	26.9	27.5
0.20	28.1	28.7	29.2	29.8	30.5
0.21	31.1	31.7	32.3	33.0	33.6
0.22	34.2	34.9	35.6	36.2	36.9
0.23	37.6	38.4	39.0	39.7	40.4
0.24	41.1	41.9	42.6	43.4	44.1

h_a (m)	0	2	4	6	8
0.25	44.9	45.6	46.4	47.2	48.0
0.26	48.8	49.6	50.4	51.2	52.0
0.27	52.9	53.7	54.6	55.4	56.3
0.28	57.2	58.1	59.0	59.9	60.8
0.29	61.7	62.7	63.5	64.5	65.4
0.30	66.4	67.3	68.3	69.3	70.3
0.31	71.3	72.3	73.3	74.3	75.3
0.32	76.4	77.4	78.5	79.5	80.6
0.33	81.7	82.8	83.9	85.0	86.1
0.34	87.2	88.3	89.5	90.6	91.8
0.35	93.0	94.1	95.3	96.5	97.7
0.36	98.9	100	101	102	104
0.37	105	106	108	109	110
0.38	112	113	114	115	117
0.39	118	119	121	122	124
0.40	125	126	128	129	131
0.41	132	134	135	136	138
0.42	139	141	142	144	145
0.43	147	149	150	152	153
0.44	155	156	158	160	161
0.45	163	165	166	168	169
0.46	171	173	175	176	178
0.47	180	181	183	185	187
0.48	189	190	192	194	196
0.49	198	199	201	203	205

h_a (m)	0	2	4	6	8
0.50	207	209	211	213	215
0.51	216	218	220	222	224
0.52	226	228	230	232	234
0.53	236	239	241	243	245
0.54	247	249	251	253	255
0.55	257	260	262	264	266
0.56	268	271	273	275	277
0.57	280	282	284	286	289
0.58	291	293	296	298	301
0.59	303	305	308	310	313
0.60	315	317	320	322	325
0.61	327	330	332	335	337
0.62	340	343	345	348	350
0.63	353	355	358	361	363
0.64	366	369	371	374	377
0.65	380	382	385	388	391
0.66	393	396	399	402	405
0.67	408	410	413	416	419
0.68	422	425	428	431	434
0.69	437	440	443	446	449
0.70	452	455	458	461	464
0.71	467	470	474	477	480
0.72	483	486	489	493	496
0.73	499	502	506	509	512
0.74	515	519	522	525	529
0.75	532	535	539	542	

TABLE 7.14. FREE-FLOW DISCHARGE THROUGH 3.0 ft H-FLUME IN
(cont.) $m^3/s \times 10^{-3}$ (l/s)

h_a (m)	0	2	4	6	8
0.00					
0.01					
0.02				0.763	0.858
0.03	0.959	1.06	1.18	1.29	1.41
0.04	1.54	1.67	1.81	1.95	2.09
0.05	2.25	2.40	2.57	2.74	2.91
0.06	3.09	3.27	3.46	3.66	3.86
0.07	4.06	4.28	4.49	4.72	4.95
0.08	5.18	5.42	5.66	5.92	6.17
0.09	6.43	6.70	6.98	7.26	7.54
0.10	7.83	8.13	8.44	8.75	9.06
0.11	9.38	9.71	10.0	10.4	10.7
0.12	11.1	11.4	11.8	12.2	12.5
0.13	12.9	13.3	13.7	14.1	14.5
0.14	14.9	15.4	15.8	16.2	16.7
0.15	17.1	17.6	18.0	18.5	19.0
0.16	19.4	19.9	20.4	20.9	21.4
0.17	21.9	22.4	23.0	23.5	24.0
0.18	24.6	25.1	25.7	26.3	26.8
0.19	27.4	28.0	28.6	29.2	29.8
0.20	30.4	31.1	31.7	32.3	33.0
0.21	33.6	34.3	35.0	35.6	36.3
0.22	37.0	37.7	38.4	39.1	39.8
0.23	40.5	41.3	42.0	42.8	43.5
0.24	44.3	45.1	45.8	46.6	47.4
0.25	48.2	49.0	49.8	50.7	51.5
0.26	52.3	53.2	54.0	54.9	55.8
0.27	56.6	57.5	58.4	59.3	60.2
0.28	61.2	62.1	63.0	64.0	64.9
0.29	65.9	66.8	67.8	68.8	69.8

h_a (m)	0	2	4	6	8
0.30	70.8	71.8	72.8	73.8	74.9
0.31	75.9	77.8	78.0	79.1	80.2
0.32	81.2	82.3	83.4	84.5	85.7
0.33	86.8	87.9	89.1	90.2	91.4
0.34	92.5	93.7	94.9	96.1	97.3
0.35	98.5	99.7	101	102	103
0.36	105	106	107	109	110
0.37	111	112	114	115	116
0.38	118	119	120	122	123
0.39	125	126	127	129	130
0.40	132	133	135	136	138
0.41	139	141	142	144	145
0.42	147	148	150	151	153
0.43	154	156	158	159	161
0.44	163	164	166	167	169
0.45	171	173	174	176	178
0.46	179	181	183	185	186
0.47	188	190	192	194	195
0.48	197	199	201	203	205
0.49	207	208	210	212	214
0.50	216	218	220	222	224
0.51	226	228	230	232	234
0.52	236	238	240	242	244
0.53	246	248	251	253	255
0.54	257	259	261	263	266
0.55	268	270	272	274	277
0.56	279	281	283	286	288
0.57	290	293	295	297	300
0.58	302	304	307	309	312
0.59	314	317	319	321	324

h_a (m)	0	2	4	6	8
0.60	326	329	331	334	336
0.61	339	341	344	347	349
0.62	352	354	357	360	362
0.63	365	368	370	373	376
0.64	378	381	384	387	389
0.65	392	395	398	400	403
0.66	406	409	412	415	418
0.67	420	423	426	429	432
0.68	435	438	441	444	447
0.69	450	453	456	459	462
0.70	465	468	471	475	478
0.71	481	484	487	490	494
0.72	497	500	503	506	510
0.73	513	516	519	523	526
0.74	529	533	536	539	543
0.75	546	550	553	556	560
0.76	563	567	570	574	577
0.77	581	584	588	592	595
0.78	599	602	606	610	613
0.79	617	620	624	628	632
0.80	635	639	643	647	650
0.81	654	658	662	666	669
0.82	673	677	681	685	689
0.83	693	697	701	705	709
0.84	713	717	721	725	729
0.85	733	737	741	745	749
0.86	753	757	762	766	770
0.87	774	778	783	787	791
0.88	795	800	804	808	813
0.89	817	821	826	830	835
0.90	839	843	848	852	857

TABLE 7.14. FREE-FLOW DISCHARGE THROUGH 4.5 ft H-FLUME IN
(cont.) $m^3/s \times 10^{-3}$ (l/s)

h_a (m)	0	2	4	6	8	h_a (m)	0	2	4	6	8	h_a (m)	0	2	4	6	8
0.00						0.25	58.1	59.1	60.0	61.0	61.9	0.50	245	247	249	251	253
0.01						0.26	62.9	63.9	64.8	65.8	66.8	0.51	255	257	260	262	264
0.02						0.27	67.8	68.9	69.9	70.9	72.0	0.52	266	268	271	273	275
0.03	1.39	1.53	1.68	1.84	2.00	0.28	73.0	74.1	75.1	76.2	77.3	0.53	277	280	282	284	287
0.04	2.17	2.35	2.53	2.72	2.91	0.29	78.4	79.5	80.6	81.7	82.8	0.54	289	291	294	296	298
0.05	3.12	3.32	3.53	3.76	3.98	0.30	84.0	85.1	86.3	87.4	88.6	0.55	301	303	305	308	310
0.06	4.22	4.46	4.70	4.95	5.21	0.31	89.8	91.0	92.2	93.4	94.6	0.56	313	315	317	320	322
0.07	5.48	5.75	6.02	6.31	6.60	0.32	95.8	97.0	98.3	99.5	101	0.57	325	327	330	332	335
0.08	6.90	7.20	7.52	7.83	8.16	0.33	102	103	105	106	107	0.58	337	340	343	345	348
0.09	8.49	8.82	9.17	9.52	9.88	0.34	109	110	111	113	114	0.59	350	353	355	358	361
0.10	10.2	10.6	11.0	11.4	11.8	0.35	115	117	118	119	121	0.60	363	366	369	371	375
0.11	12.2	12.6	13.0	13.4	13.8	0.36	122	124	125	126	128	0.61	377	380	382	385	388
0.12	14.3	14.7	15.1	15.6	16.1	0.37	129	131	132	134	135	0.62	390	393	396	399	402
0.13	16.5	17.0	17.5	18.0	18.5	0.38	137	138	140	141	143	0.63	405	407	410	413	416
0.14	19.0	19.5	20.0	20.5	21.0	0.39	144	146	148	149	151	0.64	419	422	425	427	430
0.15	21.6	22.1	22.7	23.2	23.8	0.40	152	154	155	157	159	0.65	433	436	439	442	445
0.16	24.4	25.0	25.6	26.2	26.8	0.41	160	162	164	165	167	0.66	448	451	454	457	460
0.17	27.4	28.0	28.6	29.2	30.0	0.42	169	170	172	174	176	0.67	463	466	470	473	476
0.18	30.5	31.2	31.9	32.5	33.2	0.43	177	179	181	183	184	0.68	479	482	485	488	491
0.19	33.9	34.6	35.3	36.0	36.7	0.44	186	188	190	192	193	0.69	495	498	501	504	507
0.20	37.4	38.2	38.9	39.7	40.4	0.45	195	197	199	201	203	0.70	511	514	517	520	524
0.21	41.2	42.0	42.7	43.5	44.3	0.46	205	207	208	210	212	0.71	527	530	534	537	540
0.22	45.1	45.9	46.8	47.6	48.4	0.47	214	216	218	220	222	0.72	544	547	551	554	557
0.23	49.3	50.1	51.0	51.8	52.7	0.48	224	226	228	230	232	0.73	561	564	568	571	575
0.24	53.6	54.5	55.4	56.3	57.2	0.49	234	236	238	240	243	0.74	578	582	585	589	592

TABLE 7.14. FREE-FLOW DISCHARGE THROUGH 4.5 ft H-FLUME IN $m^3/s \times 10^{-3}$ (l/s)
(cont.)

h_a (m)	0	2	4	6	8	h_a (m)	0	2	4	6	8	h_a (m)	0	2	4	6	8
0.75	596	599	603	606	610	1.00	1145	1150	1156	1161	1166	1.25	1925	1932	1939	1947	1954
0.76	614	617	621	625	628	1.01	1172	1177	1182	1188	1193	1.26	1961	1969	1976	1983	1991
0.77	632	636	639	643	647	1.02	1198	1204	1209	1215	1220	1.27	1998	2006	2013	2020	2028
0.78	650	654	658	662	666	1.03	1226	1231	1237	1242	1248	1.28	2035	2043	2050	2058	2066
0.79	669	673	677	681	685	1.04	1253	1259	1265	1270	1276	1.29	2073	2081	2088	2096	2104
0.80	689	693	696	700	704	1.05	1281	1287	1292	1299	1304	1.30	2111	2119	2127	2134	2142
0.81	708	712	716	720	724	1.06	1310	1316	1321	1327	1333	1.31	2150	2158	2165	2173	2181
0.82	728	732	736	740	744	1.07	1339	1345	1350	1356	1362	1.32	2189	2197	2205	2212	2220
0.83	748	752	757	761	765	1.08	1368	1374	1380	1386	1392	1.33	2228	2236	2244	2252	2260
0.84	769	773	777	781	786	1.09	1398	1403	1409	1415	1421	1.34	2268	2276	2284	2292	2300
0.85	790	794	798	802	807	1.10	1427	1434	1440	1446	1452	1.35	2308	2317	2325	2333	2341
0.86	811	815	820	824	828	1.11	1458	1464	1470	1476	1482	1.36	2349	2357	2366		
0.87	833	837	841	846	850	1.12	1489	1495	1501	1507	1513						
0.88	855	859	863	868	872	1.13	1520	1526	1532	1539	1545						
0.89	877	881	886	890	894	1.14	1551	1558	1564	1570	1577						
0.90	899	904	909	913	918	1.15	1583	1590	1596	1603	1609						
0.91	922	927	932	936	941	1.16	1616	1622	1629	1635	1642						
0.92	946	950	955	960	965	1.17	1648	1655	1661	1668	1675						
0.93	969	974	979	984	988	1.18	1681	1688	1695	1701	1708						
0.94	993	998	1003	1008	1013	1.19	1715	1722	1728	1735	1742						
0.95	1018	1023	1028	1032	1037	1.20	1749	1756	1763	1769	1776						
0.96	1042	1047	1052	1057	1062	1.21	1783	1790	1797	1804	1811						
0.97	1068	1073	1078	1083	1088	1.22	1818	1825	1832	1839	1846						
0.98	1093	1098	1103	1108	1114	1.23	1853	1860	1867	1875	1882						
0.99	1119	1124	1129	1134	1140	1.24	1889	1896	1903	1910	1918						

TABLE 7.15. FREE-FLOW DISCHARGE THROUGH 3.5 ft HL-FLUME IN l/s ($m^3/s \times 10^{-3}$)

h_a (m)	0	2	4	6	8
0.05	4.86	5.19	5.52	5.86	6.22
0.06	6.58	6.95	7.34	7.73	8.14
0.07	8.55	8.98	9.41	9.86	10.32
0.08	10.79	11.27	11.75	12.25	12.77
0.09	13.29	13.82	14.36	14.92	15.48
0.10	16.06	16.65	17.24	17.85	18.47
0.11	19.11	19.75	20.40	21.07	21.75
0.12	22.44	23.14	23.85	24.57	25.31
0.13	26.05	26.81	27.58	28.36	29.16
0.14	29.96	30.78	31.61	32.45	33.31
0.15	34.17	35.05	35.94	36.84	37.76
0.16	38.69	39.63	40.58	41.54	42.52
0.17	43.51	44.51	45.53	46.55	47.59
0.18	48.65	49.71	50.79	51.88	52.99
0.19	54.10	55.23	56.38	57.53	58.70
0.20	59.89	61.08	62.29	63.52	64.75
0.21	66.00	67.27	68.54	69.83	71.14
0.22	72.45	73.79	75.13	76.49	77.86
0.23	79.25	80.65	82.06	83.49	84.93
0.24	86.39	87.86	89.34	90.84	92.36
0.25	93.88	95.42	96.98	98.55	100.14
0.26	101.73	103.35	104.98	106.62	108.28
0.27	109.95	111.64	113.34	115.06	116.79
0.28	118.53	120.30	122.07	123.86	125.67
0.29	127.49	129.33	131.18	133.05	134.93
0.30	136.83	138.74	140.67	142.61	144.57
0.31	146.55	148.54	150.55	152.57	154.61
0.32	156.66	158.73	160.82	162.92	165.03
0.33	167.17	169.32	171.48	173.66	175.86
0.34	178.07	180.30	182.55	184.81	187.09
0.35	189.38	191.69	194.02	196.36	198.73
0.36	201.10	203.50	205.91	208.33	210.78
0.37	213.24	215.72	218.21	220.72	223.25
0.38	225.80	228.36	230.94	233.53	236.15
0.39	238.78	241.43	244.09	246.77	249.47
0.40	252.19	254.92	257.68	260.45	263.23
0.41	266.04	268.86	271.70	274.56	277.43
0.42	280.33	283.24	286.17	289.12	292.08
0.43	295.06	298.06	301.08	304.12	307.18
0.44	310.25	313.34	316.45	319.58	322.73
0.45	325.89	329.07	332.28	335.50	338.74
0.46	341.99	345.27	348.57	351.88	355.21
0.47	358.56	361.93	365.32	368.73	372.16
0.48	375.60	379.07	382.35	386.05	389.58
0.49	393.12	396.68	400.26	403.86	407.48
0.50	411.12	414.77	418.45	422.15	425.86
0.51	429.60	433.35	437.13	440.92	444.74
0.52	448.57	452.43	456.30	460.19	464.11
0.53	468.04	472.00	475.97	479.96	483.98
0.54	488.01	492.07	496.14	500.24	504.35
0.55	508.49	512.65	516.82	521.02	525.24
0.56	529.48	533.74	538.02	542.32	546.64
0.57	550.98	555.34	559.73	564.13	568.56
0.58	573.00	577.47	581.96	586.47	591.00
0.59	595.55	600.13	604.72	609.34	613.97

(TABLE 7.15 cont.) FREE-FLOW DISCHARGE THROUGH 3.5 ft HL-FLUME IN 1/s $(m^3/s \times 10^{-3})$

h_a (m)	0	2	4	6	8
0.60	618.63	623.31	628.01	632.74	637.48
0.61	642.25	647.03	651.84	656.67	661.53
0.62	666.40	671.30	676.22	681.16	686.12
0.63	691.10	696.11	701.14	706.19	711.26
0.64	716.35	721.47	726.61	731.77	736.95
0.65	742.16	747.39	752.64	757.91	763.21
0.66	768.52	773.87	779.23	784.61	790.02
0.67	795.46	800.91	806.39	811.89	817.41
0.68	822.96	828.52	834.12	839.73	845.37
0.69	851.03	856.71	862.42	868.15	873.91
0.70	879.68	885.49	891.31	897.16	903.03
0.71	908.92	914.84	920.78	926.75	932.74
0.72	938.75	944.79	950.85	956.93	963.04
0.73	969.17	975.33	981.51	987.71	993.94
0.74	1000.19	1006.47	1012.77	1019.10	1025.44
0.75	1031.82	1038.22	1044.64	1051.08	1057.56
0.76	1064.05	1070.57	1077.12	1083.69	1090.28
0.77	1096.90	1103.54	1110.21	1116.90	1123.62
0.78	1130.36	1137.13	1143.92	1150.74	1157.58
0.79	1164.45	1171.34	1178.26	1185.20	1192.17
0.80	1199.17	1206.19	1213.23	1220.30	1227.40
0.81	1234.52	1241.66	1248.83	1256.03	1263.25
0.82	1270.50	1277.78	1285.08	1292.40	1299.75
0.83	1307.13	1314.54	1321.97	1329.42	1336.90
0.84	1344.41	1351.94	1359.50	1367.09	1374.70
0.85	1382.34	1390.00	1397.69	1405.41	1413.15
0.86	1420.92	1428.72	1436.54	1444.39	1452.27
0.87	1460.17	1468.10	1476.06	1484.04	1492.05
0.88	1500.09	1508.15	1516.24	1524.36	1532.50
0.89	1540.67	1548.87	1557.10	1565.35	1573.63
0.90	1581.94	1590.27	1598.63	1607.02	1615.44
0.91	1623.88	1632.35	1640.85	1649.38	1657.93
0.92	1666.51	1675.12	1683.75	1692.42	1701.11
0.93	1709.83	1718.58	1727.35	1736.16	1744.99
0.94	1753.85	1762.73	1771.65	1780.59	1789.56
0.95	1798.56	1807.59	1816.65	1825.73	1834.85
0.96	1843.99	1853.16	1862.35	1871.58	1880.84
0.97	1890.12	1899.43	1908.77	1918.14	1927.54
0.98	1936.97	1946.42	1955.91	1965.42	1974.96
0.99	1984.53	1994.13	2003.76	2013.42	2023.11
1.00	2032.82	2042.57	2052.35	2062.15	2071.98
1.01	2081.85	2091.74	2101.66	2111.61	2121.59
1.02	2131.60	2141.64	2151.71	2161.81	2171.94
1.03	2182.10	2192.28	2202.50	2212.75	2223.03
1.04	2233.33	2243.67	2254.04	2264.44	2274.86
1.05	2285.32	2295.81	2306.33	2316.87	2327.45
1.06	2338.06	2348.70	2359.37	2370.07	

(TABLE 7.15 cont.) FREE-FLOW DISCHARGE THROUGH 4 ft HL-FLUME IN 1/s ($m^3/s \times 10^{-3}$)

h_a (m)	0	2	4	6	8
0.05	5.38	5.73	6.10	6.48	6.86
0.06	7.26	7.67	8.09	8.52	8.96
0.07	9.41	9.88	10.35	10.84	11.34
0.08	11.84	12.36	12.90	13.44	13.99
0.09	14.56	15.13	15.72	16.32	16.93
0.10	17.55	18.19	18.84	19.49	20.16
0.11	20.84	21.54	22.24	22.96	23.69
0.12	24.43	25.18	25.95	26.73	27.51
0.13	28.32	29.13	29.96	30.79	31.65
0.14	32.51	33.38	34.27	35.17	36.09
0.15	37.01	37.95	38.90	39.86	40.84
0.16	41.83	42.83	43.85	44.88	45.92
0.17	46.97	48.04	49.12	50.21	51.32
0.18	52.44	53.57	54.72	55.88	57.05
0.19	58.24	59.44	60.65	61.88	63.12
0.20	64.37	65.64	66.92	68.21	69.52
0.21	70.85	72.18	73.53	74.90	76.27
0.22	77.67	79.07	80.49	81.93	83.38
0.23	84.84	86.32	87.81	89.31	90.83
0.24	92.37	93.92	95.48	97.06	98.65
0.25	100.26	101.88	103.52	105.17	106.83
0.26	108.51	110.21	111.92	113.64	115.38
0.27	117.14	118.91	120.69	122.50	124.31
0.28	126.14	127.99	129.85	131.73	133.62
0.29	135.52	137.45	139.38	141.34	143.31
0.30	145.29	147.29	149.31	151.34	153.39
0.31	155.45	157.53	159.62	161.73	163.86
0.32	166.00	168.16	170.34	172.53	174.73
0.33	176.96	179.20	181.45	183.72	186.01
0.34	188.31	190.63	192.97	195.32	197.69
0.35	200.08	202.48	204.90	207.34	209.79
0.36	212.26	214.75	217.25	219.77	222.31
0.37	224.86	227.43	230.02	232.62	235.24
0.38	237.88	240.54	243.21	245.90	248.61
0.39	251.33	254.08	256.84	259.61	262.41
0.40	265.22	268.05	270.89	273.76	276.64
0.41	279.54	282.46	285.39	288.34	291.32
0.42	294.30	297.31	300.33	303.38	306.44
0.43	309.51	312.61	315.72	318.86	322.01
0.44	325.18	328.36	331.57	334.79	338.03
0.45	341.29	344.57	347.87	351.18	354.52
0.46	357.87	361.24	364.63	368.04	371.47
0.47	374.92	379.39	381.86	385.37	388.89
0.48	392.43	395.99	399.57	403.16	406.78
0.49	410.42	414.07	417.75	421.44	425.15
0.50	428.88	432.63	436.41	440.20	444.00
0.51	447.83	451.68	455.55	459.44	463.35
0.52	467.27	471.22	475.19	479.17	483.18
0.53	487.20	491.25	495.31	499.40	503.51
0.54	507.63	511.78	515.94	520.13	524.33
0.55	528.56	532.81	537.07	541.36	545.67
0.56	550.00	554.34	558.71	563.10	567.51
0.57	571.94	576.39	580.87	585.36	589.87
0.58	594.40	598.96	603.53	608.13	612.75
0.59	617.39	622.04	626.72	631.43	636.15

(TABLE 7.15 cont.) FREE-FLOW DISCHARGE THROUGH 4 ft HL-FLUME IN l/s ($m^3/s \times 10^{-3}$)

h_a (m)	0	2	4	6	8
0.60	640.89	645.66	650.44	655.25	660.08
0.61	664.92	669.80	674.69	679.60	684.54
0.62	689.49	694.47	699.47	704.49	709.53
0.63	714.60	719.68	724.79	729.92	735.07
0.64	740.24	745.44	750.65	755.89	761.15
0.65	766.44	771.74	777.07	782.41	787.79
0.66	793.18	798.59	804.03	809.49	814.97
0.67	820.48	826.00	831.55	837.13	842.72
0.68	848.34	853.98	859.64	865.32	871.03
0.69	876.76	882.51	888.29	894.09	899.91
0.70	905.75	911.62	917.51	923.42	929.36
0.71	935.31	941.30	947.30	953.33	959.38
0.72	965.46	971.55	977.67	983.82	989.99
0.73	996.18	1002.39	1008.63	1014.89	1021.18
0.74	1027.49	1033.82	1040.18	1046.56	1052.96
0.75	1059.39	1065.84	1072.31	1078.81	1085.34
0.76	1091.88	1098.45	1105.05	1111.67	1118.31
0.77	1124.98	1131.67	1138.38	1145.12	1151.89
0.78	1158.68	1165.49	1172.32	1179.19	1186.07
0.79	1192.98	1199.92	1206.88	1213.86	1220.87
0.80	1227.90	1234.96	1242.04	1249.15	1256.28
0.81	1263.44	1270.62	1277.82	1285.05	1292.31
0.82	1299.59	1306.90	1314.23	1321.59	1328.97
0.83	1336.37	1343.81	1351.26	1358.74	1366.25
0.84	1373.79	1381.34	1388.93	1396.54	1404.17
0.85	1411.83	1419.52	1427.23	1434.96	1442.73
0.86	1450.52	1458.33	1466.17	1474.04	1481.93
0.87	1489.84	1497.79	1505.76	1513.75	1521.77
0.88	1529.82	1537.89	1545.99	1554.12	1562.27
0.89	1570.44	1578.65	1586.88	1595.13	1603.42
0.90	1611.73	1620.06	1628.42	1636.81	1645.23
0.91	1653.67	1662.14	1670.63	1679.15	1687.70
0.92	1696.28	1704.88	1713.51	1722.16	1730.84
0.93	1739.55	1748.29	1757.05	1765.84	1774.66
0.94	1783.50	1792.37	1801.27	1810.20	1819.15
0.95	1828.13	1837.14	1846.17	1855.23	1864.32
0.96	1873.44	1882.58	1891.75	1900.95	1910.18
0.97	1919.43	1928.71	1938.02	1947.36	1956.73
0.98	1966.12	1975.54	1984.99	1994.46	2003.97
0.99	2013.50	2023.06	2032.65	2042.26	2051.91
1.00	2061.58	2071.28	2081.01	2090.76	2100.55
1.01	2110.36	2120.20	2130.07	2139.97	2149.90
1.02	2159.85	2169.84	2179.85	2189.89	2199.96
1.03	2210.06	2220.18	2230.34	2240.52	2250.73
1.04	2260.97	2271.24	2281.54	2291.87	2302.23
1.05	2312.61	2323.03	2333.47	2343.95	2354.45
1.06	2364.98	2375.54	2386.13	2396.75	2407.40
1.07	2418.07	2428.78	2439.52	2450.28	2461.08
1.08	2471.90	2482.76	2493.64	2504.55	2515.49
1.09	2526.47	2537.47	2548.50	2559.56	2570.65
1.10	2581.77	2592.93	2604.11	2615.32	2626.56
1.11	2637.83	2649.13	2660.46	2671.82	2683.21
1.12	2694.63	2706.09	2717.57	2729.08	2740.62
1.13	2752.19	2763.80	2775.43	2787.09	2798.79
1.14	2810.51	2822.27	2834.05	2845.87	2857.72
1.15	2869.60	2881.50	2893.44	2905.41	2917.41
1.16	2929.45	2941.51	2953.60	2965.73	2977.88
1.17	2990.07	3002.29	3014.54	3026.81	3039.13
1.18	3051.47	3063.84	3076.25	3088.68	3101.15
1.19	3113.65	3126.18	3138.74	3151.33	3163.96
1.20	3176.61	3189.30	3202.02	3214.77	3227.55
1.21	3240.37	3253.21	3266.09	3279.00	3291.94

7.6 Selected list of references

1. ACKERS, P., and HARRISON, A.J.M.: Critical-depth flumes for flow measurement in open channels. Dept.of Sci.& Industrial Research. Hydraulic Res.Sta., Hydr. Research Paper No.5. London. 1963.

2. BALLOFFET, A.: Critical flow meters (Venturi flumes). Proc.ASCE.81 (1951), Paper 743.

3. BENNET, R.S.: Cutthroat flume discharge relations. Thesis presented to Colorado State University, Fort Collins, Col., in partial fulfillment of requirements for the degree of Master of Science. 1972.

4. BOS, M.G.: The use of long-throated flumes to measure flows in irrigation and drainage canals. Agric.Water Management, 1(1977), pp.111-126. Elsevier Scientific Publishing Comp., Amsterdam.

5. BLAU, E.: Die modelmässige Untersuchung von Venturikanälen verschiedener Grösse und Form. Veröffentlichungen der Forschungsanstalt für Schiffahrt, Wasser- und Grundbau 8. Akademie-Verlag, Berlin. 1960.

6. BRITISH STANDARDS INSTITUTION: Methods of measurement of liquid flow in open channels. BS3680. Part 4. Weirs and flumes. 4A: Thin plate weirs and venturi flumes. 1965.

7. CAPLAN, F.: Nomograph for Free Flow Discharge through a Parshall Flume. Water & Sewage Works. May 1963.

8. EGGLESTON, K.O.: Effects of boundary geometry on critical and subcritical flow through measuring flumes. Utah Water Research Laboratory. College of Engineering, Utah State University. Logan, Utah. 1967.

9. ENGEL, F.V.A.E.: The venturi flume. The Engineer. 158 (1934). Aug.3, pp.104-107. Aug.10, pp.131-133. London.

10. FANE, A.C.: Report on flume experiments on Sirhind Canal. Punjab Irrigation Branch. Paper 110, Punjab Eng. Congress. 1927.

11. GWINN, Wendell R. and PARSONS, Donald A.: Discharge equations for HS, H, and HL flumes. J.of the Hydraulics Div.ASCE, Vol.102.No.HY1. Jan.1976,pp.73-88.

12. HARVEY, W.B.: Harvey's Irrigation Outlet. Punjab Irrigation Branch. 1912.

13. HOLTAN, H.N., MINCHAL, N.E., and HARROLD, L.L.: Field manual for research in agricultural hydrology. Soils & Water Conservation Research Div., Agricultural Research Service, Agricultural Handbook No.224. Washington D.C. 1962.

14. IDELCIK, I.E.: Memento des pertes de charge. Collection du Centre de recherche et d'essais de Chatou. Eyrolles. Paris, 1969.

15. INGLIS, C.C.: Notes on standing wave flumes and flume meter falls.Public Works Dept., Technical Paper No.15. Bombay. 1929.

16. JAMESON, A.H.: The development of the venturi flume. Water & Water Engineering. March 20. 1930. pp.105-107.

17. KHAFAGI, A.: Der Venturikanal. Theorie und Anwendung. Diss.-Drückerei AG. Gebr.Leemann & Co., Zürich. 1942.

18. PARSHALL, R.L.: Improving the Distribution of Water to Farmers by Use of the Parshall Measuring Flume. Soil Conservation Service. Bull.488. U.S.Dept. of Agriculture and Colorado Agricultural Experiment Station. Colorado A and M College. Fort Collins, Colorado. May 1945.

19. PARSHALL, R.L.: Measuring Water in Irrigation Channels with Parshall Flumes and Small Weirs. Soil Conservation Circular No.843. U.S.Dept. of Agriculture, May 1950.

20. PARSHALL, R.L.: Parshall Flumes of Large Size. Bull.426-A (Reprint of Bull.386). Colorado Agric.Experiment Sta., Colorado State University, Fort Collins, Colorado, March 1953.

21. PETERKA, A.J.: Water Measurement Procedures. Irrigation Operators' Workshop - 1965. Hydraulics Laboratory Report No.Hyd.-552. Bureau of Reclamation, November 15, 1965 (unpublished).

22. ROBINSON, A.R.: Parshall Measuring Flumes of Small Sizes. Technical Bulletin No.61. Agricultural Experiment Station. Colorado State University. Fort Collins, Colorado. 1957.

23. ROBINSON, A.R., and CHAMBERLAIN, A.R.: Trapezoidal flumes for open-channel flow measurement. Trans.Amer.Soc.Agri.Engnrs. 1960. 3. Nr.2, pp.120-128.

24. ROBINSON, A.R.: Simplified Flow Corrections for Parshall Flumes under Submerged Conditions. Civil Engineering ASCE. September 1965.

25. ROBINSON, A.R.: Trapezoidal flumes for measuring flow in irrigation channels. Agr.Res.Service ARS 41-140. March 1968. U.S.Dept.of Agriculture.15 pp.

26. SCHUSTER, J.C.(Ed.): Water measurement procedures. Irrigation operators' workshop. Report on REC-OCE-70-38. U.S.Bureau of Reclamation, Denver, Colorado, pp.49. 1970.

27. SKOGERBOE, G.V., HYATT, M.L., ANDERSON, R.K., and EGGLESTON, K.O.: Design and calibration of submerged open channel flow measurement structures. Part 3: Cutthroat flumes. Report WG31-4. Utah Water Res.Laboratory. College of Engineering. Utah State Unviersity. Logan, Utah. April 1957.

28. SKOGERBOE, G.V. and HYATT, M.L.: Analysis of submergence in flow measuring flumes. J.of the Hydraulics Div., ASCE. Vol.93, No.HY4, Proc.Paper 5348. July 1967. pp.183-200.

29. SKOGERBOE G.V., HYATT M.L., ENGLAND, J.D. and JOHNSON, J.R.: Design and Calibration of submerged open channel flow measurement structures. Part 2. Parshall flumes. Report WG 3/-3. Utah Water Research Laboratory. College of Eng. Utah St.University. Logan, Utah. March 1967.

30. SKOGERBOE, G.V., and HYATT, M.L.: Rectangular cutthroat flow measuring flumes. J.of the Irrigation and Drainage Div.ASCE, Vol.93, No.IR4. Dec. 1967, pp.1-33.

31. SKOGERBOE, G.V., BENNETT, R.S., and WALKER, W.R.: Generalized discharge relations for cutthroat flumes. J.of the Irrig.and Drainage Div.ASCE, Vol.98. No.IR4. Dec.1972, pp.569-583.

32. U.S.DEPARTMENT OF THE INTERIOR, U.S.BUREAU OF RECLAMATION: Water measurement manual. Second Ed. 1967. Denver, Colorado, 327 pp.

33. VEN TE CHOW: Open channel hydraulics. McGraw-Hill Book Comp., New York, 1959, pp.680.

34. WELLS, E.A., and GOTAAS, H.B.: Design of Venturi flumes in circular conduits. J.Sanit.Engng.Div.,ASCE. Paper No.2937. 1956. pp.749-771.

8 Orifices

A well defined opening in a plate or bulkhead, the top of which is placed well below the upstream water level, is classified here as an orifice.

8.1 Circular sharp-edged orifice

8.1.1 Description

A circular sharp-edged orifice, used as a measuring device, is a well-defined opening in a (metal) plate or bulkhead, which is placed perpendicular to the sides and bottom of a straight approach channel. For true orifice flow to occur, the upstream water level must always be well above the top of the opening,such that vortex-flow with air entrainment is not evident.
If the upstream water level drops below the top of the opening, it no longer performs as an orifice but as a weir (see Section 5.4).

This orifice is one of the older devices used for measuring water and formerly it was set up to discharge freely into the air,resulting in a considerable loss of head. To overcome this excessive head loss, the orifice is now arranged with the tailwater above the top of the opening. This "submerged orifice" conserves head and can be used where there is insufficient fall for a sharp-crested weir or where the head difference is too small to produce modular flow with a broad-crested weir or flume. Circular orifices have the advantage that the opening can be turned and its edges bevelled with precision on a lathe.Another advantage is that during installation no levelling is required.

In practice, circular sharp-edged orifices are fully contracted so that the bed and sides of the approach channel and the free water surface should be sufficiently remote from the control section to have no influence on the contraction of the discharging jet. The fully contracted orifice may be placed in a non-rectangular approach channel, provided that the general installation conditions comply with those explained in Section 8.1.3.
A general disadvantage of submerged orifices is that debris, weeds and sediment can accumulate upstream of the orifice, and may prevent accurate measurements. In sediment-laden water, it is especially difficult for maintenance personnel to determine whether the orifice is obstructed or completely open to flow. To prevent the overtopping of the embankments in the case of a blocked orifice, the top of the orifice wall should only be to the maximum expected upstream water level so it can act as an overflow weir.

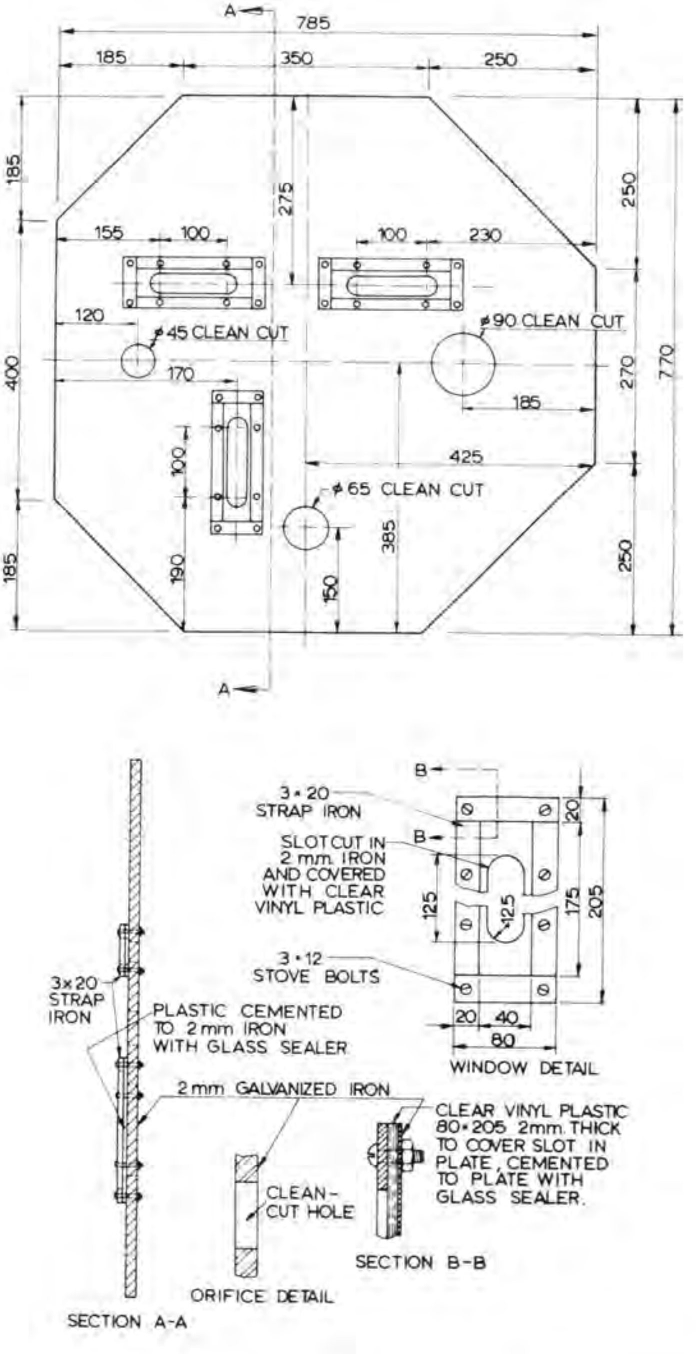

Fig.8.1. Portable orifice plate (adapted from U.S.Soil Conservation Service).

Orifice plates are simple, inexpensive and easy to install, which makes them suitable as a portable device to measure very low discharges such as furrow streamflow. An example of a portable orifice plate with three ranges of measurement is shown in Figure 8.1. The orifice plate shown contains three slots covered with clear vinyl plastic to permit the reading of the differential head from the downstream side of the plate. Since flow through this orifice must be submerged it may be necessary to restrict the downstream channel in order to raise the tailwater level above the top of the orifice.

8.1.2 Determination of discharge

The basic head-discharge equations for orifice flow, according to Section 1.12, are

$$Q = C_d C_v A\sqrt{2g(h_1 - h_2)} \tag{8-1}$$

for submerged flow conditions, and

$$Q = C_d C_v A\sqrt{2g\Delta h} \tag{8-2}$$

if the orifice discharges freely into the air. In these two equations, h_1-h_2 equals the head differential across the orifice and Δh equals the upstream head above the centre of the orifice (see Figs.1.8 and 1.19). A is the area of the orifice and equals $\frac{1}{4}\pi d^2$, where d is the orifice diameter.

Orifices should be installed and maintained so that the approach velocity is negligible, thus ensuring that C_v approaches unity.

Calibration studies performed by various research workers have produced the average C_d-values shown in Table 8.1.

The error in the discharge coefficient for a well-maintained circular sharp-crested orifice, constructed with reasonable care and skill, is expected to be of the order of 1%.

The method by which the coefficient error is to be combined with other sources of error is shown in Appendix II.

TABLE 8.1. AVERAGE DISCHARGE COEFFICIENTS FOR CIRCULAR ORIFICES (NEGLIGIBLE APPROACH VELOCITY)

Orifice diameter "d" in metres	C_d free flow	C_d submerged flow
0.020	0.61	0.57
0.025	0.62	0.58
0.035	0.64	0.61
0.045	0.63	0.61
0.050	0.62	0.61
0.065	0.61	0.60
$\geqslant$ 0.075	0.60	0.60

8.1.3 Limits of application

To ensure full contraction and accurate flow measurements, the limits of application of the circular orifice are:

a) The edge of the orifice should be sharp and smooth and be in accordance with the profile shown in Figure 5.1.

b) The distance from the edge of the orifice to the bed and side slopes of the approach and tailwater channel should not be less than the radius of the orifice. To prevent the entrainment of air, the upstream water level should be at a height above the top of the orifice which is at least equal to the diameter of the orifice.

c) The upstream face of the orifice plate should be vertical and smooth.

d) To make the approach velocity negligible, the wetted cross-sectional area at the upstream head-measurement station should be at least 10 times the area of the orifice.

e) The practical lower limit of the differential head, across the orifice is related to fluid properties and to the accuracy with which gauge readings can be made. The recommended lower limit is 0.03 m.

8.2 Rectangular sharp-edged orifice

8.2.1 Description

A rectangular sharp-edged orifice used as a discharge measuring device is a well-defined opening in a thin (metal) plate or bulkhead, which is placed perpendicular to the bounding surfaces of the approach channel. The top and bottom edges should be horizontal and the sides vertical.

Since the ratio of depth to width of irrigation canals is generally small and because changes in depth of flow should not influence the discharge coefficient too rapidly, most (submerged) rectangular orifices have a height, w, which is considerably less than the breadth, b. The principal type of orifice for which the discharge coefficient has been carefully determined in laboratory tests is the submerged, fully contracted, sharp-edged orifice. Since the discharge coefficient is not so well defined where the contraction is partially suppressed, it is advisable to use a fully contracted orifice wherever conditions permit. Where sediment is transported it may be necessary to place the lower edge of the orifice at canal bed level to avoid the accumulation of sediments on the upstream side. If the discharge must be regulated it may even be desirable to suppress both bottom and side contractions so that the orifice becomes an opening below a sluice gate.

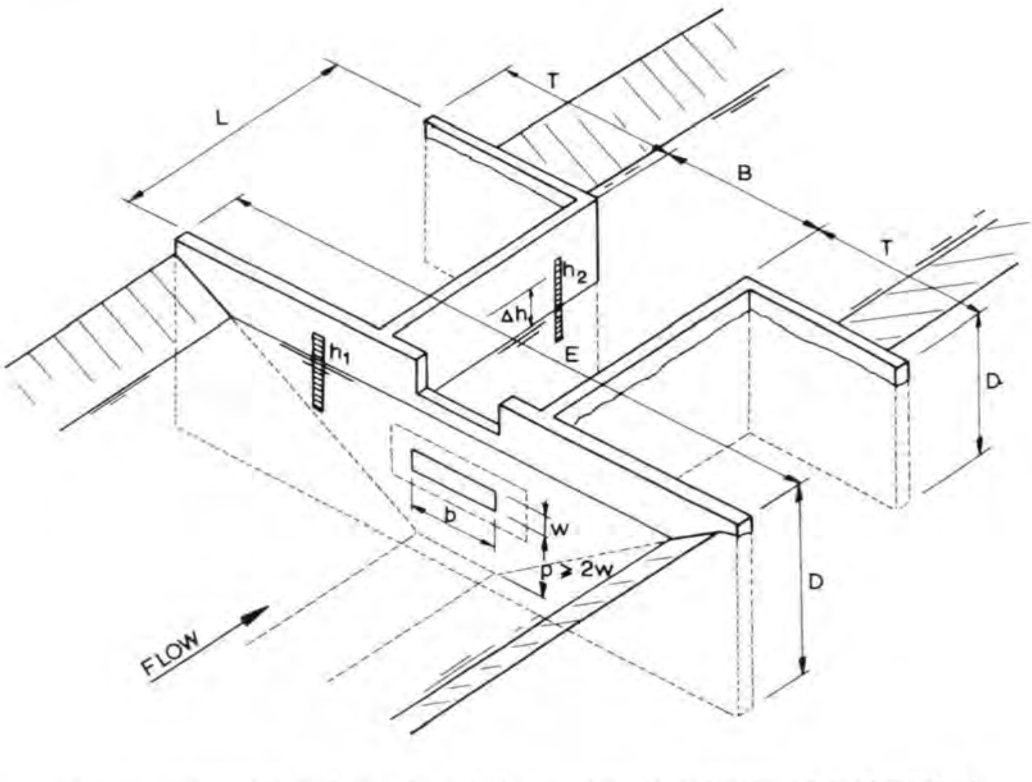

Fig. 8.2. Orifice box dimensions (adapted from U.S. Bureau of Reclamation).

A submerged orifice structure is shown in Figure 8.2. A box is provided downstream from the orifice to protect unlined canals from erosion. Both the sides and the floor of this box should be set outward from the orifice a distance of at least two times the height of the orifice. To ensure that the orifice is submerged or to cut off the flow, an adjustable gate may be provided at the downstream end of the orifice box. This gate should be a sufficient distance downstream from the orifice so as not to disturb the issuing jet.

The top of the vertical orifice wall should not be higher than the maximum expected water level in the canal, so that the wall may act as an overflow weir if the orifice should become blocked. Suitable submerged orifice-box dimensions for a concrete, masonry, or wooden structure as shown in Figure 8.2 are listed in Table 8.2.

TABLE 8.2. RECOMMENDED BOX SIZES AND DIMENSIONS FOR A SUBMERGED ORIFICE (AFTER U.S.BUREAU OF RECLAMATION)

Orifice size		Height of structure	Width of head wall	Length	Width	Length of downstream head wall
heigth	breadth					
w	b	D	E	L	B	T
0.08	0.30	1.20	3.00	0.90	0.75	0.60
0.08	0.60	1.20	3.60	0.90	1.05	0.60
0.15	0.30	1.50	3.60	1.05	0.75	0.90
0.15	0.45	1.50	4.25	1.05	0.90	0.90
0.15	0.60	1.50	4.25	1.05	1.05	0.90
0.23	0.40	1.80	4.25	1.05	0.90	0.90
0.23	0.60	1.80	4.90	1.05	1.05	0.90

8.2.2 Determination of discharge

The basic head-discharge equation for submerged orifice flow, according to Section 1.12 is

$$Q = C_d C_v A\sqrt{2g(h_1 - h_2)} \tag{8-3}$$

where $h_1 - h_2$ equals the head differential across the orifice, and A is the area of the orifice and equals the product wb. In general, the submerged orifice should be designed and maintained so that the approach velocity is negligible and the coefficient C_v approaches unity.Where this is impractical, the area ratio A^*/A_1 may be calculated and a value for C_v obtained from Figure 1.12.

For a fully contracted, submerged, rectangular orifice, the discharge coefficient $C_d = 0.61$. If the contraction is suppressed along part of the orifice perimeter, then the following approximate discharge coefficient may be used in Equation 8-3, regardless of whether the orifice bottom only or both orifice bottom and sides are suppressed

$$C_d = 0.61\ (1 + 0.15\ r) \tag{8-4}$$

where r equals the ratio of the suppressed portion of the orifice perimeter to the total perimeter.

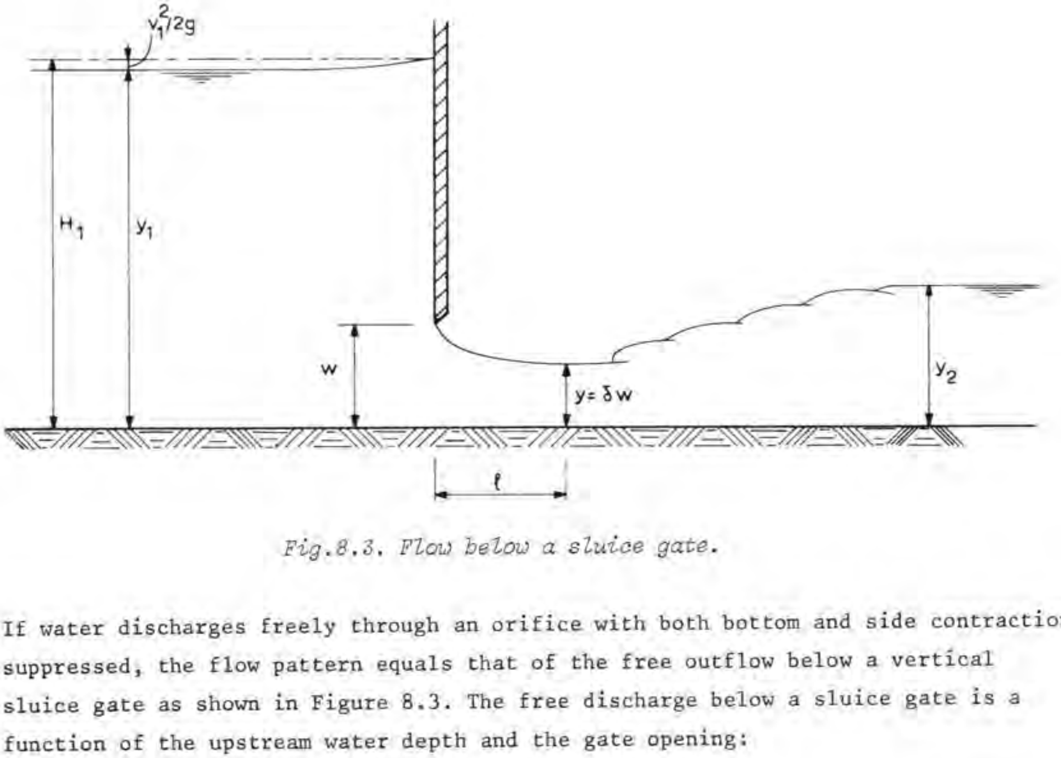

Fig.8.3. Flow below a sluice gate.

If water discharges freely through an orifice with both bottom and side contractions suppressed, the flow pattern equals that of the free outflow below a vertical sluice gate as shown in Figure 8.3. The free discharge below a sluice gate is a function of the upstream water depth and the gate opening:

$$Q = C_d C_v\ bw\sqrt{2g(y_1 - y)} \tag{8-5}$$

If we introduce the ratios $n = y_1/w$ and $\delta = y/w$, where δ is the contraction coefficient, Equation 8-5 may be written as

$$Q = C_d C_v b w^{1.5} \sqrt{2g(n - \delta)} \tag{8-6}$$

which may be simplified to

$$Q = K\, b w^{1.5} \sqrt{2g} = A\, w^{0.5}\, K\sqrt{2g} \tag{8-7}$$

where the coefficient K is a function of the ratio $n = y_1/w$ as shown in Table 8.3.

TABLE 8.3. COEFFICIENTS FOR FREE FLOW BELOW A SLUICE GATE

Ratio	Contraction coefficient	Discharge coefficient Eq.8-6	Coefficient Eq.8-7	$K\sqrt{2g}$ Eq.8-7
$n=y_1/w$	δ	C_d	K	$m^{\frac{1}{2}}\ s^{-1}$
1.50	0.648	0.600	0.614	2.720
1.60	0.642	0.599	0.641	2.838
1.70	0.637	0.598	0.665	2.946
1.80	0.634	0.597	0.689	3.052
1.90	0.632	0.597	0.713	3.159
2.00	0.630	0.596	0.735	3.255
2.20	0.628	0.596	0.780	3.453
2.40	0.626	0.596	0.823	3.643
2.60	0.626	0.597	0.865	3.832
2.80	0.625	0.598	0.905	4.010
3.00	0.625	0.599	0.944	4.183
3.50	0.625	0.602	1.038	4.597
4.00	0.624	0.604	1.124	4.977
4.50	0.624	0.605	1.204	5.331
5.00	0.624	0.607	1.279	5.664

Adapted from P.G.Franke, 1968

For field structures sufficient accuracy will be obtained if we interpolate between the following empirical values for the contraction coefficient:

$$\delta = 0.63 \quad \text{for } n = 2$$
$$\delta = 0.625 \quad \text{for } n = 3$$
$$\delta = 0.62 \quad \text{for } n = 10$$

and between the following discharge coefficients for use in Equation 8-6:

$$C_d = 0.60 \quad \text{for } 1.5 < n < 3.5$$
$$C_d = 0.605 \quad \text{for } 3.5 \leqslant n \leqslant 5.0$$
$$C_d = 0.61 \quad \text{for } n > 5.0$$

Some authors prefer to describe a sluice gate as a half-model of a two-dimensional jet as shown in Figure 1.20, the bottom of the channel being the substitute for the plane of symmetry of the jet. Hence a discharge equation similar to Equation 1-67 is used to determine the free flow below the gate. This is

$$Q = C_e A\sqrt{2gy_1} \qquad (8\text{-}8)$$

where C_e also expresses the influence of the approach velocity, since it is a function of the ratio y_1/w. The results of experiments by H.R.HENRY (1950) are plotted in Figure 8.4, which show values of C_e as a function of y_1/w and y_2/w for both free and submerged flow below the sluice gate. The C_e-values read from Figure 8.4 will result in considerable errors if the difference between y_1/w and y_2/w becomes small (< 1.0). This condition will generally be satisfied with small differential heads and thus we recommend that the submerged discharge be evaluated by the use of Equations 8-3 and 8-4.

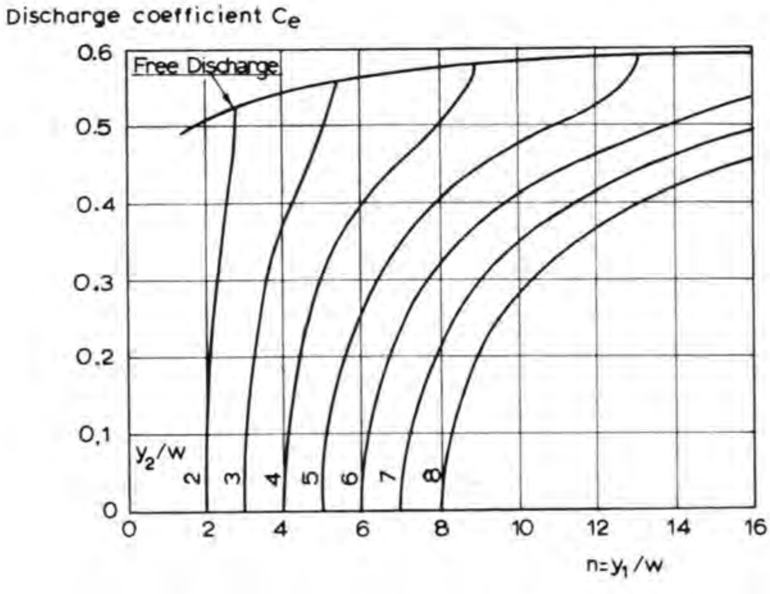

Fig.8.4. Discharge coefficient for use in Equation 8-8 (after H.R.Henry,1950).

The results obtained from experiments by HENRY, FRANKE and the U.S.Bureau of Reclaation are in good agreement.In this context it should be noted that the velocity $\sqrt{2gy_1}$ does not occur anywhere in the flow system; it simply serves as a convenient reference velocity for use in Equation 8-8.

The discharge coefficients given for the fully contracted submerged orifice (C_d=0.61) and for free flow below a sluice gate in Table 8.3 can be expected to have an error of the order of 2%. The coefficient given in Equation 8-4 for flow through a submerged partially suppressed orifice can be expected to have an error of about 3%.
The method by which the coefficient error is to be combined with other sources of error is shown in Appendix II.

8.2.3 Modular limit

Free flow below a sluice gate occurs as long as the roller of the hydraulic jump does not submerge the section of minimum depth of the jet, which is located at a distance of

$$l = w/\delta = y_1/n\delta \qquad (8\text{-}10)$$

downstream of the face of the vertical gate. To ensure such free flow, the water depth, y_2, downstream of the hydraulic jump should not exceed the alternate depth to $y = \delta w$, or according to the equation

$$y_2/w < \frac{\delta}{2}\left[\sqrt{1 + 16\left(\frac{H_1}{\delta w} - 1\right)} - 1\right] \qquad (8\text{-}11)$$

Relative numbers y_2/w worked out with the theoretical minimum contraction coefficient δ = 0.611, corresponding to high values of the ratio n, are given in Figure 8.5 as a function of y_1/w.

8.2.4 Limits of application

To ensure accurate flow measurements, the limits of application of the rectangular sharp-edged orifice are:

a) The upstream edge of the orifice should be sharp and smooth and be in accordance with the profile shown in Figure 5.1.

b) The upstream face of the orifice should be truly vertical.

c) The top and bottom edges of the orifice should be horizontal.

d) The sides of the orifice should be vertical and smooth.

e) The distance from the edge of the orifice to the bed and side slopes of the approach and tailwater channel should be greater than twice the least dimension of the orifice if full contraction is required.

f) The wetted cross-sectional area at the upstream head-measurement station should be at least 10 times the area of the orifice so as to make the approach velocity negligible; this is particularly recommended for fully contracted orifices.

g) If the contraction is suppressed along the bottom or sides of the orifice, or along both the bottom and sides, the edge of the orifice should coincide with the bounding surface of the approach channel.

h) The practical lower limit of the differential head across the submerged orifice is related to fluid properties and to the accuracy to which gauge readings can be made. The recommended lower limit is 0.03 m.

i) If the contraction along bottom and sides is suppressed, the upstream head should be measured in the rectangular approach channel.

j) The upper edge of the orifice should have an upstream submergence of 1.0 w or more to prevent the formation of air-entraining vortices.

k) A practical lower limit of $w = 0.02$ m and of $y_1 = 0.15$ m should be observed.

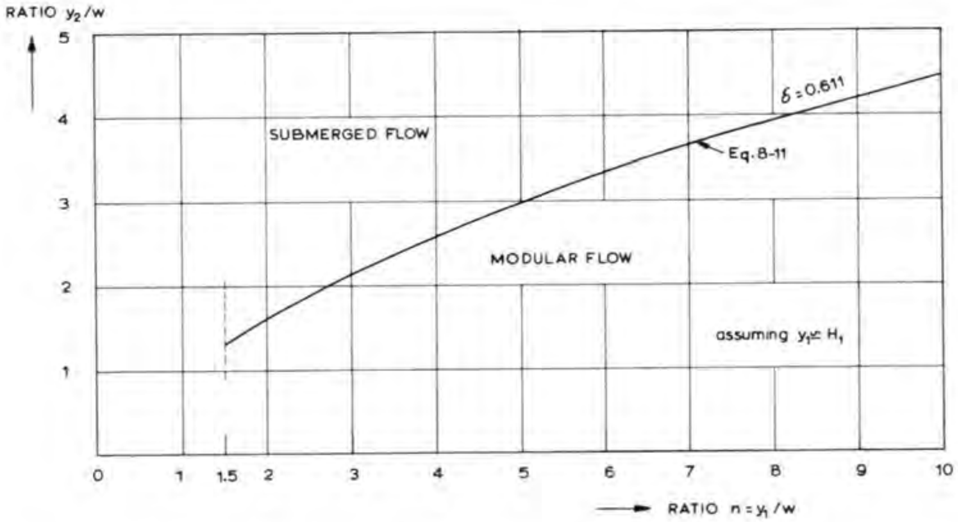

Fig.8.5. Limiting tail-water level for modular flow below a sluice gate.

8.3 Constant-head-orifice

8.3.1 Description

The constant-head-orifice farm turnout (CHO) is a combination of a regulating and measuring structure that uses an adjustable submerged orifice for measuring the flow and a (downstream) adjustable turnout gate for regulation. The turnouts are used to measure and regulate flows from main canals and laterals into smaller ditches and are usually placed at right angles to the main canal. The CHO was developed by the United States Bureau of Reclamation and is so named because its operation is based upon setting and maintaining a constant head differential, Δh, across the orifice. Discharges are varied by changing the area of the orifice. A typical constant head-orifice turnout installation is shown in Figure 8.6.

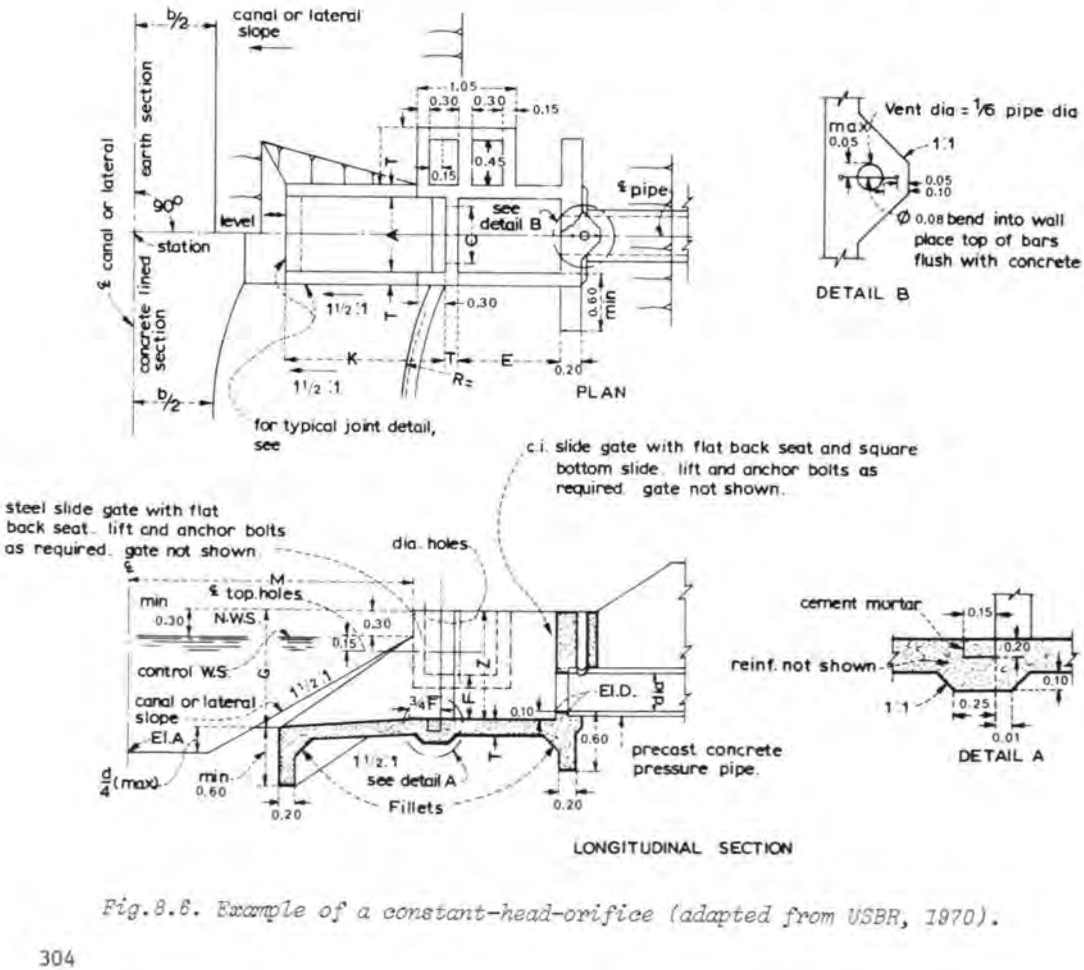

Fig.8.6. Example of a constant-head-orifice (adapted from USBR, 1970).

To set a given flow, the orifice opening A required to pass the given discharge is determined, and the orifice gate is set at this opening. The downstream turnout gate is then adjusted until the head differential as measured over the orifice gate equals the required constant-head, which usually equals 0.06 m. The discharge will then be at the required value. The rather small differential head used is one of the factors contributing to the inaccuracy of discharge measurements made by the CHO. For instance, errors of the order of 0.005 m in reading each staff gauge may cause a maximum cumulative error of 0.01 m or about 16% in Δh, which is equivalent to 8% error in the discharge. Introducing a larger differential head would reduce this type of error, but larger flow disturbances would be created in the stilling basin between the two gates. Furthermore, it is usually desirable to keep head losses in an irrigation system as low as possible. Since the downstream gate merely serves the purpose of setting a constant head differential across the orifice gate, its shape is rather arbitrary. In fact, the turnout gate shown in Figure 8.5 may be replaced by a movable weir or flap-gate if desired. If the CHO is connected to a culvert pipe that is flowing full, the air pocket immediately downstream of the turnout gate should be aerated by means of a ventilation pipe. The diameter of this pipe should be 1/6 of the culvert diameter to provide a stable flow pattern below the turnout gate. If the flow through the downstream gate is submerged, a change of tailwater level of the order of a few centimetres will cause an equivalent change of water level in the basin between the two gates. Under field conditions, the discharge in the main canal is likely to be large compared with the discharge through the turnout. Hence the head differential over the orifice gate will change with any change in tailwater level, resulting in a considerable error in the diverted flow. The reader will note that if reasonable accuracy is required in discharge measurement, the flow below the turnout gate should be supercritical at all tailwater levels. For this to occur, the turnout gate requires a minimum loss of head which may be calculated as explained in Section 8.2.2 and with the aid of Figure 8.5. The combined loss of head over the orifice gate (usually 0.06 m) and over the turnout gate (variable) to produce modular flow is considerable.

Usually the CHO is placed at an angle of 90° from the centre line of the main canal, and no approach channel is provided to the orifice gate. As a result, the flow in the main canal will cause an eddy and other flow disturbances immediately upstream of the orifice gate opening, thus affecting the flow below the orifice gate. Such detrimental effects increase as the flow velocity in the main canal increase and are greater if the CHO is working at full capacity. Full-scale tests showed a deviation of the discharge coefficient of as much as 12% about the mean C_d-values with high flow velocities (1.0 m/s) and with larger orifice gate openings.The approach flow conditions, and thus the accuracy of the CHO can be improved significantly by introducing an approach channel upstream of the orifice gate. For example, if the CHO is used in combination with a culvert under an inspection road, the CHO could be placed at the downstream end of the culvert, provided that the culvert has a free water surface.

Since the CHO is usually operated at a differential head of 0.06 m (0.20 foot), it is clear that extreme care should be taken in reading heads. Fluctuations of the water surfaces just upstream of the orifice gate and in the stilling basin downstream of the orifice can easily result in head-reading errors of one or more centimetres if the heads are read from staff gauges. This is particularly true if the CHO is working at full capacity. Tests have revealed that, with larger orifice-gate openings, staff gauge readings may show a negative differential head while piezometers show a real differential head of 0.06 m.

Head-reading errors can be significantly reduced if outside stilling wells are connected to 0.01 m piezometers placed in the exact positions shown in Figure 8.6. Two staff gauges may be installed in the stilling wells,but more accurate readings will be obtained by using a differential head meter as described in Section 2.12.

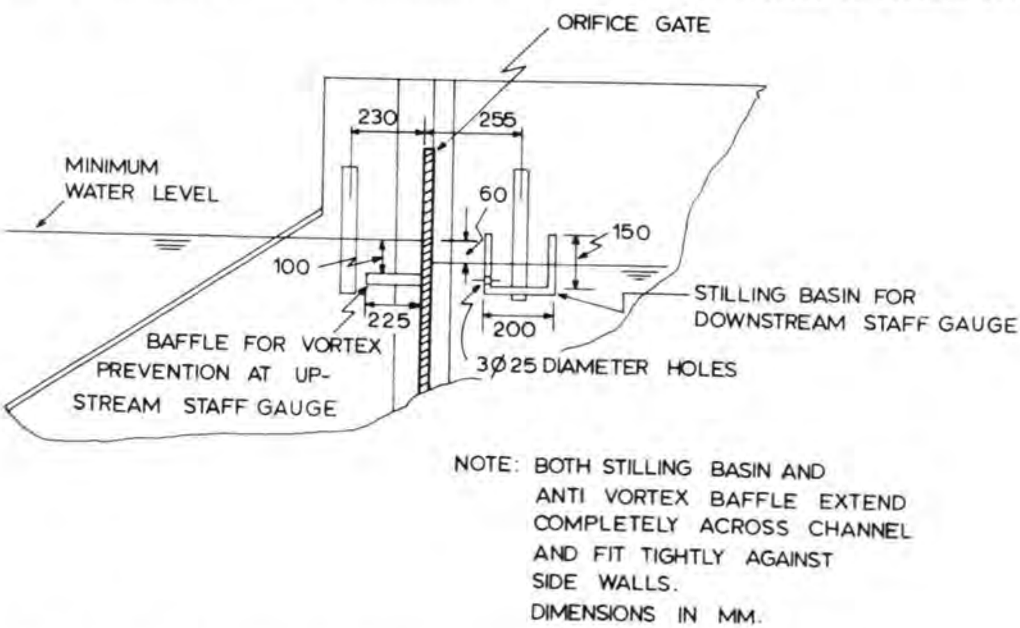

Fig.8.7. Device to reduce water level fluctuations at CHO staff gauges (after U.S.Agricultural Research Service).

Head-reading errors on existing structures equiped with outside staff gauges can be reduced by the use of a small wooden or metal baffle-type stilling basin and an anti-vortex baffle. The dimensions and position of these stilling devices, which have been developed by the U.S.Agricultural Research Service, are shown in Figure 8.7.

8.3.2 Determination of discharge

The basic head-discharge equation for a submerged orifice, according to Section 1.13 reads

$$Q = CA\sqrt{2g\Delta h} \qquad (8\text{-}12)$$

where the differential head Δh usually equals 0.06 m. The discharge coefficient C is a function of the upstream water depth, y_1, and the height of the orifice w. Experimental values of C as a function of the ratio y_1/w are shown in Figure 8.8. The reader should note that the coefficient C also expresses the influence of the approach velocity head on the flow.

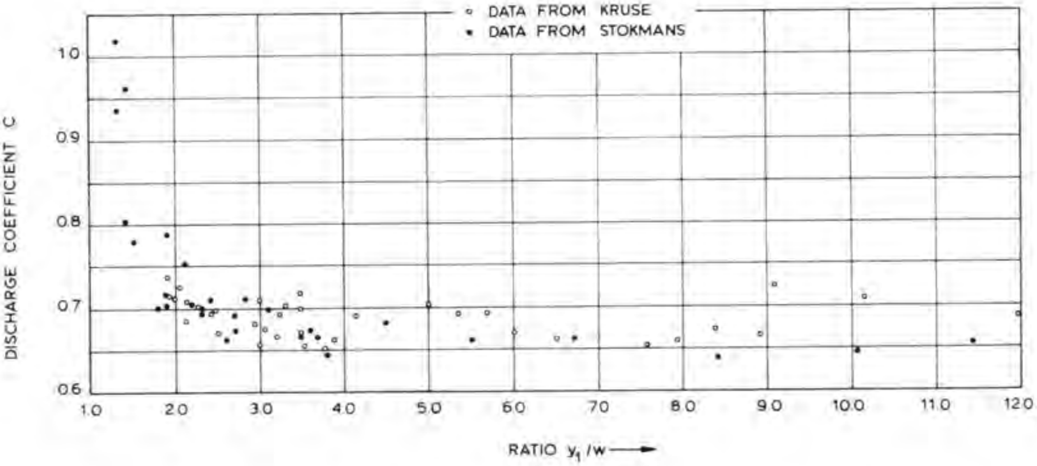

Fig.8.8. Variation of discharge coefficient, C, as a function of the ratio y_1/w (indoor tests).

From Figure 8.8 it appears that the discharge coefficient, C, is approximately 0.66 for normal operating conditions, i.e. where the water depth upstream from the orifice gate is 2.5 or more times the maximum height of the gate opening,w.

Substitution of the values $C_d = 0.66$, $\Delta h = 0.06$ m, and $g = 9.81$ m/s^2 into Equation 8.1 gives the following simple area-discharge relationship for the CHO:

$$Q = 0.716\ A = 0.716\ bw \qquad (8\text{-}13)$$

If the breadth of the orifice is known, a straight-line relationship between the orifice gate opening and the flow may be plotted for field use.

The error in the discharge coefficient given for the Constant-Head-Orifice ($C = 0.66$) can be expected to be of the order of 7%. This coefficient error applies for structures that have an even velocity distribution in the approach section. If an eddy is formed upstream of the orifice gate, however, an additional error of up to 12% may occur (see also Section 8.3.1).

The method by which the coefficient error is to be combined with other sources of error, which have a considerable magnitude, is shown in Appendix II. In this context, the reader should note that if the upstream gate is constructed with uninterrupted bottom and side walls and a sharp-edged gate, Equations 8-3 and 8-4 can be used to determine the discharge through the orifice with an accuracy of about 3%.

8.3.3 Limits of application

The limits of application of the Constant-Head-Orifice turnout are:

a) The upstream edge of the orifice gate should be sharp and smooth and be in accordance with the profile shown in Figure 8.6.

b) The sides of the orifice should have a groove arrangement as shown in Figure 8.6.

c) The bottom of the approach section upstream of the orifice gate should be horizontal over a distance of at least four times the upstream water depth.

d) To obtain a somewhat constant value for the discharge coefficient, C, the ratio y_1/w should be greater than 2.5.

e) The approach section should be such that no velocity concentrations are visible upstream of the orifice gate.

8.4 Radial or tainter gate

8.4.1 Description

The radial or tainter gate is a movable control; it is commonly used in a rectangular canal section. It has the structural advantage of not requiring a complicated groove arrangement to transmit the hydraulic thrust to the side walls, because this thrust is concentrated at the hinges. In fact, the radial gate does not require grooves at all, but has rubber seals in direct contact with the undisturbed sides of the rectangular canal section.
Figure 8.9 shows two methods by which the radial gate can be installed, either with the gate sill at stream bed elevation or with its sill raised.

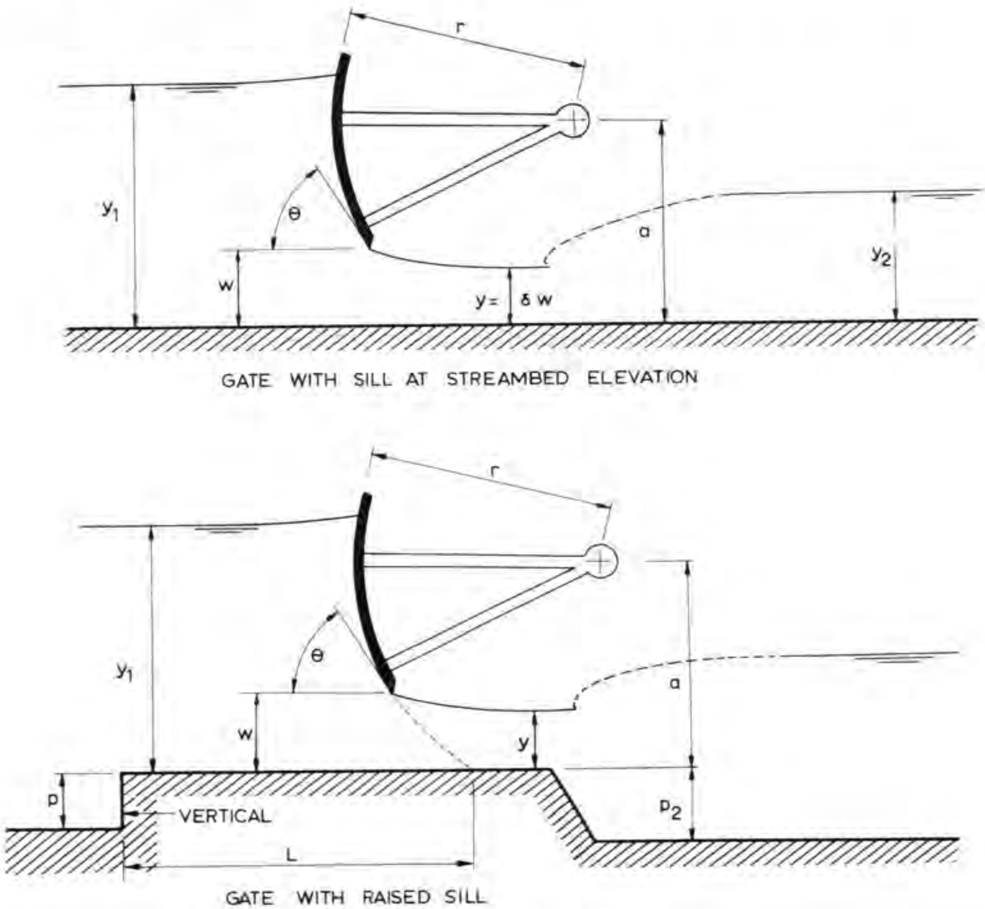

Fig.8.9. Flow below a radial or tainter gate.

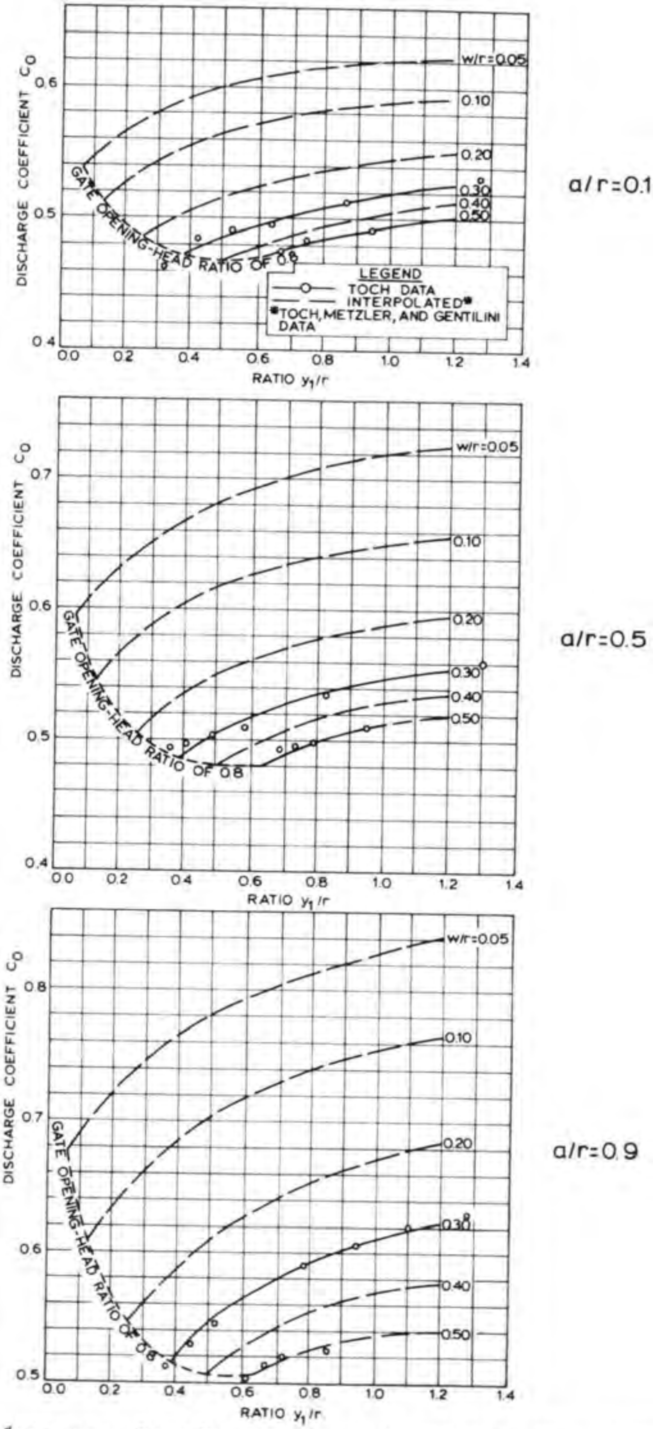

Fig. 8.10. C_o*-values as a function of* a/r*,* y_1/r *and* w/r*. (From U.S.Army Engineer Waterways Experiment Station, 1960.)*

8.4.2 Evaluation of discharge

Free flow through a partially open radial gate is commonly computed with the following equation:

$$Q = C_o C_1 \; wb\sqrt{2gy_1} \tag{8-15}$$

The coefficient, C_o, depends on the contraction of the jet below the gate, and may be expressed as a function of the gate opening w, gate radius r, trunnion height a, and upstream water depth y_1, for a gate sill at streambed elevation. Figure 8.10 gives C_o-values for a/r ratios of 0.1, 0.5, and 0.9. Coefficient values for other a/r-values may be obtained by linear interpolation between the values presented.

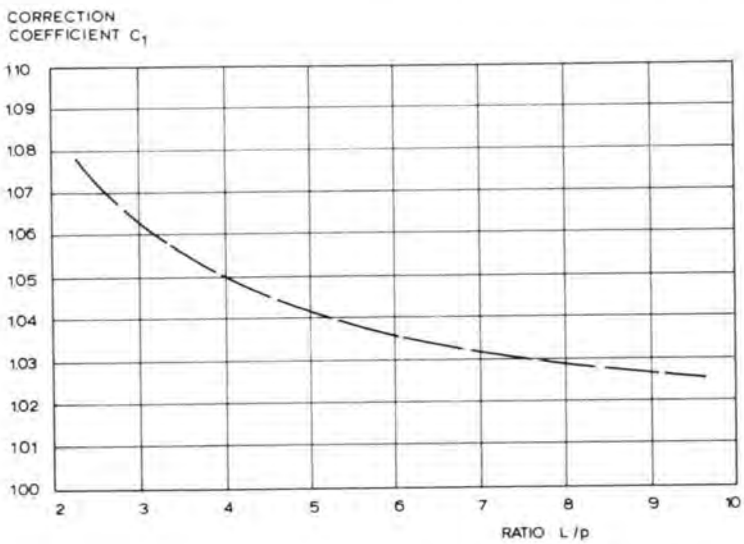

Fig.8.11. C_1-values for radial gates with raised sill. (From U.S.Army Engineer Waterways Experiment Station.)

The coefficient C_1 is a correction to C_o for gate sills above streambed elevation and depends upon sill height p and the distance between the step and the gate seat L, as shown in Figure 8.11. Insufficient information is available to determine the effects, if any, of the parameter p/r.

It should be noted that the velocity $\sqrt{2gy_1}$ in Equation 8-15 does not occur anywhere in the flow system, but simply serves as a convenient reference velocity.

The experiments on which Figure 8.10 is based showed that the contraction coefficient, δ, of the jet below the gate is mainly determined by the angle θ and to a much lesser extent by the ratio y_1/w. For preliminary design purposes, HENDERSON (1966) proposed Equation 8-16 to evaluate δ-values.

$$\delta = 1 - 0.75\ (\theta/90^{\circ}) + 0.36\ (\theta/90^{\circ})^2 \tag{8-16}$$

where θ equals the angle of inclination in degrees.

Equation 8-16 was obtained by fitting a parabola as closely as possible to TOCH's results (1952, 1955) and data obtained by VON MISES (1917) for non-gravity, two-dimensional flow through an orifice with inclined side walls.

Values of δ given by Equation 8-16 and shown in Figure 8.12 can be expected to have an error of less than 5% provided that $\theta < 90^{\circ}$.

If the discharge coefficient C_o in Equation 8-15 is to be evaluated from the contraction coefficient, we may write, according to continuity and Bernoulli:

$$C_o = \frac{\delta}{\sqrt{1 + \delta w/y_1}} \tag{8-17}$$

The discharge coefficient, C_o, given in Figure 8.10 and Equation 8-17 for free flow below a radial gate can be expected to have errors of less than 5% and between 5 and 10% respectively. The error in the correction coefficient C_1, given in

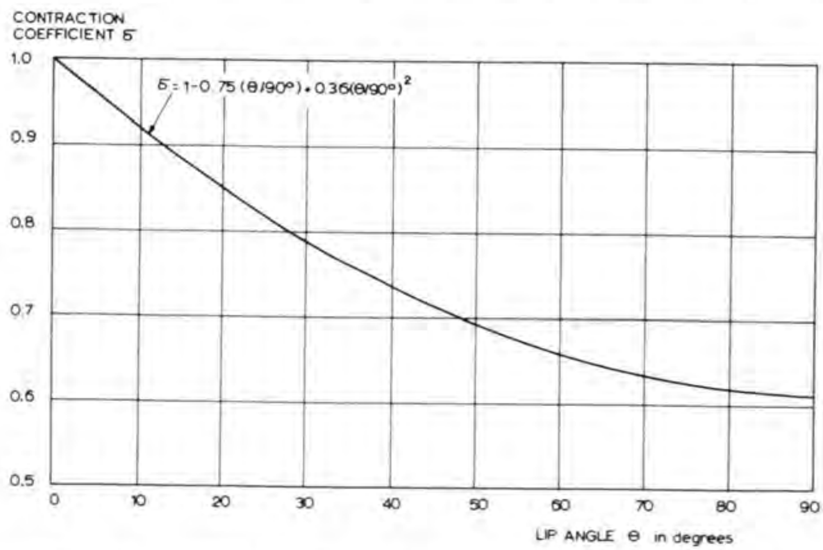

Fig.8.12. Effect of lip angle on contraction coefficient.

Figure 8.11 can be expected to have an error of less than 5%. The method by which these errors have to be combined with other sources of error is shown in Appendix II.

8.4.3 Modular limit

Modular flow below a radial gate occurs as long as the roller of the hydraulic jump does not submerge the section of minimum depth of the jet (vena contracta). To prevent such submergence, the water depth, y_2, downstream of the hydraulic jump should not exceed the alternate depth to $y = \delta w$ or according to the equation

$$y_2/w < \frac{\delta}{2}\left[\sqrt{1 + 16\left(\frac{H}{\delta w} - 1\right)} - 1\right] \tag{8-18}$$

For each radial gate the modular limit may be obtained by combining Equation 8-16 (or Figure 8.12) and Equation 8-18.
If flow below the gate is submerged, Equation 1-73 as derived in Section 1.12 may be used as a head-discharge relationship. It reads

$$Q = C_e\, bw\sqrt{2g(y_1 - y_2)} \tag{8-19}$$

Insufficient experimental data are available to present reasonably accurate C_e-values. For design purposes, however, the coefficient C_e may be evaluated from the contraction coefficient δ for free flow conditions (Fig.8.12).

A combination of the Bernoulli and the continuity equations gives for C_e

$$C_e = \frac{\delta}{\sqrt{1 - \left[\frac{\delta w}{y_1}\right]^2}} \tag{8-20}$$

It should be noted that the assumption that the contraction coefficient is the same for free flow as for submerged flow is not completely correct.

8.4.4 Limits of application

The limits of application of the radial or tainter gate are:

a) The bottom edge of the gate should be sharp and horizontal from end to end.

b) The upstream head should be measured in a rectangular approach channel that has the same width as the gate.

c) The gate opening head ratio should not exceed 0.8 ($w/y_1 \leqslant 0.8$).

d) The downstream water level should be such that modular flow occurs (see Equation 8-18).

8.5 Crump-De Gruyter adjustable orifice

8.5.1 Description

The Crump-De Gruyter adjustable orifice is a short-throated flume fitted with a vertically movable streamlined gate. It is a modification of the "adjustable proportional module", introduced by E.S.CRUMP in 1922. P.de GRUYTER (1926) modified the flume alignment and replaced the fixed "roof-block" with an adjustable sliding gate and so obtained an adjustable flume that can be used for both the measurement and regulation of irrigation water (see Fig.8.13).

Usually the orifice is placed at an angle of 90° from the centre line of the main canal which may cause eddies upstream of the orifice gate if canal velocities are high. For normal flow velocities in earthen canals, the approach section shown in Figure 8.13 is adequate. If canal velocities are high,of the order of those that may occur in lined canals, the approach section should have a greater length so that no velocity concentrations are visible upstream of the orifice gate. The structural dimensions in Figure 8.13 are shown as a function of the throat width b and head h_1.

Provided that the gate opening (w) is less than about 2/3 H_1 - in practice one takes $w \leqslant 0.63\, h_1$ - and the downstream water level is sufficiently low, supercritical flow will occur in the throat of the flume so that the flume discharge depends on the upstream water level (h_1) and the gate opening (w) only.

With the use of Equation 1-33, the discharge through the non-submerged (modular) flume can be expressed by

$$Q = C_d C_v b w \sqrt{2g(h_1 - w)} \tag{8-21}$$

where b equals the breadth of the flume throat and w is the gate opening which equals the "water depth" at the control section of the flume. To obtain modular flow, a minimal loss of head over the structure is required. This fall, Δh, is a function of both h_1 and w, and may be read from Figure 8.14, provided that the downstream transition is in accordance with Figure 8.13.

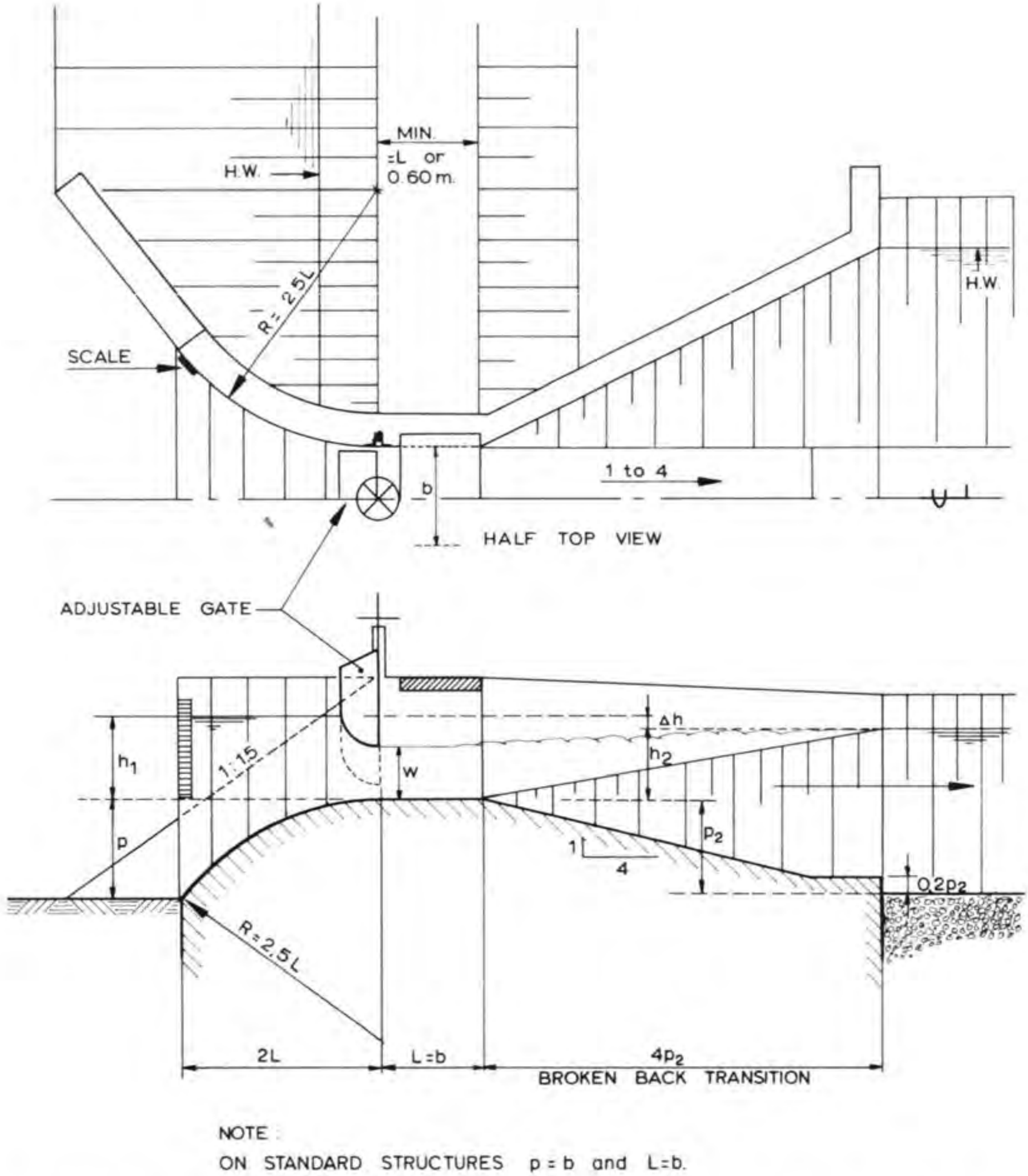

Fig.8.13. The Crump-De Gruyter adjustable orifice dimensions as a function of h_1 and b.

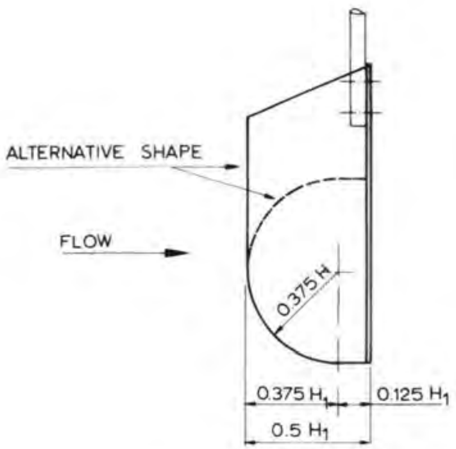

SECTION OVER ADJUSTABLE GATE

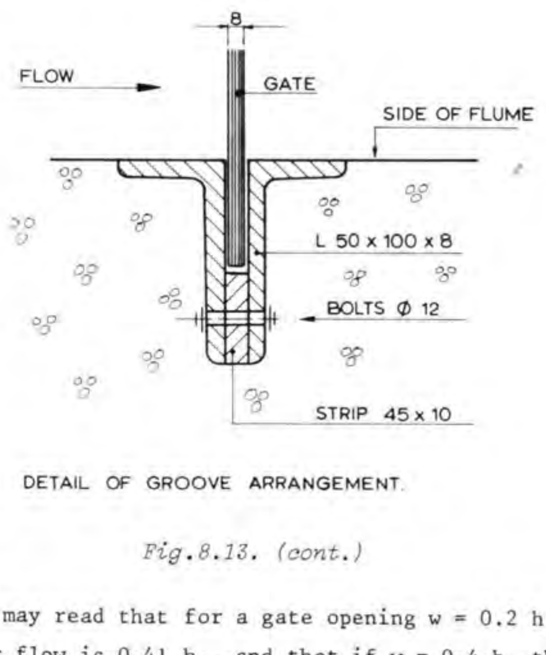

DETAIL OF GROOVE ARRANGEMENT

Fig.8.13. (cont.)

From Figure 8.14 we may read that for a gate opening $w = 0.2\ h_1$ the minimal fall required for modular flow is $0.41\ h_1$, and that if $w = 0.4\ h_1$ the minimal fall equals $0.23\ h_1$. This shows that, if h_1 remains about constant, the adjustable orifice requires a maximum loss of head to remain modular when the discharge is minimal. Therefore, the required value of the ratio $\gamma = Q_{max}/Q_{min}$ is an important design criterion for the elevation of the flume crest. If, for example, both γ and h_1 are known, the minimum loss of head, Δh, required to pass the range of discharges can be calculated from Figure 8.14. On the other hand, if both γ and

Δh are known, the minimum h_1-value, and thus the flume elevation with regard to the upstream (design) water level, is known.

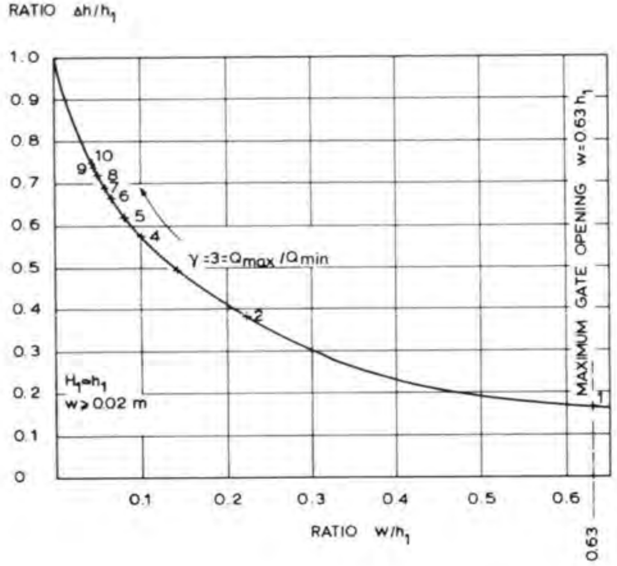

Fig.8.14. Characteristics of the Crump-De Gruyter adjustable orifice (after P.de Gruyter, 1926).

When a design value for h_1 has been selected, the minimum throat width, b, required to pass the required range of discharges under modular conditions can be calculated from the head-discharge equation and the limitation on the gate opening, which is $w \leqslant 0.63\ h_1$.

Anticipating Section 8.5.2 we can write

$$Q_{max} = 0.94\ b(0.63\ h_1)\ \sqrt{2g(h_1 - 0.63\ h_1)} \qquad (8\text{-}22)$$

which results in a minimum value of b, being

$$b \geqslant \frac{Q_{max}}{1.60\ h_1^{3/2}} \qquad (8\text{-}23)$$

With the use of Figures 8.13 and 8.14 and Equation 8-23, all hydraulic dimensions of the adjustable orifice can be determined.

TABLE 8.4: RATING TABLE FOR THE CRUMP-DE GRUIJTER ADJUSTABLE FLUME

w in metres	Upstream head over flume crest H_1 in metres																w in metres
	0.30	0.32	0.34	0.36	0.38	0.40	0.42	0.44	0.46	0.48	0.50	0.52	0.54	0.56	0.58	0.60	
	unit discharge q in m^3/s per metre																
0.02	0.044	0.045	0.046	0.048	0.049	0.050	0.052	0.054	0.055	0.056	0.057	0.058	0.059	0.060	0.061	0.062	0.02
0.03	0.064	0.068	0.070	0.072	0.074	0.076	0.078	0.080	0.082	0.084	0.085	0.087	0.088	0.090	0.092	0.094	0.03
0.04	0.084	0.088	0.090	0.094	0.097	0.100	0.102	0.105	0.108	0.110	0.113	0.116	0.118	0.120	0.122	0.124	0.04
0.05	0.104	0.108	0.112	0.116	0.119	0.122	0.126	0.130	0.133	0.136	0.140	0.143	0.146	0.149	0.152	0.154	0.05
0.06	0.122	0.127	0.132	0.137	0.142	0.146	0.150	0.154	0.158	0.162	0.165	0.168	0.171	0.174	0.178	0.182	0.06
0.07	0.140	0.145	0.150	0.156	0.162	0.167	0.172	0.177	0.182	0.186	0.190	0.195	0.200	0.204	0.208	0.212	0.07
0.08	0.156	0.163	0.170	0.176	0.182	0.188	0.194	0.200	0.206	0.211	0.216	0.221	0.226	0.231	0.236	0.241	0.08
0.09	0.172	0.180	0.187	0.194	0.201	0.208	0.215	0.222	0.228	0.234	0.240	0.246	0.252	0.258	0.263	0.268	0.09
0.10	0.186	0.195	0.204	0.212	0.220	0.228	0.235	0.242	0.249	0.256	0.263	0.270	0.276	0.282	0.288	0.294	0.10
0.11	0.200	0.210	0.219	0.228	0.237	0.246	0.253	0.262	0.270	0.278	0.285	0.292	0.300	0.308	0.314	0.320	0.11
0.12	0.212	0.223	0.234	0.244	0.254	0.264	0.274	0.283	0.292	0.300	0.308	0.316	0.323	0.330	0.338	0.346	0.12
0.13	0.224	0.236	0.248	0.259	0.270	0.280	0.290	0.300	0.310	0.319	0.328	0.337	0.346	0.354	0.362	0.370	0.13
0.14	0.234	0.247	0.260	0.273	0.286	0.297	0.308	0.319	0.330	0.340	0.350	0.359	0.368	0.377	0.386	0.395	0.14
0.15	0.242	0.257	0.272	0.286	0.299	0.312	0.324	0.335	0.346	0.358	0.370	0.380	0.390	0.400	0.410	0.420	0.15
0.16	0.250	0.266	0.282	0.298	0.312	0.326	0.339	0.352	0.364	0.376	0.388	0.399	0.410	0.420	0.430	0.440	0.16
0.17	0.256	0.274	0.292	0.308	0.324	0.339	0.354	0.368	0.381	0.394	0.406	0.418	0.430	0.442	0.453	0.464	0.17
0.18	0.260	0.280	0.299	0.318	0.334	0.350	0.366	0.381	0.396	0.410	0.424	0.437	0.450	0.462	0.474	0.486	0.18
0.19	0.262	0.284	0.305	0.325	0.344	0.362	0.380	0.396	0.410	0.425	0.440	0.454	0.468	0.480	0.492	0.504	0.19
0.20		0.288	0.310	0.331	0.352	0.372	0.390	0.408	0.424	0.440	0.456	0.472	0.486	0.498	0.512	0.525	0.20

w in metres	Upstream head over flume crest H_1 in metres																w in metres
	0.30	0.32	0.34	0.36	0.38	0.40	0.42	0.44	0.46	0.48	0.50	0.52	0.54	0.56	0.58	0.60	
	unit discharge q in m^3/s per metre																
0.21			0.316	0.338	0.360	0.380	0.400	0.419	0.438	0.454	0.472	0.488	0.502	0.518	0.532	0.546	0.21
0.22				0.342	0.366	0.388	0.408	0.428	0.448	0.466	0.484	0.502	0.518	0.532	0.548	0.564	0.22
0.23				0.344	0.370	0.394	0.417	0.438	0.458	0.478	0.496	0.514	0.532	0.550	0.566	0.582	0.23
0.24					0.374	0.400	0.424	0.446	0.468	0.488	0.508	0.528	0.548	0.566	0.584	0.600	0.24
0.25						0.404	0.427	0.452	0.476	0.498	0.519	0.540	0.560	0.578	0.596	0.615	0.25
0.26							0.432	0.458	0.482	0.506	0.528	0.549	0.572	0.592	0.612	0.631	0.26
0.27								0.462	0.489	0.514	0.538	0.562	0.583	0.604	0.624	0.646	0.27
0.28								0.464	0.493	0.520	0.546	0.570	0.594	0.616	0.638	0.659	0.28
0.29									0.496	0.525	0.552	0.578	0.604	0.628	0.650	0.672	0.29
0.30										0.528	0.558	0.586	0.612	0.636	0.660	0.684	0.30
0.31											0.562	0.590	0.618	0.644	0.669	0.694	0.31
0.32												0.594	0.624	0.651	0.679	0.704	0.32
0.33												0.600	0.628	0.658	0.687	0.714	0.33
0.34													0.632	0.662	0.694	0.720	0.34
0.35														0.666	0.698	0.728	0.35
0.36															0.700	0.732	0.36
0.37																0.738	0.37
0.38																0.742	0.38

NOTE: Valid for negligible approach velocity ($h_1 = H_1$)

8.5.2 Evaluation of discharge

As mentioned in Section 8.5.1, the basic head discharge equation for a Crump-de Gruyter adjustable orifice reads

$$Q = C_d C_v \; bw\sqrt{2g(h_1 - w)} \qquad (8\text{-}24)$$

where the discharge coefficient C_d equals 0.94 and the approach velocity coefficient can be obtained from Figure 1.12. Table 8.4 shows the unit discharge q in m^3/s per metre flume breadth as a function of h_1 and w, for negligible approach velocity ($C_v \simeq 1.0$).

If reasonable care and skill has been applied in the construction and installation of a Crump-de Gruyter adjustable orifice, the discharge coefficient may be expected to have an error of about 3%. The method by which the error in the coefficient is to be combined with other sources of error is shown in Appendix II.

8.5.3 Limits of application

The limits of application of the Crump-de Gruyter adjustable orifice are:

a) To obtain modular flow the gate opening (w) should not exceed 0.63 h_1, and the minimum fall over the structure, Δh, should be in accordance with Figure 8.14.

b) The practical lower limit of w is 0.02 m.

c) The bottom of the flume control section should be horizontal and its sides vertical.

d) The thickness of the adjustable gate in the direction of flow should be 0.5 H_1max and the upstream curvature of the gate should equal 0.375 H_1max, leaving a horizontal lip with a length of 0.125 H_1max (see Figure 8.13).

e) The minimum breadth of the flume should be in accordance with Equation 8-23, but b should not be less than 0.20 m.

f) For standard flumes p equals b; p may be changed, however, provided it remains equal to or greater than 0.20 m.

8.6 Metergate

8.6.1 Description

A metergate is rather commonly used in the USA for measuring and regulating flow to ditches. Basically, it is a submerged orifice arranged so that its area is adjustable by a vertical screw lift. It may also be regarded as a submerged calibrated valve gate at the upstream end of a pipe section.

A typical metergate installation is shown in Figure 8.15. Constructional details of the gate with a rectangular gate leaf are shown in Figure 8.16.

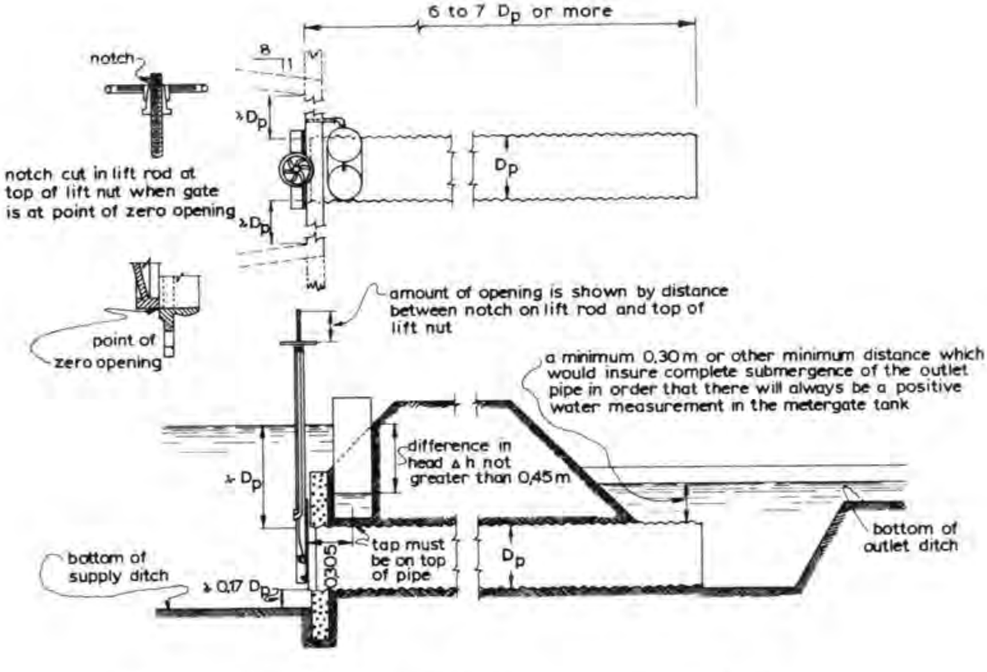

Fig. 8.15. Metergate installation (courtesy of ARMCO).

Usually the metergate is placed at right angles to the centre line of the main canal or lateral from which it diverts flow. If the flow velocity in the main canal becomes significant, it will cause eddies and other flow disturbances along the upstream wingwalls that form the approach to the gate. To prevent such disturbances from reducing the flow through the metergate, the approach to the gate should be shaped so that no velocity concentrations are visible

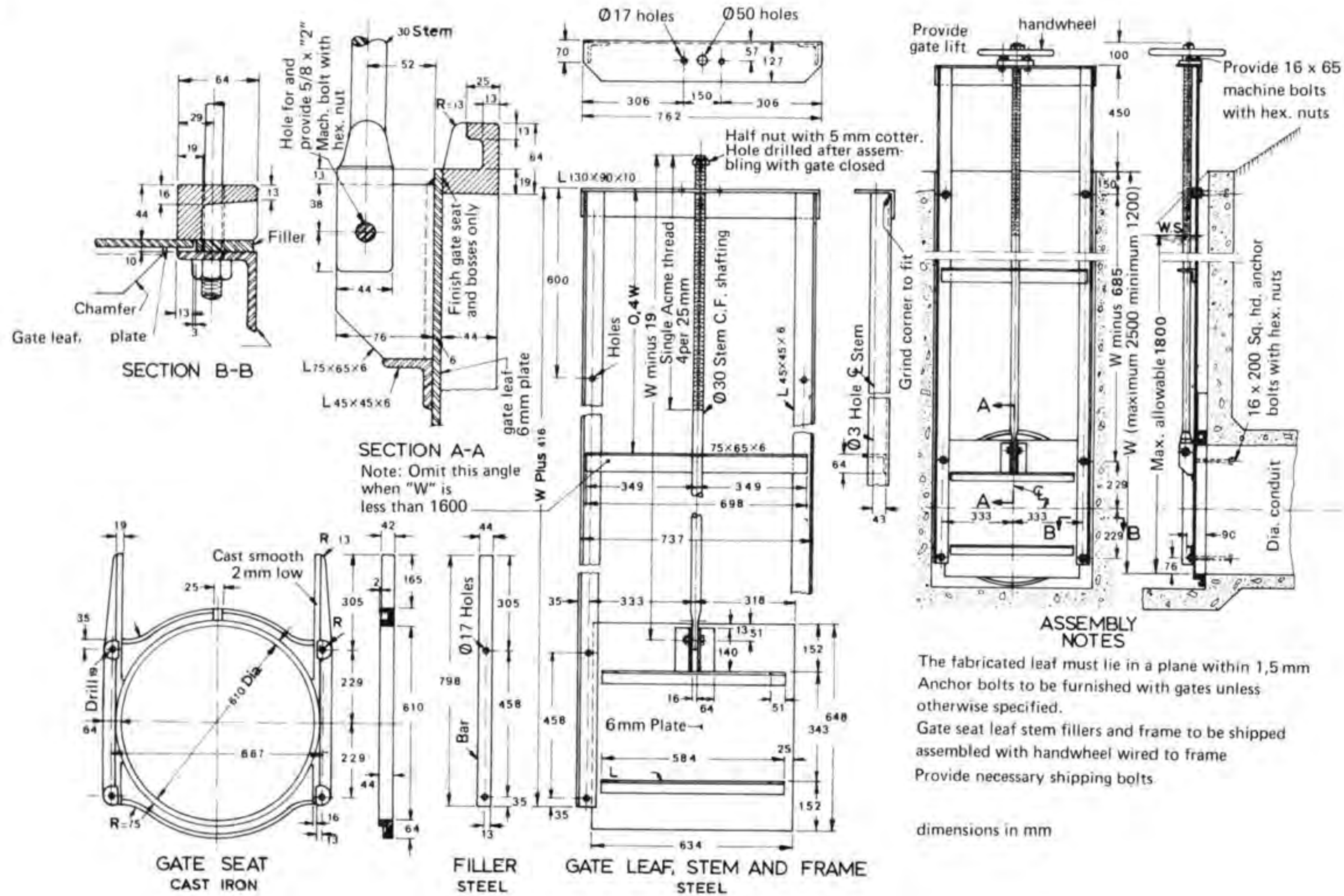

Fig.8.16. Example of screw lift vertical gate (after USBR, 1945).

on the water surface upstream of the orifice. To achieve this, the approach section should have a minimum length of about 5 D_p, where D_p equals the diameter of the pipe and also the diameter of the gate opening.

As explained in Section 1.12, the flow through a submerged orifice is directly related to the differential head over the opening. It is essential that the stilling well intakes (piezometers) be located exactly as they were in the original calibrated metergate.

The upstream piezometer should be placed in the vertical headwall, at least 0.05 m from the gate frame and also 0.05 m from any change in headwall alignment if viewed from the top. The intake should be flush with the headwall surface and at least 0.05 m below minimum water level during operation.

For the downstream piezometer, two locations are possible, depending on the method of discharge evaluation:

- on the centre line of the top of the pipe, at exactly 0.3048 m (1 foot) downstream from the downstream face of the gate. This location is used on most commercially-manufactured[1] gates. The discharge is read from tables which are supplied with each gate;

- on the centre line of the top of the pipe at $D_p/3$ downstream from the downstream gate face. This location is recommended by the U.S.Bureau of Reclamation and is supported by the present writers.The discharge can be evaluated by using equation 8-25 and Figure 8.18 (see Section 8.6.2).

If corrugated pipe is used, the downstream piezometer should always be at the top of a corrugation.

The piezometer location at exactly 0.3048 m downstream from the downstream gate face means that the various metergates are not hydraulic scale models of each other. Another disadvantage is that for small pipe diameters the downstream piezometer is situated in a region with a rapid change of pressure, as illustrated in Figure 8.17. As a result any minor displacement of the piezometer from the tested location will cause large errors in the determination of the differential pressure.

---

[1] *The metergate is commercially manufactured by ARMCO Steel Corporation,P.O.Box 700 Middletown, Ohio 45042, USA. Our listing of this supplier should not be construed as an endorsement of this company or their product by the present writers.*

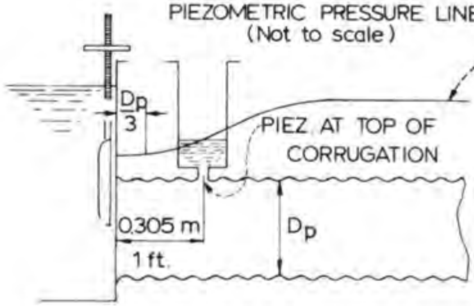

Fig.8.17. Effect of piezometer location on measured head.

Flow through the metergate is proportional to the square root of the head difference, Δh, between the two stilling wells, which may be measured by one of the differential head meters described in Section 2.12. The practical lower limit of Δh is related to the accuracy with which piezometer readings can be made. The recommended lower limit is 0.05 m. If practicable, the upstream water level should be kept at a height which ensures that the metergate operates under large differential heads.

To ensure that the downstream stilling well contains sufficient water for a reading of head to be taken, the pipe outlet must have sufficient submergence.This submergence depends,among other things, on the friction losses in the downstream pipe and the maximum head differential over the stilling wells.On field installations the head differential is usually limited to 0.45 m while the meter pipe must be longer than 6 D_p or 7 D_p so that a submergence of 0.30 m will usually be sufficient. A method by which the required submergence can be calculated is shown in Section 8.6.3.

8.6.2 Evaluation of discharge

Flow through a metergate may be evaluated by the following formula:

$$Q = C_e A_p \sqrt{2g(h_1 - h_w)} \qquad (8\text{-}25)$$

where $A_p = \frac{1}{4}\pi D_p^2$ is the nominal area of the pipe. It should be noted that the coefficient C_e is not the same as the discharge coefficient introduced in the orifice equation derived in Section 1.12, where the orifice area (A) appears in the discharge equation.

Figure 8.18 gives C_e-values as a function of the gate opening for gates with either a rectangular or a circular gate leaf, and with their downstream pressure tap at $D_p/3$ downstream from the downstream face of the gate. The curve for circular leaves was derived from tables published by ARMCO; that for rectangular leaves was taken from the U.S.Bureau of Reclamation, 1961.

Although the curves in Figure 8.18 were obtained for particular approach conditions, all approach sections that comply with the conditions outlined in Section 8.6.4 may be used in combination with the C_e-curves shown. This was demonstrated by tests, conducted by the U.S.Bureau of Reclamation (1961), which showed that C_e-values are not influenced by approach conditions if the gate opening remains less than 50%; in the range from 50% to 75%, the C_e-value may increase slightly. Gate openings greater than 75% are not recommended for discharge regulation since, in this range, the C_e-value shows considerable variation (see also Figure 8.20).

The discharge coefficient shown in Figure 8.18 may be expected to have an error of less than 3% for gate openings up to 50%, and an error of less than 6% for gate openings up to 75%. The method by which this error is to be combined with

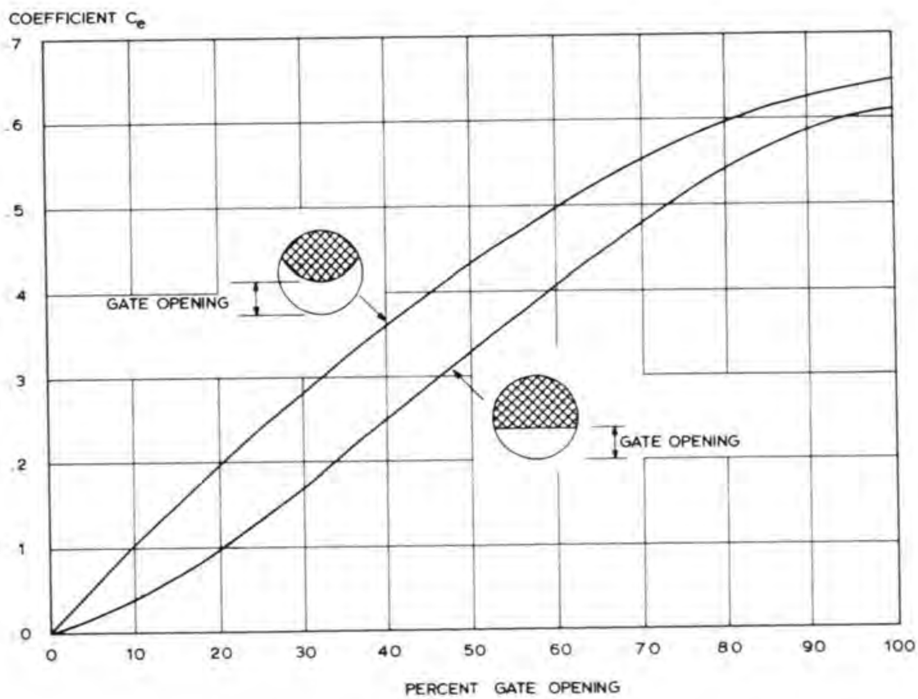

Fig.8.18. C_e-values for pressure tap located at D/3.

other sources of error is shown in Appendix II.

Each commercially-manufactured metergate is accompanied by a discharge table (Imperial units). Generally, these tables are sufficiently accurate, but the U.S. Bureau of Reclamation in some instances found errors of 18% or more. Discharge tables are available for gates ranging from 0.20 m (8") to 1.22 m (48").

Provided that water rises sufficiently high in the downstream stilling well, the degree of submergence does not affect the accuracy of the meter.

8.6.3 Metergate installation

For a metergate to function properly it must be installed at the proper elevation and be of the proper size. To aid in the selection of gate size and elevation we give the following suggestions in the form of an example:

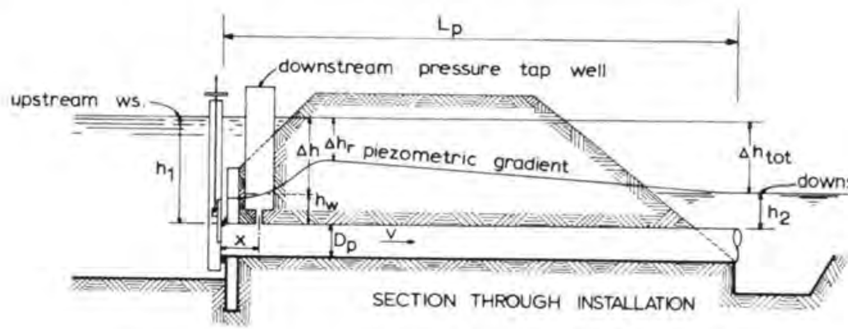

Fig.8.19. Example of metergate installation (USBR, 1961).

Given:

- Upstream water surface elevation 100.00 m.
- Downstream water surface elevation 99.70 m (thus $\Delta h_{tot} = 0.30$ m).
- Turnout discharge 0.140 m^3/s.
- Depth of water in downstream measuring well, h_w, should be 0.15 m above crown of metergate.
- Length of metergate pipe, $L_p = 8.50$ m.
- Submergence of metergate inlet, h_1, should not be less than D_p above the crown of the pipe.
- A metergate with rectangular leaf is used.

Find:

1. Metergate size.
2. Elevation at which metergate should be placed.

1: Metergate size

a) When downstream scour is a problem, an exit velocity has to be selected that will not cause objectionable erosion, say $v \leqslant 0.90$ m/s. From $A_p = Q/v$ we find $A_p \geqslant 0.140/0.90 = 0.156\ m^2$ or $D_p \geqslant 0.445$ m.
An 18-inch ($D_p = 0.457$ m) metergate is required.

b) When downstream scour is not a problem, we select a metergate that operates at gate openings not exceeding 75% (see Section 8.6.2). For 75% gate opening the coefficient $C_e = 0.51$ (Fig.8.18) and the maximum differential head $\Delta h \simeq 1.8\ \Delta h_r$ (Fig.8.20). Taking into account some losses due to friction in the pipe, we assume $\Delta h \simeq 1.60\ \Delta h_{tot} = 1.60 \times 0.30 = 0.48$ m. From Equation 8-25: $Q = C_e A_p\ (2g\Delta h)^{0.5}$ we obtain the minimum area of the pipe: $A_p \geqslant 0.0895\ m^2$ and thus $D_p \geqslant 0.34$ m. Our initial estimate is a 14-inch metergate ($D_p = 0.356$ m).

c) Check capacity of selected gate. It is common practice to express the loss of hydraulic head as a function of the velocity head, $v^2/2g$.

For a metergate the velocity head in the pipe can be found by substituting the continuity equation $Q/A_p = v$ into Equation 8-25, which leads to

$$\bar{v} = C_e\sqrt{2g\Delta h} \qquad (8\text{-}26)$$

or

$$\frac{v^2}{2g} = C_e^2\ \Delta h \qquad (8\text{-}27)$$

The total (available) loss of head over the structure, Δh_{tot}, equals the sum of the energy loss over the gate, the friction losses in the meterpipe, and the exit losses, so that:

$$\Delta h_{tot} = \Delta h_{gate} + \xi_f\ v^2/2g + \xi_{ex}\ v^2/2g \qquad (8\text{-}28)$$

If we assume that no recovery of kinetic energy occurs at the pipe exit (ξ_{ex}=1.0), we can write

$$\Delta h_{tot} = \Delta h_r + \xi_f\ v^2/2g \qquad (8\text{-}29)$$

where Δh_r denotes the drop of piezometric head to a recovery point downstream of the downstream pressure tap which equals the energy losses over the gate plus the velocity head in the meterpipe.

The substitution of Equation 8-27 and division by Δh leads to

$$\Delta h_{tot}/\Delta h = \Delta h_r/\Delta h + \xi_f C_e^2 \qquad (8\text{-}30)$$

where the friction loss coefficient ξ_f equals fL_p/D_p (assume f = 0.025 for concrete and steel pipes) and values of C_e and $\Delta h_r/\Delta h$ can be obtained from Figures 8.18 and 8.20 respectively as a function of the gate opening.

SYMBOL	D_p INCH	APPROACH SECTION			
		FLOOR		SIDE WALLS	
		SLOPE	DISTANCE BELOW INVERT OF ENTRANCE	VIEW IN PLAN	DISTANCE FROM EDGE OF ENTRANCE
Δ	18	LEVEL	1.0 D_p	PARALLEL	3.0 D_p
o	24	LEVEL	0.63 D_p	PARALLEL	2.25 D_p
+	24	1:2 DOWNWARD	0.17 D_p	8:1 FLARING	0.25 D_p

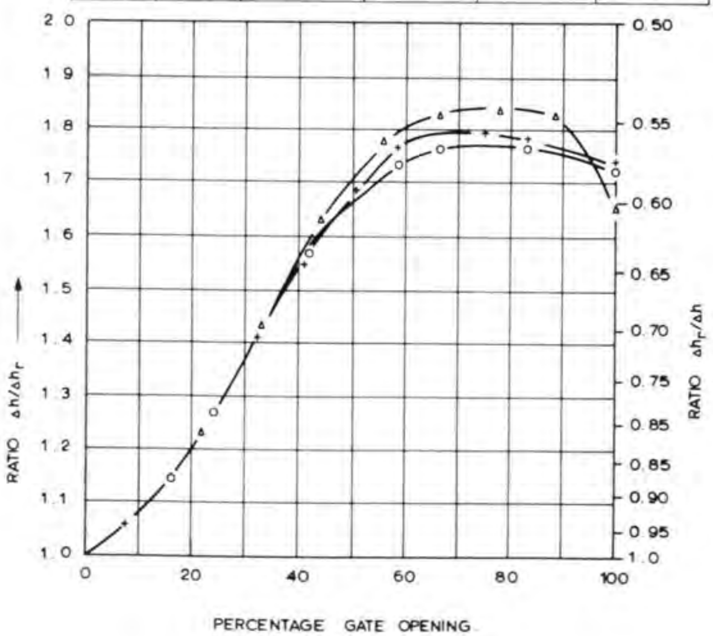

Fig.8.20. Gate opening versus $\Delta h/\Delta h_r$.

In our example $\Delta h_{tot} = 0.30$ m and $\xi_f = fL_p/D_p = 0.025 \times 8.50/0.356 = 0.60$. For 75% gate opening $C_e \simeq 0.51$ and the ratio $\Delta h/\Delta h_r \simeq 1.80$, so that according to Equation 8-30 the maximum value of $\Delta h = 0.42$ m. Using this adjusted value of Δh, turnout capacity at 75% gate opening equals

$$Q \simeq 0.51 \times \tfrac{1}{4}\pi \times 0.356^2 \; (2g \times 0.42)^{\frac{1}{2}} \simeq 0.146 \text{ m}^3/\text{s}$$

A 14-in metergate is adequate.

2: Elevation at which metergate should be placed

If the differential head over the metergate structure is a constant, in our example $\Delta h_{tot} = 0.30$ m, the head difference Δh measured between the two wells is at its maximum with gate openings of around 50%. Using Equation 8-30 the following Δh-values can be computed:

gate opening	35%	40%	50%	55%	60%	75%
Δh (m)	0.399	0.437	0.452	0.458	0.454	0.422

- To meet the requirement of water surface 0.15 m above the crown of the pipe (0.05 m above bottom of well) in the downstream well, elevation of crown entrance would be set at

$$EL = 100.00 - \Delta h_{max} - h_w = 100.00 - 0.46 - 0.15 = 99.39 \text{ m}$$

- To meet the upstream submergence requirement, h_1, of 1.0 D_p, the crown of the pipe entrance should be set at EL = $100.00 - D_p \simeq 99.64$ m.

The depth requirement for a measurable water surface in the downstream well is the governing factor and the metergate should be set with its crown of entrance not higher than EL = 99.39 m.

8.6.4 Limits of applications

The limits of application of the metergate are:

a) The crown of the pipe entrance should have an upstream submergence of 1.0 D_p or more.

b) Submergence of the pipe outlet should be such that the water surface in the downstream well is not less than 0.15 m above the crown of the pipe.

c) The approach channel should be such that no velocity concentrations are visible upstream of the gate (see Fig.8.15).

d) The length of the gate pipe should be 6 D_p to 7 D_p or more.

e) The head differential over the stilling wells should not be less than 0.05 m. Its practical upper limit is about 0.45 m.

f) During operation (flow measurement), gate openings should not be greater than 75%.

g) If Figure 8.18 is used to obtain C_e-values, the downstream pressure tap should be located at exactly $D_p/3$ downstream from the downstream face of the gate.

h) The downstream pressure tap should be located on the centre line of the top of the pipe. The intake pipe should be flush with the inside surface of the pipe and absolutely vertical. If corrugated pipe is used the intake should be at the top of a corrugation.

i) The bottom of the approach section should be at least 0.17 D_p below the invert of the gate opening.

8.7 Neyrpic module

8.7.1 Description

The Neyrpic module[1] was designed to allow the passage of an almost constant flow from an irrigation canal in which the variation of the water level is restricted. The structure consists of a fixed weir sill with a 60-degree sloping upstream face and a 12-degree sloping downstream face. The weir crest is rounded, its radius equal to 0.2 h_d, where h_d is the design head. Above the weir either one or two steel plates are fixed in a well defined position. These sloping (35-degree) sharp-edged plates cause an increase of contraction of the outflowing jet when the upstream head increases. The "near constant" orifice discharge per unit width is a function of the height of the inclined blade above the weir. Since this height cannot be altered the only way to regulate flow is to combine several orifices of different widths into one structure. The minimum width of an orifice is 0.05 m which coincides with 0.005 m^3/s for the X1-type module shown in Figure 8.21.

[1] *The module was developed and is commercially manufactured by Neyrpic, Av.de Beauvert, Grenoble, France. Our listing of this supplier should not be construed as an endorsement of this company or their product by the present writers.*

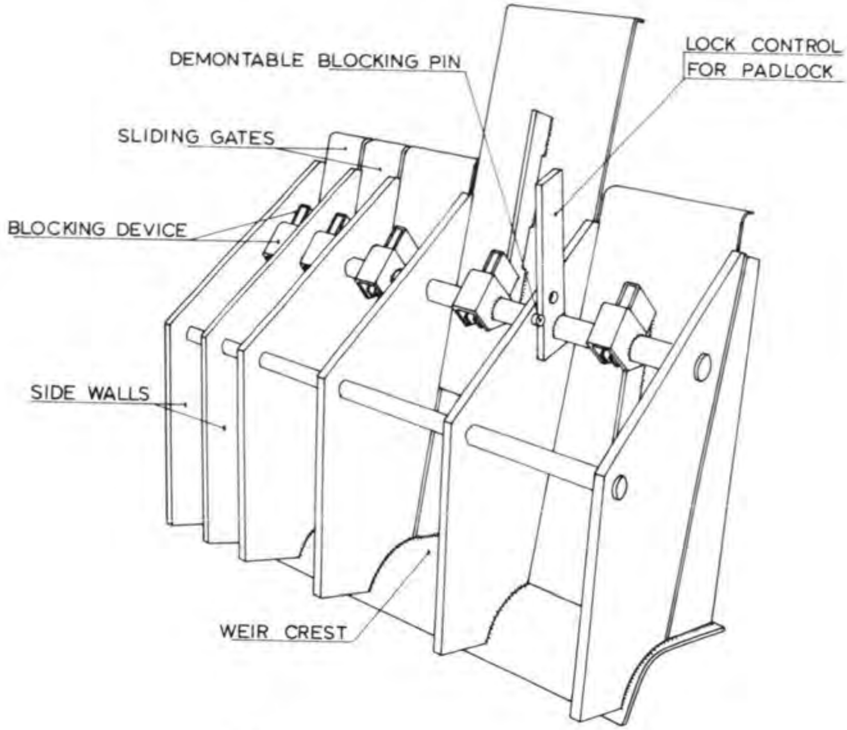

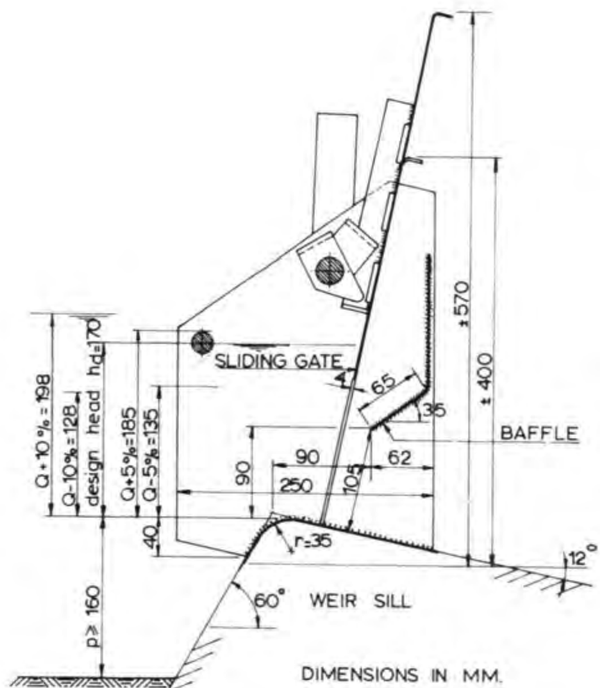

Fig.8.21. Module type X 1 dimensions (after NEYRPIC).

Photo 1. Neyrpic module type X60.

Flow through the structure is regulated by opening or closing sliding gates. These gates are locked in place either fully opened or fully closed since partially opened gates would disturb the contraction of the jet.

The gates slide in narrow grooves in the 0.01 m thick vertical steel divide plates. The position of the gates should be such that in an opened position the orifice flow pattern is not disturbed. Possible gate positions are shown in Figures 8.21 and 8.22.

Essentially two types of modules are available:

- Type X1*: This single baffle module is shown in Figure 8.21 and has a unit discharge of 0.100 m^2/s.
- Type XX2*: This double baffle module has two inclined orifice blades, the upstream one having the dual function of contracting the jet at low heads and of

* *The Roman numeral stands for the discharge in l/s per 0.10 m and the Arab numeral 1 or 2 stands for the number of baffles.*

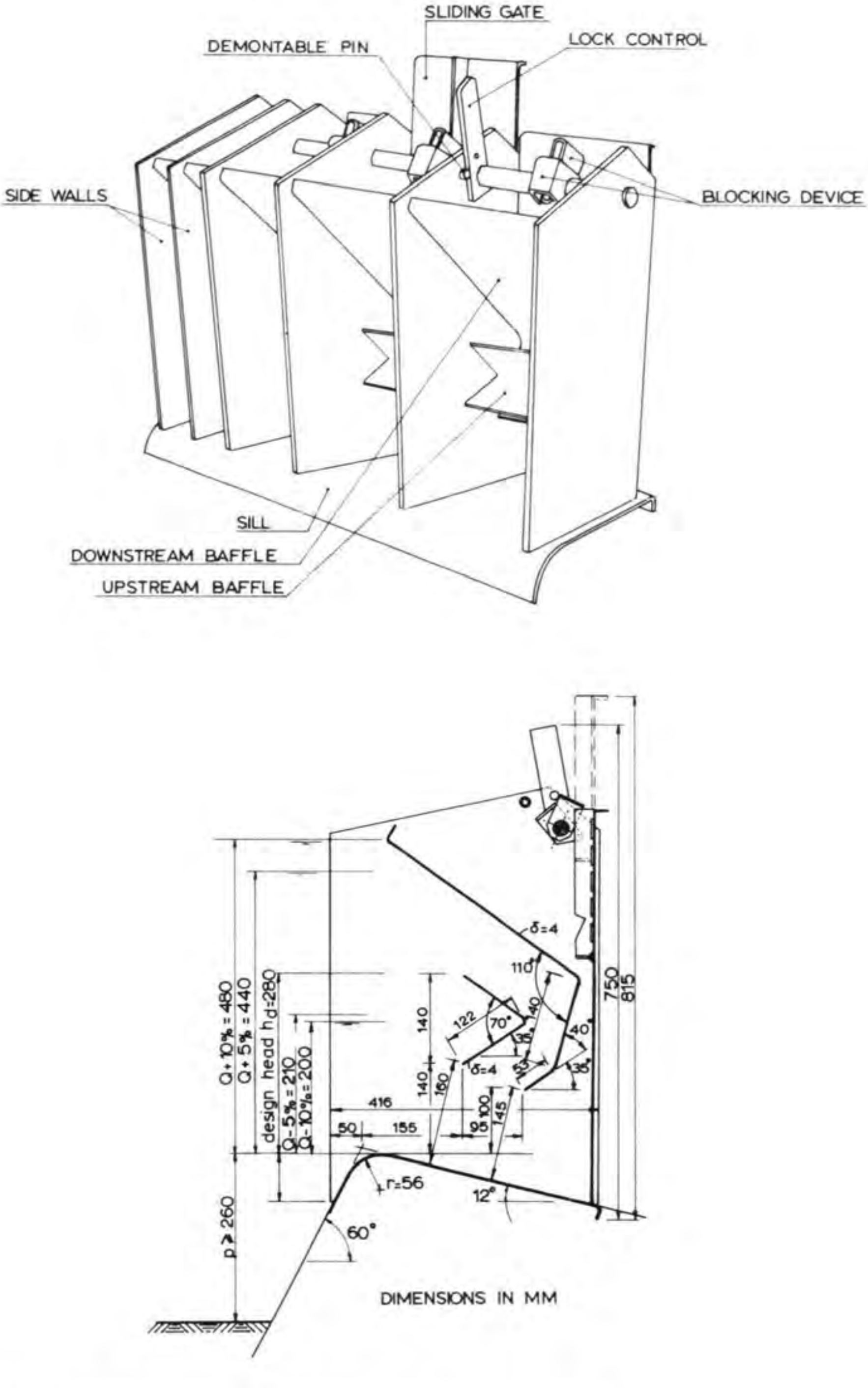

Fig.8.22. Module type XX2 dimensions (after Neyrpic).

acting as a "weir" at high heads. Water passing over the upstream blade is deflected in an upstream direction and causes additional contraction of the jet through the downstream orifice. As a result the discharge through the structure remains within narrow limits over a considerable range of upstream head. The type XX2 has a unit discharge of 0.200 m^2/s. Details of the module are shown in Figure 8.22.

If unit discharges other than those given in the examples are required, the module may be scaled up according to Froude' scale law.

8.7.2 Discharge characteristics

At low heads the upper nappe surface is not in contact with the inclined baffle plate and the structure acts as a short-crested weir with rectangular control section. According to Section 1.10, the head-discharge equation for such a weir reads:

$$Q = C_d C_v \frac{2}{3}\left[\frac{2}{3} g\right]^{0.5} bh_1^{1.5} \tag{8-31}$$

The discharge coefficient C_d is shown in Figure 8.23 as a function of the dimensionless ratio H_1/r. Since for practical reasons h_1 is used instead of H_1, the approach velocity coefficient C_v was introduced.
The value of $C_v = (H_1/h_1)^{3/2}$ is related to the ratio

$$C_d\, h_1\, b/(h_1 + p)B$$

and can be read from Figure 1.12.

If the weir discharge approximates the design discharge plus 5%, the upper nappe surface touches the inclined baffle plate and orifice flow commences. With rising head, flow passes through a transitional zone to stable orifice flow. As shown in Section 1.12 the modular discharge through an orifice equals:

$$Q = C_e\, A\sqrt{2g\Delta h} \tag{8-32}$$

where

- C_e = the effective discharge coefficient which decreases with increasing head due to contraction
- A = area of the orifice
- Δh = head over the centre of the orifice.

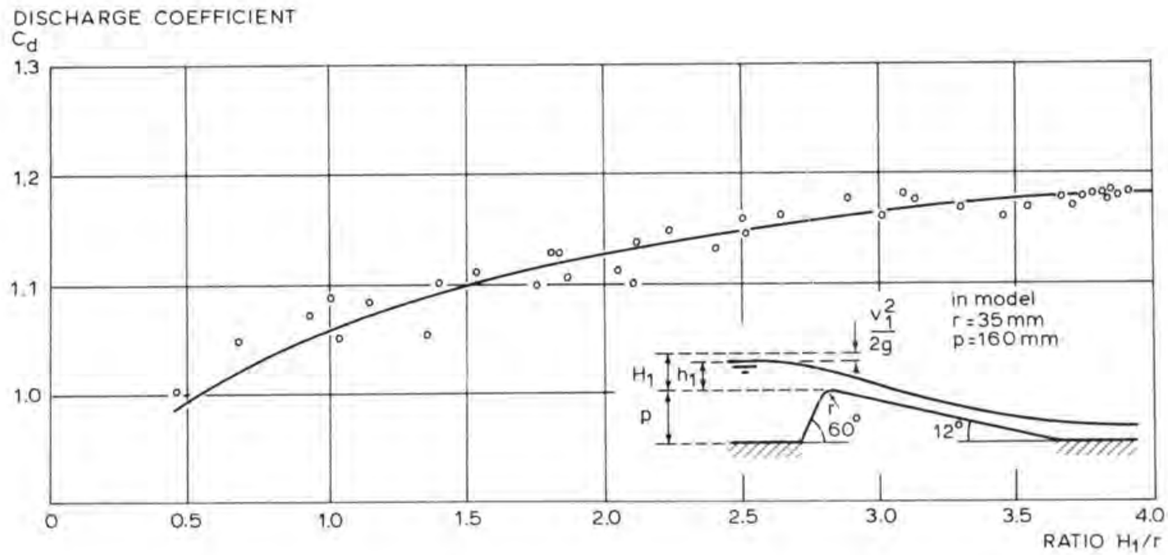

Fig. 8.23. C_d-values as a function of the ratio H_1/r.

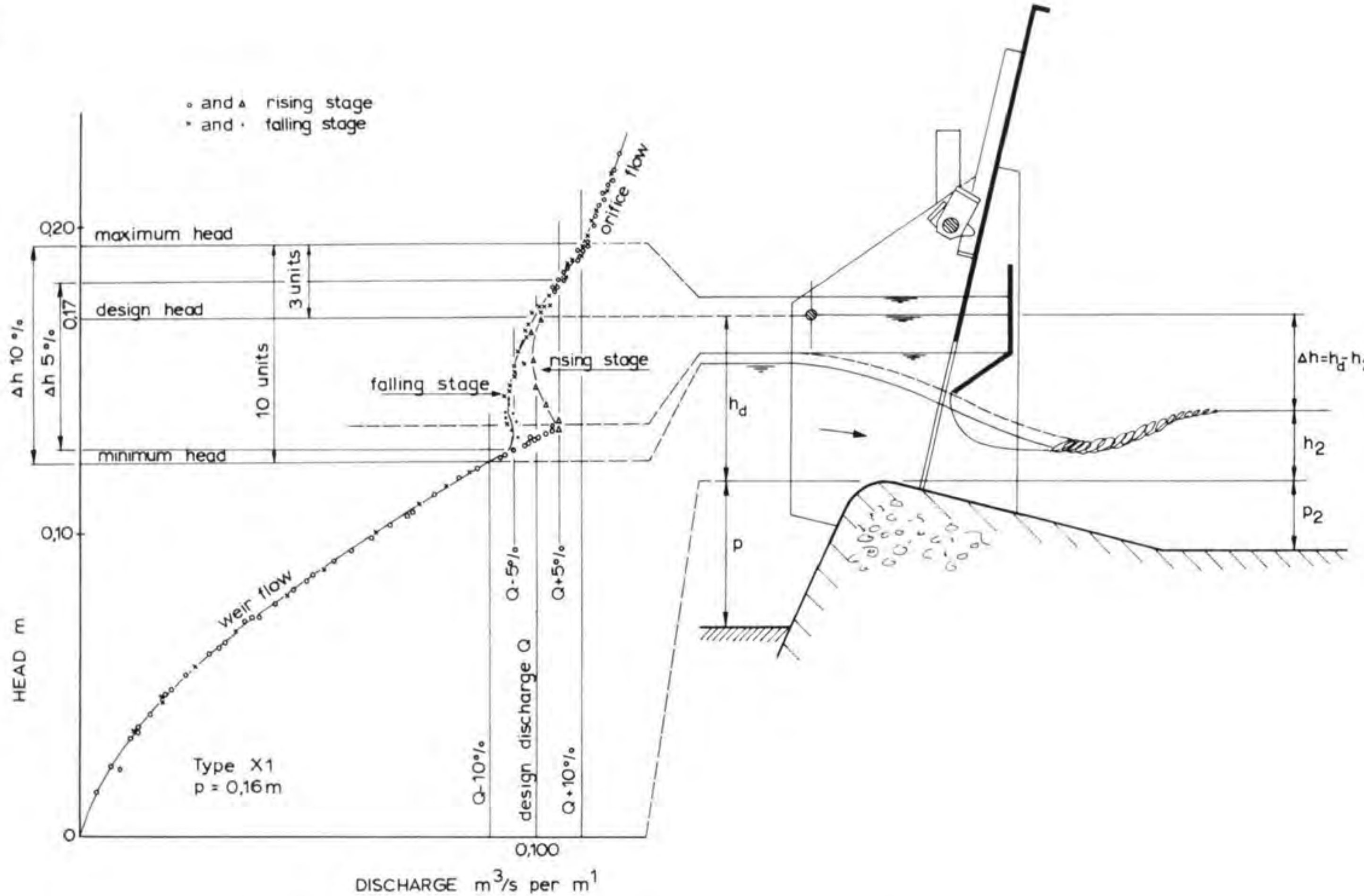

Fig.8.24. Discharge characteristics of Neyrpic module Type X1.

For the XX2-type module, flow characteristics are almost the same as those of the X1-type until the head h_1 rises above the upstream baffle. The only difference is that the distance between the lower edge of upstream baffle and weir crest is such that the baffle touches the upper nappe surface at design discharge Q instead of at Q + 5%. Figure 8.22 shows that the upstream baffle is overtopped if the upstream head exceeds design head.

As soon as the overflowing water becomes effective (at Q =+ 5%) the upstream orifice gradually submerges and flow decreases until the smaller downstream orifice becomes effective. Flow characteristics of the XX2-type module are illustrated in Figure 8.25.

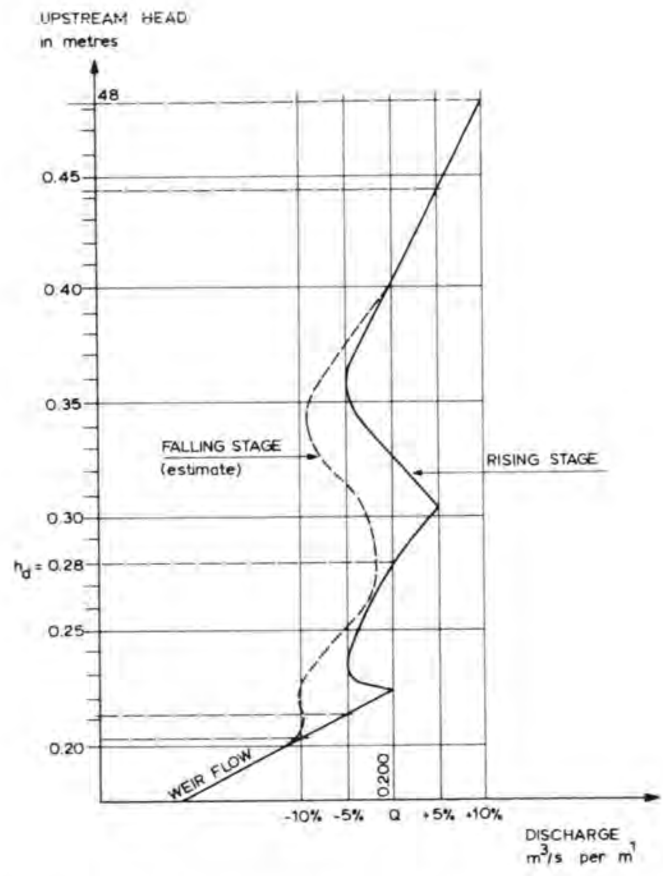

Fig.8.25. Discharge characteristics of Neyrpic module type XX2 (rising stage).

The discharge through a module constructed with reasonable care and skill and in accordance with the dimensions shown in Figures 8.21 and 8.22 will vary some 10% around the design discharge provided that the upstream head is kept between given limits.

Sometimes the upstream head is maintained between narrower limits, so that the discharge deviates no more than 5% from the design value. Due to the difference in the module's behaviour with either rising or falling stage, however, the 5% range is not well defined.

To keep the module functioning properly, frequent maintenance is required.

8.7.3 Limits of application

The limits of application of the Neyrpic module are:

a) The upstream water level should be kept between the limits shown in Figures 8.21 and 8.22.

b) To reduce the influence of the approach velocity on the flow pattern through the module, the ratio h_d/p should not exceed unity.

c) To prevent the tailwater channel bottom from influencing the flow pattern through the orifice, the ratio p_2/h_d should not be less than 0.35.

d) To obtain modular flow, the ratio h_2/h_d should not exceed 0.60.

8.8 Danaïdean tub

8.8.1 Description

The Danaïdean tub is a vessel which receives a flow of water from above and discharges it through a (circular) orifice or a (rectangular) slot in its bottom. After some time the water surface in the Danaïdean tub stabilizes to a head h_1, being the head that makes the orifice discharge at the same rate as water flows into the tub ($Q = Q_{in} = Q_{out}$). The head h_1 can be read by means of a piezometer as shown in Figure 8.26. If the area A of the orifice is known, the discharge can be calculated (see Section 8.8.2). If the head-discharge equations are to be applicable, however, the contraction of the jet must not be hindered. Therefore, the bottom of the tub must have a minimum clearance of d/δ to the free water surface below the tub. Here δ denotes the ratio of the cross-sectional area of the fully contracted jet to that of the efflux section. The ratio δ is known as the contraction coefficient.

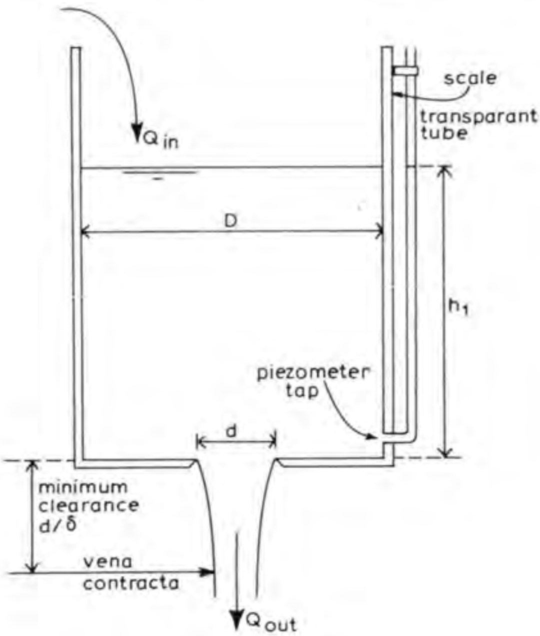

Fig.8.26. Danaïdean tub (circular).

The bottom of the tub must be smooth and plane so that the velocity component along the bottom (upstream face of orifice plate) is not retarded. Provided that the tub bottom has a perfectly plane surface, it may be horizontal or sloping under an angle β as shown in Figure 8.27.

8.8.2 Evaluation of discharge

To determine the discharge through the opening in the Danaïdean tub, we use an equation similar to Equation 1-67. This reads:

$$Q = C_d \, A\sqrt{2gh_1} \tag{8-33}$$

The discharge coefficient, C_d, depends on the contraction of the jet, which, obviously, is a function of the boundary geometry of the tub. Sufficient values of the contraction coefficient are given in Table 8.5 to permit interpolation for any boundary condition.

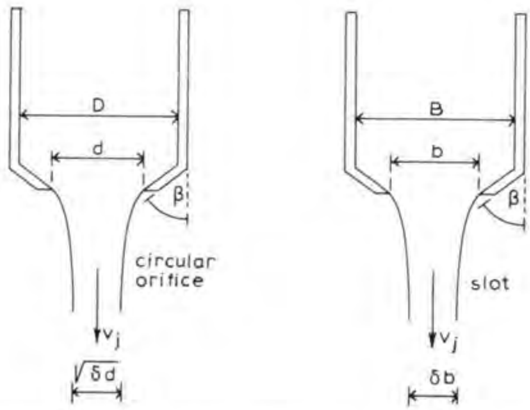

Fig.8.27. Definition sketch for orifice (circular) and slot (rectangular).

TABLE 8.5. COEFFICIENTS OF JET CONTRACTION

$\frac{b}{B}$ or $\frac{d}{D}$	$\beta = 45^0$ δ	$\beta = 90^0$ δ	$\beta = 135^0$ δ	$\beta = 180^0$ δ
0.0	0.746	0.611	0.537	0.500
0.1	0.747	0.612	0.546	0.513
0.2	0.747	0.616	0.555	0.528
0.3	0.748	0.622	0.566	0.544
0.4	0.749	0.631	0.580	0.564
0.5	0.752	0.644	0.599	0.586
0.6	0.758	0.662	0.620	0.613
0.7	0.768	0.687	0.652	0.646
0.8	0.789	0.722	0.698	0.691
0.9	0.829	0.781	0.761	0.760
1.0	1.000	1.000	1.000	1.000

(after VON MISES, 1917)

By using the contraction coefficient in the continuity and pressure velocity equations (Bernoulli), ROUSE (1948) gives the following relationships for the discharge coefficient of water flowing through a slot:

$$C_d = \frac{\delta}{\sqrt{1 - \delta^2\ (b/B)^2}} \tag{8-34}$$

The corresponding expression for C_d for discharge from an orifice reads

$$C_d = \frac{\delta}{\sqrt{1 - \delta^2 \; (d/D)^4}} \tag{8-35}$$

Since the right-hand term of each equation is a function of quantities depending on boundary geometry, the discharge coefficient C_d can be evaluated. A typical plot of C_d versus boundary geometry is shown in Figure 8.28 to indicate its trend in comparison with that of δ.

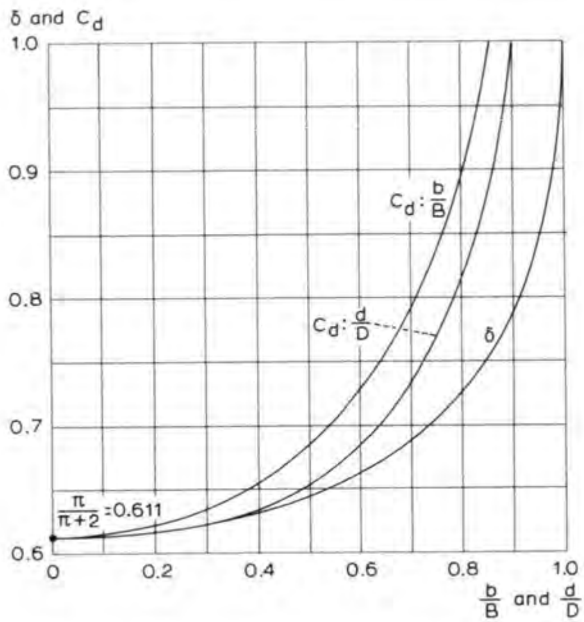

Fig. 8.28. Variation of efflux coefficients with boundary proportions. Valid if $\beta = 90^o$. (After ROUSE, 1949.)

If reasonable care and skill has been applied in the construction and installation of a Danaïdean tub, the discharge coefficient may be expected to have an error of about 2%. The method by which this error is to be combined with other sources of error is shown in Appendix II.

The reader may be interested to note that the discharge equation and related coefficient values given also apply if the orifice is placed at the end of a straight pipe which discharges its jet free into the air.

8.8.3 Limits of application

The limits of application of the Danaïdean tub are:

a) The edge of the opening should be sharp and be in accordance with the profile shown in Figure 5.1.

b) The ratios b/B and d/D should not exceed 0.8.

c) The contraction of the jet must not be hampered. To ensure this, the bottom of the tub must have a minimum clearance of d/δ (or b/δ) above the downstream water level.

8.9 Selected list of references

1. AL-KHOUDARI, N.:The module à masque type-X. Agric.Univ.Wageningen. M.Sc.Thesis 1973. 39 pp.

2. ARMCO DRAINAGE & METAL PRODUCTS INC.: Water measurement tables. Portland, Oregon 1951.

3. FRANKE, P.G., and VALENTIN, F.: The determination of discharge below gates in case of variable tailwater conditions. J.of Hydraulics Res. 7 (1969), No.4, pp.433-447.

4. GENTILINI, B.:Flow under inclined or radial sluice gate. Technical and experimental results. La Houille Blanche 1947, Vol.2.

5. GRUYTER, P.de: Een nieuw type aftap - tevens meetsluis. De Waterstaats-ingenieur. 1926 (No.12) and 1927 (No.1). Batavia, Java.

6. HENDERSON, F.M. Open channel flow. The MacMillan Comp., New York 1966. 522 pp.

7. HENRY, H: Discussion to Diffusion of submerged jets. Transitions of the American Society of Civil Engineers. 115 (1950)., pp.687-697.

8. KRUSE, E.A.:The constant-head orifice farm turnout. U.S.Dept.of Agric. Report ARS 41-93, Fort Collins, Col. 1965. 24 pp.

9. METZLER, D.E.: A Model Study of Tainter Gate Operation. State Univ.of Iowa Master's Thesis. August 1948.

10. MISES, R.von: Berechnung von Ausfluss und Überfällzahlen. Z.des Vereines deutscher Ingenieure 61 (1917). No.21, pp.447-452; No.22, pp.469-474; No.23, pp.493-498. Berlin.

11.NEYRPIC: Irrigation canal equipment. Ets Neyrpic, Grenoble, France. 1955. 32 pp.

12. ROMIJN, D.G.: Meetsluizen ten behoeve van irrigatiewerken. Handleiding uitgegeven door de "Vereniging van Waterstaat-ingenieur in Nederlandsch-Indië." Bandung 1938. 58 pp.

13. SCHUSTER, J.C.: Water measurement procedures. Irrigation operators' workshop. U.S.Bureau of Reclamation, Denver, Col.1970. Report REC-OCE-70-38. 49 pp.

14. STOKMANS, J.A.: Metingen aan de constant-head-orifice-turnout. Agric. Univ., Wageningen. M.Sc.Thesis not published. (1970)

15. TOCH, A.: The Effect of a Lip Angle Upon Flow Under a Tainter Gate. State Univ.of Iowa Master's Thesis, February 1952.

16. U.S.ARMY ENGINEER WATERWAYS EXPERIMENT STATION: Model Study of the spillway for New Lock and Dam No.1. St.Lucie Canal, Florida. Technical Memorandum No.153-1, Vicksburg, Miss., June 1939.

17. U.S.ARMY ENGINEER WATERWAYS EXPERIMENT STATION: Spillway for New Cumberland Dam, Ohio River, West Virginia. Technical Memorandum No.2-386, Vicksburg, Miss.,July 1954.

18. U.S.ARMY ENGINEER WATERWAYS EXPERIMENT STATION: Stilling Basin for Warrior Dam, Ohio River, West Virginia. Technical Report No.2-485, Vicksburg, Miss., July 1958.

19. U.S.ARMY ENGINEER WATERWAYS EXPERIMENT STATION: Spillways and Stilling Basins, Jackson Dam, Tombigbee River, Alabama. Technical Report No.2-531, Vicksburg, Miss., January 1960.

20. U.S.ARMY ENGINEER WATERWAYS EXPERIMENT STATION: Hydraulic design criteria. Sheets 320-4 to 320-7. Vicksburg, Miss. 1960.

21. U.S.BUREAU OF RECLAMATION: Water measurement manual. U.S.Gov.printing office, Washington. Second Ed. 1967. 326 pp.

22. U.S.SOIL CONSERVATION SERVICE: National Engineering Handbook. Chap.9, Section 15: Measurement of irrigation water. U.S.Government printing office, Washington. 1962. 70 pp.

9 Miscellaneous structures

9.1 Divisors

9.1.1 Description

Many of the world's older irrigation systems are co-operative stock companies in which the individual water users have rights to proportional parts of the supply of water furnished by their canal system, the divisions being in the ratio of the stock owned in the canal company. Under this system it was often considered unnecessary to measure the water so long as each user got his proportionate part of it. This led to the use of divisors or division boxes as have been described by CONE (1917). These divisors, however, are not recommended for use as measuring devices where any considerable reliability is required, and will not be described here. Our attention will be confined to divisors which can be used both for measuring and for making a fair division of the water.

Most divisors are built to divide the flow in a ditch into two ditches, but they are sometimes made to divide the flow into three parts or more. The divisor consists essentially of a short-crested weir and a movable partition board. The partition board is hinged as shown in Figure 9.1. Provision is usually made for locking the board to a timber or steel profile across the weir crest when the desired set has been made.

Photo 1. Proportional divisor with fixed pier in between the two weirs.

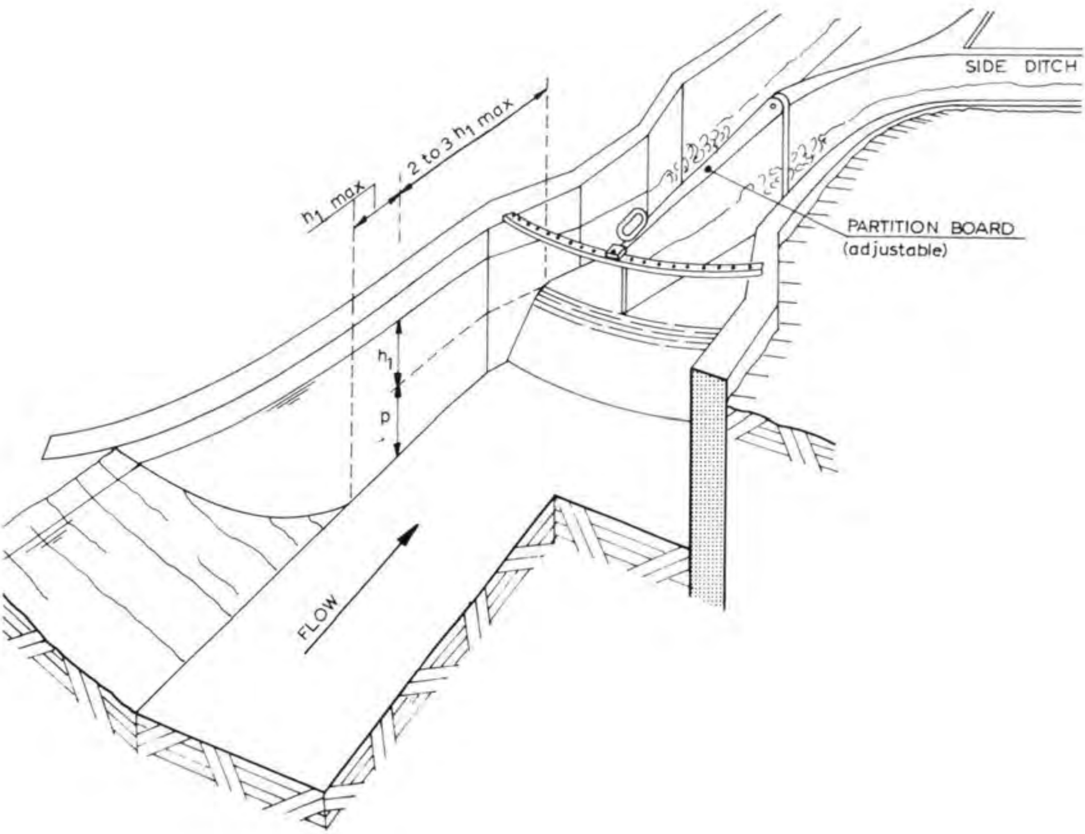

Fig.9.1. Divisor (adapted from Neyrpic).

The structure shown in Figure 9.1 was designed by Neyrpic and consists of a slightly curved weir sill with a 60-degree sloping upstream face and a 12-degree sloping downstream face. The weir crest is rounded, its radius being equal to $r = 0.2\ h_1 max$, where $h_1 max$ is the maximum upstream head. Viewed from above, the weir crest is curved with a minimum radius of 1.75 b; the crest width b should not be less than $2\ H_1 max$.

The upstream head, h_1, is to be measured in a rectangular approach channel at a distance of between $2\ h_1 max$ and $3\ h_1 max$ upstream from the weir crest.

The upstream edge of the partition board should be sharp (≤ 0.005 m thick) and should be located immediately downstream of the weir crest, in the area where flow is super-critical.

A disadvantage of sharp-edged partition boards is that trash and floating debris are caught, so that frequent maintenance is required to obtain a proportional division of water.

The flow-wise weir profile is not a determining factor in the proportional division of water. In principle, any short-crested weir is suitable, especially the triangular profile two-dimensional weir (Section 6.3) and the cylindrical crested weir (Section 6.7).

9.1.2 Evaluation of discharge

According to Section 1.10, the basic head-discharge equation for a short-crested weir with a rectangular control section reads

$$Q = C_d C_v \frac{2}{3}\left[\frac{2}{3} g\right]^{\frac{1}{2}} b h_1^{1.5} \tag{9-1}$$

where the approach velocity coefficient C_v may be read from Figure 1.12 as a function of the area ratio $C_d A^* / A_1$. The discharge coefficient of the Neyrpic weir profile is a function of the ratio H_1/r as shown in Figure 9.2.

The modular C_d-values shown in Figure 9.2 are valid if the weir crest is sufficiently high above the average bed of both the approach and tailwater channel so as not to influence the streamline curvature above the weir crest. To ensure this, the ratio p/H_1 should not be less than 0.33 and the ratio p_2/H_1 should not be less than 0.35. To obtain modular flow, the ratio H_2/H_1 should not exceed 0.60. It should be noted that the weir width b is measured along the curved weir crest.

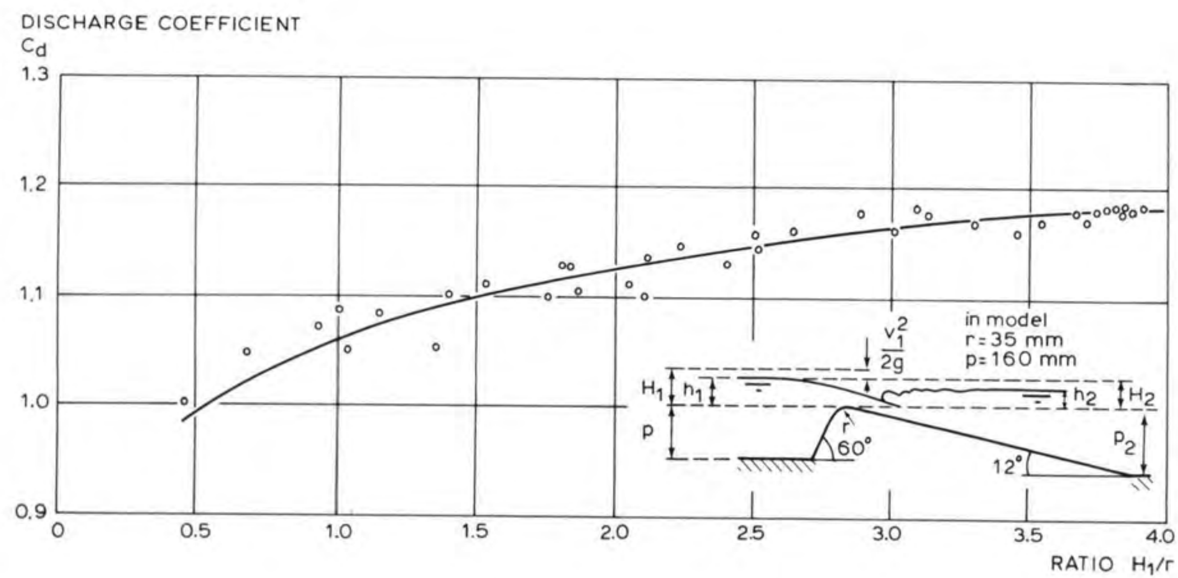

Fig.9.2. C_d-values as a function of the ratio H_1/r.

The accuracy of the discharge coefficient of a well maintained divisor which has been constructed with reasonable care and skill will be sufficient for field conditions. The error in the product C_dC_v may be expected to be less than 5 per cent. The method by which this error is to be combined with other sources of error is shown in Appendix II.

9.1.3 Limits of application

The limits of application of a divisor equipped with a Neyrpic weir crest are:

a) The upstream head over the weir crest h_1 should be measured at a distance of 2 to 3 times $h_1$max upstream from the weir crest. The recommended lower limit of h_1 = 0.06 m.

b) To prevent water surface instability in the approach channel, the ratio p/H_1 should not be less than 0.33.

c) To prevent the tailwater channel bottom from influencing the flow pattern over the weir crest, the ratio p_2/H_1 should not be less than 0.35.

d) To reduce boundary layer effects of the vertical side walls, the ratio b/H_1 should not be less than 2.0.

e) To obtain sensibly two-dimensional flow over the weir crest, the horizontal radius of curvature of the weir crest should not be less than 1.75 b.

f) The ratio H_1/r should not be less than 0.20.

g) To obtain modular flow, the ratio H_2/H_1 should not exceed 0.60.

9.2 Pipes and small syphons

9.2.1 Description

On irrigated farms, short sections of pipe are frequently used to distribute water over the fields. Commonly used for this purpose are plastic, aluminium, or galvanized steel pipes and siphons. Some examples are shown in Figure 9.3.

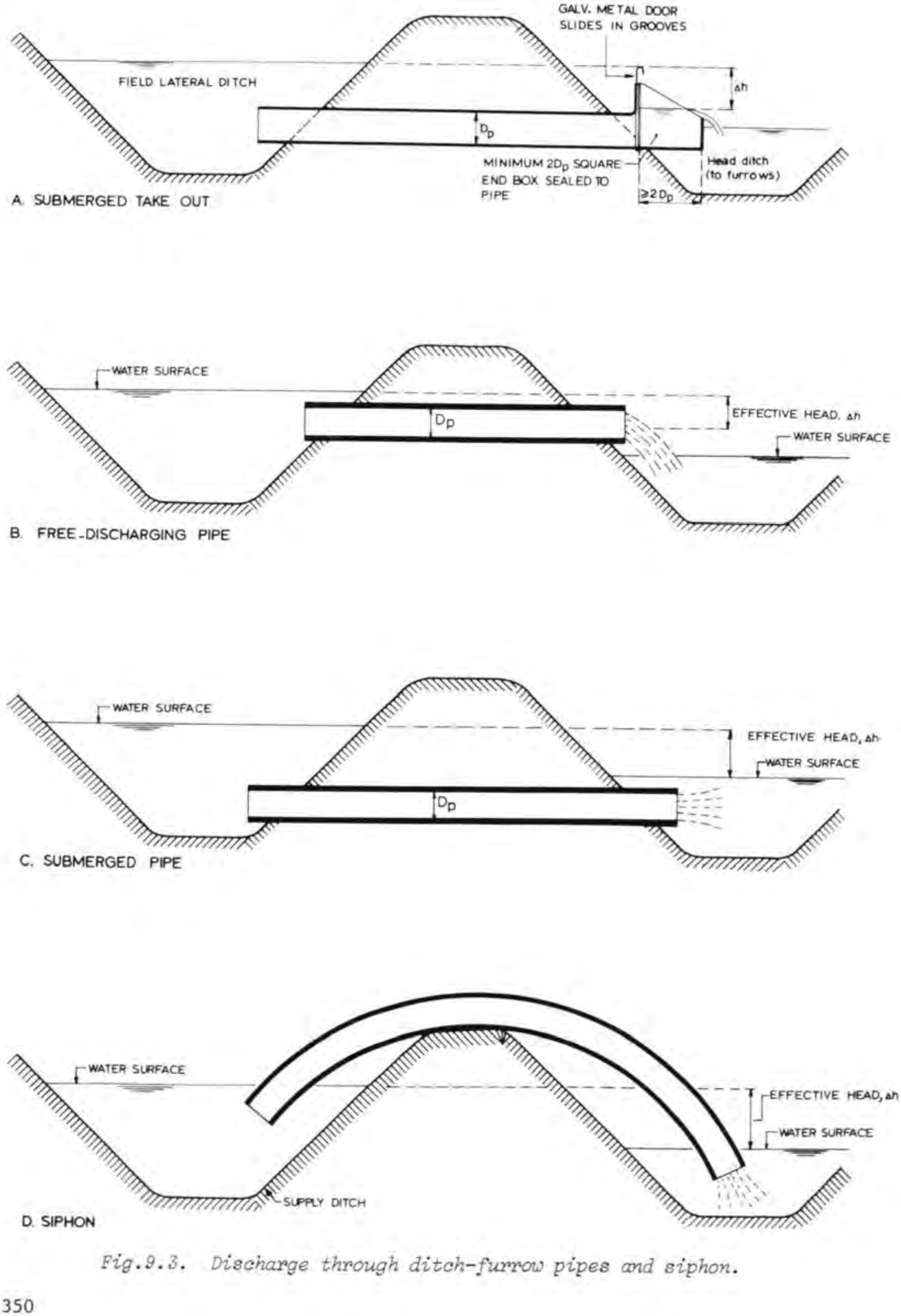

Fig.9.3. Discharge through ditch-furrow pipes and siphon.

If such pipes are to be used to estimate discharges, the hydraulic losses at the entrance and exit of the pipe have to be known. To prevent these losses from varying too greatly, we have drawn up instructions for use which are listed under the limits of application (Section 9.2.3).

The effective (differential) head, Δh, over the pipe or siphon has to be measured as accurately as possible, but the installation also has to be practical. For field measurements a transparent hose acting as a siphon, as illustrated in Figure 9.4, will be found useful. By keeping the hose in a vertical position Δh can be read from a scale.

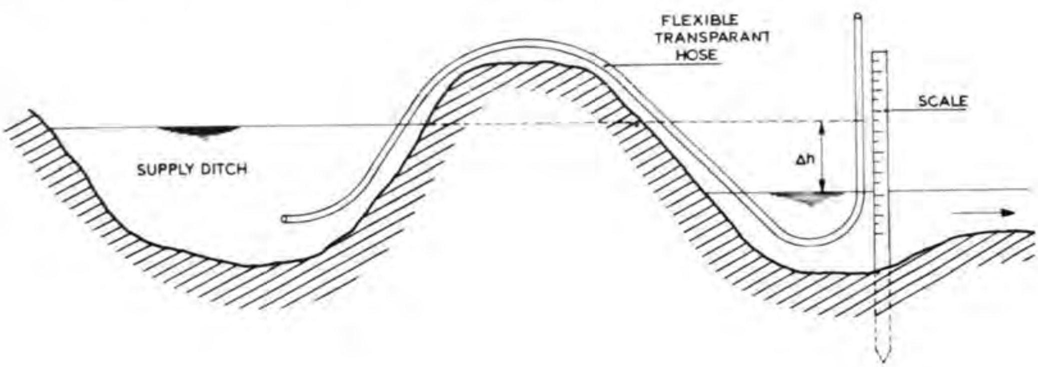

Fig.9.4. Method of head measurement.

Since tailwater level will drop as soon as the device is installed, the meter has to be placed and read quickly to obtain a reasonably accurate Δh-value.

9.2.2 Evaluation of discharge

From a hydraulical viewpoint, two types of pipes (or siphons) can be distinguished

- "small diameter pipe", being a pipe with a length L considerably more than D_p ($L > 20\ D_p$).
- "large diameter pipe", which has a relatively short length of $6\ D_p \leqslant L \leqslant 20\ D_p$.

For either pipe the discharge can be evaluated with the equation

$$\Delta h = \xi \frac{v^2}{2g} \tag{9-3}$$

where

v = average flow velocity in pipe

ξ = head loss coefficient

Substituting the continuity equation into Equation 9-3 yields

$$Q = \frac{\pi}{4} D_p^2 \left[\frac{2g\Delta h}{\xi}\right]^{0.5} \qquad (9\text{-}4)$$

For "small diameter pipes" friction losses in the pipe play a significant role and the head loss coefficient is estimated to equal

$$\xi = 1.9 + f \frac{L}{D_p} \qquad (9\text{-}5)$$

or for pipes with a length between 1.00 and 1.50 m, i.e. average L = 1.25 m

$$\xi = 1.9 + \frac{1.25\ f}{D_p} \qquad (9\text{-}6)$$

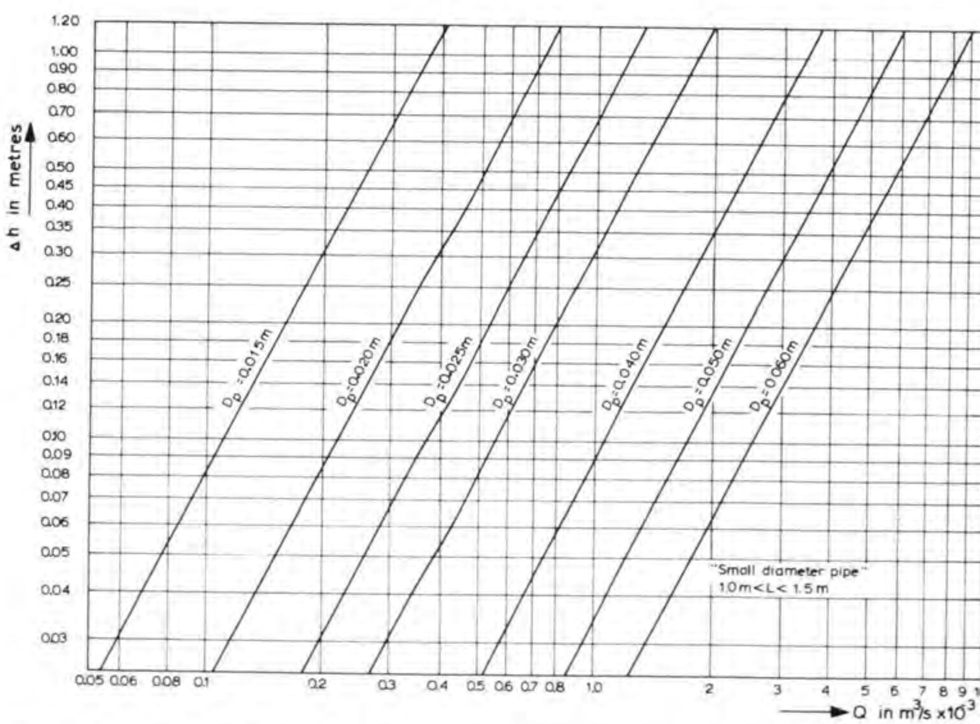

Fig.9.5. Rates of flow through smooth pipes or siphons.

where f is the friction loss coefficient of Darcy-Weissbach for an equivalent sand roughness $k = 5 \times 10^{-5}$. f is a function of the Reynoldsnumber R_e and the parameter D_p/k. If $R_e > 10^5$, $k = 5 \times 10^{-5}$ and $300 < D_p/k < 1200$ it follows that $0.028 > f > 0.019$.

For the "large diameter pipes" entrance and exit losses are the most significant sources of hydraulic losses and the head loss coefficient is estimated to equal

$$\xi = 2.1 \tag{9-7}$$

A combination of Equations 9-4 and 9-6 results in Figure 9.5, from which the pipe discharge can be read as a function of Δh and D_p for small diameter pipes. A combination of Equations 9-4 and 9-7 produces Figure 9.6, from which similar information about large diameter pipes can be obtained.

The error in the discharge read from Figures 9.5 and 9.6 is expected to be about 10%. The method by which this discharge error is to be combined with errors in Δh and D_p is shown in Appendix II.

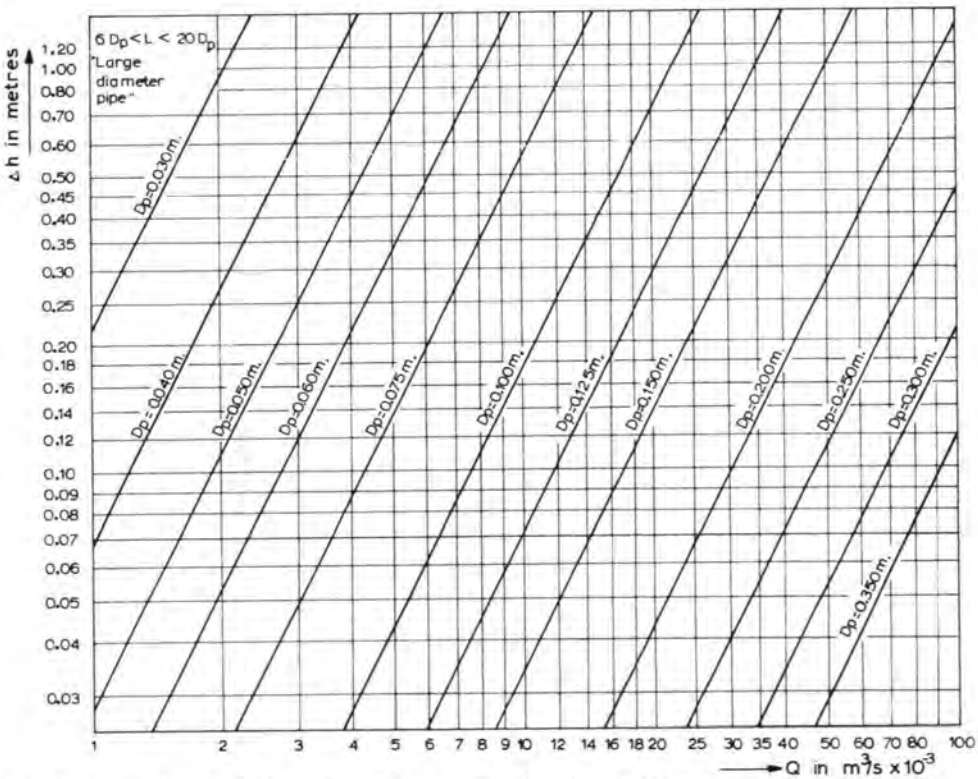

Fig.9.6. Rates of flow through smooth pipes or siphons.

9.2.3 Limits of application

To produce a reasonably accurate estimate of the discharge through a pipe or siphon, the following limits of application are considered essential.

a) Pipes should have clear cut edges (no rounding-off) and a constant diameter from entrance to end. The pipe entrance should protrude from the ditch embankment and the flow velocity in the ditch should be less than one third of the average velocity in the pipe.

b) The pipe should be made of "technically smooth material". For $D_p \leqslant 0.05$ m, PVC or aluminium are suitable, while if $D_p > 0.05$ m galvanized steel is also suitable.

c) To prevent air-bubbles from collecting at the top of a siphon, it is recommended that $\bar{v} \geqslant 1.3\,(g\,D_p \sin\alpha)^{0.5}$, where α denotes the angle of the downstream siphon limb from the horizontal.

d) To eliminate bend-losses, the radius of bends should not be less than $8\,D_p$.

e) No air-entraining vortex should be visible at the pipe entrance.

f) The exit cross-section of the pipe has to flow entirely full. For a free discharging horizontal pipe, this occurs if $Q \geqslant 1.18\,g^{0.5}\,D_p^{2.5}$ m^3/s. (See also Sections 9.4 and 9.5.)

g) The recommended lower limit of Δh is 0.03 m. The recommended lower limit of D_p is 0.015 m for "small diameter pipes" and 0.03 m for "large diameter pipes".

9.3 Fountain flow from a vertical pipe

9.3.1 Description

Fountain flow from a vertical pipe into the air can occur during pumping tests, or when there is flow from pressure conduits or from artesian wells. Such flow can occur either as weir flow or as jet flow.

Weir flow. Water discharges from the pipe with sub-critical flow and is similar to flow over a curved sharp-crested weir. Weir flow occurs if the height to which the water rises above the pipe is equal to or less than $0.37\,D_p$.

Jet flow. Water discharges from the pipe with supercritical flow. Jet flow occurs if the height of the jet exceeds $1.4\,D_p$, as determined by sighting over the jet to obtain the average rise.

The principal difficulty of measuring the discharge from a vertical pipe is to get an accurate measurement of the height to which the water rises above the end of the pipe. This is usually done with a sighting rod.
As shown in Figure 9.7, the sighting rod is attached to the pipe from which the jet is to come. To obtain proper head readings, we have to set the movable arm at the head at which the water stays the longest time. Thus we measure its average head, not the maximum head.

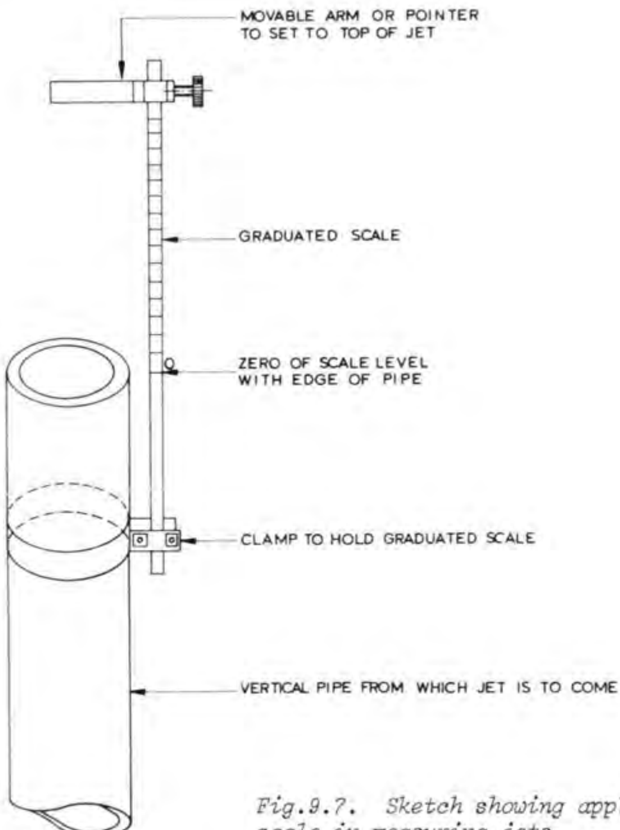

Fig.9.7. Sketch showing application of movable pointer and scale in measuring jets.

9.3.2 Evaluation of discharge

The discharge from a vertical pipe can be estimated by using the equations given by LAWRENCE and BRAUNWORTH (1906), which for sighting rod readings in the metric system are:

$$Q = 5.47\ D_p^{1.25}\ h_s^{1.35} \tag{9-8}$$

and

$$Q = 3.15\ D_p^{1.99}\ h_s^{0.53} \tag{9-9}$$

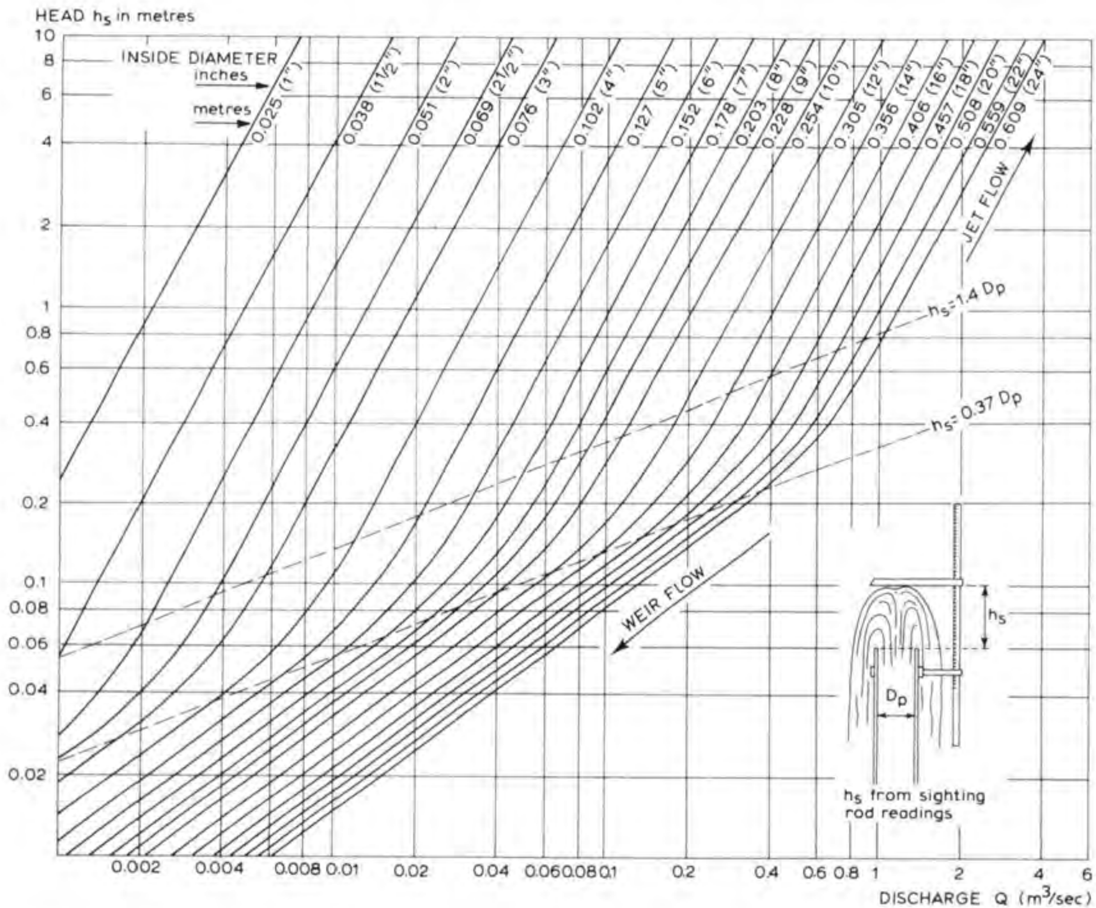

Fig.9.8. Discharge from vertical pipes.

Equation 9-8 is valid for weir flow ($h_s \leqslant 0.37\ D_p$) and Equation 9-9 is valid for jet flow ($h_s \geqslant 1.4\ D_p$). For jet heights between $0.37\ D_p$ and $1.4\ D_p$, the flow is somewhat less than given by either of these equations. Figure 9.8, prepared from LAWRENCE and BRAUNWORTH data, shows flow rates in m^3/s for standard pipes and for jet heights up to 4.0 m.

The accuracy with which the jet flow can be evaluated may be expected to be about 15% for sighting rod readings. For weir flow these accuracies are about 20%.

9.3.3 Limits of application

The limits of application that enable a reasonable estimate of the discharge from a vertical pipe are:

a) Pipes should have clear cut edges and a constant diameter over at least a length of 6 D_p.

b) Pipes should be vertical for at least a length of 6 D_p from the top of the pipe.

c) The practical range of pipe diameters is $0.025\ m \leqslant D_p \leqslant 0.609\ m$.

d) The practical range of heads is $0.03\ m \leqslant h \leqslant 4.0\ m$.

9.4 Flow from horizontal pipes

9.4.1 Description

Flow from a horizontal pipe can be estimated by using either the California pipe method[1] developed by VAN LEER (1922) or the trajectory method developed at Purdue University by GREEVE (1928). The California pipe method applies only to pipes flowing less than half full, whereas the more general trajectory method applies equally well to both partially and completely filled pipes.

[1] The California pipe method is identical to the brink depth method for circular canals.

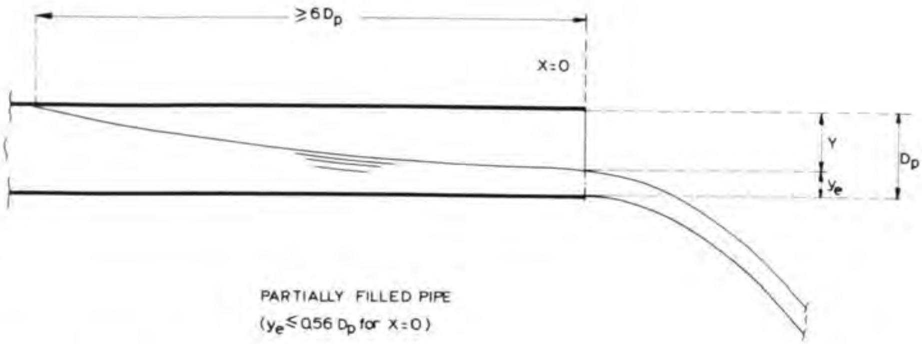

Fig.9.9. Dimension sketch partially filled pipe.

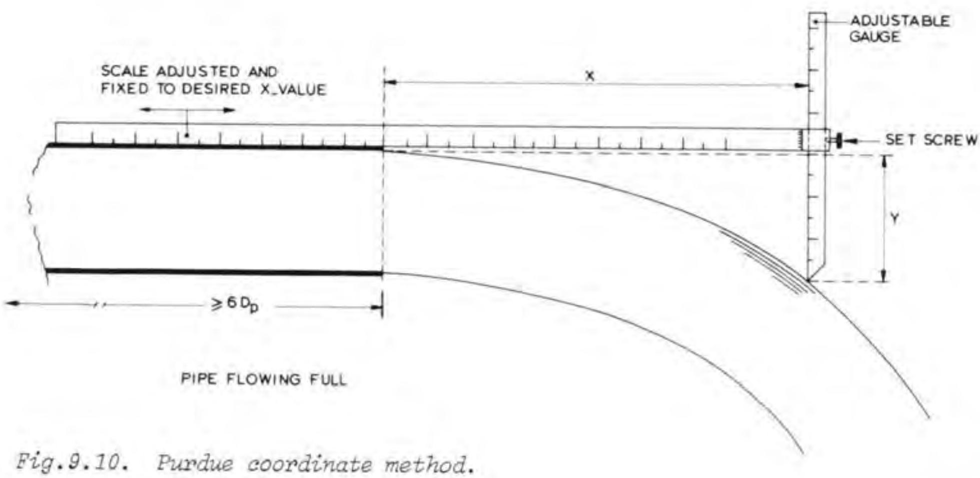

Fig.9.10. Purdue coordinate method.

The California pipe method consists of measuring the end depth at the pipe outlet and is valid if $y_e = D_p - Y \leqslant 0.56\ D_p$ (see Fig.9.9).

The Purdue trajectory method consists of measuring two coordinates of the upper surface of the jet as shown in Figure 9.10. If the pipe is flowing with a depth of less than $0.56\ D_p$ at the outlet, the vertical distance from the upper inside surface of the pipe to the surface of the flowing water, Y, can be measured at the outlet of the pipe where $X = 0$. For higher discharges, Y can be measured at horizontal distances X from the pipe outlet of 0.15, 0.305 or 0.46 metre.

Photo 2. Flow from a horizontal pipe.

9.4.2 Evaluation of discharge

California pipe method ($X = 0$)

The California pipe method is based on the unique relationship between the depth, y_e, of flow at the pipe outlet and the pipe discharge, Q. A dimensionless plot of this relationship is shown in Figure 9.11.

Provided that $y_e \leq 0.56\ D_p$ the pipe discharge can be calculated from this figure for any diameter D_p. Discharge values in $m^3/s \times 10^{-3}$ for 2- to 6-inch diameter (0.05 to 0.15 m) standard pipes are shown in Figure 9.13. A as a function of $Y = D_p - y_e$.

The user will experience difficulty in making the measurement Y exactly at the brink. Since the upper nappe surface is curved, any small error in the location of the gauge will cause large errors in Y. Actually, the only method by which Y can be measured accurately is by installing a point gauge at the center line of the pipe exactly above the brink (see also Figure 9.10). Since the upper nappe surface at the brink is instable, the accuracy of the Y-value can be greatly improved by repeating its measurement and taking the average value.

The error in the discharge value as derived from Figure 9.11 for partially filled pipes may be expected to be less than 3 per cent. The method by which the various errors have to be combined with other sources of error is shown in Appendix II.

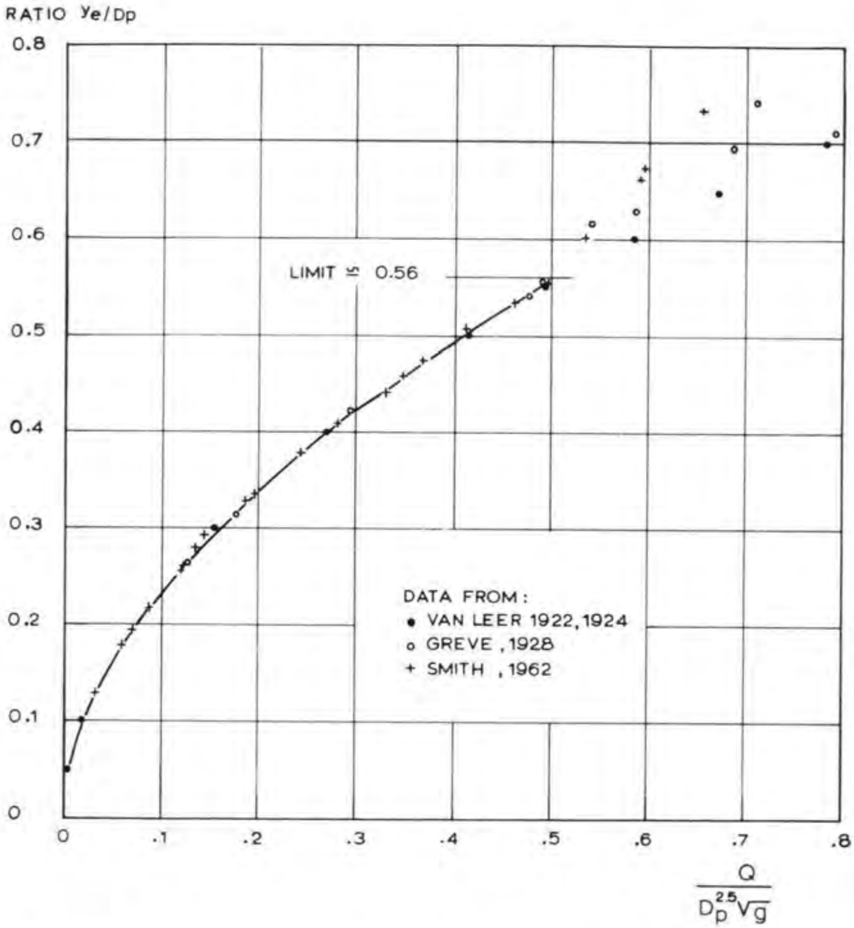

Fig.9.11. Flow from horizontal pipes by California pipe method or brink depth method.

Purdue trajectory method

The shape of the jet from a horizontal pipe can be interpreted by the principle of a projectile (Fig.9.12).

According to this principle, it is assumed that the horizontal velocity component of the flow is constant and that the only force acting on the jet is gravity. In time t, a particle on the upper surface of the jet will travel a horizontal distance X from the outlet of the pipe equal to

$$X = v_o t \tag{9-12}$$

where v_o is the velocity at the point where X = 0. In the same time t, the particle will fall a vertical distance Y equal to

$$Y = \frac{1}{2} gt^2 \tag{9-13}$$

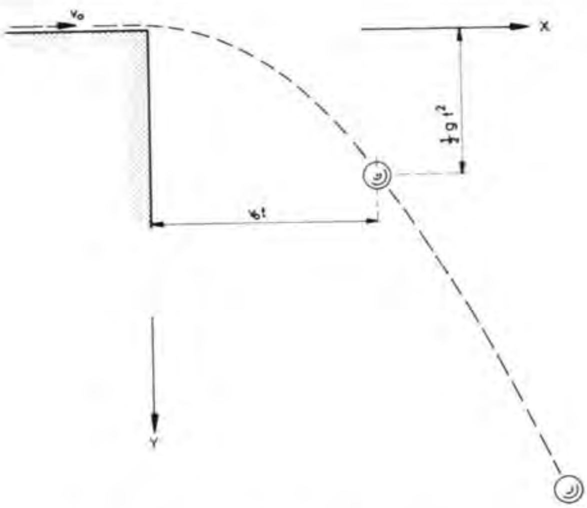

Fig.9.12. Derivation of jet profile by the principle of projectile.

Eliminating t from the above two equations and multiplying each term by the inside pipe area $\frac{1}{4} \pi D_p^2$ and a discharge coefficient leads to

$$Q = C_d \frac{1}{4} \pi D_p^2 \sqrt{g \frac{X^2}{2Y}} \tag{9-14}$$

Discharge values in $m^3/s \times 10^{-3}$ (l/s) for 2- to 6-inch diameter (0.05 to 0.15 m) standard pipes are shown in graphs in Figure 9.13-B to D.

Due to the difficulty of making the vertical measurement Y in the Purdue trajectory method ($y_e > 0.56 D_p$ or pipe flowing full), the error in flow measurement found by using Figure 9.13 may be expected to be about 10 to 15 per cent.

If this error is not to be exceeded, the pipe should be truly horizontal and straight for at least 6 times D_p from the outlet. If it slopes downward, the discharge taken from Figure 9.13 will be too low. If it slopes upward, the discharge will be too high.

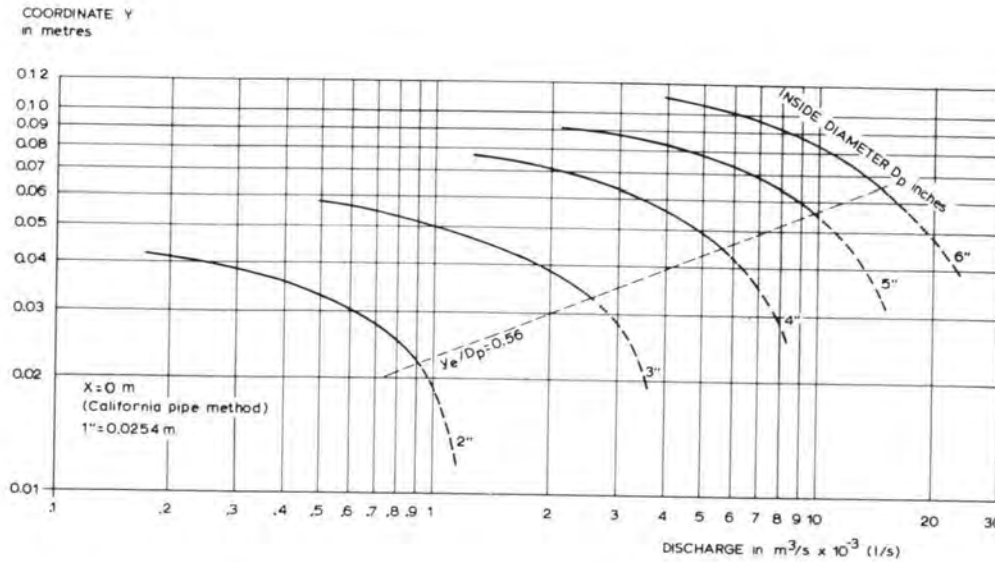

Fig.13.A. Flow from horizontal pipes by either Purdue trajectory method or by California pipe method.

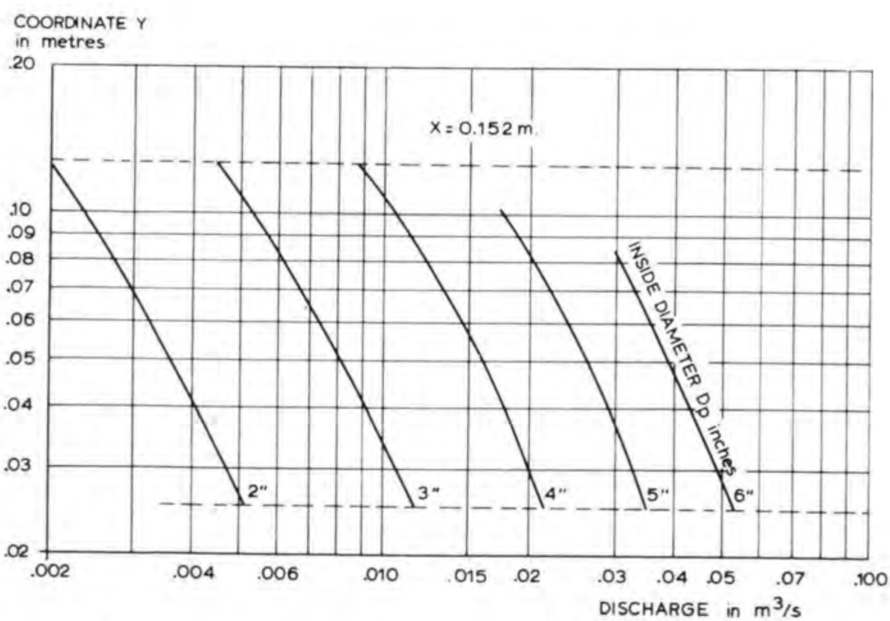

Fig.13.B. (cont.)

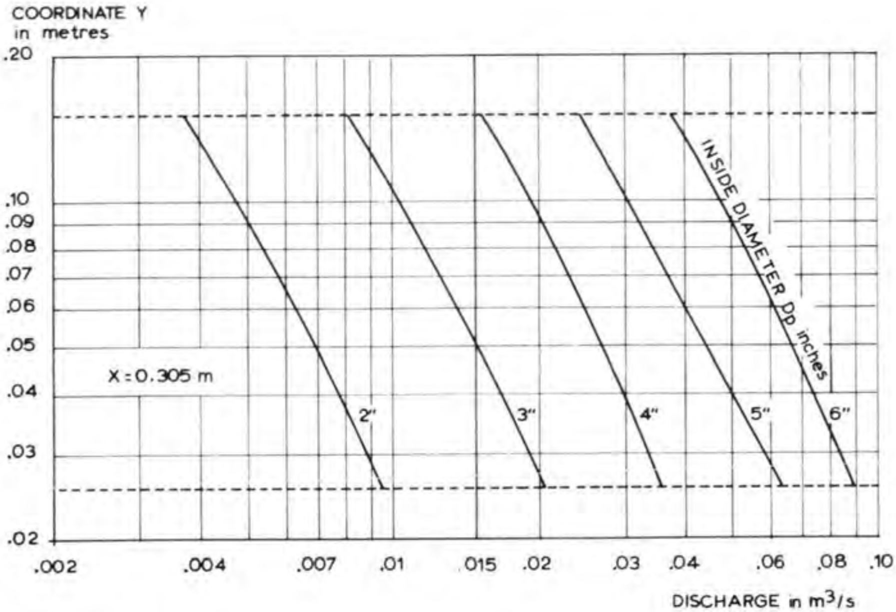

Fig.13.C. (cont.)

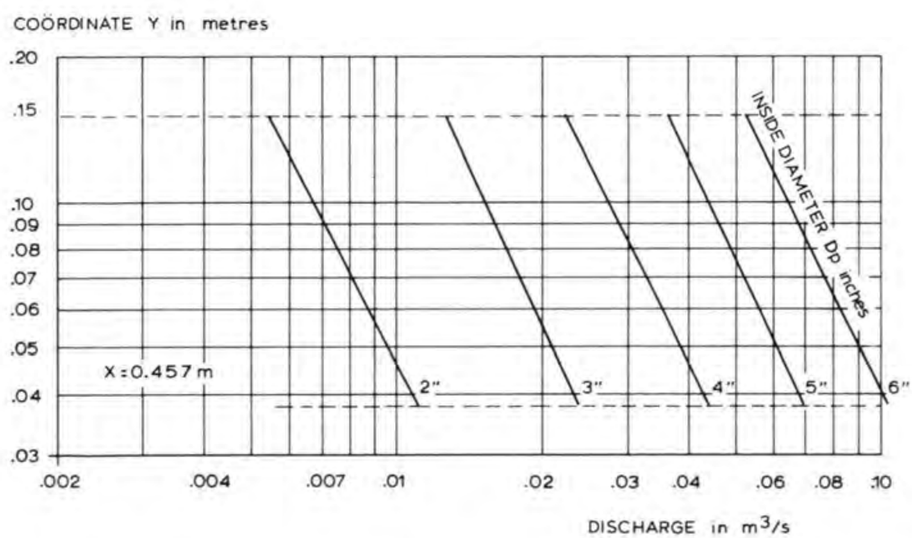

Fig.13.D. (cont.)

9.4.3 Limits of application

The limits of application that enable a reasonably accurate estimate of the discharge from a horizontal pipe are:

a) Pipes should have clear cut edges and a constant diameter over at least a length of 6 D_p from the outlet.

b) Pipes should be straight and truly horizontal over at least a length of 6 D_p from the outlet.

c) Pipes must discharge freely into the air.

9.5 Brink depth method for rectangular canals

9.5.1 Description

When the bottom of a low gradient canal drops suddenly, a free overfall is formed which, since flow changes to supercritical, may be used as a discharge measurement device. In principle, any canal cross section can be used for flow measurement provided that the free overfall is calibrated.

Sufficiently accurate experimental data, however, are only available for rectangular and circular cross sections. Since the circular section was treated in Section 9.4, we will confine our remarks here to the brink depth method for rectangular canals.

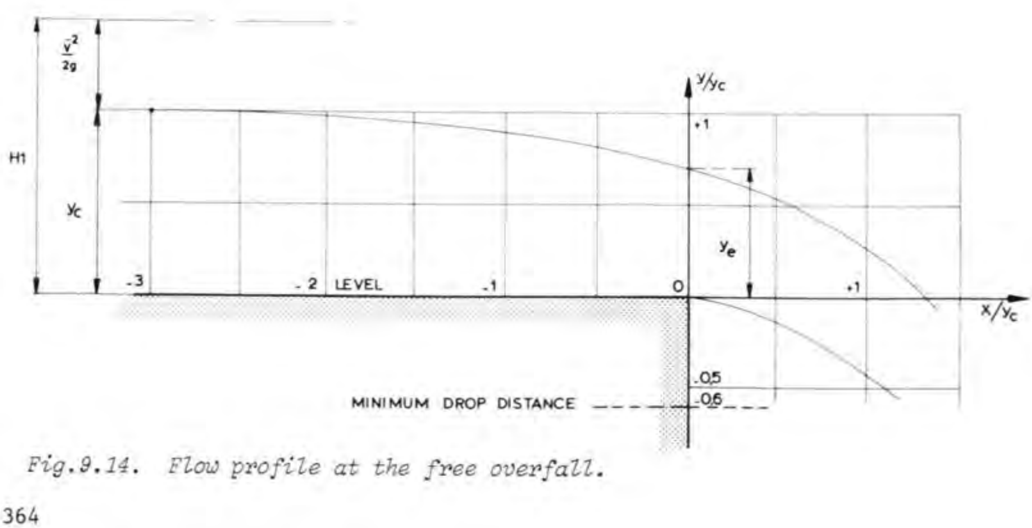

Fig.9.14. Flow profile at the free overfall.

The simplest case of a free overfall is that of a rectangular canal with sidewalls continuing downstream on either side of the free nappe over a distance of at least 0.3 H_1max, so that at the brink the atmosphere has access only to the upper and lower side of the nappe. This is a two-dimensional case with a "confined nappe", and is the only form of the problem for which serious attempts have been made to find a solution. Some experiments, however, have been made on a free overfall with "unconfined nappe", i.e. where the side walls end at the sudden drop.

In the situation shown in Figure 9.14, flow takes place over a confined drop which is sharp enough (usually 90 degrees) to guarantee complete separation of the nappe. The bottom of the tailwater channel should be sufficiently remote so as not to influence the streamline curvature at the brink section. To ensure that, this does not happen, the drop distance should be greater than 0.6 y_c.

The user will experience difficulty in making the measurement y_e exactly at the brink. Since the upper nappe surface is curved, any small error in the location of the gauge will cause large errors in y_e. Actually, the only method by which y_e can be measured accurately is by installing a point gauge in the middle of the canal exactly above the brink. Since a point gauge is vulnerable to damage, however, a staff gauge, with its face flush with the side wall, will be found more practical. The location of the brink should be marked on the gauge face to enable y_e readings to be made. The brink depth as measured at the side wall will be higher than that in the middle of the canal, because of side wall effects. To limit the effect of roughness on the brink depth as measured with a staff gauge, the side walls as well as the bottom of the canal should be smooth. If the brink depth is measured with a point gauge, no significant influence of roughness is found, as is illustrated for three values of the equivalent sand roughness, k, in Figure 9.15.

9.5.2 Evaluation of discharge

If we assume that the streamlines in the rectangular canal are straight and parallel, we may, according to Equation 1-26, write the specific energy in the canal as

$$H_o = y + \alpha \frac{q^2}{2gy^2} \qquad (9\text{-}15)$$

Differentiation of H_o to y, while Q remains constant leads to

$$\frac{dH_o}{dy} = 1 - \alpha \frac{q^2}{gy^3} \tag{9-16}$$

If the depth of flow is critical ($y = y_c$), dH_o/dy equals zero, and we may write

$$y_c = \sqrt[3]{\frac{\alpha q^2}{g}} \tag{9-17}$$

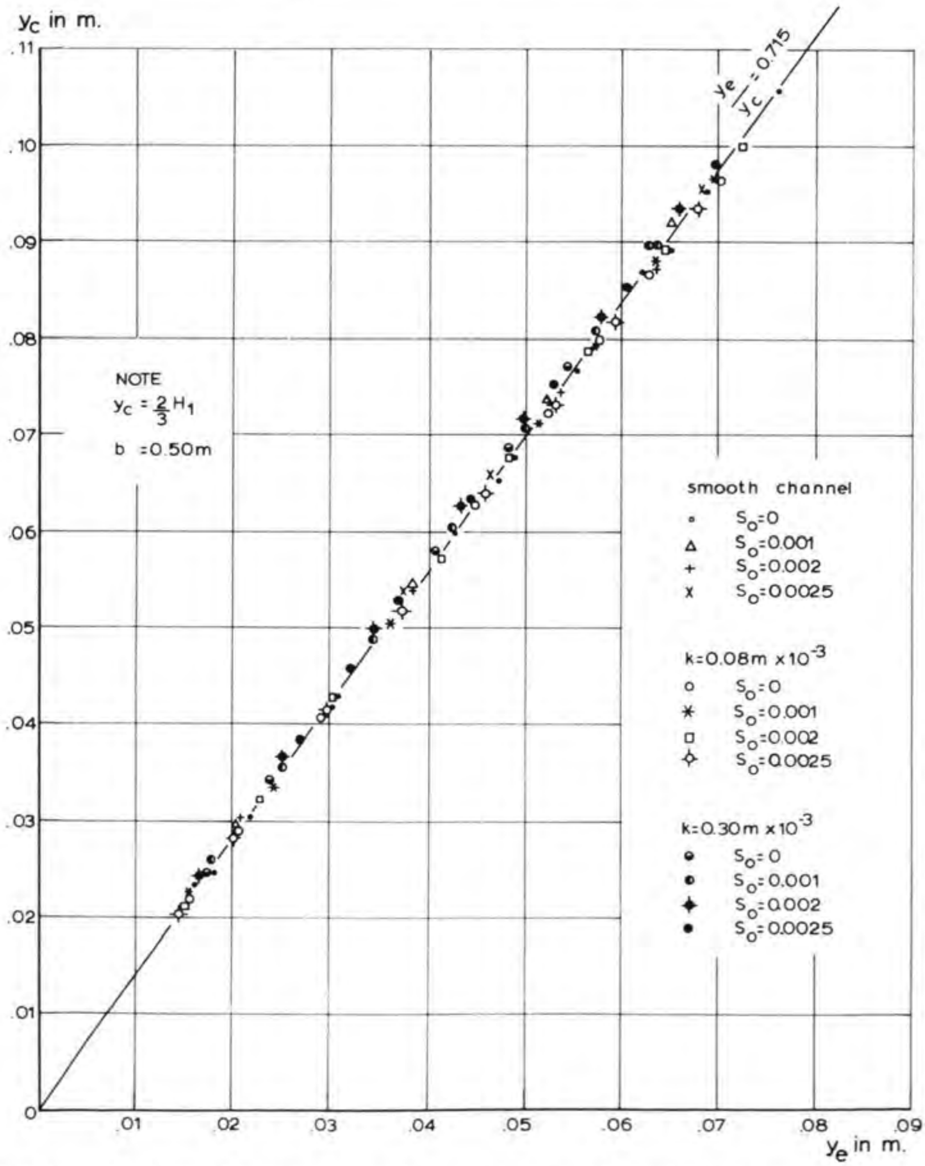

Fig.9.15. Relation between y_e and y_c (after Kraijenhoff van de Leur and Dommerholt, 1972).

Assuming $\alpha = 1$ and substituting $Q = bq$ leads to

$$Q = b\sqrt{g}\, y_c^{3/2} \tag{9-18}$$

The experiments of ROUSE (1936), and further experiments by various authors, showed that for a confined nappe the brink section has a flow depth equal to

$$y_e = 0.715\, y_c \tag{9-19}$$

resulting in the discharge equation

$$Q = b\sqrt{g} \left[\frac{y_e}{0.715}\right]^{3/2} = 5.18\, b y_e^{3/2} \tag{9-20}$$

As shown in Figure 9.15, slight variations in the roughness of the canal boundaries and in the canal bottom slope are of little significance on the ratio y_e/y_c. If the free overfall has an unconfined nappe, however, the ratio y_e/y_c is somewhat less than in the two-dimensional case, being equal to 0.705.

For a free overfall which is constructed and maintained with reasonable care and skill, the coefficients 0.715 and 0.705 can be expected to have an error of the order of 2% and 3% respectively, provided y_e is measured in the middle of the channel. If y_c is measured at the side walls an additional error in y_e occurs due to boundary roughness (see Section 9.4.2 for other possible errors). The method by which these errors are to be combined with other sources of error is shown in Appendix II.

9.5.3 Limits of application

The limits of application of the brink depth method for rectangular canals are:

a) Perpendicular to the flow, the brink should be truly horizontal and the side walls of the rectangular approach canal should be parallel from end to end.

b) To obtain a uniform velocity distribution, the length of the approach channel should not be less than 12 y_c.

c) The longitudinal slope of this approach channel should preferably be zero but not more than $s = 0.0025$.

d) The practical lower limit of y_e is related to the magnitude of the influence of fluid properties and the accuracy with which y_e can be measured. The recommended lower limit is 0.03 m.

e) The y_e-value should be measured in the middle of the canal, preferably by means of a point gauge.

f) The width of the canal should not be less than 3 y_c nor less than 0.30 m.

g) To obtain free flow, the drop height should not be less than 0.6 y_c.

9.6 Dethridge meter

9.6.1 Description

The Dethridge meter is a rather commonly used device for measuring the volume of irrigation water supplied to farms from main and lateral canals in Australia. The meter was designed by J.S.Dethridge of the State Rivers and Water Supply Commission, Victoria, in 1910. This Commission provided the present information on the standard device, of which today about 20,000 are in operation in irrigation areas throughout Australia.
The meter consists of an undershot water wheel turned by the discharging water passing through its emplacement, which is a short concrete outlet specially formed to provide only the minimum practicable clearance of the lower half of the wheel at its sides and round the lowest 70 degrees of its circumference.
Two standard sizes of the meter are used: the 1.524 m (5 ft) diameter "large" meter which is suitable for discharges from 0.040 m^3/s to 0.140 m^3/s, and the "small", 1.219 m (4 ft) diameter meter for discharges from 0.015 m^3/s to 0.070 m^3/s. The main dimensions of both meters, which are similar in general form, are shown in Figure 9.16.
The wheel is made up of a cylinder of 2 mm thick mild steel sheet, bearing eight external vanes of the same material, each welded against the surface of the cylinder on a widely distended "V", with the root of the "V" leading in the direction of the wheel's rotation. At the root of each vane is a small air vent so that compartments between the vanes can fill completely with water while being submerged by rotation of the wheel. The outer corners of the vanes are chamferred.
The internal bracing used to consist of three crossed pairs of timber spokes ($\pm$ 0.10 × 0.05 m) placed at the middle and both ends of the cylinder. Today they have given way to ø 16 mm steel rods in parallel pairs, welded on either side of the 25 mm internal diameter pipe-axle of the wheel (see Fig.9.17).

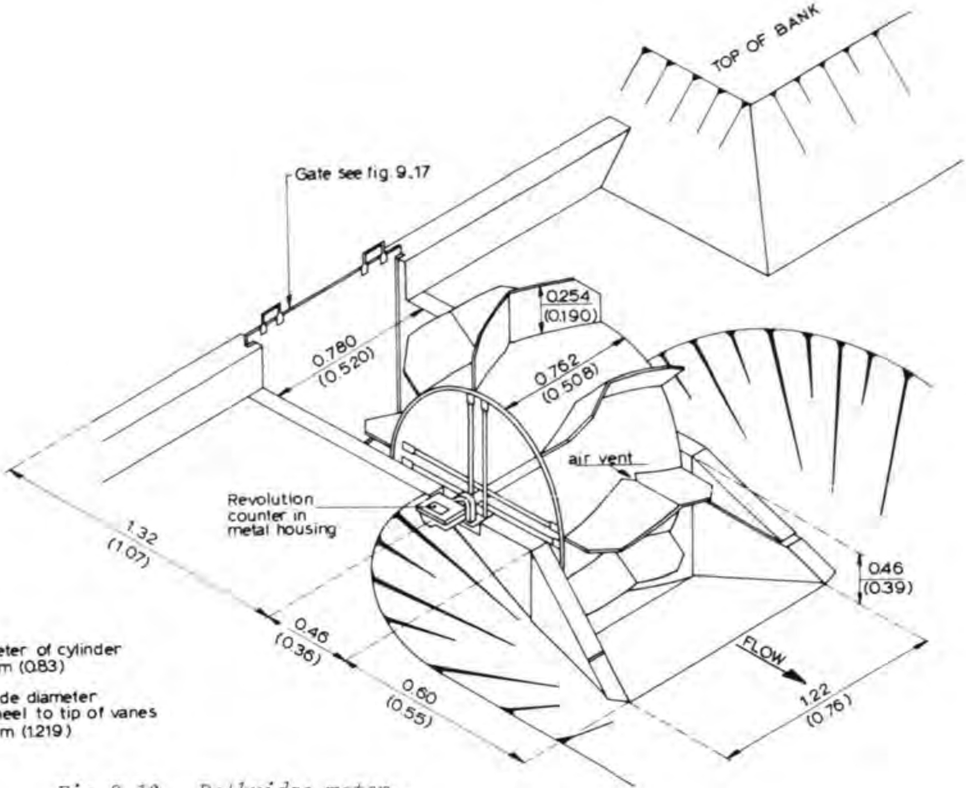

Fig.9.16. Dethridge meter.

The concrete structure in which the wheel has been placed has upstream of the wheel a simple rectangular section, with level floor in the vicinity of the wheel. At the wheel the walls remain plane and parallel but the floor is intended to accomodate an arc of about 70 degrees of the wheel's circumference. Immediately downstream of the wheel the walls are flared outward and the floor is sloped up to a lip of sufficient height (see Fig.9.17) to ensure submergence of the passage swept by the vanes under the wheel.

Most Dethridge meters are equiped with cheap wooden bearing blocks,usually seasoned Red Gum or other durable hardwood, dressed to dimensions shown in Fig.9.18. A disadvantage of these blocks is that they wear and are not always replaced in time so that the wheel may scrape on the concrete. A variety of more permanent type bearings was tested under the supervision of the above mentioned Commission and it appeared that the best installation would be a non-corrosive ball bearing which does not require any maintenance. Details of the type adapted as standard by the State Rivers and Water Supply Commission, Victoria, are shown in Fig. 9.18.

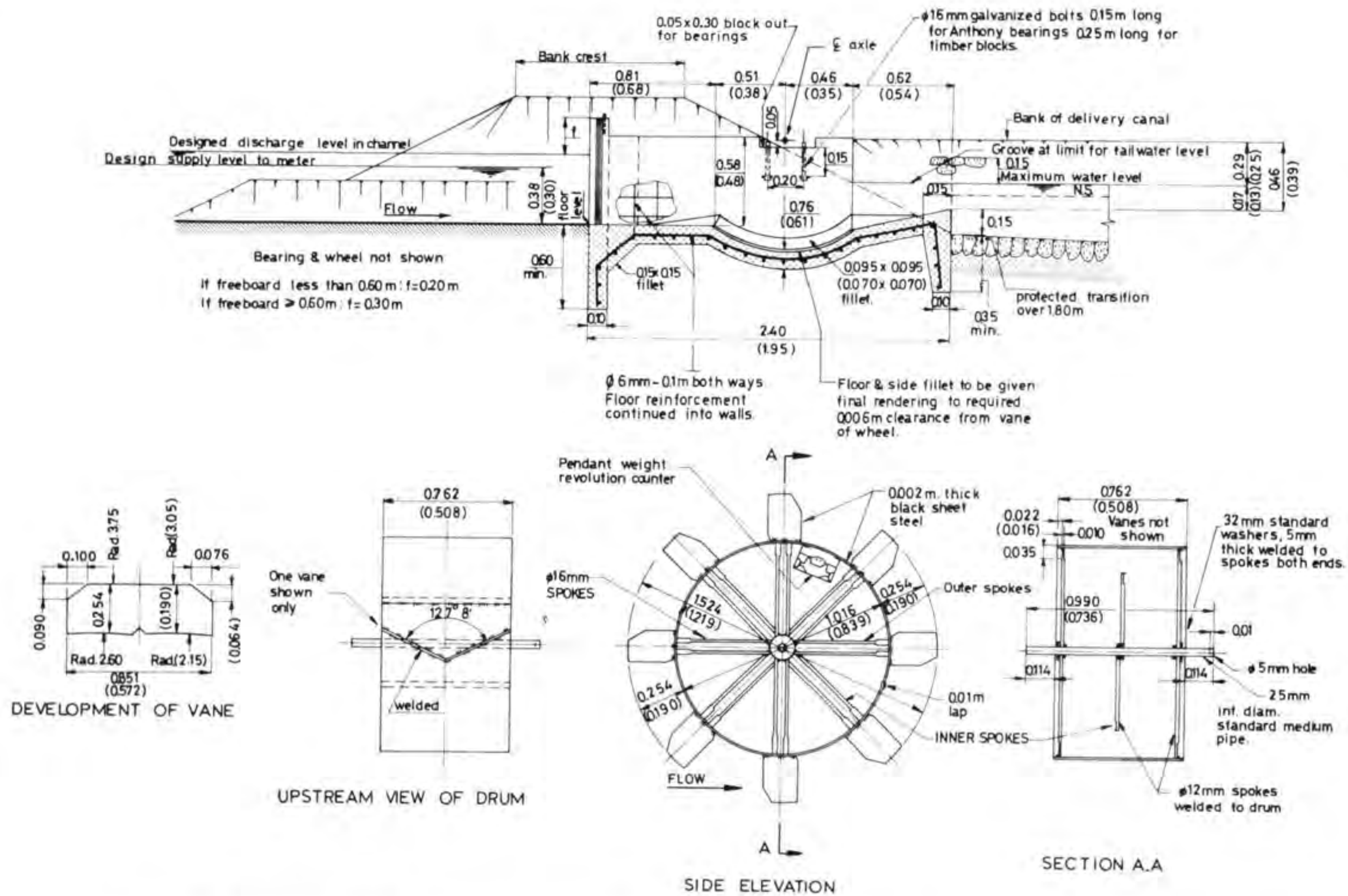

Fig.9.17. Dethridge meter dimensions (small meter dimensions shown between brackets, if different from large meter).

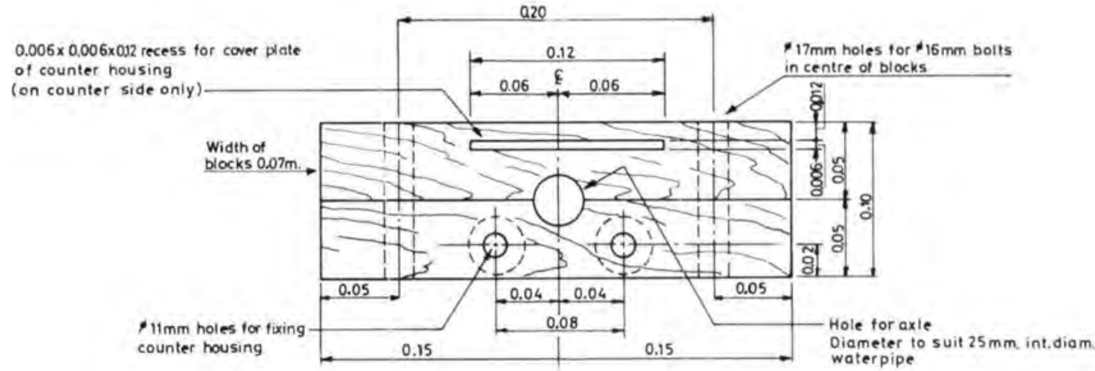

TIMBER AXLE BLOCK (dimensions in mm)

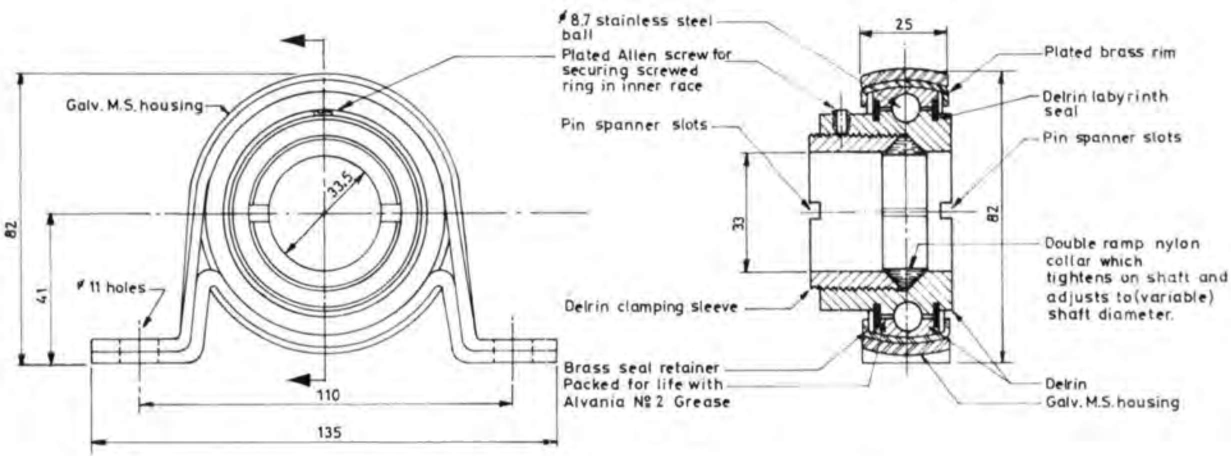

ANTHONY BEARING DETAILS (dimensions in mm)

Fig. 9.18. Alternative wheel bearing arrangements.

The operational life of revolution counters mounted to the wheel axle is quite irregular due to their fragile construction, the wire connection to the axle, and the jerky motion of the wheel. None of the counters in use can be considered satisfactory but recent (since 1966) tests showed that a pendulum actuated revolution counter fitted in a sealed casing inside the drum of the wheel may be satisfactory (see Figure 9.17).

It is important that the Dethridge meter be installed at the correct level in relation to full supply level in the undivided irrigation canal, so as to make the best use of the generally limited head available. The standard setting of the large meter is to have the floor of the concrete structure, at entry, 0.38 m below design supply level to the meter, being full supply level at the next check downstream of the meter. For the small meter this depth is 0.30 m. If excess head over the meter is available the depth may be increased up to 0.90 m, with the necessity of course, of correspondingly increasing the height of the sluice gate and head wall (see also Fig.9.17).

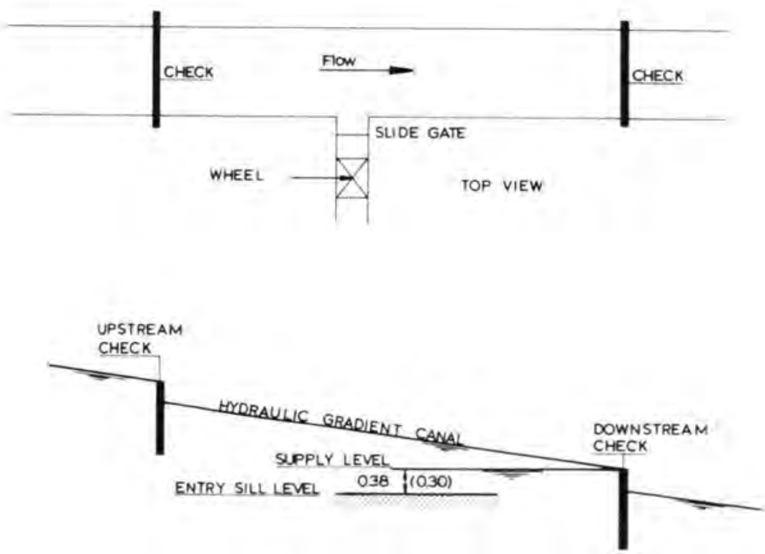

Fig.9.19. Setting of meter in relation to supply canal.

Supply level should not exceed 0.90 m above the meter sill at entry to avoid the jet below the sluice gate from driving the wheel. This "Pelton" wheel effect reduces the volume of water supplied per revolution. Discharge regulations are usually effectuated by adjusting a sluice gate immediately upstream of the wheel. Provided that supply level does not exceed 0.90 m above the meter sill at entry, the gate may be hand-operated. Gates may be locked in place as shown in Figure 9.20.

The main advantage of the Dethridge meter is that it registers a volume of supplied water; it is simple and robust in construction, operates with small head loss, and it will pass ordinary floating debris without damage to or stoppage of the wheel.

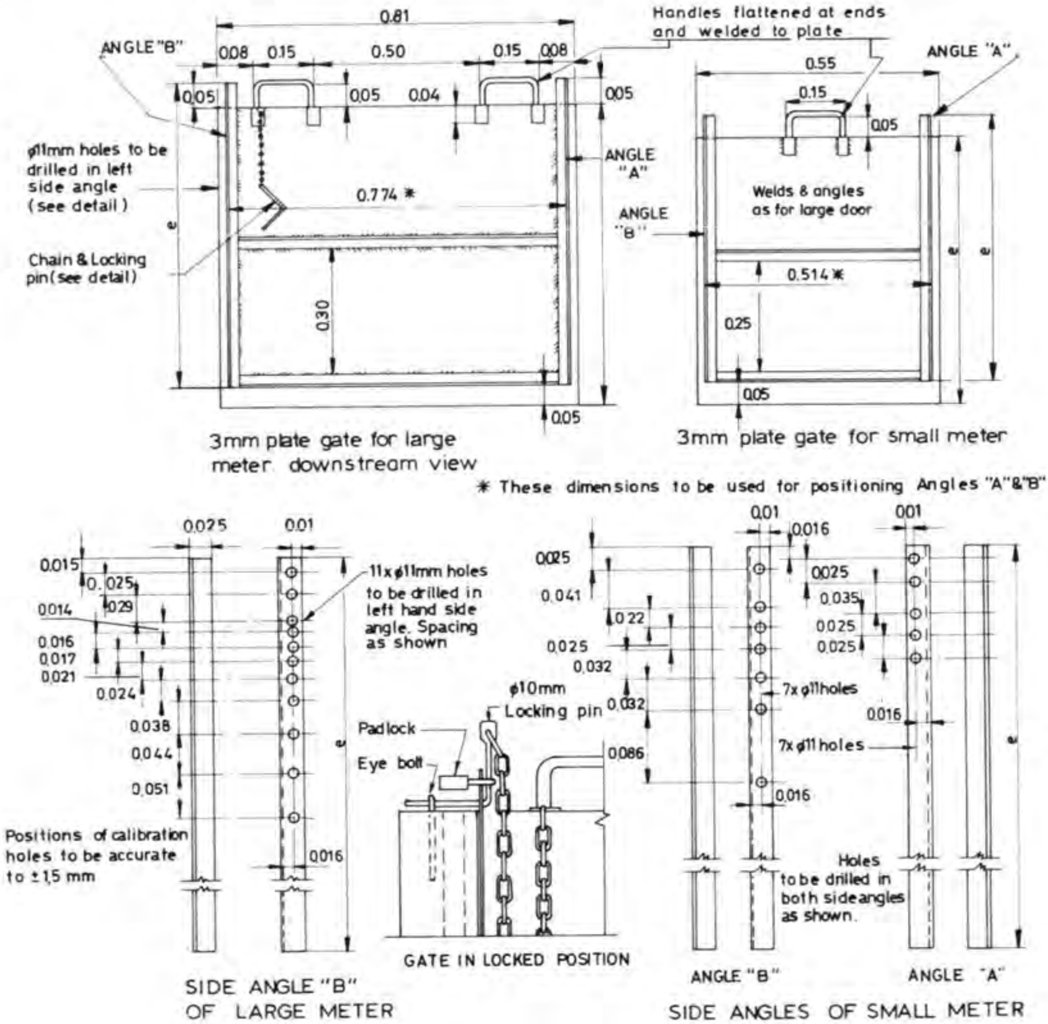

NOTE : Angle "A" of large meter has no holes

Fig.9.20. Gate dimensions.

9.6.2 Evaluation of flow quantity

If there were no clearances between the wheel and the concrete structure, the meter would give an exact measurement of the water passing through it, as each revolution of the wheel would pass an invariable quantity. With the provision for the necessary clearances, however, leakage occurs through the clearance space at a rate dependent not only on the rotation of the wheel, but dependent also on other factors such as the difference in water levels immediately upstream and downstream of the wheel, and the depth of submergence.

For free flow over the end sill, rating curves for both wheels are given in Figure 9.21.

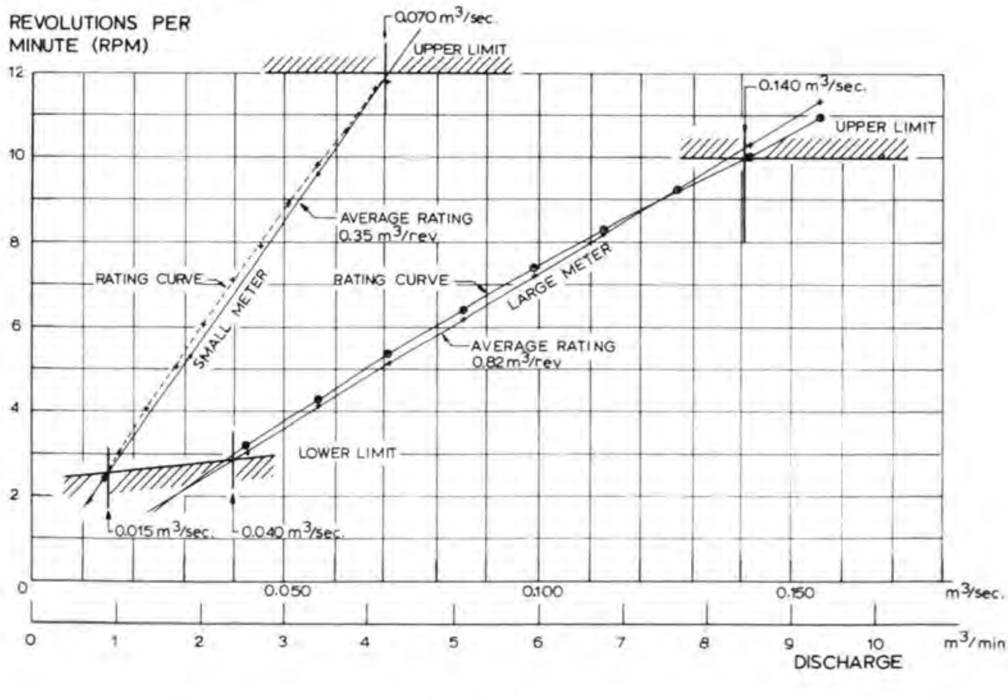

Fig.9.21. Rating curves for free flow over end sill for large and small meter.

As shown, the quantity of water passed per revolution of the wheel varies to some extent with the running speed of the wheel. For the conversion of revolutions to water quantity supplied, constant ratios are assumed, being 0.82 m^3/rev for the large wheel and 0.35 m^3/rev for the small wheel. Leakage around the wheel increases, and thus more water is supplied than registered, if there are large bottom clearances, large side clearances, high tailwater levels, and if the wheel is rotating at less than about three revolutions per minute.

The positive error resulting from excessive side clearances is smaller than that from bottom clearances. Increase in supply level has only a small effect on the rating.

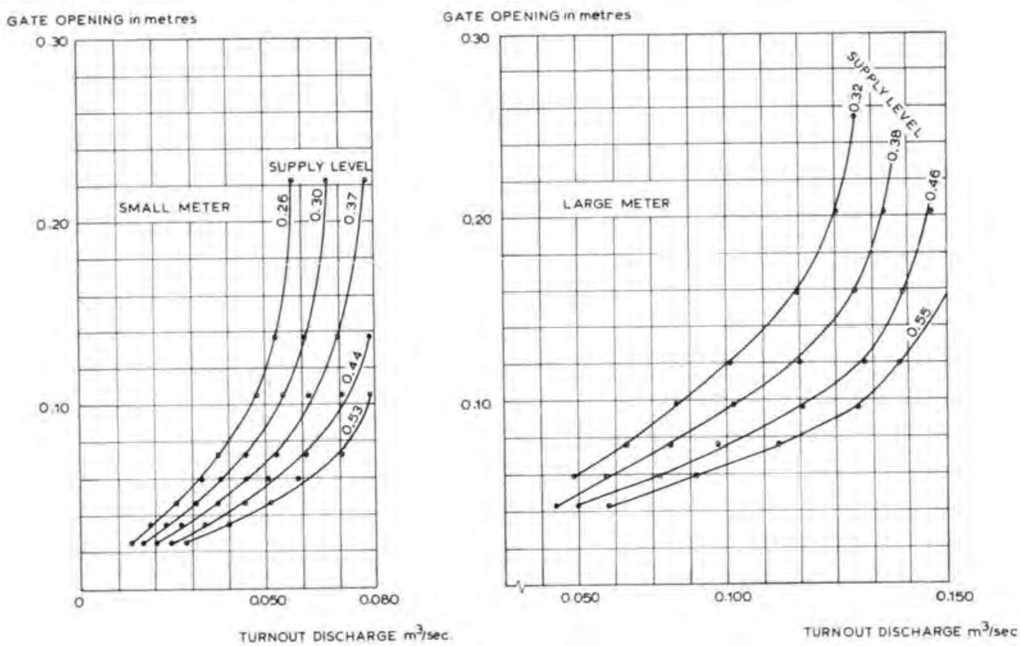

Fig.9.22. Gate calibration curves for Dethridge meters.

A Dethdridge meter which has been constructed and installed with reasonable care and skill may be expected to measure the total quantity of water passsing through it with an error of less than 5%. It is obvious that this quite reasonable degree of accuracy for the measurement of irrigation deliveries can only be achieved if adequate and regular maintenance is provided.

9.6.3 Regulation of discharge

As mentioned in Section 9.6.1, the discharge through the Dethridge meter is regulated by a sluice gate. Provided that flow over the end sill is modular, meter discharge can be set by adjusting the gate opening according to Figure 9.22.

If the meter is submerged, the most convenient method of setting a flow rate is to adjust the sliding gate so that the wheel makes the required revolutions per

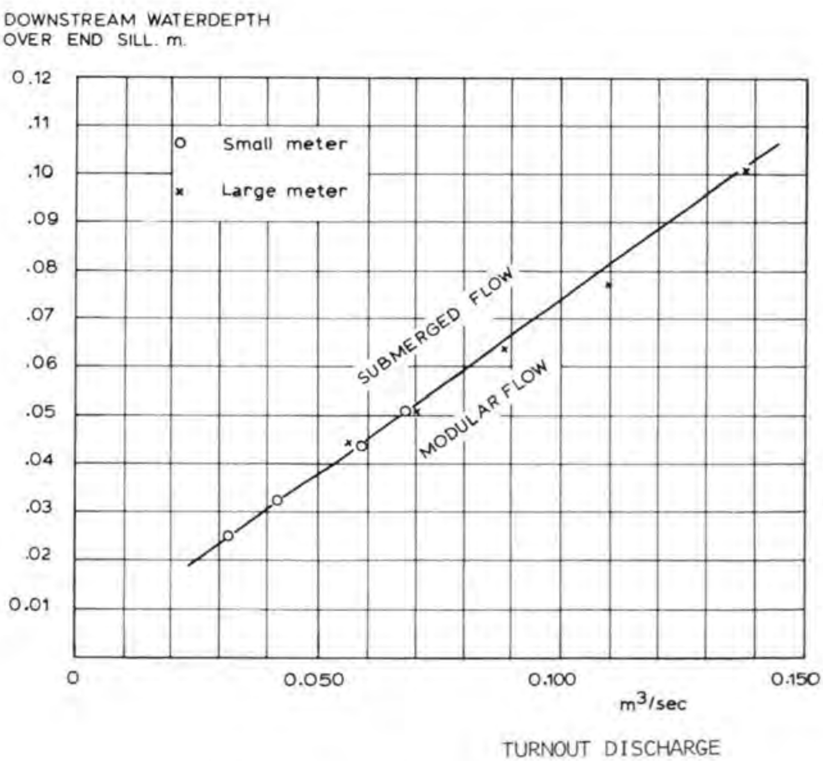

Fig.9.23. Approximate limits of tailwater for modular flow over downstream lip.

minute to pass this flow. Figure 9.21 may be used for this purpose, provided that tailwater levels remain less than 0.17 m over the end sill to avoid excessive leakage through the clearances of the large wheel. For the small wheel this value is 0.13 m.

Approximate limits of tailwater level to obtain modular flow through the Dethridge meter are shown in Figure 9.23 for both meters.

9.6.4 Limits of application

The limits of application of the Dethridge meter are:

a) The practical lower limit for the supply level over the entry sill is 0.38 m for the large meter and 0.30 m for the small meter. The upper limit for this supply level is 0.90 m for both meters.

b) Tailwater level should not be more than 0.17 m over the end sill of the large meter. This value is 0.13 m for the small meter.

c) The wheel should neither make less than about 3 r.p.m.nor more than about 10 to 12 r.p.m. Consequently, the discharge capacity ranges between 0.040 m^3/s and 0.140 m^3/s for the large meter and between 0.015 m^3/s and 0.070 m^3/s for the small meter (see also Fig.9.21).

d) Clearance between the floor and side fillets of the structure and the wheel should not exceed 0.006 m for both meters. Clearance between the side walls and the wheel should not exceed 0.009 m for the large meter and 0.006 m for the small meter.

9.7 Propeller meters

9.7.1 Description[1]

Propeller meters are commercial flow measuring devices used near the end of pipes or conduits flowing full, or as "in-line" meters in pressurized pipe systems. The meters have been in use since about 1913 and are of many shapes, kinds, and sizes. The material presented in this section applies to all makes and models of meters, in general, and serves to provide a better understanding of propeller operation.

---

[1] *The information presented in this section is for the major part an abstract from an excellent review on propeller meters by SCHUSTER and USBR (1970 and 1967).*

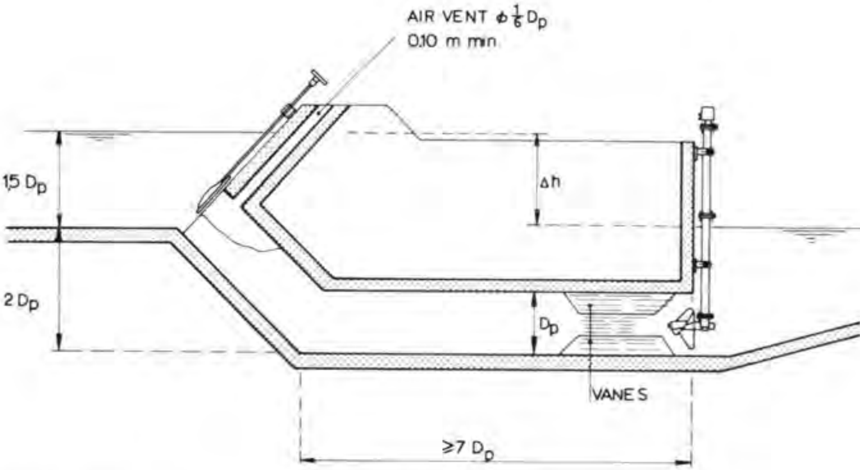

Fig.9.24. Typical propeller meter installation.

Propeller meters utilize a multibladed propeller (two to six blades) made of metal, plastic, or rubber, rotating in a vertical plane and geared to a totalizer in such a manner that a numerical counter can totalize the flow in cubic feet, cubic metres, or any other desired volumetric unit. A separate indicator can show the instantaneous discharge in any desired unit. The propellers are designed and calibrated for operation in pipes and closed conduits and should always be fully submerged. The propeller diameter is always a fraction of the pipe diameter, usually varying between 0.5 to 0.8 D_p. The measurement range of the meter is usually about 1 to 10; that is the ratio $\gamma = Q_{max}/Q_{min} \simeq 10$. The meter is ordinarily designed for use in water flowing at 0.15 to 5.0 m/s although inaccurate registration may occur for the lower velocities in the 0.15 to 0.45 m/s range. Meters are available for a range of pipe sizes from 0.05 to 1.82 m in diameter.

The principle involved in measuring discharges is not a displacement principle as in the Dethridge meter described earlier, but a simple counting of the revolutions of the propeller as the water passes it and causes it to rotate. Anything that changes the pattern of flow approaching the meter, or changes the frictional resistance of the propeller and drive gears and shafts, affects the accuracy of the meter registration.

9.7.2 Factors affecting propeller rotation

Spiral flow

Spiral flow caused by poor entrance conditions from the canal to the measuring culvert is a primary cause of discharge determination errors. Depending on the direction in which the propeller rotates, the meter will over or under register. Flow straightening vanes inserted in the pipe upstream from the propeller will help to eliminate errors resulting from this cause. Meter manufacturers usually specify that vanes be several pipe diameters in length and that they be located in a straight, horizontal piece of pipe just upstream from the propeller. The horizontal pipe length should not be less than 7 D_p. Vanes are usually made in the shape of a plus sign to divide the pipe into equal quarters. Because the area taken up by the vanes near the centre of the pipe tends to reduce the velocity at the centre of the propeller such a vane type has a negative influence on the registered discharge (about 2%) and some manufacturers suggest using vanes that do not meet in the middle. One or two diameters of clear pipe, however, between the downstream end of the vanes and the propeller will nullify any adverse effects caused by either type of vane.

If straightening vanes are not used, a long length of straight horizontal pipe (30 or more diameters long) may be required to reduce registration errors.

Velocity profiles

Changes in velocity distribution, or velocity profile, also influence registration. If the distance between the intake and the propeller is only 7 or so diameters long, the flow does not have time to reach its normal velocity distribution, and a blunt, rather evenly distributed velocity pattern results as shown in Figure 9.25, Case A. On the other hand, if the conduit length is 20 to 30 diameters or longer, the typical fully developed velocity profile as shown in Figure 9.25, Case B, occurs.

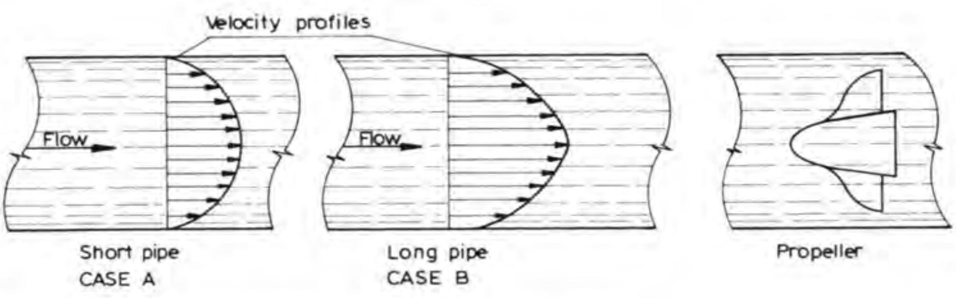

Fig.9.25. Velocity profiles (after Schuster, 1970).

Here, the velocity of flow near the centre of the pipe is high compared with the velocity near the walls. A meter whose propeller diameter is only one-half the pipe diameter would read 3 to 4 per cent higher than it would in the flat velocity profile. A larger propeller could therefore be expected to produce a more accurate meter because it is driven by more of the total flow in the line. Laboratory tests show this to be true. When the propeller diameter exceeds 75 per cent of the pipe diameter, the changes in registration due to variations of the velocity profile are minor.

Propeller motion

Since the meter, in effect, counts the number of revolutions of the propeller to indicate the discharge, any factor that influences the rate of propeller turning affects the meter registration. Practically all propeller effects reduce the number of propeller revolutions which would otherwise occur, and thus result in under-registration. Propeller shafts are usually designed to rotate in one or more bearings. The bearing is contained in a hub and is protected from direct contact with objects in the flow. However, water often can and does enter the bearing. Some hubs trap sediment, silt, or other foreign particles, and after these work into the bearing a definite added resistance to turning becomes apparent. Some propellers are therefore designed for flow through cleaning action so that particles do not permanently lodge in the bearings. Care should be taken in lubricating meter bearings. Use of the wrong lubricant (perhaps none should be used) can increase the resistance to propeller motion, particularly in cold water. It should also be established that the lubricant is reaching the desired bearing or other surfaces after it is injected. For some meters, the manufacturers do not recommend lubrication of the bearings.

Floating moss or weeds can foul a propeller unless it is protected by screens. Heavy objects can break the propeller. With larger amounts, or certain kinds, of foreign material in the water, even screens may not solve the problem.

The propeller meter will require continuous maintenance. Experience has shown that maintenance costs can be reduced by establishing a regular maintenance programme, which includes lubrication and repair of meters, screen cleaning, replacement about every 2 years, and general maintenance of the turnout and its approaches. In a regular programme many low-cost preventive measures can be made routine and thereby reduce the number of higher cost curative measures to be faced at a later time. Maintenance costs may be excessive if meters are used in sediment-laden water.

Effect of meter setting

Unless the meter is carefully positioned in the turnout, sizeable errors may result. For example, a meter with an 0.30 m propeller in an 0.60 m diameter pipe discharging 0.22 m^3/s, set with the hub centre 0.025 m off the centre of the pipe, showed an error of 1.2 per cent. When the meter was rotated 11.5° in a horizontal plane (8 mm measured on the surface of the 76 mm-diameter vertical meter shaft housing), the error was 4 per cent; for 23°, the error was 16 per cent (under-registration).

Effect of outlet box design

The geometry of the outlet box downstream from the flow meter may also affect meter accuracy. If the outlet is so narrow as to cause turbulence, boils, and/or white water, the meter registration may be affected.

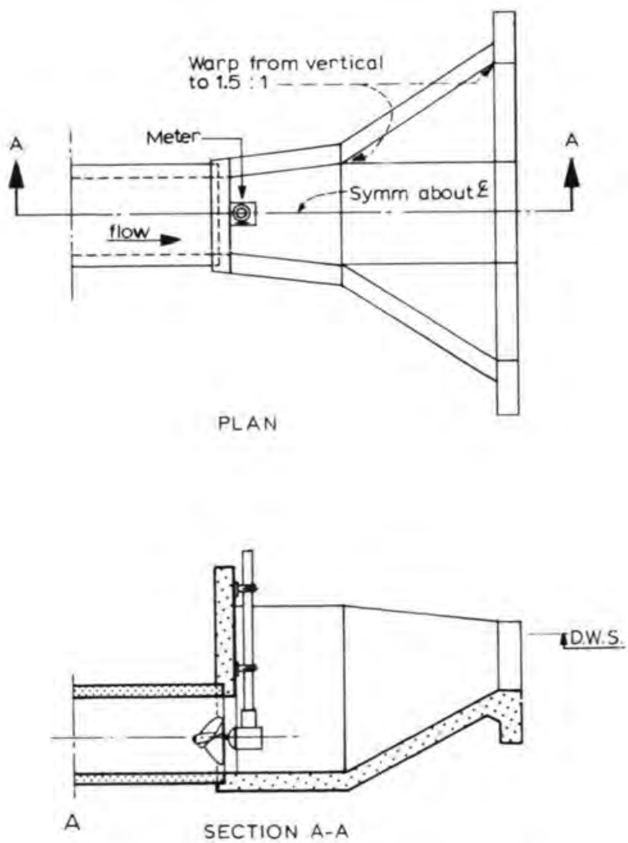

Fig.9.26. Outlet box design (after SCHUSTER, 1970).

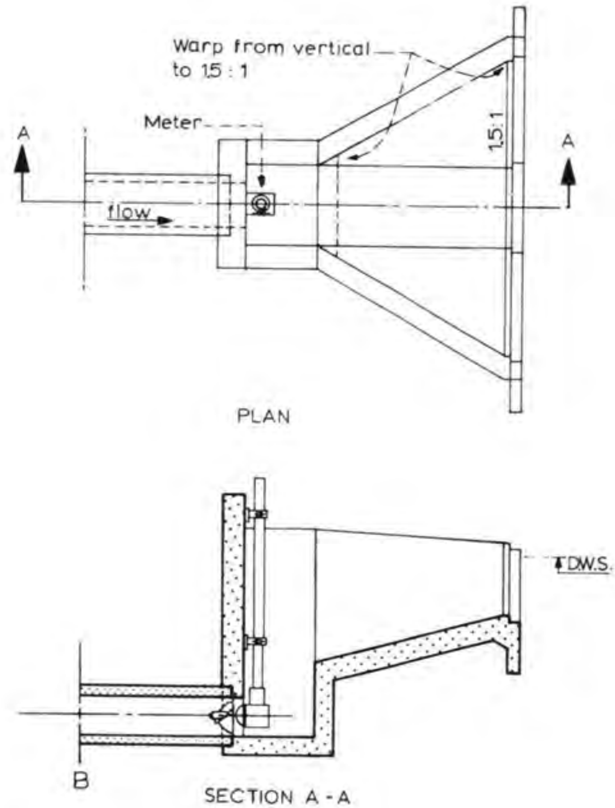

Fig.9.26. (cont.)

Figure 9.26 shows two designs of outlet boxes (to scale). Design B is believed to be the smallest outlet box that can be built without significantly affecting the meter calibration. The vertical step is as close to the meter as is desirable. Larger outlet structures - those providing more clearance between the meter and the vertical step - would probably have less effect on the registration. More rapidly diverging walls than those shown in Figure 9.26 should be avoided since they tend to produce eddies over the meter and/or surging flow through the meter and/or surging flow through the turnout. This has been observed as a continuously swinging indicator which follows the changing discharge through the meter. The surging may often be heard as well as seen. Large registration errors can occur when rapidly or continually changing discharges are being measured.

9.7.3 Head losses

Head losses across a propeller meter are usually regarded as being negligible, although there is evidence that losses may run as high as two velocity heads.

In many cases turnout losses including losses through the pipe entrance, screens, sand trap, pipe, etc., are large enough to make the losses at the meter seem negligible. Some allowance for meter losses should be made during turnout design, however, and the meter manufacturer can usually supply the necessary information. Table 9.1 may serve to give an impression of the head losses that occur over a typical propeller meter installation as shown in Figures 9.24, and in which the horizontal pipe length is 7 D_p.

TABLE 9.1. HEAD LOSSES OVER PROPELLER METER INSTALLATION (AFTER USBR, 1967)

Q, m³/s	D_p, m	Δh, m
0.085	0.30	0.50
0.140	0.36	0.54
0.280	0.46	0.66

9.7.4 Meter accuracy

The accuracy of most propeller meters, stated in broad terms, is within 5 per cent of the actual flow. Greater accuracy is sometimes claimed for certain meters and this may at times be justified, although it is difficult to repeat calibration tests, even under controlled conditions in a laboratory, to within 2 per cent. A change in lubricating practice or lubricant, along with a change in water temperature, can cause errors of this magnitude. A change in line pressure (the head on the turnout entrance) can cause errors of from 1 to 2 per cent.

9.7.5 Limits of application

The limits of application of the propeller meter for reasonable accuracy are:

a) The propeller should be installed under the conditions it was calibrated for.

b) To reduce errors due to always existing differences in velocity profiles between calibration and field structure, the propeller diameter should be as large as practicable. For a circular pipe a propeller diameter of 0.75 D_p or more is recommended.

c) The minimum length of the straight and horizontal conduit upstream from the propeller is 7 D_p, provided flow straightening vanes are used.

d) If no flow straightening vanes are used, a straight horizontal pipe without any flow disturbances and with a minimum length of 30 D_p should be used upstream from the propeller.

e) The flow velocity in the pipe should be above 0.45 m/s for best performance. In sediment-laden water the velocity should be even higher to minimize the added friction effect produced by worn bearings.

9.8 Selected list of references

1. CONE, V.M.: Divisors. The Agric.Exp.Sta. Fort Collins, Col., Bulletin 228. 1917. 52 pp.

2. DELLEUR, J.W., DOOGE, J.C.I., and GENT, K.W.: Influence of slope and roughness on the free overfall. Proc.of the American Society of Civil Engineers, Vol.82, 1956. No.HY 4, Paper No.1o38.

3. DETHRIDGE, J.S.: An Australian water meter for irrigation supplies. Engineering News, 7 (1913), No.26, Dec.25, p.1283, New York.

4. DISKIN, M.H.: End depth at a drop in trapezoidal channels. Proc.of the American Society of Civil Engineers, Vol.87, July 1961, No.HY 4, Paper No.2851.

5. GREEVE, F.W.: Measurement of pipe flow by the coordinate method. Purdue Engineering Exp.Sta., Bulletin 32, 1928.

6. ISO: Second Draft proposal for an ISO Recommendation on liquid flow measurement in open channels by weirs and flumes. Brink depth method for measurement of flow at a free overfall. ISO/TC 113/WG 2 (secretariat 26)95, December 1967.

7. KRAIJENHOFF VAN DE LEUR, D.A., and DOMMERHOLT, A.: Brink depth method for flow measurements. Supplementary data from The Netherlands to ISO/TC 113/WG2 (secretariat-26)95, December 1972.

8. LAWRENCE, F.E., and BRAUNWORTH, P.L.: Fountain flow of water in vertical pipes. American Society of Civil Engineers. Transactions vol.57, pp.256-306. 1906.

9. LEER, B.R.van: The California pipe method of water measurement. Engineering News-Record, Aug.3, 1922, Aug.21, 1924.

10. MEACHAM, I.: Water measurement in Victorian irrigation districts. The Dethridge meter. Ann.Bulletin, International Commission on Irrigation and Drainage, New Delhi, 1956, pp.14-16.

11. MURLEY, K.: Dethridge meter investigations. Aqua. Vol.17, May 1966, No.9, pp.202-211. Off.J.State Rivers and Water Supply Commission. Victoria, Austr.

12. NEOGY, B.N.: Brink Depth for trapezoidal broad-crested weir. Proc.of the Am.Society of Civil Engineers. December 1972, No.HY 12, Paper No.9427. 1972.

13. NEYRPIC: Irrigation canal equipment. Neyrpic, Grenoble, 1955. 32 pp.

14. ROHWER, C.: Discharge of pipes flowing partly full. Civil Engineering, Oct.1943.

15. ROUSE, H.: Discharge Characteristics of the free overfall. Civil Engineering, April 1936, Vol.6, No.4.

16. SCHUSTER, J.C.: Water measurement procedures. Irrigation operators' workshop. Div.of general research, Engineering and Research Centre, Bureau of Reclamation, Denver Col. Report REC-OCE-70-38, Sept.1970, 49 pp.

17. SCOTT, V.E., and HOUSTON, C.E.: Measuring irrigation water. Circular 473. California Agricultural Exp.Sta., Univ. of California. January 1959.

18. SMITH, C.D.: Brink Depth for a circular channel. Proc.Am.Soc.Civ.Engnrs. November 1962, No.HY6, Paper No.3327. 1962.

19. UNITED STATES BUREAU OF RECLAMATION. Water Measurement Manual. Denver, Colorado, 1967. 327 pp.

Appendix I
Basic equations of motion in fluid mechanics

1.1 Introduction

It is assumed that the reader of this book is familiar with the basic laws of fluid mechanics. Nevertheless, some of these laws will be discussed in this appendix to summarise material and to emphasize certain subjects which are important in the context of discharge measurement structures in open channels.

1.2 Equation of motion-Euler

In fluid mechanics we consider the motion of a fluid under the influence of forces acting upon it. Since these forces produce an unsteady motion, their study is essentially one of dynamics and must be based on Newton's second law of motion:

$$F = ma \tag{1}$$

where F is the force required to accelerate a certain mass (m) at a certain rate (a). If we consider the motion of an elementary fluid particle (dx dy dz) with a constant mass-density (ρ), its mass (m) equals

$$m = \rho \, dx \, dy \, dz \tag{2}$$

The following forces may act on this particle:

a) The normal pressures (p) exerted on the lateral faces of the elementary volume by the bordering fluid particles.

b) The mass forces, which include in the first place the gravitational force and in the second the power of attraction of the moon and the sun and the Coriolis force. These forces, acting on the mass (ρ dx dy dz) of the fluid particle, are represented together by their components in the X-, Y-, and Z-direction. It is common practice to express these components per unit of mass, and therefore as accelerations; for example, the gravitational force is expressed as the downward acceleration g.

c) Friction. There are forces in a fluid which, due to friction, act as shear forces on the lateral faces of the elementary particle (dx dy dz).

To prevent complications unnecessary in this context, the shear force is regarded as a mass force.
Gravitation and friction are the only mass forces we shall consider. If the fluid is in motion, these two forces acting on the particle (dx dy dz) do not have to be in equilibrium, but may result in an accelerating or decelerating force (pos.or neg.). This net force is named:

d) Net impressed force. This force equals the product of the mass of the particle and the acceleration due to the forces of pressure and mass not being in equilibrium. The net impressed force may be resolved in the X-, Y-, and Z-direction.

If we assume that the pressure at a point P is the same in all directions even when the fluid is in motion, and that the change of pressure intensity from point to point is continuous over the elementary lengths dx, dy, and dz, we may define the normal pressures acting, at time t, on the elementary particle as indicated in Figure A 1.1.

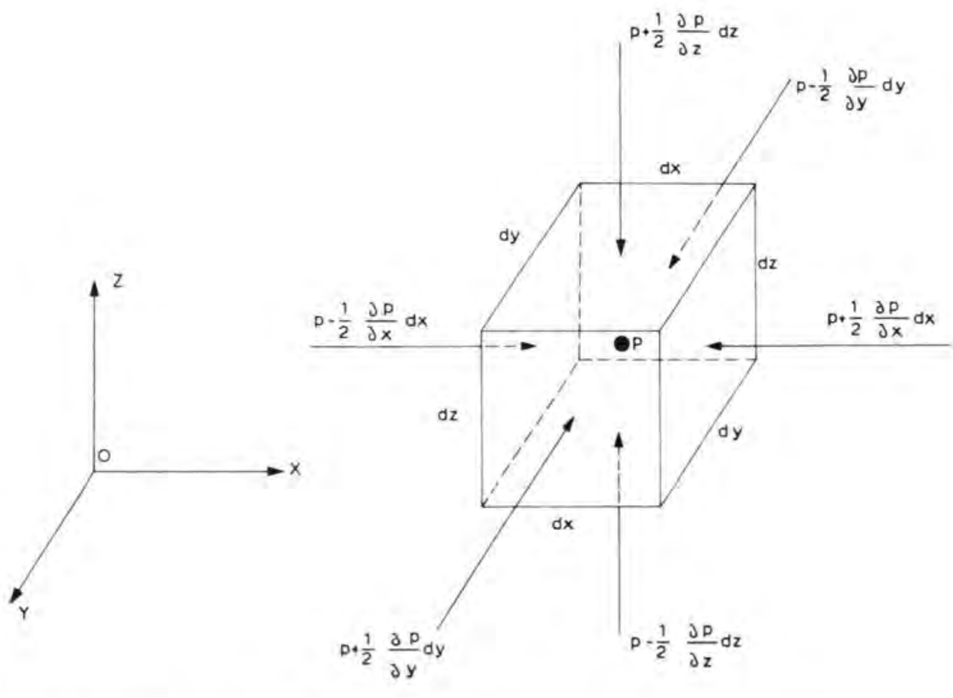

Fig.A 1.1. Pressure distribution on an elementary fluid particle.

Acting on the left-hand lateral face (X-direction) is a force

$$+ \left(p - \tfrac{1}{2}\frac{\partial p}{\partial x}\,dx\right) dy\ dz$$

while on the right-hand face is a force:

$$- \left(p + \tfrac{1}{2}\frac{\partial p}{\partial x}\,dx\right) dy\ dz$$

The resulting normal pressure on the elementary fluid particle in the X-direction equals

$$- \frac{\partial p}{\partial x}\,dx\ dy\ dz \tag{3}$$

The resultant of the combined mass forces in the X-direction equals

$$\rho\ dx\ dy\ dz\ k_x$$

where k_x is the acceleration due to gravitation and friction in the X-direction.

Hence in the X-direction, normal pressure and the combined mass forces on the elementary particle result in a total force

$$F_x = - \frac{\partial p}{\partial x}\,dx\ dy\ dz + k_x\rho\ dx\ dy\ dz \tag{4}$$

Similarly, for the forces acting on the mass (ρ dx dy dz) in the Y- and Z-direction, we may write

$$F_y = - \frac{\partial p}{\partial y}\,dx\ dy\ dz + k_y\ \rho\ dx\ dy\ dz \tag{5}$$

and

$$F_z = - \frac{\partial p}{\partial z}\,dx\ dy\ dz + k_z\ \rho\ dx\ dy\ dz \tag{6}$$

The reader should note that in the above equations k_x, k_y, and k_z have the dimension of an acceleration.

In a moving liquid the velocity varies with both position and time (Fig.A 1.2). Hence:

$$v = f(x,\ y,\ z,\ t) \tag{7}$$

and as such

$$v_x = f_x(x, y, z, t)$$

$$v_y = f_y(x, y, z, t)$$

and

$$v_z = f_z(x, y, z, t)$$

If we consider the X-direction first, we may write that at the time (t + dt) and at the point (x + dx, y + dy, z + dz) there is a velocity component in the X-direction which equals

$$v_x + dv_x$$

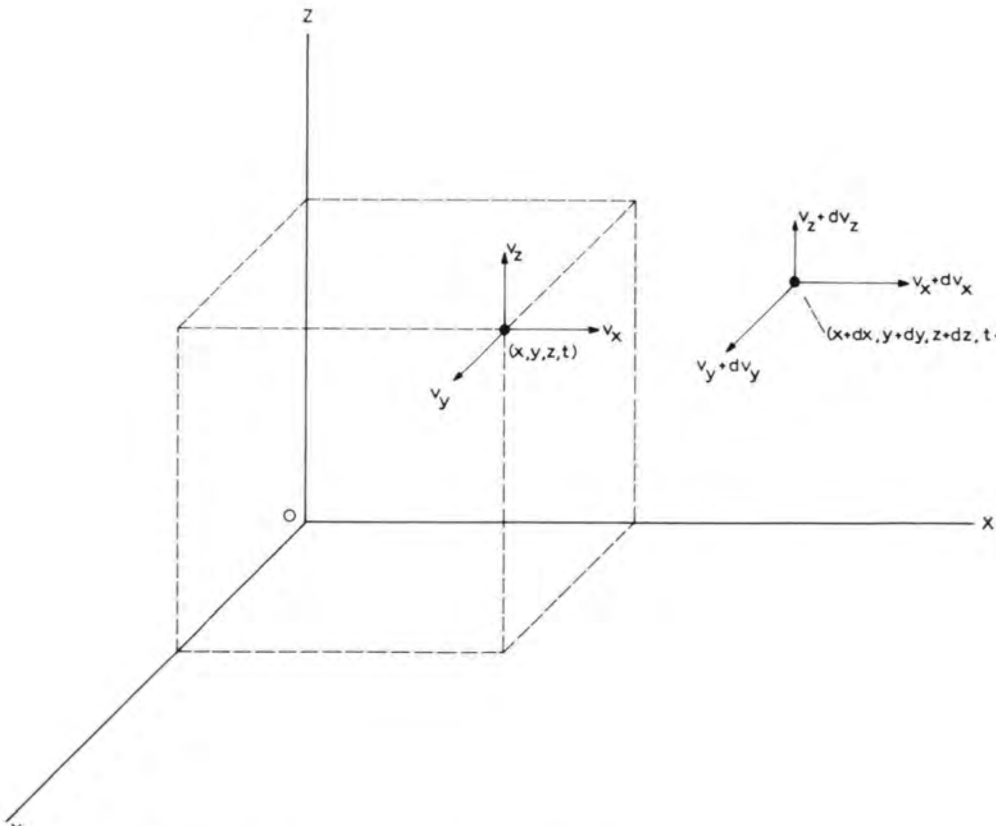

Fig.A 1.2. The velocity as a function of time and position.

The total differential of v_x is equal to

$$dv_x = \frac{\partial v_x}{\partial t} dt + \frac{\partial v_x}{\partial x} dx + \frac{\partial v_x}{\partial y} dy + \frac{\partial v_x}{\partial z} dz \tag{8}$$

In Figure A 1.3 we follow a moving fluid particle over a time dt,and see it moving along a pathline from point (x, y, z) towards point (x + dx, y + dy, z + dz), where it arrives with another velocity component ($v_x + dv_x$).

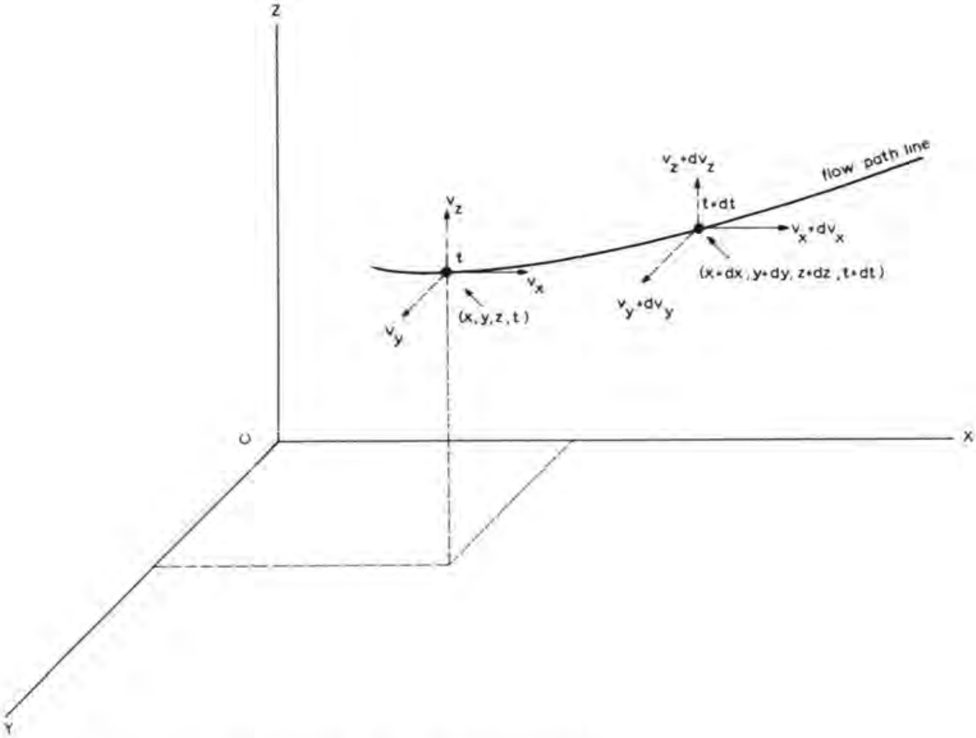

Fig.A 1.3. The flow path of a fluid particle.

The acceleration of the fluid particle in the X-direction consequently equals

$$a_x = \frac{dv_x}{dt} \tag{9}$$

while the elementary variations in time and space equal

$$dx = v_x \; dt \tag{10}$$

$$dy = v_y \; dt \tag{11}$$

$$dz = v_z \; dt \tag{12}$$

Equation 8, which is valid for a general flow pattern, also applies to a moving fluid particle as shown in Figure A 1.3, so that Equations 10 to 12 may be substituted into Equation 8, giving

$$dv_x = \frac{\partial v_x}{\partial t} dt + \frac{\partial v_x}{\partial x} v_x dt + \frac{\partial v_x}{\partial y} v_y dt + \frac{\partial v_x}{\partial z} v_z dt \tag{13}$$

and after substitution of Equation 9

$$a_x = \frac{dv_x}{dt} = \frac{\partial v_x}{\partial t} + \frac{\partial v_x}{\partial x} v_x + \frac{\partial v_x}{\partial y} v_y + \frac{\partial v_x}{\partial z} v_z \tag{14}$$

and similarly:

$$a_y = \frac{dv_y}{dt} = \frac{\partial v_y}{\partial t} + \frac{\partial v_y}{\partial x} v_x + \frac{\partial v_y}{\partial y} v_y + \frac{\partial v_y}{\partial z} v_z \tag{15}$$

$$a_z = \frac{dv_z}{dt} = \frac{\partial v_z}{\partial t} + \frac{\partial v_z}{\partial x} v_x + \frac{\partial v_z}{\partial y} v_y + \frac{\partial v_z}{\partial z} v_z \tag{16}$$

Substitution of Equations 2, 4, and 14 into Equation 1 gives

$$- \frac{\partial p}{\partial x} dx \; dy \; dz + k_x \; \rho \; dx \; dy \; dz =$$

$$\rho \; dx \; dy \; dz \left[\frac{\partial v_x}{\partial t} + \frac{\partial v_x}{\partial x} v_x + \frac{\partial v_x}{\partial y} v_y + \frac{\partial v_x}{\partial z} v_z \right]$$

or

$$\frac{\partial v_x}{\partial t} + \frac{\partial v_x}{\partial x} v_x + \frac{\partial v_x}{\partial y} v_y + \frac{\partial v_x}{\partial z} v_z = - \frac{1}{\rho} \frac{\partial p}{\partial x} + k_x \tag{17}$$

In the same manner we find for the Y- and Z-direction

$$\frac{\partial v_y}{\partial t} + \frac{\partial v_y}{\partial x} v_x + \frac{\partial v_y}{\partial y} v_y + \frac{\partial v_y}{\partial z} v_z = - \frac{1}{\rho} \frac{\partial p}{\partial y} + k_y \tag{18}$$

$$\frac{\partial v_z}{\partial t} + \frac{\partial v_z}{\partial x} v_x + \frac{\partial v_z}{\partial y} v_y + \frac{\partial v_z}{\partial z} v_z = - \frac{1}{\rho} \frac{\partial p}{\partial z} + k_z \tag{19}$$

These are the Eulerian equations of motion, which have been derived for the general case of unsteady non-uniform flow and for an arbitrary Cartesian coordinate system. An important simplification of these equations may be obtained by selecting a coordinate system whose origin coincides with the observed moving fluid particle (point P). The directions of the three axes are chosen as follows:

s-direction: the direction of the velocity vector at point P, at time t. As defined, this vector coincides with the tangent to the streamline at P at time t ($v_s = v$).

n-direction: the principal normal direction towards the centre of curvature of the streamline at point P at time t. As defined, both the s- and n-direction lie in the osculating plane.

m-direction: the binormal direction perpendicular to the osculating plane at P at time t (see also Chapter 1).

If we assume that a fluid particle is passing through point P at time t with a velocity v, the Eulerian equations of motion can be written as:

$$\frac{\partial v_s}{\partial t} + \frac{\partial v_s}{\partial s} v_s + \frac{\partial v_s}{\partial n} v_n + \frac{\partial v_s}{\partial m} v_m = - \frac{1}{\rho} \frac{\partial p}{\partial s} + k_s \qquad (20)$$

$$\frac{\partial v_n}{\partial t} + \frac{\partial v_n}{\partial s} v_s + \frac{\partial v_n}{\partial n} v_n + \frac{\partial v_n}{\partial m} v_m = - \frac{1}{\rho} \frac{\partial p}{\partial n} + k_n \qquad (21)$$

$$\frac{\partial v_m}{\partial t} + \frac{\partial v_m}{\partial s} v_s + \frac{\partial v_m}{\partial n} v_n + \frac{\partial v_m}{\partial m} v_m = - \frac{1}{\rho} \frac{\partial p}{\partial m} + k_m \qquad (22)$$

Due to the selection of the coordinate system, there is no velocity perpendicular to the s-direction; thus

$$v_n = 0 \qquad \text{and} \qquad v_m = 0 \qquad (23)$$

(Note that $\frac{\partial v_s}{\partial t} \neq 0$, $\frac{\partial v_n}{\partial t} \neq 0$, and $\frac{\partial v_m}{\partial t} \neq 0$)

Therefore the equations of motion may be simplified to:

$$\frac{\partial v_s}{\partial t} + \frac{\partial v_s}{\partial s} v_s = - \frac{1}{\rho} \frac{\partial p}{\partial s} + k_s \qquad (24)$$

$$\frac{\partial v_n}{\partial t} + \frac{\partial v_n}{\partial s} v_s = - \frac{1}{\rho} \frac{\partial p}{\partial n} + k_n \qquad (25)$$

$$\frac{\partial v_m}{\partial t} + \frac{\partial v_m}{\partial s} v_s = - \frac{1}{\rho} \frac{\partial p}{\partial m} + k_m \qquad (26)$$

Since the streamline at both sides of P is situated over an elementary length in the osculating plane, the variation of v_m in the s-direction equals zero. Hence, in Equation 26

$$\frac{\partial v_m}{\partial s} = 0 \tag{27}$$

In Figure A 1.4 an elementary section of the streamline at P at time t is shown in the osculating plane.

It can be seen that

$$\tan d\beta = \frac{\frac{\partial v_n}{\partial s} ds}{v_s + \frac{\partial v_s}{\partial s} ds} = \frac{ds}{r} \tag{28}$$

or

$$\frac{\partial v_n}{\partial s} = \frac{v_s + \frac{\partial v_s}{\partial s} ds}{r} \tag{29}$$

In the latter equation, however, $\frac{\partial v_s}{\partial s} ds$ is infinitely small compared with v_s; thus we may rewrite Equation 29 as

$$\frac{\partial v_n}{\partial s} = \frac{v_s}{r} \tag{30}$$

or

$$\frac{\partial v_n}{\partial s} v_s = \frac{v_s^2}{r} \tag{31}$$

Substitution of Equations 27 and 31 into Equations 26 and 25 respectively gives Euler's equations of motion as follows

$$\frac{\partial v_s}{\partial t} + \frac{\partial v_s}{\partial s} v_s = -\frac{1}{\rho}\frac{\partial p}{\partial s} + k_s \tag{32}$$

$$\frac{\partial v_n}{\partial t} + \frac{v_s^2}{r} = -\frac{1}{\rho}\frac{\partial p}{\partial n} + k_n \tag{33}$$

$$\frac{\partial v_m}{\partial t} = -\frac{1}{\rho}\frac{\partial p}{\partial m} + k_m \tag{34}$$

These equations of motion are valid for both unsteady and non-uniform flow. Hereafter, we shall confine our attention to steady flow, in which case all terms $\partial../\partial t$ equal zero.
Equations 32, 33, and 34 are of little use in direct applications, and they tend to repel engineers by the presence of partial derivative signs; however, they help one's understanding of certain basic equations, which will be dealt with below.

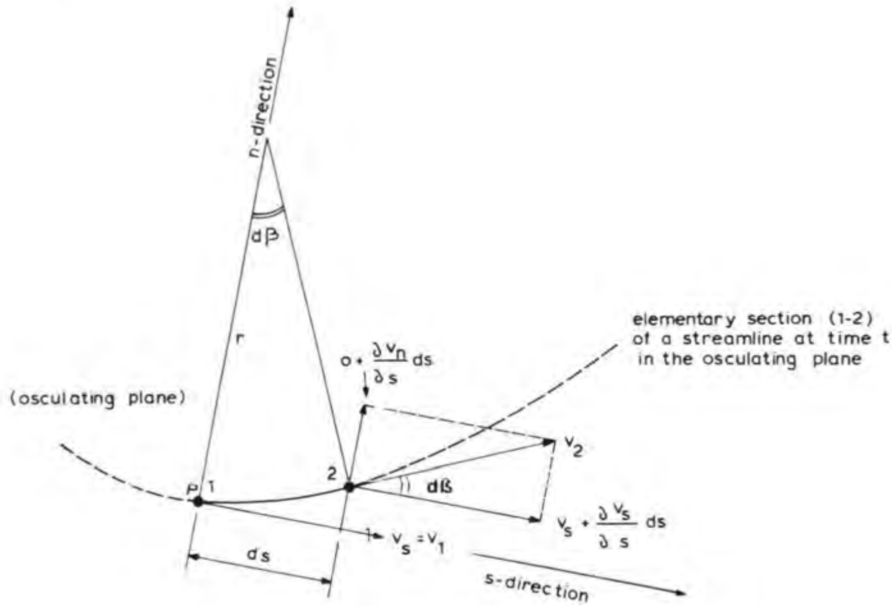

Fig.A 1.4. Elementary section of a streamline.

1.3 Equation of motion in the s-direction

If we follow a streamline (in the s-direction) we may write $v_s = v$, and the partial derivatives can be replaced by normal derivatives because s is the only dependent variable. (Thus ∂ changes into d). Accordingly, Equation 32 reads for steady flow

$$\frac{dv}{ds} v = - \frac{1}{\rho} \frac{dp}{ds} + k_s \qquad (35)$$

where k_s is the acceleration due to gravity and friction.

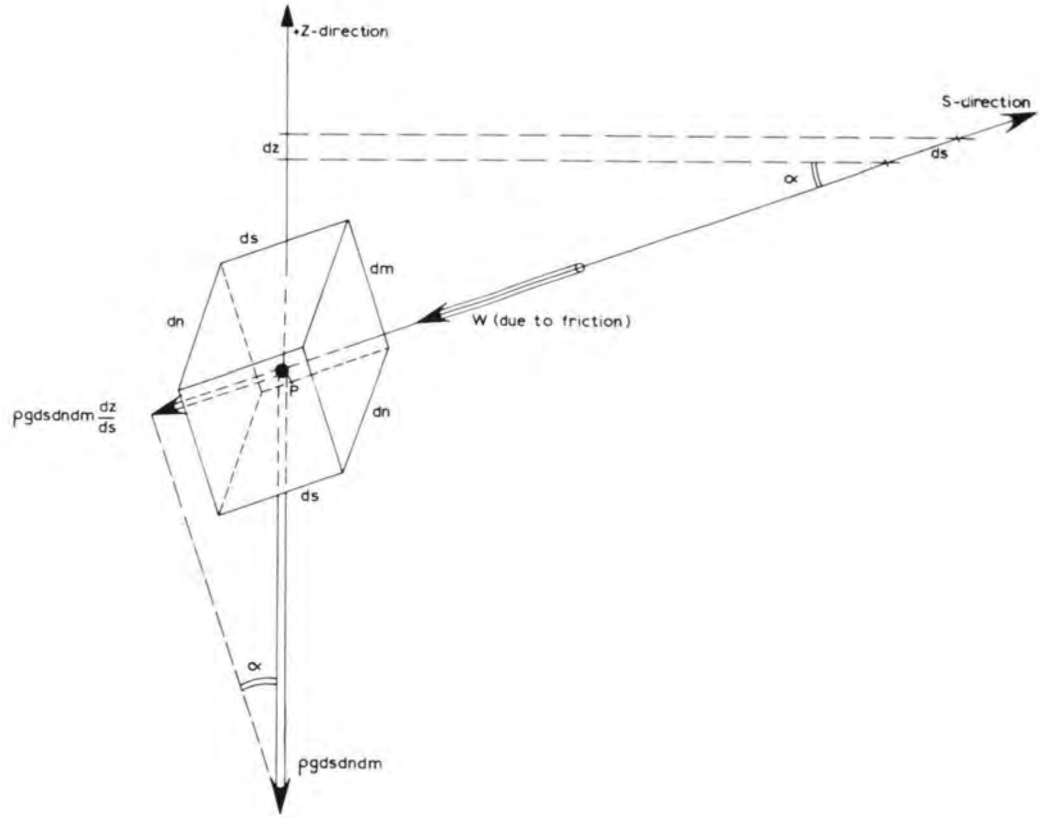

Fig.A 1.5. Forces due to gravitation and friction acting on an elementary fluid particle.

We now define the negative Z-direction as the direction of gravity. The weight of the fluid particle is

$$- \rho \ g \ ds \ dn \ dm$$

of which the component in the s-direction is

$$- \rho \ g \ ds \ dn \ dm \ \frac{dz}{ds}$$

and per unit of mass

$$\frac{-\rho \ g \ ds \ dn \ dm \ \frac{dz}{ds}}{\rho \ ds \ dn \ dm} = - \ g \ \frac{dz}{ds} \tag{36}$$

The force due to friction acting on the fluid particle in the negative s-direction equals per unit of mass

$$- w = \frac{- W}{\rho \ ds \ dn \ dm} \tag{37}$$

The acceleration due to the combined mass-forces (k_s) acting in the s-direction accordingly equals

$$k_s = - w - g \frac{dz}{ds} \tag{38}$$

Substitution of this equation into Equation 35 gives

$$\frac{dv}{ds} v = - \frac{1}{\rho} \frac{dp}{ds} - g \frac{dz}{ds} - w \tag{39}$$

or

$$\rho \ v \frac{dv}{ds} + \frac{dp}{ds} + \rho \ g \frac{dz}{ds} = - \rho \ w \tag{40}$$

or

$$d \ (\tfrac{1}{2} \ \rho \ v^2 + p + \rho \ g \ z) = - \rho \ w \ ds \tag{41}$$

The latter equation indicates the dissipation of energy per unit of volume due to local friction. If, however, the decelerating effect of friction is neglected, Equation 41 becomes

$$\frac{d}{ds} \ (\tfrac{1}{2} \ \rho \ v^2 + p + \rho \ g \ z) = 0 \tag{42}$$

Hence

$$\tfrac{1}{2} \ \rho \ v^2 + p + \rho \ g \ z = \text{constant} \tag{43}$$

where

$\frac{1}{2} \rho v^2$ = kinetic energy per unit of volume

$\rho g z$ = potential energy per unit of volume

p = pressure energy per unit of volume

If Equation 43 is divided by ρg, an equation in terms of head is obtained, which reads

$$v^2/2g + p/\rho g + z = \text{constant} = H \tag{44}$$

where

$v^2/2g$ = the velocity head
$p/\rho g$ = the pressure head
z = the elevation head
$p/\rho g+z$ = the piezometric head
H = the total energy head.

The last three heads all refer to the same reference level (see Figure 1.3, Chapter 1).

The Equations 43 and 44 are alternative forms of the well-known Bernoulli equation, and are valid only if we consider the movement of an elementary fluid particle along a streamline under steady flow conditions (pathline) with the mass-density (ρ) constant, and that energy losses can be neglected.

1.4 Piezometric gradient in the n-direction

The equation of motion in the n-direction reads for steady flow (see Eq.33)

$$\frac{v^2}{r} = - \frac{1}{\rho}\frac{dp}{dn} + k_n \tag{45}$$

Above, the ∂ has been replaced by d since n is the only independent variable. The term v^2/r equals the force per unit of mass acting on a fluid particle which follows a curved path with radius $\underline{r}$ at a velocity $\underline{v}$ (centripetal acceleration). In Equation 45, k_n is the acceleration due to gravity and friction in the n-direction. Since $v_n = 0$, there is no friction component. Analogous to its component in the direction of flow here the component due to gravitation can be shown to be

$$k_n = - g \frac{dz}{dn} \tag{46}$$

Substitution into Equation 45 yields

$$\frac{v^2}{r} = - \frac{1}{\rho}\frac{dp}{dn} - g \frac{dz}{dn} \tag{47}$$

which, after division by g, may be written as

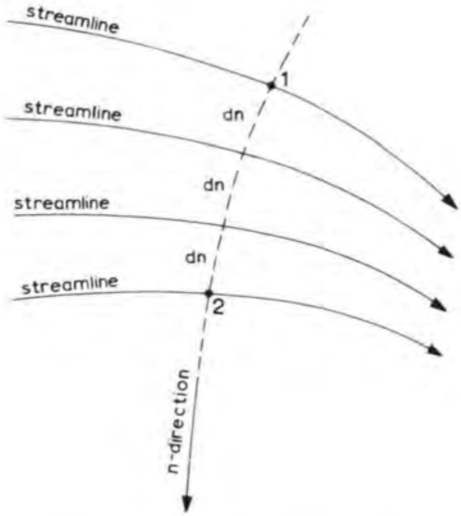

Fig.A 1.6. The principal normal direction

$$d\left(\frac{p}{\rho g} + z\right) = - \frac{v^2}{gr}\, dn \tag{48}$$

After integration of this equation from point 1 to point 2 in the n-direction, we obtain the following equation for the change of piezometric head in the n-direction:

$$\left[\frac{p}{\rho g} + z\right]_1 - \left[\frac{p}{\rho g} + z\right]_2 = \frac{1}{g} \int_1^2 \frac{v^2}{r}\, dn \tag{49}$$

where $(p/\rho g + z)$ equals the piezometric head at point 1 and 2 respectively and

$$\frac{1}{g} \int_1^2 \frac{v^2}{r}\, dn$$

is the loss of piezometric head due to curvature of the streamlines.

1.5 Hydrostatic pressure distribution in the m-direction

Perpendicular to the osculating plane, the equation of motion, according to Euler, reads for steady flow

$$- \frac{1}{\rho} \frac{dp}{dm} + k_m = 0 \tag{50}$$

Since there is no velocity component perpendicular to the osculating plane ($v_m = 0$), there is no friction either. The component of the acceleration due to gravity in the m-direction is obtained as before, so that

$$k_m = - g \frac{dz}{dm} \tag{51}$$

Substitution of this acceleration in the equation of motion (Eq.50) gives

$$- \frac{1}{\rho} \frac{dp}{dm} - g \frac{dz}{dm} = 0 \tag{52}$$

which may be written as

$$\frac{d}{dm} \left(\frac{p}{\rho g} + z \right) = 0 \tag{53}$$

It follows from this equation that the piezometric head in the m-direction is

$$\frac{p}{\rho g} + z = \text{constant} \tag{54}$$

irrespective of the curvature of the streamlines.

In other words, perpendicular to the osculating plane, there is a hydrostatic pressure distribution.

Appendix II
The overall accuracy of the measurement of flow

2.1 General principles

Whenever a flow rate or discharge is measured, the value obtained is simply the best estimate of the true flow rate which can be obtained from the data collected; the true flow rate may be slightly greater or less than this value. This appendix describes the calculations required to arrive at a statistical estimate of the range which is expected to cover the true flow rate.

The usefulness of the flow rate measurement is greatly enhanced if a statement of possible error accompanies the result. The error may be defined as the difference between the true flow rate and the flow rate which is calculated from the measured water level (upstream head) with the aid of the appropriate head-discharge equations.

It is not relevant to give an absolute upper bound to the value of error. Due to chance, such bounds can be exceeded. Taking this into account, it is better to give a range which is expected to cover the true value of the measured quantity with a high degree of probability.

This range is termed the uncertainty of measurement, and the confidence level associated with it indicates the probability that the range quoted will include the true value of the quantity being measured. In this appendix a probability of 95% is adopted as the confidence level for all errors.

2.2 Nature of errors

Basically there are three types of error which must be considered (see Fig.1):

a) Spurious errors (human mistakes and instrument malfunctions)
b) Random errors (experimental and reading errors)
c) Systematic errors (which may be either constant or variable)

NOTE: Sections 1 and 2 of this appendix are based on a draft proposal of an ISO standard prepared by KINGHORN

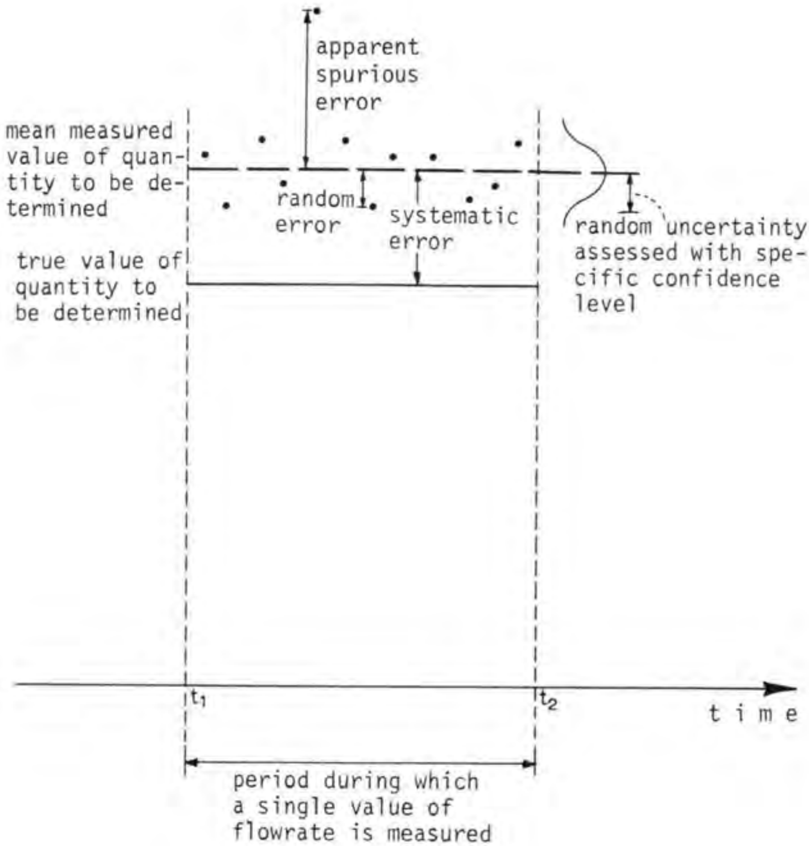

Fig.A 2.1. Illustration of terms.

Spurious errors are errors which invalidate a measurement. Such errors cannot be incorporated into a statistical analysis with the object of estimating the overall accuracy of a measurement and the measurement must be discarded.Steps should be taken to avoid such errors or to recognize them and discard the results. Alternatively, corrections may be applied.

Random errors are errors that affect the reproducibility of measurement. It is assumed that data points deviate from the mean in accordance with the laws of chance as a result of random errors. The mean random error of a summarized discharge over a period is expected to decrease when the number of discharge measurements during the period increases.As a result, the integrated flow over a long period of observation will have a mean random error that approaches zero. It is emphasized that this refers to time-dependent errors only, and that the length of time over which observations should be made has to be several times the period of fluctuations of flow.

Systematic errors are errors which cannot be reduced by increasing the number of measurements so long as equipment and conditions remain unchanged.

Whenever there is evidence of a systematic error of a known sign, the mean error should be added to (or subtracted from) the measurement results. A residual systematic error should be assessed as half the range of possible variation that is due to this systematic error.

A strict separation of random and systematic errors has to be made because of their different sources and the different influence they have on the total error. This influence will depend on whether the error in a single measurement is concerned, or that in the sum of a series of measurements.

2.3 Sources of errors

For discharge measurement structures, the sources of error may be identified by considering a generalized form of head-discharge equation:

$$Q = w\, C_d\, C_v\, f\sqrt{g}\, b\, h_1^u \qquad (1)$$

where w and u are numerical constants which are not subject to error. The acceleration due to gravity, g, varies from place to place, but the variation is small enough to be neglected in flow measurement.

So the following errors remain to be considered:

δC = error in product $C_d\, C_v$

δf = error in drowned flow reduction factor f

δb = error in dimensional measurement of weir; e.g. the width of the weir b or the weir notch angle θ

δh = error in h_1 and/or Δh

The error δC of each of the standard structures described in Chapters 4 to 9 is given in the relevant sections on evaluation of discharge. These errors are considered to be constant and systematic. This classification is not entirely correct because C_d and C_v are functions of h_1. However, the variations in C_d and C_v as a function of h_1 are sufficiently small to be neglected.

When flow is modular, the drowned flow reduction factor f is constant (f=1.0) and is not subject to error. As a result, for modular flow $\delta f = 0$. When flow is non-modular (submerged) the error δf consists of a systematic error, δf_n, being the error in the numerical value of f, and of systematic and random errors caused by the fact that f is a function of the submergence ratio $S_h = H_2/H_1 \approx H_2/h_1$.

The error δb depends on the accuracy with which the structure as constructed can be measured, and is also a systematic error. In practice this error may prove to be insignificant in comparison with other errors. The error δh_1 has to be split into a random error δh_R and a systematic error δh_S. Those errors may contain many contributory errors. Possible sources of contributory errors are:

- (i) internal friction of the recording system
- (ii) inertia of the indication mechanism
- (iii) instrument errors
- (iv) zero setting
- (v) settling or tilting sideways of the structure with time
- (vi) the crest not being level, or other construction faults not included in δb
- (vii) improper maintenance of the structure (this also may cause an extra error δC)
- (viii) reading errors

We have to be careful in recognizing whether an error is random or systematic. Some sources can cause either systematic or random errors, depending on circumstances. Internal friction of the recorder, for example, causes a systematic error of a single measurement or a number of measurements in a period when either rising or falling stage is being considered, but a random error if the total discharge through an irrigation canal per season is being considered. On natural streams, however, falling stage may occur over a much longer period than rising stage and here the internal friction of the recorder once again results in a systematic error. Also zero setting may cause either a systematic or a random error. If a single measurement or measurements within the period between two zero settings are considered,the error will be systematic; it will be random if one is considering the total discharge over a period which is long in comparison with the interval between zero settings. The errors due to (iii), (v), and (vi) are considered to be systematic, that due to (viii) being random.

In the following sections the term relative error will frequently be found. By this we mean the error in a quantity divided by this quantity. For example, the relative error in h_1 equals $X_{h_1} = \delta h_1/h_1$.

2.4 Propagation of errors

The overall error in the flow Q is the resultant of various contributory errors, which themselves can be composite errors. The propagation of errors is to be based upon the standard deviation of the errors. The standard deviation σ out of a set of measurements on Y may be estimated by the equation

$$\sigma^2 = \frac{\sum_{i=1}^{n} (Y_i - \bar{Y})^2}{n - 1} \tag{2}$$

where

$\bar{Y}$ = the arithmetic mean of the n-measurements of the variable Y

Y_i = the value obtained by the i^{th} measurement of the variable Y

n = the total number of measurements of Y.

The relative standard deviation σ' equals σ divided by the observed mean. Hence

$$\sigma' = \frac{1}{\bar{Y}} \left[\frac{\sum_{i=1}^{n} (Y_i - \bar{Y})^2}{(n - 1)} \right]^{\frac{1}{2}} \tag{3}$$

The relative standard deviation of the mean σ'_Y, of n-measurements is given by

$$\sigma'_Y = \frac{\sigma'}{\sqrt{n}} \tag{4}$$

If Equations 2 to 4 cannot be used to estimate the relative standard deviation, it may be estimated by using the relative error of the mean for a 95% confidence level, X_i. The value of X_i is either given (X_c), or must be estimated.

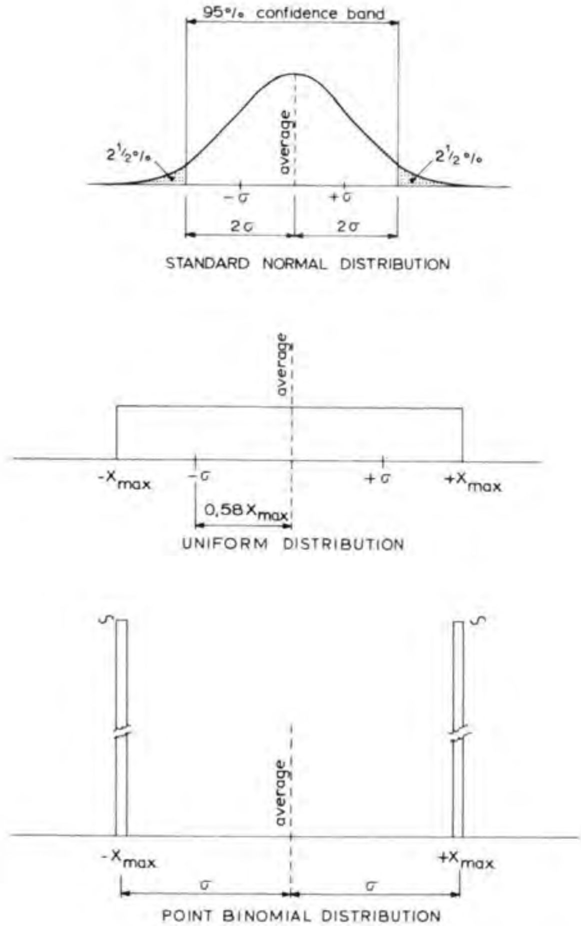

Fig.A 2.2. Possible variation of measured values about the average (actual) value.

To estimate σ' it is necessary to know the distribution of the various errors. In this context we distinguish three types of distribution (see Fig.A 2.2):

- normal distribution: For practical purposes it is assumed that the distribution of the errors in a set of measurements under steady conditions can be sufficiently closely approximated by a normal distribution. If σ' is based on a large number of observations, the error of the mean for a 95% confidence level equals approximately two times σ' ($\sigma' = 0.5\ X$). This factor of two assumes that n is large. For $n = 6$ the factor should be 2.6; $n = 10$ requires 2.3 and $n = 15$ requires 2.1.

- uniform distribution: For errors X having their extreme values at either $+X_{max}$ or $-X_{max}$ with an equal probability for every error size in this range, σ' equals 0.58 X_{max} ($\sigma' = 0.58\ X_{max}$).

- point binomial distribution: For errors X which always have an extreme value of either $+X_{max}$ or $-X_{max}$, with an equal probability for each of these values, σ' equals 1.0 X_{max} ($\sigma' = X_{max}$).

To determine the magnitude of composite errors the standard deviation has to be used. The composite standard deviation can be calculated with the following equation

$$\sigma'_T = \left[\sum_{i=1}^{k} G_i\ \sigma'_i \right]^{\frac{1}{2}} \qquad (5)$$

in which

$$G_i = \frac{\partial T}{\partial F_i} \frac{F_i}{T} \qquad (6)$$

where

σ'_T = relative standard deviation of the composite factor T

σ'_i = relative standard deviation of the factor F_i

F_i = relevant factor influencing Q; the error of this factor is uncorrelated with the errors in other contributory factors of Equations 5 and 6; F_i may itself be a composite factor

It is emphasized that only factors with uncorrelated errors can be introduced in Equation 5. This means that it is incorrect to determine σ'_Q by substituting σ'_c, σ'_f, σ'_b, and σ'_h into Equation 5 because the errors in f and h_1 are correlated. One must start from relevant (=contributing to δC, δb, δf and δh_1) errors or standard deviations which are mutually independent. For weirs and flumes, those independent errors are generally δC, δb, δf_n[†], δh_1 (containing δh_{1R} and δh_{1S}) and δH_2 (containing δH_{2R} and δH_{2S}). The first three errors are systematic errors. The last two errors are often composite errors themselves, and their magnitude has to be determined with the use of Equations 5 and 6.

† δf_n is the error in the numerical value of f and has no relation to δh_1. Systematic and random errors in f caused by its relation to h_1 and H_2 are not independent and cannot be substituted into Equation 5.

Substitution into Equation 6 of the independent factors contributing to the overall error in Q and their relative standard deviations yields the first two terms of the following equations.

$$G_c = \frac{\partial Q}{\partial C}\frac{C}{Q} = 1$$

$$G_b = \frac{\partial Q}{\partial b}\frac{b}{Q} = 1$$

$$G_{f_n} = \frac{\partial Q}{\partial f_n}\frac{f}{Q} = 1$$

$$G_{h_1} = \frac{\partial Q}{\partial h_1}\frac{h_1}{Q} = u - \frac{\partial f}{\partial S_h}\frac{S_h}{f}$$

$$G_{H_2} = \frac{\partial Q}{\partial H_2}\frac{H_2}{Q} = \frac{\partial f}{\partial S_h}\frac{S_h}{f}$$

The righthand side of these equations is found by partial differentiation of Equation 1 to C, b, f_n, h_1, and H_2 respectively. In doing so we have to take into account that f is a function of $S_h \simeq H_2/h_1$. Putting

$$\frac{\partial f}{\partial S_h}\frac{S_h}{f} = \frac{\Delta f}{\Delta S_h}\frac{S_h}{f} = G \tag{7}$$

and substituting the above information into Equation 5 gives

$$\sigma'_Q = \left[\sigma'^2_c + \sigma'^2_b + \sigma'^2_{fn} + (u-G)^2\,\sigma'^2_{h_1} + G^2\,\sigma'^2_{H_2}\right]^{\frac{1}{2}} \tag{8}$$

As has been mentioned in the section on sources of error, we have to distinguish between systematic and random errors because of their different influences on the accuracy of measured volumes over long periods. Using the given information on the character of various errors, we can divide Equation 8 into two equations; one for random errors and the other for systematic errors, as follows:

$$\sigma'_{QR} = \left[(u-G)^2\,\sigma'^2_{h_1R} + G^2\,\sigma'^2_{H_2R}\right]^{\frac{1}{2}} \tag{9}$$

$$\sigma'_{QS} = \left[\sigma'^2_c + \sigma'^2_b + \sigma'^2_{fn} + (u-G)^2\,\sigma'^2_{h_1S} + G^2\,\sigma'^2_{H_2S}\right]^{\frac{1}{2}} \tag{10}$$

For most discharge measuring structures, the error δf_n is unknown. We know, however, that if f does not deviate much from unity (near modular flow), the error δf_n is negligible. For low values of f ($f <$ appr.0.8), the error in the numerical value of f, δf_n, becomes large, but then the absolute value of G becomes so large that the structure ceases to be an accurate measuring device. As mentioned, δf_n is usually unknown and therefore it is often assumed that $\delta f_n \approx 0$ and thus also $\sigma'_{f_n} \approx 0$.

To determine G we need a relationship between the drowned flow reduction factor and the submergence ratio. If we have, for example, a triangular broad-crested weir operating at a submergence ratio $H_2/H_1 = 0.925$, we can determine G (being a measure for the "slope" of the S_h-f-curve) from Figure 4.11 as

$$G = \frac{\Delta f/f}{\Delta s_h/S_h} = \frac{(0.775 - 0.825)/0.80}{(0.932 - 0.918)/0.925} = -4.1$$

It should be noted that G always has a negative value.

From Equations 9 and 10, it may be noted that σ'_Q increases sharply if $|G|$ increases, i.e. if the slope of the H_2/H_1-f-curve in Figure 4.9 becomes flat.

If flow is modular, the drowned flow reduction factor f is constant and is not subject to error (f=1.0).

Thus, $\sigma'_{f_n} = 0$ and $G = 0$, and as a consequence Equations 9 and 10 reduce to

$$\sigma'_{QR} = u\,\sigma'_{h_1R} \tag{11}$$

and

$$\sigma'_{QS} = \left[\sigma'^2_c + \sigma'^2_b + u^2\,\sigma'^2_{h_1S}\right]^{\frac{1}{2}} \tag{12}$$

It is noted again that Equations 11 and 12 are only valid if flow is modular. It can be proved that the combination of a sufficiently large number of errors not having a normal distribution tends to a composite error having a normal distribution. So we may assume that the overall error of the flow rate measurement has a normal distribution even if the overall error is the result of the combination of a few errors not having a normal distribution. Thus, the overall relative error of the flow rate for a single discharge measurement approximates

$$X_Q = 2\left[{\sigma'_{QR}}^2 + {\sigma'_{QS}}^2\right]^{\frac{1}{2}} \tag{13}$$

It should be realized that the relative error X_Q is not a single value for a given device, but will vary with discharge. It is therefore necessary to consider the error at several discharges covering the required range of measurement.

In error analysis, estimates of certain errors (or standard deviations) will often be used. There is a general tendency to underestimate errors. In some cases they may even be overlooked.

2.5 Errors in measurements of head

When errors are quoted, the reader should be aware that the general tendency is for them to be underestimated. He should also realize that errors having a 95 per cent confidence level must be estimated by the user.

Chapter 2.2 indicates that the head measurement station should be located sufficiently far upstream of the structure to avoid the area of surface drawdown, yet it should be close enough for the energy loss between the head measurement station and structure to be negligible. For each of the standard structures described in Chapters 4 to 9, the location of the head measurement station has been prescribed. In practice, however, it very often happens that this station is located incorrectly, resulting in very serious errors in head.

Insufficient depth of the foundation of the structure or the head measurement device, or both, can cause errors in the zero-setting since ground-frost and changes in soil-moisture may move the structure and device. To limit errors in zero setting it is recommended that the setting be repeated at least twice a year; for example, after a period of frost, after a rainy season, or during summer or a dry season. The reading error of a staff-gauge is strongly influenced by the reading angle and the distance between the gauge and the observer, the turbulence of the water, and the graduation unit of the gauge.

For example, a staff gauge with centimeter graduation placed in standing water can be read with a negligible systematic error and a random reading error of 0.003 m. If the same gauge is placed in an approach channel with a smooth water surface, the gauge becomes more difficult to read and a systematic reading error of 0.005 m and a random reading error of 0.005 m may be expected. Little research has been done on this subject, although ROBERTSON (1966) reports on the reading error of a gauge with graduation in feet and tenths of a foot located in reasonably still water in a river. He recorded a systematic reading error of 0.007 m and a random reading error of 0.007 m. The graduation unit of the reported gauge equaled 0.03 m.If the water surface is not smooth or the position of the observer is not optimal, or both, reading errors exceeding one or more graduation units must be expected.

It is obvious that a dirty gauge face hinders readings and will cause serious reading errors. Staff gauges should therefore be installed in locations where it is possible for the observer to clean them.

Since reading a gauge in standing water causes a smaller reading error than one read in streaming water, the use of a stilling well must be considered whenever the accuracy of head readings has to be improved. The stilling well should be designed according to the instructions given in Chapter 2.6.

When a float-operated automatic water level recorder is used great care should be given to the selection of the cable, although it is recommended that a calibrated float tape be used instead. The cable or tape should not stretch and should be made of corrosion-resistant material.

Several errors are introduced when a float-operated recorder is used in combination with a stilling well. These are:

- Lag error due to imperfections in the stilling well. This error, caused by head losses in the pipe connecting the stilling well with the approach channel during rising or falling discharges or head losses caused by a leaking stilling well, has also been considered in Chapter 2.6.

- Instrument errors, due to imperfections in the recorder. This error depends on contributory errors due to internal friction of the recorder, faulty zero setting, and back-lash in the mechanism, etc.

The magnitude of internal friction should be given by the manufacturer of the recorder. The reader should realize, however, that manufacturers are sometimes rather optimistic and that their data are valid for factory-new recorders only. Regular maintenance will be required to minimize internal friction. The error due to internal friction and those caused by a change in cable weight hanging on one side of the float wheel or submergence of the counter weight are considered

in Chapter 2.9. The magnitude of all these errors is inversely proportional to the square of the float diameter (d^2).
To give an idea of the order of magnitude of errors that may occur in automatic recorders we cite three examples:

- STEVENS (1919) reports on a recorder equipped with a ø 0.25 m float, a steel cable, and a 4 kg counter weight. The following errors were observed:

Error due to submergence of counterweight 0.0015 m. Difference in readings between falling and rising stage due to internal friction 0.002 m. An increasing total weight of cable plus counter weight hanging on one side of the cable wheel caused a registration error of 0.06%.

- ROBERTSON (1966) reports on the reading error of recorder charts. When a writing mechanism with 1:1 reduction (full scale) was used, the systematic reading error was negligible and the random error was 0.010 m. For a writing mechanism with 10:1 reduction, however, a systematic error of 0.010 m and a random error of 0.016 m was reported. No float diameter was mentioned.

- AGRICULTURAL UNIVERSITY (1966) at Wageningen reports on laboratory tests conducted under ideal conditions with a digital recorder giving a signal for a 0.003 m head interval. Equipped with a ø 0.20 m float the digital reading showed a negligible systematic error and a random error of 0.002 m. In addition, a difference of 0.002 m was found between readings for falling and rising stage. The errors found in the Wageningen tests must be regarded an absolute minimum.

It should be noted that if waves are dampened in the approach channel by means of a stilling well a systematic error may be introduced. This is a result of the non-linear relationship between the head and the discharge.

2.6 Coefficient errors

The coefficient errors presented in Chapters 4 to 9 are valid for well-maintained clean structures. To obtain the accuracies listed, sediment, debris, and algal growth must be removed regularly. To keep the structure free of weed, fungicides can be used. The best method is probably to add, say, 0.5 per cent by weight of cement copper oxide to facing concrete during mixing. Copper sulphate or another appropriate fungicide can be applied to existing concrete but frequent treatment will be required. Algal growth on non-concrete structural parts can be prevented by regular treatment with an anti-fouling paint such as that used on yachts.

It must be realized that algal growth on broad-crested weirs and flumes increases friction and "raises" the crest. Consequently algal growth has a negative influence on C_d-values. On sharp-crested weirs or sharp-edged orifices, algal growth reduces the velocity component along the weir face, causing an increase of C_d-values.

NAGLER (1929) investigated this type of influence on a sharp-crested weir whose upstream weir face was roughened with coarse sand. He found that, compared with the coefficient value of a smooth-faced weir the discharge coefficient increased by as much as 5 per cent when $h_1 = 0.15$ m and by 7 per cent when $h_1 = 0.06$ m. Algal growth on the upstream face of sharp-crested weirs may cause a "rounding-off" of the edge which, in addition to reducing the velocity component along the weir face, causes a decrease of contraction and consequently results in an increase of the discharge coefficient. For a head of 0.15 m, THOMAS (1957) reported an increase of some 2, 3, 5.5, 11, and 13.5 per cent due solely to the effect of rounding-off by radii of a mere 1, 3, 6, 12, and 19 mm respectively.

Another factor that will cause the discharge coefficient to increase is insufficient aeration of the air pocket beneath the overfalling nappe of a sharp- or short-crested weir (see also Chap.1.14).

2.7 Example of error combination

In this example all errors mentioned are expected to have a 95 per cent confidence level. We shall consider a triangular broad-crested weir as described in Chapter 4.3, flowing less-than-full, with a vertical back face, a crest length $L = 0.60$ m, a weir notch angle $\theta = 120^\circ$, and a crest height $p = 0.30$ m. According to Chapter 4.3, the following head-discharge equation applies

$$Q = C_d C_v \frac{16}{25}\sqrt{\frac{2g}{5}}\ f\ \tan\frac{\theta}{2}\ h_1^{2.5} \qquad (14)$$

Both upstream and downstream heads were measured by identical digital recorders giving a signal for every 0.003 m head difference (thus maximum reading error is 0.0015 m). The random error due to internal friction of the recorder was 0.002 m. The systematic error in zero setting was estimated to be 0.002 m due to internal friction of the recorder and 0.001 m due to the procedure used. The latter error is due to the difficulty of determining the exact elevation of the crest.

In addition to these errors, it was found that over the period between two successive zero settings the stilling well plus recorder had subsided 0.005 m more than the structure. To correct for this subsidence, all relevant head readings were increased by 0.0025 m, leaving a systematic error of 0.0025 m. The frequency distribution of the error due to subsidence is unknown, but is likely to be more irregular than a normal distribution. If subsidence occurs over a period which is short compared with the interval between two zero settings, the ratio σ_i'/X_i approaches unity. In our example we assume σ_i'/X_i to equal 0.75. The error in the discharge coefficient (including C_v) is given by the equation

$$X_c = \pm 2(21 - 20\ C_d) \text{ per cent} \tag{15}$$

The overall error in a single discharge measurement for three different states of flow has been calculated in Table 1. From this example it appears that even if accurate head registration equipment is used, the accuracy of a single measurement at low heads and at small differential heads $H_1 - H_2$ is low.

For an arbitrary hydrograph, the random error in the total discharge over a long period equals zero. If, however, the hydrograph shows a considerably shorter period of rising stage than of falling stage, as in most streams and sometimes in irrigation canals, the internal friction of an automatic recorder (if used) causes a systematic error which cannot be neglected.

The factor that has the greatest influence on the accuracy of discharge measurements is the accuracy with which the head h_1 or the differential head Δh can be measured. This warrants a careful choice of the equipment used to make such head measurements. This holds especially true for structures where the discharge is a function of the head differential, $h_1 - h_2$, across the structure, as it is for instance for submerged orifices.

If h_1 and h_2 are measured independently by two separate gauging systems, the errors of both measurements have to be combined by using Equation 5. In doing so, the errors have to be expressed as percentage errors of the differential head $(h_1 - h_2)$, thus not of h_1 and h_2 separately. If a differential head meter as described in Chapter 2.12 is used to measure $(h_1 - h_2)$, errors due to zero-

TABLE 1. EXAMPLES OF ACCURACY COMPUTATION

Source of error	Type of error	Ratio σ'_i/X_i	State of flow: $h_1 = 0.06$ m $C_d = 0.920$, $H_2 =$ nil $f = 1.0$	$h_1 = 0.40$ m $C_d = 0.996$, $H_2 = 0.30$ m $f = 1.0$	$h_1 = 0.40$ m $C_d = 0.996$, $H_2 = 0.37$ m $f = 0.80$
C_d C_v	S	0.50	$\sigma'_c = 2.6\%$	$\sigma'_c = 1.1\%$	$\sigma'_c = 1.1\%$
procedure of zero setting	S	0.50	$\sigma'_{h1} = 0.8\%$	$\sigma'_{h1} = 0.1\%$	σ'_{h1} $(= \sigma'_{H2}) = 0.1\%$
internal friction-zero setting	S	1.0	$\sigma'_{h1} = 3.3\%$	$\sigma'_{h1} = 0.5\%$	σ'_{h1} $(= \sigma'_{H2}) = 0.5\%$
internal friction	R	1.0	$\sigma'_{h1} = 3.3\%$	$\sigma'_{h1} = 0.5\%$	σ'_{h1} $(= \sigma'_{H2}) = 0.5\%$
subsidence	S	0.75	$\sigma'_{h1} = 3.1\%$	$\sigma'_{h1} = 0.45\%$	σ'_{h1} $(= \sigma'_{H2}) = 0.45\%$
digital reading	R	0.58	$\sigma'_{h1} = 1.5\%$	$\sigma'_{h1} = 0.23\%$	σ'_{h1} $(= \sigma'_{H2}) = 0.23\%$
crest level	S	0.50	$\sigma'_{h1} = 0.8\%$	$\sigma'_{h1} = 0.13\%$	σ'_{h1} $(= \sigma'_{H2}) = 0.13\%$
Calculated value	**Equation used**				
σ'_{h_1R}	5		$\sigma'_{h_1R} = 3.6\%$	$\sigma'_{h_1R} = 0.55\%$	$\sigma'_{h_1R} = \sigma'_{H_2R} = 0.55\%$
σ'_{h_1S}	5		$\sigma'_{h_1S} = 4.7\%$	$\sigma'_{h_1S} = 0.70\%$	$\sigma'_{h_1S} = \sigma'_{H_2S} = 0.70\%$
G	7				G = -4.1
σ'_{QR}	9 or 11		$\sigma'_{QR} = 9\%$	$\sigma'_{QR} = 1.40\%$	$\sigma'_{QR} =$ 3.9%
σ'_{QS}	10 or 12		$\sigma'_{QS} = 12\%$	$\sigma'_{QS} = 2.05\%$	$\sigma'_{QS} >$ 5.6% [1]
X_Q	13		$X_Q = 30\%$	$X_Q = 4.95\%$	$X_Q >$ 13.6% [1]

[1] *σ'_{QS} and X_Q are greater than values shown because the systematic error of the f-value is unknown and not included in this computation*

settings and in some cases due to reading of one head are avoided, thereby providing more accurate measurements.

2.8 Error in discharge volume over long period

If during a "long" period a great number of single discharge measurements ($n > 15$) are made and these measurements are used in combination with head readings, to calculate the discharge volume over an irrigation season or hydrological year, the percentage random error $X_{vol.R}$ tends to zero and can be neglected.

The systematic percentage error $X_{vol.S}$ of a volume of water measured at a particular station is a function of the systematic percentage error of the discharge (head) at which the volume was measured. Since the systematic percentage error of a single measurement decreases if the head increases, a volume measured over a long period of low discharges will be less accurate than the same volume measured over a (shorter) period of higher discharge. As a consequence we have to calculate $X_{vol.S}$ as a weighted error by use of the equation

$$X_{vol.S} = 2 \frac{\int Q\sigma'_{QS}dt}{\int Qdt} \tag{16}$$

which may also be written as

$$X_{vol.S} = 2 \frac{\sum_{i=1}^{k} Q_i \sigma'_{QS} \Delta t}{\sum_{i=1}^{k} Q_i \Delta t} \tag{17}$$

where

Δt = period between two successive discharge measurements

By using Equations 16 and 17 the reader will note that the value of $X_{vol.S} = X_{vol}$ will be significantly lower than the single value X_Q and will be reasonably small, provided that a sufficient number of measurements are made over the period considered.

2.9 Selected list of references

1. AGRICULTURAL UNIVERSITY, Wageningen: Voortgezet onderzoek van registrerende waterstands meters. Hydraulica Laboratorium. Nota No.4, 15 pp. 1966.

2. BRITISH STANDARD INSTITUTION: Measurement of liquid flow in open channels. Part 4: Weirs and flumes. 4B: Long base weirs. BS 3680. London 1969.BSI. 39 pp.

3. KINGHORN, F.C.: Draft proposal for an ISO standard on the calculation of the uncertainty of a measurement of flowrate. Doc.No.ISO/TC 30/WG 14:24 E. 1975.

4. NAGLER, F.A.: Discussion of precise weir measurements. Transaction ASCE. Vol.93. 1929. p.115.

5. ROBERTSON, A.I.G.S.: The magnitude of probable errors in water level determination at a gauging station. Water Resources Board. TN 7, Reading, England. 1966. Reprinted 1970.

6. STEVENS, J.C.: The accuracy of water-level recorders and indicators of the float type. Transactions ASCE. Vol.83. 1919.

7. THOMAS, C.W.: Common errors in measurement of irrigation water. Journal Irrigation and Drainage Div.Proc.Am.Soc.of Civ.Eng. Vol.83, No.IR 2 2, Sept.1957. Paper 1361, pp.1-24.

Appendix III
Side weirs and oblique weirs

3.1 Introduction

Most of the weirs described in this book serve mainly to measure discharges. Some, however, such as those described in Chapters 4 and 6, can also be used to control upstream water levels. To perform this dual function, the weirs have to be installed according to the requirements given in the relevant chapters. Since these weirs are usually relatively wide with respect to the upstream head, the accuracy of their flow measurements is not very high. Sometimes the discharge measuring function of the weir is entirely superseded by its water level control function, resulting in a contravention in their installation rules. The following weirs are typical examples of water level control structures.

Side weir: This weir is part of the channel embankment, its crest being parallel to the flow direction in the channel. Its function is to drain water from the channel whenever the water surface rises above a predetermined level so that the channel water surface downstream of the weir remains below a maximum permissible level.

Oblique weir: The most striking difference between an oblique weir and other weirs is that the crest of the oblique weir makes an angle with the flow direction in the channel. The reason for this is that the width (b) of the weir crest must be greater than the width of the channel so that with a change in discharge the water surface upstream of the weir remains between narrow limits. Some other weir types which can maintain such an almost constant upstream water level will also be described.

3.2 Side weirs

3.2.1 General

In practice, sub-critical flow will occur in almost all rivers and irrigation or drainage canals in which side weirs are constructed. Therefore, we shall restrict our attention to side weirs in canals where the flow remains subcritical.

The flow profile parallel to the weir, as illustrated in Figure A 3.1, shows an increasing depth of flow.

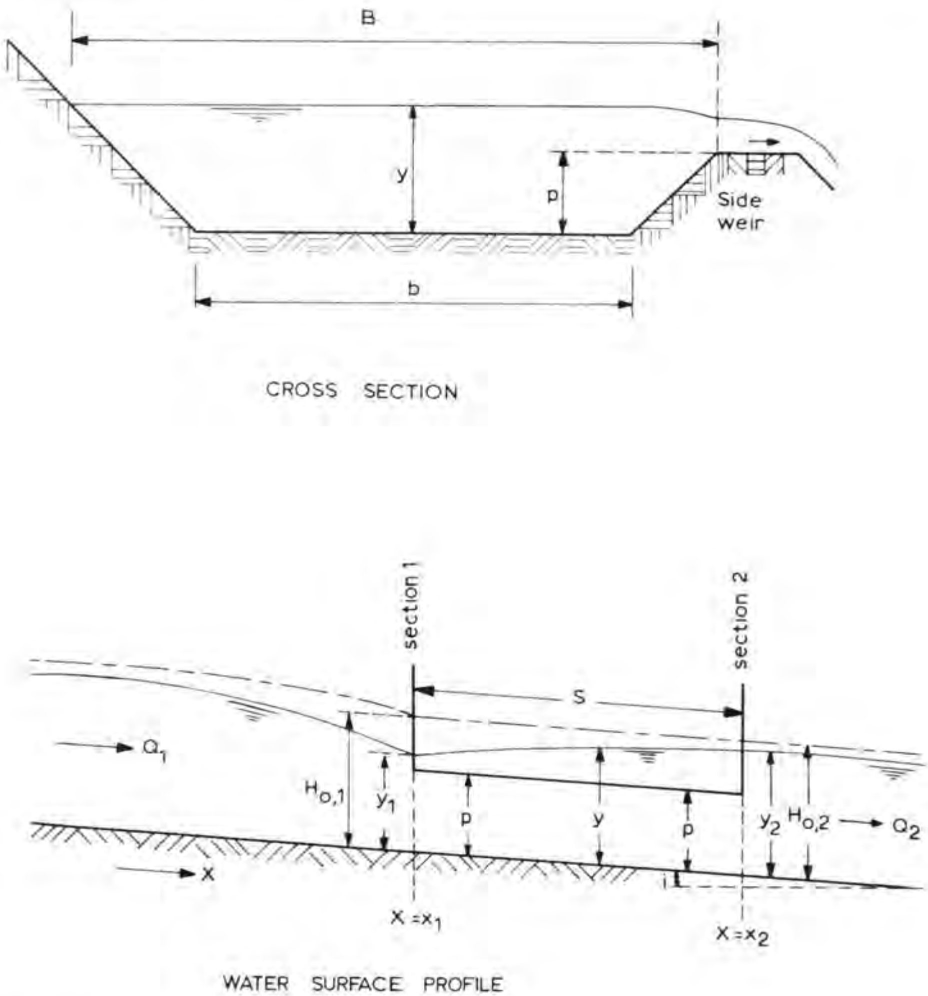

Fig.A 3.1. Dimension sketch of side weir.

The side weir shown in Figure A 3.1 is broad-crested and its crest is parallel to the channel bottom. It should be noted, however, that a side weir need not necessarily be broad-crested. The water depth downstream of the weir y_2 and also the specific energy head $H_{o,2}$ are determined by the flow rate remaining in the channel (Q_2) and the hydraulic characteristics of the downstream channel. This water depth is either controlled by some downstream construction or, in the case of a long channel, it will equal the normal depth in the downstream channel.

Normal depth is the only water depth which remains constant in the flow direction at a given discharge (Q_2), hydraulic radius, bottom slope, and friction coefficient of the downstream channel.

3.2.2 Theory

The theory on flow over side weirs given below is only applicable if the area of water surface drawdown perpendicular to the centre line of the canal is small in comparison with the water surface width of this canal. In other words, if $y - p < 0.1\ B$.

For the analysis of spatially varied flow with decreasing discharge, we may apply the energy principle as introduced in Chapter 1, Sections 1.6 and 1.8. When water is being drawn from a channel as in Figure A 3.1, energy losses in the overflow process are assumed to be small,and if we assume in addition that losses in specific energy head due to friction along the side weir equal the fall of the channel bottom, the energy line is parallel to this bottom.We should therefore be able to write

$$H_{o,1} = y_1 + \frac{Q_1^2}{2g\ A_1^2} = y_2 + \frac{Q_1^2}{2g\ A_1^2} = H_{o,2} \tag{1}$$

If the specific energy head of the water remaining in the channel is (almost) constant while at the same time the discharge decreases, the water depth y along the side weir should increase in downstream direction as indicated in Figures A 3.1 and 3.2, which is the case if the depth of flow along the side weir is subcritical (see also Chapter 1, Fig.1.9).

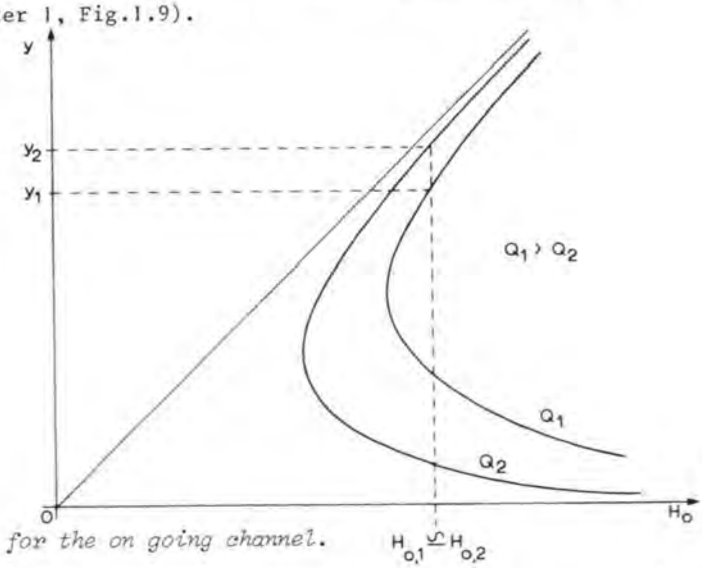

Fig.A 3.2. H_o-y diagram for the on going channel.

Far upstream of the side weir, the channel water depth y_0 equals the normal depth related to the discharge Q_1 and the water has a specific energy $H_{o,0}$, which is greater than $H_{o,2}$. Over a channel reach upstream of the weir, the water surface is drawn down in the direction of the weir. This causes the flow velocity to increase and results in an additional loss of energy due to friction expressed in the loss of specific energy head $H_{o,0} - H_{o,2}$. Writing Equation 1 as a differential equation we get

$$\frac{dH_o}{dx} = \frac{dy}{dx} + \frac{d}{dx}\frac{Q^2}{2gA^2} \tag{2}$$

or

$$\frac{dH_o}{dx} = 0 = \frac{dy}{dx} + \frac{1}{2g}\left[\frac{2Q}{A^2}\frac{dQ}{dx} - \frac{2Q^2}{A^3}\frac{dA}{dx}\right] \tag{3}$$

The continuity equation for this channel reach reads $dQ/dx = -q$, and the flow rate per unit of channel length across the side weir equals

$$q = C_s \frac{2}{3}\left[\frac{2}{3} g\right]^{0.5} (y - p)^{1.5} \tag{4}$$

The flow rate in the channel at any section is

$$Q = A\sqrt{2g(H_o - y)}$$

and finally

$$\frac{dA}{dx} = B\frac{dy}{dx}$$

so that Equation 3 can be written as follows

$$\frac{dy}{dx} = \frac{4C_s}{3^{1.5}B} \quad \frac{(H_o - y)^{0.5}(y-p)^{1.5}}{A/B + 2y - 2H_o} \tag{5}$$

where C_s denotes the effective discharge coefficient of the side weir. Equation 4 differs from Equation 1-36 (Chap.1) in that, since there is no approach velocity towards the weir crest, y has been substituted for H_o.

Equation 5, which describes the shape of the water surface along the side weir, can be further simplified by assuming a rectangular channel where B is constant and $A/B = y$, resulting in

$$\frac{dy}{dx} = \frac{4C_s}{3^{1.5}B} \; \frac{(H_o-y)^{0.5}\,(y-p)^{1.5}}{3\,y - 2\,H_o} \tag{6}$$

For this differential equation DE MARCHI (1934) found a solution which was confirmed experimentally by GENTILINI (1938) and COLLINGE (1957) and reads

$$x = \frac{3^{1.5}B}{2C_s}\left[\frac{(2H_o-3p)}{(H_o-p)}\left(\frac{H_o-y}{y-p}\right)^{0.5} - 3\,\arcsin\left(\frac{H_o-y}{H_o-p}\right)^{0.5}\right] + K \tag{7}$$

where K is an integration constant. The term in between the square brackets may be denoted as $\phi(y/H_o)$ and is a function of the dimensionless ratios $y/H_{o,2}$ and $p/H_{o,2}$ as shown in Figure A 3.3.

If p, y_2, and $H_{o,2}$ are known, the water surface elevation at any cross section at a distance $(x - x_2)$ along the side weir can be determined from the equation[1]

$$x-x_2 = \frac{3^{1.5}B}{2C_s}\left[\phi(y/H_{o,2}) - \phi(y_2/H_{o,2})\right] \tag{8}$$

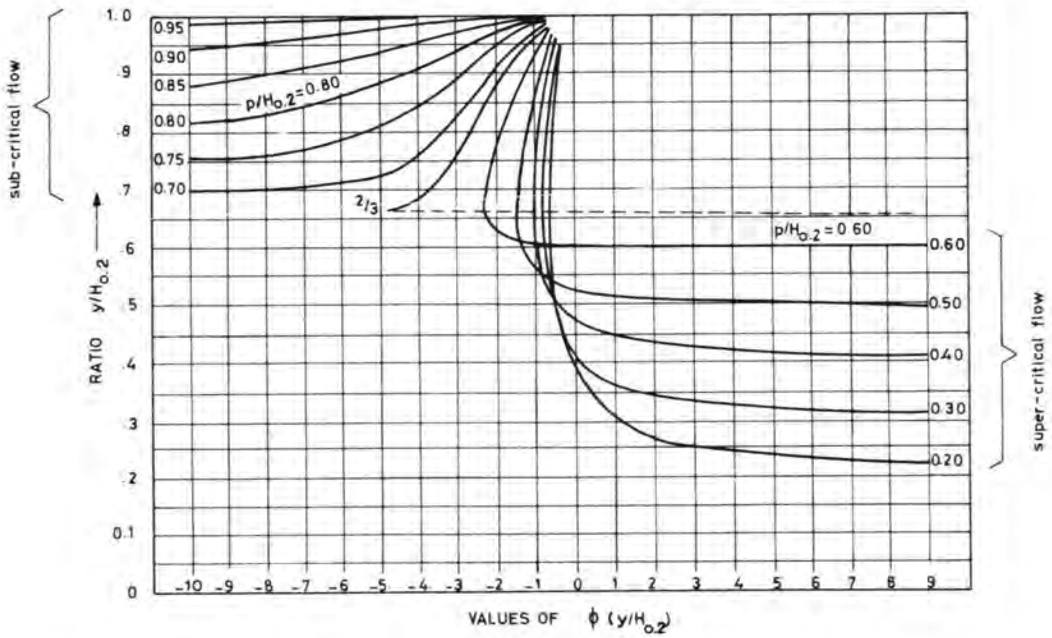

Fig.A 3.3 Values of $\phi(y/H_{o,2})$ for use in Equation 8.

[1] *If the flow along the weir is supercritical and no hydraulic jump occurs along the weir and the same simplifying assumptions are retained, Eqs.1 to 8 are also valid. Greater discrepancies, however, occur between theory and experimental results. Also, the water surface profile along the weir has a shape different from that shown in Fig.A 3.1.*

If the simplifying assumptions made to write Equation 1 cannot be retained, or, in other words, if the statement

$$\int \frac{v^2}{C^2R} - S \tan i \ll y_2 - y_1 \tag{9}$$

is not correct, the water surface elevation parallel to the weir can only be obtained by making a numerical calculation starting at the downstream end of the side weir (at $x = x_2$). This calculation also has to be made if the cross section of the channel is not rectangular.

For this procedure the following two equations can be used

$$y_u - y_d = -\frac{(v_u+v_d)(v_u-v_d)}{2g} + \left[\frac{v_d^2}{C^2R_d} - i\right] \Delta x \tag{10}$$

$$v_uA_u - v_dA_d = C_s \frac{2}{3}\left[\frac{2}{3} g\right]^{0.5} (y_d-p)^{1.5} \Delta x \tag{11}$$

where

- Δx = length of the considered channel section
- u = subscript denoting upstream end of section
- d = subscript denoting downstream end of section
- C = coefficient of Chézy
- R = hydraulic radius of channel

It should be noted that before one can use Equations 10 and 11 sufficient information must be available on both A and R along the weir. The accuracy of the water surface elevation computation will depend on the length and the chosen number of elementary reaches Δx.

3.2.3 Practical C_s-value

The reader will have noted that in Equations 3 to 9 an effective discharge coefficient C_s is used. For practical purposes, a value

$$C_s = 0.95\ C_d \tag{12}$$

may be used, where C_d equals the discharge coefficient of a standard weir of similar crest shape to those described in Chapters 4 and 6.

If Equations 4 to 11 are used for a sharp-crested side weir, the reader should be aware of a difference of $\sqrt{3}$ in the numerical constant between the head-discharge equations of broad-crested and sharp-crested weirs with rectangular control section. In addition it is proposed that the discharge coefficient (C_e) of a sharp-crested weir be reduced by about 10% if it is used as a side weir. This leads to the following C_s-value to be used in the equations for sharp-crested side weirs

$$C_s = 0.90 \sqrt{3}\, C_e \approx 1.55\, C_e \tag{13}$$

3.2.4 Practical evaluation of side weir capacity

Various authors proposed simplified equations describing the behaviour of sharp-crested side weirs along rectangular channels. However, discrepancies exist between the experimental results and the equations proposed, and it follows that each equation has only a restricted validity.

In this Appendix we shall only give the equations as proposed by FORCHHEIMER (1930), which give an approximate solution to the Equations 3 and 4 assuming that the water surface profile along the side weir is a straight line. The Forchheimer equations read:

$$\Delta Q = C_s \frac{2}{3} \sqrt{\frac{2}{3} g}\; S\left[\frac{y_1 + y_2}{2} - p\right]^{1.5} \tag{14}$$

and

$$\xi_1 = \frac{y_2 - y_1}{v_1^2/2g - v_2^2/2g - \Delta H_o} \tag{15}$$

where

ΔH_o = the loss of specific energy head along the side weir due to friction. ΔH_o can be estimated from

$$\Delta H_o = \{(v_1 - v_2)/2\}^2\; S/C^2R - iS \tag{16}$$

The most common problem is how to calculate the side weir length S, if $\Delta Q = Q_1 - Q_2$, y_2 and p are known. To find S an initial value of y_1 has to be estimated, which is then substituted into the Equations 14 and 15. By trial and error y_1 (and thus S) should be determined in such a way that $\xi_1 = 1.0$.

The equations 14 and 15 are applicable if

$$Fr_1 = v_1/\sqrt{gy_1} < 0.75 \tag{17}$$

and

$$y_1 - p \geqslant 0 \tag{18}$$

If the above limits do not apply, the water depth y_1 at the entrance of the side weir and the side weir length S required to discharge a flow $Q_1 - Q_2$ should be calculated by the use of Equation 1, which reads

$$H_{o,2} = y_1 + \frac{Q_1^2}{2gA_1^2} = y_2 + \frac{Q_2^2}{2gA_2^2} \tag{19}$$

In combination with the equation

$$-S = x_1 - x_2 = 2.73 \frac{B}{C_d} \left[\phi(y_1/H_{o,2}) - \phi(y_2/H_{o,2})\right] \tag{20}$$

The latter equation is a result of substituting Equation 12 into Equation 8. In using Equation 20 the reader should be aware that the term $x_1 - x_2$ is negative since $x_1 < x_2$. As mentioned before, values of $\phi(y/H_{o,2})$ can be read from Fig.A 3.3 as a function of the ratios $p/H_{o,2}$ and $y/H_{o,2}$.

3.3 Oblique weirs

3.3.1 Weirs in rectangular channels

According to AICHEL (1953), the discharge q per unit width of crest across oblique weirs placed in a rectangular canal as shown in Figure A 3.4 can be calculated by the equation

$$q = \left[1 - \frac{h_1}{p} \beta\right] q_n \tag{21}$$

where

q_n = the discharge over a weir per unit width if the same type of weir had been placed perpendicular to the canal axis ($\varepsilon = 90^\circ$).

β = a dimensionless empirical function of the angle of the weir crest (in degrees) with the canal axis.

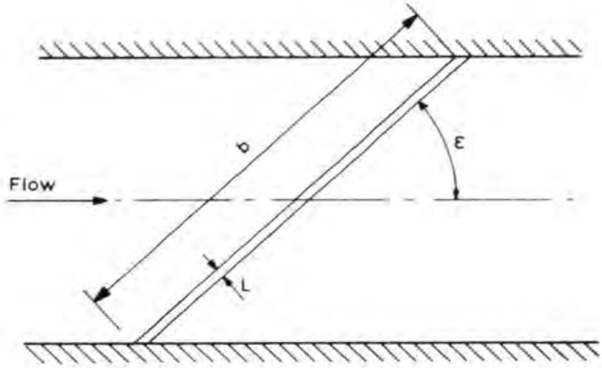

Fig.A 3.4. Oblique weir in channel having rectangular cross section.

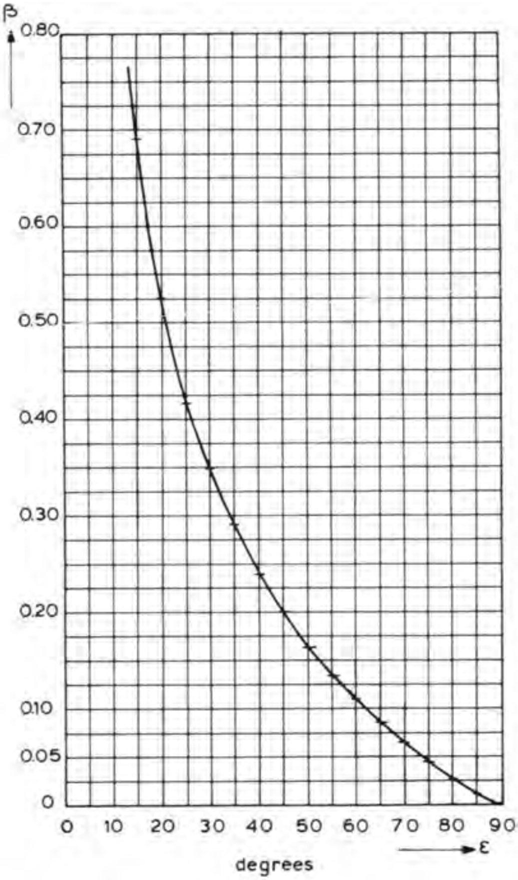

Fig.A 3.5. β-values as a function of ε.

Equation 21 is valid provided that the length of the weir crest L is small with respect to the weir width b and the upstream weir face is vertical. Values of the β coefficient are available (see Fig.A 3.5) for

$$h_1/p < 0.62 \qquad \text{and} \qquad \varepsilon > 30^{\circ} \tag{22}$$

or

$$h_1/p < 0.46 \qquad \text{and} \qquad \varepsilon > 30^{\circ} \tag{23}$$

3.3.2 Weirs in trapezoidal channels

Three weir types, which can be used to suppress water level variations upstream of the weir are shown in Figure A 3.6. Provided that the upstream head over the weir crest does not exceed 0.20 m (h_1 < 0.20 m) the unit weir discharge q can be estimated by the equation

$$q = r\, q_n \tag{24}$$

where

q_n = the discharge across a weir per unit width if the weir had been placed perpendicular to the canal axis (see Chaps.4 and 6)

r = a reduction factor as shown in Figure A 3.6.

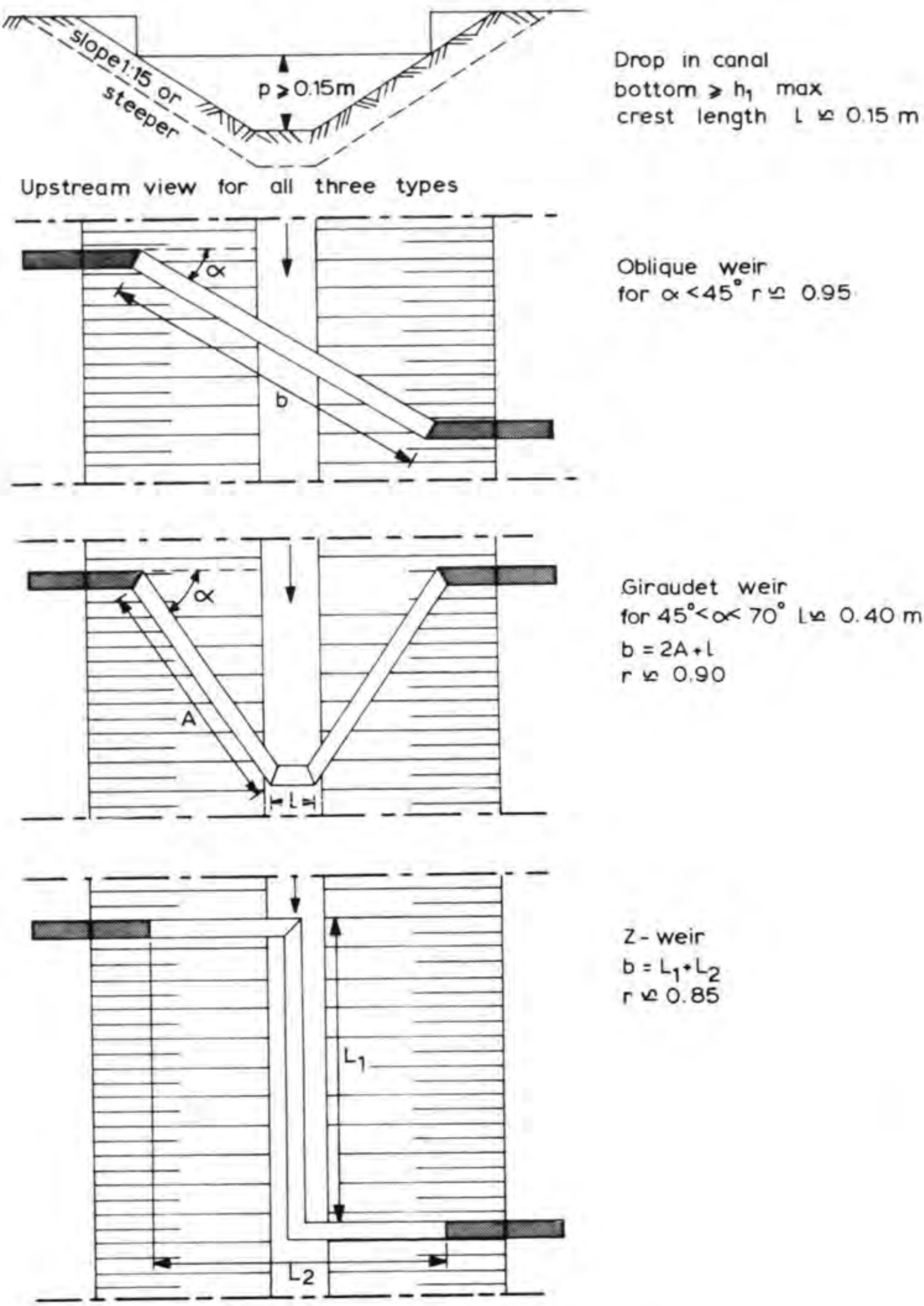

Fig.A 3.6. Weirs in trapezoidal channels.

3.4 Selected list of references

1. AICHEL, O.G.: Abflusszahlen für schiefe Wehre. (Discharge ratios for oblique weirs.) Z.VDI 95 (1953). No.1, Jan.1, pp.26-27.

2. COLLINGE, V.K.: The discharge capacity of side weirs. Proc.of the Inst. of Civil Engineers, Vol.6, 1957. Febr., pp.288-304.

3. ENGELS, H.: Versuche über Streichwehre. Mitt.aus dem Dresdener Flussbau-Laboratorium. Forschungsarbeiten auf dem Gebiete des Ingenieurwesens No. 200. Berlin 1917.

4. ENGELS, H.: Weitere Versuche über Streichwehre. Mitt. aus dem Dresdener Flussbau-Laboratorium. Forschungsarbeiten auf dem Gebiete des Ingenieurwesens no.201. 55 pp. Berlin 1920.

5. FORCHHEIMER, Ph.: Hydraulik. 3.Aufl., 1930, pp.406-408.

6. FRAZER, W.: The behaviour of side weirs in prismatic rectangular channels. Proc.of the Inst.of Civil Eng., Vol.6, 1957. Febr., pp.305-328.

7. GENTILINI, B.: Richerche sperimentali sugli sfioratori longitudinali (prima serie di prove). L'Energie Elettrica, 15 (1938), Sept. No.9, pp.583-595. Milano.

8. HENDERSON, F.M.: Open Channel Flow. MacMillan Comp. New York. 1966, 521 pp.

9. DE MARCHI, G.: Saggio di teoria de funzionamente degli stramazzi laterali. L'Energie Elettrica, 11 (1934), Nov., pp.849-860. Milano.

10. SCHAFFERNAK, F.: Streichwehrberechnung. Österreichische Wochenschrift f.d.öffentl.Baudienst. Heft 36, 1918.

11. SCHMIDT, M.: Zur Frage des Abflusses über Streichwehre. Mitt.Nr.41. Inst.für Wasserbau der Tech.Universität Berlin-Charlottenburg, 1954.

12. SCHMIDT, M.: Die Berechnung von Streichwehren. Die Wasserwirtschaft, 1954-1955, pp.96-100.

13. VEN TE CHOW: Open channel hydraulics. McGraw-Hill, New York, 680 pp.

Appendix IV
Suitable stilling basins

4.1 Introduction

Unless a weir or flume is founded on rock, a downstream stilling basin will be necessary. The floor of the stilling basin should be set at such a level that the hydraulic jump, if formed, occurs on the sloping downstream weir face or at the upstream end of the basin floor so that the turbulence in the jump will abate to a level which will not damage the unprotected downstream channel bed. Calculations for the floor level should be made for several discharges throughout the anticipated range of modular flow. To aid the engineer in designing a suitable stilling basin, hydraulic design criteria of a number of devices are given below.

4.2 Straight drop structures

4.2.1 Common drop

Illustrated in Figure A 4.1 is a drop structure that will dissipate energy if installed downstream of a weir with a vertical back face.

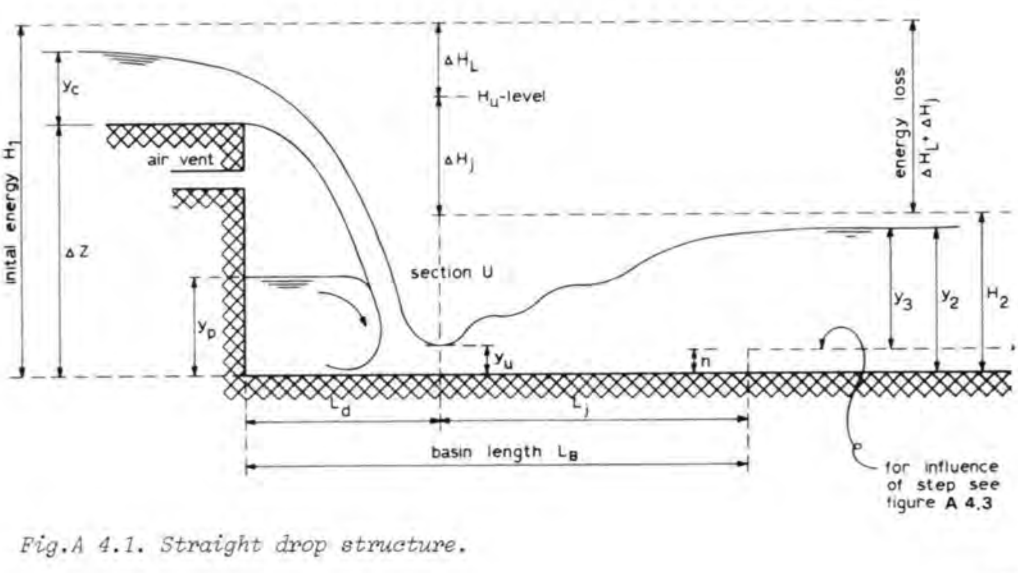

Fig.A 4.1. Straight drop structure.

The aerated free falling nappe will strike the basin floor and turn downstream at Section U. Beneath the nappe a pool is formed which supplies the horizontal thrust required to turn the nappe downstream. Because of the impact of the nappe on the basin floor and the turbulent circulation in the pool beneath the nappe, an amount of energy ΔH_L is lost. This energy loss has been determined in experiments by MOORE (1943), the results of which are shown in Figure A 4.2.

This figure shows that, with the basin floor as reference level, the energy loss at the base of a straight drop may be as much as 50% of the initial energy. Further energy will be dissipated in the hydraulic jump downstream of Section U. The loss of energy head ΔH_j over the jump is a function of the Froude number $Fr_u = v_u/(g\ A_u/B)^{\frac{1}{2}}$ of the incoming nappe; values of ΔH_j may be read from Figure A 4.2. The reader may note that the energy head H_2 downstream of the jump does not vary greatly with $\Delta z/y_c$ and is about equal to 2.5 y_c. This value of 2.5 y_c provides a satisfactory basis for design purposes.

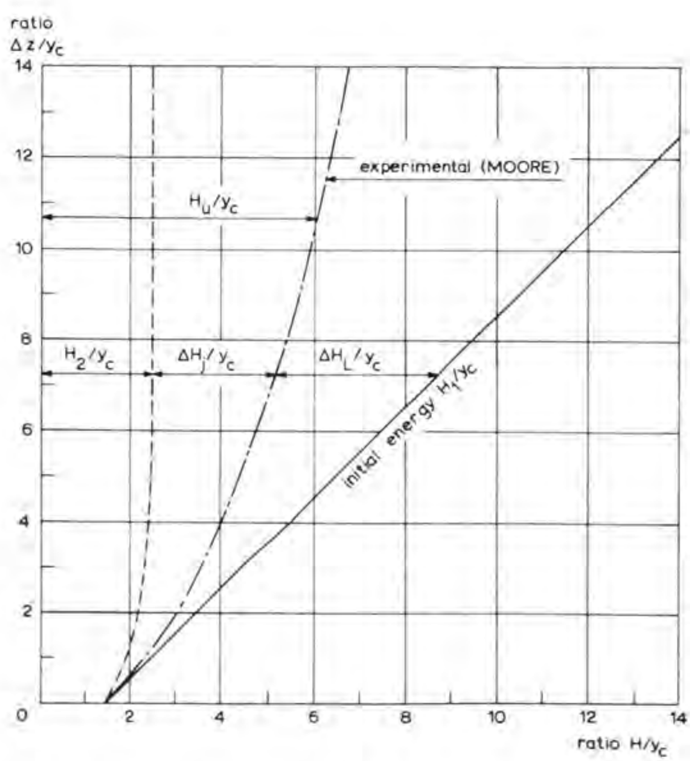

Fig.A 4.2. Energy dissipation at the base of a straight drop.

The geometry of the straight drop structure can be related to the following independent variables

- drop height Δz in metres
- unit weir discharge q in m^2/s

These two variables can be expressed in a dimensionless ratio by expressing q in terms of critical depth as

$$y_c = \sqrt[3]{\frac{q^2}{g}} \tag{1}$$

which after division of both terms by the drop height leads to

$$\frac{y_c}{\Delta z} = \sqrt[3]{\frac{q^2}{g \Delta z^3}} \tag{2}$$

The dimensionless ratio in the right-hand term of this equation is known as the drop number

$$D = \frac{q^2}{g \Delta z^3} \tag{3}$$

RAND (1955) found that the flow geometry at straight drops can be described by the following exponential functions of the drop number, which fit the experimental measurements made by himself and others with an error of 5 per cent or less.

The functions are:

$$L_d/\Delta z = 4.30\ D^{0.27} \tag{4}$$

$$y_p/\Delta z = 1.00\ D^{0.22} \tag{5}$$

$$y_u/\Delta z = 0.54\ D^{0.425} \tag{6}$$

$$y_2/\Delta z = 1.66\ D^{0.27} \tag{7}$$

In Equations 6 and 7, y_u is the initial depth and y_2 the sequent depth before and after a hydraulic jump in which a loss of energy head ΔH_j is involved. The values of y_u and y_2 may also be related to each other through the Froude number $Fr_u = v_u/\sqrt{gy_u}$ at Section U as

$$\frac{y_2}{y_u} = \tfrac{1}{2}\left[\sqrt{(1 + 8\ Fr_u^2)} - 1\right] \tag{8}$$

Equation 8, by approximation, may be written as

$$\frac{y_2}{y_u} = 1.4\ Fr_u - 0.4 \tag{9}$$

which is the equation of a straight line as shown in Fig.A 4.3 for the situation $y_3 = y_2$. To localize the hydraulic jump immediately below the straight drop we recommend that an upward step at the end of the basin floor be added as a standard design feature.

From experimental data FORSTER and SKRINDE (1950) have developed a diagram which permits the prediction of the performance of a given abrupt step when v_u, y_u, y_2, y_3, and n are known. In Figure A 4.3, a point (Fr_u, y_3/y_u) lying above the mentioned line $y_3 = y_2$ represents the condition of $y_3 > y_2$, in which case the abrupt step results only in an increased submergence. For a point situated between the lines $y_3 = y_2$ and the lower limit of the experimental range, the position of the point relative to the corresponding n/y_u curve gives the effect of the abrupt step on the flow pattern. The diagram shown in Figure A 4.3 was developed for an abrupt step at $L_j = 5(n + y_3)$ downstream of Section U.

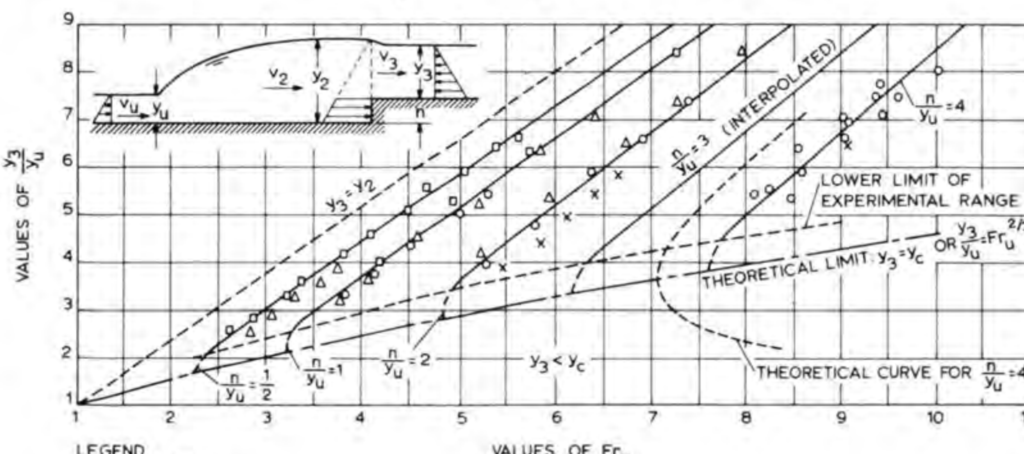

LEGEND
□ n = 0.0238 m
△ n = 0.0366 m
○ n = 0.0539 m
× n = 0.0079 m
n < 0

Fig.A 4.3. Experimental relations between Fr_u, y_3/y_u and n/y_u for an abrupt rise.
(After FORSTER & SKRINDE, 1950).

For design purposes, Figure A 4.3 can be used to determine the dimensions L_j and n of a stilling basin downstream of Section U if Fr_u and y_3 are known. The procedure to find the largest required value of n if Fr_u, y_u, and y_3 are known is as follows:

Define for the flow condition at or near maximum discharge the situation of the point (Fr_u, y_3/y_u) and by interpolation that of the corresponding value of the ratio n/y_u. Repeat this exercise for other discharges within the anticipated range of discharge and use the highest n-value for the design. A minimum tailwater level y_3 to prevent the jump from being washed out can thus also be determined.

The straight drop spillway will still be effective if the tailwater level does not reach critical depth above the weir crest, i.e. as long as the weir flow is modular.

4.2.2 USBR basin

The USBR has developed an alternative basin which is especially suitable if tailwater level is greater than the sequent depth and varies independently of the flow rate.

This impact block type basin was developed for low heads, and gives a good energy dissipation over a wide range of tailwater levels. The energy dissipation is principally by turbulence induced by the impingement of the incoming jet upon the impact blocks. The required tailwater level, therefore, is more or less independent of the drop distance Δz.

The linear hydraulic dimensions of the structure as shown in Figure A 4.4 are:

total basin length (for L_d-values see Fig.A4.5)	$L_B = L_d + 2.55\ y_c$
basin length to upstream face of impact block	$L_d + 0.8\ y_c$
minimum tailwater depth required	$y_2 \geq 2.15\ y_c$
optimum impact block height	$0.8\ y_c$
width and spacing of impact blocks	$(0.40 \pm 0.15)\ y_c$
optimum end sill height	$0.4\ y_c$
minimum side wall height	$y_2 + 0.85\ y_c$

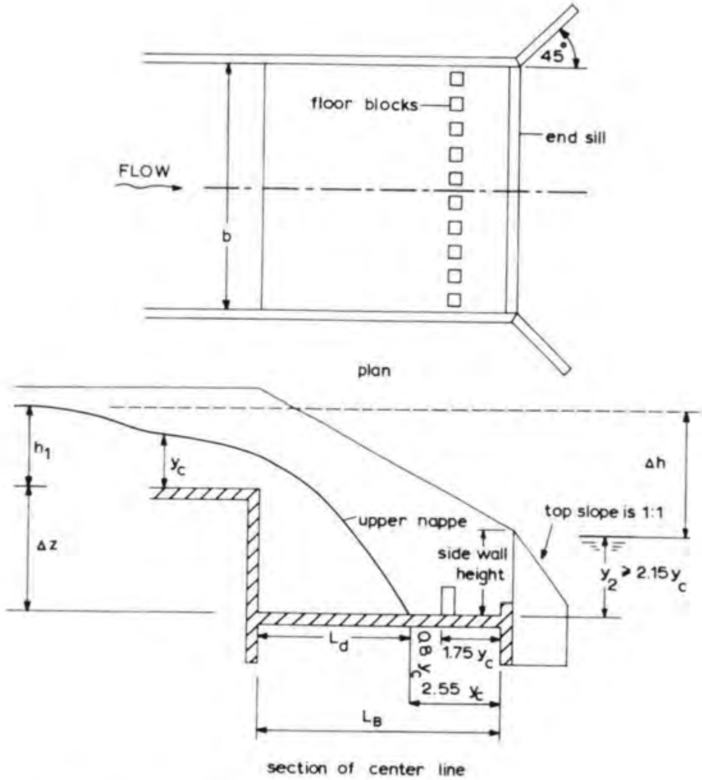

Fig.A 4.4. Impact block type basin.

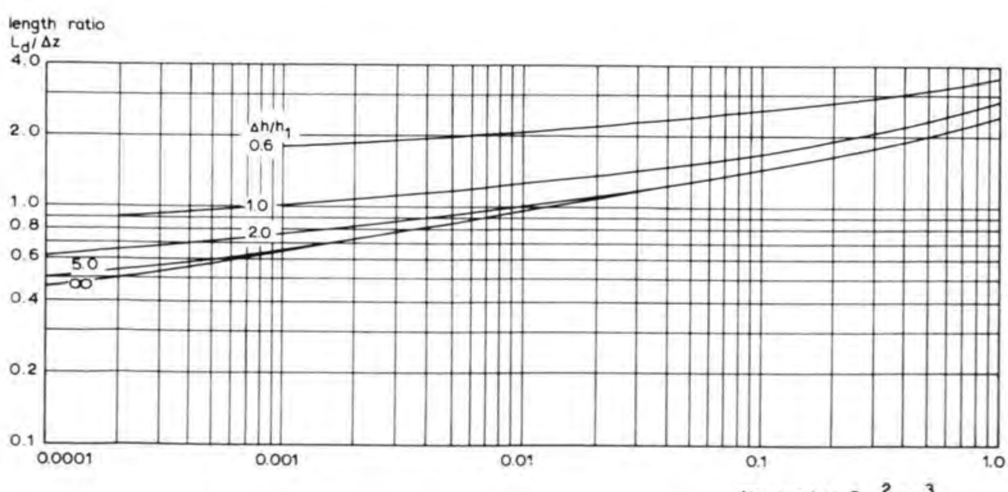

Fig.A 4.5. Values of the length ratio $L_d/\Delta z$ (after USBR, 1960).

Viewed from above, floor blocks should be square and should occupy between 50 and 60 per cent of the stilling basin width. As has already been discussed for a rising tailwater level, the length ratio $L_d/\Delta z$ is influenced by the rate of submergence. Fig.A 4.5 shows values of $L_d/\Delta z$ as a function of the ratio $\Delta h/h_1$ and the drop number **D**.

4.3 Inclined drops or chutes

4.3.1 Common chute

Downstream from the control section of either a weir or flume, a sloping downstream face or expansion is a common design feature. The slope of the downstream face usually varies between 1 in 4 and 1 in 6. By approximation we may write that the flow velocity over the downstream face equals

$$v_u = q/y_u \tag{10}$$

where q is the unit discharge on the downstream face and

y_u is the water depth at a particular point on the downstream apron.

Values of y_u may be determined by the use of Table 1. The symbols used in Table 1 are defined in Figure A 4.6.

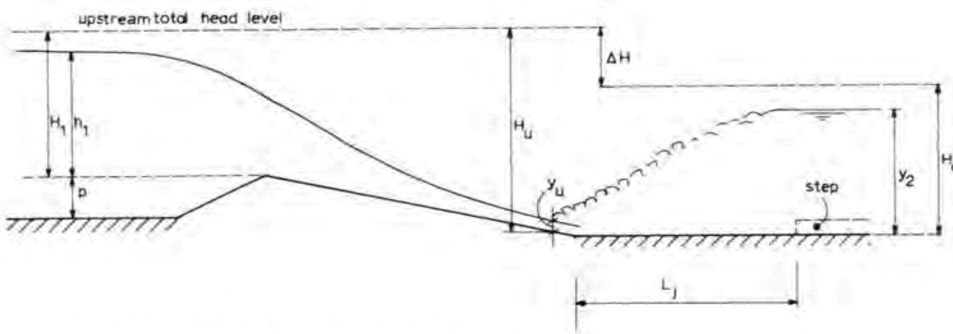

Fig.A 4.6. Definition sketch to Table 1.

A hydraulic jump will form in the horizontal (rectangular) basin provided that the tailwater depth is greater than the sequent depth y_2 to y_u and v_u. Minimum values of y_2 may be read from Figure A 4.3 for rectangular basins. The length of

TABLE 1. DIMENSIONLESS QUANTITIES

y_u/y_c	H_u/y_c	$H_{0.2}/y_c$	$\Delta H/y_c$
1.00000	1.50000	1.50000	0.00000
0.97580	1.50091	1.50088	0.00003
0.95310	1.50352	1.50330	0.00022
0.93175	1.50768	1.50700	0.00068
0.91161	1.51327	1.51175	0.00152
0.89258	1.52017	1.51738	0.00279
0.87455	1.52828	1.52374	0.00454
0.85745	1.53752	1.53070	0.00682
0.84120	1.54780	1.53818	0.00962
0.82571	1.55906	1.54609	0.01297
0.81096	1.57124	1.55434	0.01690
0.79687	1.58425	1.56288	0.02137
0.78339	1.59811	1.57168	0.02643
0.77050	1.61272	1.58065	0.03207
0.75812	1.62806	1.58985	0.03821
0.74626	1.64408	1.59913	0.04495
0.73485	1.66077	1.60851	0.05226
0.72389	1.67807	1.61830	0.05977
0.71333	1.69595	1.62751	0.06844
0.70317	1.71440	1.63707	0.07733
0.69336	1.73341	1.64673	0.08668
0.67476	1.77293	1.66602	0.10691
0.65739	1.81439	1.68528	0.12911
0.64111	1.85761	1.70451	0.15310
0.62582	1.90247	1.72361	0.17886
0.61142	1.94890	1.74255	0.20635
0.59785	1.99675	1.76133	0.23542
0.58501	2.04601	1.77991	0.26610
0.57284	2.09659	1.79831	0.29828
0.56129	2.14833	1.81648	0.33185
0.55033	2.20126	1.83440	0.36686
0.53988	2.25530	1.85212	0.40318
0.52992	2.31046	1.86961	0.44085
0.52042	2.36659	1.88689	0.47970
0.51133	2.42369	1.90395	0.51974
0.50263	2.48172	1.92077	0.56095
0.49430	2.54068	1.93736	0.60332
0.48631	2.60051	1.95374	0.64677
0.47863	2.66123	1.96995	0.69128
0.47126	2.72266	1.98592	0.73674
0.46416	2.78496	2.00170	0.78326
0.45733	2.84793	2.01722	0.83071
0.45074	2.91174	2.03261	0.87913
0.44439	2.97629	2.04783	0.92846
0.43826	3.04146	2.06277	0.97869
0.43233	3.10733	2.07760	1.02973
0.42661	3.17391	2.09223	1.08168
0.42107	3.24117	2.10666	1.13451

(Table 1 cont.)

y_u/y_c	H_u/y_c	$H_{o.2}/y_c$	$\Delta H/y_c$
0.4157	3.3090	2.1210	1.1880
0.4105	3.3774	2.1351	1.2423
0.4055	3.4466	2.1490	1.2976
0.3959	3.5865	2.1765	1.4100
0.3868	3.7287	2.2033	1.5254
0.3782	3.8731	2.2296	1.6435
0.3701	4.0197	2.2553	1.7644
0.3625	4.1683	2.2805	1.8878
0.3551	4.3194	2.3050	2.0144
0.3482	4.4714	2.3294	2.1420
0.3416	4.6256	2.3531	2.2725
0.3353	4.7817	2.3765	2.4052
0.3293	4.9398	2.3993	2.5405
0.3236	5.0994	2.4217	2.6777
0.3181	5.2606	2.4439	2.8167
0.3128	5.4236	2.4656	2.9580
0.3077	5.5881	2.4870	3.1011
0.3028	5.7542	2.5080	3.2462
0.2982	5.9217	2.5287	3.3930
0.2937	6.0911	2.5491	3.5420
0.2893	6.2614	2.5691	3.6923
0.2852	6.4334	2.5889	3.8445
0.2811	6.6068	2.6084	3.9984
0.2773	6.7817	2.6276	4.1541
0.2735	6.9577	2.6465	4.3112
0.2699	7.1354	2.6652	4.4702
0.2263	7.3140	2.6837	4.6303
0.2629	7.4941	2.7018	4.7923
0.2549	7.9499	2.7463	5.2036
0.2474	8.4130	2.7894	5.6236
0.2405	8.8840	2.8313	6.0527
0.2340	9.3619	2.8719	6.4900
0.2280	9.8466	2.9116	6.9350
0.2223	10.3379	2.9501	7.3878
0.2170	10.8361	2.9876	7.8485
0.2120	11.3403	3.0267	8.3136
0.2072	11.8509	3.0602	8.7907
0.2027	12.3671	3.0952	9.2719
0.1985	12.8893	3.1294	9.7599
0.1945	13.4175	3.1630	10.2545
0.1906	13.9510	3.1957	10.7553
0.1870	14.4901	3.2280	11.2621
0.1835	15.0343	3.2596	11.7747
0.1802	15.5841	3.2904	12.2937
0.1770	16.1362	3.3211	12.8157
0.1739	16.6985	3.3508	13.3477
0.1710	17.2637	3.3801	13.8836
0.1682	17.8330	3.4090	14.4240

After Water Resources Board (1966)

such a horizontal basin equals that part of the basin which is situated downstream of Section U in Figure A 4.1, and equals $L_j = 5(n + y_3)$.

It is recommended that a tabulation be made of the Froude number Fr_u near the toe of the downstream face, and of the depth of flow y_u throughout the anticipated discharge range. The sequent depth rating should be plotted with the stage-discharge curve of the tailwater channel to ensure that the jump forms on the basin floor.

4.3.2 SAF Basin

An alternative stilling basin suitable for use on low-head structures was developed at the St.Anthony Falls Hydraulic Laboratory (SAF-basin) of the University of Minnesota. The basin is used as a standard by the U.S.Soil Conservation Service, and has been reported by BLAISDELL (1948, 1949). The general dimensions of the SAF-basin are shown in Figure A 4.7.

The design parameters for the SAF-basin are as follows.

TABLE 2. DESIGN PARAMETERS OF THE SAF-BASIN

$Fr_u = v_u/(gA_u/B)^{\frac{1}{2}}$	L_B/y_2	TW/y_2
1.7 to 5.5	$4.5/Fr_u^{0.76}$	$1.1 - Fr_u^2/120$
5.5 to 11	$4.5/Fr_u^{0.76}$	0.85
11 to 17	$4.5/Fr_u^{0.76}$	$1.0 - Fr_u^2/800$

where y_2 is the theoretical sequent depth of the jump corresponding to y_u as shown in Figure A 4.3 (use $y_3 = y_2$ curve). The height of the end sill is given by $C = 0.07\ y_2$ and the freeboard of the sidewall above the maximum tailwater depth to be expected during the life of the basin is given by $z = y_2/3$.

The sidewalls of the basin may be parallel or they may diverge. Care should be taken that the floor blocks occupy between 40 and 55% of the stilling basin width, so that their width and spacing must be increased with the amount of divergence of the sidewalls.The effect of air entrainment should not be taken into account in the design of the basin; however, its existence within the stilling basin calls for a generous freeboard ($y_2/3$).

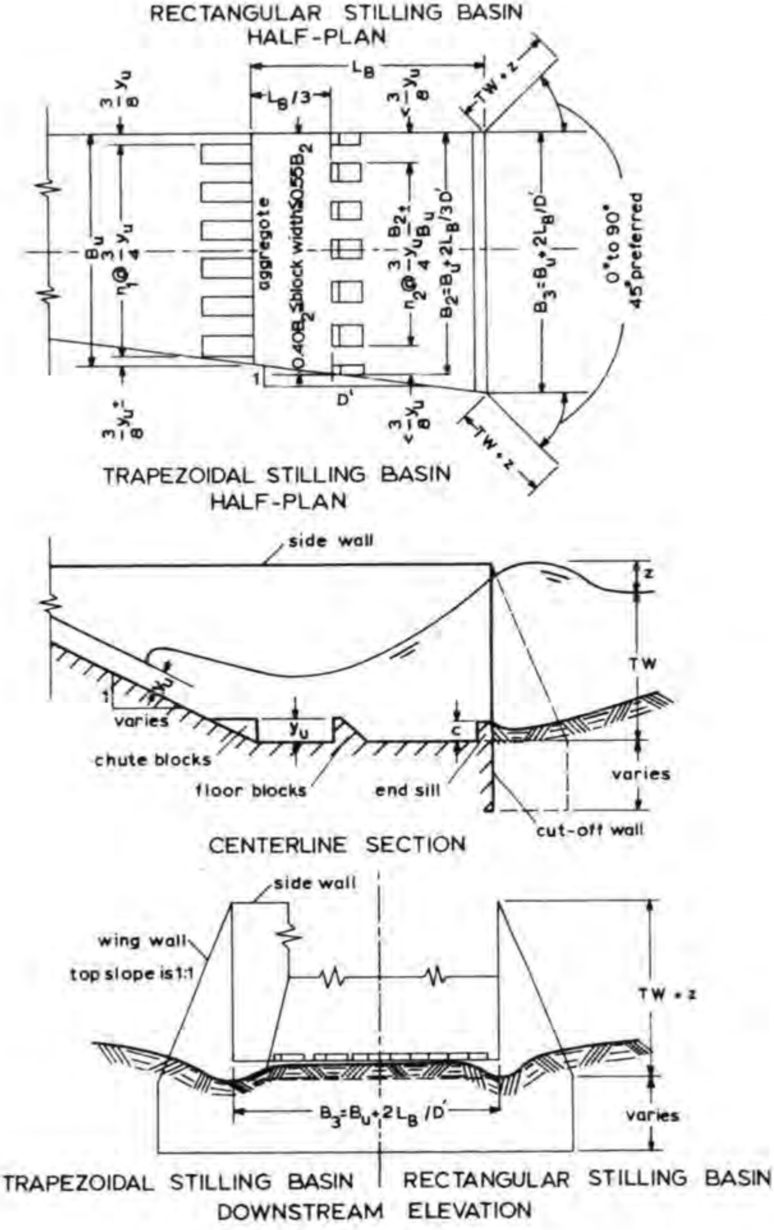

Fig.A 4.7. SAF-basin dimensions.

Design A: Tailwater depth calculated by $TW/y_2 = 1.1 - Fr_u^2/120$ *(see Table 2).*

Design B: Tailwater depth is 15% greater than in Design A.

PHOTOS: 1:20 scale model of SAF stilling basin discharging 1200 m^3/s *in prototype.*
$b = 40.0$ *m,* $\Delta H = 3.50$ *m.*

4.4 Riprap protection

To prevent bank damage by erosive currents passing over the end sill of a basis or leaving the tail of a structure, riprap is usually placed on the downstream channel bottom and banks. Several factors affect the stone size required to resist the forces which tend to move riprap. In terms of flow leav-

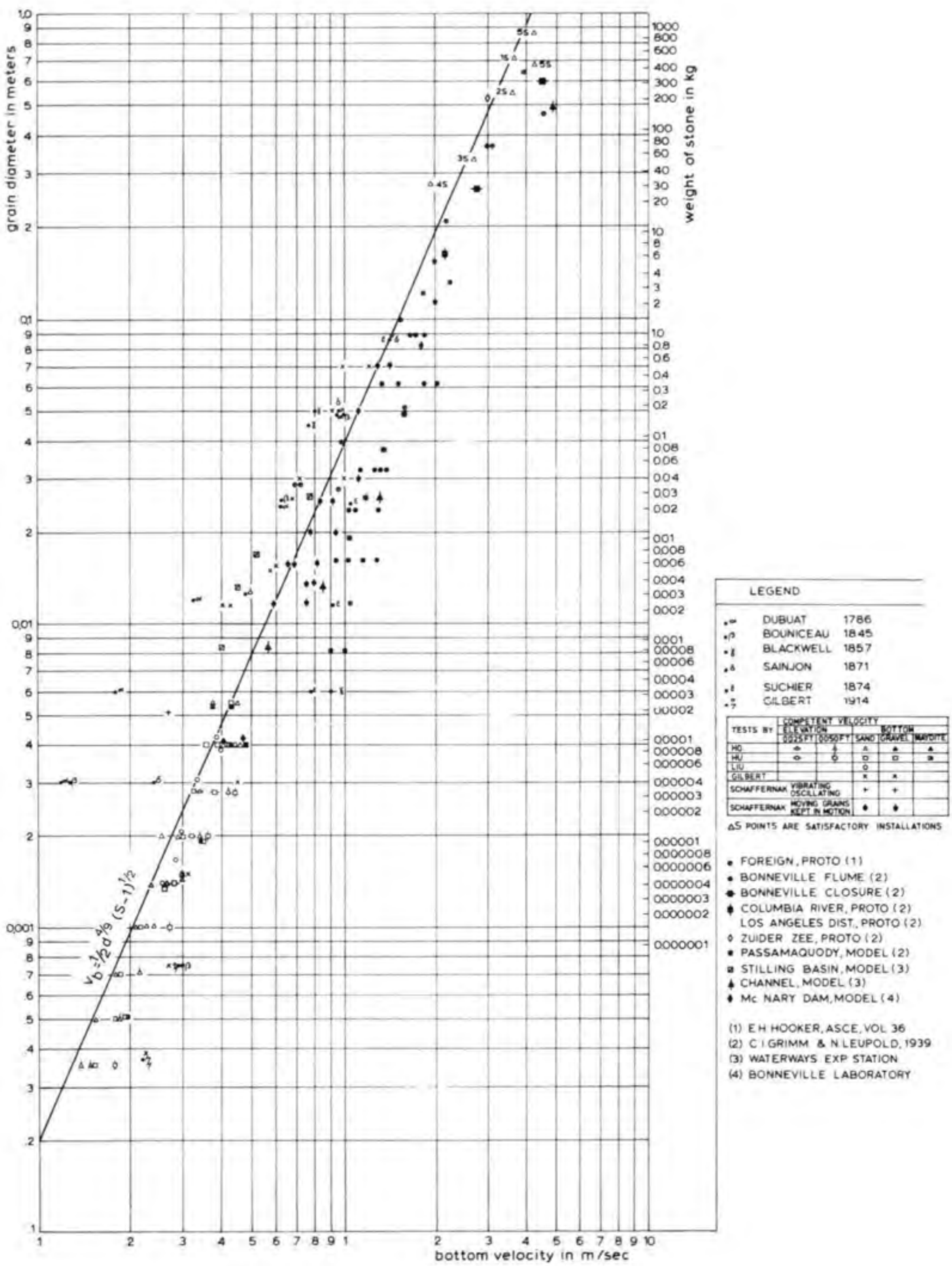

Fig.A 4.8. Curve to determine maximum stone size.

ing a structure, these factors are velocity, flow direction, turbulence, and waves. The purpose of this section is to give the design engineer a tool to determine the size of riprap to be used downstream from discharge measurement devices or stilling basins and to determine the type of filter or bedding material placed below the riprap.

4.4.1 Determining maximum stone size in riprap mixture

From published data, a tentative curve was selected showing the minimum stone diameter as a function of the bottom velocity. This curve is shown in Fig.A 4.9. Downstream of stilling basins, the conception "bottom velocity" is difficult to define because of the highly turbulent flow pattern. The velocity at which the water strikes the riprap is rather unpredictable unless the basin is tested.

For practical purposes, however, PETERKA (1958) recommends that, to find the stone diameter in Fig. A 4.9, use be made of the average velocity based on discharge divided by cross-sectional area at the end sill of the stilling basin. More than 60% of the riprap mixture should consist of stones which have length, width, and thickness dimensions as nearly alike as is practicable, and be of curve size or larger; or the stones should be of curve weight or heavier and should not be flat slabs.

4.4.2 Filter material placed beneath riprap

Besides the size and weight of the individual stones other factors that affect the satisfactory installation of a protective construction are the gradation of the entire mass of riprap, the type of filter material placed beneath the riprap, the thickness of each layer, and its possible permeability to water and sand.

permeability to water

To prevent a filter layer from lifting by water entering the channel through bottom or banks, the permeability to water of the construction as a whole and of each separate filter layer must be greater than that of the underlying material. For this to occur:

$$\frac{\Delta H_n}{D_n} < \frac{\Delta H_{n-1}}{D_{n-1}} < \frac{\Delta H_{n-2}}{D_{n-2}} \quad \text{etc.} \tag{11}$$

where ΔH_n equals the energy head loss over the top riprap layer and D_n equals the thickness of this n-th layer. The subscript n-1, n-2, etc. stands for each subsequent underlying layer (see Fig.A 4.9).

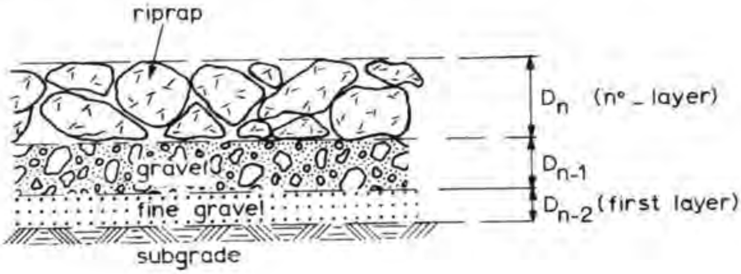

Fig.A 4.9. Example of filter construction.

To maintain a sufficient permeability to water the following condition must be observed:

$$\frac{d_{15}\ n^{e}\text{-layer}}{d_{15}\ (n-1)^{e}\text{-layer}} = \ldots = \frac{d_{15}\ \text{first layer}}{d_{15}\ \text{subgrade}} = 5 \text{ to } 40 \tag{12}$$

where d_{15} equals the diameter of the sieve opening whereby 15% of the total weight of the sample passes the sieve. Depending on the shape and gradation of the grains, roughly the following ratios can be used in Equation 12

- homogeneous round grains (gravel)	5 - 10
- homogeneous angular grains (broken gravel, rubble)	6 - 20
- well-graded grains	12 - 40

To prevent the filter from clogging, it is advisable that d_5 of a layer be larger than 0.75 mm.

permeability to sand

A riprap protection may fail because waves or groundwater flowing into the channel remove material from beneath the riprap (n^o-layer). To prevent the loss of fine material from an underlying filter layer or the subgrade, the following requirements with regard to imperviousness to sand must be met

$$\frac{d_{15}\ n^{e}\text{-layer}}{d_{85}\ (n-1)^{e}\text{-layer}} = \ldots = \frac{d_{15}\ \text{first layer}}{d_{85}\ \text{subgrade}} \leqslant 5 \tag{13}$$

and

$$\frac{d_{50}\ n^{e}\text{-layer}}{d_{50}\ (n-1)^{e}\text{-layer}} = \ldots = \frac{d_{50}\ \text{first layer}}{d_{50}\ \text{subgrade}} = 5 \text{ to } 60 \tag{14}$$

As before, the ratio in Equation 14 depends on the shape and gradation of the grains as follows:

- homogeneous round grains (gravel) 5 - 10
- homogeneous angular grains (broken gravel, rubble) 10 - 30
- well-graded grains 12 - 60

The requirements in this section describe the sieve curves of the successive filter layers. Provided that the sieve curve of the riprap layer (n^e layer) and the subgrade are known, other layers can be plotted.

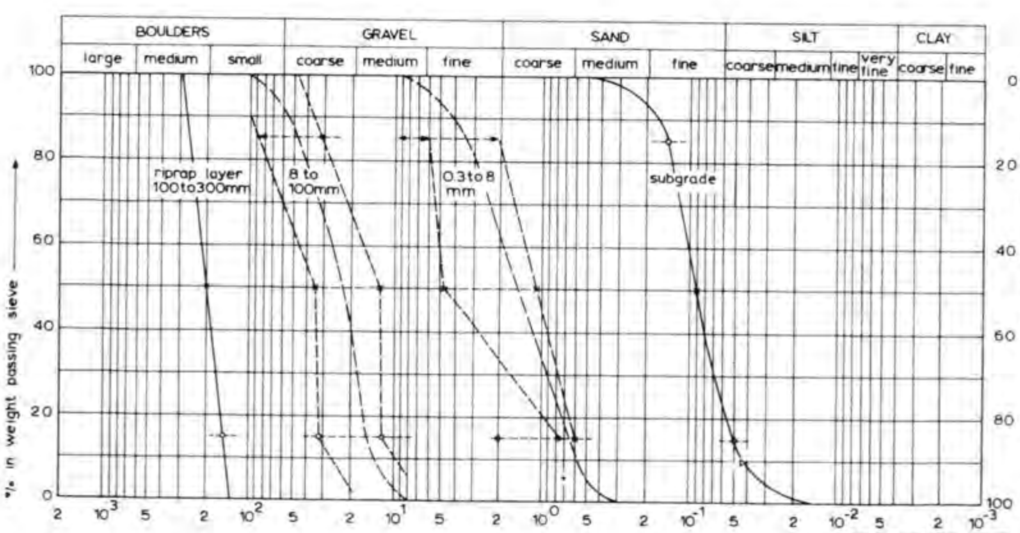

Fig.A 4.10. Sieve curves of a filter construction (after L.van Bendegom,1969).

In practice one should use materials that have a grain size distribution which is locally available, since it is uneconomical to compose a special mixture. To provide a stable and effectively functioning filter, the sieve curves for subgrade and filter layers should run about parallel for the small-diameter grains.

An example of plotting sieve curves of the various layers of a riprap protection is shown in Figure A 4.10.

4.4.3 Filter construction

To obtain a fair grain size distribution throughout a filter layer, each layer should be sufficiently thick.The following thicknesses must be regarded as a minimum for a filter construction made in the dry

- sand, fine gravel	0.05 to 0.10 m	
- gravel	0.10 to 0.20 m	
- stones	1.5 to 2	times the largest stone diameter

With filters constructed under water, these thicknesses have to be increased considerably to compensate for irregularities in the subgrade and because it is more difficult to apply an even layer under water.

Many variations can be made on the basic filter construction. One or more of the layers can be replaced with other materials. With some protective linings, only the riprap layer (n^o layer) is maintained, while the underlying layers are replaced by one single layer. For example

- concrete blocks on a nylon filter
- stones on braided azobé slabs on plastic filter
- gabions on fine gravel
- nylon-sand mattresses

The usual difficulty with these variants is their perviousness to underlying sand.The openings in each layer should not be greater than $0.5 \times d_{85}$ of the underlying material. If openings are greater, one should not replace all underlying layers but maintain as many layers (usually one) as are needed to prevent the subgrade from being washed through the combined layer.

At structure-to-filter and filter-to-unprotected channel "joints", the protective construction is most subject to damage. This is because the filter layer is subject to subsidence while the (concrete) structure itself is well founded. Underlying material (subgrade) may be washed out at these joints if no special measures are taken. It is recommended that the thickness of the filter construction be increased at these places. Some examples of common constructional details are shown in Fig.A4.11.

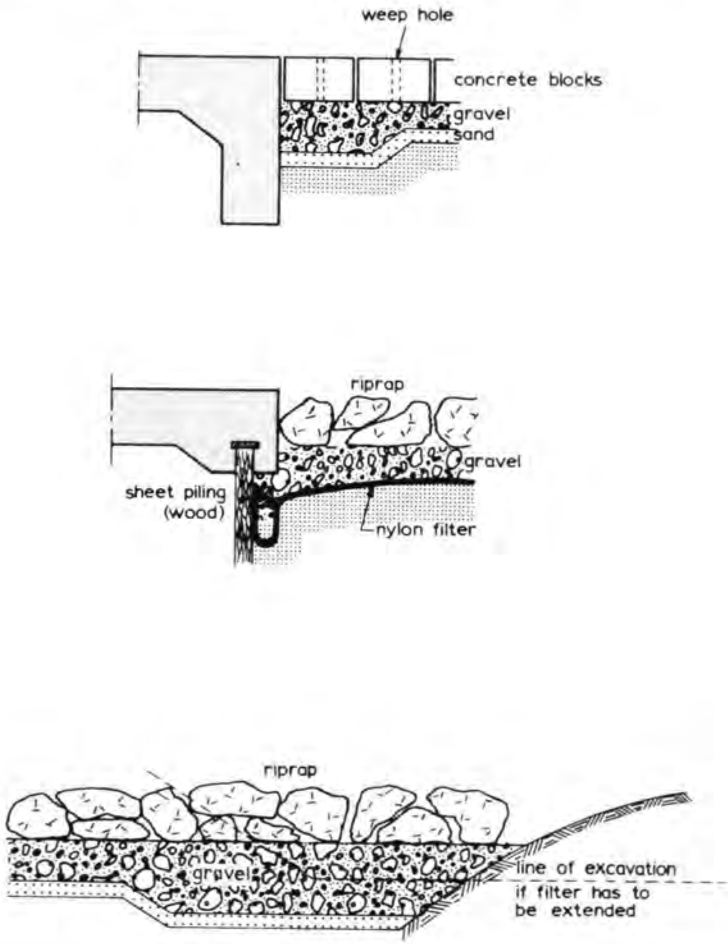

Fig.A 4.11.Examples of filter construction details (after L.van Bendegom,1969).

As a rule of thumb we may suggest a length of riprap protection which is neither less than 4 times the (maximum) normal depth in the tailwater channel, nor less than the length of the earth transition, nor less than 1.50 m.

4.5 Selected list of references

1. VAN BENDEGOM, L. et al.: Principles governing the design and construction of economic revetments for protecting the banks of rivers and canals for ocean and inland navigation. 20th Intern.navigation Congr.Paris, 43 pp. 1969.

2. BERRY, N.K.: The start of bed load movement. Thesis. Univ.of Colorado, USA, 1948.

3. BLAISDELL, F.W.: The SAF stilling basin. U.S.Dept.of Agric.Soil Conservation Service. St.Anthony Falls Hydraulic Laboratory, Minneapolis, Minn., Dec.1943.

4. BLAISDELL, F.W.: The SAF stilling basin. A structure to dissipate the destructive energy in high-velocity flow from spillways. U.S.Dept.of Agric. Service in cooperation with the Minnesota Agric.Exp.Sta. & St.Anthony Falls Hydraulic Laboratory. Agric.Handbook 156. Washington D.C. U.S.Gov.Printing Office, 1959.

5. CANALS AND RELATED STRUCTURES. Commissioner's office, Denver (Col.). U.S.Dept.of the Interior, Bureau of Recl.Design Standards 3. 1961.

6. DESIGN OF SMALL DAMS. U.S.Dept.of the Interior. Bureau of Recl., Washington D.C. U.S.Gov.Printing Office. 1960. 611 pp.

7. DORT, J.A.van, BOS, M.G.: Drainage principles and applications. Chapt.29: Main drainage systems. Int.Institute for Land Recl.& Improvement. Publication 16. Vol.IV. Wageningen 1974. pp.124-224.

8. FORSTER, J.W., SKRINDE, R.A.: Control of the hydraulic jump by sills. Transactions, American Society of Civil Engineers. Vol.115, 1950. pp.973-987.

9. HENDERSON, F.M.: Open Channel Flow. MacMillan Co., New York 1966.522 pp.

10. MAVIS, F.T., LAUSHEY, L.M.: A reappraisal of the beginnings of bed movement-competent velocity. Proc.of the Int.Assoc.for Hydraulic Research. March 1948. Stockholm. pp.213-218.

11. MOORE, W.L.: Energy loss at the base of a free overfall. Trans.of the Amer.Soc.of Civ.Engineers. 1943. Vol.108, pp.1343-1392. Paper No.2204.

12. PETERKA, A.J.: Hydraulic design of stilling basins and energy dissipators. U.S.Dept.of the Interior. Bureau of Recl.Water Resources Techn.Publ. Engineering Monograph No.25, 1964. 223 pp.

13. RAND, W.: Flow geometry at straight drop spillways. Proc.Amer.Soc.of Civil Engineers. Vol.8. Sept.1955. No.791.

14. VLUGTER, H.: 12½ Jaar hydrodynamische research aan waterloopkundige modellen in Nederlandsch Indië. De Ingenieur in Ned.Indië. No.9. 1941.

Appendix V
Tables

5.1 Factors for conversion of units

Adapted from King H.W. and E.F.Brater, 1963

To reduce A to B, multiply A by F. To reduce B to A, multiply B by G.

Unit A	Factor F	Factor G	Unit B
LENGTH			
Miles	63,360. ∷	.000015783	Inches
Miles	5,280. ∷	.00018939	Feet
Miles	1,609.35	.00062137	Meters
Miles	1.60935	.62137	Kilometers
Kilometers	3,280.83	.00030480	Feet
Meters	3.2808	.30480	Feet
Yards	36. ∷	.027778	Inches
Feet	12. ∷	.083333	Inches
Meters	39.370	.025400	Inches
Inches	2.5400	.39370	Centimeters
Nautical miles	6,080.20	.00016447	Feet
Nautical miles	1.1516	.86836	Miles
Fathoms	6. ∷	.16667	Feet
Gunter's chains	66. ∷	.0151515	Feet
Rods	16.5 ∷	.060606	Feet
SURFACE			
Square miles	27,878,400. ∷	.000000035870	Square feet
Square miles	640. ∷	.0015625 ∷	Acres
Square miles	259.000	.0038610	Hectares
Acres	43,560. ∷	.000022957	Square feet
Acres	4,046.9	.00024710	Square meters
Hectares	2.47104	.40469	Acres
Hectares	10,000. ∷	.0001 ∷	Square meters
Square feet	144. ∷	.0069444	Square inches
Square inches	6.4516	.15500	Square centimeters
Square meters	10.764	.092902	Square feet

∷ *Exact values*

(Table 1. cont.)

Unit A	Factor F	Factor G	Unit B
VOLUME			
Cubic feet	1,728. *	.00057870	Cubic inches
Cubic inches	16.387	.061024	Cubic centimeters
Cubic meters	35.3145	.028317	Cubic feet
Cubic meters	1.3079	.76456	Cubic yards
Cubic feet	7.4805	.13368	U.S.gallons
Cubic feet	6.2321	.16046	Imperial gallons
Cubic feet	28.317	.035314	Liters
U.S.gallons	231. *	.0043290	Cubic inches
Imperial gallons	277.274	.0036065	Cubic inches
Liters	61.0234	.016387	Cubic inches
U.S.gallons	3.7854	.26417	Liters
Imperial gallons	1.2003	.83311	U.S.gallons
Imperial gallons	4.5437	.22009	Liters
U.S.bushels	1.2445	.80356	Cubic feet
Fluid ounces	1.8047	.55411	Cubic inches
Acre-feet	43,560. *	.000022957	Cubic feet
Acre-feet	1,613.3	.00061983	Cubic yards
Acre-feet	1,233.5	.00081071	Cubic meters
Acre-inches	3,630. *	.00027548	Cubic feet
Millions U.S.gallons	133,681.	.0000074805	Cubic feet
Millions U.S.gallons	3.0689	.32585	Acre-feet
Feet depth on 1 square mile	27,878,400. *	.000000035870	Cubic feet
Feet depth on 1 square mile	640. *	.0015625 *	Acre-feet
Inches depth on 1 square mile	2,323,200. *	.00000043044	Cubic feet
Inches depth on 1 square mile	53.333	.01875 *	Acre-feet

* Exact values

(Table 1. cont.)

Unit A	Factor F	Factor G	Unit B
VELOCITIES			
Miles per hour	1.4667	.68182	Feet per second
Meters per second	3.2808	.30480	Feet per second
Meters per second	2.2369	.44704	Miles per hour
Knots	1.1516	.86836	Miles per hour
Knots	1.6889	.5921	Feet per second
DISCHARGE			
Cubic metre per second	35.3145	.028317	Second-feet
Cubic metre per second	1000. ::	.001 ::	Litre per second
Cubic metre per second	86,400. ::	.000011574	Cubic metre per 24 hours
Cubic metre per second	15,850.20	.00006309	U.S.gallon per minute
Second-feet	28.317	.03531	Litre per second
Second-feet	60. ::	.016667	Cubic feet per minute
Second-feet	86,400. ::	.000011574	Cubic feet per 24 hours
Second-feet	448.83	.0022280	U.S.gallons per minute
Second-feet	646,317.	.0000015472	U.S.gallons per 24 hours
Second-feet	1.9835	.50417	Acre-feet per 24 hours
Second-feet	723.98	.0013813	Acre-feet per 365 days
Second-feet	50. ::	.02 ::	Miner's inches, Idaho
Second-feet	50. ::	.02 ::	Miner's inches, Kansas
Second-feet	50. ::	.02 ::	Miner's inches, Nebraska
Second-feet	50. ::	.02 ::	Miner's inches, New Mexico
Second-feet	50. ::	.02 ::	Miner's inches, N.Dakota
Second-feet	50. ::	.02 ::	Miner's inches, S.Dakota
Second-feet	40. ::	.025 ::	Miner's inches, Arizona
Second-feet	40. ::	.025 ::	Miner's inches, California
Second-feet	40. ::	.025 ::	Miner's inches, Montana
Second-feet	40. ::	.025 ::	Miner's inches, Oregon
Second-feet	38.4 ::	.026042	Miner's inches, Colorado
Millions U.S.gallons per day	1.5472	.64632	Second-feet
Inches depth per hour	645.33	.0015496	Second-feet per square mile
Inches depth per day	26.889	.037190	Second-feet per square mile

:: Exact values

(Table 1. cont.)

Unit A	Factor F	Factor G	Unit B
DISCHARGE (cont.)			
Second-feet per square mile	1.0413	.96032	Inches depth per 28 days
Second-feet per square mile	1.0785	.92720	Inches depth per 29 days
Second-feet per square mile	1.1157	.89630	Inches depth per 30 days
Second-feet per square mile	1.1529	.86738	Inches depth per 31 days
Second-feet per square mile	13.574	.073668	Inches depth per 365 days
Second-feet per square mile	13.612	.073467	Inches depth per 366 days
Acre-inches per hour	1.0083 +	.99173 +	Second-feet
Cubic-feet per minute	7.4805	.13368	U.S.gallons per minute
Cubic-feet per minute	10,772.	.000092834	U.S.gallons per 24 hours
U.S.gallons per minute	1,440. ::	.00069444	U.S.gallons per 24 hours
PRESSURES ($0^{o}C = 32^{o}F$)			
Atmospheres (mean)	14.697	.068041	Pounds per square inch
Atmospheres (mean)	29.921	.033421	Inches of mercury
Atmospheres (mean)	760.	.0013158	Millimeters of mercury
Atmospheres (mean)	33.901	.029498	Feet of water
Atmospheres (mean)	1.0333	.96778	Kilograms per square cm
Inches of mercury	1.1330	.88261	Feet of water
Pounds per square inch	2.0359	.49119	Inches of mercury
Pounds per square inch	51.711	.019338	Millimeters of mercury
Feet of water	62.416	.016022	Pounds per square foot
Pounds per square inch	2.3071	.43344	Feet of water
WEIGHT			
Pounds	7,000. ::	.00014286	Grains
Grams	15.432	.064799	Grains
Kilograms	2.2046	.45359	Pounds
Long tons (2240 pounds)	1.12 ::	.89286	Short tons
Long tons	1.0160	.98421	Metric tons (1,000 kg)
POWER			
Horsepower	550. ::	.0018182	Foot-pounds per second
Kilowatts	1.3405	.746	Horsepower
Kilowatts	8,760. ::	.00011416	Kilowatt-hours per year
Horsepower	8,760. ::	.00011416	Horsepower-hours per year
Horsepower	6,535.	.00015303	Kilowatt-hours per year

:: Exact values + Usually taken as unity

5.2 Conversion of inches to millimetres

Inches	milli-metres	Inches	milli-metres	Inches	milli-metres	Inches	milli-metres
1/32"	0.79	19/32"	15.08	1 5/16"	33.34	2 7/8"	73.02
1/16"	1.59	5/8"	15.87	1 3/8"	34.92	3"	76.20
3/32"	2.38	21/32"	16.67	1 7/16"	36.51	3 1/8"	79.37
1/8"	3.17	11/16"	17.46	1 1/2"	38.10	3 1/4"	82.55
5/32"	3.97	23/32"	18.26	1 9/16"	39.69	3 3/8"	85.72
3/16"	4.76	3/4"	19.05	1 5/8"	41.27	3 1/2"	88.90
7/32"	5.56	25/32"	19.84	1 11/16"	42.86	3 5/8"	92.07
1/4"	6.35	13/16"	20.64	1 3/4"	44.45	3 3/4"	95.25
9/32"	7.14	27/32"	21.43	1 13/16"	46.04	3 7/8"	98.42
5/16"	7.94	7/8"	22.22	1 7/8"	47.62	4"	101.60
11/32"	8.73	29/32"	23.02	1 15/16"	49.21	4 1/4"	107.95
3/8"	9.52	15/16"	23.81	2"	50.80	4 1/2"	114.30
13/32"	10.32	31/32"	24.62	2 1/8"	53.97	4 3/4"	120.65
7/16"	11.11	1"	25.40	2 1/4"	57.15	5"	127.00
15/32"	11.91	1 1/16"	26.99	2 3/8"	60.32	5 1/4"	133.35
1/2"	12.70	1 1/8"	28.57	2 1/2"	63.50	5 1/2"	139.70
17/32"	13.49	1 3/16"	30.16	2 5/8"	66.67	5 3/4"	146.05
9/16"	14.29	1 1/4"	31.75	2 3/4"	69.85	6"	152.40
1/20"	1.27	6/20"	7.62	11/20"	13.97	16/20"	20.32
2/20"	2.54	7/20"	8.89	12/20"	15.24	17/20"	21.59
3/20"	3.81	8/20"	10.16	13/20"	16.51	18/20"	22.86
4/20	5.08	9/20"	11.43	14/20"	17.78	19/20"	24.13
5/20"	6.35	10/20"	12.70	15/20"	19.05	20/20"	25.40

(Tab.2 cont.)

Inches	milli-metres	Inches	milli-metres	Inches	milli-metres
0.10	2.54	0.41	10.41	0.72	18.28
0.11	2.79	0.42	10.66	0.73	18.54
0.12	3.05	0.43	10.92	0.74	18.79
0.13	3.30	0.44	11.18	0.75	19.05
0.14	3.56	0.45	11.43	0.76	19.30
0.15	3.81	0.46	11.68	0.77	19.55
0.16	4.06	0.47	11.93	0.78	19.81
0.17	4.32	0.48	12.19	0.79	20.06
0.18	4.57	0.49	12.44	0.80	20.32
0.19	4.83	0.50	12.70	0.81	20.57
0.20	5.08	0.51	12.95	0.82	20.82
0.21	5.33	0.52	13.20	0.83	21.08
0.22	5.59	0.53	13.46	0.84	21.33
0.23	5.84	0.54	13.71	0.85	21.59
0.24	6.10	0.55	13.97	0.86	21.84
0.25	6.35	0.56	14.22	0.87	22.09
0.26	6.60	0.57	14.47	0.88	22.35
0.27	6.86	0.58	14.73	0.89	22.60
0.28	7.11	0.59	14.98	0.90	22.86
0.29	7.37	0.60	15.24	0.91	23.11
0.30	7.62	0.61	15.49	0.92	23.36
0.31	7.87	0.62	15.74	0.93	23.62
0.32	8.13	0.63	16.00	0.94	23.87
0.33	8.38	0.64	16.25	0.95	24.13
0.34	8.64	0.65	16.51	0.96	24.38
0.35	8.89	0.66	16.76	0.97	24.63
0.36	9.14	0.67	17.01	0.98	24.89
0.37	9.39	0.68	17.27	0.99	25.14
0.38	9.65	0.69	17.52	1.00	25.40
0.39	9.90	0.70	17.78		
0.40	10.16	0.71	18.03		

Subject index

A

B

C

D

E

I

J

K

L

M

S

Z

LIST OF AVAILABLE PUBLICATIONS

PUBLICATIONS

(3/D) Erich H. Jacobi. *Flurbereinigung in Europa.* 1961, 157 pp.
(6) *A priority scheme for Dutch land consolidation projects.* 1960, 84 pp.
(7) *An assessment of investments in land reclamation from the point of view of the national economy.* 1969, 65 pp.
(8) F. Hellinga. *Local administration of water control in a number of European countries.* 1960, 46 pp.
(9) L. F. Kamps. *Mud distribution and land reclamation in the eastern Wadden Shallows.* 1963, 91 pp.
(11) P. J. Dieleman, ed. *Reclamation of salt affected soils in Iraq.* 1963, 175 pp.
(12) C. H. Edelman. *Applications of soil survey in land development in Europe.* 1963, 43 pp.
(13) L. J. Pons, and I. S. Zonneveld. *Soil ripening and soil classification.* 1975, 128 pp.
(14) G. A. W. van de Goor and G. Zijlstra. *Irrigation requirements for double cropping of lowland rice in Malaya.* 1968, 68 pp.
(15) D. B. W. M. van Dusseldorp. *Planning of service centres in rural areas of developing countries.* 1971, 159 pp.
(16) *Drainage principles and applications.* Vols I/IV (1972–1974), 1455 pp.
(17) *Land evaluation for rural purposes.* 1973, 116 pp.
(19) M. G. Bos, and J. Nugteren. *On irrigation efficiencies.* 1978, 140 pp. revised edition
(20) M. G. Bos, ed. *Discharge Measurement Structures.* 1976, 464 pp.
(21) N. A. de Ridder and A. Erez. *Optimum use of water resources.* 1977, 250 pp.
(22) FAO. *A Framework for land evaluation.* 1977, 87 pp.
(23) K. J. Beek. *Land Evaluation for Agricultural Development.* 1978, 336 pp.

BULLETINS

(1) W. F. J. van Beers. *The auger hole method.* 1958, 32 pp. Rev. offprint 1970.
(1/D) W. F. J. van Beers. *Die Bohrloch-Methode.* 1962, 32 pp.
(3) W. F. J. van Beers. *Acid Sulphate Soils.* 1962, 31 pp.
(4) B. Verhoeven. *On the calciumcarbonate content of young marine sediments.* 1963, 27 pp.
(5) P. J. Dieleman and N. A. de Ridder. *Studies of salt water movement in the Bol Guini Polder, Chad Republic.* 1964, 40 pp.
(6) A. J. de Groot. *Mud transport studies in coastal waters from the western Scheldt to the Danish Frontier.* 1964.
(7) *Code of practice for the design of open watercourses and ancillary structures.* 1964, 80 pp.
(8/F) W. F. J. van Beers. *Quelques nomogrammes pour le calcul des espacements des drains.* 1966, 21 pp.
(9) D. J. Shaw. *The Managil South-Western extension to the Gezira Scheme.* 1965, 37 pp.
(10) F. Homma. *A viscous fluid model for demonstration of groundwater flow to parallel drains.* 1968, 32 pp.
(11) G. P. Kruseman, and N. A. de Ridder. *Analysis and evaluation of pumping test data.* 1970, 2nd ed. 200 pp.
(11/F) G. P. Kruseman, and N. A. de Ridder. *Interpretation et discussion des pompages d'essai.* 1973, 2nd ed. 213 pp.
(11/S) G. P. Kruseman, and N. A. de Ridder. *Análisis y evaluación de los datos de ensayos por bombeo.* 1975, 212 pp.
(12) J. G. van Alphen, and F. de los Rios Romero. *Gypsiferous soils.* 1971, 44 pp.
(13) J. H. Edelman. *Groundwater hydraulics of extensive aquifers.* 1972, 216 pp.
(14) Ch. A. P. Takes. *Land settlement and resettlement projects.* 1975, 44 pp.
(15) W. F. J. van Beers. *Computing drain spacings.* 1978, 47 pp. revised edition. R. J. Oosterbaan.
(16) C. A. Alva, J. G. van Alphen et al. *Problemas de drenaje y salinidad en la Costa Peruana.* 1976, 116 pp.

BIBLIOGRAPHIES

(4) L. F. Abell, and W. J. Gelderman. *Annotated bibliography on reclamation and improvement of saline and alkali soils.* 1964, 59 pp.
(5) C. A. de Vries, and B. C. P. H. van Baak. *Drainage of agricultural lands.* 1966, 28 pp.
(6) J. G. van Alphen, and L. F. Abell. *Annotated bibliography on reclamation and improvement of saline and sodic soils* (1966–1960). 43 pp.
(7) C. A. de Vries. *Agricultural extension in developing countries.* 125 pp.
(8) C. J. Brouwer, and L. F. Abell. *Bibliography on cotton irrigation.* 1970, 41 pp.
(9) S. Raadsma, and G. Schrale. *Annotated bibliography on surface irrigation methods.* 1971, 72 pp.
(10) R. H. Brook. *Soil survey interpretation.* 1975, 64 pp.
(11) *Land and water development.* 1975, 80 pp.
(12) *Land and water development.* 1976, 96 pp.
(13) L. F. Abell. *Abstract Journals on Irrigation, drainage and water resources engineering.* 1978, 47 pp.
(14) B. C. P. H. van Baak. *Land and water development*, 1977, 168 pp.

ANNUAL REPORTS: free of charge

Information about exchange and sale of ILRI publications can be obtained from:

INTERNATIONAL INSTITUTE FOR LAND RECLAMATION AND IMPROVEMENT/ILRI
P.O. BOX 45, 6700 AA WAGENINGEN/THE NETHERLANDS